Inflammation and Colorectal Cancer:

Elucidation of the cellular and molecular mechanisms by which interleukin 22 contributes to the development and progression of colorectal cancer



Sarah McCuaig

St. Hilda's College

Nuffield Department of Medicine

University of Oxford

A thesis submitted for the degree of

Doctor of Philosophy

Trinity 2017

Abstract

Sarah McCuaig | DPhil Thesis Abstract | St. Hilda's College | Trinity 2017

Inflammation and Colorectal Cancer:
Elucidation of the cellular and molecular mechanisms by which interleukin 22 contributes to the development and progression of colorectal cancer

Colorectal cancer (CRC) is a molecularly heterogeneous disease driven by the complex interplay between genetic factors, such as oncogenic mutations, and microenvironmental factors, such as aberrant immunity. Notably, interleukin 22 (IL-22), which plays a critical role in intestinal epithelial repair, promotes CRC progression in murine models of both colitis-associated and sporadic CRC. However, the phenotypes associated with IL-22/IL-22 receptor expression in human CRC remain uncharacterized and the molecular mechanisms of IL-22-dependent tumourigenesis are not understood. Thus the primary aim of this study was to understand the mechanisms by which IL-22 contributes to the development and progression of human colorectal cancer.

Specific driving mutations in human CRC critically influence the impact of the IL-22 pathway on disease progression. The *KRAS* oncogene is mutated in roughly 40% of colorectal cancers and carries a minor adverse prognostic impact. However, using independent training and validation cohorts in tumour transcriptomic datasets totalling 1820 patients, we identified that in patients with high tumoural expression of either or both subunits of the heterodimeric IL-22 receptor (*IL22RA1, IL10RB*), *KRAS* mutation markedly worsens prognosis. Using a panel of CRC cell lines and primary human organoids, we confirmed that this prognostic association is due to a functional interaction between IL-22 and mutant *KRAS* by observing that IL-22 enhances chemoresistance, 3-dimensional clonogenicity, and proliferation specifically in CRC cells with both high IL-22 receptor levels and *KRAS* mutations. Taking unbiased RNA-sequencing and proteomic approaches, we identified non-cell autonomous and cell autonomous pathways by which IL-22 may interact with *KRAS* to promote malignancy. IL-22 enhanced ELR^+ CXC chemokine expression, which may condition a tumour-promoting immune microenvironment, and induced the Myc pathway, which may augment proliferation and glycolytic flux, in *KRAS* mutant cells.

Collectively, this work has revealed that an IL-22 signal is interpreted differently in the presence or absence of mutant *KRAS*. Our data points toward a method to identify a subset of poor prognosis IL-22 receptor-high, *KRAS* mutant CRC patients and we hypothesise that blockade of the IL-22 pathway in these patients may have therapeutic benefit.

Acknowledgements

I express my deepest gratitude to my supervisor Professor Fiona Powrie, for the autonomy that she has given me to pursue interesting questions at the intersection of human immunology and cancer biology, and to explore the realm of clinical translation. I thank her for her scientific guidance and for the example that she has set for me of the power of a positive outlook despite life's many demands. I am also indebted to Professor Tim Maughan. When we first shared our clinical findings with Tim, he embraced our immunological perspective on colon cancer with enthusiasm, he facilitated a collaboration with Professor Sabine Tejpar to confirm our findings, and he was the voice of clinical reason as we put together a proposal for an experimental study of therapeutic IL-22 blockade in CRC. Tim has really served as our bridge to Oncology at Oxford and we hope that this will be a lasting and mutually beneficial link. I will also be forever grateful for my Canadian compatriot in the lab, Dr. Nathan West. Nathan has been a sounding board for experimental ideas, a go-to for all questions cancer-related, and a proofreader extraordinaire. Despite his own heavy workload, Nathan has always made time for discussion and his mentorship has been instrumental to my development as a scientist. I am also incredibly grateful for the insightful input, infectious enthusiasm, and generous donation of cell lines from Dr. Simon Leedham.

As it relates to this project, I would like to acknowledge Professor Sabine Tejpar of KU Leuven, for providing us access to transcriptomic data from the PETACC3 clinical trial as a confirmation cohort. Moreover, I would like to thank our collaborators at the Swiss Institute of Bioinformatics, Mauro Delorenzi and in particular Dr. David Barras. David performed the confirmation cohort analysis for this project and has graciously guided me through RNA-sequencing analysis by sharing code and always being prompt to answer questions. Moreover, I thank Professor Doreen Cantrell and Dr. Mahima Swamy of the University of Dundee for performing the proteomics and in particular to Mahima for assisting with the raw data analysis. I thank Suzanne Page in the Oxford Molecular Diagnostics Centre for facilitating access to tumour mutation status data and Dr. Marc Van de Wetering of the Hubrecht Institute, Utrecht for providing us with human organoid protocols. I am very appreciative of the guidance provided by Dr. Ahmed Hegazy around expansion of primary human T cells and to Dr. Matthias Friedrich for keeping me company during the many late evenings processing samples and for preparing some of the matched normal organoid cultures. This work would not have been possible without Cloe Vassart, James Chivenga, Ngonidzashe Charumbira, and David Maldonado-Perez who consented patients and collected samples from the operating theatres for this study. Moreover, I thank Dr. Lai Mun Wang and the team of pathologists at the JR Hospital who have stayed late on countless evenings to biopsy fresh resections for us. However, I am most indebted to the patients, who in the midst of the distress of a cancer diagnosis, have generously consented to use of their tissue for research.

What has made my DPhil experience the most fulfilling is the privilege of working everyday alongside colleagues in the Powrie Lab who are not only excellent scientists from whom I have learned much, but who are also kindhearted, social, and caring people. Thank you to each one of you!

I am forever grateful to the Rhodes Trust for providing me the opportunity to study at Oxford. The people I have met in Oxford have shaped my experience and I am particularly thankful for my dear friend Suzana, with whom I have spent hours running around the Oxford countryside, bantering about science.

I would not be where I am today, if it were not for a long line of awe-inspiring science teachers and professors; Mr. Burndt, Mr. Vrolyk, Dr. Dixon, and Dr. Martin to name a few. Nor would I be here without the enduring support of my family. I thank my parents, in particular, for their encouragement of my scholarly pursuits over the years, even if at times, it has come at the expense of time spent with family. To my fiancé Kit, for his unending patience with late nights and weekends spent in the lab, for the way in which he values and respects the work that I do, and for the balance and perspective that he brings to my life. Thank you for the memories we have made in Oxford, they will last a lifetime.

And finally to my grandfather, Bop, who instilled a love of science in me from a very early age. I will always remember our long dinner table conversations, your eagerness to teach, and your equal eagerness to learn for your 95 long years.

Collaborator Contributions

A number of individuals contributed to work in this thesis. Their contributions are highlighted below and are also specifically indicated in the body of the thesis.

Basic patient stratification: Dr. Nathan West performed the initial basic stratification of patients in the GSE39582 cohort.

PETACC3 confirmation cohort analysis: Professor Sabine Tejpar (KU Leuven), kindly provided us access to transcriptomic data from the PETACC3 Clinical Trial. Dr. David Barras (Swiss Institute of Bioinformatics), under the direction of Dr. Mauro Delorenzi, performed the confirmation cohort and combined cohort analysis using this dataset. Dr. Barras also performed the CMS subtyping analysis of *IL22RA1*-high, *KRAS* mutant tumours.

Investigation of IL-22 receptor dynamics: Lucy Garner was a rotation DPhil student in the lab who performed a series of experiments to explore IL-22 receptor dynamics in *KRAS* mutant and wild type isogenic cells, under my direction.

Guidance and assistance with RNA-sequencing analysis: Dr. Barras simultaneously performed RNA-sequencing raw data alignment, processing, basic principal component and differential expression analysis with me to confirm that my methodology was sound. Moreover, Dr. Barras shared code for more complex interaction analyses and he performed single sample GSEA analysis on the data generated in this experiment.

Label-free proteomics and raw data analysis: Protein prepared for LC-MS/MS was sent to the University of Dundee where, in collaboration with Professor Doreen Cantrell and Dr. Mahima Swamy, the samples were analysed. Dr. Swamy performed the MaxQuant analysis on the raw data.

Table of Contents

ABSTRACT i

ACKNOWLEDGEMENTS iii

COLLABORATOR CONTRIBUTIONS v

TABLE OF CONTENTS vii

LIST OF ABBREVIATIONS xiv

1 INTRODUCTION 1

1.1 The yin and yang of inflammation in cancer 2

1.1.1 The basics of an immune response 2

1.1.2 Antitumour immunity 7

1.1.3 Tumour-promoting inflammation 9

1.2 The etiology of colorectal cancer 11

1.2.1 Colorectal cancer epidemiology: the stats 11

1.2.2 Inside-out: oncogenes as drivers of CRC 13

1.2.3 Outside-in: inflammation as a driver of CRC 18

1.3 The IL-23 pathway in gastrointestinal health and disease 24

1.3.1 IL-23: upstream regulators and downstream effectors 24

1.3.2 Maintaining the barrier: homeostatic function of the IL-23 pathway in the gut 26

1.3.3 Too much of a good thing: the IL-23 pathway in CRC 27

1.4 IL-22: a friend in health, a foe in CRC 30

1.4.1 IL-22: A double-edged sword 30

1.4.2 IL-22 receptor and signalling 30

1.4.3 IL-22 and colorectal cancer in murine models 32

1.4.4 IL-22 in human gastrointestinal cancer 33

1.5 Tumour adaptations to cytokines in CRC 34

1.5.1 Silencing of tumour-suppressor genes normally augmented by cytokine signalling 35

1.5.2 Inflammatory modulation by loss of p53 35

1.5.3 Inflammatory modulation by oncogenic *KRAS* 36

1.6 Cytokines as therapeutic targets in CRC 38

1.6.1 The challenge of cytokine networks 39

1.6.2 Patient stratification based on interactions with oncogenes 42

1.7 Uncovering the role of the IL-22 pathway in human CRC 44

1.7.1 Primary aims 44

1.7.2 Thesis outline 44
2 MATERIALS AND METHODS 47
2.1 Prospective collection and analysis of fresh CRC and matched normal adjacent tissue 48
2.1.1 Patient identification and consent 48
2.1.2 Fresh tissue collection and processing 48
2.1.3 Immunohistochemical analysis of IL-22RA1 on formalin fixed, paraffin embedded (FFPE) tumour and matched normal sections 49
2.1.4 Whole tissue flow cytometric analysis of IL-22RA1 expression 50
2.1.5 Whole tissue RNA extraction and qPCR analysis 53
2.1.6 Polyclonal T cell expansion from tumour and matched normal adjacent tissue 54
2.2 Colorectal cancer cell line culture and experimentation 58
2.2.1 Source and maintenance culture of cell lines used 58
2.2.2 Flow cytometric analysis of IL-22RA1 expression 59
2.2.3 Basic cytokine stimulation experiments 59
2.2.4 T cell supernatant stimulation experiments 60
2.2.5 RNA extraction and qPCR 61
2.2.6 Immunoblotting 61
2.2.7 Phosflow 63
2.2.8 Chemoresistance assays 64
2.2.9 Clonogenic outgrowth assays 65
2.2.10 Proliferation assays 66
2.2.11 siRNA knockdown experiments 67
2.2.12 Lactate Assays 68
2.3 Primary human CRC and normal adjacent colon tissue organoid culture and experimentation 68
2.3.1 Crypt isolation and culture of normal human colonic organoids 68
2.3.2 Tumour cell isolation and culture of CRC organoids 71
2.3.3 Organoid passaging, freezing, and establishment from frozen stocks 72
2.3.4 KRAS mutation typing in CRC organoids 73
2.3.5 Basic cytokine stimulation experiments 75
2.3.6 Organoid proliferation assays 75
2.3.7 T cell supernatant stimulation experiments 76
2.3.8 RNA extraction and qPCR 77
2.3.9 Flow cytometric analysis of IL-22RA1 77
2.3.10 Phosflow 78

2.3.11 Confocal microscopy 78
2.4 In silico analysis in tumour transcriptomic datasets 79
2.4.1 Description of CRC transcriptomic datasets 79
2.4.2 Statistical analyses for clinical outcome in tumour transcriptomic datasets 81
2.4.3 Gene set enrichment analysis comparing proximal and distal tumours 82
2.4.4 Immune metagene signature comparison between proximal and distal tumours 83
2.5 RNA-Sequencing DLD-1 isogenic cell line 83
2.5.1 Sample preparation 83
2.5.2 Library preparation, RNA-sequencing, and data processing 84
2.5.3 Data analysis 85
2.6 Label-free proteomics DLD-1 isogenic cell line 87
2.6.1 Sample preparation 87
2.6.2 Label-free LC-MS/MS 88
2.6.3 Data analysis 88
2.7 Statistical Analysis 89
3 IDENTIFICATION OF AN IL-22 RECEPTOR-HIGH, *KRAS* MUTANT POOR PROGNOSIS COLORECTAL CANCER SUBTYPE 91
3.1 Introduction 92
3.2 Results 98
3.2.1 *IL23A* is elevated in human colorectal tumours compared to normal adjacent mucosa 98
3.2.2 IL-22RA1 is differentially expressed in tumours from different colorectal cancer patients 102
3.2.3 *KRAS* mutation is prognostic in patients whose tumours express high levels of the interleukin 22-receptor gene. 108
3.2.4 *IL22RA1* does not interact with other common oncogenic driving mutations in colorectal cancer. 115
3.2.5 *KRAS* mutation does not stratify patients with high expression of the interleukin 6 or interleukin 17 receptors. 118
3.2.6 Unbiased analysis of cytokines and cytokine receptors that interact with *KRAS* mutation. 120
3.2.7 High expression of either or both subunits of the heterodimeric IL-22R confers poor prognosis in *KRAS* mutant CRC. 124
3.2.8 The prognostic interaction between *KRAS* mutation and *IL22RA1* occurs preferentially in proximal colorectal cancer. 130

3.2.9 IL-22R-high tumours classify predominately as CMS2 136
3.3 Discussion 138
3.3.1 Main conclusions 138
3.3.2 *IL23A* is elevated in CRC compared to matched normal tissue 138
3.3.3 Heterogeneous expression of IL-22RA1 in human CRC 141
3.3.4 Identification of a novel prognostic link between *IL22RA1* and *KRAS* mutation 144
3.3.5 Stratification of *IL22RA1*-high, *KRAS* mutant CRC patients for immunomodulatory therapy in the clinic 147
3.3.6 Concluding Remarks 148
4 IL-22 SYNERGISES WITH MUTANT *KRAS* TO PROMOTE MALIGNANCY 151
4.1 Introduction 152
4.2 Results 159
4.2.1 Selection of a panel of CRC lines to mirror the clinical molecular subtypes of interest 159
4.2.2 *OLFM4* is induced in an IL-22-specific manner in IL-22R-high cells 162
4.2.3 IL-22 promotes chemoresistance in IL-22R-high, *KRAS* mutant T84 and DLD-1 cells 165
4.2.4 IL-22 promotes clonogenic outgrowth in IL-22R-high, *KRAS* mutant T84 and DLD-1 cells 166
4.2.5 Characterisation of a DLD-1 *KRAS* mutant and wild type isogenic cell line pair 171
4.2.6 IL-22 promotes chemoresistance and enhances proliferation specifically in *KRAS* mutant and not wild type DLD-1 isogenic cells 174
4.2.7 IL-22 enhances phosphorylation of S6 (pS235/236) ribosomal protein in *KRAS* mutant but not wild type DLD-1 isogenic cells 179
4.2.8 Dynamic regulation of IL-22RA1 upon ligand binding is comparable between *KRAS* mutant and wild type DLD-1 isogenic cells 183
4.2.9 Establishment and validation of primary human CRC organoids as an accurate *ex vivo* model to functionally explore the IL-22-*KRAS* synergy 188
4.2.10 IL-22 induces proliferation in *KRAS* mutant organoids. 203
4.3 Discussion 209
4.3.1 Main conclusions 209
4.3.2 IL-22 promotes chemoresistance, clonogenic outgrowth, and proliferation in a *KRAS*-dependent manner 209

4.3.3 Convergence of IL-22 signalling and mutant *KRAS* on AKT, ribosomal protein S6, and *S100A9* activation and induction hint at possible mechanisms mediating malignant progression 214
4.3.4 Oncogenic *KRAS* does not directly modulate IL-22RA1 expression or dynamic regulation 217
4.3.5 The study of primary normal adjacent and CRC organoids reveals unique differences between homeostasis and malignancy 218
4.3.6 Concluding remarks 220
5 ELUCIDATION OF THE MECHANISMS OF IL-22-*KRAS* SYNERGY 223
5.1 Introduction 224
5.2 Results 227
5.2.1 Unbiased RNA-sequencing and proteomic approaches to identify potential mechanisms of IL-22-*KRAS* synergy. 227
5.2.2 ELR^+ CXC chemokines are potently induced by IL-22 in *KRAS* mutant compared to *KRAS* wild type cells 230
5.2.3 IL-17A expression is elevated in $CD4^+$ T cells from tumour compared to matched normal adjacent tissue 235
5.2.4 ELR^+ CXC chemokines are induced in *KRAS* mutant cells and organoids by supernatant from tumour-infiltrating $CD4^+$ T cells in an IL-22-dependent manner 240
5.2.5 *CD274* (PD-L1) is induced by IL-22 and not IL-6, specifically in *KRAS* mutant cells and organoids 245
5.2.6 The Myc pathway is uniquely induced by IL-22 and not IL-6 in *KRAS* mutant cells based on RNA-sequencing analysis 247
5.2.7 Myc knockdown attenuates *KRAS* mutant cell proliferation at baseline and following IL-22 stimulation 255
5.2.8 Preliminary evidence suggests that *MYC* transcriptional induction by IL-22 is not STAT3 dependent 258
5.2.9 *MYC* expression is correlated with *IL22RA1* expression 261
5.2.10 IL-22 enhances lactate production in *KRAS* mutant cells that is diminished by *MYC* knockdown 264
5.2.11 The high capacity glucose transporter, GLUT3, is highly induced by IL-22 in *KRAS* mutant cells based on proteomic and RNA-sequencing analyses 266
5.2.12 Myc target protein signatures are enriched in IL-22 stimulated *KRAS* mutant compared to wild type cells based on proteomic analysis 268
5.3 Discussion 270

5.3.1 Main conclusions 270
5.3.2 Conditioning a pro-tumourigenic immune microenvironment: cell extrinsic mechanisms by which IL-22 interacts with mutant *KRAS* to promote malignancy 273
5.3.3 IL-22-*KRAS* dependent induction of the master transcriptional regulator and proto-oncogene c-Myc: cell intrinsic mechanisms by which IL-22 synergises with mutant *KRAS* to promote malignancy 281
5.3.4 Concluding Remarks 289
6 FINAL DISCUSSION 291
6.1 Summary of findings 292
6.2 Clinical translation 295
6.3 Limitations and new avenues 298
REFERENCES 301
1 APPENDIX: FUTURE EXPERIMENTS 337
1.1 Unanswered scientific questions 338
1.2 IL-22RA1 expression and regulation 338
1.3 Elevated IL-23 in CRC 341
1.4 IL-22-*KRAS*-enhanced ELR^+ CXC chemokines 342
1.5 IL-22-*KRAS*-enhanced Myc pathway 342
1.6 IL-22-*KRAS* synergy in metastatic disease 345
2 APPENDIX: EXTENDED MATERIALS AND METHODS 347
2.1 Confirmation of specificity of IL-22RA1 antibodies used in this study 348
2.1.1 *IL22RA1* siRNA knockdown to confirm specificity 348
2.1.2 IL-22RA1 immunohistochemistry staining controls 351
2.2 T cell supernatant titration experiments 352
2.3 Production of Noggin, R-spondin, Wnt3A conditioned media 355
2.3.1 Rspondin and Noggin conditioned media production 355
2.3.2 Wnt-3A conditioned media preparation 356
2.4 Taqman probes used in this study 357
2.5 DLD-1 isogenic cell line generation 358
3 APPENDIX: RNA-SEQUENCING AND PROTEOMICS EXTENDED DATA 359
3.1 RNA-Sequencing 360
3.1.1 Differential expression analysis 360
3.1.2 Pathway analysis 368

3.2 Proteomics 369
3.2.1 Differential expression analysis 369
3.2.2 Pathway analysis 372
4 APPENDIX: CLINICAL DATA 375

List of Abbreviations

Abbreviation	
5-FU	5 fluorouracil
AKT	protein kinase B
AOM	azoxymethane
APC	adenomatous polyposis coli gene
BRAF	v-Raf murine sarcoma viral oncogene homolog B (B-Raf) gene
CAC	colitis-associated cancer
CAF	cancer-associated fibroblast
CRC	colorectal cancer
CTL	cytotoxic T lymphocyte
CXCL-1,2,3,5	chemokine (C-X-C motif) ligand 1,2,3,5
DSB	double stranded breaks
DSS	dextran sodium sulphate
ERK	extracellular signal-regulated kinase
FDR	false discovery rate
GDP	guanosine diphosphate
GLUT3	glucose transporter 3 (solute carrier family 2, facilitated glucose transporter member 3)
gMFI	geometric mean fluorescence intensity
GSEA	Gene Set Enrichment Analysis
GTP	guanosine triphosphate
GTPase	GTP hydrolase
Hh	*Helicobacter hepaticus*
iBAQ	intensity based absolute quantification
IBD	inflammatory bowel disease
ICAM-1	intercellular adhesion molecule 1
IFNγ	interferon gamma
IL-	interleukin
IL-10RB	interleukin 10 receptor beta subunit
IL-22RA1	interleukin 22 receptor alpha subunit
ILC	innate lymphoid cell
iNOS	inducible nitric oxide synthase
ITS	insulin-transferrin-selenium
JNK	c-Jun N-terminal kinase
KRAS	Kirsten rat sarcoma viral oncogene homolog (K-Ras) gene
Lgr5	leucine rich repeat containing G protein-coupled receptor 5
MAPK	mitogen-activated protein kinase
MDSC	myeloid-derived supressor cell

Abbreviation	
MEK	mitogen-activated protein kinase kinase
MHC	major histocompatibility complex
MSI	microsatellite instable
MSigDB	The Molecular Signatures Database
MUT	mutant
NF-κB	nuclear factor kappa-light-chain-enhancer of activated B cells
NT	no treatment
PD-L1	programmed death-ligand 1
PI3K	phosphoinositide 3-kinase
PIK3CA	phosphatidylinositol-4,5-bisphosphate 3-kinase catalytic subunit alpha gene
PMA	phorbol 12-myristate 13-acetate
RAGE	receptor for advanced glycation end products
RORγt	RAR-related orphan receptor gamma T
RPKM	reads per kilobase of transcript per million mapped reads
RPLPO	large ribosomal protein
RSK	ribosomal protein S6 kinase
S6	ribosomal protein S6
SAPK	stress-activated protein kinase
SOCS3	supressor of cytokine signalling 3
STAT3	signal transducer and activator of transcription 3
TAM	tumour-associated macrophage
Th1	T helper 1
Th17	T helper 17
TIL	tumour-infiltrating leukocyte
TNFα	tumour necrosis factor alpha
TP53	gene encoding the p53 tumour supressor protein
WT	wild type

1 Introduction

Note: Components of this introduction were adapted from a review: West, N.R.*, McCuaig, S*, Franchini, F, and Powrie, F. 2015. "Emerging Cytokine Networks in Colorectal Cancer." *Nature Reviews Immunology* 15(10). **Denotes co-first authors.* Where relevant, figures prepared by S. McCuaig for this review are indicated.

1.1 The yin and yang of inflammation in cancer

Carcinogenesis is the result of a complex interplay between cell intrinsic and extrinsic processes that promote sustained proliferation, resistance to apoptosis, reprogramming and reorganization of the stromal environment, and genomic instability. Inflammation, although necessary for damage repair and anti-tumour immunity, can influence these processes to promote neoplasia. As such, inflammation in now regarded as an enabling characteristic for the acquisition of the core hallmarks of cancer (Hanahan and Weinberg, 2011).

1.1.1 The basics of an immune response

1.1.1.1 Innate and adaptive immunity

The evolution of the immune system was driven by the necessity to protect the host from cellular damage caused by acute inflammation or sterile injury (Shalapour and Karin, 2015). The innate immune system, which is more evolutionary ancient than the adaptive immune system, forms the first line of defense. Its activation is directly triggered by the recognition of sequences of bacterial or viral structures known as pathogen-associated-molecular patterns (PAMPs), or components of host cells released upon acute injury and death known as damage-associated-molecular patterns (DAMPs), by antigen-presenting cells (Janeway, 1989; Iwasaki and Medzhitov, 2015).

Upon activation, antigen-presenting cells such as dendritic cells and macrophages, upregulate major histocompatibility complex (MHC) class I and II and costimulatory

molecules, and produce inflammatory cytokines and chemokines that attract and activate T cells to direct the adaptive immune response. Activated adaptive immune cells, T cells and B cells, then amplify the initial inflammatory response in a targeted fashion (Iwasaki and Medzhitov, 2015).

1.1.1.2 $CD8^+$ and $CD4^+$ T cells

The predominate pool of peripheral T cells express αβ T cell receptors (TCRs) and respond to processed peptide components of PAMPs and DAMPs (termed antigens) presented in the context of MHC class I and II molecules by antigen-presenting cells (Germain, 1994). Notably, all nucleated cells of the human body express MHC class I. Antigens presented on MHC class I alert the immune system to intracellular infection and target the infected cells for destruction. While antigens presented on MHC class II orchestrate a response against extracellular infections (Germain, 1994). As such, two distinct lineages of αβ T cells exist to recognise MHC class I or II associated peptides and their effector functions are specialised accordingly (Germain, 2002). These lineages are defined by the expression of either CD8 or CD4 co-receptors, which recognise the ligands of the TCR in the context of MHC class I or II respectively and are required for T cell activation (Swain, 1983; Janeway, 1992). Activated $CD8^+$ T cells (cytotoxic T lymphocytes) exert direct cell-killing function via the production of perforin and granzymes. By contrast, activated $CD4^+$ T cells (T helper (Th) cells) do not mediate direct killing, but orchestrate a wide range of immunologic responses including the maturation of B cells into antibody-producing plasma cells, and the activation of $CD8^+$ T cells and macrophages (Kim and Cantor, 2014). $CD4^+$ T cells differentiate into diverse sublineages in order to execute these varied effector functions (Sher and Coffman, 1992; Kim and Cantor, 2014).

1.1.1.3 T cell subsets with specialised effector functions

This $CD4^+$ T cell polarisation is controlled in part by the strength of the TCR-MHC and co-stimulatory receptor-ligand interaction, but critically by specific cytokines in the microenvironment (DuPage and Bluestone, 2016). These inductive cytokines are messengers serving as a conduit between environmental cues (e.g. microbes) and gene expression in $CD4^+$ T cells, which dictates their effector function. Each $CD4^+$ T cell subset senses different inductive cytokines, which regulate expression of a program of transcription factors, leading to the production of selected effector cytokines to optimally control the specific type of pathogen or damage, or to limit immune pathology (Figure 1.1) (DuPage and Bluestone, 2016). Mosmann and Coffman first described T helper 1 (Th1) and T helper 2 (Th2) cells in the 1980s based on their capacity to produce interferon γ (IFNγ) and interleukin 4 (IL-4) respectively (Mosmann *et al.*, 1986). IFNγ-producing Th1 cells enhance the priming and expansion of $CD8^+$ T-cells, recruit natural killer (NK) cells, and activate macrophages to phagocytose intracellular pathogens (Gazzinelli *et al.*, 1991; Kim and Cantor, 2014). While Th2 cells that secrete IL-4, IL-5, and IL-13 are critical in defense against extracellular pathogens (e.g. helminths) and promote allergic responses (Finkelman *et al.*, 1991; Kim and Cantor, 2014). However, the binary Th1/Th2 classification of $CD4^+$ T cells could not explain the complexity of their function and several additional $CD4^+$ T cell subsets have since been identified (Figure 1.1). $CD4^+$ regulatory T cells (Tregs) play a critical role in self-tolerance and limiting immune pathology (Sakaguchi, Takahashi and Nishizuka, 1982; Powrie *et al.*, 1993; Wing and Sakaguchi, 2012). Th17 cells are polarised by a combination of transforming growth factor β (TGF-β), IL-1β, and IL-6 and are stabilised and maintained by the key microbe-driven cytokine IL-23 (Harrington *et al.*, 2005; Park *et al.*, 2005; Cua and

Tato, 2010; Burkett, Zu Horste and Kuchroo, 2015). They confer protection against fungal infections, in particular, via the secretion of the key effector cytokines IL-17A, IL-17F, and IL-22 (Stockinger and Veldhoen, 2007).

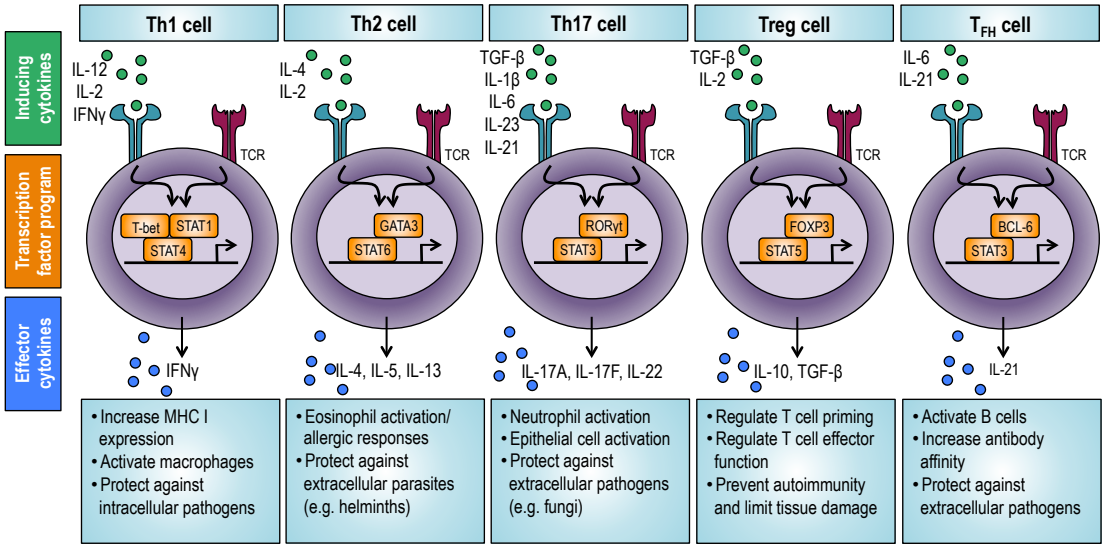


Figure 1.1 CD4$^+$ T cell subsets: inductive cytokines, defining transcription factors, and effector cytokines.

CD4$^+$ T cells are polarised into subsets with distinct effector functions by TCR activation and cytokines in the microenvironment (green). These cytokines induce a transcriptional program directed by master transcriptional regulators specific to each subset (orange). The unique transcriptional program in each subset regulates the production of characteristic effector cytokines (blue) that are important in the control of specific types of pathogens or other immune pathologies. TCR, T cell receptor; T_{FH}, T follicular helper cell; STAT, signal transducer and activator; RORγt, retinoic acid receptor-related orphan receptor γ t, BCL-6, B cell lymphoma 6; GATA3, GATA-binding protein 3; Treg, regulatory T cell; FOXP3, forkhead box P3. (Figure adapted from DuPage and Bluestone, 2016)

In recent years, populations of innate lymphoid cells (ILCs) have been discovered that lack expression of somatically rearranged T cell receptors and thus do not exhibit antigen specificity (Artis and Spits, 2015). Nevertheless, subsets of ILCs have been identified which mirror CD4$^+$ T cell subsets to a degree, based on their transcription factor profiles and effector cytokine expression. Broadly, group 1 ILCs (ILC1s), group 2 ILCs (ILC2s), and group 3 ILCs (ILC3s), are similar to Th1, Th2, and Th17 cells respectively (Buonocore *et al.*, 2010; Geremia *et al.*, 2011; Spits *et al.*, 2013). ILCs serve critical functions in host defense against infection, but also in tissue repair and regulation of interactions with the commensal microbiota (Artis and Spits, 2015).

1.1.1.4 Preventing collateral damage

Despite the sophisticated coordination of the immune response, inflammation can cause severe collateral damage when responses are inappropriately directed (e.g. autoimmunity) or left unchecked (e.g. chronic inflammation). In fact, Th17 cells were first discovered due to their pathogenic role in models of autoimmunity [experimental autoimmune encephalomyelitis (Langrish *et al.*, 2005), collagen-induced arthritis (Murphy *et al.*, 2003)] and chronic inflammatory diseases [psoriasis (Wilson *et al.*, 2007), inflammatory bowel disease (Uhlig *et al.*, 2006; Yen *et al.*, 2006; Ahern *et al.*, 2010)]. As such, multiple negative regulatory mechanisms to minimize immunopathology are part of a robust immune response. For instance, professional immune regulatory adaptive immune cells, Tregs, can dampen inflammatory responses (Tanoue, Atarashi and Honda, 2016). Moreover, inhibitory receptors and ligands are induced on T cells and antigen-presenting cells respectively during chronic viral infections to limit immunopathology caused by an unrestrained response (Nguyen and Ohashi, 2014).

1.1.1.5 Immune infiltrates in tumours

Rudolf Virchow was the first to identify inflammatory infiltrates within tumours in the late nineteenth century (Grivennikov, Greten and Karin, 2010). While thought to be exclusively involved in tumour surveillance and antitumour immunity, the presence of immune cells at tumour sites is now understood to also have a pro-tumorigenic role. Moreover, some of the aforementioned negative regulatory responses may limit maximal antitumour immunity. Thus, inflammation can play both a beneficial and deleterious role in cancer (Figure 1.2).

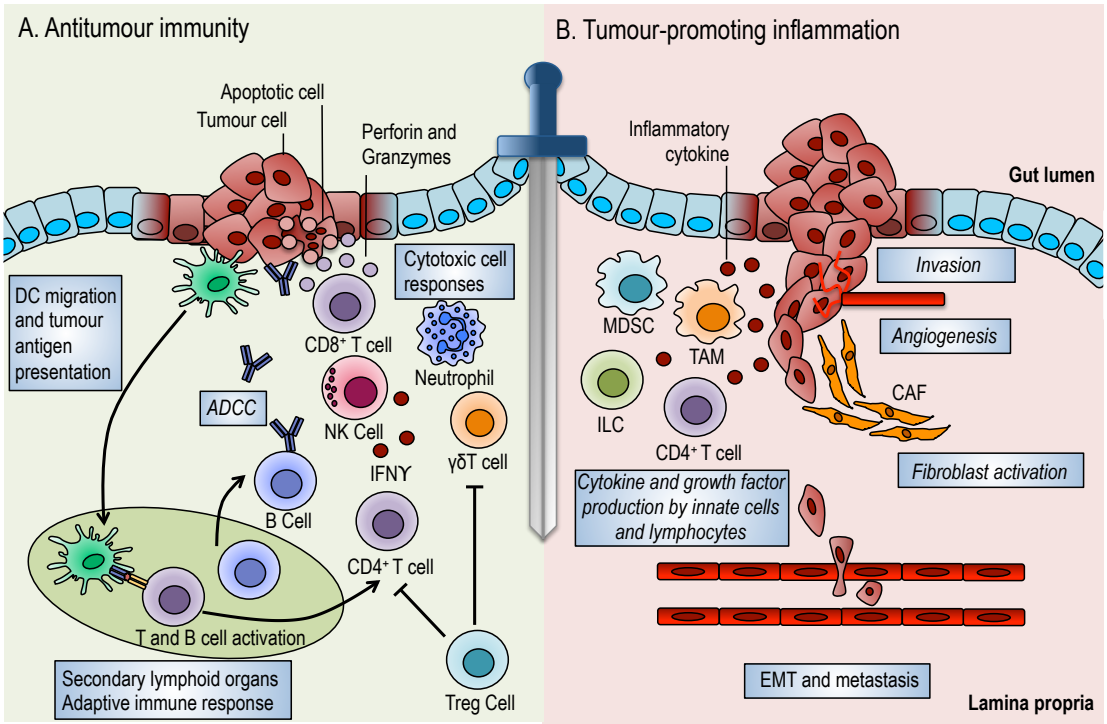


Figure 1.2 The double-edged sword of inflammation in cancer

The immune system can have profound but disparate roles in the pathogenesis of cancer. Many new therapeutic approaches in cancer immunology aim to potentiate antitumour immunity (**A**). Mechanistically, dendritic cells (DCs) sample tumour antigens and activate tumour-specific B cells and T cells in secondary lymphoid organs (e.g. Lymph nodes) to initiate cytolytic and/or humoural responses (e.g. Antibody-dependent cell-mediated cytotoxicity ADCC). IFNγ-producing $CD4^+$ T cells, cytotoxic $CD8^+$ T cells, and NK cells drive a conventional antitumour immune response. New evidence supports a role for γδ T cells in antitumour immunity. These responses are restrained by Treg cells that can impair antitumour immunity, but also inflammatory responses that promote tumourigenesis. By contrast, non-specific inflammation (**B**) results in the production of inflammatory cytokines by myeloid derived suppressor cells (MDSCs), tumour-associated macrophages (TAMs), $CD4^+$ T cells, and innate lymphoid cells (ILCs). Many of these cytokines can act directly on transformed epithelial cells to promote proliferation, inhibition of apoptosis, invasion, angiogenesis, epithelial to mesenchymal transition (EMT), and metastasis. Cancer associated fibroblasts (CAFs) can also produce cytokines and growth factors that act directly on tumour cells or modulate the microenvironment. (Figure prepared by S.McCuaig for NRI)

1.1.2 Antitumour immunity

The field of cancer immunology has received unprecedented attention in recent years due to the development of clinically efficacious therapeutics that harness the capacity of the immune system to recognise and mount a response against a tumour – termed antitumour immunity (Couzin-Frankel, 2013). Decades after Virchow first observed inflammatory infiltrates in tumours, it was Paul Ehrlich who first hypothesised that the immune system could be harnessed to treat established tumours; the earliest

description of immunotherapy (Ehrlich, 1909). In the 1950's, Burnet and Thomas then proposed the immune surveillance hypothesis (Burnet, 1970), suggesting that malignant cells could be recognized and eradicated by the immune system before they developed into detectable tumours. Central to this hypothesis was the idea that somatic mutations in cancer result in the expression of tumour-specific antigens (neoantigens) that can activate antitumour immunity and mediate early rejection of malignant cells.

Antitumour immunity is executed predominately by antigen-specific IFNγ-producing $CD4^+$ Th1 cells and $CD8^+$ T cells, and innate natural killer cells (Medler, Cotechini and Coussens, 2015). Antigens, typically foreign substances of microbial origin or peptide products of somatically mutated proteins, are processed and presented by MHC class I on APCs such as dendritic cells, macrophages, and B cells (Medler, Cotechini and Coussens, 2015). Antigen-specific $CD8^+$ T cells engage with APCs via direct binding of the peptide-MHC I complex with its cognate T cell receptor (TCR). Subsequent engagement of costimulatory molecules induces $CD8^+$ T cell proliferation and antigen-specific cytolytic attack (Medler, Cotechini and Coussens, 2015). While solid tumours are known to contain tumour antigen-specific T cells, a potent antitumour immune response is not always observed. Induction of tolerance or diminished cytolytic capacity can result due to immunosuppressive cells and cytokines such as IL-10, expression of ligands that engage immune checkpoint inhibitory receptors, and downregulation of MHC class I by tumour cells (Shalapour and Karin, 2015). Therapeutic strategies that subvert these regulatory mechanisms and unleash $CD8^+$ T cell responses have shown durable responses in several malignancies. Inhibition of immune checkpoint molecules, particularly cytotoxic T

lymphocyte-associated protein 4 (CTLA-4) or the programmed death 1 (PD-1) pathway have shown therapeutic efficacy in the treatment of melanoma, non-small cell lung carcinoma, bladder, and kidney cancers (Medler, Cotechini and Coussens, 2015). Adoptive transfer of T cells harbouring chimeric antigen receptors (CAR-T cells) directed against tumour antigens has shown success predominately in hematological malignancies (Porter *et al.*, 2011; Garfall *et al.*, 2015; Brown *et al.*, 2016). Finally in 2015, a first-in-class oncolytic virus that selectively replicates in tumour cells and potentiates antitumour immunity received FDA approval for use in melanoma after demonstrating clinical benefit in a Phase III clinical trial (Andtbacka *et al.*, 2015). Despite the promise of immune checkpoint blockade, CAR-T cells, and oncolytic viruses, the vast majority of patients are refractory to such therapies (Schumacher, Kesmir and van Buuren, 2015). Whether due to low neoantigen load, induction of negative regulatory receptors, or the presence of immunosuppressive cells and cytokines, in many solid malignancies the balance is tipped from antitumour immunity to immunosuppressive pro-tumourigenic inflammation.

1.1.3 Tumour-promoting inflammation

Chronic inflammation is an aberrant and prolonged response to a disruption in tissue homeostasis. Similarly, tumourigenesis is often a deregulated reparative or growth response. Thus decades ago an analogy was drawn between chronic inflammation and tumourigenesis as “wounds that do not heal” (Dvorak, 1986). Globally, up to 20% of cancers are associated with an overt microbial infection (Elinav *et al.*, 2013). However, a number of inflammatory insults or conditions have been linked to increased risk of cancer (Table 1.1). Solid malignancies that do not arise in a pre-existing inflammatory context also elicit inflammatory responses. Several cells types including $CD4^+$ T cells, innate lymphoid cells, tumour-associated macrophages, and

myeloid-derived suppressor cells produce inflammatory cytokines in the tumour microenvironment. Many of these cytokines can act directly on transformed cells to promote proliferation, inhibition of apoptosis, invasion, angiogenesis, epithelial mesenchymal transition, and metastasis (Hanahan and Weinberg, 2011). More recently, it has been appreciated that these cytokines can activate cancer-associated fibroblasts (CAFs) to produce cytokines and growth factors that modulate both neoplastic cells and the tumour microenvironment. Whether inflammation is an initiating factor or consequence of tumourigenesis, it is likely part of a homeostatic response to cellular damage that has been commandeered by tumour cells for their own gain.

Pathological inflammatory condition or inflammatory insult	Malignancy
Inflammatory bowel disease	Colorectal carcinoma
Pelvic inflammatory disease	Ovarian carcinoma
Gingivitis (inflammation of the gum tissue) and lichen planus	Oral squamous cell carcinoma
Sialadenitis (inflammation of the salivary gland)	Salivary gland carcinoma
Lichen sclerosus (a skin condition)	Vulvar carcinoma
Gastric acid-associated Barrett's metaplasia and reflux oesophagitis	Oesophageal carcinoma
Bile acids	Cholangiosarcoma and colorectal carcinoma
Silica, asbestos, smoking-associated silicosis, bronchitis	Lung carcinoma
Chronic indwelling urinary catheter	Bladder carcinoma
TRYP1 mutation-associated pancreatitis and alcoholism-associated pancreatitis	Pancreatic carcinoma
UV irradiation-associated skin inflammation	Melanoma
Asbestos	Mesothelioma

Table 1.1 Pathological inflammatory conditions or inflammatory insults that are associated with malignancy.

TYRP1, trypsinogen (Table adapted from (Elinav *et al.*, 2013))

Unlike the dozens of clinical studies underway to test new therapies and combinations that potentiate antitumour immunity, a comparatively small number of therapies have been developed to specifically target pro-tumourigenic inflammation. In the past two years, a monoclonal antibody that targets the receptor for the main survival and differentiation factor of tumour-associated macrophages (TAMs), colony stimulating factor 1 receptor (CSF-1R), was developed. In early phase trials anti-CSF-1R (emactuzumab) treatment reduced macrophage infiltration into tumours of patients suffering from various solid malignancies and showed clinical efficacy in rare diffuse-type tenosynovival giant cell tumours (Ries *et al.*, 2014; Cassier *et al.*, 2015). Studies of CSF-1R blockade in other solid malignancies are currently recruiting or ongoing (NCT02760797, NCT02923739).

Therapeutic strategies which combine potentiation of antitumour immunity with suppression of pro-tumourigenic inflammation will be necessary to harness the full anti-tumourigenic capacity of the immune system and moreover may be the key to increasing response rates to existing immune-activating therapies.

1.2 The etiology of colorectal cancer

1.2.1 Colorectal cancer epidemiology: the stats

Colorectal cancer is a prime example of a solid malignancy in which unleashing anti-tumour immunity through immune checkpoint blockade has been largely unsuccessful (Brahmer *et al.*, 2012; Topalian *et al.*, 2012), except for in a small subset of patients with mismatch repair-deficient tumours (Le *et al.*, 2015; Llosa *et al.*, 2015). The poor response in microsatellite stable tumours may be a consequence of reduced neoantigen load and inflammation that is directly protumourigenic.

Chronic intestinal inflammation predisposes patients to colorectal cancer (CRC); ulcerative colitis in particular increases the risk of CRC development 2.4 fold (Jess, Rungoe and Peyrin–Biroulet, 2012). However, the risk of colitis-associated cancer (CAC) in patients with inflammatory bowel disease (IBD) has declined considerably in the last two decades, in large part due to better control of inflammation and advances in preventative screening practices (Longo, Beaugerie and Itzkowitz, 2015; Dulai, Sandborn and Gupta, 2016). Nonetheless, sporadic CRCs also elicit an inflammatory response that has a critical role in determining the fate of CRC (Grivennikov, Greten and Karin, 2010). Sporadic CRCs account for the vast majority of colorectal cancer, which is the third most common malignancy worldwide and the fourth leading cause of cancer-related deaths (Arnold *et al.*, 2017). While in countries that fall highest on the human development index (HDI) (UK, Canada, USA, Australia, New Zealand) overall CRC incidence and mortality rates have stabilised or declined, increasing rates of CRC in low and middle income countries coincide rapid social and economic changes and the adoption of more western lifestyles (Arnold *et al.*, 2017). Despite declining overall rates of CRC in high HDI countries, the incidence of proximal colorectal cancers continues to rise (Cheng *et al.*, 2011). Furthermore, a recent study demonstrated that age-specific CRC risk for individuals born since 1990 is double that for those born between 1950-1990 in the United States (Siegel *et al.*, 2017). Collectively, the global burden of CRC is predicted to increase by 60% by 2030 (Arnold *et al.*, 2017).

In the UK, the clinical management of CRC typically involves resection of the primary tumour and adjuvant chemotherapy for locally advanced and metastatic disease (high-risk stage II, stage III, stage IV) (NICE, 2014). Standard of care

chemotherapeutic regimens include a combination of 5-fluoruracil, oxaliplatin, folinic acid and or irinotecan (NICE, 2014). In some instances front line, or second line therapy can include biologic agents like Cetuximab, an anti-epidermal growth factor receptor antibody, however the presence of *KRAS* mutation is a contraindication for Cetuximab therapy (NICE, 2013). Over the past decade, a large CRC Subtyping Consortium has advanced understanding of the molecular heterogeneity of colorectal cancer (Guinney *et al.*, 2015) and increasingly clinical studies which aim to stratify patients for targeted therapies based on predominately the genetic features of their disease are underway (ie. FOCUS-4 http://www.focus4trial.org/).

1.2.2 Inside-out: oncogenes as drivers of CRC

1.2.2.1 The adenoma to carcinoma sequence and beyond

Colorectal cancer is one of the most extensively studied cancers from a genetic perspective. While a minority of colorectal cancers (~10%) are the consequence of heritable genetic defects (Familial adenomatous polyposis (FAP) – inherited autosomal dominant germline mutation in the adenomatous polyposis coli (APC) gene; hereditary non-polyposis colorectal cancer (HNPCC or Lynch syndrome) – germline mutation in mismatch repair (MMR) genes), the vast majority of sporadic CRCs follow a step-wise accumulation of well-documented somatic mutations (Bogaert and Prenen, 2014). The so-called adenoma to carcinoma sequence, first elucidated by Fearon and Vogelstein, posits that CRCs arise from premalignant polyps that develop into carcinomas (Fearon and Vogelstein, 1990). While genome sequencing studies have identified over 80 mutations in a single colorectal tumour, fewer than 15 of these mutations are predicted to be true drivers of disease (Wood *et al.*, 2007). These driving mutations occur in tumour suppressor-genes, among which

APC and *TP53* are the most common, and oncogenes, among which *KRAS*, *PIK3CA,* and *BRAF* are the most common (Longo and Strum, 2016) (Figure 1.3).

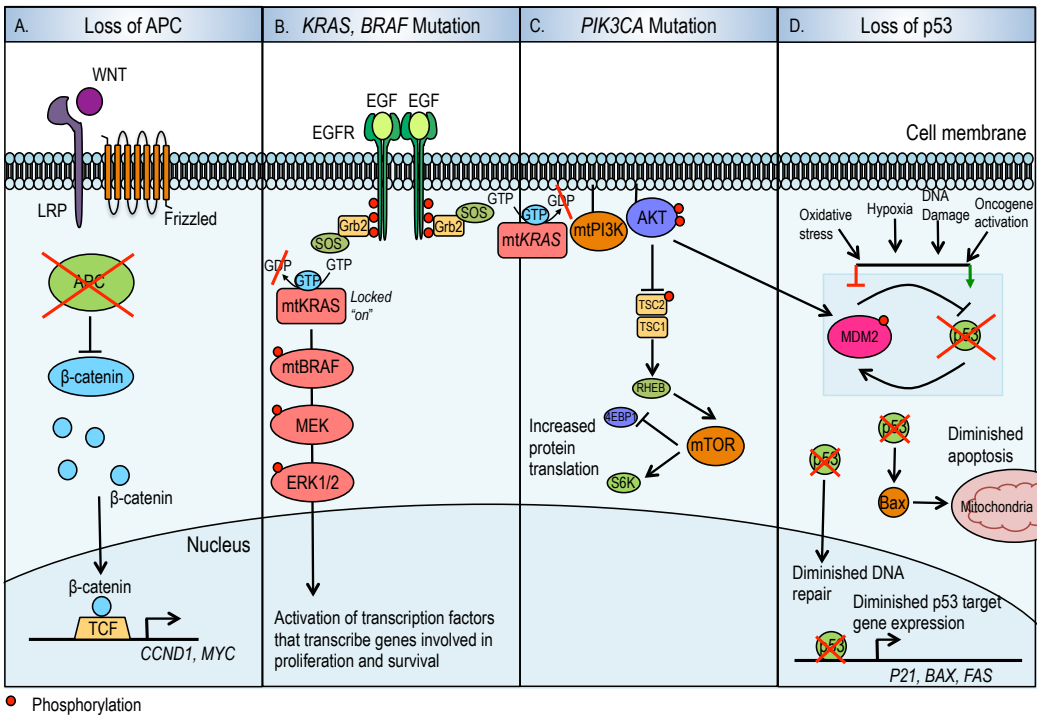


Figure 1.3 Loss of major tumour suppressors and activation of key oncogenes in CRC.

(A) Under homeostatic settings, APC sequesters β-catenin in the cytoplasm. Activation of the Wnt pathway results in proteolytic degradation of APC and translocation of β-catenin to the nucleus where it induces the transcription of growth-promoting genes (e.g. *CCND1*, cyclin D1; *MYC,* c-Myc). Loss of APC results in constitutive activation of the Wnt pathway.
(B) Ras proteins (e.g KRAS) function downstream of receptor tyrosine kinase growth factor receptors (e.g. EGFR; epidermal growth factor receptor). KRAS is a small GTPase that binds GTP in its active state and subsequently hydrolyses GTP to GDP. Mutations in codons 12 and 13 of *KRAS* lock KRAS in its GTP-bound state, resulting in its constitutive activation. KRAS can directly activate BRAF, a protein kinase that is also constitutively activated by somatic mutation in 5-10% of CRCs. BRAF phosphorylates MEK leading to downstream activation of ERK1/2, which phosphorylates and activates transcription factors that transcribe genes involved in proliferation and survival. *KRAS* and *BRAF* mutations are mutually exclusive in CRC.
(C) KRAS also activates phosphatidylinositol-4,5-bisphosphate 3-kinase (PI3K), which is encoded by *PIK3CA* and is mutated in 15-25% of CRCs. Since mutant KRAS does not efficiently activate PI3K, *KRAS* mutations are often found in conjunction with *PIK3CA* mutations in CRC. PI3K activates AKT, resulting in downstream mTOR activation. mTOR activates S6 kinases and represses the negative regulator of translation 4EBP1. The net effect is increased protein translation, which enhances cell growth and survival. Not displayed here are pathways that enhance glycolysis and angiogenesis downstream of PI3K-AKT activation.
(D) Under unstressed conditions the p53 protein is bound by MDM2 and targeted for proteasomal degradation. However, cellular stresses (e.g. DNA damage) prevent p53 association with MDM2. p53 then accumulates and activates transcription of target genes involved in cell-cycle control, apoptosis, DNA repair and it associates with BAX promoting its pro-apoptotic function. Loss of p53 results in proliferation of damaged or mutated cells. Moreover, AKT can phosphorylate MDM2 and enhance p53 degradation.

The traditional adenoma to carcinoma sequence is thought to be initiated by mutation and subsequent loss of heterozygosity at the *APC* locus (Fearon and Vogelstein, 1990). The APC protein is an inhibitor of β-catenin, which sequesters it in the cytoplasm. Activation of the Wnt pathway results in proteolytic degradation of APC and subsequent translocation of β-catenin to the nucleus where it acts as a transcription factor (Terzić *et al.*, 2010). Loss of *APC* results in constitutive activation of the Wnt pathway and aberrant epithelial cell growth. The acquisition of mutations in *KRAS* or *BRAF* leads to constitutive activation of MAPK signalling pathways. Subsequent inactivation of transforming growth factor-β (TGF-β) pathway components (ie. *SMAD2, SMAD4*), and loss of the critical tumour suppressor required to maintain genomic integrity, *TP53*, allow for aberrant outgrowth of the early adenomatous polyp into adenocarcinoma (Fearon, 2011) (Figure 1.4). Further mutations in genes that control DNA integrity result in microsatellite instability in 15% of colorectal tumours and chromosomal instability (despite microsatellite stability) in 80% of late stage CRCs (Grady and Carethers, 2008). This genetic instability results in somatic gene copy number alterations and the acquisition of further passenger mutations that contribute to the incredible heterogeneity observed in CRC resulting in varied responses to therapy and escape of host control. Importantly, only 50-60% of CRCs develop along this traditional adenoma-carcinoma sequence (Punt, Koopman and Vermeulen, 2016). Alternative routes of disease development are thought to account for other CRCs. These include the serrated pathway, characterised by a high frequency of *BRAF* mutations and colitis-associated CRC, in which early loss of *TP53* and later acquisition of *KRAS* and *APC* mutations are hallmarks (Punt, Koopman and Vermeulen, 2016) (Figure 1.4).

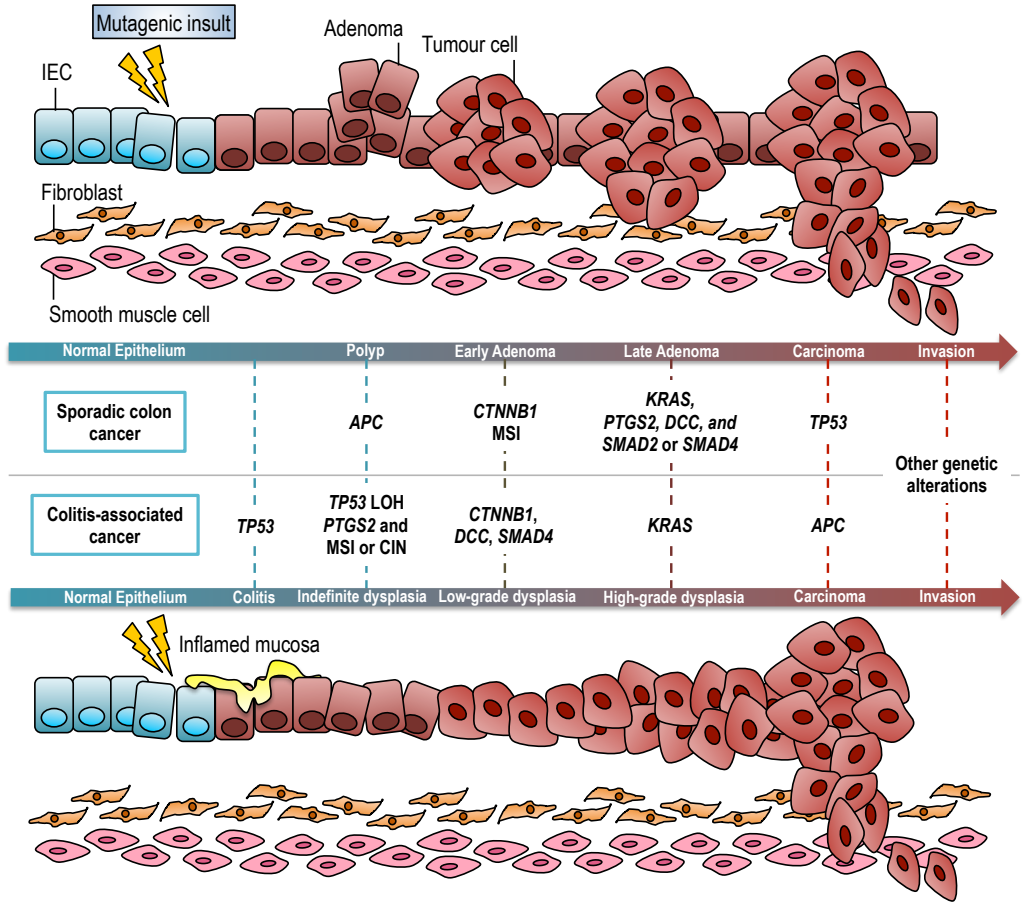


Figure 1.4 Developmental sequence of sporadic CRC versus colitis-associated cancer

Both sporadic CRC (top panel) and colitis-associated cancer (CAC) (bottom panel) are characterised by a sequence of genetic events that culminates in invasive carcinoma. Many of these genetic events are similar along these two developmental pathways including: mutation and eventual loss of heterozygosity (LOH) at the *TP53*, *APC, SMAD4* (component of the TGFβ pathway), and deleted in colon cancer (*DCC*) loci. Moreover, activating mutations are acquired in the oncogene *KRAS*, and molecules β-catenin (*CTNNB1*) and cyclooxygenase 2 (COX2; encoded by *PTGS2*). Despite the similarity in genetic events the frequency and sequence in which they occur differs. Most notably, mutation in *APC* is an early/initiating event in sporadic CRC, but a late event in CAC. By contrast, *TP53* mutations occur early in CAC but at a later stage in sporadic CRC. Morphologically, sporadic CRCs that develop along the classical adenoma-carcinoma sequence show a clear progression from adenoma to invasive carcinoma. However, CAC involves increasing histological grades of dysplasia that lead to invasive adenocarcinoma. MSI, microsatellite instability; CIN, chromosomal instability; IEC, intestinal epithelial cell. (Figure prepared by S.McCuaig for NRI)

Based on the integration of copy number, methylation status, and gene expression in 224 colorectal tumour and normal pairs, despite the striking diversity in tumours based on anatomical site or specific mutations, nearly all tumours had alterations in targets of the Myc transcription factor, which is a central regulator of growth and metabolic pathways (Cancer Genome Atlas Network and Muzny, 2012). Moreover,

the aforementioned consortium effort has identified four consensus molecular subtypes of colorectal cancer that are governed in part by their development pathways and have differing prognostic implications (Guinney *et al.*, 2015). Despite detailed understanding of the genetic events leading to CRC development, only *KRAS* mutation status, mismatch repair status, and possibly *BRAF* mutation status influence clinical decision making (Punt, Koopman and Vermeulen, 2016).

1.2.2.2 Bi-directional histogenesis of colorectal adenomas

Two opposing theories exist regarding the histogenesis of colorectal tumours. Dysplastic cells are frequently found at the luminal surface of the crypts and have alterations in the *APC* gene. This observation led the Vogelstein group to coin the "top-down model of adenoma morphogenesis" (Shih *et al.*, 2001). By contrast, more recent genetic analysis supports a model in which transformative genetic lesions in the crypt base stem cells leads to their stochastic expansion, resulting a monoclonal conversion and a monocryptal adenoma. The adenoma then spreads *via* crypt fission (Preston *et al.*, 2003). This so-called "bottom-up histogenesis" of colorectal adenomas has been supported by further evidence that $Bmi1^+$ or $Lgr5^+$ stem cells can be the initiating cells of intestinal adenomas in mice (Sangiorgi and Capecchi, 2008; Barker *et al.*, 2009). These models do not, however, account for the influence of the inflammatory microenvironment in early adenoma development. However, a genetic model of intestinal tumour initiation has revealed the potential for inflammation to influence plasticity and bidirectional conversion of intestinal epithelial cells (IECs). Specifically, NF-κB activation enhanced Wnt signalling and led to the de-differentiation of $Lgr5^-$ epithelial non-stem cells, marked by re-acquisition of characteristic stem cell gene expression and induction of tumour-initiating properties (Schwitalla, Fingerle, *et al.*, 2013).

1.2.3 Outside-in: inflammation as a driver of CRC

Historically, elucidation of the clear series of genetic events that leads to invasive adenocarcinoma established the view that cancer was fundamentally a genetic disease (Vogelstein and Kinzler, 2004). The importance of environmental factors such as the microbiota and inflammation was thought to be limited to their direct mutagenic capacity. For instance, chronic inflammation in IBD leads to elevated reactive oxygen species (ROS) production that was thought to confer cancer susceptibility (Terzić *et al.*, 2010). Moreover, expression of inducible nitric oxide synthase (iNOS) by immune cells induces oxidative DNA damage and accelerates loss of heterozygosity at the *Apc* locus (Shaked *et al.*, 2012). Though chronic inflammation is a well-known risk factor for CRC, sporadic tumours that do not develop in an overt inflammatory setting, also elicit an inflammatory response. It is now appreciated that whether inflammation precedes or follows CRC tumour development, it has a critical role in determining the fate of CRC. Antigen-driven, cytolytic responses can limit cancer progression, while non-specific inflammatory activity can in some circumstances augment it (Grivennikov, Greten and Karin, 2010). These distinct sides of tumour immunity do not act in isolation, but normally act in concert to maintain intestinal homeostasis. The gut is home to the highest density of microorganisms in the human body and the symbiosis between microbe and man has led to the development of a highly sophisticated immune system with robust peripheral tolerance mechanisms (Elinav *et al.*, 2013). Critically, complex cytokine networks direct the immune response and aberrations in these finely tuned networks can lead to CRC (West *et al.*, 2015) (Figure 1.5,Table 1.2).

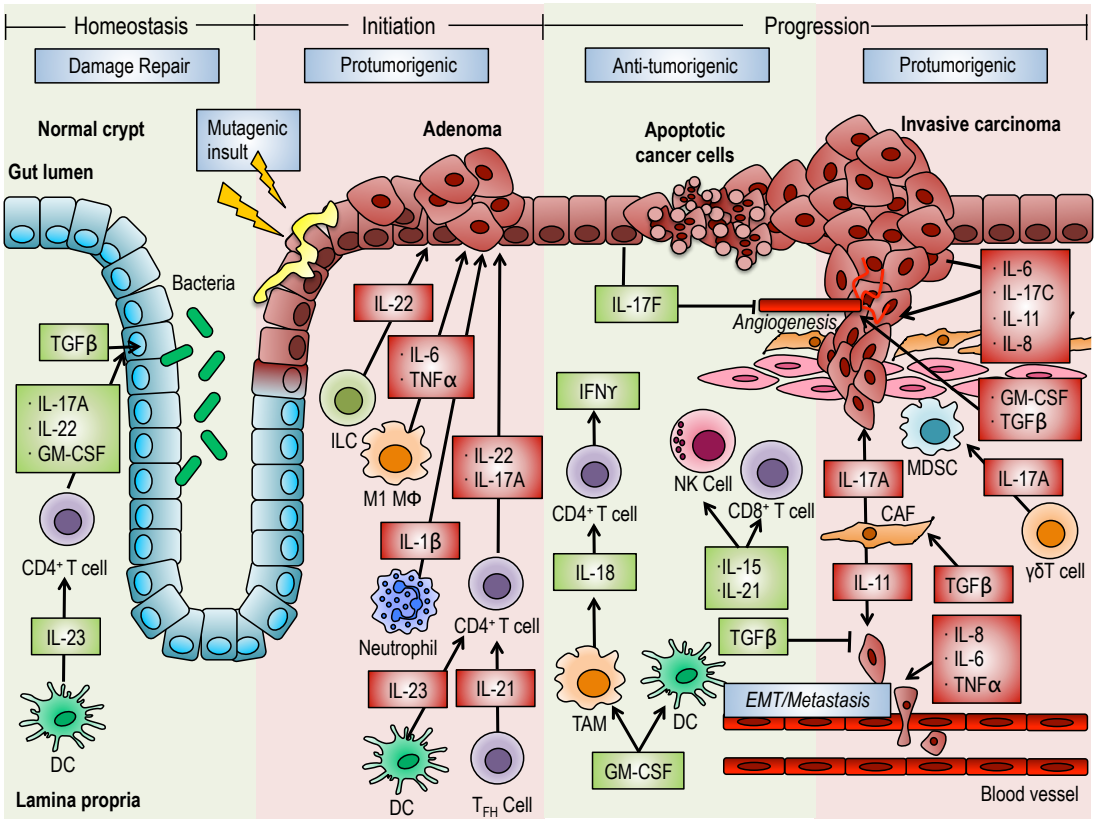


Figure 1.5 Cytokines in the pathogenesis of colorectal cancer

Cytokines are produced by innate and adaptive immune cells, fibroblasts, and cancer epithelial cells and can fuel tumourigenesis or promote anti-tumour immunity at different stages of CRC progression. IL-23, made by dendritic cells (DCs), induces the production of IL-22 and IL-17A from $CD4^+$ T cells and innate lymphoid cells (ILCs) in response to damage and microbial stimuli. These cytokines are important for mucosal tissue healing and host protection, but can also promote tumour formation and progression. At early stages of tumourigenesis, cytokines can inhibit tumour progression: IL-15 and IL-21 potentiate cytotoxic responses by $CD8^+$ T cells and NK cells; granulocyte-macrophage colony-stimulating factor (GM-CSF) activates macrophages and DCs; IL-18 induces IFNγ release; IL-17F inhibits angiogenesis; TGFβ can impair cancer cell growth and dissemination. By contrast, in well-established tumours which may have developed adaptations to resist the anti-tumour effects of certain cytokines, many cytokines can actually promote the hallmarks of cancer: proliferation, inhibition of apoptosis, angiogenesis, epithelial to mesenchymal transition (EMT), metastasis, and suppression of anti-tumour immunity. The major cell types reported to produce and respond to specific cytokines in CRC are outlined in Table 1.2 below. IEC, intestinal epithelial cell; DC, dendritic cell; TAM, tumour-associated macrophage; MDSC, myeloid-derived suppressor cell; CAF, cancer-associated fibroblast. (Figure prepared by S.McCuaig for NRI)

Cytokine	Cellular Source	Cellular Responder
TNFα	hematopoietic cells[1,2]	IECs[3], cancer cells[4]
TGFβ	CAFs[5]	cancer cells[5], CAFs[6,7]
IL-1β	TAMs[8], neutrophils[9]	IECs[9], cancer cells[8,10]
IL-6	TAMs[11], CAFs[12], mesenchymal stem cells[13]	IECs[14], cancer cells[12-14]
IL-11	CAFs[6]	cancer cells[6,15]
IL-23	DCs[16], TAMs (Cd11b+, Gr1+)[17]	hematopoietic cells[17]
IL-17A	CD4+ αβ T cells[18,19], CD8+ (Tc17 cells), γδ T cells[19], ILCs[22], CAFs[21]	cancer cells[20], CICs[21], MDSCs[19,16]
IL-17C	IECs[23]	IECs[23], cancer cells[23]
IL-17F	IECs[24]	endothelial cells[24]
IL-22	ILC3s[22], CD4+ T cells[25,26]	cancer cells[22,25,26]
IL-18	TAMs, IECs[27]	IECs[28], T cells[29,27]
IL-8	CD44+ cancer stem-like cells[30]	CD11b+Gr-1+ myeloid cells[31]
GM-CSF	cancer cells[32,33,34]	cancer cells[32], APCs[32], monocytes[33]
IL-15	cancer cells[35]	NK cells[36,37], CD8+ T cells[36], B & T cells[35]
IL-21	CD4+ T cells[37], activated NK cells[37]	NK cells[38,37], CD8 T cells[37]

Anti-tumourigenic Protumourigenic Pro/anti-tumourigenic

Table 1.2 Major cytokine producer and responder cells in CRC

IEC, intestinal epithelial cell; DC, dendritic cell; TAM, tumour-associated macrophage; MDSC, myeloid-derived suppressor cell; APC, antigen-presenting cell; CIC, cancer-initiating cell; CAF, cancer-associated fibroblast. 1.(Hale and Greer, 2012) 2.(Blatner *et al.*, 2012) 3.(Flores *et al.*, 2012) 4.(Wang *et al.*, 2013) 5.(Hawinkels *et al.*, 2014) 6.(Calon *et al.*, 2012) 7.(Calon *et al.*, 2015) 8.(Kaler, Augenlicht and Klampfer, 2009) 9.(Y Wang *et al.*, 2014) 10.(Yijing Li *et al.*, 2012) 11.(Schiechl *et al.*, 2011) 12.(Nagasaki *et al.*, 2014) 13.(Lin *et al.*, 2013) 14.(Tseng-Rogenski *et al.*, 2014) 15.(Putoczki *et al.*, 2013) 16.(He *et al.*, 2010) 17.(Grivennikov *et al.*, 2012) 18.(S. Wu *et al.*, 2009) 19.(P. Wu *et al.*, 2014) 20.(K. Wang *et al.*, 2014) 21.(Lotti *et al.*, 2013) 22.(Kirchberger *et al.*, 2013a) 23.(Song *et al.*, 2014) 24.(Tong *et al.*, 2012) 25.(Huber *et al.*, 2012) 26.(Kryczek *et al.*, 2014) 27.(Harrison *et al.*, 2015) 28.(Zaki *et al.*, 2010) 29.(Salcedo *et al.*, 2010) 30.(Hwang *et al.*, 2011) 31.(Asfaha *et al.*, 2013) 32.(Urdinguio *et al.*, 2013) 33.(Nebiker *et al.*, 2014) 34.(Yi Wang *et al.*, 2014) 35.(Mlecnik *et al.*, 2014) 36.(Rochman, Spolski and Leonard, 2009) 37.(Zhang *et al.*, 2009) 38.(Steele *et al.*, 2012)
(Table prepared by S.McCuaig for NRI)

We will briefly highlight key cytokines in the CRC microenvironment and the known mechanisms by which they promote tumourigenesis, with an ultimate focus on the IL-23 pathway.

1.2.3.1 The classical players in the CRC cytokine milieu

TNFα – Tumour necrosis factor α is a proinflammatory cytokine, produced by hematopoietic and non-hematopoietic cells, with pleiotropic functions. In cancer, it

was first identified as a tumour suppressive cytokine due to its capacity to induce apoptosis in certain cell types (Balkwill, 2009). However in CRC, it is now recognised as a critical tumour-promoting cytokine in the inflammatory milieu (Popivanova *et al.*, 2008; Erdman *et al.*, 2009; Y. Wu *et al.*, 2009; Grivennikov and Karin, 2011). High expression of the TNFα receptor 1 (TNFR1) renders intestinal epithelial cells highly sensitive to TNFα, which potently induces NF-κB signalling that can promote proliferation and resistance to apoptosis (Grivennikov and Karin, 2011). Hematopoietic cell-specific TNFα deficiency dramatically reduces spontaneous adenoma formation in an Apc^{A468} CRC model (transgenic mice express a mutant form of *Apc* encoding the APC protein) (Blatner *et al.*, 2012). Similarly, in the colitis-associated CRC model driven by dextran sodium sulphate (DSS) and azoxymethane (AOM) administration, TNFα is required for the tumour-promoting effect of obesity (Flores *et al.*, 2012). Moreover, TNFα may induce epithelial mesenchymal transition (EMT) and thus promote metastasis in CRC by augmenting SNAI1 transcription factor activity (Wang *et al.*, 2013).

IL-1β – Interleukin 1 β, like TNFα, is a potent NF-κB activator and its expression increases during CRC progression (Apte and Voronov, 2002; Cui *et al.*, 2012). By inactivating GSK3β, IL-1β actives the Wnt pathway in CRC (Kaler, Augenlicht and Klampfer, 2009) and induces chemoresistance and features associated with stemness (Yijing Li *et al.*, 2012). Neutrophils are a dominant source of IL-1β in the DSS-AOM CAC model (Y Wang *et al.*, 2014). Therapeutic blockade of IL-1β with a soluble receptor antagonist in this model attenuated tumour formation and IL-6 expression by infiltrating myeloid cells (Y Wang *et al.*, 2014).

TGFβ – Transforming growth factor β is a cytokine with important tissue protective functions in homeostasis, particularly with respect to wound healing (Wan and

Flavell, 2007). Mechanistically, TGFβ activates the serine/threonine kinase receptors TBFβR1 and TGFβR2, which then activate the intracellular proteins SMAD2 and SMAD3 that subsequently interact with SMAD4 to control gene expression (Weiss and Attisano, 2013). In CRC, TGFβ is thought to have tumour suppressive functions in early-stage disease (Kim *et al.*, 2000; Becker *et al.*, 2004; Biswas *et al.*, 2004), which is corroborated by the high frequency of inactivating mutations in TGFβ signalling components in CRC (Fleming *et al.*, 2013). However, high levels of TGFβ in human CRC are associated with poor prognosis, particularly in patients with advanced disease (Calon *et al.*, 2012). Rather than promoting tumourigenesis via direct effects on the malignant epithelium, TGFβ signalling into stromal cells drives gene expression signatures associated with poor prognosis in CRC (Calon *et al.*, 2015). Furthermore, TGFβ can induce interleukin 11 expression by cancer-associated fibroblasts (CAFs), which promotes STAT3 signalling in CRC cells and increases metastasis (Calon *et al.*, 2012).

IL-6 – Interleukin 6 is produced by diverse cell types in the CRC microenvironment and transduces signals via gp130 to potently induce STAT3 activation (Taniguchi and Karin, 2014). IL-6 is the most well studied STAT3 activator in CRC and has been shown to drive proliferation, migration, and angiogenesis in both CAC (Bollrath *et al.*, 2009; Grivennikov *et al.*, 2009) and sporadic CRC (Nagasaki *et al.*, 2014; Taniguchi and Karin, 2014). IL-6-induced STAT3 signalling in myeloid cells was recently described to promote tumour recurrence following radiotherapy (Gao *et al.*, 2013). While macrophages were classically regarded as the primary source of IL-6 in CRC, recent data supports CAF production of IL-6 in human tumours (Nagasaki *et al.*, 2014). CAF-derived IL-6 promotes tumourigenesis in human CRC through the induction of Notch1 and CD44 expression (Lin *et al.*, 2013). Upstream production of

IL-6 was recently linked to the microbiota. Bacterial biofilms, were found to be almost universally present on tumours in the proximal colon. These biolfilms were associated with increased IL-6 production in the lamina propria and enhanced epithelial STAT3 activation (Dejea *et al.*, 2014). Though causality was not established, the bacterial biofilms represent a novel driver of IL-6 production in human CRC.

1.2.3.2 Cytokines with emerging roles in CRC

IL-11 – Interleukin-11 is a member of the IL-6 cytokine family (Taniguchi and Karin, 2014) and is highly expressed in human CRC (Putoczki *et al.*, 2013). Interestingly, IL-11 is a stronger correlate of phosphorylated STAT3 than IL-6 (Putoczki *et al.*, 2013). In both $Apc^{Min/+}$ mice and DSS-AOM treated mice, genetic deletion of the IL-11 receptor alpha subunit profoundly reduced tumour formation, regardless of IL-6 activity (Putoczki *et al.*, 2013). Combined with the recent report that demonstrated that TGFβ promotes metastasis by inducing IL-11 production by CAFs (Calon *et al.*, 2012), this evidence points toward a critical role for IL-11 as a protumourigenic driver in CRC.

IL-8 (CXCL8) – Interleukin 8 is a potent neutrophil chemoattractant that signals through the CXC-chemokine receptor 2 (CXCR2) (Waugh and Wilson, 2008). Genetic alterations in the genes encoding IL-8 and CXCR2 are associated with CRC recurrence and therapeutic resistance (Gordon *et al.*, 2005; Lurje *et al.*, 2008). When transfected to overexpress *IL8*, HCT116 and Caco2 CRC cells exhibit enhanced growth and vascularisation in xenograft models (Ning *et al.*, 2011). Importantly, CXCR2 blockade with the small molecule inhibitor SCH-527123 impaired proliferation and enhanced survival and chemosensitivity to oxaliplatin in CRC xenografts (Ning *et al.*, 2012). Notably, antagonism of CXCR2 not only prevents IL-8

signalling, but also other members of the ELR$^+$ CXC chemokine family, that have known pro-tumourigenic functions in other malignancies (O'Hayer, Brady and Counter, 2009).

IL-23, IL-17A, IL-22 – IL-23 and its downstream effectors IL-17A and IL-22 are critical for maintenance of barrier integrity in the gut (Maloy and Kullberg, 2008), however they have emerged in recent years as pro-tumourigenic cytokines in both colitis-associated and sporadic CRC models (Shalapour and Karin, 2015). The following sections (1.3, 1.4) will highlight their homeostatic and pathogenic function in detail.

1.3 The IL-23 pathway in gastrointestinal health and disease

1.3.1 IL-23: upstream regulators and downstream effectors

IL-23 is a heterodimeric cytokine belonging to the IL-12 family (Oppmann *et al.*, 2000). Both IL-12 and IL-23 share a common p40 subunit (encoded by *IL12B*) that heterodimerises with p35 (*IL12A*) to form IL-12 or with p19 (*IL23A*) to form IL-23 (Oppmann *et al.*, 2000). Both cytokines are secreted predominately by antigen presenting cells such as activated dendritic cells, macrophages, and monocytes in response to microbial or damage-associated stimuli (Ngiow, Teng and Smyth, 2013). Despite their shared p40 subunit and similar modes of induction, IL-12 and IL-23 drive divergent immunological responses (Uhlig *et al.*, 2006). The IL-12 receptor is expressed on naïve CD4$^+$ T cells and promotes their differentiation into IFNγ producing Th1 cells capable of promoting anti-tumour immunity by inducing the proliferation and cytotoxic activity of NK cells and CD8$^+$ T cells (Trinchieri, 2003; Langowski *et al.*, 2006). By contrast the IL-23 receptor, comprised of IL-23R and IL-12Rβ1 (Parham *et al.*, 2002), is not expressed on naïve T cells and thus IL-23 does not promote T cell differentiation per se. However, exposure of naïve T cells to

TGFβ, IL-1β, and IL-6 induces the expression of the retinoic acid receptor-related orphan receptor-γt (RORγt), which is a lineage-specific transcription factor that drives expression of *Il23r* and *Il17a* (Ivanov *et al.*, 2006; Maloy and Kullberg, 2008; Volpe *et al.*, 2008; Gaffen *et al.*, 2014; Teng *et al.*, 2015). IL-23 expands and maintains this $CD4^+$ T helper 17 (Th17) population by signalling into IL-23R-expressing $CD4^+$ T cells. This activates STAT3 to promote transcription of *Il23r* and *Rorc* (encoding RORγt) to sustain a positive feedback loop (McGeachy *et al.*, 2009; Ghoreschi *et al.*, 2010; Teng *et al.*, 2015). Th17 cells produce a variety of inflammatory cytokines including IL-17A and IL-22 (Zheng *et al.*, 2007; Gaffen *et al.*, 2014). More recently, it has been appreciated that IL-23 sustains RORγt-expressing γδ T cells and type 3 innate lymphoid cells (ILC3s) that produce high levels of IL-17 and IL-22 (Buonocore *et al.*, 2010; Cua and Tato, 2010). The IL-17 receptor (IL-17RA, IL-17RC) is expressed on multiple hematopoietic and non-hematopoietic cell types and signalling predominately activates the NF-κB pathway (Yao *et al.*, 1995; Gaffen *et al.*, 2014). By contrast IL-22 receptor (IL-22RA1, IL-10RB) expression is limited to non-hematopoietic cells and its activation drives STAT3 signalling (Xie *et al.*, 2000; Wolk *et al.*, 2004). Thus, both IL-23 downstream effectors can mediate cross talk between the immune system and peripheral tissues (Figure 1.6).

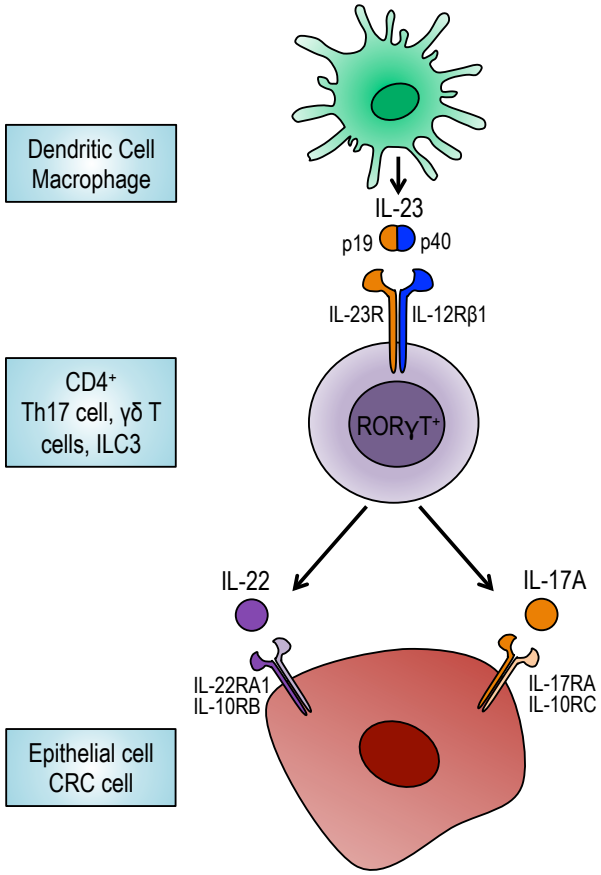


Figure 1.6 The IL-23 pathway from a cellular perspective.

Activated dendritic cells and macrophages produce IL-23, a heterodimeric cytokine comprised of a p19 and p40 subunit, in response to microbial or damage-associated stimuli. IL-23 signals through a heterodimeric receptor (IL-23R, IL-12Rβ1), expressed on $CD4^+$ Th17 cells, γδ T cells, and type 3 innate lymphoid cells, and induces the production of its downstream effectors IL-22 and IL-17A. The IL-17A receptor (IL-17RA, IL10RC) is expressed on multiple hematopoietic and non-hematopoietic cell types, while IL-22 receptor (IL-22RA1, IL10RB) expression is predominately restricted to epithelial cells. In homeostasis and colorectal cancer, IL-22 and IL-17A can provide directional signals from the immune system into the epithelium.

1.3.2 Maintaining the barrier: homeostatic function of the IL-23 pathway in the gut

The function of IL-23 was initially characterised on the basis of studies that uncovered its role in driving immune pathology (Gaffen *et al.*, 2014), however IL-23 and its downstream effectors, IL-17A and IL-22, also have important functions in mucosal immune defense and restitution and repair of the intestinal epithelium. A role for IL-23-mediated protection against extracellular pathogens was revealed when IL-$23p19^{-/-}$ mice were found to have enhanced susceptibility to and mortality following *Citrobacter rodentium* infection, a murine model of enteropathogenic *Escherichia*

coli infection (Mangan *et al.*, 2006). Evidence suggests that downstream IL-17A and IL-22, which can act directly on intestinal epithelial cells, critically maintain the single layer of epithelial cells that separates a microbe-rich intestinal lumen from the underlying host tissue. Neutralisation of IL-17A or IL-22 exacerbated disease and delayed recovery in an acute damage dextran sodium sulphate (DSS) model of colitis (Ogawa *et al.*, 2004; Sugimoto *et al.*, 2008). Mechanistically, IL-17A stimulates expression of claudins in intestinal epithelial cells to enhance tight-junction formation and maintain mucosal barrier integrity in the gut (Kinugasa *et al.*, 2000). While IL-22 promotes proliferation and migration of epithelial cells, and directly protects epithelial cells from microbial insult by inducing protective mucin and anti-microbial peptide (β-defensins, RegIIIγ, S100A8/9) production (Andoh *et al.*, 2005; Brand *et al.*, 2006; Zheng *et al.*, 2008). More recent evidence has illuminated the importance of IL-22 signalling directly into intestinal epithelial stem cells to promote epithelial regeneration following graft versus host disease-induced damage (Hanash *et al.*, 2012; Lindemans *et al.*, 2015). Thus, by controlling extracellular bacterial infections and repairing a damaged mucosal barrier, the IL-23 pathway plays a critical role in maintaining gut homeostasis.

1.3.3 Too much of a good thing: the IL-23 pathway in CRC

When high levels of IL-23 and its downstream effectors are sustained for extended periods, the consequent chronic inflammatory responses can drive IBD pathogenesis and more recently it has come to be appreciated that these cytokines can promote intestinal tumourigenesis (Teng *et al.*, 2015). Several single nucleotide poylmorphisms in the *IL23R* gene locus were identified in genome wide association studies to confer increased susceptibility to IBD (Duerr *et al.*, 2006). Indeed,

abundant evidence from murine experimental colitis models supports a pathogenic role for IL-23, IL-17A, and IL-22 in IBD in certain settings (Maloy and Kullberg, 2008; Gaffen *et al.*, 2014) and therapeutic targeting of the IL-23 pathway is being explored in the clinic (Teng *et al.*, 2015).

The first indication that IL-23 may be pro-tumourigenic came with the observation that *IL23A* mRNA was elevated in a number of human solid tumours compared to the corresponding matched normal adjacent tissue (Langowski *et al.*, 2006). Langowski *et al.* then went on to demonstrate that mice deficient in IL-12/23p40 or IL-23p19, but not IL-12p35, are resistant to carcinogen-induced skin papilloma formation, implicating IL-23 as a promoter of malignancy (Langowski *et al.*, 2006). In the gut, genetic ablation of *Il23a* reduced tumourigenesis in the murine CPC-APC sporadic CRC model, an adaptation of the classical $Apc^{Min+/-}$ model where tumours are directed to the colon by *Cdx2* Cre-mediated deletion of an *Apc* allele (Grivennikov *et al.*, 2012). Moreover, in a model of bacterially driven colitis-associated colorectal cancer in which genetically susceptible 129*SvEv.*$Rag^{-/-}$ mice were infected with the mouse pathobiont *Helicobater hepaticus* (*Hh*) and treated with the chemical carcinogen azoxymethane (AOM), IL-23 receptor blockade reduced the appearance of aberrant crypt foci and reduced tumour burden in mice with established disease (Kirchberger *et al.*, unpublished).

A pro-tumourigenic role for downstream IL-17A in CRC was first identified in $Apc^{Min/+}$ mice infected with enterotoxigenic *Bacteroides fragilis* (S. Wu *et al.*, 2009). IL-17A blockade in these animals significantly reduced tumour burden (S. Wu *et al.*, 2009). Genetic deletion of *Il17a* had a similar effect in the classical $Apc^{Min/+}$ sporadic

CRC model (Chae *et al.*, 2010). Moreover, *Il17ra* deficiency in the CPC-APC model diminished epithelial STAT3 activation and tumourigenesis (Grivennikov *et al.*, 2012). Tumourigenesis mediated by IL-17A is not restricted to sporadic disease, in the DSS-AOM colitis-associated cancer model, *Il17a-/-* mice were resistant to tumour development (Hyun *et al.*, 2012). Reciprocal bone marrow chimera experiments elucidated the important role of IL-17A signalling directly into transformed epithelial cells rather than hematopoietic cells, in promoting tumourigenesis (K. Wang *et al.*, 2014). Moreover, IL-17A blockade in the CPC-APC model sensitized animals to 5-fluoruracil chemotherapy (K. Wang *et al.*, 2014). Independent of the direct effects on the malignant epithelium, IL-17-expressing γδ T cells, induced by IL-23, are reported to attract and promote the expansion of myeloid derived suppressor cells in the tumour microenvironment to condition an immunosuppressive milieu (P. Wu *et al.*, 2014). Beyond hematopoietic cells, chemotherapy reportedly induced IL-17A production by CAFs in xenograft models (Lotti *et al.*, 2013) and IL-17A may educate tumour stromal cells to promote resistance to anti-angiogenic therapy (Chung *et al.*, 2013). Functional data from human colorectal cancer implicating the IL-23 pathway in disease pathogenesis is very limited, though it is clear that high expression of a functional Th17 mRNA signature is associated with poor prognosis (Tosolini *et al.*, 2011; Bindea *et al.*, 2013).

IL-22 is distinct from IL-17A as it cannot signal between leukocytes, but provides a directional signal into the epithelium. Though IL-22 has classically been studied for its important tissue protective function, key recent studies in pre-clinical models have illuminated its role in CRC. These will be the focus of the following section.

1.4 IL-22: a friend in health, a foe in CRC

1.4.1 IL-22: A double-edged sword

IL-22 is an IL-10 family cytokine produced predominately by Th17 and innate lymphoid cells at barrier surfaces. However in humans, IL-22 can also be produced by γδ T cells, NK cells, Th1 cells, and a subset of $CD4^+$ T cells termed Th22 cells (characterised by IL-22 and TNFα, but not IL-17 production) (Sabat, Ouyang and Wolk, 2014). As outlined in Section 1.3.2, by triggering epithelial cell proliferation, survival, and antimicrobial peptide and mucin production, IL-22 plays a critical role in the resolution of tissue damage induced by microbial insult, reactive oxygen species, and other harmful chemicals (Sugimoto *et al.*, 2008; Zheng *et al.*, 2008; Hanash *et al.*, 2012; Lindemans *et al.*, 2015). Elevated IL-22 levels are detected in the serum (Wolk *et al.*, 2007) and colon (Brand *et al.*, 2006; Geremia *et al.*, 2011) of IBD patients where it acts as a double-edged sword. While necessary for damage repair, IL-22 can promote colitis in some settings by triggering proinflammatory cytokine secretion and perpetuating the inflammatory response (Kamanaka *et al.*, 2011).

1.4.2 IL-22 receptor and signalling

IL-22 signals through a heterodimeric receptor comprised of the IL-22 receptor alpha 1 (IL-22RA1) subunit and IL-10 receptor 2 (IL10RB) subunit, which is also utilised by several other members of the IL-10 family (Xie *et al.*, 2000; Gurney, 2004). While classified as an interleukin, IL-22 does not mediate direct cross talk between leukocytes, but that between leukocytes and non-hematopoietic cells, as receptor expression is restricted to the non-hematopoetic compartment (Wolk *et al.*, 2004). At present, the regulation of expression of the IL-22 receptor is poorly understood. Studies in mice have demonstrated that GSK-3β can phosphorylate IL-22RA1 on its cytoplasmic tail and prevent its proteasomal degradation (Weathington *et al.*, 2014).

However, the human IL-22RA1 receptor lacks a GSK-3β-targeting consensus sequence and thus its stability is not likely controlled by GSK-3β. Rather it undergoes degradation mediated by the E3 ubiquitin ligase FBXW12 (Franz *et al.*, 2015). Signalling downstream of the IL-22 receptor is mediated predominately via the JAK1/TYK2/STAT3 pathway. The majority of the well-documented physiologic and pathologic functions of IL-22 are STAT3-dependent. Atypically, the intracellular domain of IL-22RA1 is constitutively associated with STAT3, allowing for rapid activation upon receptor dimerisation by phosphorylation at both tyrosine 705 (Y705) and serine 727 (S727) (Figure 1.7)(Dumoutier *et al.*, 2009; Lim and Savan, 2014). In a STAT3-dependent manner, IL-22 signalling induces expression of suppressor of cytokine signalling 3 (SOCS3). SOCS3 is capable of inhibiting signalling downstream of gp130 domain-containing cytokine receptors (ie. IL-6, IL-11, oncostatin M). However, both IL-22 receptor subunits lack SOCS3 binding sites and thus IL-22 signalling is not subject to negative feedback via SOCS3 (Yoshimura and Yasukawa, 2012). Though less extensively studied, IL-22 also induces the PI3K/AKT/mTOR signalling cascade which enables normal proliferation of human epithelial keratinocytes, is required for migration of colonic epithelial cells, and inhibits apoptosis in renal tubular epithelial cells (Mitra, Raychaudhuri and Raychaudhuri, 2012; Xu *et al.*, 2014). Moreover, *in vitro* evidence in a rat hepatoma cell line, demonstrated that IL-22 activates the three major MAPK pathways: MEK-ERK-RSK, JNK/SAPK, and p38 pathways (Lejeune *et al.*, 2002; Sabat, Ouyang and Wolk, 2014). Finally, IL-22 is capable of activating NF-κB and through synergism with STAT3, induces the expression of genes that regulate cell cycle progression and inhibition of apoptosis (Sugimoto *et al.*, 2008; Lim and Savan, 2014). Thus IL-22 is a pleiotropic cytokine capable of activating multiple signalling pathways and as such

requires careful regulation. An important component of IL-22 regulation is the IL-22 neutralising receptor, IL-22-binding protein (IL-22BP or IL-22RA2), a soluble receptor produced by $CD11c^+$ dendritic cells that sequesters IL-22 and prevents its activity (Xu *et al.*, 2001). Recent studies have identified IL-22BP as a therapeutic target in IBD, as its overexpression limits the important tissue protective properties of IL-22 (Martin *et al.*, 2016; Pelczar *et al.*, 2016). The existence of the IL-22BP, in evolutionary terms, underscores the necessity for tight regulation of the IL-22 pathway.

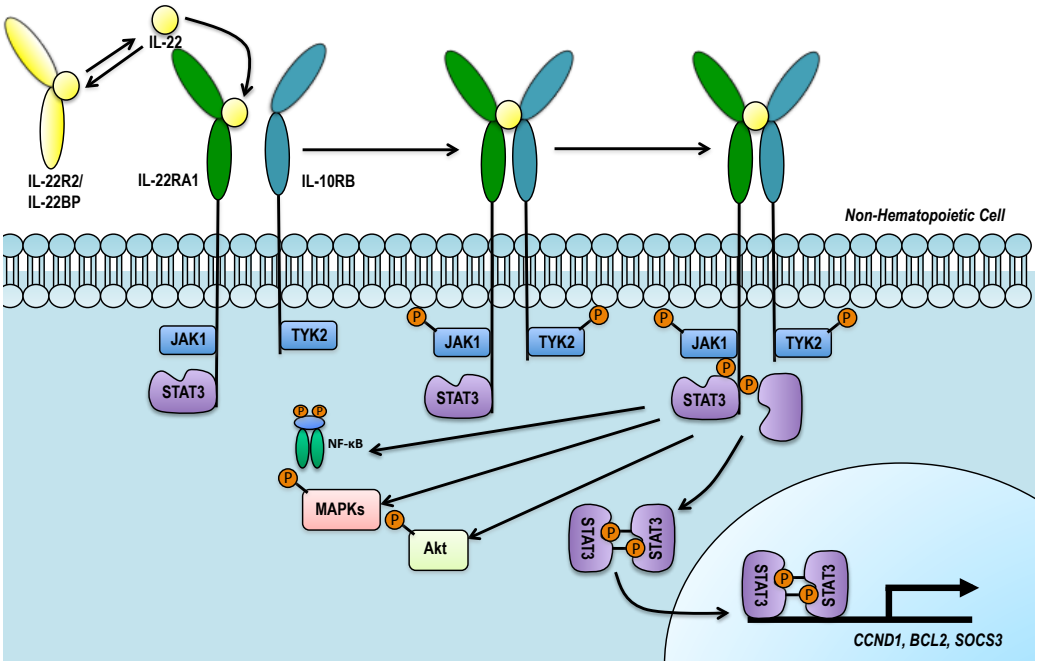


Figure 1.7 IL-22 receptor and downstream signalling.

IL-22 is a pleiotropic cytokine capable of activating multiple intracellular signalling pathways. Mechanistically, IL-22 first binds the IL-22RA1 subunit of its heterodimeric receptor, which induces a conformational change that allows for subsequent binding of the IL-10RB subunit. Receptor dimerisation results in phosphorylation of the receptor-associated JAK1/TYK2, followed by STAT3. Phosphorylated STAT3 homerdimerises with another STAT3 subunit, translocates to the nucleus, and activates the transcription of genes involved in cell proliferation, apoptosis, and antimicrobial peptide production. IL-22 is additionally known to activate mitogen-associated protein kinase (MAPKs) pathways, the AKT pathway, and NF-κB pathway.

1.4.3 IL-22 and colorectal cancer in murine models

Previous studies in our lab identified a population of colonic innate lymphoid cells ($IL\text{-}17^+IL\text{-}22^+$ ILC3s) as a dominant source of IL-22 in a model of bacterially driven

colorectal cancer. In this model genetically susceptible 129*SvEv.Rag*$^{-/-}$ mice were infected with the mouse pathobiont *Helicobater hepaticus* (*Hh*) and treated with the chemical carcinogen azoxymethane (AOM). These animals normally develop invasive adenocarcinoma in 3-5 months, but when animals with established tumours were treated with anti-IL-22 the tumours regressed (Kirchberger *et al.*, 2013a). Similarly, a pro-tumorigenic role for IL-22 was identified through manipulation of the established *Apc*$^{Min/+}$ genetic model of CRC. *Apc*$^{Min/+}$ animals crossed to IL-22BP deficient animals (*Apc*$^{Min/+}$ x *IL22bp*$^{-/-}$) developed larger and more numerous tumours, while *Apc*$^{Min/+}$ animals also lacking IL-22 (*Apc*$^{Min/+}$ x *Il22*$^{-/-}$) developed fewer colonic tumours compared to *Apc*$^{Min/+}$ controls (Huber *et al.*, 2012). Very recently, IL-22 was shown to potentiate inducible nitric oxide synthase (iNOS) expression in colonic epithelial cells in 129*SvEv.Rag*$^{-/-}$ mice after 10 weeks of *Hh* infection. Nitric oxide-mediated double-stranded DNA breaks (DSB) formed as a consequence and led to premalignant dysplasia. Inhibition of IL-22 reduced DSB and the appearance of dysplastic tissue (Wang *et al.*, 2017). Thus IL-22 seems to be required for the development and progression of both colitis-associated and sporadic CRC in certain settings. However, the precise mechanisms by which IL-22 promotes tumourigenesis remain to be elucidated.

1.4.4 IL-22 in human gastrointestinal cancer

Evidence suggesting a role for IL-22 in gastrointestinal cancer development and progression in humans is relatively sparse and largely observational. Increased infiltration of IL-22^{+} CD4^{+} T cells was observed in a cohort of gastric tumours (N=76) as compared to surrounding non-tumour tissue. Quantitatively, the amount IL-22^{+} CD4^{+} T cell infiltration increased with tumour stage and was negatively correlated with overall patient survival (Zhuang *et al.*, 2012). Elevated serum IL-22

levels were found in a group of chemoresistant (N=41) as compared to chemosensitive (N=46) CRC patients (T. Wu *et al.*, 2014). Moreover, *IL22* mRNA was found to be higher in CRC tumour sections compared to matched normal adjacent tissue (Kirchberger *et al.*, 2013a). Furthermore, Kryczek *et al.* provided the first evidence to suggest that IL-22 promotes colorectal cancer stemness. In their studies in the human DLD-1 colorectal cancer adenocarcinoma line, they demonstrated that IL-22-activated STAT3 directly induced the expression of the methyltransferase DOT1L. DOT1L in turn augmented expression of drivers of pluripotency (*SOX2, NANOG, POU5F1*) that were negatively correlated with patient prognosis (Kryczek *et al.*, 2014).

Despite the evidence to suggest a role for IL-22 in human disease, the phenotypes associated with IL-22/IL-22 receptor expression in CRC remain uncharacterized and the molecular mechanisms by which IL-22 mediates tumourigenesis are not understood. The primary aim of this thesis is to understand the role of the IL-22 pathway in human CRC. However, given the vast amount of heterogeneity in human CRC and the presence of oncogenic mutations in components of the IL-22 signalling pathway, we hypothesise that the mutational landscape of a tumour will play an important role in dictating whether IL-22 signalling is protective or pro-tumourigenic in CRC.

1.5 Tumour adaptations to cytokines in CRC

Drawing from examples of known mechanisms by which other cytokines can promote CRC development and progression, it becomes clear that tumours develop adaptations to maximize the benefit they receive from cytokine signalling. Thus it is often not the

cytokine alone, but the concerted action of cytokines and oncogenic drivers or tumour adaptations that potentiate or attenuate cytokine signaling, that results in malignant progression.

1.5.1 Silencing of tumour-suppressor genes normally augmented by cytokine signalling

One example of such an adaptation is the selective suppression cytokine target genes that may halt tumour growth. For example, expression of the gene encoding the pro-apoptotic protein kinase Cδ (PRKCDBP) is induced by TNFα in an NF-κB-dependent manner and promotes TNFα-mediated apoptosis (Lee *et al.*, 2011). Interestingly, PRKCDBP is silenced by promoter hypermethylation in over one-third of primary CRCs, thus inducing tumour cell resistance to TNFα-dependent apoptosis (Lee *et al.*, 2011). The promoter of the important negative regulator of STAT3 signalling, *SOCS3*, is similarly hypermethylated in the dysplastic colonic epithelium of patients with ulcerative colitis (Yi Li *et al.*, 2012). Attenuated SOCS3 expression was found to correlate with increased expression of the DNA methyltransferase DNMT1 (Yi Li *et al.*, 2012), which directly represses *SOCS3* (Huang *et al.*, 2016). Independently, IL-6 was shown to induce DNMT1 expression in human CRC (Foran *et al.*, 2010). Thus IL-6 signalling may be perpetuated in the tumour microenvironment by a feed-forward loop driven by repression of its negative regulator, SOCS3, and consequently enable progression from dysplasia to overt malignancy.

1.5.2 Inflammatory modulation by loss of p53

Genetic changes in CRC can directly augment pro-tumourigenic inflammation. *TP53* encodes the tumour suppressor protein p53 and is mutated in 60-70% of CRCs (Fearon, 2011). *TP53* mutations are an early event in colitis-associated cancer development and can even be detected in the epithelium of patients with colitis before the appearance of neoplasia (Hussain *et al.*, 2000). p53 has earned the title of

"guardian of the genome" for its critical role in controlling genome integrity and preventing the outgrowth of mutant cells, however, more recently its immune-modulating function has come to be appreciated. Loss of p53 augments IL-6 signalling in CRC due to consequent diminished expression of the p53 transcriptional target microRNA-34a (miR-34a). Under physiologic settings, miR-34a represses IL-6 receptor expression and reduces IL-6-mediated epithelial mesenchymal transition (EMT) (Rokavec *et al.*, 2014). Furthermore, tumours that developed in mice with an epithelial cell-specific p53 deletion ($Trp53^{\Delta IEC}$) following AOM administration displayed a pronounced myeloid cell infiltrate, elevated levels of NF-κB-dependent cytokines and chemokines, and expression of markers of EMT (Schwitalla, Ziegler, *et al.*, 2013). Each of these features was required for the enhanced tumourigenesis and local metastasis observed in $Trp53^{\Delta IEC}$ compared to wild type control treated animals (Schwitalla, Ziegler, *et al.*, 2013). Finally, mutations in *TP53* can augment cytokine signalling through gain-of-function effects. For example, the R248W mutation leads to prolonged NF-κB activation following low level TNFα stimulation and renders mice more susceptible to CAC (Cooks *et al.*, 2013). Thus, p53 seems to exert a tumour suppressive function independent of its capacity to induce cell-cycle-arrest, apoptosis, and senescence by keeping pro-tumorigenic cytokine-signalling at bay.

1.5.3 Inflammatory modulation by oncogenic *KRAS*

40-45% of colorectal tumours harbour mutations in *KRAS* that result in constitutive activation of the Ras pathway (Sinicrope *et al.*, 2014). *KRAS* mutations are strongly associated with resistance to EGFR-targeting therapies and variably associated with resistance to standard chemotherapies (Karapetis *et al.*, 2008; Bokemeyer and Bondarenko, 2011; Van Cutsem *et al.*, 2015). Little is known about the direct influence of *KRAS* on inflammatory signalling in CRC, however tumours harbouring

mutations in *KRAS* or *NRAS* in microsatellite-stable CRC have reduced expression of genes associated with Th1-type immunity, antigen presentation, and checkpoint blockade targets (Lal *et al.*, 2015). Borrowing knowledge from other malignancies, oncogenic Ras has been shown to directly induce the production of pro-inflammatory cytokines and chemokines such as IL-6, IL-8 (CXCL8), IL-11, GM-CSF, and CXCL1 (Ancrile, Lim and Counter, 2007; O'Hayer, Brady and Counter, 2009; Pylayeva-Gupta *et al.*, 2012; Shin *et al.*, 2012). In pancreatic cancer, where greater than 90% of tumours harbour activating *KRAS* mutations (Ryan, Hong and Bardeesy, 2014), *KRAS* was shown to promote carcinogenesis in a murine model by directly augmenting IL-17 receptor alpha and intracellular adhesion molecule 1 (ICAM1) expression on epithelial cells and by conditioning a tumour microenvironment enriched in Th17 cells and inflammatory macrophages (McAllister *et al.*, 2014; Liou *et al.*, 2015). Thus, given the evidence from other malignancies, *KRAS* may directly induce cytokine and chemokine production, to tip the balance from anti-tumour immunity toward pro-tumourigenic inflammation.

Interestingly, two more recent studies in CRC have highlighted that *KRAS* may also act as a molecular switch to favour the pro-invasive properties of cytokines with known pro-apoptotic function. In murine intestinal adenomas and human CRC organoids, constitutively active *KRAS* supressed TGFβ-induced expression of the pro-apoptotic protein BIM via ERK1/2 activation, rendering the adenoma/CRC cells resistant to the tumour suppressive effects of TGFβ (Wiener *et al.*, 2014). Furthermore in murine and human CRC cells, mutant *KRAS* blocked the pro-apoptotic function of TNF-related apoptosis-inducing ligand (TRAIL or TNFSF10) and CD95

ligand (CD95L or TNFS6/FASL), but left their pro-metastatic properties intact (Hoogwater *et al.*, 2010).

In summary, there is an emerging body of evidence demonstrating that oncogenic mutations can directly alter the tumour immune microenvironment in CRC. They do this by strategically augmenting pro-inflammatory cytokine and chemokine production, silencing genes encoding negative regulators of cytokine signalling, and selectively abolishing the pro-apoptotic/anti-tumourigenic action of cytokines to maximise the growth and survival benefits conferred by cytokines in the milieu. At present it remains unknown however, whether oncogenic mutations disrupt or augment the IL-22 pathway in CRC, however this will be a focus as we explore the role of IL-22 in human CRC.

1.6 Cytokines as therapeutic targets in CRC

Despite the efficacy of therapeutic blockade of pro-tumourigenic cytokines in a number of pre-clinical CRC models (Kirchberger *et al.*, 2013a; K. Wang *et al.*, 2014; Y Wang *et al.*, 2014; Wang *et al.*, 2017), clinical trials of cytokine-targeting agents in human CRC are sparse and have been largely unsuccessful. Although abundant evidence supports a pro-tumourigenic role for IL-6 in CRC, an IL-6-specific antibody, siltuximab, failed to elicit clinical responses in a Phase I/II trial (Angevin *et al.*, 2014). Moreover, blockade of TNF with etanercept (recombinant TNF receptor), failed to treat cancer related cachexia in a Phase III trial (Jatoi *et al.*, 2007). Two Phase I/II trials of an IL-1β receptor antagonist (Anakinra) in advanced CRC are currently underway. The only success story thus far has come with the recent publication of the results of a Phase III trial investigating the efficacy of IL-1α

blockade with the MABp1 monoclonal antibody in treatment refractory CRC (Hickish *et al.*, 2017). MABp1 therapy increased lean body mass, reduced pain, fatigue, anorexia, and serum IL-6 concentrations (Hickish *et al.*, 2017), however the impact of MABp1 treatment on overall survival remains to be determined.

The relative lack of success of cytokine blockade in human CRC thus far is likely a consequence of the complexity of cytokine networks and the influence of underlying oncogenic mutations on cytokine signalling. Hence, targeting single cytokines in patients irrespective of the molecular subtype of their tumour is broadly ineffective.

1.6.1 The challenge of cytokine networks

Mutations in components of intracellular signalling pathways do not function in isolation, but as part of complex signalling networks. In much the same way cytokines, though often studied in isolation, act in concert with other cytokines. In CRC, abundant evidence has demonstrated that tumour infiltration by Th1 cells and CTLs is associated with favourable patient prognosis, while Th17 cells are linked to higher frequency of disease recurrence (Nosho *et al.*, 2010; Tosolini *et al.*, 2011; Bindea *et al.*, 2013). The human colorectal cancer cytokine milieu is dominated by high amounts of Th17 cell-derived cytokines (IL-17A, IL-17F, and IL-22), Th17 cell-polarising cytokines (IL-1β, TGFβ, IL-6) and classical proinflammatory cytokines such as TNFα (Blatner *et al.*, 2010; Cui *et al.*, 2012; Y Wang *et al.*, 2014; De Simone *et al.*, 2015). However, cytokines associated with immune regulation (ie. IL-10) (Blatner *et al.*, 2010) or Th1 and CTL responses (ie. IFNγ) are not abundant (De Simone *et al.*, 2015). In the midst of these complicated networks of, often interdependent, cytokines it is difficult to isolate which player(s) would make effective therapeutic targets. For example, previous studies in our lab demonstrated

that in a CAC model characterised by a mixed Th1 and Th17 signature, blockade of IL-22 suppressed tumourigenesis, while blockade of IL-17 or IFNγ did not have significant effects (Kirchberger *et al.*, 2013a). Moreover, in the CPC-APC model of CRC, IL-17 and IL-23 signalling are evidently pro-tumourigenic, but are not required for initial polyp formation (Grivennikov *et al.*, 2012). In a human *ex vivo* setting, neutralisation of any individual cytokine could not abolish the pro-proliferative effect conferred by treatment of CRC cells with supernatants generated from tumour infiltrating lymphocytes (De Simone *et al.*, 2015). Rather, combinatorial blockade of both STAT3 drivers (IL-6, IL-22) and NF-κB drivers (TNFα, IL-17A) was required to inhibit proliferation promoted by lymphocyte supernatants (De Simone *et al.*, 2015). Synergism between STAT3 and NF-κB is known to be a key contributor to the tumourigenic properties of the CRC cytokine milieu (Grivennikov and Karin, 2010). Therefore, rather than targeting upstream cytokines, utilising small molecule inhibitors of downstream STAT3 and NF-κB may have more potent anti-tumour effects. Notably, BP-1-102, which binds the STAT3 SH2 domain, may prevent the ability of STAT3 to enhance NF-κB signalling through direct physical interaction (Yu, Pardoll and Jove, 2009; Grivennikov and Karin, 2010; Zhang *et al.*, 2012). BP-1-102 suppressed CRC cell proliferation induced by tumour infiltrating lymphocytes and inhibited tumourigenesis when administered intravenously to $Apc^{Min/+}$ mice (De Simone *et al.*, 2015). Other strategies exist to neutralise signals from multiple cytokine pathways. For example, a novel STAT3 inhibitor that blocks induction of core stem cell genes (BBI-608) has shown signs of antitumour activity when combined with FOLFIRI chemotherapy in advanced CRC patients in a Phase Ib study (Hubbard *et al.*, 2016). Small molecule JAK1 and JAK2 inhibitors have shown encouraging results in other malignancies (Lee *et al.*, 2013; Gu *et al.*, 2014; Wen *et*

al., 2014). Moreover, effective inflammatory pathway blockade may be achieved by targeting the upstream immunologic signal that induces cytokine effectors capable of directly acting on CRC cells. For example, independently IL-23, IL-17A, and IL-22 have all been shown to promote CAC and sporadic CRC development and progression in murine models (Grivennikov *et al.*, 2012; Hyun *et al.*, 2012; Kirchberger *et al.*, 2013a; K. Wang *et al.*, 2014). Highly, effective IL-23p19 targeting antibodies were recently approved for use in psoriasis (Gordon *et al.*, 2015; Kopp *et al.*, 2015), but if deployed in CRC would theoretically inhibit the pro-tumourigenic action of both IL-17A and IL-22 by blocking their induction by IL-23.

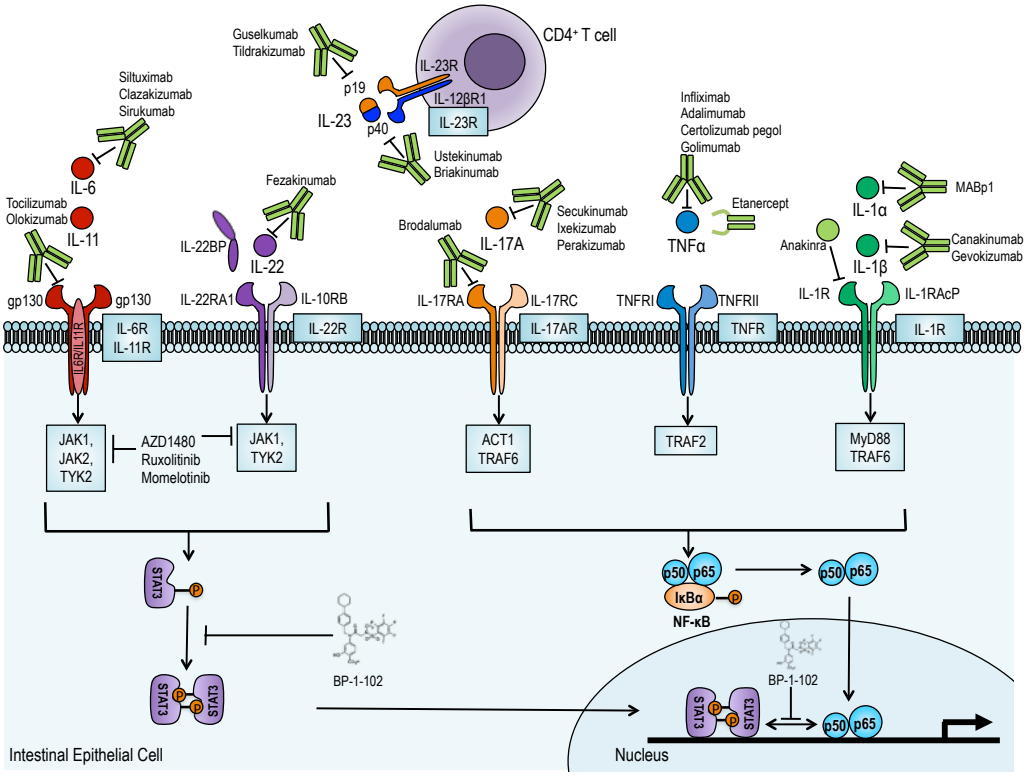


Figure 1.8 Opportunities for therapeutic intervention in cytokine signalling in CRC.

Major cytokines that can provide a directional signal from the immune system into the malignant epithelium by binding their cognate receptors expressed on intestinal epithelial cells. The cytokines highlighted here drive two critical signalling pathways: STAT3 and NF-κB. Cytokine receptor engagement results in phosphorylation of associated JAK1/2 and TYK2 molecules to activate the STAT3 pathway or activation of adaptor molecules in the NF-κB pathway culminating transcription of p50, p65 target genes. IL-23 signals into $CD4^+$ T cells and induces the production of IL-22 and IL-17A, which induce STAT3 and NF-κB respectively in epithelial cells to promote malignant progression. STAT3-NF-κB cross talk can be driven by numerous cytokines with similar biochemical functions. Numerous antibodies and soluble receptors exist to inhibit induction of cytokine signalling. Most of these drugs were developed for use in inflammatory diseases and have not been tested in CRC. Therapies which combine cytokine or cytokine-receptor-targeting antibodies and small-molecule inhibitors of downstream pathway components may prove efficacious. JAK1/2 inhibitors have shown promise in other malignancies. BP-1-102 is capable of preventing STAT3 dimerisation and STAT3-NF-κB interactions. Anakinra (IL-1β blockade) is currently in trials in advanced CRC. MABp1 (IL-1α blockade) recently showed efficacy in treatment refractory CRC. (This figure was adapted from a figure prepare by S. McCuaig for NRI)

1.6.2 Patient stratification based on interactions with oncogenes

Even still, approaches that target multiple cytokine signalling pathways simultaneously may only have efficacy in specific mutational subtypes of CRC. The evidence presented in Section 1.5 highlights that the mutational landscape can dictate the abundance of pro-tumourigenic cytokines in the milieu and whether their function is pro- or anti-tumourigenic. This knowledge has important implications for the

stratification of patients with specific oncogenic mutations to immune modulating therapies to maximise clinical benefit. For example, DNA methyltransferase inhibitors such as decitabine may have efficacy in tumours in which *SOCS3* is epigenetically silenced, by restoring negative feedback inhibition of IL-6 signalling (Gravina *et al.*, 2010; Yi Li *et al.*, 2012). Moreover, given that TNFα and IL-6 signalling is enhanced in CRC cells harbouring *TP53* mutations, perhaps etanercept (TNFα blockade) or siltuximab (IL-6 blockade) may show therapeutic efficacy if deployed specifically in patients with *TP53*-mutant tumours (Cooks *et al.*, 2013; Rokavec *et al.*, 2014). It remains to be determined whether IL-22 signalling is pathogenic in specific mutational subtypes of human CRC and how this may influence therapeutic strategies targeting this pathway.

1.7 Uncovering the role of the IL-22 pathway in human CRC

1.7.1 Primary aims

The primary aim of this thesis is to understand the cellular and molecular mechanisms by which IL-22 contributes to the development and progression of human colorectal cancer. Specifically, we seek to bring together two historically distinct perspectives on cancer to understand how oncogenic driving mutations may synergise with IL-22 signalling to promote malignancy.

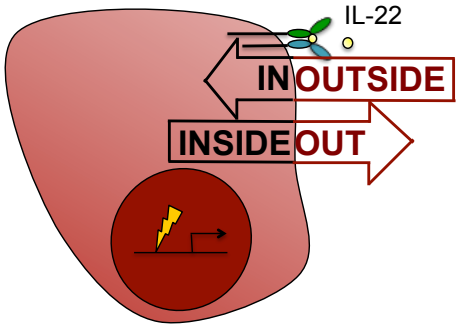


Figure 1.9 Linking an IL-22 signal from the microenvironment with oncogenic drivers.

Cytokines do not drive tumourigenesis in absence of mutations that maximize their oncogenic potential. We question how the interpretation of an IL-22 signal changes in cells harbouring specific oncogenic mutations.

1.7.2 Thesis outline

In Chapter 3, using tumour transcriptomic data from cohort studies and clinical trials totaling nearly 2000 patients, we identify a unique and prognostically important interaction between the IL-22 pathway and *KRAS* mutation. Specifically, we find that patients with high tumoural expression of the IL-22 receptor and *KRAS* mutations have dramatically worse prognosis than their *KRAS* wild type counterparts. Whether this poor prognosis is a result of a spurious association or a true biological interaction between IL-22 and *KRAS* is unclear.

Thus the primary objective in Chapter 4 is to determine whether there is a functional interaction between IL-22 and *KRAS* mutation that promotes malignant behaviour. Using a panel of colorectal cancer cell lines to recapitulate the molecular subtypes of interest, an isogenic cell line pair with matched IL-22 receptor expression differing only in the presence or absence of mutant *KRAS*, and primary tumour and matched normal organoids, we find that IL-22 promotes chemoresistance, clonogenic outgrowth, and proliferation specifically in IL-22 receptor-high, *KRAS* mutant cells. However, the precise mechanism of interaction between IL-22 and *KRAS* is not known.

Finally, in Chapter 5, we seek to identify potential mechanisms of IL-22-*KRAS* synergy using unbiased RNA-sequencing and proteomic approaches. We identify unique non-cell autonomous and cell-autonomous modalities controlled by IL-22 in *KRAS* mutant cells that may promote malignancy.

2 Materials and Methods

2.1 Prospective collection and analysis of fresh CRC and matched normal adjacent tissue

2.1.1 Patient identification and consent

Diagnosed colorectal cancer patients scheduled for colectomy at the Churchill Hospital, Oxford provided informed and written consent for research use of their resected cancer and matched normal mucosa during a pre-operative appointment under the established GI Illness Ethics through the University of Oxford Translational Gastroenterology Unit (Reference numbers: 11/YH/0020, 16/YH/0247, HTA 12217). Only the following de-identified patient clinical information was provided to investigators: tumour location, tumour stage, age, sex, and neo-adjuvant therapy. Tumour mutation status was obtained from the Oxford Molecular Diagnostics Centre. Mutational analysis was performed on FFPE tissue using massively parallel sequencing technology (Ion Torrent, PGM, ThermoFisher) that employs a targeted hotspot strategy (Ion AmpliSeq Cancer Panel, ThermoFisher). Detailed tables outlining the prospectively collected colorectal cancer tissue and corresponding clinical disease features included in this study (N=69) can found in in Appendix 4.

2.1.2 Fresh tissue collection and processing

5-7mm punch biopsies of resected tumour and 5-10cm pieces of match normal mucosa from a site distant to the tumour (clearly outside the tumour margins) were collected by pathologists at the John Radcliffe Hospital, Oxford. One $2mm^3$ piece of each tumour and matched normal tissue was preserved in RNA Later (Qiagen) and frozen for subsequent whole tissue RNA analysis. A second $2mm^3$ piece of each tumour and matched normal tissue was fixed in 4% formalin and paraffin embedded for subsequent immunohistochemical analysis. The remainder of each tumour biopsy and matched normal tissue was used for: a) whole tissue flow cytometry b) polycloncal T cell expansion c) organoid growth.

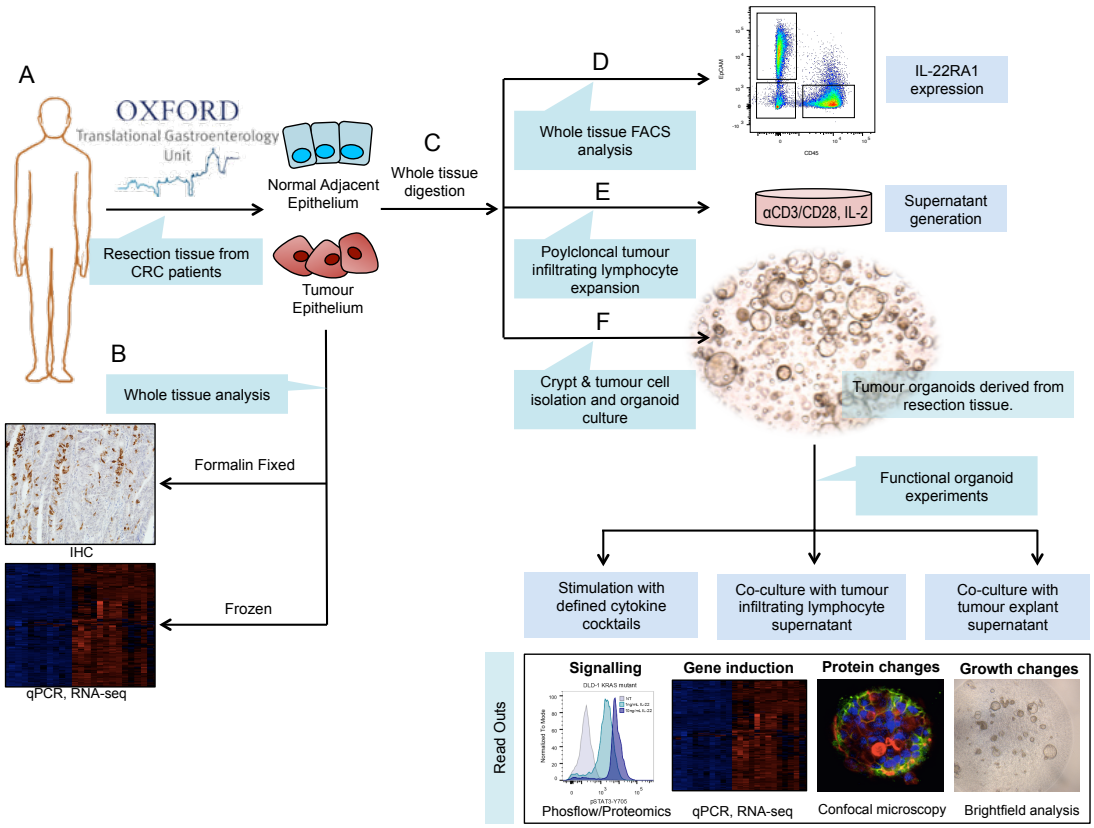


Figure 2.1 Processing of human CRC resections and matched normal adjacent tissue

(A) Tumour and matched normal adjacent tissue collected from patients undergoing colectomy at the Churchill Hospital, Oxford under GI Illness Ethics through the Translational Gastroenterology Unit.
(B) 2mm^3 piece of whole tumour and matched normal tissue were fixed in formalin for IHC analysis and frozen in RNA later for whole tissue RNA analysis.
(C) Remainder of fresh tissue was collagenase digested to generate single cell suspensions to be used for:
(D) Whole tissue flow cytometric (FACS) analysis of IL-22RA1 expression.
(E) Polyclonal T cell expansion from tumours and matched normal tissue using anti-CD3/anti-CD28 + IL-2 followed by re-stimulation and generation of T cell supernatants to use in culture with the organoids.
(F) Isolation of crypts from normal adjacent tissue and tumour cells from CRC tissue to grow organoids for banking and performing downstream functional experiments.

2.1.3 Immunohistochemical analysis of IL-22RA1 on formalin fixed, paraffin embedded (FFPE) tumour and matched normal sections

5μM FFPE sections of colorectal tumour and matched normal adjacent tissue were obtained under ethics approval from the Oxford Radcliffe Biobank and Oxford Centre for Histopathology Research (OCHRe). Antigen retrieval was performed using Dako Antigen Retrieval Solution (Dako, Agilent) and microwaving slides at full power for 15 minutes. Endogenous peroxidase activity was blocked (Avidin Biotin Blocking

Kit, Vector Laboratories) and non-specific binding of the secondary antibody was blocked using 10% normal goat serum for 1 hour at room temperature. Sections were stained with anti-human IL-22RA1 (0.27ug/mL [1:750], Atlas Antibodies; HPA042399 lot: R38731) or no primary antibody (secondary only control) (see Appendix 2.1.2) and visualized using a biotinylated goat anti-rabbit IgG secondary antibody (1:400, Vector Laboratories), detected with StrepA/B/HRP complexes (Vectastain ABC Kit, Vector Laboratories) and developed using DAB peroxidase (DAB Peroxidase (HRP) Substrate Kit, Vector Laboratories). Slides were counterstained with hematoxylin and images were acquired on an Olympus BX51 Osteometric microscope. The specificity of the IL-22RA1 antibody was determined by siRNA knockdown of *IL22RA1* in T84 CRC cells (Appendix 2.1.1).

2.1.4 Whole tissue flow cytometric analysis of IL-22RA1 expression

Tumour biopsies were minced into small pieces (<5mm) and digested in 1.5mg/mL Collagenase A (Sigma Aldrich) in RPMI with 1% Penicillin/Streptomycin (P/S) on a magnetic stirrer at 37°C. 30 minutes into the incubation, an 18G needle was used to homogenise the tissue and the tissue was digested for an additional 30 minutes. Digested tissue was then passed sequentially through an 18G needle, 21G needle, and 70uM mesh filter to generate a single cell suspension. Cells were spun (500g, 8 minutes) and washed in 1X HBSS with 1% P/S. ACK was added to the cell pellet to lyse red blood cells. Cells were washed and re-suspended in RPMI with 10% FBS, 1% P/S and incubated at 37°C in 5% CO_2 for 30 minutes to regenerate any receptors cleaved by collagenase. Cells were spun (500g, 8 minutes), washed in 1X HBSS, and re-suspended in FACS buffer (1X PBS + 0.5% BSA + 2mM EDTA). 2/3 of cells were used for full staining and 1/3 of cells were used for isotype staining. Cells were stained with the following antibody combinations (Table 2.1) in 96 well, round

bottom plates in 100uL of FACS buffer at 37°C, 5% CO_2 for 20 minutes. Stained cells were spun (500g, 8 minutes) and washed in FACS buffer 2X. After washing, cells were fixed in 100uL Fix/Lyse Solution (BD) and incubated at room temperature for 15 minutes. Fixed cells were spun (500g, 8 minutes) and washed in FACS buffer 2X. Washed cells were re-suspended in 200uL FACS buffer and flow cytometric analysis was performed on a BD LSR Fortessa X-20 following compensation. Data analysis was performed using FlowJo 10 software. Gating strategies for assessment of IL-22RA1 expression are outlined in Figure 2.2. The specificity of the IL-22RA1 antibody was determined by siRNA knockdown of *IL22RA1* in T84 CRC cells (Appendix 2.1.1).

Target Molecule	Fluorophore	Dilution	Company	Clone
Full Staining Panel				
IL-22RA1	PE	1:10	R&D	305405
EpCAM (CD326)	FITC	1:100	Biolegend	9C4
CD45	AF700	1:100	Biolegend	HI30
Live/Dead (fixable viability dye)	APC Cy7	1:1000	eBioscience	N/A
Isotype Control Panel				
Mouse IgG1, k	PE	1:10	R&D	11711
Mouse IgG2b, k	FITC	1:100	Biolegend	MPC-11
CD45	AF700	1:100	Biolegend	HI30
Live/Dead (fixable viability dye)	APC Cy7	1:1000	eBioscience	N/A

Table 2.1 IL-22RA1 whole tissue staining panel

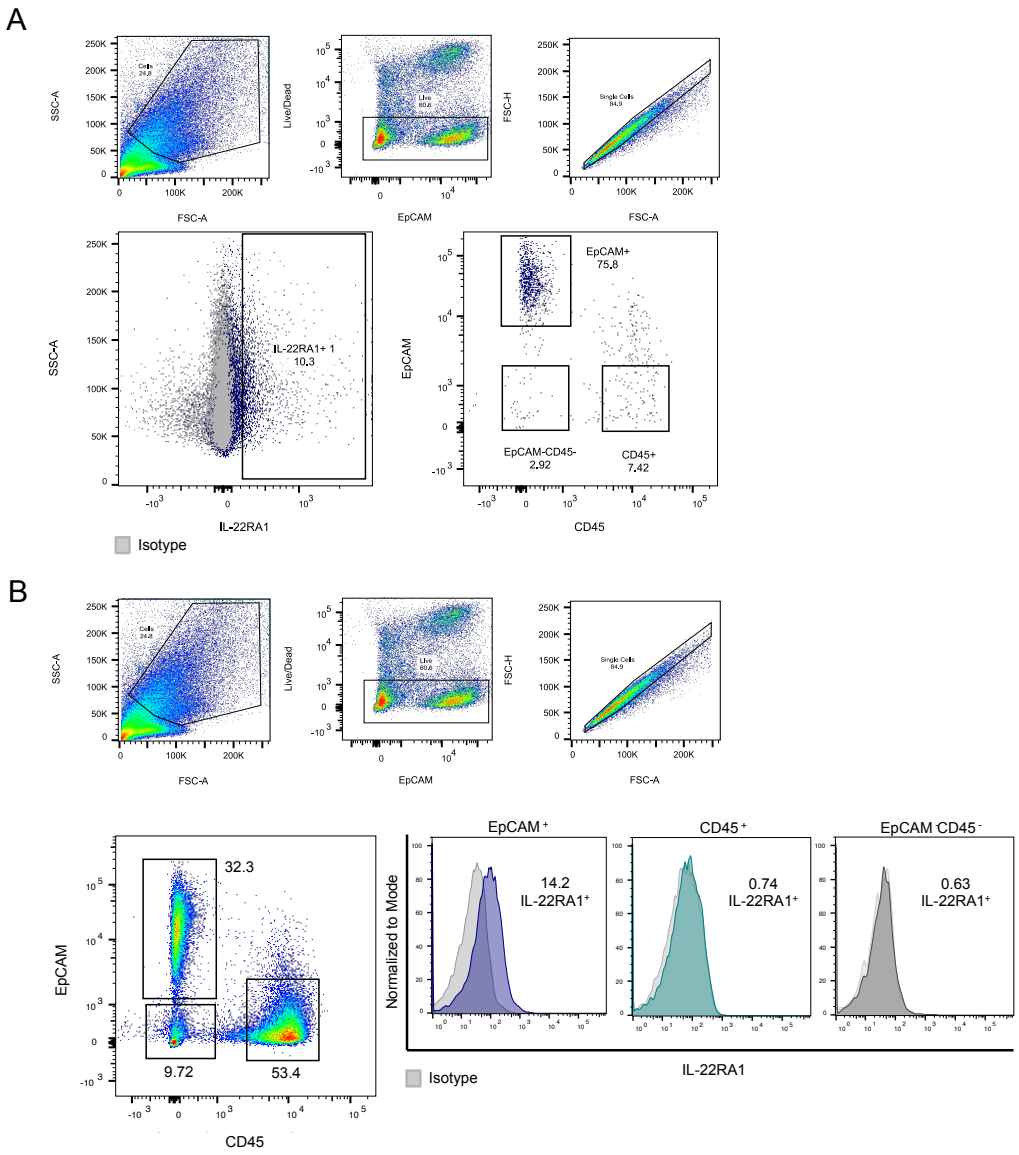


Figure 2.2 Gating strategies for assessment of IL-22RA1 cell surface expression in whole fresh tumour specimens by flow cytometry.

Two different gating strategies were employed to assess IL-22RA1 expression in whole digested tumour biopsies.

(A) To determine the relative proportion of epithelial ($EpCAM^+$), immune ($CD45^+$), and stromal ($EpCAM^-CD45^-$) cells in the total $IL\text{-}22RA1^+$ population, live, single cells were gated and $IL\text{-}22RA1^+$ cells were selected based on comparison to the matched isotype control. The entire $IL\text{-}22RA1^+$ population was then gated based on EpCAM and CD45 to identify epithelial, immune, and stromal $IL\text{-}22RA1^+$ cells.

(B) To determine the amount of surface IL-22RA1 expression in each individual cell population, live, single cells were first gated on cell lineage markers EpCAM and CD45. The proportion of $IL\text{-}22RA1^+$ cells in each cell population ($EpCAM^+$, $CD45^+$, $EpCAM^-CD45^-$) was then determined based on comparison to the matched isotype control.

2.1.5 Whole tissue RNA extraction and qPCR analysis

Fresh 2mm^3 tumour biopsies and matched normal adjacent mucosa were frozen in RNA Later (Qiagen) at -20°C immediately following tissue collection. On the day of RNA extraction, samples were thawed on ice, RNA Later was removed and 650uL of RLT Buffer (Qiagen) with β-mercaptoethanol (Sigma) was added to each sample and samples were transferred to Soft Tissue Homogenizing CK14 Kit vials (Stretton Scientific). Tissue was homogenised in the Precellys 24 (Bertin Instruments) homogeniser (30s at 3500 RPM). 650uL of 70% ethanol was added to homogenised tissue lysates and lysates were transferred to Qiagen RNeasy Minikit columns (Qiagen) for RNA extraction according to the manufacturers protocol. An on-column DNase digestion was performed for each sample using an RNAse Free DNAse Kit (Qiagen). Samples were eluted from columns in 30uL RNAse free; DNAse free H_2O and RNA concentrations and 260/280 ratios were determined on a NanoDrop 1000 (Thermo Fisher). cDNA was synthesised from 500ng RNA for each sample using the High Capacity cDNA Kit (Applied Biosciences) according to the manufacturers protocol using a C1000 Touch^{TM} Thermal Cycler (Biorad). The remaining RNA was frozen at -80°C for long-term storage. Synthesised cDNA was diluted 1:5 with RNAse free; DNAse free H_2O and used for qPCR analysis. qPCR analysis was performed using TaqMan Real-Time PCR assays (a full list of probes used in this thesis can be found in Appendix 2.4) and Precision Fast qPCR Mastermix with ROX at a lower level, with inert blue dye (PrimerDesign) in 384 well plates (FrameStar; clear wells). qPCR reactions were prepared as follows (Table 2.2):

Reagent	Volume per rxn (uL)
1:5 diluted cDNA	2
Precision Fast qPCR Master Mix	3
TaqMan Real Time PCR Assay	0.2
RNAse Free DNAse Free H2O	0.8
Total Volume	6

Table 2.2 qPCR Reaction Mix

Plates were sealed with MicroAmp ® Optical Adhesive Film (Life Technologies). Loaded, sealed plates were run on the ViiA7 Real-Time PCR System (Applied Biosystems) using the fast run method (Table 2.3).

Stage	Step	Ramp Rate	Temperature	Time
Hold Stage	1	1.9°C/s	95°C	2 minutes
PCR Stage	1	1.9°C/s	95°C	5 seconds
Number of Cycles: 40	2	1.6°C/s	60°C	20 seconds

Table 2.3 qPCR thermal profile, fast run method

Data was analysed using the ΔC_T method [$2^{-\Delta CT}$ where $\Delta C_T = C_{T(\text{target gene})} - C_{T(\text{endogenous control})}$]. Large ribosomal protein (human *RPLPO*) was used as the endogenous control for all qPCR analyses in this thesis.

2.1.6 Polyclonal T cell expansion from tumour and matched normal adjacent tissue

2.1.6.1 T cell isolation and expansion

After collecting pieces of the tumour biopsy and normal adjacent tissue for whole tissue RNA and IHC analysis, the remaining tumour biopsy (3-5mm^3) and a similar sized piece of matched normal adjacent mucosa were minced into small pieces and digested in collagenase as described in detail in 2.3.2. In the case of the tumour biopsy, 60% of the digested sample was allocated for T cell expansion and the remaining 30% of the sample was used to seed organoids as described in 2.3.2.

Lymphocytes were isolated by re-suspending cells in 1.5mL warm DMEM and layering on top of 1.5mL of room temperature Lymphoprep™ (STEMCELL Technologies) in a 5mL FACS tube. The mini gradient was centrifuged (900g, 25 minutes) at room temperature with the break off. The buffy coat at the interface was collected, washed, re-suspended and counted by Trypan Blue exclusion. Cells were seeded at a ratio of 10:1 with Gibco™ Dynabeads™ Human T-Activator CD3/CD28 (Fisher Scientific) in media containing 300 units/mL recombinant human IL-2 (Peprotech), 5% human serum, 1X Glutamax (Invitrogen), 1X Primocin (Invitrogen), and 0.1% β-mercaptoethanol. $5x10^5$-$1x10^6$ cells (depending on size of specimen) were plated in 500µL media per well in 48 well plates. Cells were expanded for 11-20 days and were sequentially transferred to 24-well, 12-well, and 6-well plates, as cells grew confluent. Fresh media was added at each step. 100µL of expanded T cells were used for RNA extraction and qPCR analysis (following the methodology described in 2.1.5).

2.1.6.2 Basic flow cytometric analysis

300µL of T cells confluent in 6 well plates following expansion were removed from each culture for flow cytometric analysis. 100µL of each sample was used for basic surface staining; the remaining 200µL was used for intracellular staining. T cells were re-stimulated in 10ng/mL phorbol 12-myristate 13-acetate (PMA) (Cayman Chemical) and 1µg/mL ionomycin (Sigma) for 30 minutes at 37°C, 5% CO_2. After 30 minutes 1X BD Golgi Plug (BD) was added and cells were incubated for an additional 2.5 hours. Cells were then washed in FACS buffer and plated in 96 well round bottom plates for staining. Cells were first stained for surface markers for 15 minutes at 4°C using the staining panel outlined in Table 2.4. Cells were then washed 2X in FACS buffer and fixed for 20 minutes at room temperature in 100µL/well 1X

BD Cell Fix (BD). After washing, cells were centrifuged in 200µL 0.05% Saponin (500g, 6 minutes) to permeabilise. Intracellular staining was conducted at 4°C for 40 minutes in 0.05% Saponin using the staining panel outlined in Table 2.4. Cells were washed once in Saponin and re-suspended in 200µL FACS buffer for acquisition. Cells reserved for basic surface staining were stained for the surface markers outlined in Table 2.5 for 15 minutes at 4°C. Cells were washed, fixed in 1X BD Cell Fix (BD) for 20 minutes at room temperature, washed again and re-suspended in 200µL FACS buffer for acquisition. Flow cytometric analysis was performed on a BD LSR Fortessa X-20 following compensation, by acquiring 30,000 cells of each condition. Data analysis was performed using FlowJo 10 software.

Target Molecule	Fluorophore	Dilution	Company	Clone
Surface Markers				
CD3	BV510	1:200	Biolegend	OKT3
CD4	PE-TxR	1:300	Biolegend	RPA-T4
CD8a	AF700	1:200	eBioscience	OKT8
Live/Dead (fixable viability dye)	APC-Cy7	1:1000	eBioscience	N/A
Intracellular Molecules				
IFNg	FITC	1:200	Biolegend	45.B3
IL-5	PE	1:100	Biolegend	JES1-39010
IL-17F	PerCP Cy5.5	1:150	BD	033-782
IL-17A	BV711	1:300	Biolegend	BL168
IL-22	PE-Cy7	1:300	eBioscience	22URTI
IL-10	Pac Blue	1:150	Biolegend	JES3-907
IL-2	BV650	1:100	Biolegend	MQI-I7H12
GM-CSF	APC	1:300	Biolegend	BVD2-21C11
TNFa	BV605	1:200	Biolegend	MAb11

Table 2.4 Intracellular T cell staining panel

Target Molecule	Fluorophore	Dilution	Company	Clone
Surface Markers				
CD45RA	BV510	1:100	Biolegend	HI100
CD14	BV650	1:100	Biolegend	M5E2
CD16	BV605	1:100	Biolegend	3G8
CD56	BV711	1:75	Biolegend	HCD56
HLADR	PerCp Cy5.5	1:75	Biolegend	L243
CD19	AF488	1:100	Biolegend	HIB19
CD3	PE-TxR	1:100	Biolegend	UCHT1
CD4	PE-Cy7	1:200	Biolegend	OKT4
CD45	AF700	1:100	Biolegend	HI30
CD25	PE	1:100	Biolegend	BC96
Live/Dead (fixable viability dye)	APC-Cy7	1:1000	eBioscience	N/A

Table 2.5 T cell surface staining panel

2.1.6.3 MACS enrichment for $CD4^+$ cells

The remaining expanded T cells were re-suspended in FACS buffer at a density of 10^7 cells per 90µL with 10µL Human CD4 Micro Beads (Miltenyi). Cells were incubated with the microbeads for 15 minutes at 4°C on a vertical rotor, then washed and run on the positive selection function (Possel) on an autoMACs® Pro Separator (Miltenyi). The negative fraction was run through the autoMACS® a second time using the DEPLETES function to increase $CD4^+$ cell yield. The purity of the final pooled $CD4^+$ cells was checked by flow cytometry.

2.1.6.4 Generation of T cell supernatants

Sorted cells were counted and cells were plated at a density of $1x10^6$ cells/mL in 24 well plates with 2mL per well in RPMI with 10% FBS, 1% P/S, and 10ng/mL PMA/1µg/mL ionomycin (PMA/iono). Cells were re-stimulated for 24 hours. Cells were then centrifuged (500g, 8 minutes), the pellet was kept for RNA analysis, and the supernatant was filtered and frozen for use in stimulation experiments with cell lines and organoids. A vehicle control supernatant was generated by incubating RMPI with 10% FBS, 1% P/S and 10ng/mL PMA/1µg/mL ionomycin for 24 hours.

2.2 Colorectal cancer cell line culture and experimentation

2.2.1 Source and maintenance culture of cell lines used

Colo205, SW948, SW480, HCT116, T84, and DLD-1 (ATCC) colorectal cancer cell lines were a generous gift from Dr. Simon Leedham and were confirmed to be mycoplasma free. A mutational analysis on the cell lines was conducted in the labs of Professor Ian Tomlinson and Dr. Simon Leedham (Table 2.6). The DLD-1 isogenic pair was purchased from Horizon Discovery Group (Parental Line (KRAS G13D): HD PAR-111 Passage 4; Wild type reverted line (KRAS+/-): HD 105-040 Passage 4) (see Appendix 2.5 for detailed description). Due to drift of the wild type reverted line (KRAS +/-) with successive passages, experiments with the isogenic pair were performed with the cells between passages 4-9. *KRAS* mutation status in the isogenic pair was confirmed in house using the qBiomarker^{TM} Somatic Mutation PCR Array Human KRAS Gene (Qiagen, Plate E Format, SMH-806ARE-12 337021) (See Section 2.3.4).

Cell line	COLO205	SW948	SW480	HCT116	T84	DLD1
Age	70	81	50		72	
Sex	M	F	M	M	M	M
Stage	D	C	B		C2	C
Grade		3				
Site	Colon- Ascites	Colon	Colon	Colon	Colon	Colon
Karyotype	Hypertriploid (78)	Hypotriploid (67)	Hypotriploid (57)	Near-diploid (45)	Hyperdiploid (56)	Near-diploid (46)
MSI	-	-	-	+	-	+
APC mutn 1	1554 ins1bp	1114 CGA->TGA	1338 CAG->TAG	None found	1488 del1bp	1417 del1bp
APC mutn 2	L	1430 CAA->TAA	L	None found	L	L
APC	205kD	160kD	170kD	Normal product	Not done	170kD
APC	Truncated 15E-J	Truncated 15E-J	Truncated 15E-J	None found	Truncated 15E-J?	Truncated 15E-F
Beta-catenin	A->G Asn287Ser x6	None found	None found	Del codon 45 x3	None found	None found
K-ras	None found	None found	GTT/GTT c12	GGC/GAC c13	GGC/GAC c13	GGT/TGT c12
p53	CODON 103/DEL 27		Arg273His	No (but E7 by DB)	E5/6, E7	Ser241Phe
p53	232		1343		819	705
p53	L	L	L	NL	Not done	NL
SMAD4	Del ex1-ex4	g1609t	5th base intron 7, g->c	None found		None found
SMAD4	No protein	D537Y	Splice disruption			
Loss 18q	yes	yes	yes	no		no

Table 2.6 Colorectal cancer cell line characteristics

Colo205 and DLD-1 cells were cultured in RPMI (Sigma) with 10% FBS, 1% P/S (Sigma). SW948, SW480, and HCT116 cells were cultured in DMEM (Sigma) with 10% FBS, 1% P/S. T84 cells were cultured in DMEM F12 Hams (DMEM Nutrient Mix F-12, D8437, Sigma) with 5% FBS, 1% P/S. Cultures were maintained in 37°C, 5% CO_2.

2.2.2 Flow cytometric analysis of IL-22RA1 expression

Adherent cells (unstimulated or stimulated) were dissociated using TrypLE (Life Technologies), filtered through 70uM filters, and counted by Trypan Blue exclusion. $2x10^5$ cells were stained using the panels for full staining and isotype control staining described in Table 2.1, though CD45 was omitted. Cells were stained for 30 minutes at room temperature, washed, fixed in 100uL Fix/Lyse Solution (BD), washed and re-suspended in 200uL FACS buffer, as described in 2.1.4. Flow cytometric analysis was performed on a BD LSR Fortessa X-20. Data analysis was performed using FlowJo 10 software.

2.2.3 Basic cytokine stimulation experiments

Cells were plated in 400µL of cell line-specific media (described in 2.2.1) at $3x10^4$ cells per well in 48 well plates and cultured overnight. Cytokines (recombinant human IL-22 [R&D Systems] and recombinant human IL-6 [Peprotech]) were prepared in cell line-specific media and 100uL of the appropriate cytokine was added to each well to achieve the following final concentrations: 1ng/mL IL-22, 10ng/mL IL-22, 1ng/mL IL-6, 10ng/mL IL-6. Triplicate wells of each condition wells were prepared. Cells were stimulated for the time indicated, media was aspirated from wells and plates were frozen in -80°C for subsequent RNA or protein extraction. Note that all cytokine stimulation experiments in the DLD-1 isogenic pair were performed in serum free

conditions with 1X ITS (Insulin, Transferrin, Selenium) (Sigma). Survival assays confirmed equal viability in both lines in serum free media with 1X ITS.

2.2.4 T cell supernatant stimulation experiments

DLD-1 isogenic cells were plated at a density of $3x10^4$ cells per well in 48 well plates and cultured overnight in 200µL serum free RPMI with 1X ITS (Sigma). In order to determine the appropriate concentration of T cell supernatant to use for stimulation, dose response stimulations were conducted (see Appendix 2.2 for results) and determined that when used at 1:100, supernatants both elicited gene expression changes and did not significantly alter cell viability (Appendix 2.2) . Therefore downstream experiments were conducted with T cell supernatants at 1:100 in the presence or absence of blocking antibodies against IL-22, IFNγ, TNFα, or matched isotype control (Table 2.7) (Table of stimulation conditions: Table 2.8). T cell stimuli (± blocking antibody) solutions were prepared in 25µL serum free RPMI with 1X ITS (Sigma) and added to the existing 200µL media in each well. Note that the vehicle control for all of the stimulations conditions that did not contain T cell supernatant was PMA/ionomycin control conditioned media, generated as described in 2.1.6 used at the same dilution as the corresponding T cell conditioned media. A 10ng/mL IL-22 condition was used as a control to both ensure that gene expression responses to IL-22 were as expected and that IL-22 blockade was efficacious. Stimulations were conducted for 24 hours. In this thesis, data is presented using a candidate $CD4^+$ tumour-infiltrating leukocyte (TIL) (0108756) supernatant and matched normal adjacent $CD4^+$ leukocyte (0108755) supernatant. Experiments were repeated on four independent days with successive DLD-1 cell passages (5-8). RNA was subsequently extracted, cDNA synthesized and qPCR performed as described in 2.2.5. Gene

expression was normalized to the vehicle control (PMA/Iono) no treatment condition for each gene and each cell line.

Blocking antibody	Stock Concentration	Dilution used	Company	Clone
anti-human IL-22	1mg/mL	1:1000	eBioscience	IL22JOP
anti-human IFNg	1mg/mL	1:100	eBioscience	NIB42
Infliximab (anti-human TNFa)	50mg/mL	1:5000	Janssen	--
Isotype: Total Rat IgG	2mg/mL	Matched to target Ab	Sigma	--

Table 2.7 Cytokine blocking antibodies and isotype controls

Stimulation Conditions
No treatment + vehicle
10ng/mL IL-22 + vehicle + isotype
10ng/mL IL-22 + vehicle + anti-IL-22
CD4+ TIL (1:100) + iso
CD4+ TIL (1:100) + aIL-22
CD4+ TIL (1:100) + aIFNg
CD4+ TIL (1:100) + aTNFa
CD4+ TIL (1:100) + aIL-22 + aIFNg
CD4+ TIL (1:100) + aIL-22 + aTNFa
CD4+ TIL (1:100) + aIL-22 + aIFNg + aTNFa
CD4+ norm (1:100) + iso
CD4+ norm (1:100) + aIL-22
CD4+ norm (1:100) + aIFNg
CD4+ norm (1:100) + aTNFa
CD4+ norm (1:100) + aIL-22 + aIFNg
CD4+ norm (1:100) + aIL-22 + aTNFa
CD4+ norm (1:100) + aIL-22 + aIFNg + aTNFa

*TIL - tumour infiltrating lymphocyte derived supernatant
*Norm - normal adjacent T cell derived supernatant

Table 2.8 T cell supernatant stimulation conditions

2.2.5 RNA extraction and qPCR

RNA was extracted from cultured monolayers of CRC lines using the Qiagen RNeasy Mini Kit (Qiagen) according to the manufacturers protocol. cDNA was synthesised using 10uL of the eluted RNA following the protocol as in 2.1.5. Finally, qPCR was performed as in 2.1.5. A full list of Taqman probes used in this thesis can be found in Appendix 2.4).

2.2.6 Immunoblotting

Protein was extracted from adherent CRC cell monolayers using a solution of 50mM Tris pH 6.8, 20mM EDTA, 5% SDS, 1mM DTT, 10% glycerol. 15-20µg of protein was loaded into pre-cast NuPAGE ® Novex 4-12% Bis-Tris Gels (Life

Technologies), separated by SDS-PAGE and transferred onto PVDF membranes using a wet transfer apparatus. Note that for HRP-based detection Hybond PVDF (Amersham) was used and for Li-COR-based detection Immobilon-FL PVDF (Millipore) was used. Non-specific background binding was blocked with 5% Skim Milk in Tris-HCl buffer containing 0.05% Tween-20 (TBST) (for HRP detection) or Odyssey ® Blocking Buffer (TBS) (Li-COR) (for Li-COR detection). Membranes were incubated with primary antibody (Table 2.9) in 2.5% BSA/TBST (for HRP detection) or Odyssey ® Blocking Buffer with 0.2% Tween-20 (for Li-COR detection) overnight at 4°C. Membranes were washed in TBST and incubated with HRP-conjugated secondary antibody (for HRP detection) or fluorescently conjugated secondary antibody (for Li-COR detection) for 1 hour at room temperature (Table 2.9). Membranes were washed in TBST and protein expression was detected using Pierce ECL Plus (Thermo Scientific) (for HRP detection) or the Odyssey CLx detection system (for Li-COR detection). Target protein was quantified on blots performed using the Li-COR system by normalizing target protein fluorescence intensity to the fluorescence intensity of simultaneously stained β-actin for each sample.

Target Molecule	Fluorophore	Dilution	Company	Clone
Primary Antibodies				
pSTAT3(Y705)	N/A	1:1000	Cell Signaling	D3A7
pSTAT3(S727)	N/A	1:1000	Cell Signaling	9134P
pAKT(S473)	N/A	1:1000	Cell Signaling	D9E
pERK1/2 (T202/Y204)	N/A	1:1000	Cell Signaling	9101
Total ERK1/2	N/A	1:1000	Cell Signaling	9102
Total STAT3	N/A	1:1000	Cell Signaling	79D7
Total c-MYC	N/A	1:1000	Cell Signaling	D84C12
p-c-MYC(S62)	N/A	1:1000	Cell Signaling	E1J4K
p-c-MYC(T58)	N/A	1:200	Santa Cruz	sc-139600
β actin (produced in mouse)	N/A	1:4000	Sigma	AC-74
Secondary Antibodies				
Goat anti-rabbit-HRP	N/A	1:1000	Cell Signaling	7074
Goat anti-mouse-HRP	N/A	1:2000	Millipore	AP308P
Goat anti-rabbit-800CW	800CW	1:15,000	LiCOR	925-32211
Goat anti-mouse-680RD	680RD	1:15,000	LiCOR	925-68070

Table 2.9 Western blot primary and secondary antibodies

2.2.7 Phosflow

DLD-1 isogenic cells were seeded at a density of $1x10^6$ cells per well in serum free RPMI containing 1X ITS (Sigma) in 6 well plates and allowed to adhere overnight. Cells were then stimulated in technical duplicates with 0-100ng/mL IL-22 (R&D Systems) (10-fold dilution series) for 30 minutes at 37°C, 5% CO_2. Following stimulation, supernatant was aspirated, cells were liberated from the plate using TrypLE (Life Technologies), the contents of each well were transferred to separate 5mL FACS tubes, and pelleted (500g, 4°C, 5 minutes). Cell pellets were re-suspended in 200µL pre-warmed Cytofix (BD) and fixed for 10 minutes at 37°C. Following fixation, cells were washed with FACS buffer and the contents of each FACS tube was transferred to 4 separate wells of a 96 well, round bottom plate to stain for each molecule of interest. Cells were pelleted in the plate (500g, 4°C, 5 minutes). Permeabilisation was performed by adding 200µL of ice-cold Perm III Buffer (BD) to each well and incubating for 30 minutes on ice. Cells were washed 3X in FACS buffer and were stained with fluorescently conjugated antibodies to phosphorylated residues on intracellular signalling proteins of interest (Table 2.10). Staining was

conducted for 1 hour at room temperature, protected from light. Cells were then washed 2X and re-suspended in 200µL FACS buffer. Flow cytometric analysis was performed on a BD LSR Fortessa X-20 by acquiring 10,000 cells of each condition. Data analysis was performed using FlowJo 10 software. The amount of phosphorylation of a given intracellular signalling protein was determined by comparing the geometric mean fluorescence intensity of the corresponding fluorophore in stimulated cells to that of the untreated control cells or for markers displaying a bimodal distribution (e.g. pS6), the frequency of positive events in the stimulated versus unstimulated condition.

Target Molecule	Fluorophore	Dilution	Company	Clone
anti-STAT3 (pY705)	AF-647	1:10	BD	4
anti-ERK1/2 (pT202/pY204)	AF-647	1:10	BD	20A (RUO)
anti-AKT (pS473)	AF-647	1:10	BD	M89-61
anti-S6 (pS235/236)	AF-488	1:10	BD	N7-548

*Note cells were stained in a total volume of 25uL in 96 well round bottom plates.

Table 2.10 Phosflow ® antibodies

For experiments where Rapamycin was used to determine the dependency of ribosomal protein S6 phosphorylation on mTOR signalling, DLD-1 *KRAS* mutant cells were plated as described above. Cells were stimulated with 100nM Rapamycin (Sigma) ± 10ng/mL IL-22 for 30 minutes. Fixation, permeabilisation, intracellular staining, and flow cytometry was conducted as described above.

2.2.8 Chemoresistance assays

Colo205, SW480, T84, and DLD-1 cells were seeded at a density of $1x10^4$ cells per well in 48 well plates in cell line-specific media and left to adhere overnight. Note that chemoresistance assays on the DLD-1 isogenic pair were conducted in serum free RPMI with 1X ITS. Cells were pretreated for 48 hours with 10ng/mL IL-22 (R&D Systems), then subjected to 5-fluorouracil (5µM-1000µM) (Sigma) or vehicle control (DMSO) for an additional 48 hours. 50µg of methylthiazolyldiphenyl-tetrazolium

bromide (MTT) (Sigma) was added to each well 2 hours prior to the end of the incubation. At the end of the 48-hour incubation, supernatants were aspirated and formazan particles were solubilized with DMSO and transferred to a flat bottom 96 well plate (Costar). Absorbance was measured at 570nm on a BMG SPECTROstar NANO Microplate Reader (BMG Labtech).

2.2.9 Clonogenic outgrowth assays

Colo205, SW480, T84, and DLD-1 cells were pretreated for 48 hours in 24 wells plates with 10ng/mL IL-22. Cells were trypsinized, filtered to single cells using a 70μM filter, and 1000 cells/well were seeded into 96 well low-binding plates (Corning) in 1% methylcellulose in IMDM (R&D Systems), 20ng/mL recombinant EGF (Sigma), 20ng/mL basic FGF (Peprotech), 1X ITS (Sigma) in serum free DMEM/RPMI. 10ng/mL IL-22 was also added in continuous stimulation conditions. 3-4 replicate wells of each condition were seeded for each independent assay. Cells were incubated for 7 days in 37°C, 5% CO_2. Bright-field microscopic images were taken of each well at 4X magnification and spheres were measured and enumerated using the Edge Detection and Analyze Particle functions on ImageJ (Figure 2.3). Spheres with 2-dimensional perimeters under 500μM were excluded from the analysis. For RNA analysis of spheres, spheres from technical replicate wells were pooled, methylcellulose was dissolved by re-suspending in PBS, spheres were pelleted and lysed in RLT Buffer (Qiagen) containing β-mercaptoethanol. RNA extraction, cDNA synthesis, and qPCR was performed as described in 2.2.5.

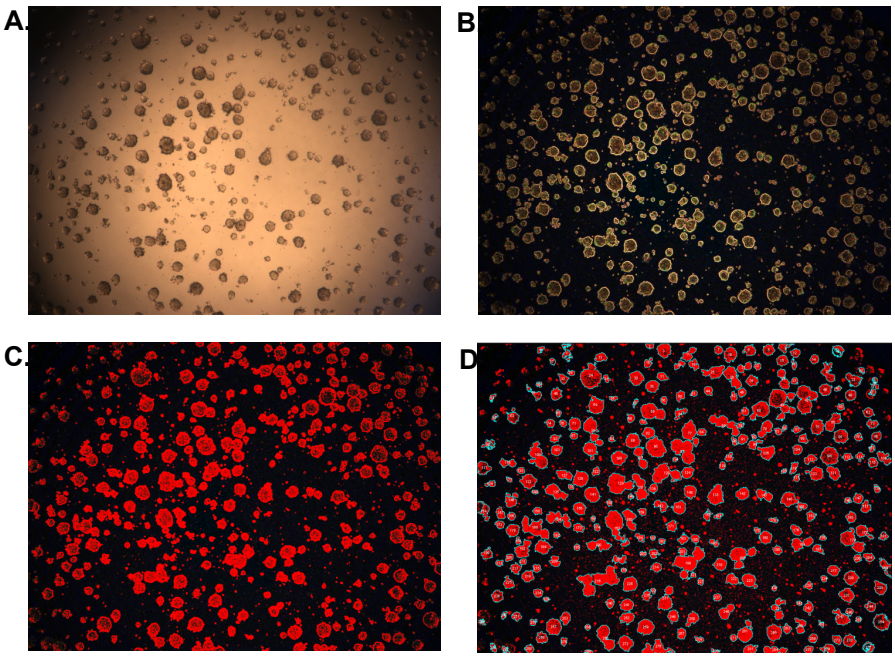


Figure 2.3 ImageJ sphere measurement and enumeration methodology.

(A) Brightfield images of each well were taken at 4X magnification.
(B) Spheres were detected in ImageJ using the "Find Edges" function.
(C) The colour threshold was adjusted to 40.
(D) The "Analyse Particle" function was used to measure the sphere perimeter.

2.2.10 Proliferation assays

DLD-1 isogenic cells were seeded at a density of $1x10^4$ cells per well in 48 well plates in serum free RPMI with 1X ITS (Sigma) and allowed to adhere overnight. Cells were stimulated with 10ng/mL IL-22 for 96 hours. Cellular viability/proliferation was measured by adding 50µg of MTT to each well 2 hours prior to the end of the IL-22 incubation. At the end of the 96-hour incubation, supernatants were aspirated, formazan particles were solubilized with DMSO and transferred to a flat bottom 96 well plate (Costar). Absorbance was measured at 570nm on a BMG SPECTROstar NANO Microplate Reader (BMG Labtech). The ratio of the OD_{570} with IL-22 compared to the no treatment condition was used to assess viability in the DLD-1 isogenic pair.

2.2.11 siRNA knockdown experiments

DLD-1 isogenic cells were seeded at a density of $3x10^4$ cells per well in 48 well plates in serum free RPMI with 1X ITS (Sigma) and allowed to adhere overnight. 5nmol siRNA (Table 2.11) was diluted in 250µL 1X siRNA Diluent Buffer (Dharmafect) for a 20µM working stock. The optimal siRNA transfection dose was determined for each siRNA by performing titration experiments with 10nM, 20nM, and 40nM siRNA. siRNA was incubated with DharmaFect 2 (Dharmacon) in Opti-MEM (Thermo Fisher) for 20 minutes prior to transfection to allow complex formation. Cells were transfected with 0.8µL DharmaFect 2 and the appropriate siRNA concentration (si*MYC* 40nM, si*STAT3* 20nM) per well. Note that the cells were also transfected with control siRNA (Table 2.11) at the concentration corresponding to that of the target gene siRNA. Cells were transfected for 48 hours at which point RNA and protein were extracted to determine efficiency of knockdown. Media was replaced with serum free RPMI with 1X ITS (Sigma) and the appropriate stimulus was added. For survival assays conducted following *MYC* knockdown, cells were stimulated with 10ng/mL IL-22 for 48 hours following knockdown. Supernatants were collected for Lactate Assays (described in 2.2.12) and cells were incubated with MTT 2 hours prior to the end of the incubation to assay for survival as described in 2.2.10. For gene and protein induction assays conducted following *STAT3* knockdown, cells were stimulated with 10ng/mL IL-22 for 24 hours following knockdown. qPCR and Western Blot analyses of the appropriate target genes and proteins was subsequently conducted.

Target Molecule	Concentration	Company	Reference
Target gene siRNA			
ON-TARGET Plus Human MYC SMARTpool	40nM	Dharmacon	4609
ON-TARGET Plus Human STAT3 SMARTpool	20nM	Dharmacon	6774
Control siRNA			
ON-TARGET Plus control pool	40nM or 20nM	Dharmacon	001810-10

Table 2.11 Target and control siRNA.

2.2.12 Lactate Assays

Lactate assays were performed using a Lactate Assay Kit (Sigma, MAK064) according to the manufacturer's instructions. Briefly, supernatants collected from *MYC* siRNA knockdown experiments were centrifuged (13,000g, 10 minutes, 4°C) to remove insoluble debris. Samples were diluted 1:50 and 25µL of each diluted sample was further diluted in 25µL Lactate Assay Buffer (Sigma) and loaded into 96 well flat bottom plates (Costar). A standard curve was prepared according to the manufacturer's instructions (0-10nM). 50µL of master mix containing Lactate Enzyme Mix (Sigma) and Lactate Probe (Sigma) was added to each well, and the plate was incubated for 30 minutes at room temperature protected from light. Absorbance was measured at 570nm on a BMG SPECTROstar NANO Microplate Reader (BMG Labtech). Lactate concentration was determined by interpolating from the standard curve.

2.3 Primary human CRC and normal adjacent colon tissue organoid culture and experimentation

2.3.1 Crypt isolation and culture of normal human colonic organoids

Note: The protocols in this section were adapted from human normal colonic organoid culture protocols generously provided by Marc van de Wetering (Hubrecht Institute, Netherlands).

Muscle and fat tissue was removed from normal adjacent colon resections to isolate the mucosa. A $2cm^2$ piece was cut into smaller 2-$3mm^2$ pieces and submerged in

15mL freshly prepared 1X Complete Chelating Solution (CCS) (Table 2.12). Mucosal pieces were shaken vigorously by hand in 1X CCS, the pieces were allowed to settle by gravity, the supernatant was removed and this wash process was repeated 2X. 500uL 0.5M EDTA was added to 50mL 1X CCS with DTT for longer wash steps. Mucosal pieces were shaken at 4°C in EDTA/CCS/DTT for 45 minutes, vortexed for 30 seconds and the supernatant was discarded. This step was repeated, but the supernatant containing crypts was collected and kept on ice. 15mL of ADF^{+++} was added to the mucosal pieces, vortexed for 30 seconds, the supernatant was collected on ice and combined with the existing crypts. This process was repeated until crypts were no longer liberated from the mucosal tissue (1-2 more washes). The collected supernatants were centrifuged (700 RPM, 4°C, 3 minutes). Crypts pellets were gently re-suspended in 10mL Advanced DMEM/F-12 (Life Technologies) with 1x Glutamax (Invitrogen), 10mM HEPES (Sigma), 1% Pen/Strep (Sigma) [herein referred to as ADF^{+++}], and centrifuged (700 RPM, 4°C, 3 minutes) to wash. This process was repeated 2X. Before the last wash, the pellet was first re-suspended in 1mL of ADF^{+++} and a 5uL aliquot was used to count the crypts. Following the last wash, the pellet was re-suspended in a sufficient amount of reduced growth factor basement membrane extract 2 (Cultrex, BME 2 RGF Organoid Matrix, Path Clear, Amsbio) [herein referred to as BME] to allow for seeding of 100-300 crypts per 10uL of BME. 10uL droplets of crypts re-suspended in BME were seeded in 48 well plates. Plates were inverted to allow for proper dome formation and incubated at 37°C for 20 minutes to allow BME to solidify. After BME solidification, 200uL of pre-warmed Colon Normal Media (CNM) (Table 2.13) (see Appendix 2.3 for description of production of Noggin, R-spondin, Wnt3A conditioned media) was added to each well.

PBS was added to the wells at the edge of the plate to prevent media evaporation from the organoid wells. Media was refreshed every 2-3 days during continuous culture.

Chemical	Concentration in 5X Stock (mM)	Amount for 500mL 5X Stock (g)
Na2HPO4	28	1.97
KH2PO4	40	2.7
NaCl	480	14
KCl	8	0.3
Sucrose	220	37.5
D-sorbitol	274	25

Make to 500mL with MilliQ H2O. Adjust pH to 7.0-7.3.

Prepare 1X complete chelating solution by diluting 1:5 in MillQ H2O and adding 1:2000 2M DTT just before use.

Table 2.12 5X Complete Chelating Solution

Reagent	Final concentration	Volume for 100mL Media	Company	Product Code
ADF+++		20mL		
Rspondin-1 conditioned media	20%	20mL		
Noggin conditioned media	10%	10mL		
Wnt-3A conditioned media	50%	50mL		
50X B27	1X	2mL	Invitrogen	17504-044
500mM N-acetylcysteine	1.25mM	250uL	Sigma	A9165
1M Nicotinamide	10mM	1mL	Sigma	N0636
500ug/mL Recombinant human EGF	50ng/mL	10uL	Invitrogen	PMG8043
5mM TGFB receptor inhibitor A83-01	500nM	10uL	Tocris	2939
30mM p38 inhibitor	10uM	33uL	Sigma	S7067
100uM Prostaglandin E2	10nM	10uL	Tocris	2296
100uM Gastrin	10nM	10uL	Sigma	G9145
500X Primocin	1X	200uL	Invitrogen	ant-pm-1
100mM Rho kinase inhibitor Y-27632	10nM	10uL	Abmole	Y-27632

Table 2.13 Colon normal media (CNM)

2.3.2 Tumour cell isolation and culture of CRC organoids

Note: The protocols in this section were adapted from human tumour colonic organoid culture protocols generously provided by Marc van de Wetering (Hubrecht Institute, Netherlands).

After collecting pieces of the tumour biopsy for whole tissue RNA and IHC analysis, the remaining biopsy (3-5mm^3) was minced into small pieces using a scalpel. Tumour pieces were submerged in 10mL Tumour Digestion Media (Table 2.14) in a 15mL falcon tube and incubated at 37°C for 1 hour with 200 RPM shaking. After 1 hour, liberated single cells were filtered through a 70uM cell strainer, and 1mL FBS was added to quench the collagenase. Cells were pelleted (500g, 4°C, 8 minutes). The pellet was washed 3X with 10mL ADF^{+++} by successive cycles of re-suspension, spinning (500g, 4°C, 8 minutes), and supernatant disposal. Following the final wash, the pellet was re-suspended in BME and plated at different dilutions in 10uL BME per well, in 48 well plates. Plates were inverted and incubated at 37°C for 20 minutes to allow for BME solidification. 200uL of pre-warmed Colon Tumour Media (Table 2.15) (see Appendix 2.3 for description of production of Noggin, R-spondin conditioned media) was then added to each well and PBS was added to peripheral wells of the plate to prevent media evaporation. Media was refreshed every 2-3 days during continuous culture.

Reagent	Final concentration	Volume for 10mL Media	Company	Product Code
ADF+++		10mL		
15mg/mL Collagenase A	1mg/mL	666L	Sigma	11088793001
100mM Rho kinase inhibitor Y-27632	10nM	1uL	Abmole	Y-27632

Table 2.14 Tumour Digestion Media

Reagent	Final concentration	Volume for 100mL Media	Company	Product Code
ADF+++		70mL		
Rspondin-1 conditioned media	20%	20mL		
Noggin conditioned media	10%	10mL		
50X B27	1X	2mL	Invitrogen	17504-044
500mM N-acetylcysteine	1.25mM	250uL	Sigma	A9165
1M Nicotinamide	10mM	1mL	Sigma	N0636
500ug/mL Recombinant human EGF	50ng/mL	10uL	Invitrogen	PMG8043
5mM TGFB receptor inhibitor A83-01	500nM	10uL	Tocris	2939
30mM p38 inhibitor	10uM	33uL	Sigma	S7067
100uM Prostaglandin E2	10nM	10uL	Tocris	2296
100uM Gastrin	10nM	10uL	Sigma	G9145
500X Primocin	1X	200uL	Invitrogen	ant-pm-1
100mM Rho kinase inhibitor Y-27632	10nM	10uL	Abmole	Y-27632

Table 2.15 Colon Tumour Media (CTM)

2.3.3 Organoid passaging, freezing, and establishment from frozen stocks

2.3.3.1 Organoid passaging

Following initial seeding, organoids were allowed to grow for 3-4 days (normal colon organoids) or 7 days (tumour organoids) prior to the first passage. Since normal organoids are established from crypts, crypt closure results in more rapid initial organoid formation than tumour organoids, which are derived from single tumour cells. To passage, the contents of each well were pipetted up and down to break up the BME and transferred into one 15mL falcon tube. Organoids were pelleted, supernatant was discarded, and the pellet was re-suspended in 5mL TrypLE (Life Technologies) and incubated for 5 minutes in a 37°C water bath. After 5 minutes, the tube was vigorously vortexed to further dissociate organoids. 1mL FBS was added to the organoids suspended in TrypLE and the contents were pelleted. The supernatant was discarded and the pellet was re-suspended in the appropriate amount of BME for seeding 10uL per well of a 48 well plate. For the first passage (P1) organoids were typically passaged 1:1. Upon the second passage, organoids were expanded by passaging 1:2-1:3. For continuous culture, organoids were passaged once weekly and confluent wells were passaged 1:3-1:4 as appropriate.

2.3.3.2 Organoid freezing

After the first or second organoid passage from initial seeding (depending on efficiency of organoid expansion), 15 confluent wells of organoids were collected in a 15mL falcon tube 2-3 days after their last passage. Organoids were washed in cold ADF^{+++} and left on ice for 5 minutes to dissolve BME. Organoids were vigorously pipetted up and down and then spun to pellet (500g, 4°C, 3 minutes). After pelleting, the pellet was washed again in ADF^{+++}, and the pellet was re-suspended in 1.5mL of Recovery Cell Freezing Medium (Invitrogen, 12648-010). 500uL was added to 3 cryovials. Cryovials were initially frozen in -80°C and then transferred to liquid nitrogen for long-term storage.

2.3.3.3 Organoid establishment from frozen stocks

To re-establish organoid cultures from banked frozen stocks, frozen vials were rapidly thawed in a 37°C water bath and 1mL of 37°C ADF^{+++} was added to dilute the freezing medium. Cells were transferred to a 15mL falcon tube and an additional 15mL of ADF^{+++} was added. Cells were spun at a low speed (600 RPM, 3 minutes, 4°C). The pellet from one cryovial was re-suspended in 40uL BME and organoids were plated in 4 wells, 10uL/well in 48 well plates, inverted, incubated at 37°C to allow BME to solidify, and 200uL pre-warmed CNM or CTM was added as appropriate. Typically, much organoid death was observed after thawing and required 3-5 passages to expand for experiments.

2.3.4 KRAS mutation typing in CRC organoids

Organoids from 2-3 confluent wells were re-suspended in 10mL PBS to wash and pelleted. The pellet was re-suspended in 200uL PBS to which 20uL of Proteinase K (Qiagen) was added. Genomic DNA was extracted using the QiaAmp DNA MiniKit (Qiagen) according to the manufacturers protocol for Cells, Blood, and Body Fluids.

DNA was eluted from the spin columns in 100uL DNase/RNase Free H_2O. DNA concentration, 260/280 and 260/230 ratios were determined using a NanoDrop 1000 (Thermo Fisher). Only DNA with 260/280 and 260/230 ratios greater than 1.8 and 1.7 respectively were used for subsequent analysis. *KRAS* mutation status was determined using a qBiomarker^{TM} Somatic Mutation PCR Array Human KRAS Gene (Qiagen, Plate E Format, SMH-806ARE-12 337021). This qPCR-based array detects 20 different somatic mutations in the human *KRAS* gene (Table 2.16). The assay was carried out according to the manufacturer's protocol for the 384-well plate format. Six independent organoid lines were assayed per plate in addition to *KRAS* mutant and wild type controls. Plates were run on the ViiA7 Real-Time PCR System (Applied Biosystems), importantly with the baseline set to 8-20 cycles and the threshold set to 0.1 to appropriately detect amplification. Data was analysed using the Excel-based PCR array Data Analysis Template from www.sabiosciences.com/somaticmutationdataanalysis.php. Results of the qBiomarker assay for each organoid were always compared to results of the diagnostic whole tumour tissue mutation analysis (Oxford Molecular Diagnostics Centre). See (Chapter 4, Table 4.1) for a list of established organoids and their corresponding mutation status.

Nucleotide Change	Amino Acid Change	Mutation Frequency
c.35G>A	p.G12D	0.287
c.35G>T	p.G12V	0.191
c.38G>A	p.G13D	0.101
c.34G>T	p.G12C	0.098
c.35G>C	p.G12A	0.047
c.34G>A	p.G12S	0.045
c.34G>C	p.G12R	0.028
c.37G>T	p.G13C	0.007
c.183A>C	p.Q61H	0.003
c.37G>A	p.G13S	0.002
c.182A>T	p.Q61L	0.002
c.183A>T	p.Q61H	0.002
c.436G>A	p.A146T	0.002
c.37G>C	p.G13R	0.002
c.182A>G	p.Q61R	0.002
c.34_35GG>TT	p.G12F	0.001
c.38G>C	p.G13A	0.001
c.181C>A	p.Q61K	0.001
c.38_39GC>AT	p.G13D	0.001
c.38G>T	p.G13V	0.001

Table 2.16 *KRAS* mutations detected in qBiomarker assay

2.3.5 Basic cytokine stimulation experiments

Systematically, newly established organoids were subjected to basic cytokine stimulation assays between passages 2-4. Following their last passage, organoids were seeded into 10 wells of 48 well plates in 10uL BME per well. Organoids were grown for 3-4 days, refreshing the media every 2 days. One day prior to stimulation, fresh media (200uL) was added to each well. Cytokines (IL-22 and IL-6) were prepared in ADF^{+++} and 50uL of the appropriate cytokine was added to each well to achieve the following final concentrations: 1ng/mL IL-22, 10ng/mL IL-22, 1ng/mL IL-6, 10ng/mL IL-6. Duplicate wells of each condition as well as two no treatment control wells were prepared. Organoids were stimulated for 24 hours, media was aspirated, and plates were frozen in -80°C for subsequent RNA extraction.

2.3.6 Organoid proliferation assays

Two confluent wells of each organoid line were dissociated to single cells with TrypLE, re-suspended in 80uL BME and used to seed 12 wells of organoids in 5uL BME in 96 well plates. Following BME solidification, triplicate wells of each: no

treatment in full CTM, no treatment in CTM without EGF, 1ng/mL IL-22 in full CTM, 1ng/mL IL-22 in CTM without EGF were prepared and 200uL of the appropriate stimulus was added to each well. 48 hours following initial seeding, the media was refreshed with the same stimulations as described above. 96 hours after initial seeding all wells were imaged at low magnification (4X) on an inverted microscope for macroscopic growth evaluation. The media was refreshed again with the appropriate stimulations containing 10% Alamar Blue (BioRad) and incubated for an additional 5 hours. Absorbance was measured at 570nm and 600nm as a reference on a BMG SPECTROstar NANO Microplate Reader (BMG Labtech). The percent difference in alamar blue reduction for each condition compared to the full CTM no treatment condition was determined as described in Figure 2.4.

$$\text{Percentage difference between treated and control cells} = \frac{(O2 \times A1) - (O1 \times A2)}{(O2 \times P1) - (O1 \times P2)} \times 100$$

Where:

O1 = molar extinction coefficient (E) of oxidized alamarBlue® (Blue) at 570 nm (80586)
O2= E of oxidized alamarBlue® at 600 nm (117216)
A1 = absorbance of test wells at 570 nm
A2 = absorbance of test wells at 600 nm
P1 = absorbance of no treatment wells at 570 nm
P2 = absorbance of no treatment wells at 600 nm

Figure 2.4 Computation of percent difference in alamar blue reduction between treated and control organoids

2.3.7 T cell supernatant stimulation experiments

3-5 days after passage, organoids from confluent wells in 48 well plates were used at 1:4 to seed into 96 well plates in 5µL BME per well in 150µL CTM. One day after seeding, organoids were stimulated with T cell supernatants as described in 2.2.4, however stimulations were prepared in CTM as base media. Organoids were stimulated for 24 hours after which supernatant was aspirated and plates were frozen in -80°C for subsequent RNA extraction and qPCR as described in 2.3.8.

2.3.8 RNA extraction and qPCR

RNA was extracted from organoids by adding 150uL RLT Buffer (Qiagen) with β-mercaptoethanol (Sigma) to each well of frozen BME-embedded organoids and pipetting up and down to solubilise. RNA was then extracted following the procedures described in 2.1.5. cDNA was synthesised using 10uL of the eluted RNA, subsequently following the protocol as in 2.1.5. Finally, qPCR was performed as in 2.1.5.

2.3.9 Flow cytometric analysis of IL-22RA1

Four confluent wells of organoids were collected into cold PBS in a 15mL falcon tube and pelleted (500g, 4°C, 5 minutes). Supernatant was discarded and the pellet was re-suspended in 5mL TrypLE, incubated for 5 minutes in a 37°C water bath, and vortexed vigorously to dissociate organoids to single cells. 1mL of FBS was added to the dissociated cells and cells were pelleted (500g, 4°C, 5 minutes). The pellet was re-suspended in 400uL of FACS Buffer (1x PBS + 0.5% BSA + 2mM EDTA) and 200uL of cell suspension was seeded into two wells of a 96 well round bottom plate. Cells were pelleted (500g, 4°C, 5 minutes), washed in 150uL FACS Buffer, and then stained in 50uL FACS Buffer using the staining panel described in Table 2.1, omitting CD45. One well was stained for IL-22RA1 and one well was stained using matched isotype controls as in Table 2.1 for 40 minutes at 4°C. Stained cells were centrifuged (500g, 4°C, 8 minutes) and washed in FACS buffer 2X. After washing, cells were fixed in 100uL Fix/Lyse Solution (BD) and incubated at room temperature for 15 minutes. Fixed cells were centrifuged (500g, 4°C, 8 minutes) and washed in FACS buffer 2X. Washed cells were re-suspended in 200uL FACS buffer and flow cytometric analysis was performed on a BD LSR Fortessa X-20 following compensation. Data analysis was performed using FlowJo 10 software.

2.3.10 Phosflow

Organoids of a given line were seeded at equal density into 9 wells of a 48 well plate, 10uL BME per well. One day prior to phosflow, when wells were confluent, 200µL of fresh CTM was added to each well. IL-22 (R&D Systems) was prepared in ADF^{+++} and 50uL of the appropriate concentration was added to each well to achieve the following final concentrations: 1ng/mL, 10ng/mL. Triplicate wells of each condition as well as 3 no treatment wells were prepared. Organoids were stimulated for 30 mintues, media was aspirated and single cell suspensions of organoids were prepared as described for basic flow cytometric analysis in 2.3.9. Cells were then fixed, permeabilised, stained with fluorophore-conjugated antibodies against phosphorylated residues on intracellular signalling molecules of interest (Table 2.10), and intracellular flow cytometry was performed as described in 2.2.7.

2.3.11 Confocal microscopy

Organoids were seeded onto autoclaved 9mm diameter glass coverslips (VWR) in 24 well plates with 10uL of BME containing organoids per coverslip. BME was spread with a 200uL pipet tip to create a thin layer and was allowed to solidify at 37°C for 20 minutes. 400uL of organoid media (CTM or CNM) with stimuli as appropriate was added and organoids were incubated for 24 hours. Supernatant was aspirated from each well following the stimulation, and wells were washed with warm PBS. 200uL of 4% paraformaldehyde was added to each well and organoids were fixed for 20 minutes at room temperature. Wells were washed 2X with room temperature 1X Tris buffered saline (TBS). Organoids were permeabilised by adding 500uL of ice-cold methanol to each well and incubating at -20°C for 10 minutes. Wells were washed 3X with 1X TBS. 400uL of 10% goat serum in 1X TBS was added to each well and organoids were incubated for 1 hour at room temperature to block non-specific

antibody binding. Primary antibody solutions were made up in 1X TBS, 400uL per well. The following primary antibodies were used in conjunction with mouse anti-E-cadherin (1:300, 610181, clone 36/E-cadherin, BD): Phospho-Stat3 (Tyr705) XP Rabbit mAb (1:1000, 9145, clone D3A7, Cell Signaling), anti-human IL-22RA1 (1:750, Atlas Antibodies; HPA042399 lot: R38731), c-Myc Rabbit mAb (1:800, 5605, clone D84C12, Cell Signaling). Organoids were incubated with primary antibodies overnight at 4°C. Wells were washed 3X with 1X TBS and stained with secondary antibodies: goat anti-rabbit IgG Alexa Fluor 555 conjugated secondary antibody (1:400, Life Technologies; A32732) and goat anti-mouse IgG Alex Fluor 488 conjugated secondary antibody (1:400, Life Technologies; A11001) for 1 hour at room temperature. Slides were washed and nuclei were stained with Hoechst (1:20,000, Life Technologies) for 10 minutes at room temperature. Wells were washed 3X with 1X TBS and coverslips were removed from each well, inverted, and mounted onto Superfrost Plus slides (VWR). Images were acquired on an Olympus FV1200 IX83 Confocal System.

2.4 In silico analysis in tumour transcriptomic datasets

2.4.1 Description of CRC transcriptomic datasets

The GSE39397 superseries (Calon *et al.*, 2012) comprised of expression profiles of cell populations from human CRCs sorted 3 ways (GSE39395, N=8) and 4 ways (GSE39396, N=6) into epithelial, immune, and stromal cells was used to assess cell-specific expression of *IL23A, IL22RA1,* and *IL10RB*. Prior to analysis, the genes of interest were median-normalised and log2 transformed.

Four different colorectal cancer transcriptomic datasets comprising 2,332 patients were used for the prognostic studies in this thesis. The French National Cartes

d'Identite des Tumeurs (CIT) cohort [GSE39582; (Marisa *et al.*, 2013)] contains 469 patients with stage II/III CRC who underwent surgery between 1987 and 2007 at seven different centres. Patients who received pre-operative chemotherapy/radiotherapy were excluded from the study. RNA from fresh frozen primary tumours was assessed using the HG-U133A Affymetrix platform, which contains one probe that detects *IL22RA1* (220056_at). The seven most frequent *KRAS* mutations in codons 12 and 13 were assessed using Taqman probes for allelic discrimination. Six such mutations are represented in this cohort (G12A, G12C, G12D, G12S, G12V, G13D). This cohort was used for initial discovery/training analysis.

The Pan-European Trials in Alimentary Tract Cancers (PETACC3) cohort (NCT00026273) was used as a validation set. 752 stage II (n=108) and stage III (n=644) CRC patients were used from the PETACC3 clinical trial (Popovici *et al.*, 2012; Roth *et al.*, 2012). PETACC3 is a randomized phase III adjuvant chemotherapy trial investigating the efficacy of irinotecan added to fluorouracil (FU) and leucovorin (folinic acid). Gene expression from PETACC3 patients was obtained using the ALMAC Colorectal Cancer DSA platform (Craigavon, Northern Ireland), which is a customized Affymetrix chip that includes 61,528 probe sets mapping to 15,920 unique Entrez Gene IDs. The PETACC3 dataset contains three different probes for *IL22RA1*. The probe used in analysis was that which displayed the greatest variation in the dataset (ADXCRAD_BX089163_s_at).

Finally, a merged dataset comprising stage II/III CRC patients of GSE39582 (Marisa *et al.*, 2013), PETACC3 (Popovici *et al.*, 2012; Roth *et al.*, 2012), TCGA (Cancer

Genome Atlas Network and Muzny, 2012), and ALMAC (Kennedy *et al.*, 2011), representing 1,820 patients, was used as an additional confirmation cohort (referred to in tables as the "Combined" dataset). The ALMAC dataset was obtained from ArrayExpress (www.ebi.ac.uk/arrayexpress) on the A-AFFY-101 platform (customized Affymetrix chip) and is a merge of E-MTAB-863 and E-MTAB-864 (Kennedy *et al.*, 2011). Clinical information on overall survival was available for 1,734 patients and on relapse-free survival for 1,499 patients. Gene expression profiles of the datasets were merged at the gene level, then normalized and corrected for batch effects using the *Combat* R package.

For the individual analyses of the GSE39582 and PETACC3 datasets, gene expression profiles from each of the datasets were used independently (not normalised to the others). Tumours proximal to the splenic flexure were defined as proximal and tumours distal to the splenic flexure were classified as distal.

2.4.2 Statistical analyses for clinical outcome in tumour transcriptomic datasets

All analyses were performed using R software (version 3.03). Receiver operator characteristic (ROC) analysis was performed to determine an optimal *IL22RA1* cutpoint based on log2 expression values in the training cohort (GSE39582). The presence or absence of disease relapse at last follow-up was used as the binary variable in this analysis. The *IL22RA1* cutoff value associated with the maximum Youden index (J = sensitivity + specificity −1) was found to be the 67th percentile. This value was used for all downstream analyses of *IL22RA1* in both the training and validation datasets, and was also used for analyses of additional cytokine/cytokine receptor genes. Contingency analysis (Fisher's exact test) was used to assess association of clinicopathological features with *IL22RA1* expression status.

Probabilities associated with Fisher's exact test were corrected for multiple comparisons using the Bonferroni method. Univariate, multivariate, and interaction analyses of relapse-free survival (RFS) and overall survival (OS) were performed using Cox's proportional hazard regression models constructed in the *survival* R package. Interaction analyses were used to assess specific interaction between *KRAS* mutation status and the expression of cytokine and cytokine receptor genes. Hazard ratios (HRs) were estimated with model coefficients and 95% confidence intervals (CIs) and *P* values were computed with Wald tests. Time-to-event curves were prepared using Kaplan-Meier methods in GraphPad Prism 7.

2.4.3 Gene set enrichment analysis comparing proximal and distal tumours

Gene set enrichment analyses (GSEA) for immune pathways comparing proximal and distal tumours were performed as follows. Expression data from the combined cohort were merged at the gene level using gene symbol; batch effects due to independent cohorts were corrected using the *ComBat* function from the *sva* R package (version 3.14.0) (Johnson, Li and Rabinovic, 2007). Differential expression analysis between proximal (right-sided) and distal (left-sided) tumours using the *limma* R package (version 3.24.4) was performed (Smyth, 2004). By using the t-statistics from the differential expression analysis as a weighting factor, a preranked Gene Set Enrichment Analysis (GSEA) using the GenePattern web interface from the Broad Institute (genepattern.broadinstitute.org/) was performed. GSEA was run on two different gene signatures selected from the MSigDB portal (http://www.broadinstitute.org/gsea/msigdb): (i) hallmark_inflammatory_response (MSigDB ref: M5932) and (ii) immune_reponse (MSigDB ref: M19817).

2.4.4 Immune metagene signature comparison between proximal and distal tumours

Relative log2 expression values of genes characteristic of distinct immune subsets were compared between proximal (n = 181) and distal (n = 267) tumours from patients in the training cohort. The combined average of the log2 expression of the markers indicated for each immune subtype was determined. Markers of each distinct immune subtype are indicated in Table 2.17.

Cell population	Metagene signature
Dendritic cells (DC)	*CD208, CD209, CD83*
Neutrophils	*CD66B, FCGR3B*
Macrophages	*MSR1, CD14, CD68, CSF1R*
Cytotoxic cells	*GNLY, GZMA, GZMB, GZMH, GZMK*
B cells	*MS4A1, CD19, CD22, CD79A*
T cells	*CD2, CD274, CD28, CD3E*

Table 2.17 Immune metagene signatures

2.5 RNA-Sequencing DLD-1 isogenic cell line

2.5.1 Sample preparation

DLD-1 isogenic cells were seeded at 120,000 cells per well in 12-well plates in 800uL serum free RPMI with 1X ITS (Sigma) and allowed to adhere overnight. Cytokines were prepared in RPMI with 1X ITS (Sigma). 200uL of cytokine stimulus or RPMI, 1X ITS (Sigma) control was added to each well as appropriate for final concentrations of 10ng/mL IL-22 (R&D Systems) or 10ng/mL IL-6 (Peprotech). Cells were stimulated for 2 hours or 24 hours. RNA was extracted by adding 150uL RLT Buffer (Qiagen) with β-mercaptoethanol (Sigma) to each well. 150uL of 70% ethanol was added to each lysed sample and the contents were transferred to Qiagen RNeasy Minikit columns (Qiagen). RNA was extracted following the procedures described in 2.1.5. RNA concentration and 260/280 ratios were determined on a NanoDrop 1000 (Thermo Fisher). cDNA was synthesised from 500ng RNA from each sample using

the High Capacity cDNA Kit (Applied Biosciences) according to the manufacturers protocol using a C1000 Touch™ Thermal Cycler (Biorad) and used for quality control qPCR. Three independent experiments were performed with cells at passages 6, 7, 8 (Figure 2.5).

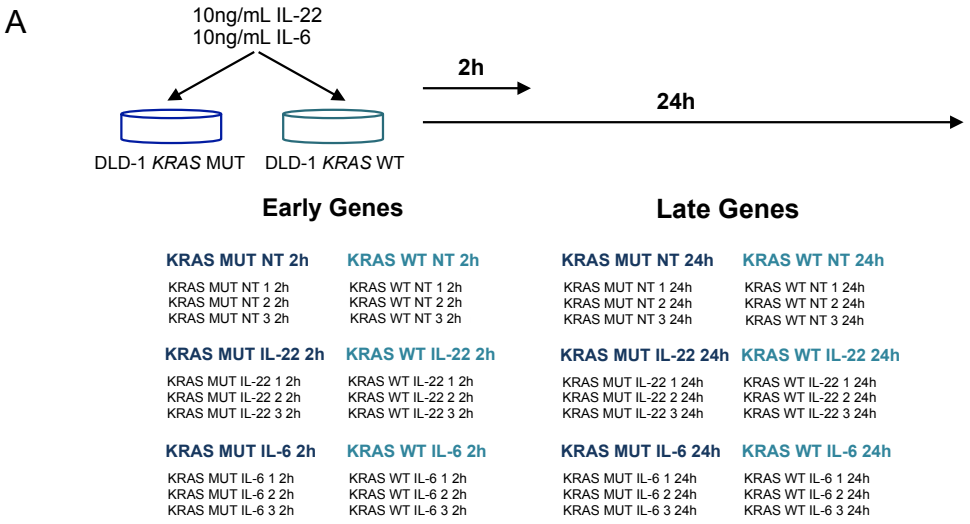


Figure 2.5 Samples for RNA-sequencing

(A) DLD-1 isogenic cells were stimulated for 2h or 24h with 10ng/mL IL-22 or IL-6 in serum free media containing 1X ITS. Three independent experiments (1,2,3) were performed with successive cell passages 6,7,8.

2.5.2 Library preparation, RNA-sequencing, and data processing

Library preparation, RNA-sequencing, and quality control were performed on a service basis by the High-Throughput Genomics Group (Wellcome Trust Centre for Human Genetics, Oxford). Bioanalysis of RNA was performed and all samples had RIN=10. Samples were normalised to 1ug total RNA and the mRNA fraction was isolated by polyA selection. Libraries were prepared using the TruSeq Stranded mRNA Kit (Illumina) following the manufacturer's instructions. The prepared libraries were size-selected and multiplexed and paired-end sequenced using the Illumina HiSeq4000 platform (Illumina) over three lanes of a flow cell. "Strandedness" was tested as part of internal quality control and the proportion of

reads mapping to the correct strand was found to be very high for the samples in this dataset (Figure 2.6).

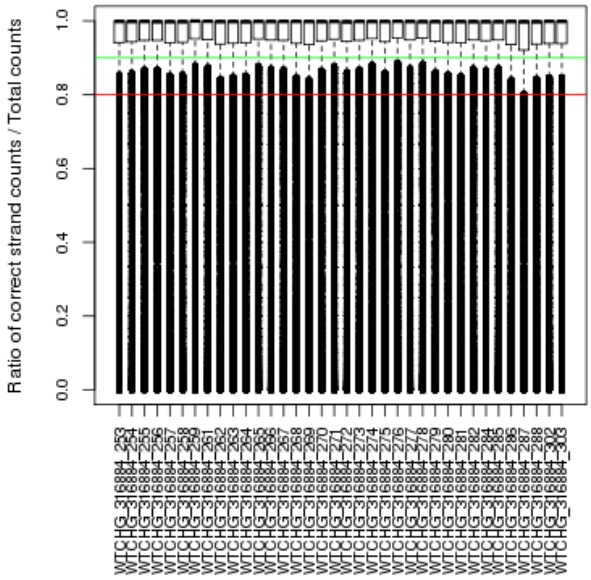


Figure 2.6 Proportion of reads mapping to the correct strand

Raw data was processed using a pipeline invoked by bcbio-nextgen (http://bcbio-nextgen.readthedocs.io/en/latest/contents/pipelines.html#rna-seq). Adapter trimming was performed using cutadapt, alignment was performed using hisat2, indexing was performed with SAMBAMBA, mapped reads were quantified using featurecounts.

2.5.3 Data analysis

Clustering analysis was performed on all 36 samples using correlation distance metrics and the average linkage agglomeration algorithm (R package *nclust* version 1.9.0; http://bcf.isb-sib.ch/Resources.html) on log transformed Reads Per Kilobase of transcript per Million (log2(RPKM+1)) values for each gene. Principal component analysis (R package *prcomp* version 3.3.1) was subsequently performed on all samples. These analyses confirmed that experimental replicates clustered together.

2.5.3.1 Differential expression analysis

Differential expression analysis was performed using the generalised linear model (GLM) implemented in the *edgeR* package (version 3.16.0). Note that original read counts were used as input into *edgeR* to allow for accurate estimatation of the mean-variance relationship in the data. The GLM approach was used to assess the contrasts highlighted in Table 2.18. Genes fom each contrast were ranked according to log2 fold change and false discovery rate (FDR) values. Generally genes with log2 fold change greater than 2 and FDR <0.05 were considered to be differentially regulated. Specific statistical cutoffs are indicated in the results for each comparison. Tables/heatmaps of top differentially regulated genes for the contrasts highlighted in Table 2.18 are contained in Appendix 3.1.1. Heat mapping was performed using the *pheatmap* package (version 1.0.8).

Differentially expressed genes in:	Contrast
KRAS MUT cells with IL-22 after 2h	*KRAS* MUT 2h IL-22 - *KRAS* MUT 2h NT
KRAS WT cells with IL-22 after 2h	*KRAS* WT 2h IL-22 - *KRAS* WT 2h NT
KRAS MUT cells with IL-22 after 24h	*KRAS* MUT 24h IL-22 - *KRAS* MUT 24h NT
KRAS WT cells with IL-22 after 24h	*KRAS* WT 24h IL-22 - *KRAS* WT 24h NT
KRAS MUT IL-22 stimulated but not *KRAS* WT IL-22 stimulated cells after 2h	(*KRAS* MUT 2h IL-22 - *KRAS* MUT 2h NT)-(KRAS WT 2h IL-22 - KRAS WT 2h NT)
KRAS MUT IL-22 stimulated but not *KRAS* WT IL-22 stimulated cells after 24h	(*KRAS* MUT 24h IL-22 - *KRAS* MUT 24h NT)-(KRAS WT 24h IL-22 - KRAS WT 24h NT)
IL-22 but not IL-6 stimulated *KRAS* MUT but not WT cells after 2h	[(*KRAS* MUT 2h IL-22 - *KRAS* MUT 2h NT)-(KRAS MUT 2h IL-6 - KRAS MUT 2h NT)]-[(KRAS WT 2h IL-22 - KRAS WT 2h NT)-(KRAS WT 2h IL-6 - KRAS WT 2h NT)]
IL-22 but not IL-6 stimulated *KRAS* MUT but not WT cells after 24h	[(*KRAS* MUT 24h IL-22 - *KRAS* MUT 24h NT)-(KRAS MUT 24h IL-6 - KRAS MUT 24h NT)]-[(KRAS WT 24h IL-22 - KRAS WT 24h NT)-(KRAS WT 24h IL-6 - KRAS WT 24h NT)]

Table 2.18 Contrasts used in differential expression analysis

2.5.3.2 Pathway analysis

Pathway analyses were performed by single sample GSEA (ssGSEA) using the GenePattern web interface from the Broad Institute (genepattern.broadinstitute.org/). The Hallmark collection of well-annotated gene sets from the MSigDB portal (http://www.broadinstitute.org/gsea/msigdb) was used. Enrichment scores from ssGSEA were used for differential analysis using the generalised linear model as

implemented in the *limma* package (version 3.30.0) using the contrasts outlined in Table 2.18. Differentially expressed pathways with an adjusted p-value <0.01 were considered significant. Heat mapping was performed using the *pheatmap* package (version 1.0.8). Heat maps for the top differentially regulated pathways for the contrasts highlighted in Table 2.18 are contained in Appendix 3.1.2.

2.6 Label-free proteomics DLD-1 isogenic cell line

2.6.1 Sample preparation

DLD-1 isogenic cells were seeded at $10x10^6$ cells per plate in 10cm plates in 9.5mL serum free RPMI with 1X ITS (Sigma) and allowed to adhere overnight. Cytokines were prepared in RPMI with 1X ITS (Sigma). 500uL of cytokine stimulus or RPMI, 1X ITS (Sigma) control was added to each plate as appropriate for final a concentration of 10ng/mL IL-22 (R&D Systems). Cells were stimulated for 24 hours. Fresh, keratin-free lysis buffer (Table 2.19) was prepared. Cells were washed two times, with ice cold PBS, then lysed in 500uL lysis buffer on ice.

Reagent	Final concentration	Volume for 5mL Media	Company
Ultrapure 10% SDS solution	4%	2mL	ThermoFisher
Triethylammonium bicarbonate (TEAB)	100mM	0.5mL	Sigma
Tris(2-carboxyethyl)phosphine (TCEP)	10mM	100uL	ThermoFisher
Ultrapure H2O	--	2.4mL	ThermoFisher

Table 2.19 Proteomics cell lysis buffer

Lysate was harvested into LoBind Eppendorf tubes (2mL) (Sigma), vortexed for 30 seconds and boiled for 5 minutes at 95°C. Samples were cooled at room temperature for 5 minutes and snap frozen. Four independent experiments were performed with cells at passage 5, 6, 7, 8 (Figure 2.7) (Note: Experiments with cells at passage 6, 7, 8 were performed in parallel with experiments for RNA-sequencing).

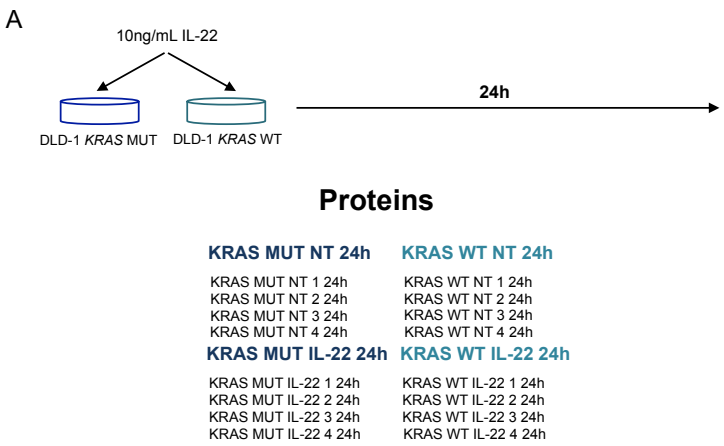


Figure 2.7 Samples for label-free proteomics

(A) DLD-1 isogenic cells were stimulated for 24h with 10ng/mL IL-22 in serum free media containing 1X ITS. Four independent experiments (1,2,3,4) were performed with successive cell passages 5,6,7,8.

2.6.2 Label-free LC-MS/MS

Label-free LC-MS/MS was performed at the University of Dundee Proteomics Unit (Dundee, Scotland) in collaboration with Professor Doreen Cantrell and Dr. Mahima Swamy. Cells were lysed and digested with trypsin/Lys-C, peptides were separated into 16 fractions using an Ultimate 3000 HPLC (Thermo Scientific), and each fraction was analysed using an LTQ-Orbitrap Velos Pro mass spectrometer (Thermo Scientific) coupled to an Ultimate 3000 RSLC Nano sysem (Thermo Scientific). MaxQuant (Tyanova, Temu and Cox, 2016) was used for data normalization, peak-picking, database searching, peptide and protein identification. Over 9000 proteins were identified in each sample.

2.6.3 Data analysis

2.6.3.1 Differential expression analysis

Relative iBAQ (intensity-based absolute quantification) intensities, which are an approximation of protein copy numbers based on the sum of peptide-feature intensities of all peptides matching to a specific protein, divided by the number of theoretically observable peptides, were used for differential expression analysis. Two-

tailed, paired T-tests were used to compare relative iBAQ intensities for the IL-22 stimulated versus no treatment condition for the *KRAS* mutant and wild type line. Proteins for which log2 fold change > 1 and P<0.05 were considered significantly differentially regulated. The top differentially regulated proteins unique to each line and shared between the lines were identified (Appendix 3.2.1).

2.6.3.2 Pathway analysis

Protein set enrichment analysis (PSEA-Quant) (http://pseaquant.scripps.edu/) (Lavallée-Adam *et al.*, 2014; Lavallée-Adam and Yates, 2016) was used to perform pathway analysis. Inherent in the PSEA-Quant algorithm is a permutation scheme that models protein abundance dependencies and annotation biases and has been validated for label-free proteomic analysis (Lavallée-Adam *et al.*, 2014). Analysis of the ratio of the fold changes in iBAQ values for *KRAS* mutant IL-22 stimulated over unstimulated cells compared to *KRAS* wild type IL-22 stimulated over unstimulated cells was performed. The positional, curated, motif, computational, oncogenic, immunologic pathways from the MSigDB (totaling 11,812 pathways) were used in this analysis. The pathways for which P<0.001, with an FDR-q value of less than 0.05 were considered significant. A list of differentially induced pathways can be found in Appendix 3.2.2.

2.7 Statistical Analysis

For the analysis of gene expression in prospectively collected tumour and matched normal tissue, *in vitro* experiments in cell lines, and *ex vivo* experiments in primary organoids, all statistical tests were two-sided and are specified in figure legends with exact p-values displayed. Differences were considered significant when $P<0.05$. All bar charts display mean ± SEM, box and whisker plots display the 5^{th}-95^{th} percentile, single dots represent a value from an individual patient (often the average of technical

duplicates). D'Agostino-Pearson Omnibus normality tests were performed, when appropriate ($n>8$), and determined the use of parametric versus non-parametric tests. Parametric tests were used when $n<8$. These analyses were performed using GraphPad Prism 7. Specific statistical analyses for tumour transcriptomic data, RNA-sequencing, and proteomic analysis are described in 2.4.2, 2.5.3, 2.6.3.

3 Identification of an IL-22 receptor-high, *KRAS* mutant poor prognosis colorectal cancer subtype

3.1 Introduction

Colorectal cancer (CRC), is a molecularly heterogeneous disease thought to be driven by the interplay of genetic factors, such as activating mutations in oncogenes like *KRAS*, environmental influences, such as the gut microbiota, and aberrant immunity (Terzić *et al.*, 2010; Elinav *et al.*, 2013). Chronic intestinal inflammation is a well-known risk factor for colorectal cancer (Jess, Rungoe and Peyrin–Biroulet, 2012). Sporadic CRCs that do not arise in a colitic context also elicit inflammatory responses (Hanahan and Weinberg, 2011). Once thought to be exclusively involved in immune surveillance and anti-tumour immunity, intratumoural leukocytes are now understood to also have pro-tumourigenic roles. As such, inflammation is regarded as an enabling characteristic for the acquisition of the core hallmarks of cancer (Hanahan and Weinberg, 2011). Leukocyte-derived cytokines that modulate cancer cell proliferation, survival, and dissemination are central linchpins in this relationship (West *et al.*, 2015).

Whether specific cytokines play a beneficial or deleterious role in cancer is largely context dependent. Logically, cancers therefore develop adaptations to exploit the growth and survival benefits conferred through cytokine signalling. For example, *TP53*, which encodes the p53 tumour suppressor, is mutated in 60-70% of CRCs and often coupled with loss of heterozygosity at this locus (Fearon, 2011). Loss of p53 has been found to augment interleukin 6 (IL-6) signalling in CRC by reducing expression of microRNA-34a (miR-34a), a p53 transcriptional target that normally represses IL-6 receptor expression and reduces epithelial-mesenchymal-transition (EMT) mediated by IL-6 (Rokavec *et al.*, 2014). Furthermore, gain-of-function mutations in *TP53* prolong tumour necrosis factor alpha (TNFα)-induced nuclear factor kappa-B (NF-

κB) signalling and consequently renders mice harbouring this mutation more susceptible to colitis associated cancer (Cooks *et al.*, 2013).

Oncogenic Ras isoforms modulate inflammatory pathways in cancer by directly inducing aberrant production of pro-inflammatory cytokines (e.g. IL-6, IL-8, IL-11, granulocyte monocyte colony stimulating factor [GM-CSF]), chemokines (e.g. CXC chemokine ligand 1 [CXCL1]), and cytokine receptors (Ancrile, Lim and Counter, 2007; O'Hayer, Brady and Counter, 2009; Pylayeva-Gupta *et al.*, 2012; Shin *et al.*, 2012; McAllister *et al.*, 2014). Furthermore, oncogenic Ras can influence cytokine signal transduction pathways and downstream biological effects (Hoogwater *et al.*, 2010; Wiener *et al.*, 2014). A major Ras isoform, KRAS, is a critical driver of mitogenic signalling and is negatively regulated by its intrinsic GTPase activity. Mutations that inactivate this self-limiting aspect of KRAS occur in 40-45% of colorectal cancers (Sinicrope *et al.*, 2014) in which they drive constitutive activation of the Ras-Raf-MEK-ERK pathway. However, the influence of mutant *KRAS* on cytokine signalling in CRC has not been extensively characterised. *KRAS* mutations are strongly associated with resistance to EGFR-targeted therapy and variably associated with resistance to standard chemotherapies (Karapetis *et al.*, 2008; Bokemeyer and Bondarenko, 2011; Van Cutsem *et al.*, 2015). Efforts to generate effective KRAS inhibitors have been largely unsuccessful, making *KRAS*-mutant CRC a disease subtype with unmet clinical need. Despite the well-described mechanisms of *KRAS*-driven carcinogenesis, *KRAS* mutations are not strongly prognostic in stage II/III CRC patients who receive adjuvant chemotherapy (González-Aguilera *et al.*, 2004; Westra *et al.*, 2005; Roth *et al.*, 2010). However,

given the cytokine modulating capacity of the Ras family, *KRAS* mutations may be prognostic in specific subtypes of cytokine-driven cancer.

Interleukin 23 (IL-23) and interleukin 12 (IL-12) are heterodimeric cytokines of the same family that share a common p40 subunit. The p40 subunit (encoded by *IL12B*) heterodimerizes with p19 (*IL23A*) to form IL-23 or with p35 (*IL12A*) to form IL-12 (Oppmann *et al.*, 2000). Both cytokines are secreted by activated dendritic cells, monocytes, and macrophages in response to damage-associated or microbial stimuli, while their respective receptors are expressed predominately on $CD4^+$ T cells, natural killer (NK) cells, natural killer T (NKT) cells, and innate lymphoid cells (Ngiow, Teng and Smyth, 2013). Despite their similarities, IL-23 and IL-12 drive divergent immunologic responses upon cytokine receptor engagement. IL-12 initiates a classical Th1, interferon gamma (IFNγ) dominated response and is known to promote anti-tumour immunity by inducing the proliferation and cytotoxic activity of NK cells and $CD8^+$ T cells (Trinchieri, 2003; Langowski *et al.*, 2006). On the contrary, IL-23 expands and maintains retinoid acid receptor-related orphan receptor γt (RORγt) expressing $CD4^+$ Th17 and innate lymphoid cell populations that produce interleukin 17A (IL-17A) and interleukin 22 (IL-22) (Langrish *et al.*, 2005; Buonocore *et al.*, 2010; Gaffen *et al.*, 2014). These cytokines play essential roles in host defence and damage repair in the gut (Ogawa *et al.*, 2004; Stockinger and Veldhoen, 2007; Sugimoto *et al.*, 2008; Zheng *et al.*, 2008; Sano *et al.*, 2015; Aden *et al.*, 2016), but can be protumourigenic when present chronically or in the context of specific mutations. For example, genetic ablation of *Il23a* reduced tumourigenesis in the murine CPC-APC sporadic CRC model, an adaptation of the classical $Apc^{Min+/-}$ model where tumours are directed to the colon by *Cdx2* Cre-mediated deletion of an *Apc*

allele (Grivennikov *et al.*, 2012). Similarly, previous work in our group demonstrated that in a colitis associated cancer (CAC) model (129*SvEv.Rag*$^{-/-}$ mice infected with *Helicobacter hepaticus* and treated with azoxymethane), antibody blockade of the IL-23 receptor reduced tumour burden in animals with established colon carcinomas (Kirchberger et al., *unpublished*).

Relatedly, IL-17A, a critical downstream effector of IL-23, has been linked to the development and progression of both sporadic CRC (S. Wu *et al.*, 2009; Chae *et al.*, 2010; Grivennikov *et al.*, 2012; K. Wang *et al.*, 2014) and CAC (Hyun *et al.*, 2012) in murine models. Notably, in human CRC, high expression of a functional Th17 cell mRNA signature is associated with poor prognosis (Tosolini *et al.*, 2011; Bindea *et al.*, 2013).

Furthermore, IL-22 is an IL-10 cytokine superfamily member secreted by $CD4^+$ T cells and innate lymphoid cells in the tumour microenvironment downstream of IL-23, which provides a directional signal from the immune compartment to the malignant epithelium. Work from our group demonstrated that IL-22 blockade attenuates tumourigenesis in *Helicobacter hepaticus* infected, AOM treated 129*SvEv.Rag*$^{-/-}$ mice with established invasive adenocarcinoma (Kirchberger *et al.*, 2013b). Almost simultaneously, a protumourigenic role for IL-22 was identified through manipulation of the well-established *Apc*$^{Min/+}$ genetic model of CRC (Huber *et al.*, 2012). Furthermore, IL-22 has been associated with human gastrointestinal cancer progression (Zhuang *et al.*, 2012), resistance to FOLFOX (Folinic acid, 5-fluoruracil, oxaliplatin) chemotherapy in human CRC (T. Wu *et al.*, 2014), and has been described to promote colorectal cancer stemness (Kryczek *et al.*, 2014).

IL-22 signals through a heterodimeric receptor comprised of the IL-22 receptor alpha 1 subunit (IL-22RA1) and an IL-10 receptor beta (IL-10RB) subunit, which is also utilized by several other members of the IL-10 family (Xie *et al.*, 2000; Gurney, 2004). Expression of IL-22RA1 is reported to be restricted to the epithelium of mucosal tissues, while IL-10RB is more widely expressed in the hematopoietic, epithelial, and stromal compartments (Gurney, 2004). IL-22 receptor engagement potently activates Janus kinase 1 (JAK1), tyrosine kinase 2 (TYK2), and signal transducer and activator of transcription 3 (STAT3). Although not as extensively characterised, IL-22 also activates mitogen activated protein kinase (MAPK) pathways, and the phosphatidylinositol-3-kinase (PI3K)/Akt cascade (Mitra, Raychaudhuri and Raychaudhuri, 2012; Xu *et al.*, 2014). Finally, IL-22 has been shown to activate NF-κB, which, through synergism with STAT3, induces expression of genes involved in cell cycle progression and inhibition of apoptosis (Lim and Savan, 2014). Oncogenic *KRAS* has the potential to influence virtually all of the signal transduction pathways downstream of IL-22, but a specific interaction between IL-22 signalling and *KRAS* mutation has not been described.

In light of the multitude of evidence pointing toward a pro-tumorigenic role for IL-23 and its downstream effectors IL-17A and IL-22 in murine models, here we seek to determine the importance of this pathway in human CRC, which remains relatively unknown. Taking an interdisciplinary approach we bring together two historically distinct perspectives on cancer, in which either somatic mutations or inflammation and microenvironmental signals are viewed as oncogenic drivers, and explore the prognostic consequence of cytokine signalling in the context of specific driving mutations. Due to the extensive previous work in our lab, which elucidated the

importance of IL-22 in murine CAC, we focus on IL-22 as a key IL-23 downstream effector.

In this chapter we use prospectively collected fresh colorectal tumour and matched normal adjacent tissue in addition to analyses of large tumour transcriptomic datasets to:

1. Characterise the cytokine microenvironment in human colorectal tumours compared to matched normal adjacent tissue, with a particular focus on IL-23.
2. Explore the expression and distribution of the interleukin 22 receptor, as a stable marker of IL-22 activity, in CRC.
3. Determine the prognostic consequence of having high or low interleukin 22 receptor expression in CRC on its own and in the context of key oncogenic driving mutations, using independent training and validation CRC cohorts totalling over 1,800 patients.

3.2 Results

3.2.1 *IL23A* is elevated in human colorectal tumours compared to normal adjacent mucosa

Given the extensive evidence of a deleterious role for IL-23 and its downstream effectors IL-22 and IL-17A in both colitis associated and sporadic murine models of CRC (S. Wu *et al.*, 2009; Grivennikov *et al.*, 2012; Huber *et al.*, 2012; Hyun *et al.*, 2012; Kirchberger *et al.*, 2013b; K. Wang *et al.*, 2014), we sought to understand whether the IL-23 pathway plays a role in human colorectal cancer. The IL-23 pathway is critical for maintenance of barrier integrity under homeostatic settings in the colon (Maloy and Kullberg, 2008). Therefore we first investigated how amounts of IL-23 in human colorectal tumours compare to those in the normal adjacent mucosa. Biopsies from colorectal tumours and normal adjacent mucosa taken from outside the tumour margins were collected from patients undergoing colectomy at the Churchill Hospital, Oxford, UK. Whole tissue mRNA analysis for a panel of inflammatory cytokines was conducted on fresh frozen biopsies (N=69 patients) comparing cytokine expression in the tumour to normal adjacent tissue (Figure 3.1 A). Expression of the key proinflammatory mediator *TNF* was unchanged between tumours and matched normal adjacent tissue (Figure 3.1 A). *IL6*, which has a well-established deleterious role in murine CRC models (Bollrath *et al.*, 2009; Grivennikov *et al.*, 2009), was elevated in tumours compared to matched normal adjacent tissue from individual patients, however expression was very heterogeneous in the prospective cohort (Figure 3.1 A). Interestingly, the amount of *IL23A* expression was elevated almost universally in tumours compared to matched normal adjacent tissue (Figure 3.1 B). In direct contrast, *IL12A* expression was reduced in almost every tumour compared to matched normal adjacent tissue (Figure 3.1 B).

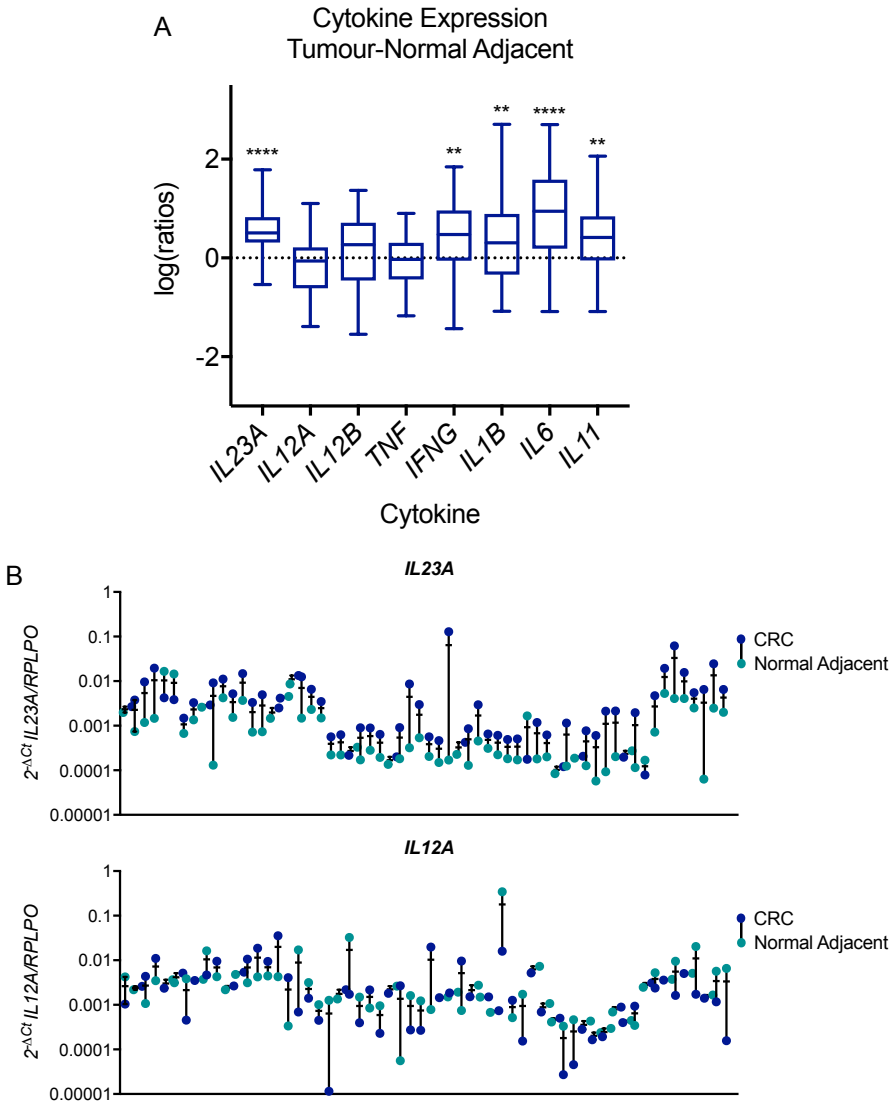


Figure 3.1 *IL23A* is elevated in human colorectal tumours compared to normal adjacent mucosa.

Biopsies from colorectal tumours and matched normal adjacent mucosa, distant from the tumour margins, were collected prospectively from N=69 patients undergoing colectomy. Fresh frozen whole tissue RNA analysis via qPCR was performed.

(A) Box and whisker plots representing the ratio of tumour to normal adjacent [log(tumour)-log(normal adjacent)] expression of a panel of inflammatory cytokines. Whiskers are 5-95th percentile. N=69 patients.

(B) Relative expression of *IL23A* and *IL12A* in tumour (CRC) and matched normal adjacent tissue. Each dot represents a single sample with CRC and Normal adjacent expression from one patient connected with a vertical line. N=69 patients.

Statistical significance was determined using ratio paired T-tests. Where exact p-values are not indicated: **p<0.01, ***p<0.0001. P<0.05 is significant.

We next wanted to confirm that the *IL23A* signal in the human colorectal tumours was indeed coming from the hematopoietic compartment. IL-23 is reported to be produced by activated dendritic cells and macrophages/monocytes (Ngiow, Teng and Smyth, 2013), but its cell specific expression has not been studied extensively in human CRC. Using a publically available microarray dataset [GSE39397 (Calon *et al.*, 2012)], in which two different cell sorting strategies were employed to sort human CRCs into the immune, epithelial, and stromal compartments, we interrogated *IL23A* mRNA expression. Interestingly, when tumours (N=6) were sorted four ways into epithelial ($EpCAM^+$), immune ($CD45^+$), stromal (FAP^+), and endothelial ($CD31^+$) cells, *IL23A* was expressed in the $CD45^+$ immune cells, but marked expression was also present in the $EpCAM^+$ epithelial cells (Figure 3.2 A). Negligible *IL23A* expression was observed in the FAP^+ stromal cells or $CD31^+$ endothelial cells (Figure 3.2 A). When tumours (N=8) were only sorted three ways, into epithelial ($EpCAM^+CD45^-$), immune ($EpCAM^-CD45^+$), and stromal ($EpCAM^-CD45^-$) cells, *IL23A* expression was significantly higher in the immune compartment compared to the epithelial or stromal compartments (Figure 3.2 B). However, an appreciable amount of *IL23A* was expressed in the epithelial cells, which was significantly higher than that in the stromal cells (Figure 3.2 B). Thus, *IL23A* expression in the malignant epithelium may contribute to the elevated *IL23A* expression seen in whole tumour tissue mRNA analysis.

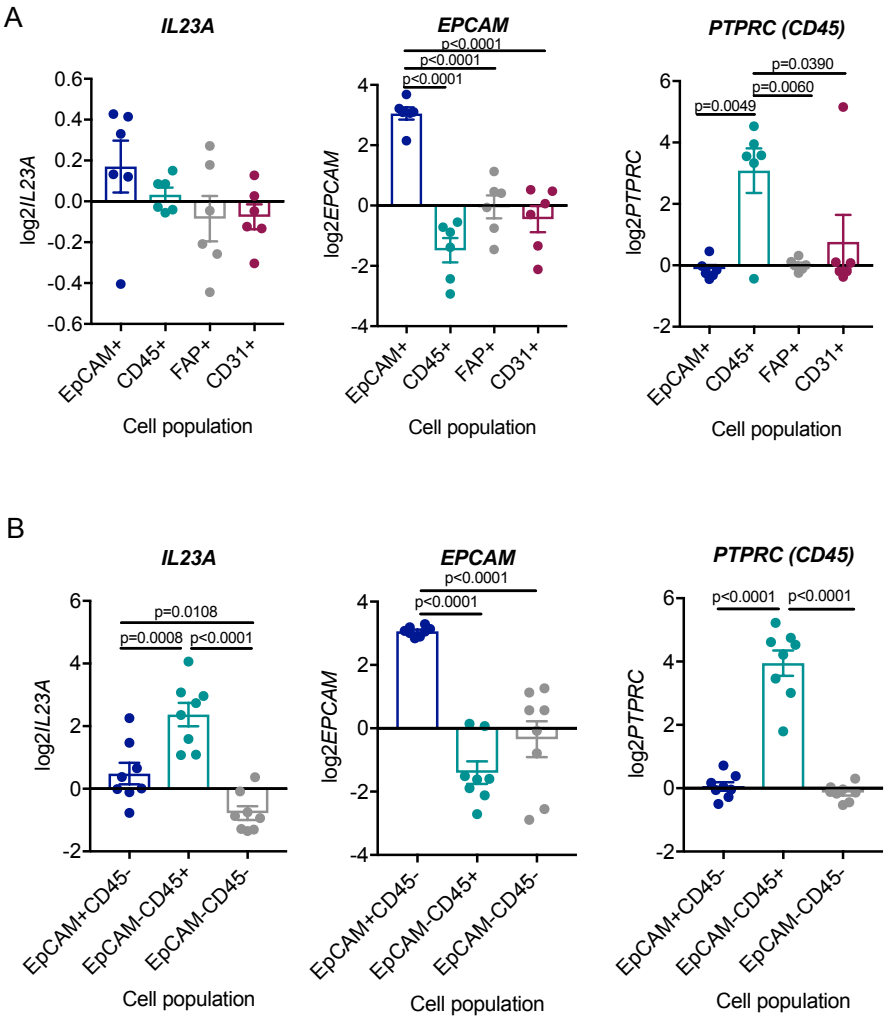


Figure 3.2 *IL23A* mRNA is expressed in both immune and epithelial cells in human CRC.

(A) Gene expression in cells from N=6 independent colorectal tumours sorted four ways based on epithelial ($EpCAM^+$), immune ($CD45^+$), stromal (FAP^+), and endothelial ($CD31^+$) markers from GSE39397 cohort (Calon 2012). RNA was extracted and microarrays were performed. Expression is the median normalised log2 expression from each of the indicated gene probes. The purity of the sorted populations is indicated by enrichment of *EPCAM* and *PTPRC* (encoding CD45) in the $EpCAM^+$ and $CD45^+$ compartments respectively.

(B) Gene expression in cells from N=8 independent colorectal tumours sorted based on epithelial ($EpCAM^+CD45^-$), immune ($EpCAM^-CD45^+$), and stromal ($EpCAM^-CD45^-$) markers from GSE39397 cohort (Calon 2012). RNA was extracted and microarrays were performed. Expression is the median normalised log2 expression from each of the indicated gene probes. The purity of the sorted populations is indicated by enrichment of *EPCAM* and *PTPRC* (encoding CD45) in the $EpCAM^+CD45^-$ and $EpCAM^-CD45^+$ compartments respectively.

Statistical significance was determined using a one-way ANOVA with Tukey's post test for multiple comparisons. $P<0.05$ is significant.

3.2.2 IL-22RA1 is differentially expressed in tumours from different colorectal cancer patients

Given the elevated expression of *IL23A* observed in human CRC tumours compared to normal adjacent tissue, we next sought to understand whether components of the IL-23 pathway hold prognostic significance in human CRC. We detected a minor poor prognostic consequence of having high tumoural *IL23A* expression in a cohort of 457 stage II/III CRC patients (GSE39582) in terms of relapse free survival (RFS *HR*=1.456, 95% CI=1.044-2.132, *P*=0.00289) and overall survival (OS *HR*=1.337, 95% CI=0.956-1.934, *P*=0.0891). However, since IL-23 and its downstream effectors IL-22 and IL-17A are cytokines produced intermittently by leukocytes during periods of immune activity, we focussed our initial analysis on the IL-22 receptor alpha subunit (IL-22RA1), which is stably expressed and required for IL-22 signalling (Xie *et al.*, 2000; Gurney, 2004). Additionally, IL-22RA1 expression is reported to be restricted to the epithelial compartment (Gurney, 2004; Nagalakshmi *et al.*, 2004). This simplifies the interpretation of an *IL22RA1* signal from whole tumour tissue RNA analysis, as it is not complicated by levels of infiltrating leukocytes.

IL-22RA1 expression was assessed in formalin fixed, paraffin embedded (FFPE) sections of resected colorectal tumours and matched normal adjacent tissue (Figure 3.3 A). In normal adjacent sections where crypt cross-sectional architecture was intact, IL-22RA1 staining occurred in a regular pattern in the epithelial cells of the crypt, most visible at 40X magnification (Figure 3.3 A). Notably, not every crypt epithelial cell stained positively (Figure 3.3 A). This is consistent with existing murine data, which suggests that IL-22RA1 is expressed by specific epithelial cell subsets in the crypts (Hanash *et al.*, 2012; Lindemans *et al.*, 2015). In tumour sections, where normal crypt architecture was completely lost, the IL-22RA1

expression was more irregular, but was similarly restricted to specific cells within the epithelial compartment (Figure 3.3 A). There was marked heterogeneity in the amount of IL-22RA1 expression in colorectal tumours from different patients, with some patients expressing high amounts (Figure 3.3 A Patient 1) in contrast to other patients where IL-22RA1 was barely detectable (Figure 3.3 A Patient 3). This same heterogeneity was observed upon whole tissue mRNA analysis of *IL22RA1* in prospectively collected tumour biopsies (N=69 patients) (Figure 3.3 B). *IL22RA1* expression was higher in matched normal adjacent compared to CRC tissue and the range of expression between patients was narrower (Figure 3.3 B). Interestingly, tumoural *IL22RA1* expression was highly correlated to *IL22RA1* expression in the normal adjacent tissue (Figure 3.3 C).

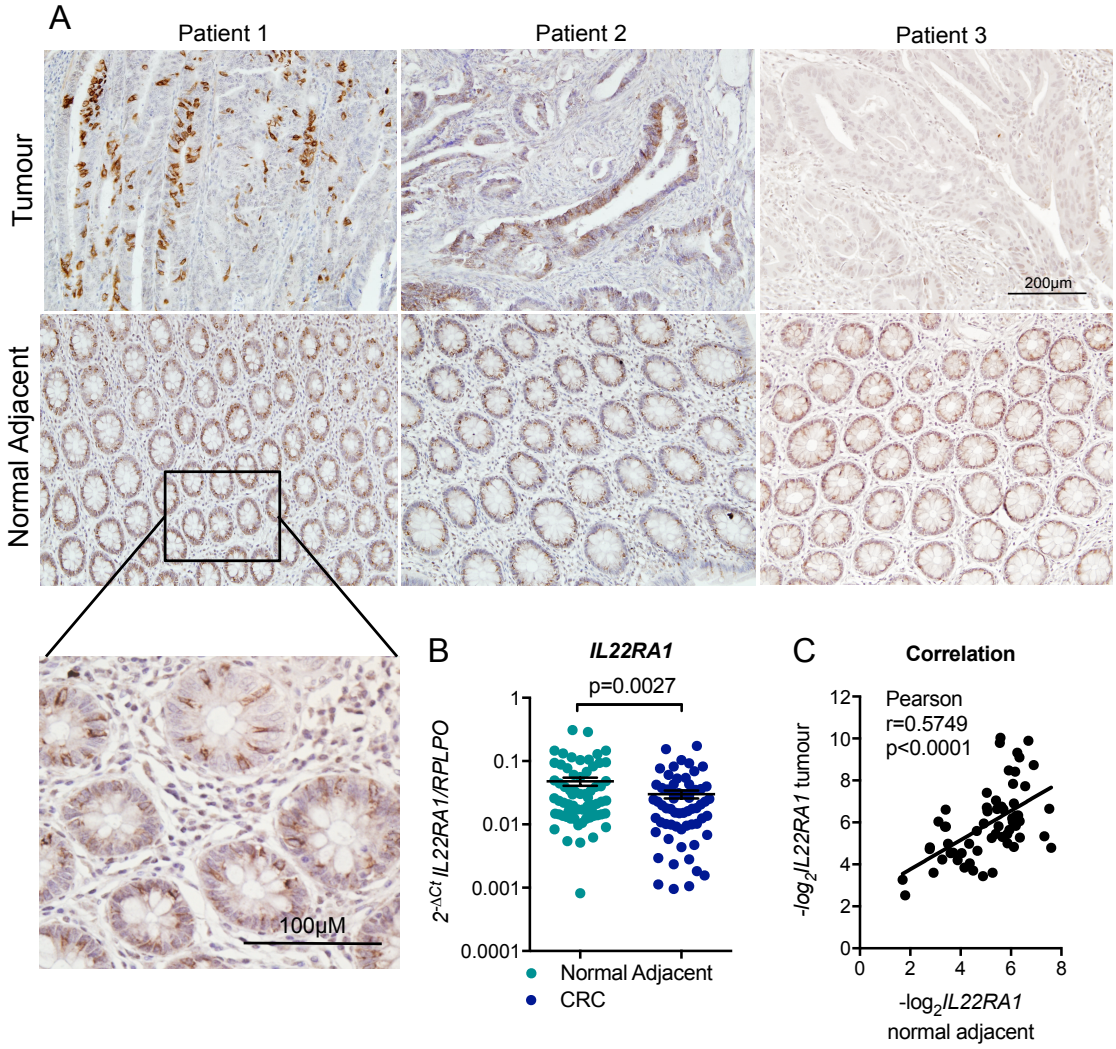


Figure 3.3 IL-22RA1 is differentially expressed in tumours from different colorectal cancer patients.

(A) Immunohistochemical analysis of IL-22RA1 expression in 3 representative colorectal tumours and matched normal adjacent mucosa (20X magnification). Region of normal adjacent mucosa from Patient 1 highlighted at 40X magnification. See Appendix 2.1.2 for negative control staining.

(B) *IL22RA1* expression in fresh/frozen whole tumour and matched normal adjacent tissue. N=69 patients. Statistical significance was determined using a ratio paired T-test comparing tumour (CRC) and matched normal expression for each patient. P<0.05 is significant.

(C) Pearson Correlation analysis of *IL22RA1* expression in tumour versus matched normal adjacent tissue. N=69 patients.

Early descriptions of IL-22 and its cognate IL-22RA1 subunit suggested that expression of the receptor was restricted to epithelial cells and some stromal cell populations (Gurney, 2004; Nagalakshmi *et al.*, 2004). Immunohistochemical analysis of colorectal cancer FFPE sections where both malignant epithelium and an immune infiltrate were visible supports these early observations, since positive IL-22RA1 staining was not visible in the morphologically distinct immune infiltrate (Figure 3.4 A). To systematically determine which cell compartment is the dominant source of IL-22RA1 expression, flow cytometric analysis of fresh CRC biopsies from patients undergoing colectomy was conducted. Single cell suspensions of digested whole tumour were stained for the epithelial marker EpCAM, the hematopoietic lineage marker CD45, and IL-22RA1. EpCAM negative, CD45 negative cells were considered stromal cells for the purposes of this analysis. Live, single, IL-22RA1 positive (IL-22RA1$^+$) cells were gated and the relative contribution of each cell compartment to the total IL-22RA1$^+$ population was assessed (see Chapter 2. Figure 2.2A for gating strategy). EpCAM$^+$ epithelial cells were the dominant IL-22RA1$^+$ cell type. The percentage of total IL-22RA1$^+$ cells that was EpCAM$^+$ was significantly higher than those that were CD45$^+$ or EpCAM$^-$CD45$^-$ (N=7 patients) (Figure 3.4 B). In order to assess the amount of IL-22RA1 expression in each cell compartment, live, single cells were first gated on cell subset specific markers (EpCAM, CD45) and IL-22RA1 expression was assessed in each subpopulation (See Chapter 2. Figure 2.2B for gating strategy). As was observed in the immunohistochemical analysis of IL-22RA1 in CRC sections, the amount of IL-22RA1 expression was highly variable in the EpCAM$^+$ compartment between different patients (Figure 3.4 C, D). IL-22RA1 expression was negligible in the EpCAM$^-$CD45$^-$ cells and CD45$^+$ cells, however two outlying patients had high IL-22RA1 expression in the immune compartment (Figure

3.4 C). We confirmed that IL-22RA1 is predominantly expressed by the epithelium, by assessing *IL22RA1* mRNA in publically available data from sorted human CRCs [GSE39397 (Calon *et al.*, 2012)]. Indeed *IL22RA1* expression is enriched specifically in $EpCAM^{+}CD45^{-}$ cells and negligible expression is present in immune and stromal populations (Figure 3.5 A).

In summary, IL-22RA1 expression is heterogeneous in tumours from different colorectal cancer patients and epithelial cells are the dominant cell type expressing IL-22RA1 in the tumour.

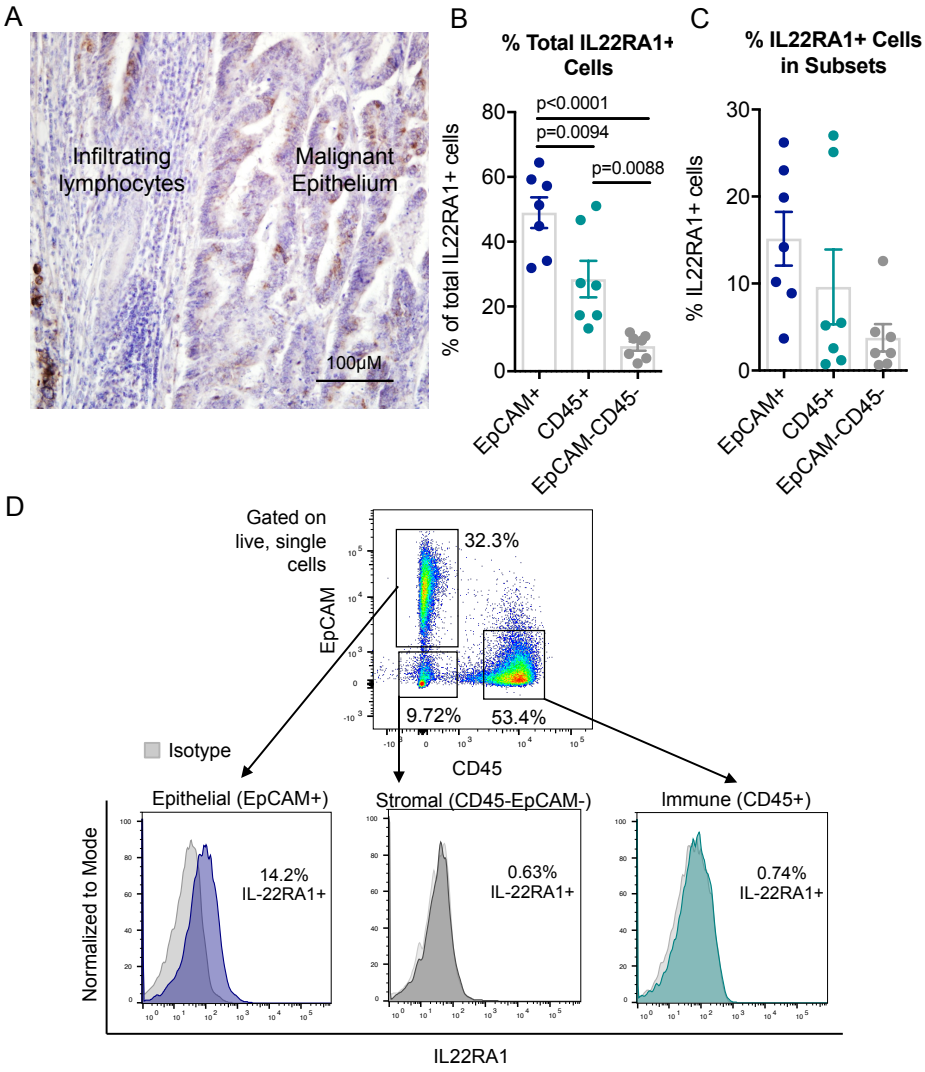


Figure 3.4 IL-22RA1 is expressed predominately on epithelial cells within CRC.

(A) Immunohistochemical analysis of IL-22RA1 in a representative CRC section with a large lymphocytic infiltrate.

(B) Flow cytometric analysis of IL-22RA1 expression in cell suspensions generated from fresh CRC biopsies obtained from patients undergoing colectomy. Cells were gated on live, single, IL-22RA1+ cells. IL-22RA1 positivity was determined by comparison to a matched isotype control. Data represent the relative proportion of each of the major cells types (EpCAM+ [Epithelial], CD45+ [Immune], EpCAM-CD45- [Stromal]) in the IL-22RA1+ population. Each point represents an independent patient [N=7]. Statistical significance was determined using a one-way ANOVA with Tukey's post test for multiple comparisons. P<0.05 is significant. (Gating strategy Chapter 2 Fig.2.2A)

(C) Flow cytometric analysis of IL-22RA1 in samples as described in B. Cells were first gated on live, single cells, and then IL-22RA1 expression was assessed in each subpopulation compared to matched isotype control. Each point represents an independent patient [N=7]. (Gating strategy Chapter 2 Fig.2.2B)

(D) Representative flow cytometry plots showing flow cytometric analysis described in C. Histograms represent IL-22RA1 staining compared to matched isotype control staining for each subpopulation.

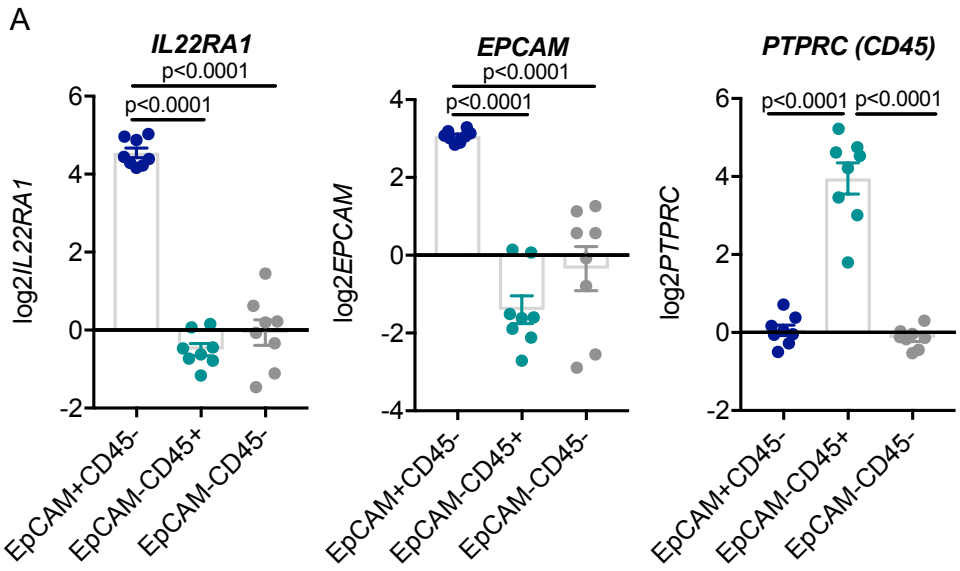


Figure 3.5 *IL22RA1* mRNA is predominately expressed by epithelial cells within human colorectal tumours.

(A) Gene expression in cells from N=8 independent colorectal tumours sorted based on epithelial ($EpCAM^+CD45^-$), immune ($EpCAM^-CD45^+$), and stromal ($EpCAM^-CD45^-$) markers from GSE39397 cohort (Calon *et al.*, 2012). RNA was extracted and microarrays were performed. Expression is median normalised log2 expression from each of the indicated gene probes. The purity of the sorted populations is indicated by enrichment of *EPCAM* and *PTPRC* (encoding CD45) in the $EpCAM^+CD45^-$ and $EpCAM^-CD45^+$ compartments respectively. Statistical significance was determined using a one-way ANOVA with Tukey's post test for multiple comparisons. $P<0.05$ is significant.

3.2.3 *KRAS* mutation is prognostic in patients whose tumours express high levels of the interleukin 22-receptor gene.

Given the observed heterogeneity of expression of IL-22RA1 in tumours from different colorectal cancer patients, we next sought to determine whether IL-22RA1 expression impacts CRC patient survival. *IL22RA1* gene expression was first assessed in stage II/III CRC specimens using transcriptomic-profiling data from a publically available, population-based cohort (GSE39582, N=566) (Marisa *et al.*, 2013), which we used as a training/discovery dataset. Findings were validated using gene expression data from randomized stage III CRC patients enrolled in the PETACC3 (NCT00026273) phase III clinical trial (N=752) (Popovici *et al.*, 2012; Roth *et al.*, 2012). Finally, a merged dataset comprising stage II/III CRC patients of the

GSE39582, PETACC3, and two additional independent cohorts, TCGA and ALMAC, representing 2332 patients, was used as an additional confirmation cohort (referred to in tables as the "Combined" dataset) (Figure 3.6 A). After excluding patients with missing data or non-stage II/III tumours the number of patients that remained for analysis of *IL22RA1* expression are outlined in the CONSORT diagram below (Figure 3.6 A). [1]

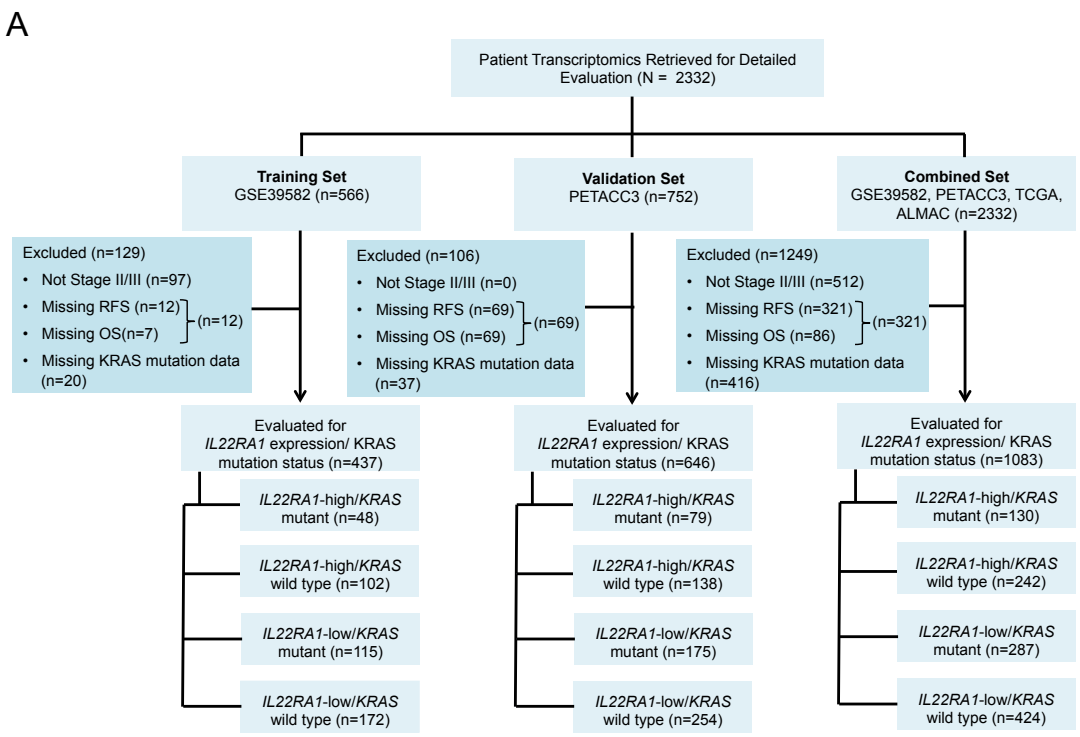


Figure 3.6 CONSORT diagram illustrating training and validation set methodology.

(A) Training and validation set approach used to assess the prognostic consequence of having high or low expression of *IL22RA1* in the presence or absence of *KRAS* mutation. The total number of patients in each cohort, excluded patients, and number of patients in each molecular subtype of interest are indicated. (RFS data is missing from the TCGA dataset, thus numbers for RFS versus OS analysis in the combined cohort differ significantly.)

[1] Note that the PETACC3 dataset is a proprietary dataset from the PETACC3 clinical trial. Through a collaboration with Professor Sabine Tejpar (KU, Leuven), use of the PETACC3 dataset as a validation set was possible. Dr. David Barras, a collaborating bioinformatician at the Swiss Institute of Bioinformatics (Lausanne, Switzerland) conducted the confirmation analysis in the PETACC3 dataset and combined cohort. Data from his analyses are included in the tables in this chapter.

IL22RA1 was expressed as a continuous variable with a roughly normal distribution in the cohorts (Figure 3.7 A). Therefore, to determine an optimal cut-off value to classify tumours as *IL22RA1*-high versus *IL22RA1*-low, receiver operator characteristic (ROC) analysis was performed using log2 *IL22RA1* expression values in the training cohort (GSE39582). The presence or absence of disease relapse at last follow-up was used as the binary variable in this analysis. The *IL22RA1* cut-off value associated with the maximum Youden index (J = sensitivity + specificity – 1) was found to be the 67th percentile. This value was used for all downstream analyses of *IL22RA1* in both the training, validation, and combined cohorts.

A contingency analysis (Fisher's exact test) was performed to assess the association of clinicopathological features with *IL22RA1* expression status. High *IL22RA1* expression was found to be associated with distal tumour location (distal to the splenic flexure) and microsatellite stable (MSS) tumours. *IL22RA1* expression was not associated with *KRAS* mutation status, *BRAF* mutation status, gender, or tumour stage (II versus III) (Figure 3.7 B).

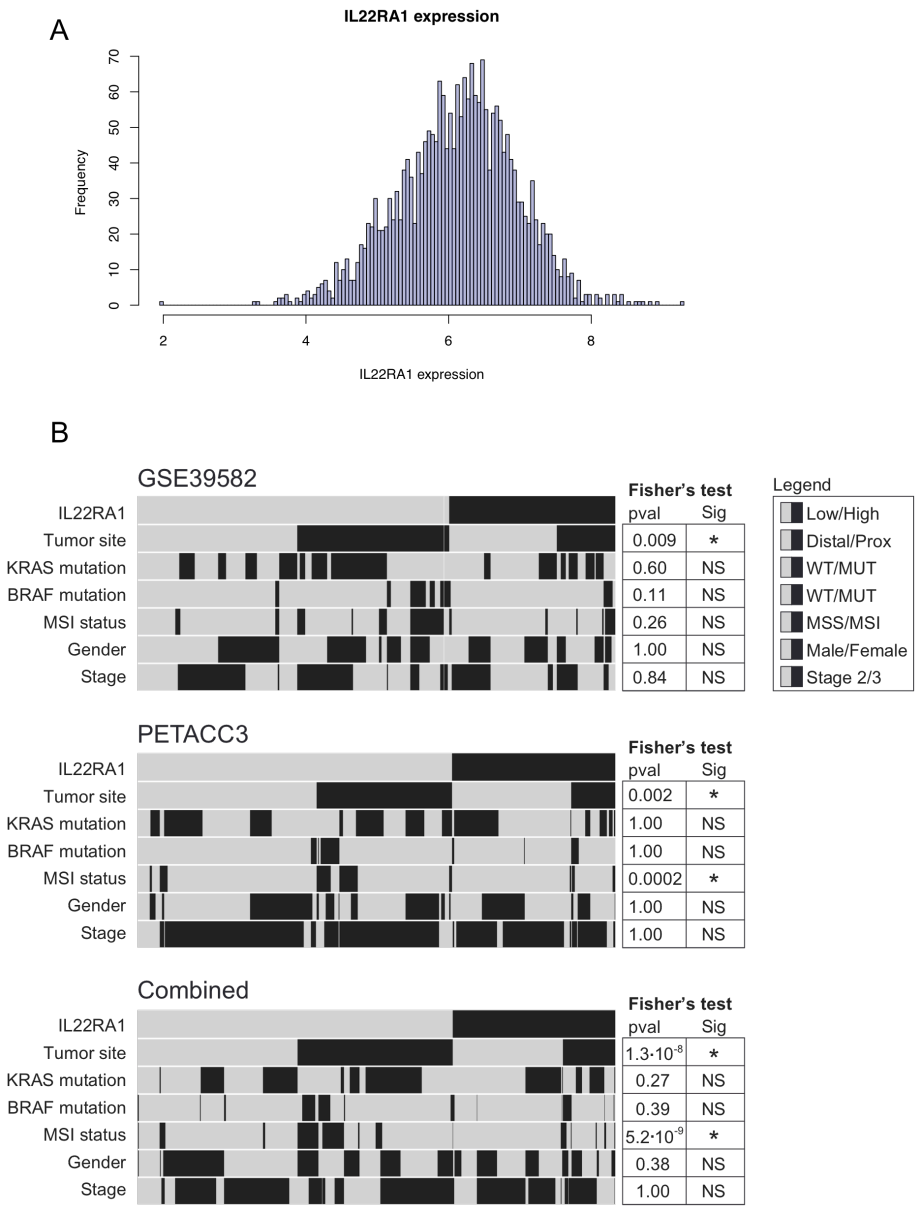


Figure 3.7 High *IL22RA1* expression is associated with distally located tumours and microsatellite stability.

(A) Distribution of *IL22RA1* expression in combined GSE39582, PETACC3, and TCGA datasets (n=1188). Patients for whom clinical information was not complete were removed from this analysis.

(B) Fisher's exact test were used to examine the association of *IL22RA1* expression (low/high) with: tumour location (distal to the splenic flexure [distal]/proximal to the splenic flexure [proximal]), *KRAS* mutation status (WT/MUT), BRAF mutation status (WT/MUT), microsatellite stability (microsatellite stable [MSS]/microsatellite instable [MSI]), gender (male/female), and stage (2/3) in the training (GSE39582), confirmation (PETACC3), and combined cohorts. *p<0.05, Fisher's exact test.

To determine the prognostic consequence of having high or low tumoural *IL22RA1* expression, patients in the training cohort (GSE39582) were stratified based on *IL22RA1* expression, relapse-free survival (RFS), and overall survival (OS). Univariate Cox's proportional hazard regression models demonstrated that *IL22RA1* expression had no impact on relapse-free survival (Figure 3.8 A) or overall survival (Figure 3.9 A) in the training cohort.

Given the capacity for oncogenic Ras to modulate inflammation and the potential for Ras involvement in IL-22 signalling, we tested the hypothesis that *KRAS* mutation is prognostic specifically in patients with high *IL22RA1* expression. Consistent with prior reports (Roth *et al.*, 2010), activating *KRAS* mutations were weakly associated with poor clinical outcome (Figure 3.8 B, Figure 3.9 B). However, among cases with high *IL22RA1* expression, *KRAS* mutations were strongly associated with poor RFS (*HR*=2.93, 95% CI=1.59-5.43, *P*=0.0006) (Figure 3.8 C) and OS (*HR*=2.45, 95% CI=1.38-4.36, *P*=0.0023) (Figure 3.9 C). In contrast, *KRAS* mutations had no prognostic impact in patients with *IL22RA1*-low tumours in terms of RFS (*HR*=1.16, 95% CI=0.76-1.78, *P*=0.4840) (Figure 3.8 D) or OS (*HR*=1.05, 95% CI=0.69-1.61, *P*=0.813) (Figure 3.9 D).[2] This prognostic association between *IL22RA1* and *KRAS* was validated in the PETACC3 clinical trial confirmation cohort (Table 3.1). Finally, in the large combined cohort totalling 1,820 patients, the negative prognostic effect of *KRAS* mutation in patients with *IL22RA1*-high tumours was marked (RFS *HR*=2.05, 95% CI=1.45-2.89, *P*<0.0001; OS *HR*=1.65, 95% CI=1.09-2.50, *P*=0.018) (Table 3.1).

[2] Note that this initial stratification in the GSE39582 cohort was performed by N. West.

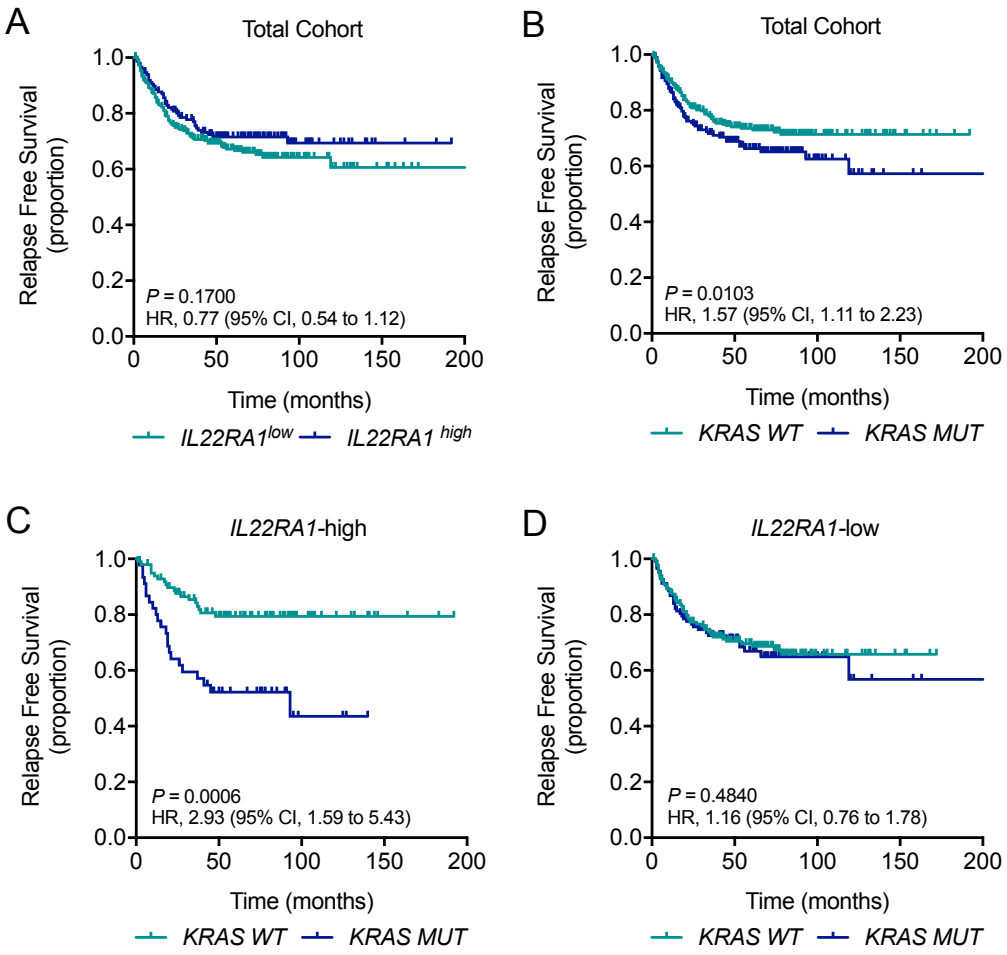


Figure 3.8 High *IL22RA1* expression promotes poor relapse free survival in *KRAS* mutant CRC.

Relapse free survival (RFS) in Stage II/III patients in the GSE39582 training cohort estimated using Kaplan-Meier methods.

(A) RFS in the training cohort based on *IL22RA1* expression. *IL22RA1*-high and low is defined by a cutpoint at the 67th percentile determined using Receiver operator characteristic (ROC) analysis in the training cohort. This cutpoint was used to define *IL22RA1*-high and low in all downstream analyses.
(B) RFS in the training cohort based on *KRAS* mutation status.
(C) RFS among *IL22RA1*-high patients based on *KRAS* mutation status.
(D) RFS among *IL22RA1*-low patients based on *KRAS* mutation status.

P values were computed using Wald-tests. Hazard ratios (HR) are univariate Cox proportional hazard ratios with 95% confidence intervals.

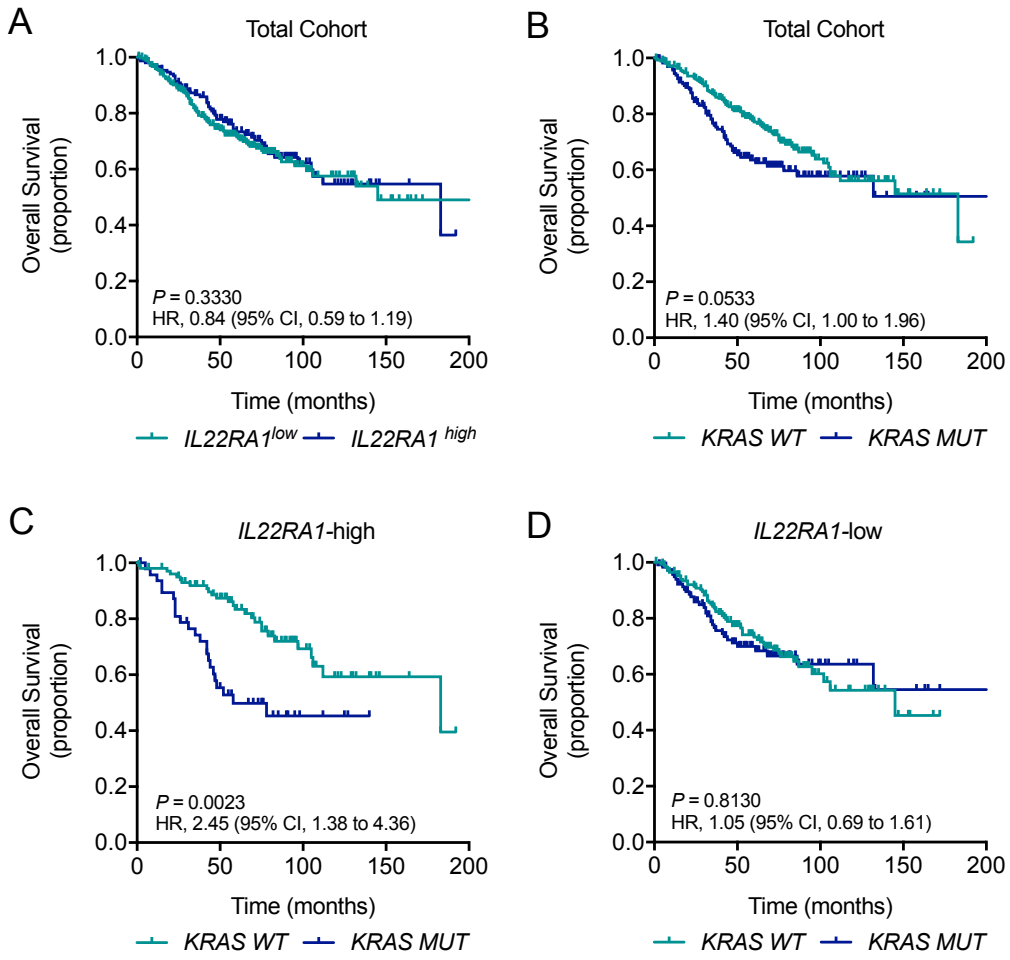


Figure 3.9 High *IL22RA1* expression promotes poor overall survival in *KRAS* mutant CRC.

Overall survival (OS) in Stage II/III patients in the GSE39582 training cohort estimated using Kaplan-Meier methods.

(A) OS in the training cohort based on *IL22RA1* expression. *IL22RA1*-high and low is defined by a cutpoint at the 67th percentile determined using Receiver operator characteristic (ROC) analysis in the training cohort. This cutpoint was used to define *IL22RA1*-high and low in all downstream analyses.
(B) OS in the training cohort based on *KRAS* mutation status.
(C) OS among *IL22RA1*-high patients based on *KRAS* mutation status.
(D) OS among *IL22RA1*-low patients based on *KRAS* mutation status.

P values were computed using Wald-tests. Hazard ratios (HR) are univariate Cox proportional hazard ratios with 95% confidence intervals.

Table 3.1. Survival analysis (RFS and OS) for Stage II, III patients of GSE39582, PETACC3 and combined dataset (univariate analysis)

		RFS			OS		
	No.	*P*	HR	95% CI	*P*	HR	95% CI
GSE39582							
IL22RA1^{high} / IL22RA1^{low}	157 / 312	0.1700	0.77	0.54 to 1.12	0.3330	0.84	0.59 to 1.19
KRAS mut / KRAS WT	169 / 279	**0.0103**	**1.57**	**1.11 to 2.23**	0.0533	1.40	1.00 to 1.96
Within IL22RA1^{low}: KRAS mut / KRAS WT	120 / 176	0.4840	1.16	0.76 to 1.78	0.8130	1.05	0.69 to 1.61
Within IL22RA1^{high}: KRAS mut / KRAS WT	49 / 103	**0.0006**	**2.93**	**1.59 to 5.43**	**0.0023**	**2.45**	**1.38 to 4.36**
Within KRAS WT: IL22RA1^{high} / IL22RA1^{low}	103 / 176	**0.0365**	**0.57**	**0.34 to 0.97**	0.0650	0.64	0.40 to 1.03
Within KRAS mut: IL22RA1^{high} / IL22RA1^{low}	49 / 120	0.1860	1.43	0.84 to 2.42	0.1930	1.43	0.84 to 2.43
PETACC3							
IL22RA1^{high} / IL22RA1^{low}	247 / 505	0.4160	1.11	0.86 to 1.43	0.7300	0.95	0.70 to 1.28
KRAS mut / KRAS WT	283 / 425	**0.0215**	**1.34**	**1.04 to 1.72**	**0.0051**	**1.51**	**1.13 to 2.02**
Within IL22RA1^{low}: KRAS mut / KRAS WT	194 / 278	0.2660	1.19	0.87 to 1.63	0.1260	1.32	0.92 to 1.88
Within IL22RA1^{high}: KRAS mut / KRAS WT	89 / 147	**0.0149**	**1.68**	**1.11 to 2.56**	**0.0070**	**2.00**	**1.21 to 3.30**
Within KRAS WT: IL22RA1^{high} / IL22RA1^{low}	147 / 278	0.8800	0.97	0.68 to 1.39	0.3890	0.83	0.54 to 1.27
Within KRAS mut: IL22RA1^{high} / IL22RA1^{low}	89 / 194	0.1040	1.38	0.94 to 2.02	0.3670	1.22	0.79 to 1.89
Combined							
IL22RA1^{high} / IL22RA1^{low}	590 / 1230	0.9200	0.99	0.83 to 1.19	0.4170	0.93	0.77 to 1.12
KRAS mut / KRAS WT	515 / 881	**0.0006**	**1.43**	**1.16 to 1.75**	**0.0054**	**1.35**	**1.09 to 1.66**
Within IL22RA1^{low}: KRAS mut / KRAS WT	361 / 570	0.1800	1.19	0.92 to 1.53	0.5030	1.09	0.84 to 1.42
Within IL22RA1^{high}: KRAS mut / KRAS WT	154 / 311	**0.0000**	**2.05**	**1.45 to 2.89**	**0.0001**	**2.07**	**1.44 to 2.96**
Within KRAS WT: IL22RA1^{high} / IL22RA1^{low}	311 / 570	0.1390	0.80	0.60 to 1.07	**0.0468**	**0.74**	**0.55 to 1.00**
Within KRAS mut: IL22RA1^{high} / IL22RA1^{low}	154 / 361	**0.0465**	**1.37**	**1.00 to 1.87**	0.0660	1.36	0.98 to 1.89

Table 3.1 Univariate survival analysis of stage II/III CRC patients in training, validation, and combined cohorts based on *IL22RA1* and *KRAS* mutation status.

Univariate Cox proportional hazard survival analyses were performed to determine the prognostic consequence of having high or low *IL22RA1* expression in the context of *KRAS* mutation in the training (GSE39582), confirmation (PETACC3), and combined cohorts. *IL22RA1*-high and low is defined by a cutpoint at the 67th percentile determined using Receiver operator characteristic (ROC) analysis in the training cohort. This cutpoint was used to define *IL22RA1*-high and low in all downstream analyses. Cox proportional hazard ratios (HR) for relapse free survival (RFS) and overall survival (OS) are displayed with 95% confidence intervals (95% CI). Significant results are bolded. Patient numbers (No.) in each subgroup are indicated.

3.2.4 *IL22RA1* does not interact with other common oncogenic driving mutations in colorectal cancer.

Sporadic and colitis-associated colorectal cancers are characterised by the sequential acquisition of somatic gain-of-function mutations in oncogenes and loss-of-function mutations in tumour suppressors. Activating point mutations in *KRAS* are among the most common oncogene mutations in CRC, with an estimated frequency of approximately 40% (Fearon, 2011). Activating mutations in *BRAF,* encoding BRAF protein directly downstream of KRAS in the Ras-Raf-MEK signalling cascade, are much more infrequent and are estimated to occur in roughly 5-10% of CRCs (Fearon, 2011). Activating *BRAF* mutations are mutually exclusive with activating *KRAS* mutations (Popovici *et al.*, 2012). *APC*, which encodes the adenomatous polyposis

coli (APC) protein, is the most commonly mutated tumour suppressor gene in CRC, with mutations found in 80% of CRC patients (Fearon, 2011; Cancer Genome Atlas Network and Muzny, 2012). Inactivating mutations in *APC* are thought to be an initiating event in sporadic CRC and are believed to be rate-limiting in adenoma development (Fearon and Vogelstein, 1990). Finally, allelic loss of *TP53* coupled with inactivating mutations occur in an estimated 60-70% of CRCs (Fearon, 2011) and p53 is known to be an important regulator of inflammatory pathways (Cooks, Harris and Oren, 2014).

To determine whether *IL22RA1* was prognostic in other mutational subtypes of CRC, we stratified patients according to *IL22RA1* and mutations for which data were available. *TP53* mutation status did not stratify patients with high *IL22RA1* expression in terms of RFS or OS (Figure 3.10 C, D), as was the case for *KRAS* mutation. Indeed, in contrast to *KRAS* mutation, patients with *IL22RA1*-low, *TP53* mutant tumours had modestly poorer RFS (*HR*=1.69, 95% CI=1.04-2.75, *P*=0.032) and OS (*HR*=1.65, 95% CI=1.01-2.71, *P*=0.043) (Figure 3.10 E, F).

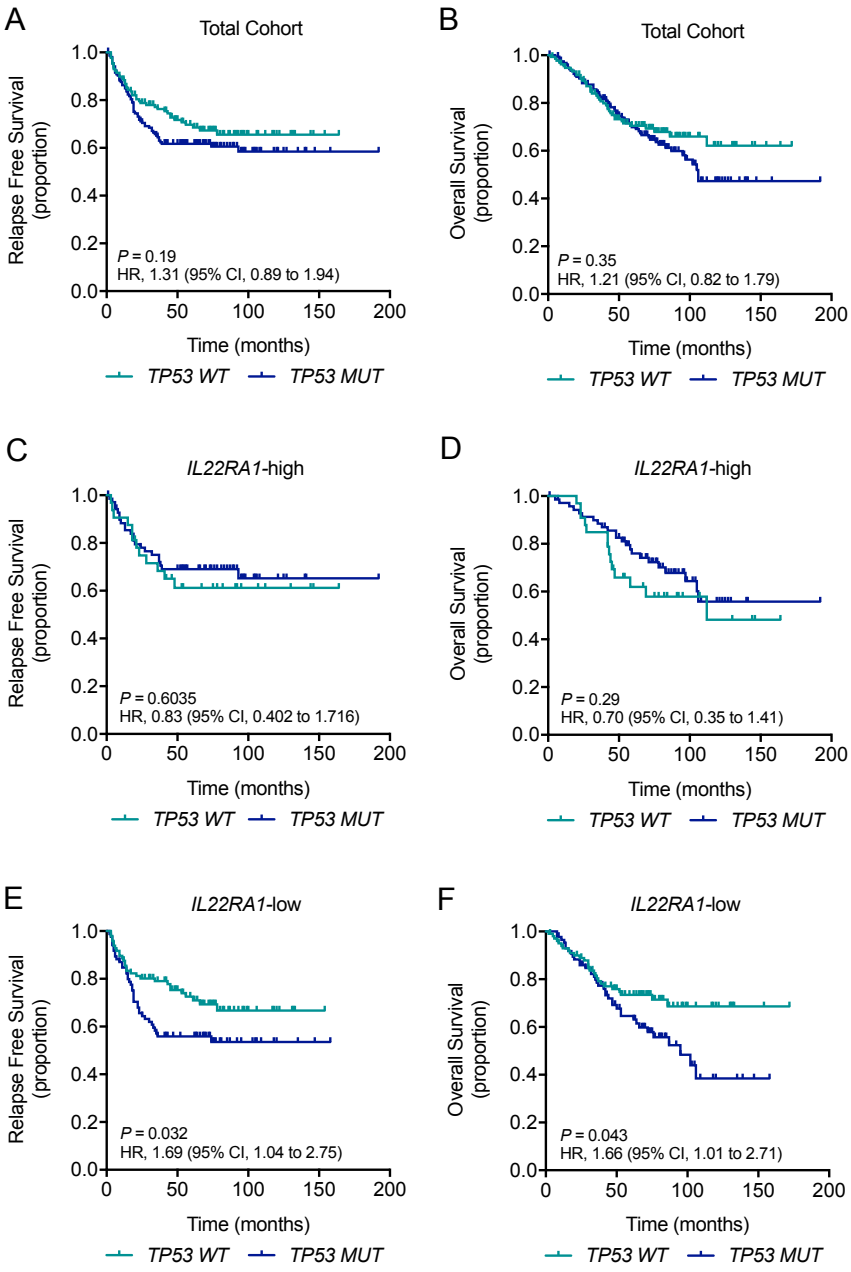


Figure 3.10 *TP53* mutation status does not stratify patients with high *IL22RA1* expression.

Relapse free survival (RFS) and overall survival (OS) in Stage II/III patients in the GSE39582 training cohort estimated using Kaplan-Meier methods.

(A) RFS in the training cohort based on *TP53* mutation status.
(B) OS in the training cohort based on *TP53* mutation status.
(C) RFS among IL22RA1-high patients based on *TP53* mutation status.
(D) OS among IL22RA1-high patients based on *TP53* mutation status.
(E) RFS among IL22RA1-low patients based on *TP53* mutation status.
(F) OS among IL22RA1-low patients based on *TP53* mutation status.

P values were computed using Wald-tests. Hazard ratios (HR) are univariate Cox proportional hazard ratios with 95% confidence intervals.

Due to the low prevalence of *BRAF* mutations in CRC, only N=6 *IL22RA1*-high, *BRAF* mutant patients were present in the training cohort, precluding robust survival analyses. However, we conducted a multivariate Cox proportional hazard test for interaction between *IL22RA1* and *KRAS* mutation in the combined cohort that included the following covariates: *BRAF* mutation status, gender, tumour site (proximal vs distal), and microsatellite stability or instability. The interaction between *IL22RA1* and *KRAS* mutation was found to be highly significant in terms of RFS (*HR*=1.99, 95% CI=1.24-2.89, *P*=0.0031), and therefore independent of *BRAF* mutation (Table 3.2).

3.2.5 *KRAS* mutation does not stratify patients with high expression of the interleukin 6 or interleukin 17 receptors.

Data from preclinical models suggest that numerous cytokines may influence CRC progression. Interleukin 6 (IL-6), for example, has a well-documented role in CRC and drives similar signal transduction pathways to IL-22 (Bollrath *et al.*, 2009; Grivennikov *et al.*, 2009). A role for interleukin 17A (IL-17A) in CRC has also been elucidated in preclinical models (S. Wu *et al.*, 2009; Chae *et al.*, 2010; Grivennikov *et al.*, 2012; Hyun *et al.*, 2012; K. Wang *et al.*, 2014) and high expression of a functional Th17 signature associates with poor prognosis in human CRC (Tosolini *et al.*, 2011). The production of IL-17A, like IL-22, is induced by IL-23, and IL-6 is a critical driver of Th17 cell differentiation.

To determine whether the level of expression of the IL-6 receptor (*IL6R*) or IL-17 receptor (*IL17RA*) impacts prognosis depending upon *KRAS* mutation status, Cox proportional hazard tests for interaction were performed. Patients in the top tertile (33%) of expression for each cytokine receptor gene were classified as “high”. Tests

for interaction were performed by including cytokine receptor expression and *KRAS* mutation status, as well as their cross product, in the Cox proportional hazard model and testing the significance of the cross product term for each cytokine receptor gene. This interaction analysis was performed in the combined cohort to ensure adequate power to detect interactions in subgroup analyses. The interaction between *IL22RA1* expression and *KRAS* mutation was highly significant in univariate analysis in terms of both RFS (*HR*=1.76, 95% CI=1.17-2.63, *P*=0.0065) and OS (*HR*=1.65, 95% CI=1.09-2.50, *P*=0.0179) (Table 3.2). This interaction was independent of *BRAF* mutation status, microsatellite stability or instability, gender, and tumour site, as determined in multivariate interaction analyses (Table 3.2). However no interaction between *IL6R* or *IL17RA* expression and *KRAS* mutation status was detectable (Table 3.2).

Therefore, despite the fact that IL-6 induces similar downstream signalling pathways to IL-22 or that the production of IL-17A is also induced by IL-23, the interaction between cytokine receptor gene expression and *KRAS* mutation is unique to *IL22RA1*.

Table 3.2 Coxph interaction analysis (RFS and OS) for stage II, III patients from combined dataset (GSE39582, PETACC3, TCGA, ALMAC)

	RFS			OS		
Univariate	***P***	**HR**	**95% CI**	***P***	**HR**	**95% CI**
*IL22RA1 * KRAS mut*	**0.0065**	**1.76**	**1.17 to 2.63**	**0.0179**	**1.65**	**1.09 to 2.50**
*IL6R * KRAS mut*	0.4763	1.16	0.77 to 1.75	0.2205	1.30	0.85 to 1.98
*IL17RA * KRAS mut*	0.5082	1.15	0.76 to 1.76	0.4399	0.84	0.55 to 1.30
*Site * KRAS mut*	0.9535	0.99	0.66 to 1.48	0.8421	0.96	0.64 to 1.43
Multivariate (BRAF, MSI status, Gender, Tumour site)						
*IL22RA1 * KRAS mut*	**0.0031**	**1.89**	**1.24 to 2.89**	0.0640	1.52	0.98 to 2.36
*IL6R * KRAS mut*	0.6282	1.11	0.73 to 1.70	0.3577	1.23	0.79 to 1.93
*IL17RA * KRAS mut*	0.7419	1.08	0.69 to 1.68	0.6561	0.90	0.56 to 1.43

Table 3.2 *KRAS* mutation interacts with *IL22RA1* but not *IL6R* or *IL17RA* in univariate and multivariate interaction analyses.

Univariate and multivariate Cox proportional hazard interaction analyses were performed to determine whether *IL22RA1*, *IL6R* or *IL17RA* interacts with *KRAS* mutation in Stage II/III patients the combined cohort. The top tertile for each receptor gene was classified as "high". Cox proportional hazard ratios (HR) for relapse free survival (RFS) and overall survival (OS) are displayed with 95% confidence intervals (95% CI). Significant interactions are bolded. Covariates included in the multivariate analysis were: BRAF mutation status, microsatellite stability/instability status, gender, and tumour site.

3.2.6 Unbiased analysis of cytokines and cytokine receptors that interact with *KRAS* mutation.

Although *IL6R* and *IL17RA* expression did not interact with *KRAS* mutation, this does not exclude the possibility that other cytokine pathways interact with *KRAS* mutation. Therefore, to determine whether other cytokines and/or their cognate receptors stratify patients with *KRAS* mutations in terms of survival, Cox proportional hazard interaction analyses were performed on all cytokine and cytokine receptor genes (classifying the highest expression tertile for each gene as "high") and *KRAS* mutation status in the combined cohort. While several cytokine/cytokine receptor genes interacted with *KRAS* mutation, *IL22RA1* was the top hit (Table 3.3). Remarkably, *IL10RB*, which encodes the second subunit of the heterodimeric IL-22 receptor, was a similarly strong interactor (Table 3.3, Table 3.4). Detailed survival analysis in the training cohort (GSE39582) revealed that like *IL22RA1*, patients whose tumours were *IL10RB*-high and *KRAS*-mutant had dramatically worsened prognosis compared to

their *KRAS* wild type counterparts in terms of both RFS (*HR*=3.62, 95% CI=1.95-6.70, *P*<0.0001, Figure 3.11 C) and OS (*HR*=2.43, 95% CI=1.33-4.45, *P*=0.0039, Figure 3.11 D). *KRAS* mutation was not prognostic in *IL10RB*-low patients (Figure 3.11 E, F). Though this association did not quite reach statistical significance in the confirmation cohort (PETACC3), in the larger combined cohort, the association between *IL10RB* expression and *KRAS* mutation was highly significant (RFS *HR*=1.89, 95% CI=1.36-2.63, *P*=0.0002; OS *HR*=1.73, 95% CI=1.21-2.48, *P*=0.0027) (Table 3.5).

Table 3.3 Results of unbiased interaction coxph survival analysis between cytokines/cytokine receptors and KRAS mutation in combined dataset

	RFS	OS
Name	***P***	***P***
*IL22RA1 * KRAS mut*	**0.0065**	**0.0179**
*IL10RB * KRAS mut*	**0.0177**	**0.0463**
*IL13RA2 * KRAS mut*	**0.0403**	0.2549
*IL3RA * KRAS mut*	**0.0489**	0.0731
*IL1RAP * KRAS mut*	0.1176	**0.0437**
*IL17RD * KRAS mut*	0.1593	**0.0044**
*IL4R * KRAS mut*	0.3131	0.7395
*IL32 * KRAS mut*	0.5130	**0.0362**

Table 3.3 Unbiased Coxph interaction analysis between cytokines/cytokine receptors and *KRAS* mutation in combined dataset.

Univariate Cox proportional hazard interaction analyses were performed on all cytokine and cytokine receptor genes (classifying the highest expression tertile for each gene as “high”) and *KRAS* mutation status in the combined cohort. Cox proportional hazard ratios (HR) for relapse free survival (RFS) and overall survival (OS) are displayed. Significant interactions are bolded.

Table 3.4 Survival analysis (RFS and OS) for Stage II, III patients of GSE39582, PETACC3 and combined dataset (univariate analysis)

	RFS			OS		
Name	***P***	**HR**	**95% CI**	***P***	**HR**	**95% CI**
Within **IL22RA1^{low}**: KRAS mut / KRAS WT	0.18000	0.84	0.66 to 1.08	0.50300	1.09	0.84 to 1.42
Within **IL22RA1^{high}**: KRAS mut / KRAS WT	**0.00005**	**2.05**	**1.45 to 2.89**	**0.00008**	**2.07**	**1.44 to 2.96**
Within **IL10RB^{low}**: KRAS mut / KRAS WT	0.12500	1.22	0.95 to 1.58	0.17100	1.20	0.92 to 1.56
Within **IL10RB^{high}**: KRAS mut / KRAS WT	**0.00017**	**1.89**	**1.36 to 2.63**	**0.00267**	**1.73**	**1.21 to 2.48**
Within **IL13RA2^{low}**: KRAS mut / KRAS WT	**0.00002**	**1.69**	**1.33 to 2.15**	**0.00126**	**1.51**	**1.18 to 1.94**
Within **IL13RA2^{high}**: KRAS mut / KRAS WT	0.81300	0.95	0.65 to 1.40	0.89000	1.03	0.69 to 1.53
Within **IL3RA^{low}**: KRAS mut / KRAS WT	0.11600	1.22	0.95 to 1.57	0.18200	1.19	0.92 to 1.55
Within **IL3RA^{high}**: KRAS mut / KRAS WT	**0.00021**	**1.92**	**1.36 to 2.71**	**0.00336**	**1.71**	**1.19 to 2.44**
Within **IL1RAP^{low}**: KRAS mut / KRAS WT	**0.00096**	**1.50**	**1.18 to 1.90**	**0.00435**	**1.45**	**1.12 to 1.86**
Within **IL1RAP^{high}**: KRAS mut / KRAS WT	0.23800	1.26	0.86 to 1.86	0.42500	1.17	0.80 to 1.72
Within **IL17RD^{low}**: KRAS mut / KRAS WT	**0.00041**	**1.57**	**1.22 to 2.02**	**0.00006**	**1.68**	**1.30 to 2.16**
Within **IL17RD^{high}**: KRAS mut / KRAS WT	0.38900	1.16	0.82 to 1.65	0.48500	0.87	0.60 to 1.28
Within **IL4R^{low}**: KRAS mut / KRAS WT	0.05210	1.29	1.00 to 1.66	0.07580	1.27	0.98 to 1.65
Within **IL4R^{high}**: KRAS mut / KRAS WT	**0.00142**	**1.73**	**1.23 to 2.41**	**0.02300**	**1.50**	**1.06 to 2.13**
Within **IL32^{low}**: KRAS mut / KRAS WT	**0.01920**	**1.34**	**1.05 to 1.70**	0.23700	1.16	0.90 to 1.50
Within **IL32^{high}**: KRAS mut / KRAS WT	**0.01350**	**1.59**	**1.10 to 2.31**	**0.00180**	**1.84**	**1.26 to 2.71**

Table 3.4 Univariate Coxph survival analysis for cytokines and cytokine receptors found to interact with *KRAS* in unbiased screen.

Univariate Cox proportional hazard survival analyses were performed on all cytokines and cytokine receptors found to interact with *KRAS* in the combined cohort. Cox proportional hazard ratios (HR) for relapse free survival (RFS) and overall survival (OS) are displayed with 95% confidence intervals (95% CI). Significant results are bolded.

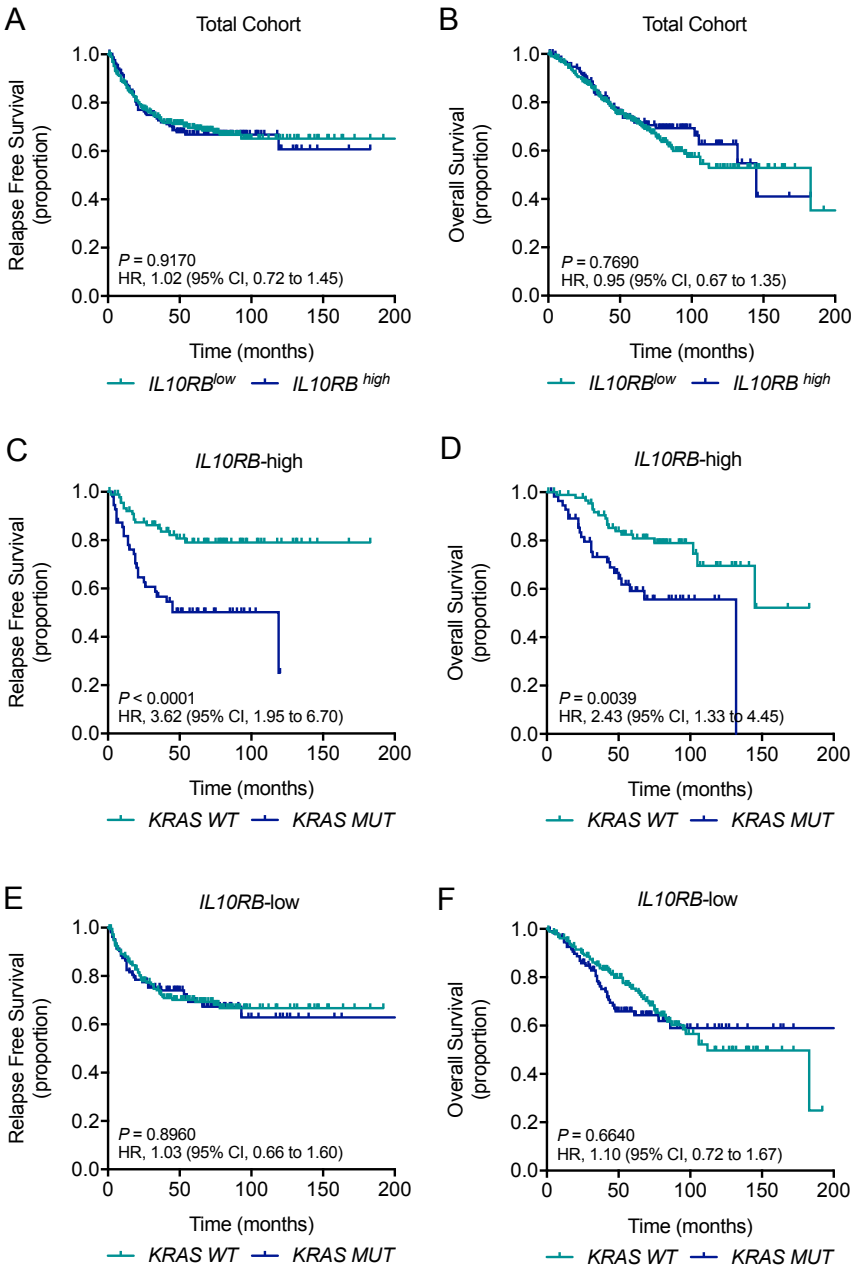


Figure 3.11 High expression of *IL10RB*, the second subunit of the heterodimeric IL-22R, confers poor relapse free and overall survival in *KRAS* mutant CRC.

Relapse free survival (RFS) and overall survival (OS) in Stage II/III patients in the GSE39582 training cohort estimated using Kaplan-Meier methods.

(A) RFS in the training cohort based on *IL10RB* expression. *IL10RB*-high and low is defined by a cutpoint at the 67th percentile
(B) OS in the training cohort based on *IL10RB* expression.
(C) RFS among *IL10RB*-high patients based on *KRAS* mutation status.
(D) OS among *IL10RB*-high patients based on *KRAS* mutation status.
(E) RFS among *IL10RB*-low patients based on *KRAS* mutation status.
(F) OS among *IL10RB*-low patients based on *KRAS* mutation status.

P values were computed using Wald-tests. Hazard ratios (HR) are univariate Cox proportional hazard ratios with 95% confidence intervals.

Table 3.5 Survival analysis (RFS and OS) for Stage II, III patients of GSE39582, PETACC3 and combined dataset (univariate analysis)

		RFS			OS		
	No.	*P*	HR	95% CI	*P*	HR	95% CI
GSE39582							
IL10RB^{high} / IL10RB^{low}	157 / 312	0.9170	1.02	0.72 to 1.45	0.7690	0.95	0.67 to 1.35
KRAS mut / KRAS WT	169 / 279	**0.0103**	**1.57**	**1.11 to 2.23**	0.0533	1.40	1.00 to 1.96
Within IL10RB^{low}: KRAS mut / KRAS WT	112 / 187	0.8960	1.03	0.66 to 1.60	0.6640	1.10	0.72 to 1.67
Within IL10RB^{high}: KRAS mut / KRAS WT	57 / 92	**0.0000**	**3.62**	**1.95 to 6.70**	**0.0039**	**2.43**	**1.33 to 4.45**
Within KRAS WT: IL10RB^{high} / IL10RB^{low}	92 / 187	**0.0256**	**0.53**	**0.30 to 0.93**	0.0938	0.65	0.40 to 1.08
Within KRAS mut: IL10RB^{high} / IL10RB^{low}	57 / 112	**0.0196**	**1.84**	**1.10 to 3.07**	0.2840	1.34	0.79 to 2.27
PETACC3							
IL10RB^{high} / IL10RB^{low}	248 / 504	**0.0131**	**1.36**	**1.07 to 1.74**	0.2820	1.17	0.88 to 1.57
KRAS mut / KRAS WT	283 / 425	**0.0215**	**1.34**	**1.04 to 1.72**	**0.0051**	**1.51**	**1.13 to 2.02**
Within IL10RB^{low}: KRAS mut / KRAS WT	189 / 280	0.0856	1.33	0.96 to 1.84	**0.0302**	**1.51**	**1.04 to 2.18**
Within IL10RB^{high}: KRAS mut / KRAS WT	94 / 145	0.0981	1.39	0.94 to 2.05	0.0577	1.57	0.99 to 2.51
Within KRAS WT: IL10RB^{high} / IL10RB^{low}	145 / 280	0.0520	1.40	1.00 to 1.96	0.3140	1.23	0.82 to 1.86
Within KRAS mut: IL10RB^{high} / IL10RB^{low}	94 / 189	0.0580	1.44	0.99 to 2.10	0.2920	1.26	0.82 to 1.94
Combined							
IL10RB^{high} / IL10RB^{low}	590 / 1230	0.1190	1.15	0.96 to 1.37	0.4830	1.07	0.89 to 1.28
KRAS mut / KRAS WT	515 / 881	**0.0006**	**1.43**	**1.16 to 1.75**	**0.0054**	**1.35**	**1.09 to 1.66**
Within IL10RB^{low}: KRAS mut / KRAS WT	347 / 585	0.1250	1.22	0.95 to 1.58	0.1710	1.20	0.92 to 1.56
Within IL10RB^{high}: KRAS mut / KRAS WT	168 / 296	**0.0002**	**1.89**	**1.36 to 2.63**	**0.0027**	**1.73**	**1.21 to 2.48**
Within KRAS WT: IL10RB^{high} / IL10RB^{low}	296 / 585	0.7310	0.95	0.71 to 1.27	0.4440	0.89	0.66 to 1.20
Within KRAS mut: IL10RB^{high} / IL10RB^{low}	168 / 347	**0.0172**	**1.45**	**1.07 to 1.97**	0.1680	1.26	0.91 to 1.75

Table 3.5 Univariate survival analysis of stage II/III CRC patients in training, validation, and combined cohorts based on *IL10RB* expression and *KRAS* mutation status.

Univariate Cox proportional hazard survival analyses were performed to determine the prognostic consequence of having high or low *IL10RB* expression in the context of *KRAS* mutation in the training (GSE39582), confirmation (PETACC3), and combined cohorts. *IL10RB*-high and low is defined by a cutpoint at the 67th percentile. Cox proportional hazard ratios (HR) for relapse free survival (RFS) and overall survival (OS) are displayed with 95% confidence intervals (95% CI). Significant results are bolded. Patient numbers (No.) in each subgroup are indicated.

3.2.7 High expression of either or both subunits of the heterodimeric IL-22R confers poor prognosis in *KRAS* mutant CRC.

Given that *IL22RA1* and *IL10RB* were the top two hits in an unbiased screen for cytokine and/or cytokine receptors that interact with *KRAS* mutation, we next sought to determine whether co-expression of high levels of both subunits of the heterodimeric IL-22R have an additive effect resulting in worsened prognosis in *KRAS* mutant tumours. Patients were classified into six groups based on *KRAS* mutation status, *IL22RA1*, and *IL10RB* expression level. *KRAS*-mutant tumours with high expression of both IL-22R subunits displayed the lowest five-year relapse free survival rates of the six subgroups in the discovery cohort (GSE39582) (Figure 3.12 A). This finding was confirmed in the confirmation (PETACC3) and combined

cohorts (Table 3.6). Detailed survival analysis revealed that *KRAS* mutation was more strongly associated with poor outcome among tumours with high *IL22RA1* and *IL10RB* expression (RFS *HR*=3.81, 95% CI=1.55-9.36, *P*=0.0036; OS *HR*=3.90, 95% CI=1.51-10.9, *P*=0.0050) than among tumours with high expression of either IL-22R subunit alone (Table 3.7). This finding was confirmed in the combined cohort (Table 3.7). Based on data from the training cohort, 4.9% of stage II/III CRC patients are predicted to stratify into the subgroup of poorest prognosis. However collectively, 18.9% of stage II/III CRC patients are predicted to be *KRAS* mutant and have high expression of either or both subunits of the heterodimeric IL-22R (Figure 3.12 B). This represents approximately 50% of *KRAS* mutant patients.

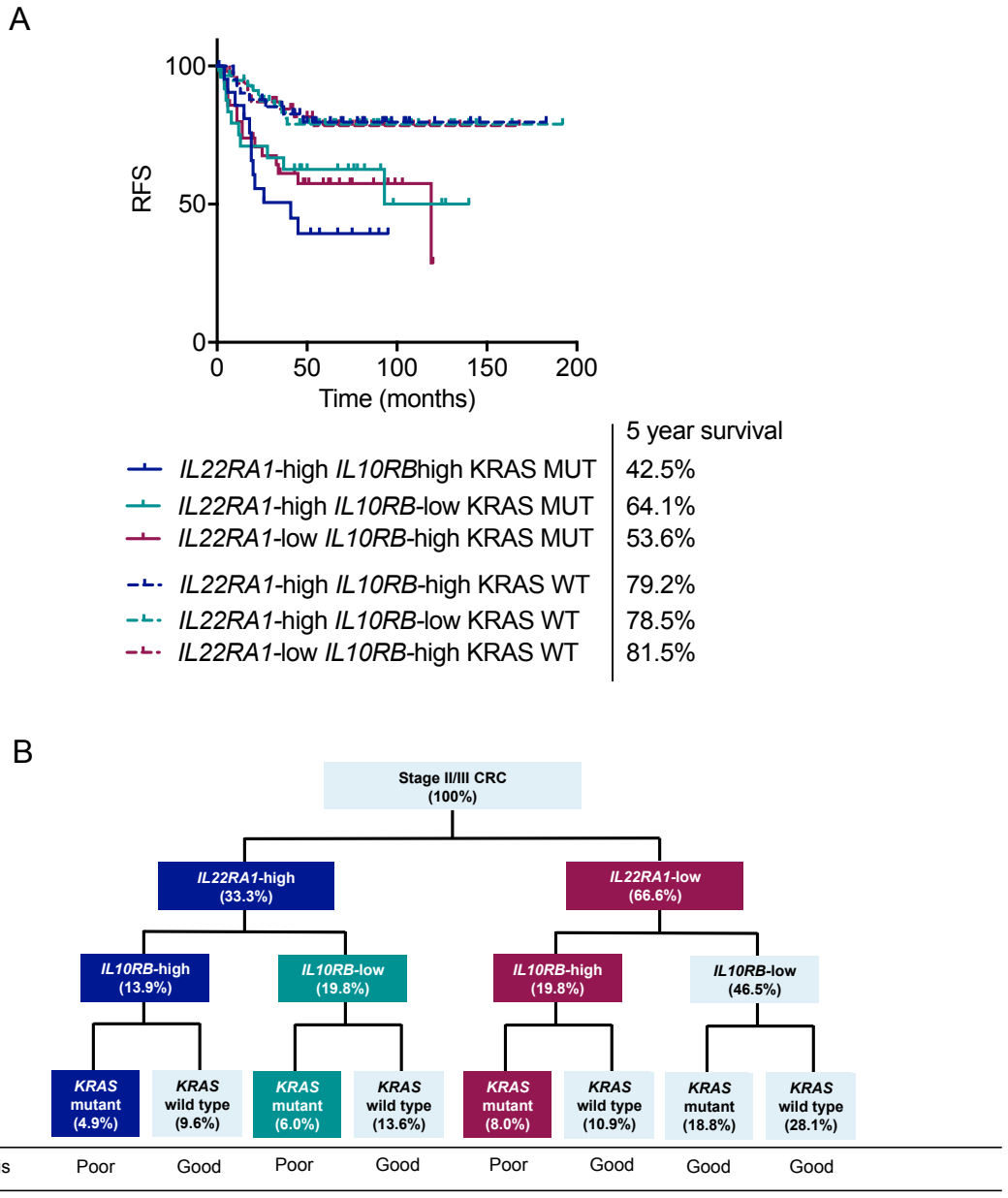


Figure 3.12 High expression of either or both subunits of the heterodimeric IL-22R confers poor prognosis in *KRAS* mutant CRC.

(A) Relapse free survival (RFS) in Stage II/III patients in the GSE39582 training cohort estimated using Kaplan-Meier methods. Patients stratified based on both *IL22RA1* and *IL10RB* expression and *KRAS* mutation status. *IL22RA1*-high/low and *IL10RB*-high/low is defined by a cutpoint at the 67th percentile for each gene. 5-year (60 month) survival proportions for each molecular subtype are displayed.

(B) Relative proportions of Stage II/III patients in the GSE39582 training cohort whose tumours were categorized based on *IL22RA1* expression, *IL10RB* expression, and *KRAS* mutation status. The predicted prognosis of each molecular subtype is displayed.

Table 3.6	5 year relapse-free survival (RFS)		
	GSE39582	**PETACC3**	**Combined**
IL22RA1^{high}/IL10RB^{high}: KRAS WT	79.2%	58.7%	68.1%
IL22RA1^{high}/IL10RB^{low}: KRAS WT	78.5%	71.3%	73.4%
IL22RA1^{low}/IL10RB^{high}: KRAS WT	81.5%	60.3%	69.3%
IL22RA1^{low}/IL10RB^{low}: KRAS WT	65.3%	68.5%	66.2%
IL22RA1^{high}/IL10RB^{high}: KRAS mut	42.5%	50.0%	47.9%
IL22RA1^{high}/IL10RB^{low}: KRAS mut	64.1%	53.9%	55.8%
IL22RA1^{low}/IL10RB^{high}: KRAS mut	53.6%	52.5%	54.8%
IL22RA1^{low}/IL10RB^{low}: KRAS mut	70.7%	65.5%	66.9%

	5 year overall survival (OS)		
	GSE39582	**PETACC3**	**Combined**
IL22RA1^{high}/IL10RB^{high}: KRAS WT	84.1%	79.9%	81.3%
IL22RA1^{high}/IL10RB^{low}: KRAS WT	82.5%	82.8%	81.3%
IL22RA1^{low}/IL10RB^{high}: KRAS WT	76.5%	74.2%	73.6%
IL22RA1^{low}/IL10RB^{low}: KRAS WT	71.3%	78.7%	73.3%
IL22RA1^{high}/IL10RB^{high}: KRAS mut	45.8%	69.2%	55.5%
IL22RA1^{high}/IL10RB^{low}: KRAS mut	59.0%	72.0%	66.1%
IL22RA1^{low}/IL10RB^{high}: KRAS mut	65.8%	63.3%	66.8%
IL22RA1^{low}/IL10RB^{low}: KRAS mut	71.1%	73.1%	71.2%

Table 3.6 5-year relapse free and overall survival in patients with high expression of either or both subunits of the heterodimeric IL-22R.

Patients stratified based on both *IL22RA1* and *IL10RB* expression and *KRAS* mutation status. *IL22RA1*-high/low and *IL10RB*-high/low is defined by a cutpoint at the 67th percentile for each gene. For each molecular subtype 5 year (60 month) relapse free survival (RFS) and overall survival (OS) proportions in Stage II/III patients in the training cohort (GSE39582), confirmation cohort (PETACC3), and combined cohort estimated using Kaplan-Meier methods are displayed.

Table 3.7 Survival analysis (RFS and OS) for Stage II, III patients of GSE39582, PETACC3 and combined dataset (univariate analysis)

		RFS				OS		
	No.	*P*	HR	95% CI	No.	*P*	HR	95% CI
GSE39582								
Within IL22RA1^{high}/IL10RB^{high}: KRAS mut / KRAS WT	22 / 43	**0.0036**	**3.81**	**1.55 to 9.36**	22 / 43	**0.0050**	**3.90**	**1.51 to 10.09**
Within IL22RA1^{high}/IL10RB^{low}: KRAS mut / KRAS WT	26 / 58	0.0623	2.26	0.96 to 5.32	26 / 59	0.1220	1.82	0.85 to 3.91
Within IL22RA1^{low}/IL10RB^{high}: KRAS mut / KRAS WT	34 / 49	**0.0038**	**3.50**	**1.50 to 8.20**	34 / 49	0.1730	1.75	0.78 to 3.91
Within IL22RA1^{low}/IL10RB^{low}: KRAS mut / KRAS WT	81 / 124	0.3140	0.76	0.45 to 1.29	83 / 126	0.6980	0.90	0.54 to 1.50
PETACC3								
Within IL22RA1^{high}/IL10RB^{high}: KRAS mut / KRAS WT	30 / 61	0.1910	1.51	0.81 to 2.80	30 / 61	0.2260	1.62	0.74 to 3.52
Within IL22RA1^{high}/IL10RB^{low}: KRAS mut / KRAS WT	50 / 77	**0.0388**	**1.84**	**1.03 to 3.29**	50 / 77	**0.0178**	**2.25**	**1.15 to 4.39**
Within IL22RA1^{low}/IL10RB^{high}: KRAS mut / KRAS WT	55 / 79	0.2940	1.31	0.79 to 2.17	55 / 79	0.2100	1.45	0.81 to 2.61
Within IL22RA1^{low}/IL10RB^{low}: KRAS mut / KRAS WT	119 / 175	0.5120	1.14	0.77 to 1.70	119 / 175	0.3070	1.26	0.81 to 1.98
Combined								
Within IL22RA1^{high}/IL10RB^{high}: KRAS mut / KRAS WT	53 / 103	**0.0028**	**2.17**	**1.31 to 3.60**	**57 / 122**	**0.0012**	**2.53**	**1.44 to 4.44**
Within IL22RA1^{high}/IL10RB^{low}: KRAS mut / KRAS WT	77 / 139	**0.0048**	**1.97**	**1.23 to 3.16**	**86 / 174**	**0.0122**	**1.83**	**1.14 to 2.95**
Within IL22RA1^{low}/IL10RB^{high}: KRAS mut / KRAS WT	87 / 130	**0.0169**	**1.71**	**1.10 to 2.65**	102 / 164	0.2160	1.35	0.84 to 2.16
Within IL22RA1^{low}/IL10RB^{low}: KRAS mut / KRAS WT	200 / 294	0.9870	1.00	0.73 to 1.36	236 / 377	0.9460	1.01	0.74 to 1.38

Table 3.7 Univariate survival analysis of stage II/III CRC patients in training, validation, and combined cohorts based on *IL22RA1, IL10RB,* and *KRAS* mutation status.

Univariate Cox proportional hazard survival analyses were performed to determine the prognostic consequence of having high or low *IL22RA1* and/or *IL10RB* expression in the context of *KRAS* mutation in the training (GSE39582), confirmation (PETACC3), and combined cohorts. *IL22RA1*-high/low and *IL10RB*-high/low is defined by a cutpoint at the 67th percentile for each gene. Cox proportional hazard ratios (HR) for relapse free survival (RFS) and overall survival (OS) are displayed with 95% confidence intervals (95% CI). Significant results are bolded. Patient numbers (No.) in each subgroup are indicated.

Similar to *IL22RA1*, when *IL10RB* expression was examined in prospectively collected tumours and matched normal adjacent tissue (N=69), *IL10RB* expression was found to be higher in normal adjacent mucosa compared to the tumour (CRC) tissue (Figure 3.13 A). Like *IL22RA1*, *IL10RB* expression in the tumour tissue was highly correlated with that in the normal adjacent tissue (Figure 3.13 B). Likely due to the widespread expression of *IL10RB* on numerous cell types (Figure 3.13 C), compared to the more restricted expression of *IL22RA1* to the epithelium (Figure 3.4, Figure 3.5), *IL22RA1* and *IL10RB* expression were not highly correlated in the training, validation, or combined cohorts (Figure 3.13 D). However, when *IL22RA1* and *IL10RB* expression were compared in prospectively collected tumour tissue (N=69), expression was highly correlated (Figure 3.13 E). This conflicting data may be the consequence of higher sensitivity of detection of the receptor subunits by qPCR in the prospective cohort as compared to microarray in the large retrospectively assessed cohorts.

In summary, the prognostic impact of having high expression of both subunits of the heterodimeric IL-22R in *KRAS* mutant tumours, underscores the possibility of functional synergism between IL-22 signalling and oncogenic *KRAS* that promotes malignant progression.

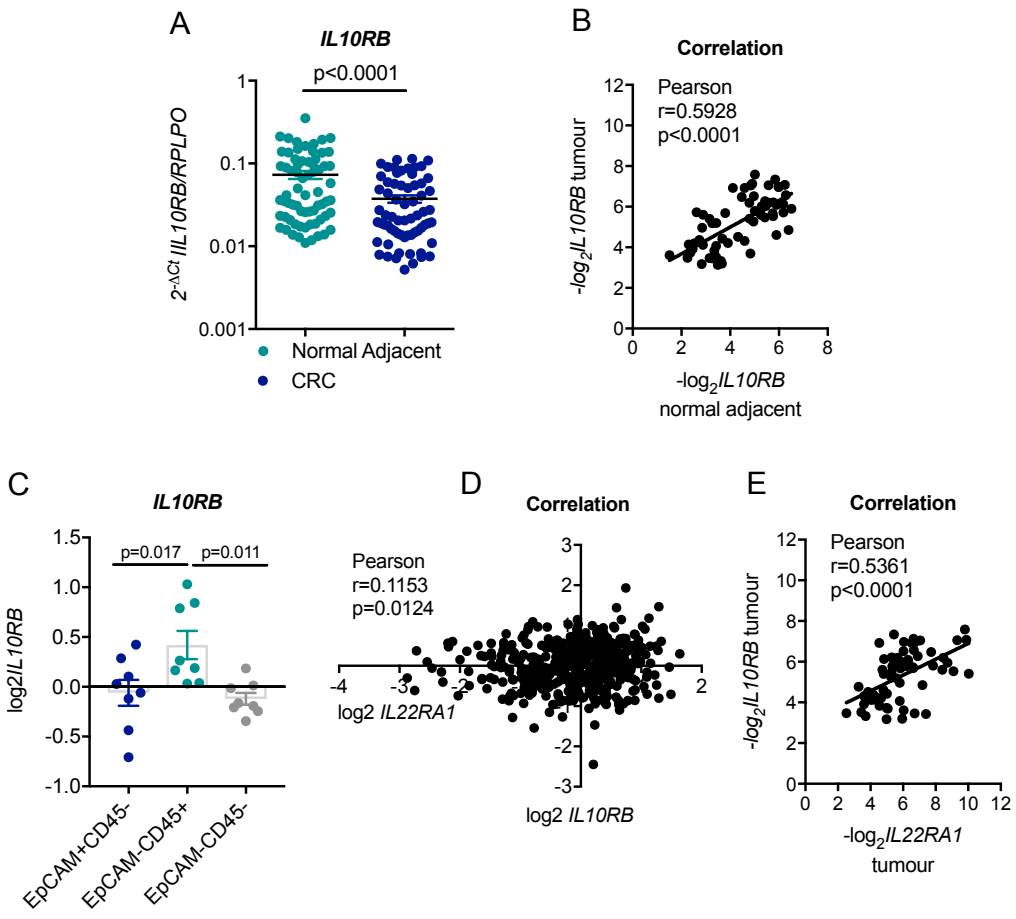


Figure 3.13 *IL10RB* expression is lower in tumour compared to normal adjacent tissue but *IL10RB* tumoural expression is correlated to expression in the normal adjacent tissue.

(A) *IL10RB* expression in fresh/frozen whole tumour and matched normal adjacent tissue. N=69 patients. Statistical significance was determined using a ratio paired T-test comparing tumour (CRC) and matched normal expression for each patient.

(B) Pearson Correlation analysis comparing tumour to matched normal adjacent tissue *IL10RB* expression. N=69 patients.

(C) *IL10RB* expression in cells from N=8 independent colorectal tumours sorted based on epithelial ($EpCAM^+CD45^-$), immune ($EpCAM^-CD45^+$), and stromal ($EpCAM^-CD45^-$) from GSE39397 cohort (Calon *et al.*, 2012). RNA was extracted from sorted cells and microarrays were performed. Expression is the median normalised log2 expression from the *IL10RB* probe. Statistical significance was determined using a one-way ANOVA with Tukey's post test for multiple comparisons.

(D) Pearson Correlation analysis comparing tumoural *IL22RA1* to *IL10RB* expression in GSE39582 training cohort. N=469 patients.

(E) Pearson Correlation analysis comparing tumoural *IL22RA1* to *IL10RB* expression in prospectively collected fresh/frozen whole tumour tissue. N=69 patients.

3.2.8 The prognostic interaction between *KRAS* mutation and *IL22RA1* occurs preferentially in proximal colorectal cancer.

There are clear clinical and molecular differences between proximal and distal CRCs, deriving in part from the differing embryonic origins of the proximal and distal colon (Missiaglia *et al.*, 2014; Maus *et al.*, 2015). Notably, proximal CRCs are more commonly associated with microsatellite instability and immune activation (Guinney *et al.*, 2015). The microbiota is also known to change along the length of the colon, both in terms of the relative proportions of given phyla and in terms of its structural arrangement (Drewes, Housseau and Sears, 2016). Recently, bacterial biofilms were found to be present specifically on proximal but not distal colorectal tumours (Dejea *et al.*, 2014). Given that IL-23 and its downstream effector IL-22 are produced in response to microbial signals in the gut, we first sought to determine whether immune/inflammatory signatures differed in proximal versus distal tumours.

We first performed gene set enrichment analysis (GSEA) on proximal (N=626) versus distal (N=832) tumours in the combined cohort. In line with previous reports, enrichment of "inflammatory response" and "immune response" signatures was observed in proximal tumours (Figure 3.14 A). Furthermore, specific examination of immune cell subsets using metagene signatures in the training cohort (GSE39582), revealed elevated expression of metagene signatures associated with dendritic cells, macrophages, neutrophils, B cells, T cells, and cytotoxic T cells in the proximal versus distal colon (Figure 3.14 B). In light of these observations, we next focussed more specifically on the immune effectors of interest, IL-23 and IL-22, and assessed the expression of *IL23A* and *IL22* among *IL22RA1*-high, *KRAS* wild type versus mutant tumours in the proximal and distal colon. Interestingly, *IL23A* expression trended towards being higher in proximal, *KRAS* mutant versus wild type, *IL22RA1*-

high tumours. However, there was no difference in *IL23A* expression between *KRAS* mutant and wild type tumours in the distal colon (Figure 3.14 C). Moreover, *IL22* expression was significantly higher in *IL22RA1*-high, proximal, *KRAS* mutant versus wild type tumours. Again, *IL22* expression in *IL22RA1*-high, distal *KRAS* mutant and wild type tumours was similar (Figure 3.14 C). It should also be noted that *IL22* expression was similar between *IL22RA1*-high, *KRAS* mutant tumours in the proximal and distal colon (Figure 3.14 C).

Therefore, there are clear differences in the inflammatory microenvironment in proximal versus distal colorectal tumours that have the potential to influence the prognostic interaction between *IL22RA1* expression and *KRAS* mutation.

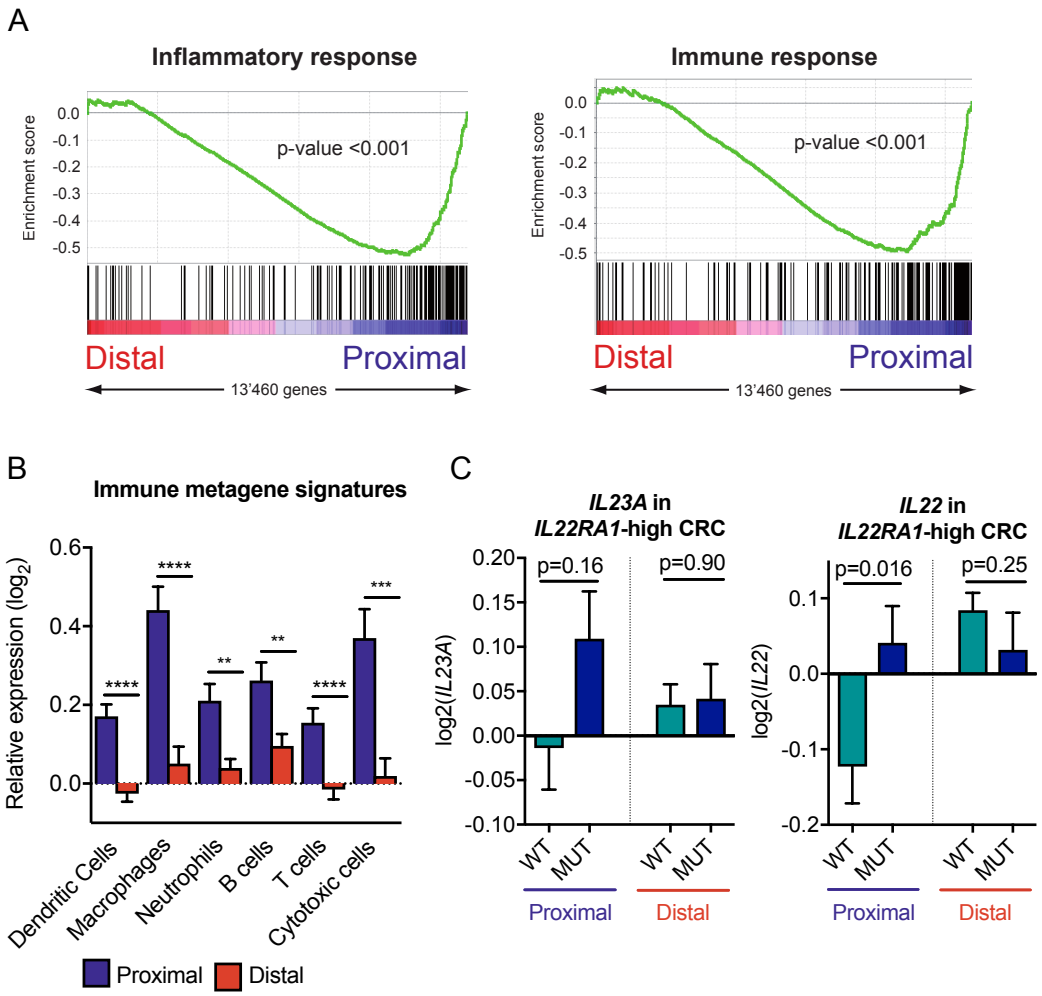


Figure 3.14 Inflammation metagene signatures are enriched in proximal compared to distal CRCs and *IL22* expression is enriched in proximal, *IL22RA1*-high, *KRAS* mutant compared to WT CRCs.

(A) Gene set enrichment analysis (GSEA) comparing enrichment of the Inflammatory Response and Immune Response signatures in proximal [N=598] versus distal [N=795] tumours from the combined cohort. (This analysis was conducted by D. Barras)

(B) Analysis of immune subsets defined by metagene signatures in proximal [N=192] versus distal [N=277] tumours in the GSE39582 training set. Log_2 expression values display immune metagene signature enrichment. Metagenes were calculated as the geometric means of *CD208*, *CD209*, *CD83* (dendritic cells); *MSR1*, *CD14*, *CD68*, *CSF1R* (macrophages); *CD66B*, *FCGR3B* (neutrophils); *GNLY*, *GZMA*, *GZMB*, *GZMH*, *GZMK* (cytotoxic cells); *MS4A1*, *CD19*, *CD22*, *CD79A* (B cells); *CD2*, *CD247*, *CD3E*, *CD28* (T cells). Statistical significance was determined using Mann-Whitney U tests. $^{**}P \leq 0.01$, $^{***}P \leq 0.001$, $^{****}P < 0.0001$. (This analysis was conducted by N. West, figure modified by S. McCuaig)

(C) Log_2 expression of *IL23A* and *IL22* among *IL22RA1*-high patients in the proximal colon comparing *KRAS* wild type (WT) [N=20] to mutant (MUT) [N=22] and in the distal colon comparing WT [N=85] to MUT [N=27] in the GSE329582 training set. Statistical significance was determined using Mann-Whitney U tests. $P < 0.05$ is considered significant.

Given that we observed elevated expression of *IL23A* and its downstream effector *IL22* in *IL22RA1*-high, proximal, *KRAS* mutant versus wild type tumours, we hypothesised that the prognostic consequence of having high *IL22RA1* expression in the context of *KRAS* mutation would be most profound in proximal colorectal tumours. We therefore first stratified patients based on tumour location (proximal versus distal to the splenic flexure), and then examined the impact of *IL22RA1* expression and *KRAS* mutation status on survival. Indeed, the poor prognosis associated with high *IL22RA1* and *KRAS* mutation was predominately evident in proximal tumours in the training cohort both in terms of RFS (*HR*=4.23, 95% CI=1.38-13.01, *P*=0.012) (Figure 3.15 A) and OS (*HR*=9.41, 95% CI=2.13-41.60, *P*=0.003) (Figure 3.15 B). This observation was confirmed in both the confirmation cohort (PETACC3) and combined cohort (Table 3.8). It should be noted that in the combined cohort, *KRAS* mutation was still significantly poorly prognostic in terms of RFS in *IL22RA1*-high, distal tumours (*HR*=1.64, 95% CI=1.07-2.54, *P*=0.025); however, the effect was not as marked as in proximal tumours (*HR*=2.93, 95% CI=1.57-5.48, *P*=0.001) (Table 3.8).

BRAF mutations and microsatellite instability (MSI) are both common features of proximal tumours (Guinney *et al.*, 2015). The prognosis of patients with microsatellite instable tumours is known to be better than their microsatellite stable counterparts (Guidoboni *et al.*, 2001; Guinney *et al.*, 2015), in part because increased neoantigen load is thought to increase immune activation and anti-tumour immunity in MSI tumours. To exclude the possibility that the striking prognostic impact of *KRAS* mutation in *IL22RA1*-high, proximal tumours was a surrogate measure of the good prognosis of patients with MSI tumours, we conducted a multivariate survival

analysis which included MSI status, *BRAF* mutation status, and stage (II versus III) as covariates. *KRAS* mutation status was highly prognostic in *IL22RA1*-high, proximal tumours independent of MSI, *BRAF* mutation, and stage (Table 3.9).

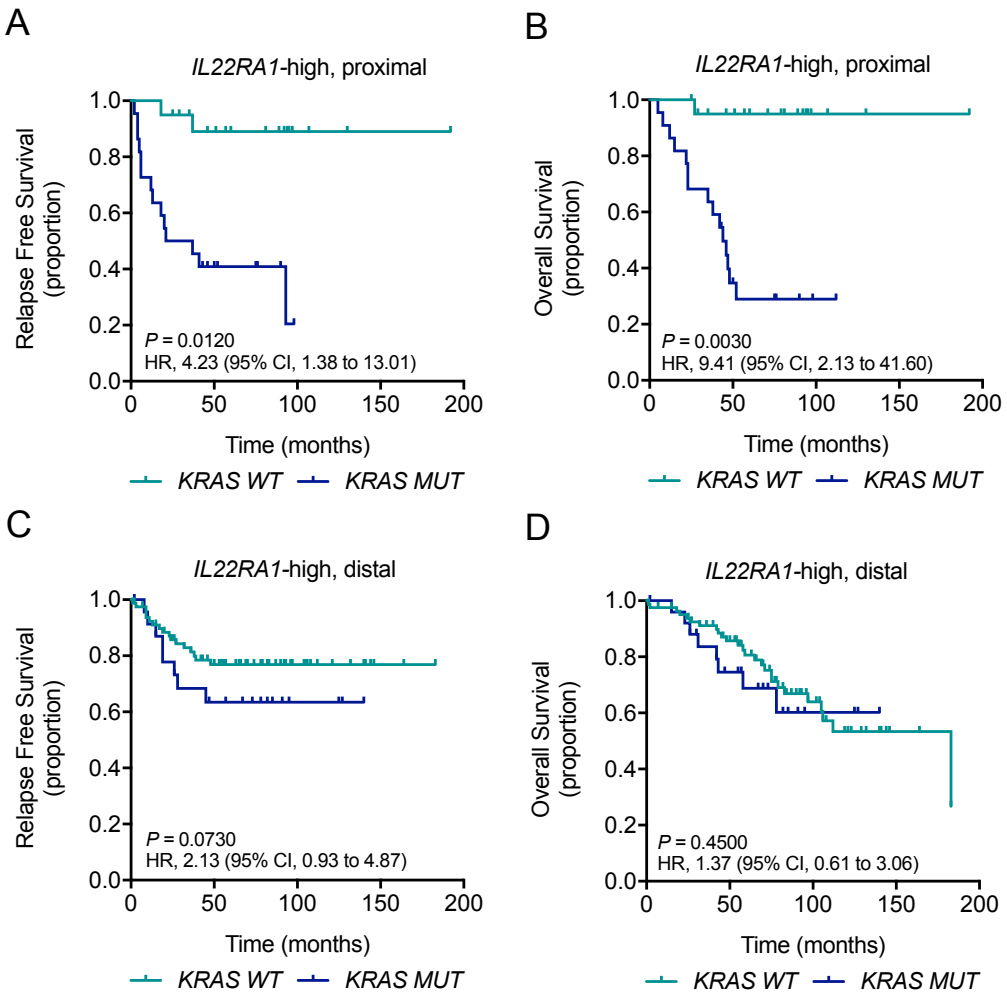


Figure 3.15 The negative prognostic effect of having high *IL22RA1* expression in the context of *KRAS* mutation is most profound in the proximal colon.

Relapse free survival (RFS) and overall survival (OS) in Stage II/III patients in the GSE39582 training cohort estimated using Kaplan-Meier methods.

(A) RFS among *IL22RA1*-high patients with tumours proximal to the splenic flexure (proximal) based on *KRAS* mutation status.
(B) OS among *IL22RA1*-high patients with proximal tumours based on *KRAS* mutation status.
(C) RFS among *IL22RA1*-high patients with tumours distal to the splenic flexure (distal) based on *KRAS* mutation status.
(D) OS among *IL22RA1*-high patients with distal tumours based on *KRAS* mutation status.

P values were computed using Wald-tests. Hazard ratios (HR) are univariate Cox proportional hazard ratios with 95% confidence intervals.

Table 3.8 Univariate survival analysis of stage II/III CRC patients in training, validation, and combined cohorts based on *IL22RA1* expression, *KRAS* mutation status, and tumour location.

			RFS			OS		
		No.	*P*	HR	95% CI	*P*	HR	95% CI
GSE39582								
IL22RA1 low	**Proximal** KRAS mut / KRAS WT	65 / 69	0.414	0.73	0.35 to 1.54	0.871	0.95	0.50 to 1.80
	Distal KRAS mut / KRAS WT	55 / 107	**0.031**	**1.77**	**1.05 to 2.97**	0.531	1.20	0.67 to 2.15
IL22RA1 high	**Proximal** KRAS mut / KRAS WT	24 / 23	**0.012**	**4.23**	**1.38 to 13.01**	**0.003**	**9.41**	**2.13 to 41.60**
	Distal KRAS mut / KRAS WT	25 / 80	0.073	2.13	0.93 to 4.87	0.450	1.37	0.61 to 3.06
PETACC3								
IL22RA1 low	**Proximal** KRAS mut / KRAS WT	88 / 111	0.252	1.32	0.82 to 2.14	0.404	1.26	0.73 to 2.17
	Distal KRAS mut / KRAS WT	106 / 167	0.635	1.11	0.73 to 1.67	0.204	1.36	0.85 to 2.18
IL22RA1 high	**Proximal** KRAS mut / KRAS WT	26 / 39	**0.008**	**2.84**	**1.31 to 6.12**	**0.033**	**2.52**	**1.08 to 5.90**
	Distal KRAS mut / KRAS WT	63 / 108	0.281	1.32	0.79 to 2.21	0.088	1.73	0.92 to 3.25
Combined								
IL22RA1 low	**Proximal** KRAS mut / KRAS WT	187 / 264	0.572	1.12	0.75 to 1.68	0.705	0.93	0.63 to 1.36
	Distal KRAS mut / KRAS WT	173 / 305	0.129	1.28	0.93 to 1.77	0.222	1.25	0.87 to 1.79
IL22RA1 high	**Proximal** KRAS mut / KRAS WT	58 / 89	**0.001**	**2.93**	**1.57 to 5.48**	**0.000**	**3.70**	**1.93 to 7.07**
	Distal KRAS mut / KRAS WT	96 / 221	**0.025**	**1.64**	**1.07 to 2.54**	0.167	1.40	0.87 to 2.25

Table 3.8 Univariate survival analysis of stage II/III CRC patients in training, validation, and combined cohorts based on *IL22RA1* expression, *KRAS* mutation status, and tumour location.

Univariate Cox proportional hazard survival analyses were performed to determine the prognostic consequence of having high or low *IL22RA1* expression in the context of *KRAS* mutation in tumours in the proximal or distal colon in the training (GSE39582), confirmation (PETACC3), and combined cohorts. *IL22RA1*-high and low is defined by a cutpoint at the 67th percentile. Cox proportional hazard ratios (HR) for relapse free survival (RFS) and overall survival (OS) are displayed with 95% confidence intervals (95% CI). Significant results are bolded. Patient numbers (No.) in each subgroup are indicated.

Table 3.9 Survival analysis (RFS and OS) for Stage II, III patients of GSE39582, PETACC3 and combined dataset (multivariate analysis)

			RFS			OS		
		No.	*P*	HR	95% CI	*P*	HR	95% CI
GSE39582								
IL22RA1 low	**Proximal** *KRAS mut / KRAS WT*		0.466	0.71	0.28 to 1.78	0.617	1.24	0.53 to 2.91
	Distal *KRAS mut / KRAS WT*		0.375	1.33	0.71 to 2.47	0.820	0.92	0.43 to 1.96
IL22RA1 high	**Proximal** *KRAS mut / KRAS WT*		**0.032**	**5.13**	**1.15 to 22.84**	**0.015**	**12.74**	**1.66 to 97.98**
	Distal *KRAS mut / KRAS WT*		0.068	2.43	0.94 to 6.32	0.740	1.18	0.44 to 3.17
PETACC3								
IL22RA1 low	**Proximal** *KRAS mut / KRAS WT*		0.205	1.42	0.83 to 2.42	0.195	1.51	0.81 to 2.83
	Distal *KRAS mut / KRAS WT*		0.071	1.51	0.97 to 2.36	**0.010**	**1.98**	**1.18 to 3.33**
IL22RA1 high	**Proximal** *KRAS mut / KRAS WT*		**0.003**	**4.87**	**1.70 to 13.96**	**0.002**	**10.75**	**2.46 to 46.89**
	Distal *KRAS mut / KRAS WT*		0.386	1.26	0.75 to 2.13	0.092	1.77	0.91 to 3.42
Combined								
IL22RA1 low	**Proximal** *KRAS mut / KRAS WT*		0.581	1.14	0.72 to 1.81	0.575	1.14	0.71 to 1.84
	Distal *KRAS mut / KRAS WT*		0.185	1.27	0.89 to 1.81	0.124	1.37	0.92 to 2.05
IL22RA1 high	**Proximal** *KRAS mut / KRAS WT*		**0.000**	**4.18**	**1.90 to 9.19**	**0.000**	**6.74**	**2.60 to 17.43**
	Distal *KRAS mut / KRAS WT*		**0.018**	**1.75**	**1.10 to 2.78**	0.098	1.55	0.92 to 2.60

The variables included in the multivariate analysis were: MSI status, BRAF mutation and Stage

Table 3.9 Multivariate survival analysis of stage II/III CRC patients in training, validation, and combined cohorts based on *IL22RA1* expression, *KRAS* mutation status, and tumour location.

Multivariate Cox proportional hazard survival analyses were performed to determine the prognostic consequence of having high or low *IL22RA1* expression in the context of *KRAS* mutation in tumours in the proximal or distal colon in the training (GSE39582), confirmation (PETACC3), and combined cohorts. *IL22RA1*-high and low is defined by a cutpoint at the 67th percentile. Cox proportional hazard ratios (HR) for relapse free survival (RFS) and overall survival (OS) are displayed with 95% confidence intervals (95% CI). Significant results are bolded. Patient numbers (No.) in each subgroup are indicated. Covariates included in the analysis were: microsatellite stability/instability (MSI) status, BRAF mutation status, and stage.

3.2.9 IL-22R-high tumours classify predominately as CMS2.

Several groups have recently proposed molecular classification schemes for CRC based on transcriptomic signatures, fuelling a large international subtyping consortium effort that defined the "consensus molecular subtypes" (CMS) of colorectal cancer in 2015 (Guinney *et al.*, 2015). The four CMS are characterized by distinct molecular signatures of: microsatellite instability and immune activation (CMS1), epithelial WNT and MYC signalling activation (CMS2), epithelial metabolic deregulation (CMS3), and stromal invasion and angiogenesis (CMS4) (Guinney *et al.*, 2015). Given that the CMS subgroups represent the most robust CRC molecular classification system at present, we sought to determine whether the poor prognosis *KRAS* mutant, *IL22RA1*-high, proximal tumours were enriched in any particular CMS subgroup. Patients were grouped based on *IL22RA1* expression, *KRAS* mutation status, and tumour site and the proportion of patients in each group that classify as CMS1, 2, 3, 4 or the unclassified (UNK) subgroups were determined using the published CMS signatures (Guinney *et al.*, 2015). Poor prognosis, *KRAS* mutant, *IL22RA1*-high, proximal (right-sided) tumours enrich in the CMS2 subgroup (35.9%). However, *KRAS* wild type, *IL22RA1*-high, proximal tumours also interestingly enrich in CMS2 (37.8%) (Figure 3.16 A). This effect seems to be driven by the level of *IL22RA1* expression alone, as when all *IL22RA1*-high tumours, regardless of site and mutation status were compared to all *IL22RA1*-low tumour, 52.5% of *IL22RA1*-high tumours classified as CMS2 compared to 24.4% of *IL22RA1*-low tumours (Figure 3.16). A large proportion of the poor prognosis *KRAS* mutant, *IL22RA1*-high, proximal tumours do not fall into any specific subgroup and are considered unclassified (UNK) (25%) (Figure 3.16 A), while a high percentage of *KRAS* wild type, *IL22RA1*-high, proximal tumours classify as CMS1 (28.6%) (Figure 3.16 A).

One of the striking differences between the *KRAS* mutant versus wild type *IL22RA1*-high, proximal tumours lies in the percentage of patients that classify as the CMS3, metabolic subtype (15.6% in *KRAS* mutant versus 4.1% in *KRAS* wild type) (Figure 3.16 A).

In summary, poor prognosis *KRAS* mutant, *IL22RA1*-high, proximal tumours do not classify well as CMS1, 2, 3, or 4. However, high *IL22RA1* expression seems to drive enrichment into CMS2 regardless of *KRAS* mutation status and tumour site.

A

IL22RA1	KRAS	Site	CMS1	CMS2	CMS3	CMS4	UNK
High	MUT	Right	6.2 %	35.9 %	15.6 %	17.2 %	25 %
Low	MUT	Right	16.8 %	12 %	26 %	26 %	19.2 %
High	WT	Right	28.6 %	37.8 %	4.1 %	16.3 %	13.3 %
Low	WT	Right	41.5 %	11.7 %	12.1 %	19.9 %	14.9 %
High	MUT	Left	4.9 %	43.1 %	17.6 %	12.7 %	21.6 %
Low	MUT	Left	7.2 %	23.8 %	22.1 %	28.2 %	18.8 %
High	WT	Left	3.2 %	64.7 %	0.4 %	18.5 %	13.3 %
Low	WT	Left	5.5 %	42.2 %	4.1 %	27.9 %	20.3 %
	IL22RA1-high		8.4 %	52.5 %	6.2 %	16.7 %	16.1 %
	IL22RA1-low		18.1 %	24.4 %	13.7 %	25 %	18.8 %

Figure 3.16 *IL22RA1*-high tumours classify predominately as CMS2.

(A) Heatmap displaying the proportion of patients in each molecular subtype of interest (rows) which classify into each of the Consensus Molecular Subtypes (CMS) of colorectal cancer (columns). The combined cohort was used to conduct the CMS classification. Right = proximal tumours, Left = distal tumours, UNK = unclassified subtype. (This analysis was conducted by D. Barras)

3.3 Discussion

3.3.1 Main conclusions

Here, we have observed that *IL23A* expression is almost universally elevated in human colorectal tumours compared to matched normal adjacent tissue. Using the GSE39582 cohort as a training set and the larger PETACC3 cohort as a validation set, we have identified a novel, prognostically important interaction between the downstream IL-22 pathway and *KRAS* mutation. High expression of either or both subunits of the heterodimeric IL-22 receptor, *IL22RA1* and *IL10RB*, distinguishes a patient subgroup in which *KRAS* mutation associates with poor outcome. The detrimental effect of having a *KRAS* mutation in the context of high *IL22RA1* expression preferentially affects tumours in the proximal colon. This association suggests a potential synergism between oncogenic *KRAS* and IL-22 signalling in colorectal cancer progression.

3.3.2 *IL23A* is elevated in CRC compared to matched normal tissue

The observation that elevated tumoural *IL23A* is a near universal feature of colorectal tumours compared to matched normal adjacent mucosa is striking. Though one might argue that the elevated *IL23A* could be attributed to generalised inflammation in the tumour compared to normal adjacent tissue, we did not observe elevated expression of other critical proinflammatory mediators like *IL12A* and *TNF*. In 2006, Langowski *et al.* surveyed a range of human solid tumours (colon, ovarian, head and neck, lung, breast, stomach, melanoma) and in line with our observations found that *IL23A* was surprisingly upregulated in carcinomas compared to matched normal adjacent tissue (Langowski *et al.*, 2006). They found a significant correlation between *IL23A* expression in CRC and expression of the myelomonocytic lineage marker *CD14* and

markers of activated neutrophils such as *SOD2*. Although they did not investigate IL-23p19 protein expression in colorectal tumours, immune fluorescence in human ovarian tumours revealed that IL-23p19 co-localised with tumour infiltrating $CD11c^+$ dendritic cells (DC), suggesting that DCs are the dominant cellular source of IL-23p19 in tumours (Langowski *et al.*, 2006). Grivennikov *et al.* have also observed elevated *IL23A* mRNA expression in their examination of a small number of human CRC tumours compared to matched normal tissue (N=7) (Grivennikov *et al.*, 2012).

By contrast to *IL23A,* we found that *IL12A* expression was unchanged or in many cases lower in tumours compared to matched normal tissue in our prospective cohort. Systematic dissection of the divergent roles of IL-23 and IL-12 by genetic deletion of either IL-23 ($p19^{-/-}$), IL-12 ($p35^{-/-}$) or both cytokines through knock-out of their shared p40 subunit ($p40^{-/-}$) was undertaken in a chemical carcinogen-induced skin papilloma model (Langowski *et al.*, 2006). While $Il12p35^{-/-}$ mice developed papillomas more rapidly and in greater numbers than wild type controls due to reduced cytotoxic T cell activity, both $Il23p19^{-/-}$ and $Il12p40^{-/-}$ animals did not develop tumours due to enhanced numbers and activity of $CD8^+$ T cells (Langowski *et al.*, 2006). The apparent yin and yang IL-23 and IL-12 in the tumour microenvironment, underscores the potential deleterious consequences of high tumoural *IL23A* and low *IL12A* expression, in favouring pro-tumorigenic over anti-tumorigenic, cytotoxic immunity. In the training cohort (GSE39582), we indeed observed a modest poor prognostic consequence of having high tumoural *IL23A* expression both in terms of relapse free and overall survival. Although not directly demonstrated for *IL23A*, these findings are in line with the observed association of a Th17 immune signature (*RORC*, *IL17A*) with poor prognosis in human CRC (Tosolini *et al.*, 2011).

The stable, elevated expression of *IL23A* in each tumour compared to normal adjacent tissue begs the question of whether the signal is coming from a transient infiltrating or resident immune population or whether another cell type such as the malignant epithelium itself is inappropriately expressing *IL23A*. It is not unprecedented for epithelial cancers to acquire the capacity to express genes classically associated with immune cells, to craft an immune suppressive tumour microenvironment that favours immune evasion (Choi *et al.*, 2012). By interrogating publically available data from sorted human CRCs, we observed appreciable *IL23A* expression in both epithelial and immune compartments. However, it remains to be determined whether the malignant epithelium in human CRC can produce functional IL-23 protein. Recently, immunohistochemical analysis of IL-23p19 in 129 human CRC sections revealed pronounced epithelial IL-23p19 expression that was modestly linked to poor clinical outcome and advanced tumour stage (Hu *et al.*, 2017). Whether this represents true epithelial IL-23p19 expression is dependent upon the specificity of the IL-23p19 polyclonal antibody used in this study and needs to be validated.

While the cell-specific expression and function of IL-23 has not been comprehensively explored in human CRC, Grivennikov *et al.* showed that in the CPC-APC mouse model of sporadic CRC, tumour multiplicity and size were diminished in animals with complete genetic deficiency of *Il23a* or *Il23r* (Grivennikov *et al.*, 2012). Based on a bone marrow chimera experiment in which CPC-APC wild type hosts received wild type or *Il23*$^{-/-}$ bone marrow, the investigators claimed that haematopoietically derived IL-23 was necessary for enhanced tumourigenesis. However, the data shows no difference in tumour number and only modest reductions in tumour size and load in animals reconstituted with *Il23*$^{-/-}$ bone

marrow (Grivennikov *et al.*, 2012). Thus the phenotype is intermediate when compared to the CPC-APC full body *Il23*$^{-/-}$ and leaves open the possibility that a radioresistant cell population, such as the epithelium, may be contributing protumourigenic IL-23.

A key future objective is to confirm that IL-23p19 expression in CRC tumours is elevated compared to matched normal adjacent mucosal tissue at the protein level, optimally by flow cytometric analysis of fresh digested and restimulated whole tumour and matched normal tissue. Furthermore, the cell types capable of expressing IL-23p19 in the tumour must be robustly characterised. This can be achieved through basic flow cytometric assessment of IL-23p19 in a panel that includes myeloid and epithelial markers in addition to cell sorting the immune, epithelial, and stromal compartments and performing qPCR on the sorted populations for *IL23A* in a larger cohort of samples. Finally, if it is observed that the malignant epithelium is capable of producing IL-23p19, supernatants from CRC cell lines or primary organoids could be used to treat naïve CD4^{+} T cells, in the presence or absence of an IL-23p19 blocking antibody, to determine whether the T cell population is skewed toward a Th17 phenotype capable of producing IL-17A and IL-22.

3.3.3 Heterogeneous expression of IL-22RA1 in human CRC

At present, knowledge of the mechanisms of IL-22RA1 regulation is limited. Due to the presence of NF-κB binding sites in its promoter, inflammatory stimuli such as LPS or TNFα have been shown to induce IL-22RA1 expression (Tachiiri *et al.*, 2003). In mice, phosphorylation of GSK-3β has been shown to stabilise IL-22RA1 expression and prevent its proteasomal degradation (Weathington *et al.*, 2014; Metz *et al.*, 2016), while in humans, IL-22RA1 proteasomal degradation is mediated by a

novel F-box protein E3 ligase FBXW12 (Franz *et al.*, 2015). Because constitutively active *KRAS* can promote NF-κB activation (Sparmann and Bar-Sagi, 2004), one might predict IL-22RA1 expression to be elevated in *KRAS* mutant tumours. However, Fisher's exact tests did not reveal an association between *IL22RA1* expression and *KRAS* mutation status in our large combined cohort.

A recent report observed elevated expression of both IL-22RA1 and IL-10RB in microsatellite stable colorectal cancer compared to microsatellite instable tumours and matched normal tissue based on IHC analysis of a small cohort of patients (N=22) (Khare *et al.*, 2015). Fisher's exact tests in our large combined cohort indeed revealed an association between high *IL22RA1* expression and microsatellite stability. However, both IHC and qPCR based analysis of IL-22RA1 expression in our prospectively collected tumour and matched normal resection tissue (N=69) revealed that IL-22RA1 expression is reduced in tumours compared to matched normal tissue. The reason for this discrepancy may lie in the specificity of the antibody utilized by Khare *et al*. as they observed abundant IL-22RA1 staining in not only epithelial cells, but also stromal cells and in some cases immune infiltrates in tumours. By contrast, the IL-22RA1 staining pattern we observed was restricted to some but not all epithelial cells in the normal and tumour tissue. These findings are consistent with the epithelial-enriched expression of IL-22RA1 that we and others (Zheng *et al.*, 2008) have observed by flow cytometric analysis, except in the case of some haematological malignancies (Gelebart *et al.*, 2011). Within the epithelium of the gut, IL-22RA1 is reported to be expressed by crypt based stem cells and Paneth cells (Hanash *et al.*, 2012; Lindemans *et al.*, 2015). However, IL-22RA1 staining in murine small intestinal crypts reveals that the differentiated cells distant from the crypt base are the

dominant IL-22RA1 expressors (Hanash *et al.*, 2012). The morphology of the IL-22RA1 expressing cells that we observe in the normal human colonic crypts is consistent with a secretory phenotype. Given the physiologic function of IL-22 to stimulate mucin and anti-bacterial peptide production, it is logical that the receptor would be expressed on specialized secretory epithelial cells like goblet or enteroendocrine cells. However, future work must combine detection of IL-22RA1 and markers of known epithelial cells subsets to systematically determine epithelial cell types that express IL-22RA1 in homeostasis. If IL-22RA1 is predominately expressed by differentiated cell subtypes within the colonic crypt, it is therefore logical that its expression would be reduced in tumours, which tend to be less differentiated. Rather than inducing IL-22RA1 expression in tumours, our results point toward a mechanism by which IL-22RA1 expression is inappropriately sustained in cancer. Paradoxically, differentiation tends to be a good prognostic indicator in cancer (Halvorsen and Seim, 1988), therefore it remains to be determined whether the epithelial cell types that express IL-22RA1 in the tumour mirror those in health or whether IL-22RA1 marks a nascent stem cell population that sustains malignant progression. Single cell RNA sequencing analysis of matched tumour and normal adjacent tissue and subsequent examination of epithelial cell signatures in *IL22RA1*-high versus low or null cells could provide important insights.

Although *IL22RA1* expression is lower in tumours compared to matched normal tissue, *IL22RA1* expression in tumours and matched normal tissue is positively correlated. Therefore, patients with high normal adjacent *IL22RA1* expression also have high tumoural *IL22RA1* expression relative to the whole cohort. This suggests that there could be underlying genetic or epigenetic factors that result in elevated

IL22RA1 expression in the normal colon, creating a permissive environment for malignant progression upon acquisition of critical driving mutations like *KRAS*. Polymorphisms in the *IL22RA1* gene have been reported and three SNPs in particular (rs4292900, rs4648936, rs16829225) have been associated with severe chronic rhinosinusitus (Endam *et al.*, 2009). However, the consequences of these polymorphisms on *IL22RA1* expression, structure, and function are not known. One SNP in *IL22* itself (rs1179251) has been shown to confer an estimated 50% increase in colon cancer risk (Thompson *et al.*, 2010). However, to our knowledge the association between polymorphisms in *IL22RA1* and colon cancer have not specifically been explored. Alternatively, despite the fact that the normal adjacent biopsies were taken at sites distant from the tumour margins, the high *IL22RA1* expression in matched normal tissue from *IL22RA1* tumours could be a consequence of field cancerization (Galandiuk *et al.*, 2012). The possible involvement of the composition and structure of the microbiota in modulating *IL22RA1* expression is discussed below.

3.3.4 Identification of a novel prognostic link between *IL22RA1* and *KRAS* mutation

Prospective analysis of the PETACC3 cohort has previously demonstrated that *KRAS* mutations alone have no prognostic value for RFS or OS in stage II/III CRC patients who receive adjuvant chemotherapy (Roth *et al.*, 2010). This is in accordance with a number of smaller retrospective studies (González-Aguilera *et al.*, 2004; Westra *et al.*, 2005). Therefore, the negative prognostic effect of *KRAS* mutation in patients with *IL22RA1*-high tumours may be due to an apparently unique synergy between IL-22 signalling and a constitutively active KRAS pathway. KRAS has been shown to induce canonical NF-κB signalling in a number of different cancers (Starczynowski *et*

al., 2011; Ling *et al.*, 2012; Margalef *et al.*, 2015) and interactions between STAT3 and NF-κB promote colorectal, gastric, and liver cancers by potently activating anti-apoptotic pathways and genes involved in cell cycle progression (Grivennikov and Karin, 2010). Dual activation of STAT3 and NF-κB by IL-22 and KRAS, respectively, may drive tumourigenesis in the context of high IL-22 receptor expression. Thus, although mutant *KRAS* is a well-described oncogenic driver, IL-22 may be an important enhancer of its pro-tumourigenic signalling. Further understanding of the basic biology is required to elucidate these synergistic mechanisms and will be the focus of the subsequent chapters in this thesis. To our knowledge this is the first reported evidence of an *IL-22RA1-KRAS* interaction in CRC.

Despite the extensively described tumour-promoting role of IL-6, which also activates STAT3, *IL6R* does not interact with *KRAS*. This could be due to differences in negative regulation of the IL-6 and IL-22 pathways. Unlike the IL-6R, the IL-22R is not subject to negative feedback by the suppressor of cytokine signalling 3 (SOCS3) (Yoshimura and Yasukawa, 2012). IL-22 induces SOCS3 expression directly via STAT3, which may stifle an IL-6 signal but enable perpetuation of IL-22 signalling. Like *IL6R*, *IL17RA* does not interact with *KRAS* despite evidence that oncogenic *KRAS* promotes IL-17 receptor expression and IL-17 signalling in a murine model of pre-invasive pancreatic neoplasia (PanIN) (McAllister *et al.*, 2014). Therefore, the deleterious effect of an upregulated cytokine pathway in *KRAS*-mutant CRC appears to be unique to IL-22.

The prognostic value of *KRAS* in *IL22RA1*-high tumours is most prominent in proximal disease and was not related to either MSI or *BRAF* mutation status. From an immunological perspective, this is logical given that proximal tumours tend to be associated with immune activation (Missiaglia *et al.*, 2014). $CD4^+$ T cells and innate lymphoid cells secrete IL-22 both in homeostasis and pathology downstream of microbially induced IL-23. We observed significantly elevated expression of *IL22* and a trend towards elevated *IL23A* in *IL22RA1*-high proximal *KRAS* mutant but not wild type tumours. In contrast, expression of both cytokines in *IL22RA1*-high distal tumours did not differ between those that were *KRAS* mutant or wild type. Perhaps then, the strength of the prognostic association between *IL22RA1* and *KRAS* mutation is most pronounced in the proximal colon in part due to substrate availability for IL-22 receptor binding and initiation of downstream signalling.

The reason why *IL23A* and *IL22* expression is elevated specifically in *IL22RA1*-high, proximal *KRAS* mutant, but not wild type tumours, remains unknown. Interestingly, bacterial biofilms were almost universally present on proximal but not distal CRCs in independent American and Malaysian cohorts (Dejea *et al.*, 2014). Moreover, in each patient with a biofilm positive tumour, a biofilm was also present on their normal adjacent mucosa (Dejea *et al.*, 2014). Biofilms are massive complexes of bacteria coated in a polymeric matrix, which invade the epithelial mucous, allowing for close interactions between microbes and the colonic epithelial cells (Drewes, Housseau and Sears, 2016). Therefore, it is possible that bacterial products such as hydrogen sulphide, secondary bile acids, reactive oxygen species, and polyamines could be directly mutagenic and involved in tumour initiation. Recently, elevated bacterially synthesized N_1N_{12}-diacetylspermine, a key regulator of cell proliferation, was

observed in biofilm positive tumours and matched normal tissue compared to biofilm negative tissue (Johnson *et al.*, 2015). Along the same lines, close epithelial contact with microbes could trigger protumourigenic inflammatory responses. In both biofilm positive tumours and matched normal tissue, enhanced epithelial proliferation, IL-6 expression, phosphorylated STAT3 (pSTAT3), and reduced E-cadherin expression compared to biofilm negative tissue was observed (Dejea *et al.*, 2014). Given that IL-23 is produced in response to microbial stimuli, IL-23 and its downstream effectors IL-17A and IL-22 may be more abundant in biofilm positive tumours. Indeed, some of the pSTAT3 signal observed in biofilm positive tumours could in fact be a consequence of IL-22 signalling. Furthermore, biofilms could modulate IL-22RA1 expression. If this is the case, the correlation between IL-22RA1 expression in tumours and matched normal tissue could be explained by the biofilm positivity at both sites. Finally, *KRAS* mutations may create a permissive environment for biofilm formation or biofilms may be casually involved in the mutation of *KRAS*. Whether through modulation of the IL-23 pathway, IL-22RA1 expression, or interaction with mutant *KRAS*, we hypothesise that the poor prognostic consequence of high tumoural *IL22RA1* expression in the context of *KRAS* mutation is enhanced in the proximal versus distal colon due to differences in the composition and structure of the intestinal microbiota.

3.3.5 Stratification of *IL22RA1*-high, *KRAS* mutant CRC patients for immunomodulatory therapy in the clinic

Based on our results, we propose a stratification strategy in which tumours from CRC patients are subjected to standard *KRAS* mutation typing paired with immunohistochemical or quantitative PCR-based examination of IL-22 receptor expression. Although both IL-22RA1 and IL-10RB contribute prognostic information,

IL-22RA1 expression is more tightly restricted to epithelial cells, and may thus be more optimally suited for use as a biomarker. CRCs harbouring *KRAS* mutations and high expression of *IL22RA1* and/or *IL10RB* are predicted to comprise approximately 19% of the total CRC population. Such patients are predicted to have lower responsiveness to conventional chemotherapy, increased frequency of disease relapse, and reduced overall survival time. Because our analyses focussed on patients with stage II or III CRC, it is not clear whether the *IL22RA1-KRAS* interaction affects the survival of patients with metastatic disease. Thus, for pre-metastatic CRCs with high IL-22 expression and *KRAS* mutation, particularly those within the proximal colon, closer monitoring and more aggressive or alternative therapeutic strategies (such as IL-23/IL-22 blockade) could be beneficial. Notably, although the overall incidence of CRC has declined in recent years, the incidence of proximal CRCs continues to rise, highlighting the need to improve clinical management of these tumours (Cheng *et al.*, 2011).

Because *IL22RA1* expression manifests as a continuous, non-biphasic variable, further prospective studies assessing *IL22RA1* expression are required—and currently on-going in our laboratory—to characterise a clinically relevant prognostic cut-point. We have demonstrated that IL-22RA1 protein is detectable in human FFPE tissue sections, raising the possibility of developing a standardized immunohistochemical assay.

3.3.6 Concluding Remarks

In conclusion, we have identified a novel CRC molecular subtype in which coincident *KRAS* mutation and high IL-22 receptor expression is associated with highly unfavourable prognosis, particularly among cancers of the proximal colon. To our

knowledge, this is the first clinical analysis of cytokine receptor expression in the context of oncogenic mutations in CRC. Our data provide additional justification for the assessment of *KRAS* mutations in CRC, which has until now been clinically beneficial only for prediction of cetuximab responsiveness. It remains to be determined whether there is a mechanistic biological interaction between IL-22 and *KRAS*, and this is the focus of the next chapter in this thesis. If indeed IL-22 synergises with mutant *KRAS* to promote malignancy, then beyond stratifying patients based on *IL22RA1* expression and *KRAS* mutation status for purely prognostic purposes, patients with *IL22RA1*-high, *KRAS* mutant tumours may benefit from therapeutic blockade of the IL-23/IL-22 pathway.

4 IL-22 synergises with mutant *KRAS* to promote malignancy

4.1 Introduction

Hitherto, we have identified a novel and prognostically important interaction between interleukin 22 receptor expression and mutant *KRAS* in colorectal cancer. Patients whose tumours express high levels of either or both subunits of the heterodimeric IL-22R have dramatically worsened prognosis compared to their *KRAS* wild type counterparts. Interestingly, simultaneous high expression of both IL-22R subunits in the context of mutant *KRAS* leads to worse 5-year survival than in *KRAS* mutant tumours with high expression of either receptor subunit alone. Furthermore, the prognostic impact of having a *KRAS* mutation in tumours with high *IL22RA1* expression is most pronounced in the proximal colon. Here, *IL22* expression is elevated in *KRAS* mutant compared to wild type, *IL22RA1*-high tumours. Thus, the most significant prognostic interaction between IL-22R and mutant *KRAS* necessitates high expression of both IL-22R subunits and high amounts of IL-22 itself. This suggests that rather than a spurious association, a true biological interaction between IL-22 signalling and mutant *KRAS* may be active in this poor prognostic subtype. Careful examination of the consequences of IL-22 signalling in *KRAS* mutant versus wild type human colorectal cancer cells expressing high or low levels of the IL-22R is required to validate the presence of a functional synergy.

Much of the current understanding of the function and signalling downstream of IL-22 has come from studying its physiologic role in microbial defence and tissue regeneration at barrier surfaces. The IL-22 receptor, as we and others have demonstrated, is expressed predominately by epithelial cells at barrier surfaces, where IL-22 signalling serves a critical pro-inflammatory function to rapidly defend against invading pathogens (Aujla *et al.*, 2008; Zheng *et al.*, 2008). Numerous reports have

highlighted the capacity of IL-22 to induce antimicrobial peptide production in keratinocytes, particularly the calcium binding proteins S100A7, S100A8, and S100A9 (Wolk *et al.*, 2006). Synergistic induction of S100A9 was observed in primary human keratinocytes stimulated with a combination of IL-22 and IL-17A (Liang *et al.*, 2006). Moreover, S100A8 and S100A9 expression was reduced in the colonic tissue of *Il22-/-* compared to wild type mice during *Citrobacter rodentium* infection (Zheng *et al.*, 2008). In hepatocytes and epithelial cells from the colon or lung, IL-22 also induces acute phase response proteins and the production of chemokines including CXCL1, CXCL2, and CXCL5, which recruit neutrophils to the sites of infection (Andoh *et al.*, 2005). IL-22 additionally plays an important role in promoting protective mucous production at barrier surfaces that prevents direct contact between epithelial cells and invading or resident microbes (Muc1, Muc3, Muc10, Muc13) (Radaeva *et al.*, 2004; Sugimoto *et al.*, 2008; Sonnenberg *et al.*, 2010).

IL-22-driven proliferation is essential for tissue regeneration following inflammatory insult or wounding. Due to its anti-apoptotic and mitogenic effects, IL-22 is tissue protective in murine models of hepatitis (Radaeva *et al.*, 2004; Zenewicz *et al.*, 2007). Deficiency of IL-22 exacerbates tissue destruction in models of intestinal inflammation, including dextran-sodium-sulphate-mediated (DSS) colitis and adoptive transfer of pathogenic T cells (Sugimoto *et al.*, 2008; Zenewicz *et al.*, 2008; Pickert *et al.*, 2009; Zindl *et al.*, 2013). More recently, an important protective function for IL-22 in intestinal epithelial stem cells was elucidated in a mismatched bone marrow transfer model of graft versus host disease (GVHD). In this model, recipient IL-22 deficiency led to increased crypt apoptosis and depletion of intestinal

epithelial stem cells (Hanash *et al.*, 2012). In a follow-up study, IL-22 was found to enhance the efficiency of murine small intestinal organoid growth through direct induction of proliferation and diminution of cell cycle checkpoint molecule expression (Cdkn1a, Cdkn2d) in $Lgr5^{+}$ intestinal epithelial stem cells (Lindemans *et al.*, 2015). Interestingly, pre-treatment of murine small intestinal epithelial cells with IL-22 prior to *ex vivo* irradiation increased the subsequent outgrowth of organoids, and the radiation itself augmented *Il22ra1* expression (Lindemans *et al.*, 2015). Importantly, treatment of mice with IL-22 in a murine GVHD model reduced GVHD pathology, despite an intact alloimmune reaction (Lindemans *et al.*, 2015).

Thus IL-22 plays a critical role in maintenance of mucosal barrier integrity under homeostatic settings. However, IL-22 is a double-edged sword and its known tissue protective functions can become pathogenic if present chronically, or we hypothesise, in the setting of certain oncogenic mutations. Evidence for the capacity of IL-22 to induce pathological inflammation in the skin (Ma *et al.*, 2008; Van Belle *et al.*, 2012), lung (Sonnenberg *et al.*, 2010), and intestine (Muñoz *et al.*, 2009) is abundant. Deregulated IL-22 responses are largely prevented through the action of its neutralising receptor, IL-22-binding protein (IL-22BP or IL-22Rα2). IL-22BP is secreted by $CD11c^{+}$ myeloid cells and sequesters soluble IL-22, thus preventing cell surface receptor engagement and downstream signalling (Xu *et al.*, 2001). Elegant work from Huber *et al.* highlighted that $Il22bp^{-/-}Apc^{min/+}$ mice developed larger and more numerous colon tumours than $Apc^{min/+}$ controls (Huber *et al.*, 2012). The very existence of IL-22BP, in evolutionary terms, underscores the necessity for tight regulation of the IL-22 pathway.

Signalling downstream of the IL-22R is mediated predominately via JAK/STAT pathways. The majority of the well-documented physiologic and pathologic functions of IL-22 are thought to be STAT3-depedent. For example, the existing evidence linking IL-22 to the initiation and progression of murine colitis-associated and sporadic colorectal cancer, implicate, though do not definitively prove, that carcinogenesis mediated by IL-22 is STAT3-dependent (Huber *et al.*, 2012; Kirchberger *et al.*, 2013b). Our clinical data point toward an important distinction between IL-22 and the more robustly studied STAT3 activator IL-6, in promoting malignant progression in the context of *KRAS* mutation. Unlike the IL6 receptor, the intracellular domain of IL-22RA1 is constitutively associated with STAT3, allowing for rapid phosphorylation at both Tyr-705 and Ser-727 upon receptor dimerization (Dumoutier *et al.*, 2009; Lim and Savan, 2014). IL-22-mediated STAT3 signalling massively induces the expression of suppressor of cytokine signalling 3 (SOCS3), which inhibits signalling downstream of cytokine receptors containing a gp130 domain (ie. IL-6, IL-11). Interestingly, both subunits of the IL-22 receptor lack SOCS3 binding sites and thus the IL-22R is not subject to feedback inhibition by SOCS3 (Yoshimura, Naka and Kubo, 2007). Thus, in a cell autonomous fashion, IL-22 may limit IL-6 signalling via SOCS3 while allowing for sustainment of its own signalling. Although not as extensively characterised, IL-22R engagement also activates several mitogen activated protein kinase (MAPK) pathways including p38 and extracellular signalling related kinase (ERK). IL-22-induced phosphatidylinositol-3-kinase (PI3K) activation is required for migration of colonic epithelial cells, and AKT activation via IL-22 enables normal proliferation of human epithelial keratinocytes and inhibits apoptosis in renal tubular epithelial cells (Mitra, Raychaudhuri and Raychaudhuri, 2012; Xu *et al.*, 2014). Finally, IL-22 has been

shown to activate NF-κB and, through synergism with STAT3, induce the expression of genes involved in cell cycle progression and inhibition of apoptosis (Lim and Savan, 2014).

Despite the abundant data from pre-clinical models implicating IL-22 and upstream IL-23 in colorectal cancer initiation and progression, the precise molecular mechanism by which IL-22 mediates tumourigenesis remains to be elucidated. In 2014, Kryczek *et al.* provided the first evidence to suggest that IL-22 promotes colorectal cancer stemness. IL-22, produced by T cells in the tumour microenvironment, was found to activate STAT3 in tumour cells, which directly induced the expression of the methyltransferase DOT1L. DOT1L in turn permitted the expression of mediators of pluripotency (*SOX2, NANOG, POU5F1*) that were negatively correlated with patient prognosis (Kryczek *et al.*, 2014). Additionally, though limited, there is some evidence to suggest that IL-22 may promote malignancy by inducing chemoresistance. Elevated serum levels of IL-22 were found in a group of chemoresistant (N=41) as compared to chemosensistive (N=46) CRC patients (Wu *et al.*, 2013). Furthermore, pretreatment of SW620 and SW480 CRC cell lines with IL-22, followed by treatment with 5 fluorouracil (5-FU) promoted chemoresistance (Wu *et al.*, 2013). Similarly, the pro-apoptotic effects of carboplatin and 5-FU were reduced when human A549 lung cancer cells were treated with recombinant IL-22 or transfected to constitutively express IL-22 (Zhang *et al.*, 2008).

To date, the only evidence of a potential link between IL-22 signalling and oncogenic *KRAS* is reported in a published conference abstract in a Kras-induced lung cancer model (Khosravi *et al.*, 2016). Genetic ablation of IL-22 in CCSP-Cre*/LSL-Kras*^{G12D}

mice reduced the number of lung tumours by 54% compared to IL-22 sufficient controls. Reduced tumour cell proliferation, STAT3 activation, and expression of the key stem cell markers NANOG, SOX2, and OCT4 was observed in CCSP-Cre*/LSL-Kras*^{G12D} *Il22*$^{-/-}$ mice (Khosravi *et al.*, 2016). Although not directly linking IL-22 and *KRAS,* another recent report found that patients with insulin receptor substrate-1 (IRS-1) deficient lung adenocarcinomas displayed reduced survival if their tumours were *KRAS* mutant but not wild type (Metz *et al.*, 2016). Mechanistically, it was found that IRS-1-silenced, *KRAS* mutant lung adenocarcinoma cells display sustained activation of STAT3 in response to IL-22, due to a prolonged IL-22RA1 half-life. IRS-1 deficiency augmented pAKT and pGSK-3β, resulting in phosphorylation of the cytoplasmic tail of IL-22RA1, which prevented its ubiquitination and degradation. This enhanced IL-22 signalling drove CXCL1 production and myeloid infiltration that was important for malignant progression in preclinical models (Metz *et al.*, 2016). Furthermore, although not linked to IL-22, evidence from a preinvasive pancreatic neoplasia (PanIN) model revealed that oncogenic *KRAS* and chronic pancreatitis synergistically induce IL-17A and IL-22 production by $CD4^+$ and γδT cells (McAllister *et al.*, 2014). Interestingly, mutant *KRAS* also directly augmented IL-17A receptor expression in the pancreatic epithelium in a cell autonomous fashion (McAllister *et al.*, 2014).

In colorectal cancer, although our analyses in tumour transcriptomic cohorts have not revealed that *IL22RA1* is elevated in *KRAS* mutant versus wild type colorectal tumours, it remains to be determined whether mutant *KRAS* can directly influence the expression or dynamic regulation of the IL-22 receptor. Furthermore, a direct link between IL-22 signalling and mutant *KRAS* in CRC has not been made to date. Given

the genetic heterogeneity in cancer, the influence and potential synergism between cell extrinsic signalling into cells harbouring oncogenic mutations in critical cytokine signalling pathways cannot be ignored.

Given the striking prognostic interaction between high expression of either or both subunits of the heterodimeric IL-22 receptor and mutant *KRAS*, we hypothesise that IL-22 signalling synergises with mutant *KRAS* to promote malignancy. Thus, the primary aim of this chapter is to determine whether there is a mechanistic biological interaction between IL-22 and mutant *KRAS* in human colorectal cancer using three experimental modalities:

1. We first selected a panel of colorectal cancer cell lines to represent the clinical molecular subtypes of interest and assessed the capacity of IL-22 to modulate stem cell marker gene expression, chemosensitivity, and clonogenic outgrowth.
2. We then confirmed our findings in an isogenic cell line pair with matched IL-22 receptor expression, differing only in the presence or absence of *KRAS* mutation. This isogenic system was also used to explore whether the dynamic regulation of IL-22RA1 is *KRAS* dependent.
3. Finally, we established primary human organoids derived from prospectively collected tumours and matched normal adjacent tissue to be a valid *ex vivo* model in which to study the IL-22-*KRAS* interaction. We then performed functional experiments in the organoids to begin to confirm the observations made using the cell lines.

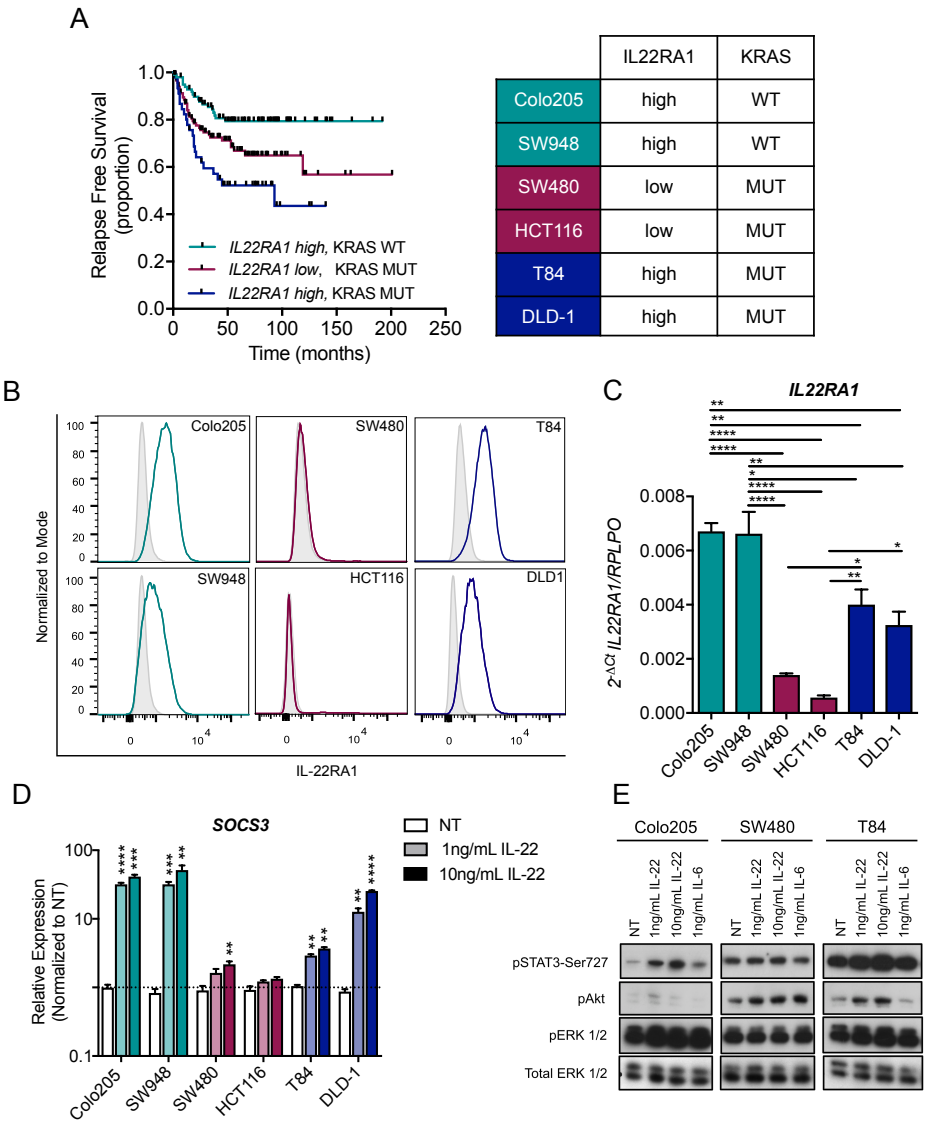
4.2 Results

4.2.1 Selection of a panel of CRC lines to mirror the clinical molecular subtypes of interest

To establish whether there is a mechanistic link between IL-22 signalling and mutant *KRAS*, we first selected a panel of CRC cell lines to recapitulate the clinical molecular subtypes of interest (Figure 4.1 A). Cell surface expression of IL-22RA1 was high in the Colo205, SW948, T84 and DLD-1 lines, but was low in the SW480 and HCT116 lines, as measured by flow cytometry (Figure 4.1 B). Q-PCR confirmed this expression pattern at the mRNA level (Figure 4.1 C). Therefore, the Colo205 and SW948 lines represented the good prognosis *IL22RA1*-high, *KRAS* WT subtype; the SW480 and HCT116 lines reflected the intermediate prognosis *IL22RA1*-low, *KRAS* MUT subtype; and the T84 and DLD-1 cells mirrored the poor prognosis *IL22RA1*-high, *KRAS* MUT subtype (Figure 4.1 A). To confirm that IL-22 signalling was active and proportional to the amount of IL-22R expressed by each line, cells were stimulated for 24 hours with 1ng/mL or 10ng/mL IL-22. Induction of *SOCS3* (encoding suppressor of cytokine signalling 3), a well-established direct transcriptional target of IL-22 (Nagalakshmi *et al.*, 2004), was measured by qPCR. Significant induction of *SOCS3* was detectable with both 1ng/mL and 10ng/mL IL-22 stimulation in each of the IL-22RA1-high lines (Colo205, SW948, DLD-1, T84), but not the IL-22RA1-low lines (SW480, HCT116) (Figure 4.1 D). The fold change in induction of *SOCS3* in the IL-22RA1-high lines was proportional to the amount of IL-22RA1 expression and not perceptibly influenced by the *KRAS* mutation status of the cell line (Figure 4.1 D). To further confirm that IL-22 signalling was active in the CRC lines, Colo205, SW480, and T84 cells were stimulated for 24h with 1ng/mL or 10ng/mL IL-22 and activation of downstream intracellular signalling pathways was evaluated by Western blot. Cells were also stimulated with 1ng/mL IL-6 as a

comparative STAT3 activator. Phosphorylation of STAT3 (S727) was evident with IL-22 stimulation in IL-22RA1-high Colo205 and T84 cells, but not in IL-22RA1-low SW480 cells (Figure 4.1 E). IL-22 did not appreciably induce phosphorylation of pERK1/2 in any of the lines assessed (Figure 4.1 E). Interestingly, marked phosphorylation of AKT (S473) was observed in the IL-22RA1-high, *KRAS* mutant T84 cells, specifically with IL-22 and not IL-6 stimulation (Figure 4.1 E). This pAKT induction was not observed in the IL-22RA1-high, *KRAS* WT Colo205 cells (Figure 4.1 E).

Therefore, IL-22 signalling is active in the panel of cell lines assessed. Furthermore, induction of the direct target gene *SOCS3* seems to be dependent on the amount of IL-22RA1 expression and independent of *KRAS* mutation status.



	IL22RA1	KRAS
Colo205	high	WT
SW948	high	WT
SW480	low	MUT
HCT116	low	MUT
T84	high	MUT
DLD-1	high	MUT

Figure 4.1 Selection of a panel of CRC lines to mirror the clinical molecular subtypes of interest.

(A) Kaplan Meier curves highlighting the clinical molecular subtypes of interest: *IL22RA1*-high, *KRAS* mutant (MUT); *IL22RA1*-high, *KRAS* wild type (WT); *IL22RA1*-low, *KRAS* mutant and table displaying the six CRC lines selected which recapitulate these subtypes.

(B) Representative histograms from flow cytometric analysis of IL-22RA1 protein expression compared to matched isotype control (grey) for each cell line.

(C) qPCR analysis of basal *IL22RA1* mRNA expression in each cell line. Data are mean ± SEM (n=3-5 independent experiments performed with n=2-3 technical replicates). Statistical significance was determined using a one-way ANOVA with Tukey's post-test for multiple comparisons: *p<0.05, **p<0.01, ***p<0.001, ****p<0.0001.

(D) qPCR analysis of *SOCS3* induction in each cell line after 24h stimulation with 1ng/mL and 10ng/mL IL-22. Data are mean ± SEM normalised to the mean *SOCS3* expression in the no treatment (NT) condition for each cell line (n=1 representative independent experiment performed with n=3 technical replicates). Statistical significance was determined using one-way ANOVAs, with Tukey's post-tests for multiple comparisons comparing the stimulation to NT conditions for each line: *p<0.05, **p<0.01, ***p<0.001, ****p<0.0001. *Cont'd next page.*

(E) Representative Western blots highlighting activation of pSTAT3-Ser727, pAKT-Ser473, and pERK 1/2 following 24h stimulation with 1ng/mL IL-22, 10ng/mL IL-22, and 1ng/mL IL-6 using ECL based detection in the Colo205, SW480 and T84 lines.

4.2.2 *OLFM4* is induced in an IL-22-specific manner in IL-22R-high cells

Having established that IL-22 signalling was active and related to IL-22RA1 expression level in the cell lines assessed, we next sought to examine the capacity of IL-22 to modulate classical hallmarks of malignancy in the CRC lines. Specifically, we wished to determine whether IL-22 could synergise with mutant *KRAS* to promote malignant behaviour.

Cancer initiating cells or cancer stem cells are thought to play a critical role in colorectal tumour initiation, perpetuation, and metastasis (Sangiorgi and Capecchi, 2008; Barker *et al.*, 2009). In light of the evidence demonstrating that IL-22 stimulates small intestinal repair through promoting intestinal epithelial stem cell-dependent regeneration (Hanash *et al.*, 2012; Lindemans *et al.*, 2015) and the recently described capacity of IL-22 to induce stemness in DLD-1 cells (Kryczek *et al.*, 2014), we first investigated whether IL-22 could induce stem cell gene expression in our panel of CRC lines. We hypothesised that IL-22 may enhance stem cell gene expression specifically in the context of *KRAS* mutation. CRC cells were stimulated for 24 hours with 1ng/mL IL-22, 10ng/mL IL-22, or 1ng/mL IL-6 as a comparative STAT3 activator, then analysed by qPCR for expression of characteristic intestinal epithelial stem cell markers. We focussed our preliminary screen on the bona fide stem cell markers *LGR5* and *OLFM4,* described extensively in the work of the Clevers' group (van der Flier *et al.*, 2009; Merlos-Suárez *et al.*, 2011; Schuijers *et al.*, 2014), and *SOX2, NANOG,* and *POU5F1* (OCT4), which were used by Kryczek *et al.* to characterise IL-22-induced stemness (Kryczek *et al.*, 2014). In contrast to the

findings of Kryczek *et al.*, we did not find that IL-22 reproducibly induced expression of *SOX2, NANOG,* or *POU5F1* in the DLD-1 line (Figure 4.2 A). *NANOG* expression was significantly induced by 1ng/mL IL-22 stimulation in the IL-22RA1-high, *KRAS* MUT T84 line, though no significant changes were observed in the other lines (Figure 4.2 A). Furthermore, *LGR5* expression was not significantly and reproducibly modulated by IL-22 stimulation. However, IL-22 (and not IL-6) stimulation did upregulate *OLFM4* expression in the IL-22RA1-high Colo205, SW948, and T84 cells (Figure 4.2 A). In line with evidence of loss of *OLFM4* in some cancers (Liu *et al.*, 2008; Besson *et al.*, 2011; Li *et al.*, 2013), we were unable to detect *OLFM4* expression in the HCT116 or DLD-1 lines (Figure 4.2 A).

In summary, IL-22 stimulation does not consistently or significantly modulate *LGR5, SOX2, NANOG,* or *POU5F1* expression at the doses used in these experiments. *OLFM4* however, is potently induced by IL-22 and not IL-6 in IL-22RA1-high cells regardless of the *KRAS* mutation status of the cell. Therefore, the poor prognosis of *IL22RA1*-high, *KRAS* mutant cells may not be a consequence of an enhanced stem cell gene expression signature. However, measuring the acquisition of stemness based on induction of stem cell marker genes is inadequate when a stem cell is defined based on its unique ability to differentiate and self-renew. Therefore, further functional assays are required to assess stemness and other malignant behaviours.

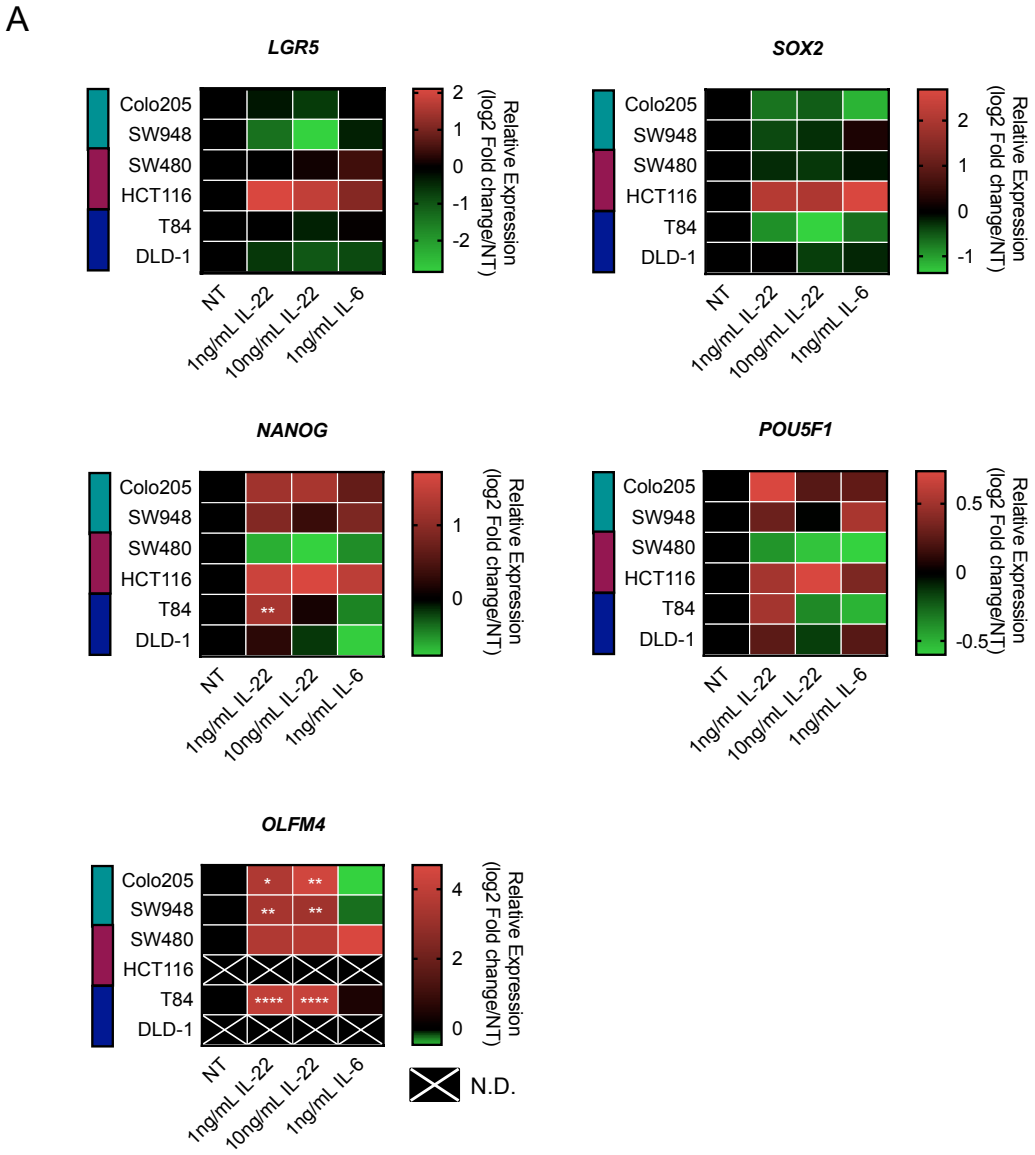


Figure 4.2 *OLFM4* is induced in an IL-22 specific manner in IL-22R-high cells.

(A) Panel of six CRC lines representing the clinical molecular subtypes of interest were stimulated for 24h with 1ng/mL IL-22, 10ng/mL IL-22, or 1ng/mL IL-6. qPCR analysis was performed to evaluate modulation of expression of the stem cell genes: *LGR5*, *SOX2*, *NANOG*, *POU5F1*, and *OLFM4*. Heat maps display the log2 fold change in gene expression between the stimulation and no treatment (NT) conditions for each line. Data represent the mean log2 fold change (n=1 experiment performed with n=3 technical replicates). Statistically significant changes are indicated on each heat map. Statistical significance was determined using ordinary one-way ANOVAs, with Dunnett's post-tests for multiple comparisons comparing the stimulation to NT conditions for each line: *p<0.05, **p<0.01, ****p<0.0001. N.D. indicates that gene expression was not detectable.

4.2.3 IL-22 promotes chemoresistance in IL-22R-high, *KRAS* mutant T84 and DLD-1 cells

In our *in silico* analysis of the prognostic association between *IL22RA1* and *KRAS* mutation, the confirmation cohort (PETACC3) was uniformly comprised of Stage II/III patients in the PETACC3 Phase III clinical trial who all received 5 fluorouracil (5-FU) in the adjuvant setting (Popovici *et al.*, 2012; Roth *et al.*, 2012). This suggested that patients with *IL22RA1*-high, *KRAS* mutant tumours were refractory to chemotherapy. We therefore sought to determine whether IL-22 could promote chemoresistance specifically in IL-22RA1-high, *KRAS* MUT cells.

Three lines representing each of the molecular subtypes of interest (Colo205, SW480, and T84), in addition to the DLD-1 line studied extensively by Kryczek *et al.*, were pre-treated for 48 hours with 10ng/mL IL-22 and then treated with 50μM 5-FU for an additional 48 hours (Figure 4.3 A). Cell viability was assessed by a colourimetric MTT assay. IL-22 promoted resistance to 5-FU specifically in the IL-22RA1-high, *KRAS* MUT T84 and DLD-1 lines (Figure 4.3 B). By contrast, the protective effect of IL-22 was substantially reduced in the IL-22RA1-high, *KRAS* WT Colo205 or IL-22RA1-low, *KRAS* MUT SW480 cells (Figure 4.3 B).

Thus, in agreement with the survival effects observed in the PETACC3 cohort, the results of these experiments suggest a possible synergism between oncogenic *KRAS* and IL-22 signalling that results in resistance to standard of care chemotherapy and malignant progression.

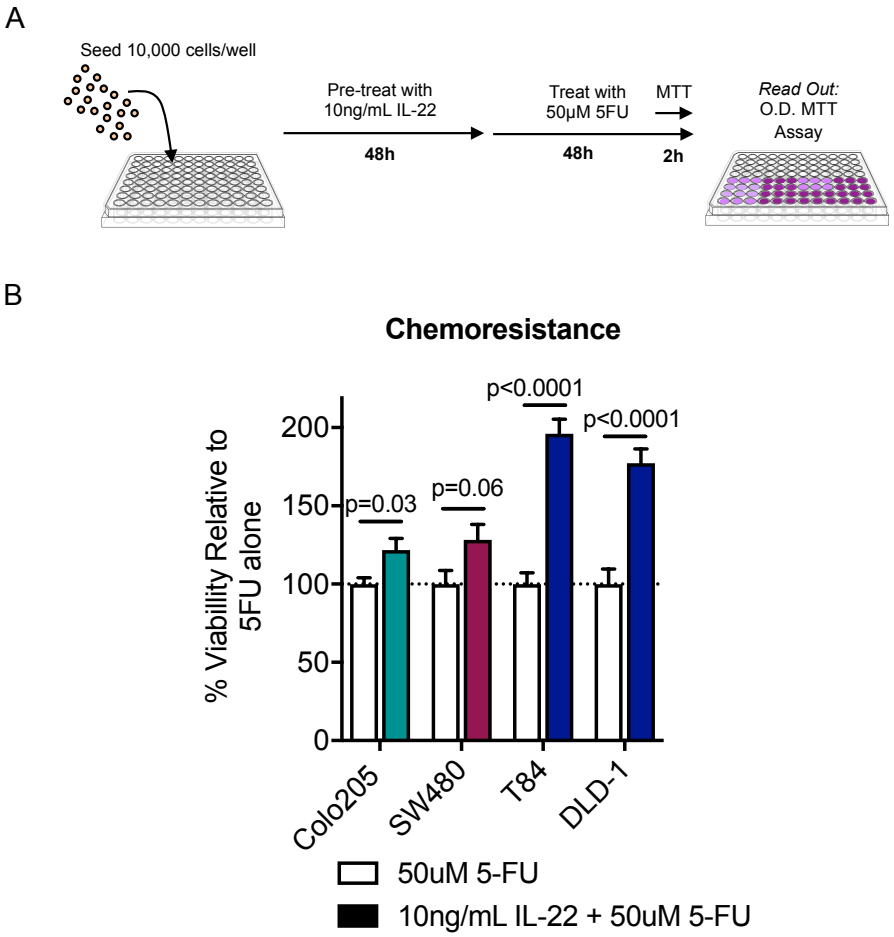


Figure 4.3 IL-22 promotes chemoresistance in IL-22R-high, *KRAS* mutant T84 and DLD-1 cells.

10,000 Colo205, SW480, T84, and DLD-1 cells were pre-stimulated or not pre-stimulated with 10ng/mL IL-22 for 48h then treated for 48h with 50μM 5 fluorouracil (5-FU) in media containing 10% FBS. 50μg MTT was added to each well 2h prior to the end of the 5-FU treatment. Formazan particles were dissolved in DMSO and absorbance was measured at 570nm to assess cell viability.

(A) Chemoresistance assay experimental workflow.
(B) Cell viability as measured by MTT assay. Raw 570nm absorbances are blank corrected and normalised to the mean of the 5-FU only condition for each independent experiment. Data are means + SEM (n=5 independent experiments performed with n=2-3 technical replicates per experiment). Statistical significance was determined using unpaired T-tests comparing the 10ng/mL IL-22 + 50μM 5-FU condition to the 50μM 5-FU only condition for each cell line. P <0.05 is considered significant.

4.2.4 IL-22 promotes clonogenic outgrowth in IL-22R-high, *KRAS* mutant T84 and DLD-1 cells

Given the capacity of IL-22 to induce chemoresistance to 5-FU specifically in IL-22RA1-high, *KRAS* MUT cells, we sought to determine whether IL-22 could enhance other malignant behaviours in a *KRAS* mutation-dependent manner. Classically,

clonogenic outgrowth assays were understood to measure proliferation, capacity for anchorage-independent growth, and resistance to apoptosis (Pastrana, Silva-Vargas and Doetsch, 2011). In addition, starting with the neural stem cell field, some have used the assay as a measure of cancer stemness (Kryczek *et al.*, 2014). Whether sphere forming assays measure stemness or stem-like behaviour remains controversial (Pastrana, Silva-Vargas and Doetsch, 2011). Typically, these sphere-forming assays, termed mammosphere assays in a breast cancer context (Stingl, 2009), are performed in liquid medium where spontaneous aggregation of single cells may lead to false positives in sphere enumeration. We therefore assessed the capacity of IL-22 to promote clonogenic outgrowth of Colo205, SW480, T84, and DLD-1 cells in three-dimensional culture in a semi-solid methylcellulose matrix to prevent spontaneous cell aggregation. Thus, each sphere formed was in theory derived from a single cell capable of clonal expansion in the culture conditions. Cells were pre-treated in monolayers with 10ng/mL IL-22 for 48 hours, then filtered to single cells and seeded at a low density (1000 cells/well) in 96 well low-binding plates and cultured for 7 days in the presence or absence of IL-22. Spheres were enumerated using an unbiased ImageJ-based edge detection approach (Chapter 2, Figure 2.3) on two-dimensional images of each well, acquired at low magnification (4x) (Figure 4.4 A). IL-22 pre-treatment enhanced clonogenic outgrowth specifically in the IL-22RA1-high, *KRAS* MUT T84 and DLD-1 cells. This effect was visible both macroscopically (Figure 4.4 B) and upon unbiased sphere enumeration (Figure 4.4 C). Additionally, IL-22 pre-treatment increased the size of T84 and DLD-1 spheres (Figure 4.4 D). Neither sphere number nor size was modulated by IL-22 in the IL-22RA1-high, *KRAS* WT Colo205 or IL-22RA1-low, *KRAS* MUT SW480 cells (Figure 4.4 C, D).

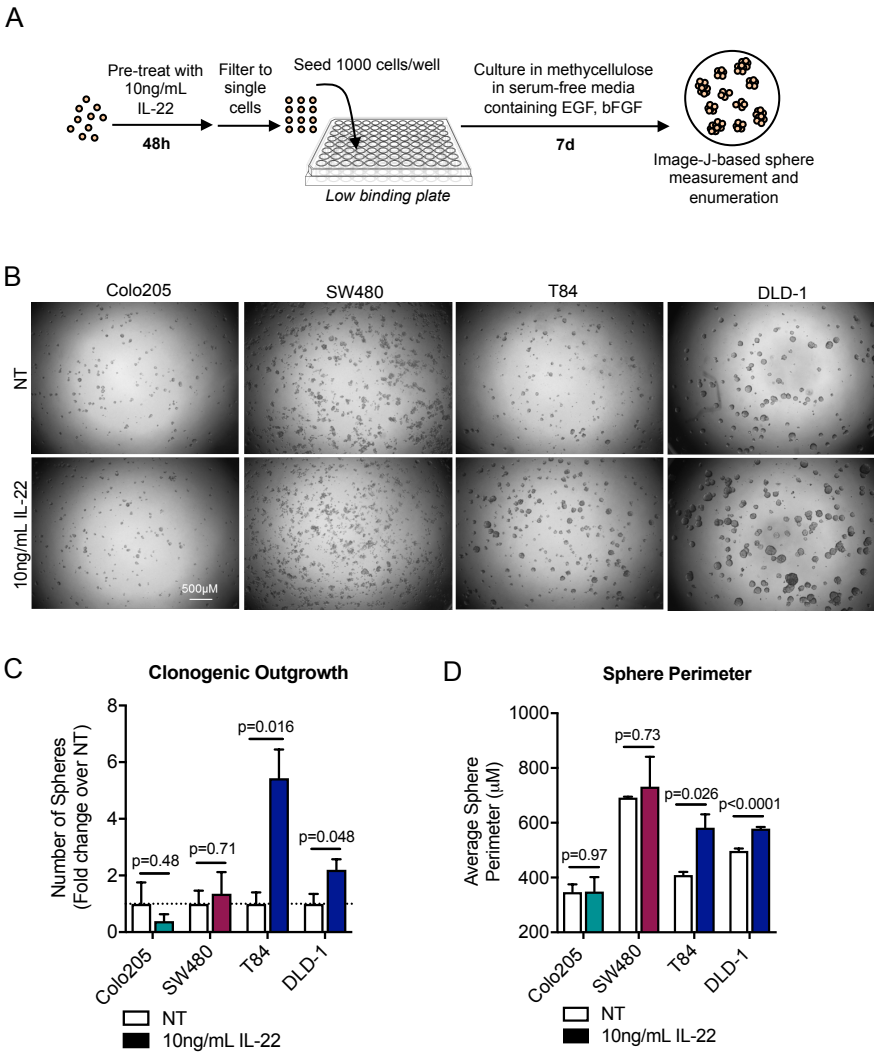


Figure 4.4 IL-22 promotes clonogenic outgrowth in IL-22R-high, *KRAS* mutant T84 and DLD-1 cells.

Colo205, SW480, T84, and DLD-1 cells were pre-treated or not pre-treated in 2D culture conditions with 10ng/mL IL-22 for 48h. Cells were then trypsinised, filtered to create a single cell suspension and 1000 cells/well were seeded into 96 well low-binding plates in serum free media containing 1% methylcellulose, 20ng/mL EGF, and 10ng/mL basic FGF. Clonogenic outgrowth was measured 7 days after seeding into sphere forming conditions. Each well was imaged and sphere numbers were quantified using an unbiased ImageJ approach (See Chapter 2.2.9 for full description)

(A) Experimental workflow for clonogenic outgrowth assay.

(B) Representative bright field microscopic images (4x magnification) of single wells of spheres 6-7 days after seeding.

(C) Quantification of number of spheres from cells that were pre-stimulated versus not pre-stimulated with 10ng/mL IL-22. Raw counts are normalised to the mean of the no treatment (NT) condition for each independent experiment. Data are means ± SEM (n=3-5 independent experiments performed with n=3 technical replicates per experiment). Perimeter cut-off to be considered a sphere was set at 500µM.

(D) Sphere perimeter measured using "Edge Detection" function in ImageJ for all spheres formed in each condition for each cell line. Data are means ± SEM (n=3-5 independent experiments performed with n=3 technical replicates per experiment).

Statistical significance for C, D was determined using unpaired T-tests comparing the 10ng/mL IL-22 condition to the NT condition for each cell line. P <0.05 is considered significant.

To determine whether enhanced clonogenic outgrowth was associated with a specific IL-22 target gene signature, we assessed gene expression in the clonogenic spheres after 7 days in culture. Q-PCR based analysis of a panel of well-annotated IL-22 target genes was conducted. Interestingly, both *SOCS3* and *MUC1* (encoding Mucin 1) were significantly induced in IL-22 stimulated as compared to untreated spheres in all CRC lines assessed (Figure 4.5 A, B). This indicated that IL-22 signalling was active, albeit to differing extents, in the clonogenic spheres derived from each line. Interestingly, *S100A9*, which encodes a calcium binding protein known to induce neutrophil chemotaxis and heterodimerise with S100A8 to form calprotectin (Damo *et al.*, 2013; Markowitz and Carson, 2013), was dramatically induced by IL-22 in the IL-22RA1-high, *KRAS* MUT T84 and DLD-1 spheres (Figure 4.5 C). It should be noted that IL-22 also induced *S100A9* expression in the IL-22RA1-high, *KRAS* WT Colo205 spheres, however the absolute amount of mRNA compared to the endogenous control was much lower than in the IL-22RA1-high, *KRAS* MUT spheres (Figure 4.5 C). Another well-characterised neutrophil chemoattractant, *CXCL1*, was induced by IL-22 in IL-22RA1-high, *KRAS* MUT T84 and DLD-1 spheres, though the induction did not reach statistical significance in the DLD-1 spheres (Figure 4.5 D). Akin to *S100A9*, *CXCL1* was also induced by IL-22 in the IL-22RA1-high, *KRAS* WT Colo205 spheres, however again the amount of mRNA compared to the endogenous control was much lower than in the IL-22RA1-high, *KRAS* MUT counterparts. Finally, IL-22 induced *OLFM4* in both Colo205 and T84 spheres, but it was undetectable in SW480 and DLD-1 spheres (Figure 4.5 E).

Therefore, IL-22 promoted clonogenic outgrowth and increased sphere size specifically in IL-22RA1-high, *KRAS* MUT cells. Furthermore, IL-22 potently induced *S100A9* expression in IL-22RA1-high, *KRAS* MUT clonogenic spheres.

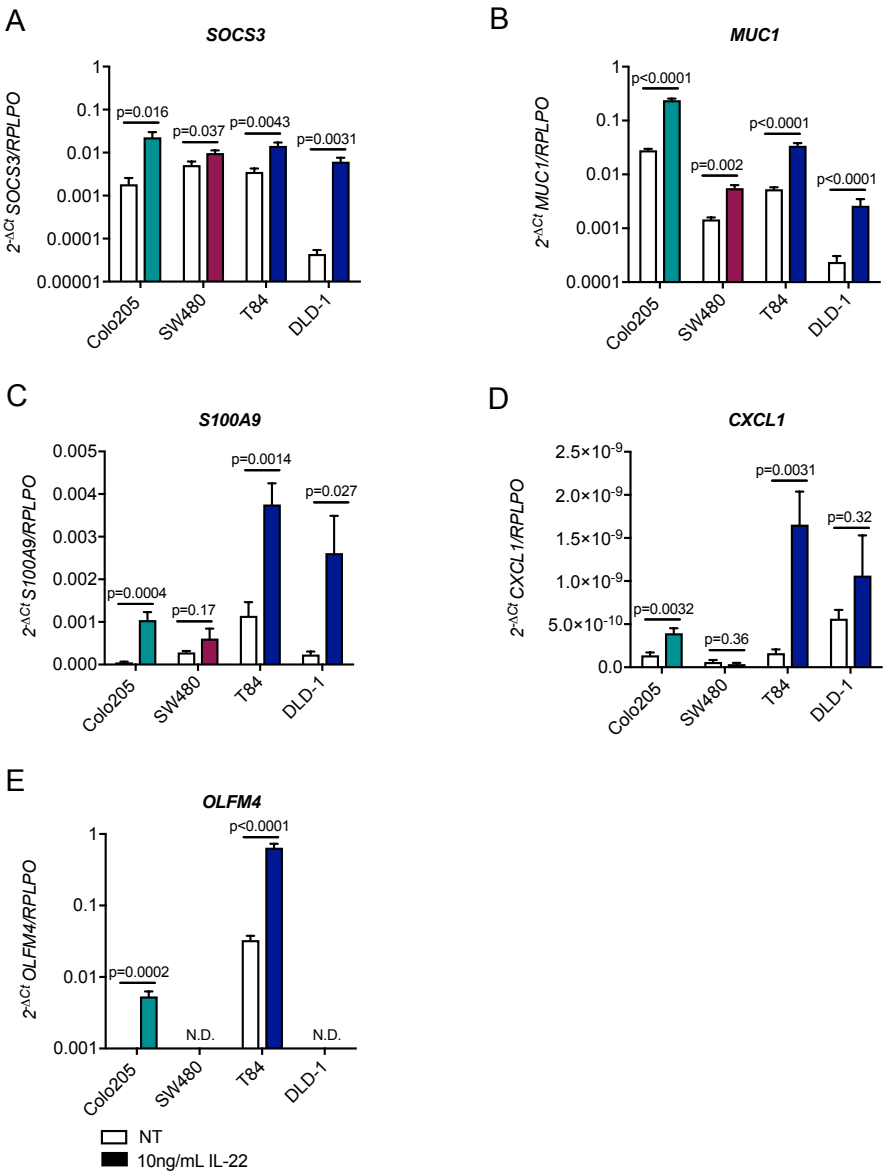


Figure 4.5 IL-22 significantly induces *S100A9* in IL-22R-high, *KRAS* mutant T84 and DLD-1 clonogenic spheres.

RNA was extracted from Colo205, SW480, T84, and DLD-1 cells pre-treated or not pre-treated for 48h with 10ng/mL IL-22 and subsequently grown under sphere forming conditions in the presence or absence of 10ng/mL IL-22 for 7 days (as described in Figure 4.4). qPCR analysis was performed for known IL-22 target genes:
(A) *SOCS3* (B) *MUC1* (C) *S100A9* (D) *CXCL1* (E) *OLFM4*
Data are mean ± SEM relative expression for each gene (n=3 independent experiments performed with n=2 technical replicates per experiment). Statistical significance was determined using unpaired T-tests comparing the 10ng/mL IL-22 condition to the NT condition for each cell line. P <0.05 is considered significant. N.D. indicates that gene expression was not detectable.

4.2.5 Characterisation of a DLD-1 *KRAS* mutant and wild type isogenic cell line pair

We have thus far established that IL-22 promotes chemoresistance and clonogenic outgrowth specifically in IL-22RA1-high, *KRAS* MUT CRC cells. However, it is impossible to definitively link the IL-22-induced malignant behaviour to an interaction with mutant *KRAS,* as each cell line was derived from a different individual and harbours a host of divergent background mutations that could be indispensible for the observed behaviour (See Chapter 2, Table 2.6 for mutation status of cell lines used). Therefore, we moved to a DLD-1 isogenic system to interrogate the specific interaction between IL-22 and mutant *KRAS*. The DLD-1 line carries an endogenous heterozygous *KRAS* G13D mutation in the parental (*KRAS* MUT) cells and a recombinant adeno-associated virus was used to knockout the mutant *KRAS* G13D allele by homologous recombination in the paired "wild type" cells (*KRAS* WT) (Horizon Discovery) (See Chapter 2.2.1 for description of isogenic cell line).

IL-22RA1 expression at both the protein (Figure 4.6 A) and mRNA (Figure 4.6 B) level was equivalent in the *KRAS* MUT and *KRAS* WT isogenic cells. Furthermore, *SOCS3* induction following 10ng/mL IL-22 stimulation for 24 hours was comparable between the *KRAS* MUT and *KRAS* WT isogenic cells (Figure 4.6 C). In accordance with the similar level of transcriptional induction of the direct STAT3 target gene *SOCS3*, phosphorylation of STAT3 (Y705) was equivalent in both lines after 24 hours of 10ng/mL IL-22 stimulation (Figure 4.6 D). Interestingly, IL-22 induced phosphorylation of AKT (S473) specifically in the *KRAS* MUT and not *KRAS* WT isogenic cells (Figure 4.6 D). The restriction of IL-22-induced pAKT (S473) to *KRAS* mutant cells supports observations made in the IL-22RA1-high, *KRAS* MUT T84 versus IL-22RA1-high, *KRAS* WT Colo205 cells (Figure 4.1 E).

Therefore, the DLD-1 isogenic pair provides a clean system with matched IL-22RA1 expression to determine whether the enhanced chemoresistance and clonogenic outgrowth capacity induced by IL-22 in *KRAS* MUT cells is specifically *KRAS* dependent.

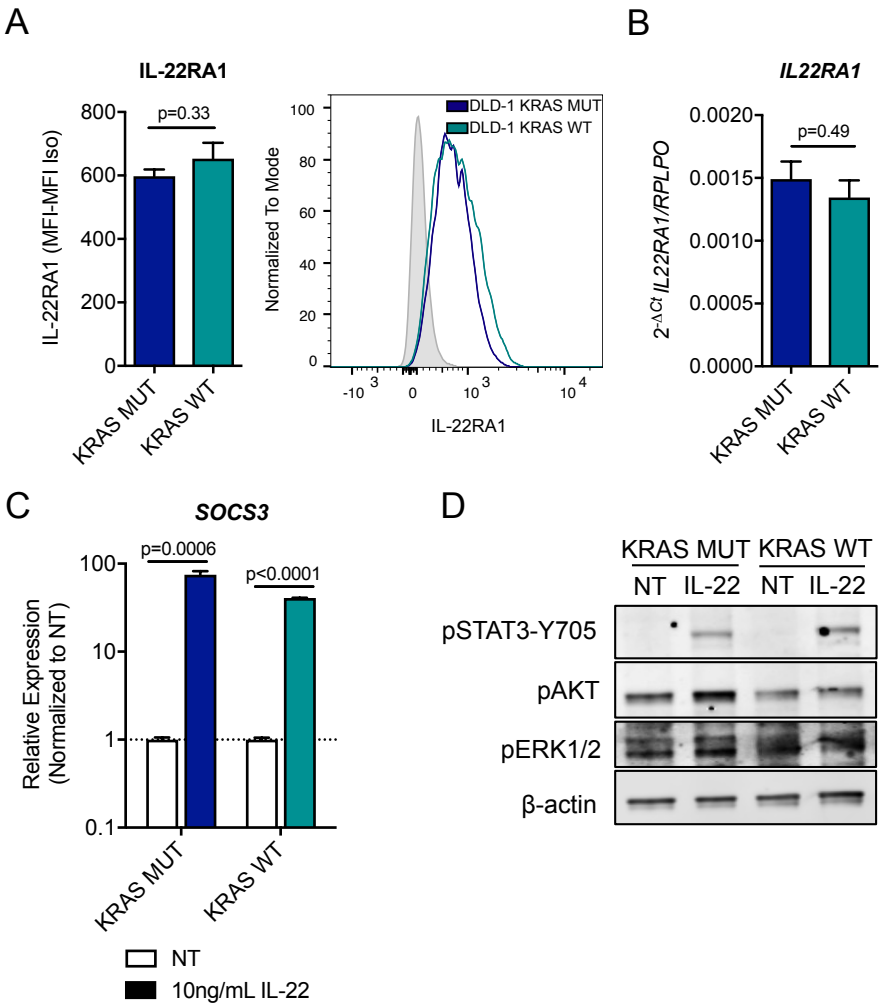


Figure 4.6 The *KRAS* mutant and wild type lines of a DLD-1 isogenic pair have comparable amounts of IL-22R expression and IL-22-induced pSTAT3.

(A) Flow cytometric analysis of IL-22RA1 protein expression at baseline in the DLD-1 isogenic cell line which harbours an endogenous *KRAS* G13D mutation in the parental line (KRAS MUT) and a deleted *KRAS* mutant allele in the partner line (KRAS WT) to revert it to *KRAS* WT. Quantification of isotype control subtracted IL-22RA1 mean fluorescence intensity (MFI) in each line. Data represent mean ± SEM (n=5 independent experiments). Statistical significance was determined using unpaired T-tests. P < 0.05 is considered significant. Representative histograms of IL-22RA1 protein expression in the *KRAS* MUT and WT isogenic pair compared to matched isotype control (grey) are displayed.

(B) qPCR analysis of basal *IL22RA1* mRNA expression in each cell line. Data are mean ± SEM (n=3 independent experiments). Statistical significance was determined using unpaired T-tests. P < 0.05 is considered significant.

(C) qPCR analysis of *SOCS3* induction in each cell line after 24h stimulation with 10ng/mL IL-22. Data are mean ± SEM normalised to the mean *SOCS3* expression in the no treatment (NT) condition for each cell line (n=3 independent experiments). Statistical significance was determined using unpaired T-tests comparing the 10ng/mL IL-22 to NT for each cell line. P <0.05 is considered significant.

(D) Representative Western blot highlighting activation of pSTAT3-Y705, pAKT-S473, and pERK 1/2 following 24h stimulation with 10ng/mL IL-22 using fluorophore-conjugated secondary antibodies and LI-COR-based detection in the DLD-1 isogenic pair.

4.2.6 IL-22 promotes chemoresistance and enhances proliferation specifically in *KRAS* mutant and not wild type DLD-1 isogenic cells

Using the DLD-1 isogenic system to confirm the specific interaction and possible synergism between IL-22 signalling and mutant *KRAS,* we first assessed whether IL-22 confers a chemo-protective effect in the isogenic cells. Cells were pre-treated for 48 hours with 10ng/mL IL-22 and subsequently subjected to 50μM 5-FU for 48 hours (Figure 4.7 A). IL-22 pre-treatment protected the *KRAS* MUT DLD-1 isogenic cells from 5-FU-induced death, but had only a very subtle protective effect in the *KRAS* WT cells (Figure 4.7 B). To determine whether IL-22 was chemo-protective over a range of 5-FU doses in the *KRAS* MUT line, cells were pre-treated with 10ng/mL IL-22 for 48 hours and then subjected to 5-FU at doses ranging from 5-1000μM. Indeed, IL-22 was chemo protective over a range of doses of 5-FU, specifically in the *KRAS* MUT cells (Figure 4.7 C).

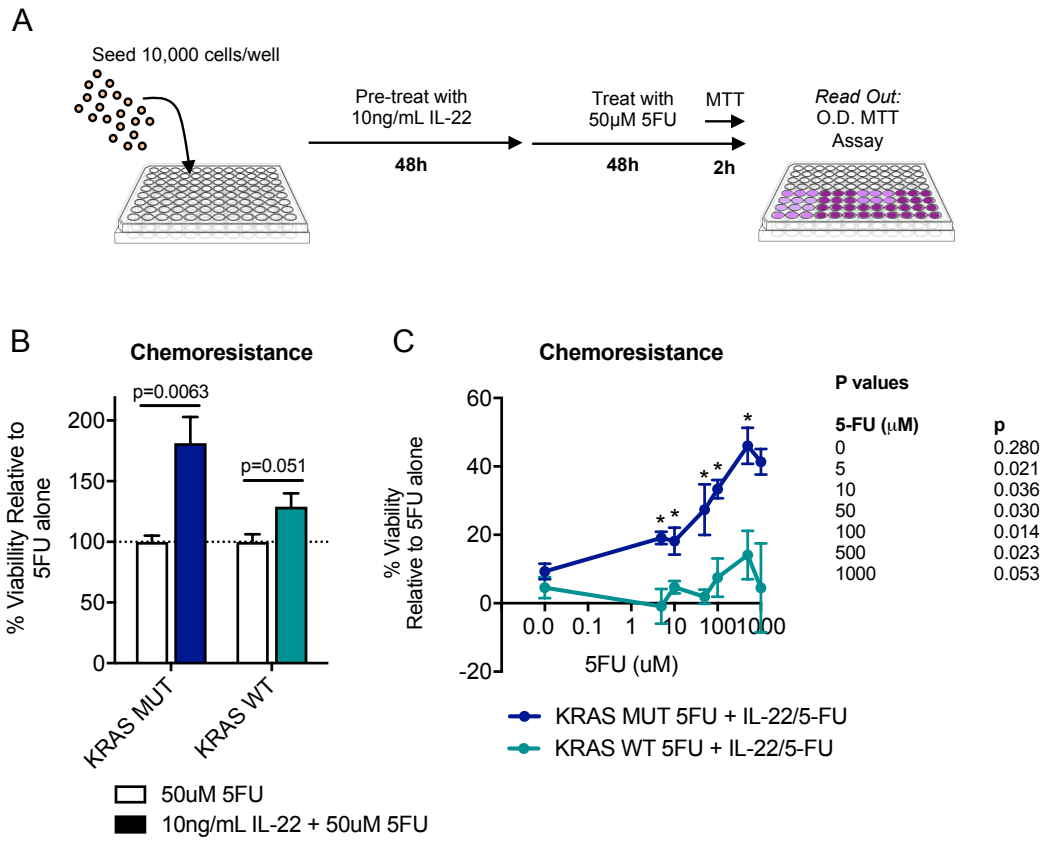


Figure 4.7 IL-22 promotes chemoresistance specifically in *KRAS* mutant isogenic DLD-1 cells.

10,000 DLD-1 *KRAS* mutant or WT isogenic cells were pre-stimulated or not pre-stimulated with 10ng/mL IL-22 for 48h then treated for 48h with 5-1000μM 5 fluorouracil (5-FU) in serum free media containing 1X ITS. 50μg of MTT was added to each well 2h prior to the end of the 5-FU treatment. Formazan particles were dissolved in DMSO and absorbance was measured at 570nm to assess cell viability.

(A) Chemoresistance assay experimental workflow.

(B) Cell viability as measured by MTT assay. Raw 570nm absorbances are blank corrected and normalised to the mean of the 5-FU only condition for each independent experiment. Data are means ± SEM (n=5 independent experiments performed with n=3 technical replicates per experiment). Statistical significance was determined using unpaired T-tests comparing the 10ng/mL IL-22 + 50μM 5-FU condition to the 50μM 5-FU only condition for each cell line. P <0.05 is considered significant.

(C) Cell viability as measured by MTT assay for cells pre-treated with 10ng/mL IL-22 and then treated with increasing doses of 5-FU. Raw 570nm absorbances are blank corrected and normalised to the mean of the 5-FU only condition for each 5-FU dose. Data are means ± SEM (n=1 independent experiment performed with n=3 technical replicates). Statistical significance was determined using multiple unpaired T-tests comparing chemoresistance in the *KRAS* MUT to WT line at each 5-FU dose. Exact p values for each dose are indicated in table adjacent to graph. P <0.05 is considered significant.

Next, to confirm that the IL-22-enhanced clonogenic outgrowth is dependent on the presence of mutant *KRAS*, DLD-1 isogenic cells were pre-treated for 48 hours with 10ng/mL IL-22 and seeded at a low density into low-binding 96 well plates in a semi-solid methylcellulose matrix. Clonogenic outgrowth was evaluated after 7 days (Figure 4.8 A). IL-22 enhanced clonogenic outgrowth in the *KRAS* MUT isogenic cells; however, the *KRAS* WT cells were severely impaired in their clonogenic outgrowth capacity at baseline (Figure 4.8 B, C). The established cut-point to classify a mass of cells as a clonogenic sphere was set to exclude spheres with perimeters less than 500μM when imaged in 2-dimensions. Very few *KRAS* WT spheres passed this threshold at baseline. To determine whether IL-22 influenced the outgrowth of smaller spheres, the sphere detection threshold was reduced to eliminate spheres with perimeters less than 200μM. Even still, IL-22 did not enhance the outgrowth of smaller spheres in the *KRAS* WT isogenic cells (Figure 4.8 C). Assessment of IL-22-dependent gene expression in this setting revealed that after 7 days, *SOCS3, MUC1,* and *S100A9* were all induced by IL-22 in both the *KRAS* MUT and WT isogenic line (Figure 4.8 D). However, IL-22-induced gene expression was modestly higher in the *KRAS* MUT versus WT spheres for all genes assessed (Figure 4.8 D).

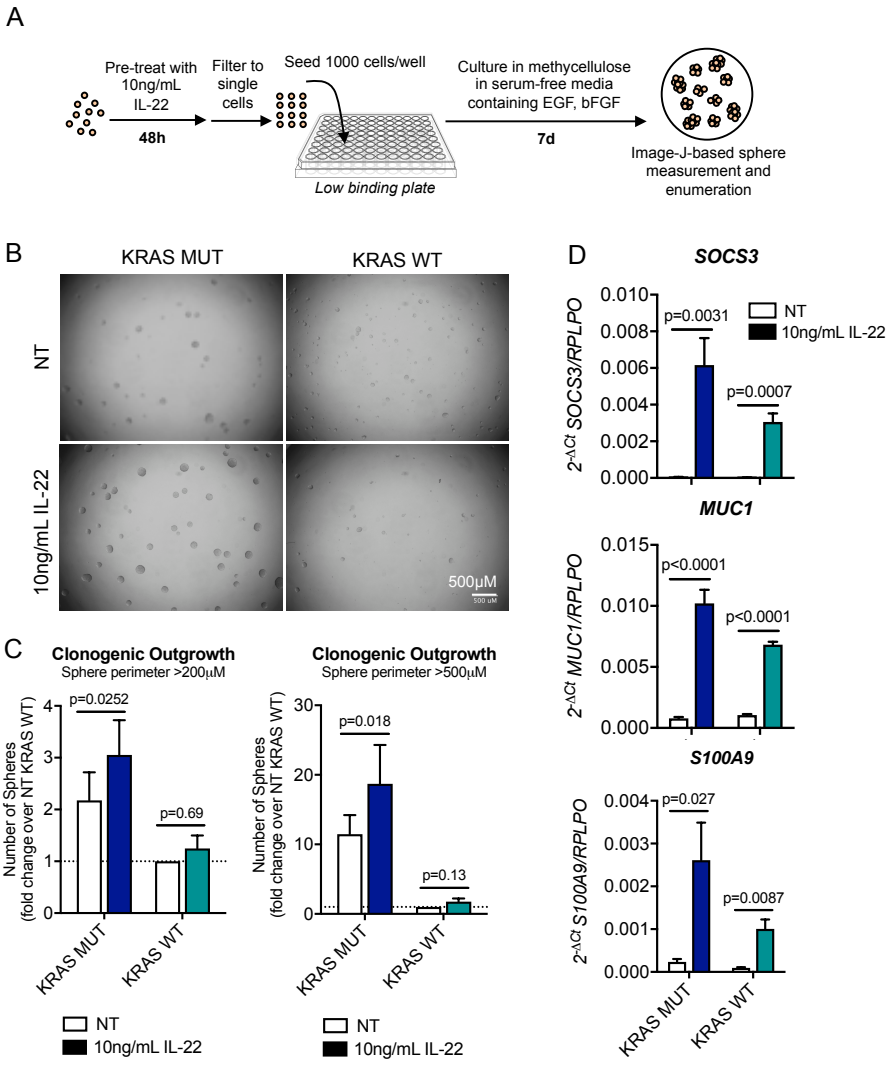


Figure 4.8 IL-22 enhances clonogenic outgrowth of *KRAS* mutant isogenic DLD-1 cells, but *KRAS* wild type isogenic DLD-1 cells have impaired clonogenic outgrowth capacity.

DLD-1 *KRAS* MUT or WT isogenic cells were pre-treated or not pre-treated in 2D culture conditions with 10ng/mL IL-22 for 48h. Cells were then trypsinised, filtered to create a single cell suspension, and 1000 cells/well were seeded into 96 well low-binding plates in serum free media containing 1% methylcellulose, 20ng/mL EGF, and 10ng/mL basic FGF. Clonogenic outgrowth was measured 7 days after seeding into sphere forming conditions. Each well was imaged and sphere numbers were quantified using an unbiased ImageJ approach (See Chapter 2.2.9 for full description)

(A) Experimental workflow for clonogenic outgrowth assay.

(B) Representative bright field microscopic images (4x magnification) of single wells of spheres 7 days after seeding.

(C) Quantification sphere number from cells that were or were not pre-stimulated with 10ng/mL IL-22. Raw counts are normalised to the mean of the no treatment (NT) condition in the *KRAS* WT line for each independent experiment. Data are means ± SEM (n=7 independent experiments performed with n=3 technical replicates per experiment). Perimeter cut-off to be considered a sphere was set at 500uM (right), however number of spheres with perimeters greater than 200uM (left) was also assessed. Statistical significance was determined using paired T-tests comparing the 10ng/mL IL-22 condition to the NT condition for each cell line. P <0.05 is considered significant. *Cont'd next page.*

(D) qPCR analysis of IL-22 target gene expression (*SOCS3*, *MUC1*, *S100A9*) in cells pre-treated or not for 48h with 10ng/mL IL-22 and subsequently grown under sphere forming conditions in the presence or absence of 10ng/mL IL-22 for 7 days. Data are mean ± SEM relative expression for each gene (n=5 independent experiments). Statistical significance was determined using unpaired T-tests comparing the 10ng/mL IL-22 condition to the NT condition for each cell line. P <0.05 is considered significant.

Due to the *KRAS* WT isogenic cells' impaired capacity for growth in 3 dimensional culture, it cannot be definitively concluded that IL-22-enhanced clonogenic outgrowth is strictly *KRAS*-dependent. Therefore instead, the capacity for IL-22 to induce proliferation in 2-dimensional culture was assessed. DLD-1 isogenic cells were treated with 10ng/mL IL-22 for 96 hours. The quantity of viable cells, as determined by MTT assay, was significantly increased by IL-22 in the *KRAS* MUT cells (Figure 4.9 A). Basal proliferation in the *KRAS* WT isogenic cells was modestly impaired compared to the *KRAS* MUT cells, but IL-22 did not significantly enhance proliferation (Figure 4.9 A).

In summary, using the isogenic DLD-1 system, we confirmed that in cells with identical IL-22RA1 expression and matched genetic backgrounds, the presence or absence of mutant *KRAS* dictates the capacity for IL-22 to induce chemoresistance and enhance proliferation in CRC cells.

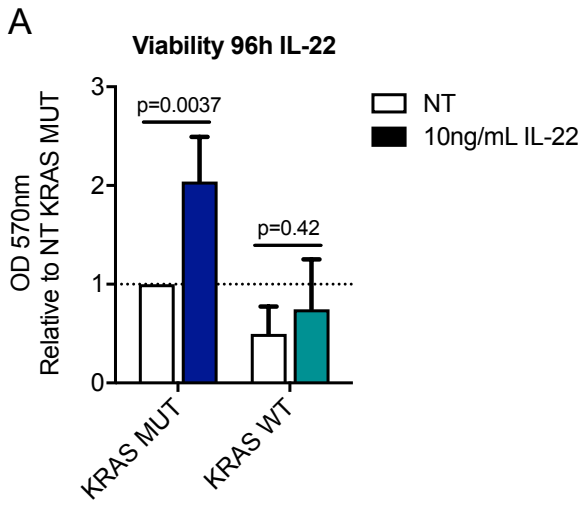


Figure 4.9 IL-22 enhances proliferation in *KRAS* mutant but not wild type DLD-1 isogenic cells.

(A) 10,000 DLD-1 KRAS MUT or WT isogenic cells were stimulated with 10ng/mL IL-22 for 96h. 50µg MTT was added to each well 2h prior to the end of the IL-22 treatment. Formazan particles were dissolved in DMSO and absorbance was measured at 570nm to assess cell viability. Raw 570nm absorbances are blank corrected and normalised to the mean of the KRAS MUT NT condition for each independent experiment. Data are means ± SEM (n=4 independent experiments performed with n=3 technical replicates per experiment). Statistical significance was determined using unpaired T-tests comparing the 10ng/mL IL-22 to the NT condition for each cell line. P <0.05 is considered significant.

4.2.7 IL-22 enhances phosphorylation of S6 (pS235/236) ribosomal protein in *KRAS* mutant but not wild type DLD-1 isogenic cells

Given, the enhanced IL-22-induced chemoresistance and proliferation in *KRAS* MUT compared to *KRAS* WT CRC cells, we next sought to determine whether there were obvious differences in activation of intracellular signalling pathways upon IL-22 stimulation that may be mediating this IL-22-*KRAS* synergy mechanistically. The Ras pathway is constitutively active in cells harbouring canonical activating mutations in *KRAS*. We thus hypothesised that either the sensitivity to IL-22 stimulation may be enhanced in *KRAS* MUT cells leading to quantitative differences in the extent of phosphorylation of key intracellular signalling molecules, or that mutant *KRAS* may act as a molecular switch, resulting in qualitative differences in the precise pathways activated upon IL-22 stimulation in *KRAS* MUT versus WT cells. Taking a

reproducible and highly quantitative approach, we performed intracellular flow cytometry with directly conjugated primary antibodies to phospho-residues on key intracellular signalling molecules (Phosflow) in DLD-1 isogenic cells following 30 minutes of IL-22 stimulation. Cells were stimulated with 0.001-100ng/mL IL-22 to allow for determination of IL-22 sensitivity differences. Importantly, all experiments were performed in serum free conditions, as serum contains various growth factors that activate the Ras pathway and may mask signalling differences in response to IL-22 in *KRAS* MUT versus WT cells. First, we predicted that phosphorylation of ERK1/2 would be enhanced at baseline in the *KRAS* MUT cells due to constitutive Ras activation. However, in light of previous evidence from Western Blot analyses (Figure 4.1, Figure 4.6), we did not expect pERK1/2 to be IL-22 inducible. Indeed, the amount of pERK1/2 in *KRAS* MUT isogenic cells was elevated at baseline compared to their *KRAS* WT counterparts (Figure 4.10 A). These differences were sustained with IL-22 stimulation, but IL-22 stimulation itself did not appreciably enhance pERK1/2 in *KRAS* MUT or WT cells (Figure 4.10 A).

Since activation of STAT3 is the most well studied pathway downstream of IL-22, we next explored STAT3-Y705 phosphorylation. Evidence from previous experiments performed with either 1ng/mL or 10ng/mL IL-22 for 24 hours, did not reveal differences between the amount of pSTAT3-Y705 in *KRAS* MUT and WT cells (Figure 4.1, Figure 4.6). This does not exclude the possibility however, that the *KRAS* MUT cells may be responsive to lower doses of IL-22 than their *KRAS* WT counterparts. Interestingly, the induction of pSTAT3-Y705 was identical between *KRAS* MUT and WT cells over the entire range of IL-22 doses tested (Figure 4.10 B).

Finally, evidence from previous experiments suggested that activation of AKT (S473) might be enhanced by IL-22 specifically in *KRAS* MUT cells (Figure 4.1, Figure 4.6). mTORC1 is a key downstream target of AKT which activates cellular S6 kinases that in turn phosphorylate ribosomal-S6 protein (LoRusso, 2016). Ribosomal S6 protein is a critical component of the 40S ribosomal subunit and its phosphorylation is required for translation initiation. It is therefore a key regulator of cell growth and proliferation (Ruvinsky and Meyuhas, 2006). Phosphorylation of ribosomal S6 specifically at the S235/236 sites has also been reported to be modulated by the Ras/ERK pathway (Roux *et al.*, 2007). Given the proliferation-enhancing capacity of IL-22 in *KRAS* MUT cells, we hypothesised that IL-22 may induce pS6 (S235/236) specifically in *KRAS* MUT cells. Indeed, IL-22 enhanced pS6 (S235/236) at higher doses of IL-22 (10-100ng/mL) in *KRAS* MUT isogenic cells (Figure 4.10 C). By contrast, the amount of pS6 (S235/236) was modestly lower at baseline in *KRAS* WT isogenic cells and IL-22 stimulation did not induce its phosphorylation (Figure 4.10 C). To determine whether this IL-22-induced pS6 (235/236) in the *KRAS* MUT cells was mTOR-dependent, cells were treated with 100nM rapamycin for 30 minutes in the presence or absence of 10ng/mL IL-22. Rapamycin treatment alone reduced basal levels of pS6 (S235/236) in the *KRAS* MUT cells (Figure 4.10 D, E). Furthermore, treatment of IL-22-stimulated *KRAS* MUT cells with rapamycin prevented induction of pS6 (S235/236). Therefore, in the DLD-1 *KRAS* MUT cells, IL-22-induced pS6 (S235/236) induction appears to be mTOR-dependent.

In summary, though activation of STAT3 by IL-22 is identical between *KRAS* MUT and WT DLD-1 isogenic cells, IL-22 uniquely induces pS6 (S235/236) in *KRAS* MUT cells possibly in an mTOR-dependent manner. Elevated pS6 may enhance protein

translation and contribute to the enhanced growth and survival of *KRAS* MUT cells in response to IL-22 stimulation.

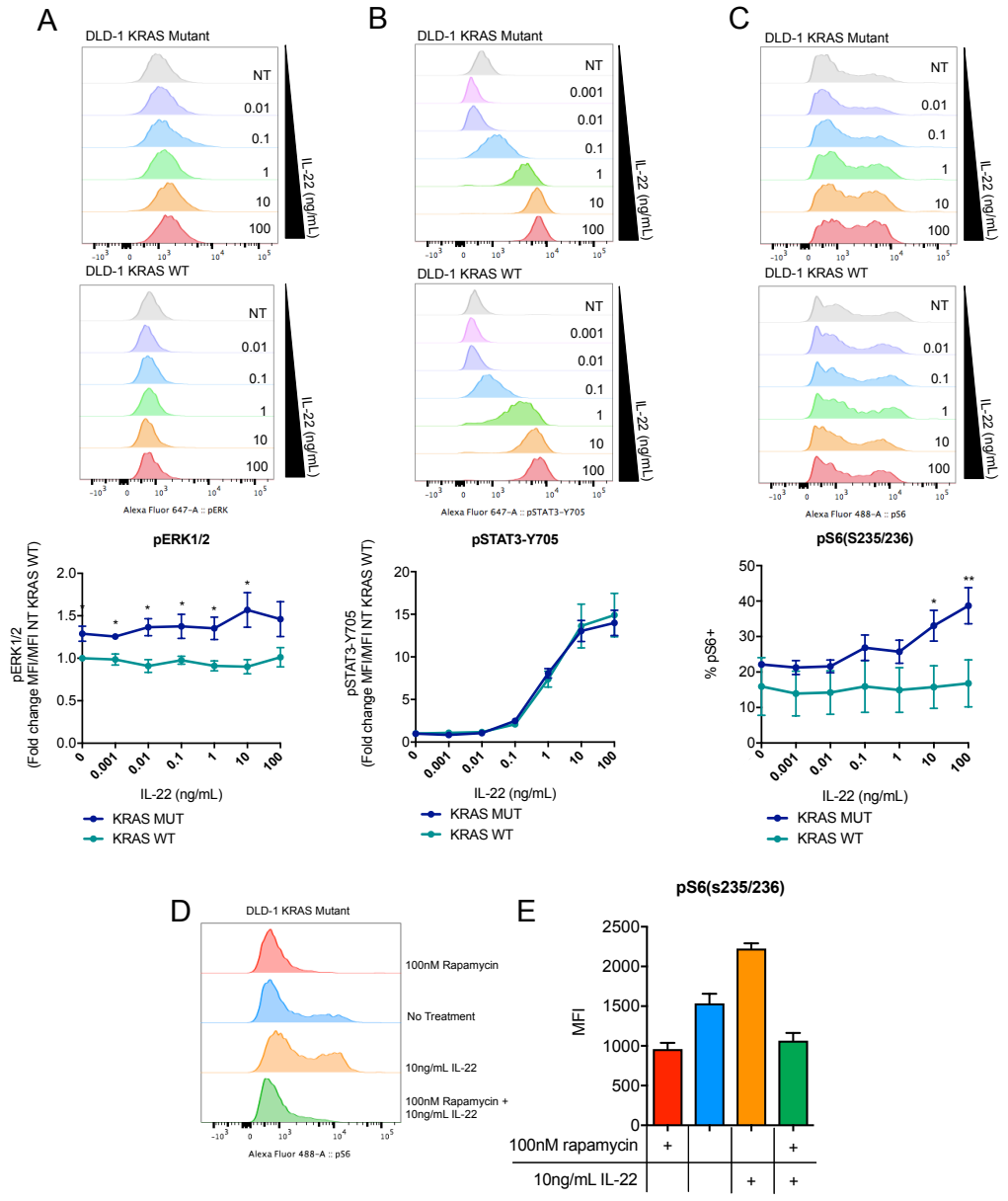


Figure 4.10 IL-22 enhances S6 (p235/236) phosphorylation in *KRAS* mutant but not wild type DLD-1 isogenic cells.

DLD-1 *KRAS* MUT or WT isogenic cells were stimulated for 30 minutes with 0.001-100ng/mL IL-22. Cells were rapidly fixed, permeabilised and stained with fluorophore-conjugated Phosflow antibodies. Intracellular flow cytometry was performed to assess phosphorylation of key cell signalling molecules in response to increasing doses of IL-22. Representative histograms from flow cytometric analysis of:

(A) pERK1/2 (B) pSTAT3-Y705 are shown with the corresponding quantification. Data represent the mean ± SEM of the fold change in mean fluorescence intensity (MFI) over the MFI of the NT condition in the KRAS WT line for each independent experiment (n=4 independent experiments). Statistical significance was determined using multiple unpaired T-tests comparing fold change MFI in the KRAS MUT to WT line at each IL-22 dose. *p<0.05. *Cont'd next page.*

(C) pS6-S235/236 is shown with the corresponding quantification. Data represent the mean ± SEM of the frequency of positive events (%$S6^+$) gating out the low intensity events in the bimodal distribution based on the NT condition (n=3 independent experiments). Statistical significance was determined using multiple unpaired T-tests the comparing the frequency of $S6^+$ cells in the *KRAS* MUT to WT line at each IL-22 dose. *p<0.05.

(D) (E) Cells were treated with 100nM rapamycin with and without 10ng/mL IL-22 for 30 minutes. Intracellular flow cytometry was performed as in (A)(B)(C) to assess pS6-S235/236. Representative histograms are shown with corresponding quantification. Data are the mean ± SEM MFI for each condition (n=1 independent experiment performed with n=2 technical replicates).

4.2.8 Dynamic regulation of IL-22RA1 upon ligand binding is comparable between *KRAS* mutant and wild type DLD-1 isogenic cells

Though examination of differences in intracellular signalling pathways under acute IL-22 stimulation conditions (30 minutes) may provide some clues as to how IL-22 and mutant *KRAS* synergise to promote malignancy, the temporal maintenance of a sustained IL-22 signal is likely important in both the development and progression of CRC. Our evidence suggests that the magnitude of an IL-22 signal in the epithelium is proportional to the level of IL-22RA1 surface expression (Figure 4.1). *IL22RA1* expression did not differ between *KRAS* MUT and *KRAS* WT CRC in retrospective analysis of nearly 2000 patients (Chapter 3.2.3, Figure 3.7 B). Furthermore, we observed comparable *IL22RA1* expression in the *KRAS* MUT and WT DLD-1 isogenic pair (Figure 4.6). Interestingly, in prospectively collected CRC and matched normal adjacent tissue, *IL22RA1* expression was higher in normal adjacent compared to matched tumour tissue (Chapter 3.2.2, Figure 3.3 B). Therefore, when comparing tumour to matched normal tissue within an individual, we asked whether *IL22RA1* expression patterns differed between *KRAS* MUT and WT patients. First, we compared *IL22RA1* expression in prospectively collected whole tumour and matched normal adjacent tissue from *KRAS* MUT (N=21) and WT (N=27) patients. Interestingly, in *KRAS* WT patients, *IL22RA1* expression was higher in normal adjacent compared to tumour tissue; however, there was no difference in *IL22RA1* expression in normal and tumour tissue derived from *KRAS* MUT patients (Figure

4.11 A). This was not the case with *IL10RB,* where by contrast expression was elevated in normal adjacent compared to tumour tissue in both *KRAS* MUT and WT patients (Figure 4.11 B).

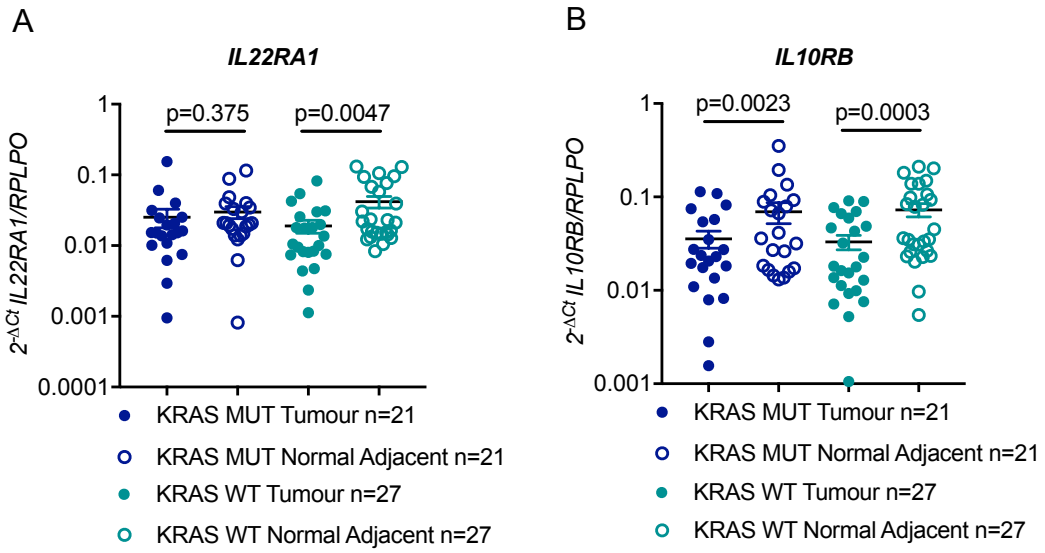


Figure 4.11 *IL22RA1* is higher in matched normal compared to tumour tissue in *KRAS* wild type CRC, but is unchanged in normal and tumour tissue in *KRAS* mutant CRC.

Whole tissue qPCR analysis of *IL22RA1* and *IL10RB* expression in N=21 *KRAS* MUT tumours and matched normal adjacent tissue and N=27 *KRAS* WT tumours and matched normal adjacent tissue collected prospectively.

(A) *IL22RA1*
(B) *IL10RB*

Each data point represents a single patient. Statistical significance was determined using Wilcoxon matched-pairs signed rank tests between tumours and corresponding normal adjacent tissue for each genotype. P <0.05 is considered significant.

Though not specifically studied for IL-22RA1, it has been well described for other cytokine receptors that surface expression is transiently downregulated upon ligand binding. This is thought to be a negative regulatory mechanism to prevent excessive, sustained activation of the downstream pathway (de Weerd and Nguyen, 2012; Cendrowski, Mamińska and Miaczynska, 2016). Whether this recycling of the receptor at the cell surface is mirrored by transcriptional downregulation of receptor mRNA expression is less well understood. However, since *IL22RA1* expression was no different between matched normal and tumour tissue in *KRAS* MUT patients, while

tumoural *IL22RA1* expression was lower in *KRAS* WT tumours versus matched normal tissue, we questioned whether this was a consequence of inappropriately sustained receptor expression in the *KRAS* MUT tumours. We therefore explored the dynamic regulation of IL-22RA1 protein and mRNA in the DLD-1 *KRAS* MUT and WT isogenic CRC cells.

First, cells were stimulated for 2-24 hours with 10ng/mL IL-22. IL-22RA1 surface protein expression was monitored by flow cytometric analysis and mRNA expression was evaluated by qPCR. Within 2 hours, surface IL-22RA1 expression was diminished by roughly 50% in both *KRAS* MUT and WT cells (Figure 4.12 A, B). Surface IL-22RA1 reached a minimum (>60% reduction compared to baseline) by 4 hours and this was sustained in both *KRAS* MUT and WT isogenic cells over a 24 hour period (Figure 4.12 A, B). mRNA expression of *IL22RA1* over the stimulation time course diminished modestly in *KRAS* MUT cells, however *IL22RA1* expression in *KRAS* WT cells was much more sporadic (Figure 4.12 E).

Given that repression of surface IL-22RA1 expression upon IL-22 stimulation was comparable between *KRAS* MUT and WT cells, we next explored whether receptor recovery after ligand removal was more rapid in the *KRAS* MUT cells. *KRAS* MUT and WT isogenic cells were stimulated with 10ng/mL IL-22 for 24 hours. Fresh media was then applied and recovery of IL-22RA1 surface expression from its supressed state at 24 hours was monitored for an additional 24 hours. Surface IL-22RA1 recovery was indistinguishable between *KRAS* WT and MUT cells and receptor expression was nearly restored to baseline 24 hours following the IL-22 wash-off (Figure 4.12 C, D). Interestingly, though *IL22RA1* mRNA expression returned to

baseline by 4 hours post IL-22 wash-off in the *KRAS* MUT isogenic cells, *IL22RA1* expression did not recover in the *KRAS* WT cells (Figure 4.12 F). In fact, transcriptional repression of *IL22RA1* continued over the 24 hour IL-22 wash-off period (Figure 4.12 F).

Therefore, downregulation of IL-22RA1 surface expression and receptor recovery following IL-22 wash-off is comparable between *KRAS* MUT and WT isogenic DLD-1 cells. The sustained *IL22RA1* transcriptional repression in *KRAS* WT as compared to *MUT* cells must be confirmed in other CRC lines and primary cells to ascertain whether *KRAS* directly modulates the dynamic regulation of *IL22RA1* at the transcriptional level. Nevertheless, given that the transcriptional differences did not translate to differences at the surface protein level, one can surmise that differential regulation of *IL22RA1* expression does not explain the IL-22-*KRAS* synergy, at least in this DLD-1 isogenic system.

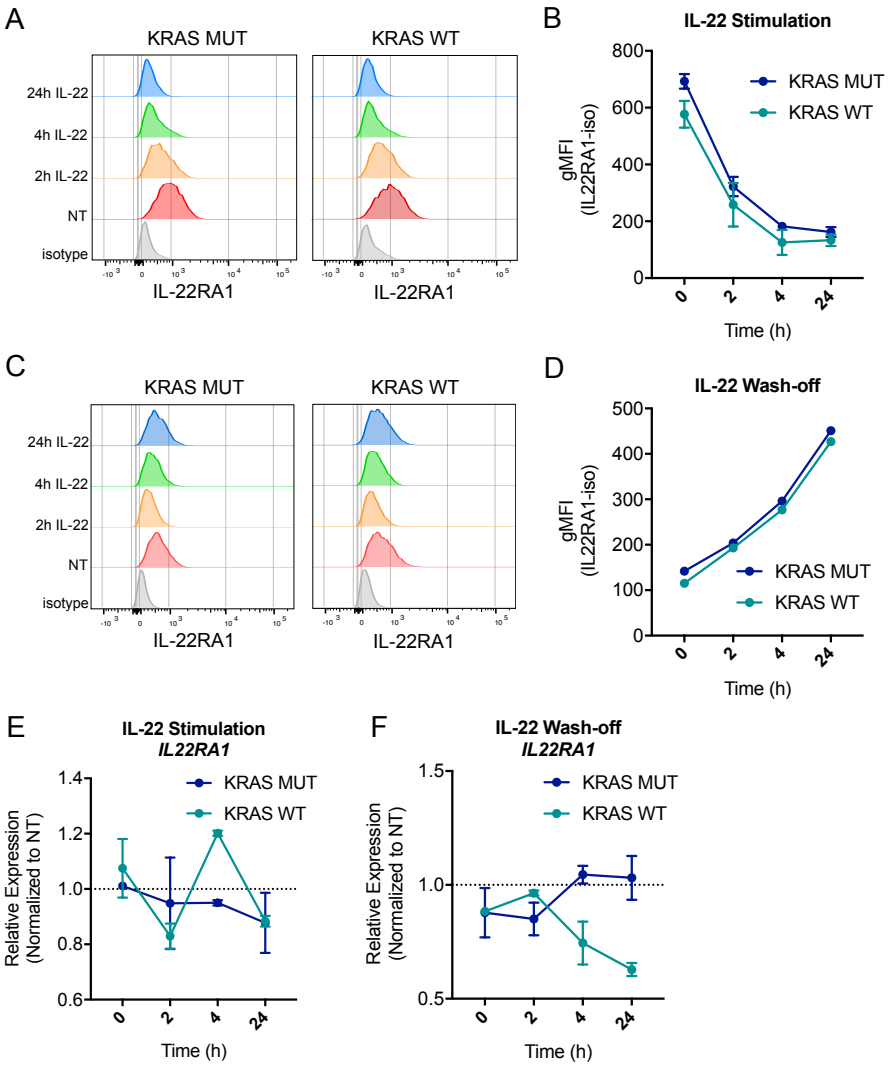


Figure 4.12 Dynamic regulation of IL-22RA1 is comparable between *KRAS* mutant and wild type DLD-1 isogenic cells.

(A) Representative histograms of flow cytometric analysis of surface IL-22RA1 expression on DLD-1 *KRAS* MUT and WT isogenic cells stimulated for 2, 4, and 24h with 10ng/mL IL-22 (IL-22 Stimulation).

(B) Quantification of isotype control subtracted IL-22RA1 geometric mean fluorescence intensity (gMFI) in each line. Data represent mean ± SEM (n=3 independent experiments). Statistical significance was assessed using unpaired T-tests between *KRAS* MUT and WT gMFI IL-22RA1 at each timepoint. No significant differences were observed.

(C) Representative histograms of flow cytometric analysis of surface IL-22RA1 expression on DLD-1 *KRAS* MUT and WT isogenic cells that were stimulated for 24h with 10ng/mL IL-22. IL-22 was then washed off and IL-22RA1 surface expression recovery was measured at 2, 4, and 24h after IL-22 wash-off (IL-22 Wash-off).

(D) Quantification of isotype control subtracted IL-22RA1 geometric mean fluorescence intensity (gMFI) in each line (n=1 independent experiment).

(E) (F) qPCR analysis of *IL22RA1* mRNA expression at each timepoint for the IL-22 Stimulation and IL-22 Washoff experiments. Data represent mean ± SEM (n=1 independent experiment performed with n=2 technical replicates).

Note: These experiments were performed by Lucy Garner, a first year rotation Wellcome Trust DPhil student supervised by S. McCuaig. Figures were prepared by S. McCuaig.

4.2.9 Establishment and validation of primary human CRC organoids as an accurate *ex vivo* model to functionally explore the IL-22-*KRAS* synergy

Until now, we have identified a unique and prognostically important interaction between IL-22 signalling and mutant *KRAS* which promotes malignancy. Our evidence for this synergy is derived from retrospective analyses of whole tumour tissue from large transcriptomic cohorts, prospective analysis of whole CRC tumour and matched normal adjacent tissue, and functional experimentation in a panel of cell lines and an isogenic pair which mirror the molecular CRC subtypes of interest. In an effort to functionally validate the IL-22-*KRAS* synergy in prospectively collected primary colorectal cancers, we established and validated the use of primary human organoids as an accurate *ex vivo* model.

Using methodology developed by Hans Clevers *et al.* (Sato *et al.*, 2011), prospectively collected tumour biopsies and matched normal adjacent tissue from patients undergoing colectomy at the Churchill Hospital, Oxford were grown in organoid forming conditions. Briefly, normal adjacent mucosa was separated from the underlying serosa and crypts were liberated by successive incubations with EDTA. Crypts were seeded into basement membrane extract (BME) and grown in a defined media containing Wnt-3A, R-spondin, and Noggin. In parallel, tumour biopsies were rapidly digested in collagenase, dissociated to single cells, seeded into basement membrane extract, and grown in media containing R-spondin and Noggin. Due to hyperactivity of the Wnt pathway in most colorectal tumours, Wnt-3A is not required for tumour organoid growth (Sato *et al.*, 2011; van de Wetering *et al.*, 2015). Detailed methodology describing the crypt and tumour cell isolation as well as the preparation of the defined media (including production of Wnt-3A, R-spondin, and Noggin

conditioned media) can be found in Chapter 2.3 and Appendix 2.3. Organoids were first passaged seven days following their initial seeding (P1) at which point they were frozen for banking and kept in continuous culture for downstream experiments.

4.2.9.1 *IL23A* is elevated in primary human CRC-derived organoids as compared to those from matched normal tissue

Prior to investigating the IL-22-*KRAS* synergy, we first utilised the organoid system to interrogate epithelial expression of IL-23, the upstream regulator of IL-22. Given our observation that *IL23A* is elevated in colorectal tumours compared to matched normal adjacent whole tissue (Chapter 3.2.1 Figure 3.1 A, B) and that, counter to the existing dogma, *IL23A* can be detected in the malignant epithelium in sorted human tumours (Chapter 3.2.1 Figure 3.2 A, B), we wanted to determine whether *IL23A* is expressed in CRC-derived organoids. Furthermore, we wished to examine whether *IL23A* expression is elevated in organoids from CRC versus matched normal tissue at baseline. CRC and matched normal organoids (Figure 4.13 A) were grown from prospectively collected tissue. Basal *IL23A* expression was assessed by qPCR in CRC and normal adjacent organoids between passages 2-4. Examination of *IL23A* in paired CRC and matched normal organoids revealed that *IL23A* is expressed in both tumour and normal adjacent epithelium. Importantly, *IL23A* expression is elevated in tumour compared to matched normal organoids, though the amount of expression relative to the endogenous control is variable from patient to patient (Figure 4.13 B). Even still, despite inter-patient variability, when we assessed *IL23A* expression in a larger cohort of CRC (N=13) and normal adjacent-derived (N=15) organoids, *IL23A* expression was elevated in CRC compared to normal adjacent-derived organoids (Figure 4.13 C). Thus, in line with data from sorted human CRC tumours, *IL23A* is expressed in the malignant epithelium. Moreover, as was observed in whole tumour tissue, *IL23A*

expression is elevated in tumour compared to normal adjacent-derived organoids. While these findings need to be confirmed at the protein level, these observations provide early evidence that CRC cells may augment IL-23 expression as an adaptive mechanism to condition the immune microenvironment to favour their proliferation and survival by locally induced IL-22 and IL-17A production by immune cells.

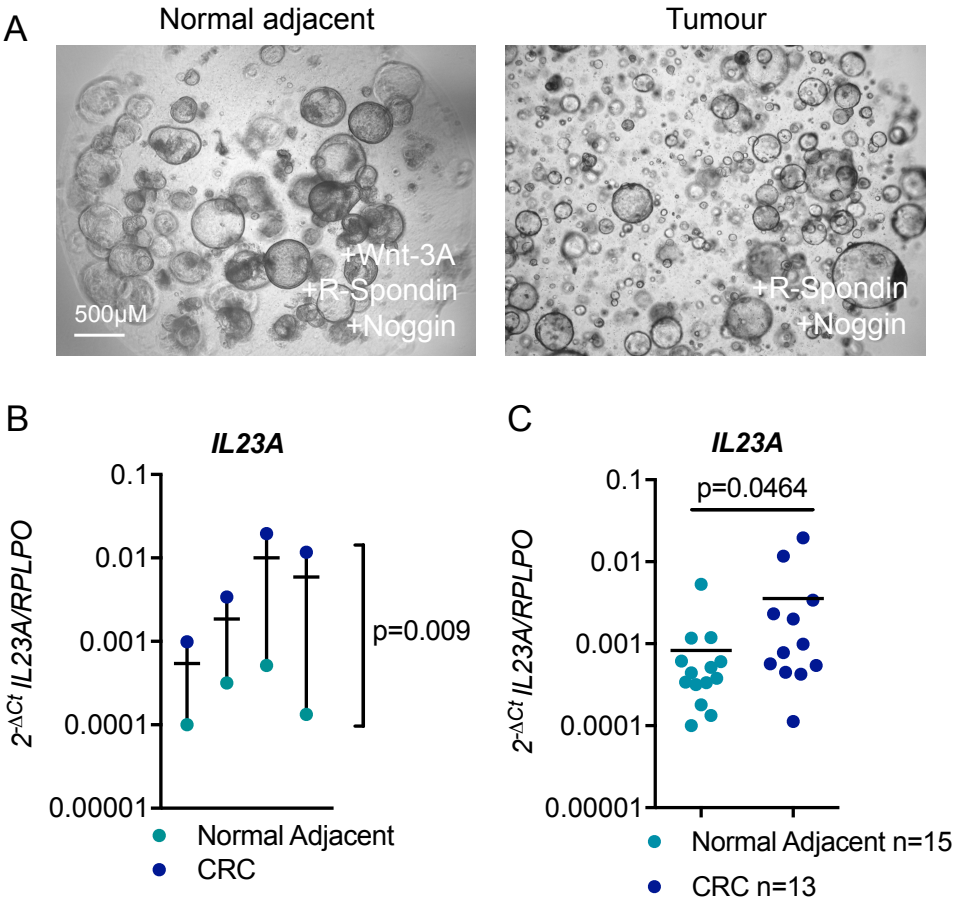


Figure 4.13 *IL23A* is elevated in CRC-derived versus normal adjacent-derived organoids at baseline.

(A) Brightfield microscopy of organoids derived from colorectal tumour biopsies and matched normal adjacent tissue grown in basement membrane extract in the appropriate organoid media (4x magnification). Matched normal adjacent organoids require Wnt3A, R-Spondin, and Noggin to support growth, while tumour organoids require only R-Spondin and Noggin.

(B) qPCR analysis of *IL23A* in normal adjacent and matched CRC (N=4) derived organoids at baseline. Ratio-paired T-test. P <0.05 is considered significant.

(C) qPCR analysis of *IL22RA1* and *IL10RB* in normal adjacent (N=15) and CRC (N=13) derived organoids at baseline. Mann Whitney U test. P <0.05 is considered significant.

Each dot represents the mean gene expression from technical duplicates in an organoid derived from an individual patient.

4.2.9.2 IL-22RA1 expression in primary human CRC organoids accurately recapitulates that in the whole tumour tissue

Prior to utilising the primary organoids for functional experiments to validate the observed synergy between IL-22 and mutant *KRAS*, we first had to ascertain whether IL-22 receptor expression in the organoids accurately reflected that in the whole tumour tissue. This was a critical first step as it is *IL22RA1* expression in the whole tumour tissue that stratified patients prognostically based on *KRAS* mutation.

IL22RA1 and *IL10RB* expression was assessed in CRC and matched normal organoids from prospectively collected resection tissue at baseline between passages 2-4. Mirroring the whole tissue (Figure 4.14 A, B), *IL22RA1* (Figure 4.14 C) and *IL10RB* (Figure 4.14 D) expression was higher in matched normal compared to CRC-derived organoids. *IL22RA1* CRC organoid expression was highly correlated with the matched whole tumour tissue *IL22RA1* expression (Figure 4.14 E). By contrast, *IL10RB* expression in CRC organoids did not correlate with matched whole tumour tissue *IL10RB* expression (Figure 4.14 F). This is logical however; unlike the epithelial cell-restricted expression of *IL22RA1*, *IL10RB* is highly expressed on infiltrating immune cells as well as epithelial cells. Thus, the organoid *IL10RB* expression reflects only the contribution of the epithelium to the *IL10RB* expression in the whole tumour tissue.

Importantly, both components of the heterodimeric IL-22 receptor are expressed in tumour and normal adjacent tissue-derived organoids, and *IL22RA1* expression in tumour-derived organoids is highly correlated to that in the matched whole tumour tissue.

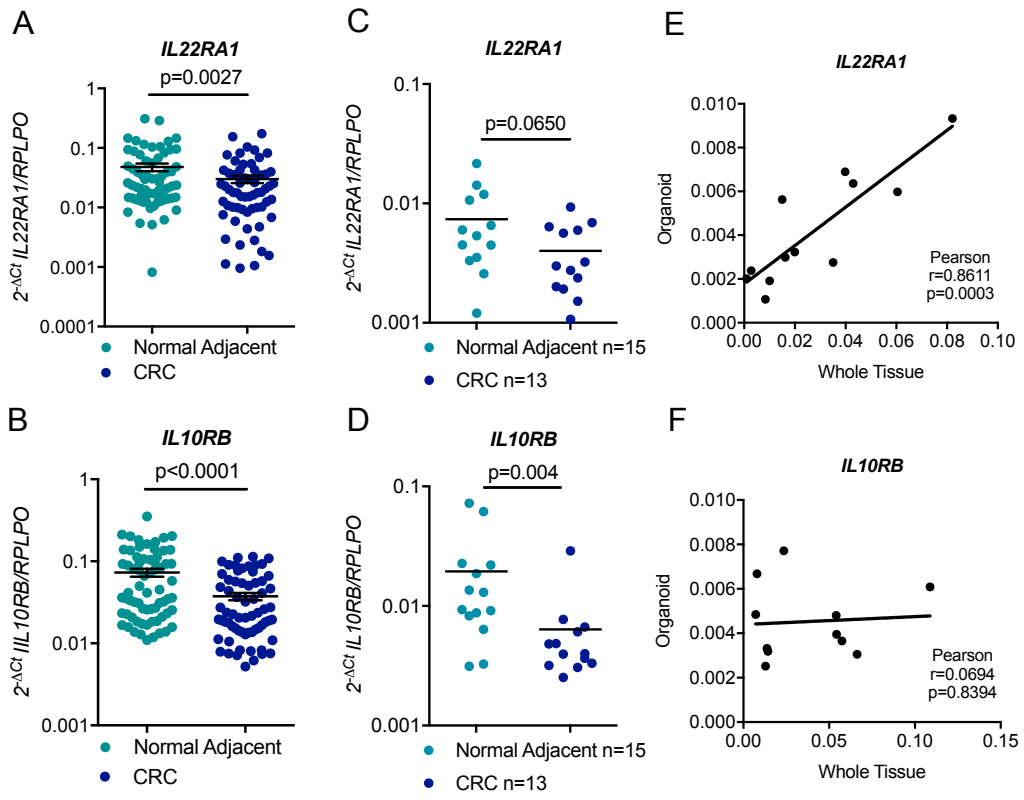


Figure 4.14 *IL22RA1* in primary human CRC and matched normal adjacent organoids accurately recapitulates that in the tumour tissue.

(A) (B) Whole tissue qPCR analysis of *IL22RA1* and *IL10RB* in prospectively collected CRCs and matched normal adjacent tissue. N=69, ratio paired T-test. P <0.05 is considered significant.

(C) (D) qPCR analysis of *IL22RA1* and *IL10RB* in normal adjacent (N=15) and CRC (N=13) derived organoids at baseline. Mann Whitney U test. P <0.05 is considered significant.

(E) (F) Pearson correlation between CRC organoid and matched whole CRC tissue *IL22RA1* or *IL10RB* expression from N=12 patients. Exact Pearson r statistics and p values are displayed. P <0.05 is considered significant.

Each dot represents the mean gene expression from technical duplicates in an organoid derived from an individual patient.

To confirm that IL-22RA1 protein was also appropriately expressed on primary CRC organoids, organoids were dissociated to single cells and analysed for IL-22RA1 surface expression using flow cytometry. As expected, all of the cells in the organoids were epithelial, as determined by expression of EpCAM (Figure 4.15 A). IL-22RA1 surface protein expression was assessed on live, single, $EpCAM^+$ cells and gates were set using matched isotype controls (Figure 4.15 A). The isotype subtracted geometric mean fluorescence intensity (gMFI) of IL-22RA1 was determined for each CRC organoid. Like whole tumour tissue, IL-22RA1 expression was heterogeneous between organoids derived from tumours from different patients (Figure 4.15 B). IL-22RA1 protein expression was concordant with *IL22RA1* mRNA expression from the same organoid, though Pearson Correlation analysis did not reach statistical significance, likely due to low sample size (N=8) (Figure 4.15 C). Finally, to assess the cellular distribution of IL-22RA1 in CRC organoids, whole organoids were fixed and stained using the same IL-22RA1 antibody that was used for whole tissue IHC analysis. Confocal microscopic analysis revealed cell surface IL-22RA1 staining in the organoids. However, similar to whole tissue, IL-22RA1 was not expressed by every cell (Figure 4.15 D).

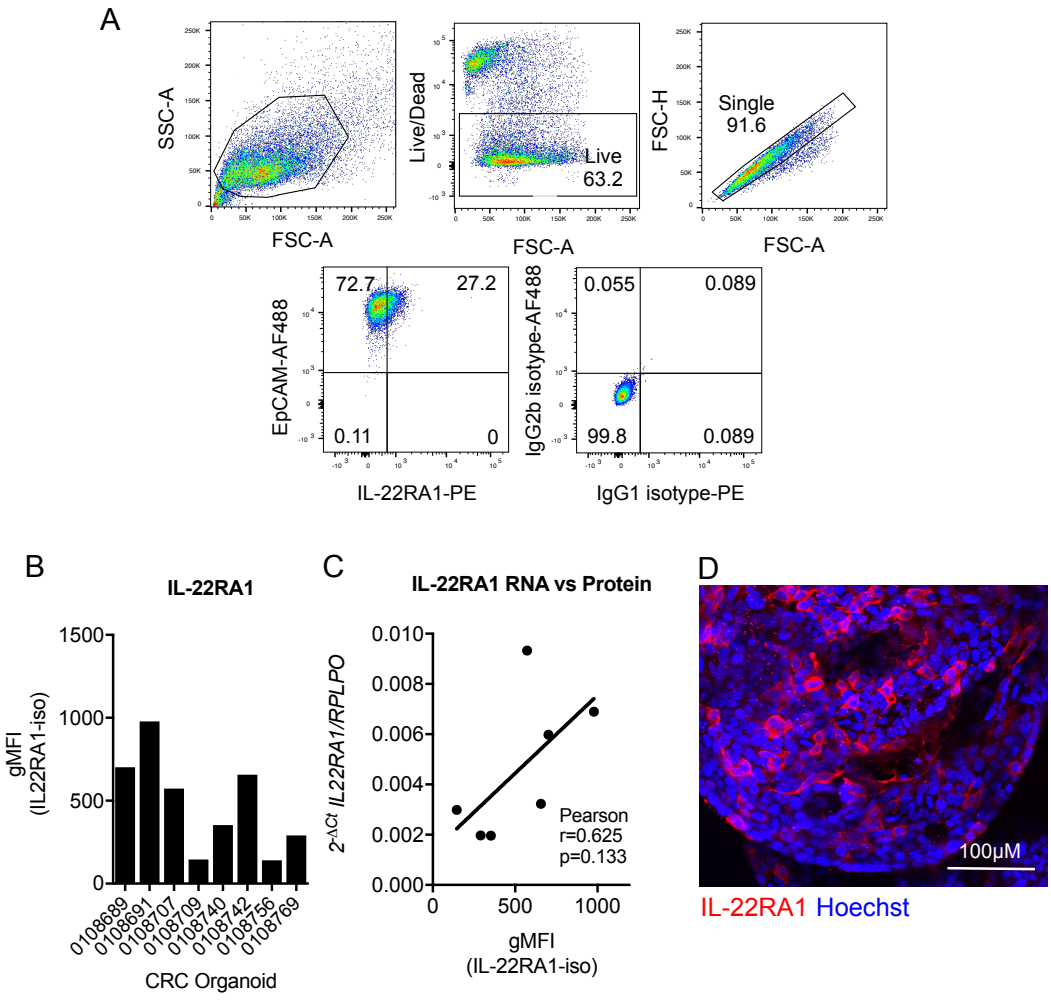


Figure 4.15 IL-22RA1 protein expression is heterogeneous on organoids derived from different CRC patients.

(A) Representative plots displaying gating strategy for flow cytometric analysis of IL-22RA1 protein expression on primary human organoids. Expression of IL-22RA1 on live, single, $EpCAM^+$ cells was assessed. Gates for IL-22RA1 positivity are set for each organoid by comparing to staining with matched IgG1 PE conjugated isotype control.

(B) Quantification of isotype control subtracted basal IL-22RA1 geometric mean fluorescence intensity (gMFI) in N=8 CRC-derived organoid lines.

(C) Pearson correlation between basal IL-22RA1 organoid protein expression as determined by flow cytometric analysis and basal *IL22RA1* organoid mRNA expression as determined by qPCR analysis. Each dot represents an organoid line derived from one CRC patient. Exact Pearson r statistics and p values are displayed. P <0.05 is considered significant.

(D) Representative confocal microscopic image of IL-22RA1 protein expression in a primary CRC derived organoid. Hoechst staining marks nuclei. (20x magnification).

4.2.9.3 IL-22 signalling is active in primary human organoids

After establishing that the organoids expressed IL-22RA1 at the mRNA and protein level and that the amount of expression in the organoids mirrored that in whole tissue, we next needed to establish that the receptor was functional. Since IL-22 stimulation

reproducibly results in phosphorylation of STAT3-Y705 regardless of mutation status if adequate IL-22RA1 is expressed, pSTAT3-Y705 and its direct transcriptional target *SOCS3* were used to confirm active IL-22 signalling in the organoids. CRC organoids were treated for 30 minutes with 1ng/mL IL-22, then rapidly fixed and stained to detect STAT3-Y705 phosphorylation. Confocal microscopic analysis revealed robust STAT3-Y705 phosphorylation upon IL-22 stimulation (Figure 4.16 A). Taking a more quantitative approach, pSTAT3-Y705 was also assessed by intracellular flow cytometry (Phosflow). Organoids were stimulated with 1ng/mL or 10ng/mL IL-22 for 30 minutes and were subsequently dissociated to single cells, fixed, permeabilised, and stained for pSTAT3-Y705. Flow cytometric analysis revealed a dose-dependent induction of pSTAT3-Y705 following IL-22 stimulation (Figure 4.16 B). In the CRC organoids derived from the two patients used as representative examples, pSTAT3-Y705 was enhanced in Patient 2 compared to Patient 1 (Figure 4.16 C). Logically, *SOCS3* induction was also enhanced upon 24-hour IL-22 stimulation in organoids derived from Patient 2 (Figure 4.16 D). Moreover, IL-22RA1 expression as assessed by flow cytometry was higher in Patient 2 compared to Patient 1 (Figure 4.16 E). Thus, IL-22 signalling is active in CRC-derived organoids and the extent of pSTAT3-Y705 and *SOCS3* induction seems to be proportional to IL-22RA1 expression, as was observed in the CRC lines. This observation was validated in CRC organoids derived from 13 independent patients, which were stimulated for 24h with IL-22. A significant dose-dependent induction of *SOCS3* was observed in all organoids (Figure 4.16 F) and the amount of *SOCS3* induction correlated with the amount of *IL22RA1* expression (Figure 4.16 G).

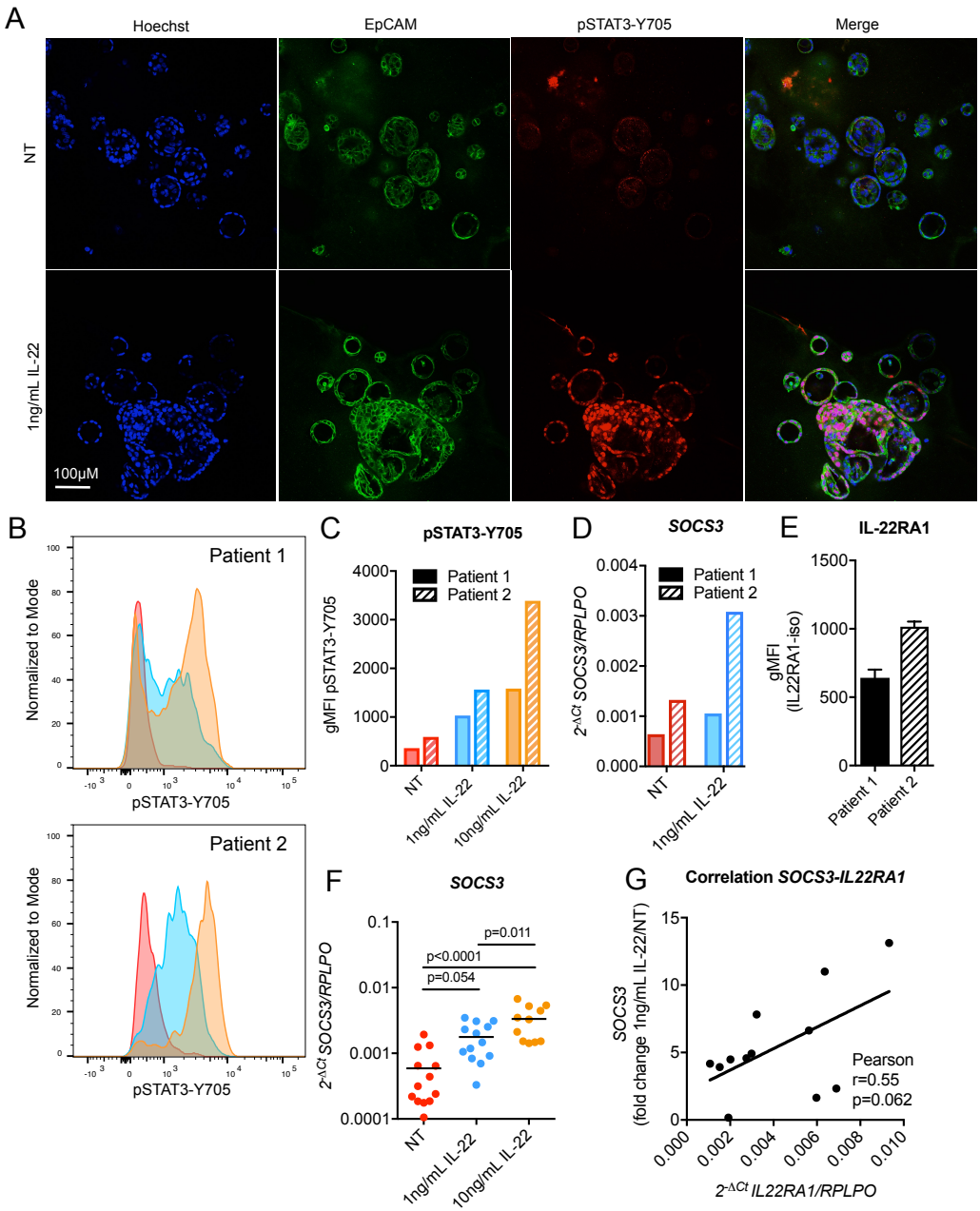


Figure 4.16 IL-22 signalling is active in primary human organoids and pSTAT3-Y705 and *SOCS3* induction are related to the amount of *IL22RA1* expression.

(A) Representative confocal microscopic images of pSTAT3-Y705 induction in primary CRC organoids stimulated for 30 minutes with 1ng/mL IL-22. Hoechst marks nuclei, EpCAM marks epithelial cells.

(B) Representative histograms of intracellular flow cytometric analysis (Phosflow) of pSTAT3-Y705 in primary CRC organoids stimulated for 30 minutes with IL-22. Organoids derived from N=2 independent CRCs. Red = NT, blue = 1ng/mL IL-22, orange = 10ng/mL IL-22.

(C) Quantification of geometric mean fluorescence intensity (gMFI) of pSTAT3-Y705 in each organoid line after 30 minutes of 1ng/mL or 10ng/mL IL-22 stimulation. Organoids derived from N=2 independent CRCs.

(D) qPCR analysis of *SOCS3* induction following 24h 1ng/mL IL-22 stimulation in the matched organoids from (B)(C).

(E) Flow cytometric analysis of basal IL-22RA1 surface expression in the matched organoids from (B) (C). Data represent 2 technical replicates. *Cont'd next page.*

(F) qPCR analysis of *SOCS3* induction following 24h of 1ng/mL or 10ng/mL IL-22 stimulation in N=13 independent CRC derived organoid lines. Each dot represents an organoid line derived from a single CRC. Statistical significance was evaluated using a one-way ANOVA with Tukey's post test for multiple comparisons. P <0.05 is considered significant.

(G) Pearson correlation analysis of *SOCS3* induction after 24h 1ng/mL IL-22 stimulation and basal *IL22RA1* mRNA expression. Each dot represents the mean gene expression from technical duplicates of an organoid line (N=12) derived from one CRC patient. Exact Pearson r statistics and p values are displayed. P <0.05 is considered significant.

4.2.9.4 *SOCS3*, *MUC1*, and *OLFM4* are universally higher in normal adjacent organoids, while *S100A9* is elevated in IL-22 stimulated CRC-derived organoids

Having established that IL-22 signalling is active in the organoids, we next sought to explore differences in both the basal and induced expression of a number of classical IL-22 target genes in normal adjacent compared to tumour-derived organoids to understand global differences between homeostasis and malignancy. Organoids between passages 2-4 were stimulated for 24 hours with 1ng/mL or 10ng/mL IL-22 and gene expression was assessed by qPCR. First, the expression of each gene of interest relative to the endogenous control in each organoid was compared between normal adjacent (N=15) and CRC-derived organoids (N=13). Interestingly, *SOCS3, MUC1,* and *OLFM4* expression was elevated in normal adjacent compared to CRC-derived organoids at baseline and upon IL-22 stimulation (Figure 4.17 A, B, C). By contrast, *S100A9* expression trended towards being basally elevated in CRC-derived organoids, but was significantly elevated compared to their normal adjacent counterparts after IL-22 stimulation (Figure 4.17 D).

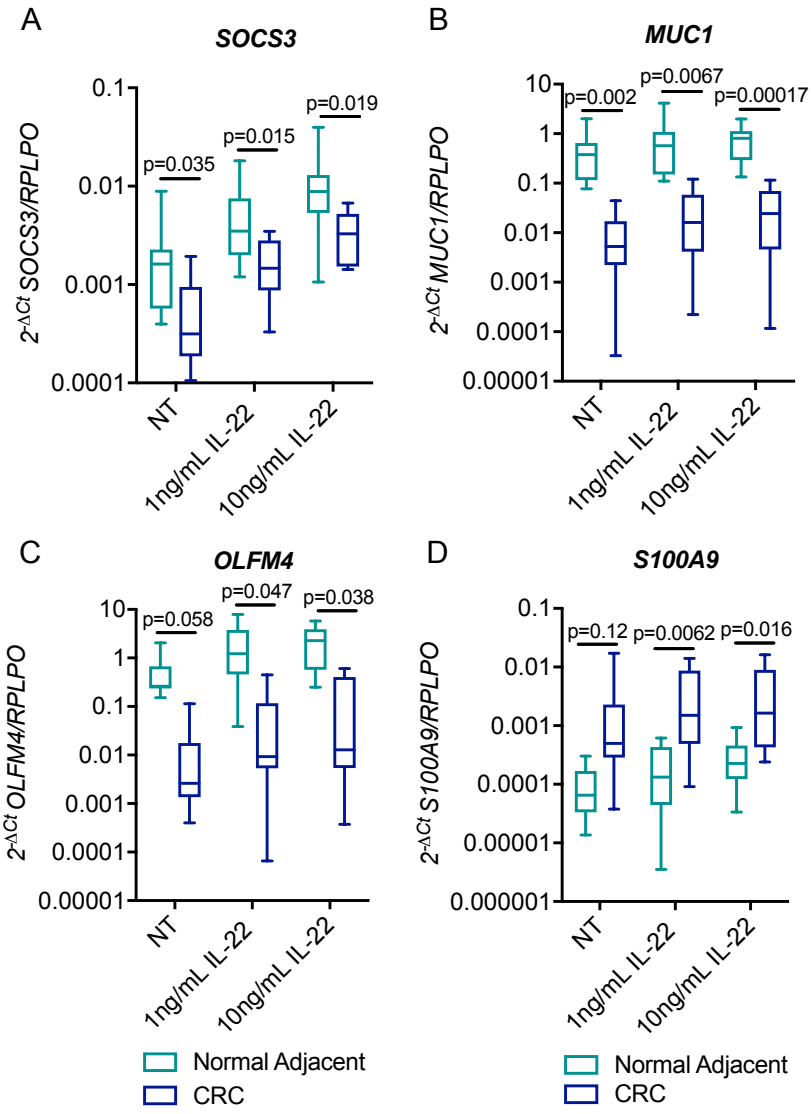


Figure 4.17 *SOCS3*, *MUC1, OLFM4* are universally higher in normal adjacent organoids, while *S100A9* is elevated in CRC derived organoids following IL-22 stimulation.

CRC and matched normal adjacent organoids generated from prospectively collected resection tissue were stimulated between passages 2-4 for 24h with 1ng/mL, 10ng/mL IL-22. qPCR analysis was performed for key IL-22 target genes:

(A) *SOCS3*
(B) *MUC1*
(C) *OLFM4*
(D) *S100A9*

Box and whisker plots represent the 5-95th percentile of relative expression of each gene for each condition in N=15 normal adjacent derived organoids and N=13 CRC derived organoids. Stimulations were performed in technical duplicate for each line. Statistical significance was evaluated using unpaired T-tests comparing normal adjacent to CRC-derived organoid expression for each of the NT and IL-22 stimulation conditions. P <0.05 is considered significant.

Given the basal differences in IL-22 target gene expression between normal adjacent and CRC-derived organoids observed; we next determined whether expression of each gene was significantly modulated upon IL-22 stimulation. Thus the fold change in gene induction following 24-hour IL-22 stimulation compared to no treatment was determined for each organoid. Despite the lower average *IL22RA1* expression in the CRC-derived organoids compared to their normal adjacent counterparts (Figure 4.14), they seemed to be equally sensitive to IL-22 stimulation as is evident in the consistent and significant induction of downstream target genes (*SOCS3, MUC1, S100A9*) (Figure 4.18 A, B, D). The amount of IL-22-induced *OLFM4* varied considerably from one organoid line to the next and thus its induction was not statistically significant (Figure 4.18 C).

In summary, expression of *SOCS3,* an important negative regulator of STAT3 signalling, and *MUC1*, a key component of the mucous barrier that protects the epithelium from invading microbes, was elevated in matched normal compared to CRC-derived organoids at baseline. By contrast basal and IL-22-induced expression of *S100A9*, an antimicrobial peptide with well-established pro-tumourigenic function (Cheng *et al.*, 2008; Ichikawa *et al.*, 2011; Markowitz and Carson, 2013), was elevated in CRC organoids. Thus tumours, possibly through somatic mutation or epigenetic adaptation, may selectively favour induction of IL-22 targets that promote tumourigenesis over those with important homeostatic function.

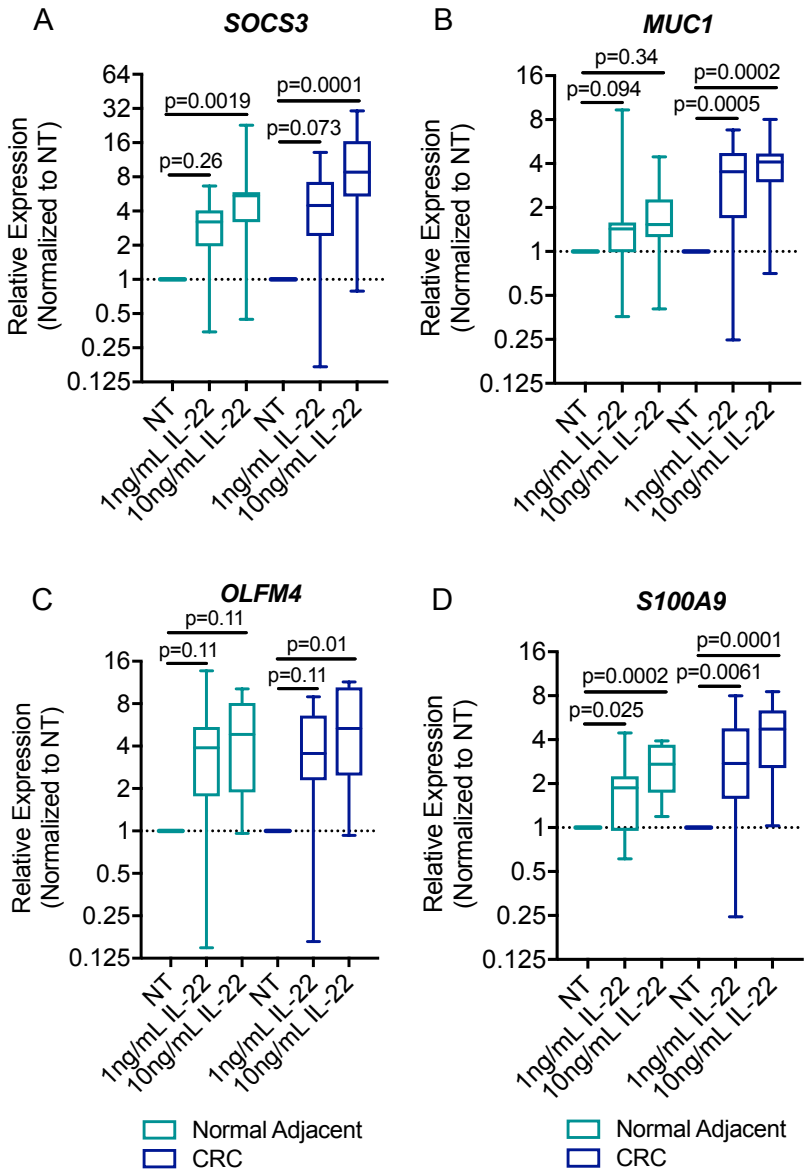


Figure 4.18 IL-22 target genes *SOCS3*, *MUC1,* and *S100A9* are induced with IL-22 stimulation in normal adjacent and tumour derived organoids.

CRC and matched normal adjacent organoids generated from prospectively collected resection tissue were stimulated between passages 2-4 for 24h with 1ng/mL, 10ng/mL IL-22. qPCR analysis was performed for key IL-22 target genes:

(A) *SOCS3*
(B) *MUC1*
(C) *OLFM4*
(D) *S100A9*

Box and whisker plots represent the 5-95th percentile of relative expression of each gene for each condition in N=15 normal adjacent derived organoids and N=13 CRC derived organoids. Stimulations were performed in technical duplicate for each line. Expression is normalised to the NT condition for each independent organoid to observe the fold change in the genes studied. Statistical significance was evaluated using one-way ANOVA with Dunnett's post test for multiple comparisons, comparing each stimulation to the NT condition for normal adjacent and CRC derived organoids independently. P <0.05 is considered significant.

4.2.9.5 *KRAS* mutations detected in whole tumour tissue are also present in the corresponding organoids.

Finally, it was necessary to confirm that *KRAS* mutations present in the whole tumour tissue at the time of resection were also present in the corresponding tumour-derived organoids. Van de Wetering *et al.* have previously reported that key oncogenic driving mutations in organoids derived from human tumours match those detected in whole tissue biopsies and are stable over successive passages (van de Wetering *et al.*, 2015). FFPE sections of colorectal tumours from patients undergoing colectomy at the Churchill Hospital are used to perform mutational analysis in the Oxford Molecular Diagnostics Centre as part of routine pathology using massively parallel sequencing technology. *KRAS* mutation status is of particular importance in colorectal cancer for clinical decision-making, as it is an established contraindication for cetuximab treatment according to NICE guidelines (NICE, 2013). The mutational profile of each prospectively collected tumour was obtained. Independently, using a qPCR-based assay with probes specific for 20 known mutational variants in *KRAS* (qBiomarker, Qiagen), we determined *KRAS* mutation status in each organoid using DNA extracted between passages 2-8. *KRAS* mutation status in the organoids reproducibly reflected that in the whole tissue from which it was derived, except in the case of two patients with rare variants, not present in the qPCR-based assay that were detected by massively parallel sequencing in FFPE sections (Table 4.1).

ORB #	Oxford Molecular Diagnostics Mutational Analysis from FFPE	qBiomarker Mutation Analysis on orgnaoids	KRAS Mutation Call
108740	c.35G>A, p.G12D, COSM521	c.35G>A, p.G12D, COSM521	MUT
108790	c.35G>A, p.G12D, COSM521	c.35G>A, p.G12D, COSM521	MUT
108870	c.35G>T, p.G12V, COSM520	c.35G>T, p.G12V, COSM520; c.34_35GG>TT, p.G12F, COSM512	MUT
108689	Mutation of uncertain clinical significance: c.35_36insAGCTGG, p.A11_G12dup, COSM1562186	None detected	MUT (uncertain clinical significance)
108691	Mutation of uncertain clinical significance: c.35_36insAGCTGG, p.A11_G12dup, COSM1562186	None detected	MUT (uncertain clinical significance)
108858	c.38G>C, p.G13A, COSM533	c.38G>C, p.G13A, COSM533	MUT (uncertain clinical significance)
108707	None detected	None detected	WT
108742	None detected	None detected	WT
108769	None detected	None detected	WT
108802	None detected	None detected	WT
108898	None detected	None detected	WT

Diagnostic mutational analysis was not available for organoids 0108709, 0108719

Table 4.1 *KRAS* mutation status in organoids and matched whole tumour tissue.

In summary, we have validated that the IL-22 receptor is expressed and functional in primary human colonic organoids and mirrors that in the whole tumour tissue. Additionally, we have identified global gene expression differences in normal adjacent and CRC-derived organoids at baseline and following IL-22 stimulation. Finally, we have confirmed that organoid *KRAS* mutation status matches that of the whole tissue from which it was derived, except in the case of rare variants of unknown clinical significance not detected by the qPCR-based assay. Therefore, the organoid system provides an accurate *ex vivo* model of human CRC in which to interrogate the functional synergy between IL-22 and mutant *KRAS*.

4.2.10 IL-22 induces proliferation in *KRAS* mutant organoids.

Next, organoids were stratified based on *KRAS* mutation status and functional responses to IL-22 were evaluated. First, we confirmed that the pattern of IL-22 target gene induction was comparable to that observed in *KRAS* mutant versus wild type CRC lines following 24-hour 1ng/mL IL-22 stimulation. Like the DLD-1 isogenic cells, *SOCS3* expression at baseline (Figure 4.19 A) and fold induction after IL-22 stimulation (Figure 4.19 B) was comparable between *KRAS* mutant and wild type organoids. Moreover *MUC1* expression was similar regardless of the *KRAS* mutation status of the organoid (Figure 4.19 A, B). By contrast, *S100A9* expression trended towards being elevated in *KRAS* mutant compared to wild type organoids at baseline (Figure 4.19 A) and was significantly induced following IL-22 stimulation (Figure 4.19 B), as was the case in *IL22RA1*-high, *KRAS* mutant CRC clonogenic spheres (Figure 4.5, Figure 4.8).

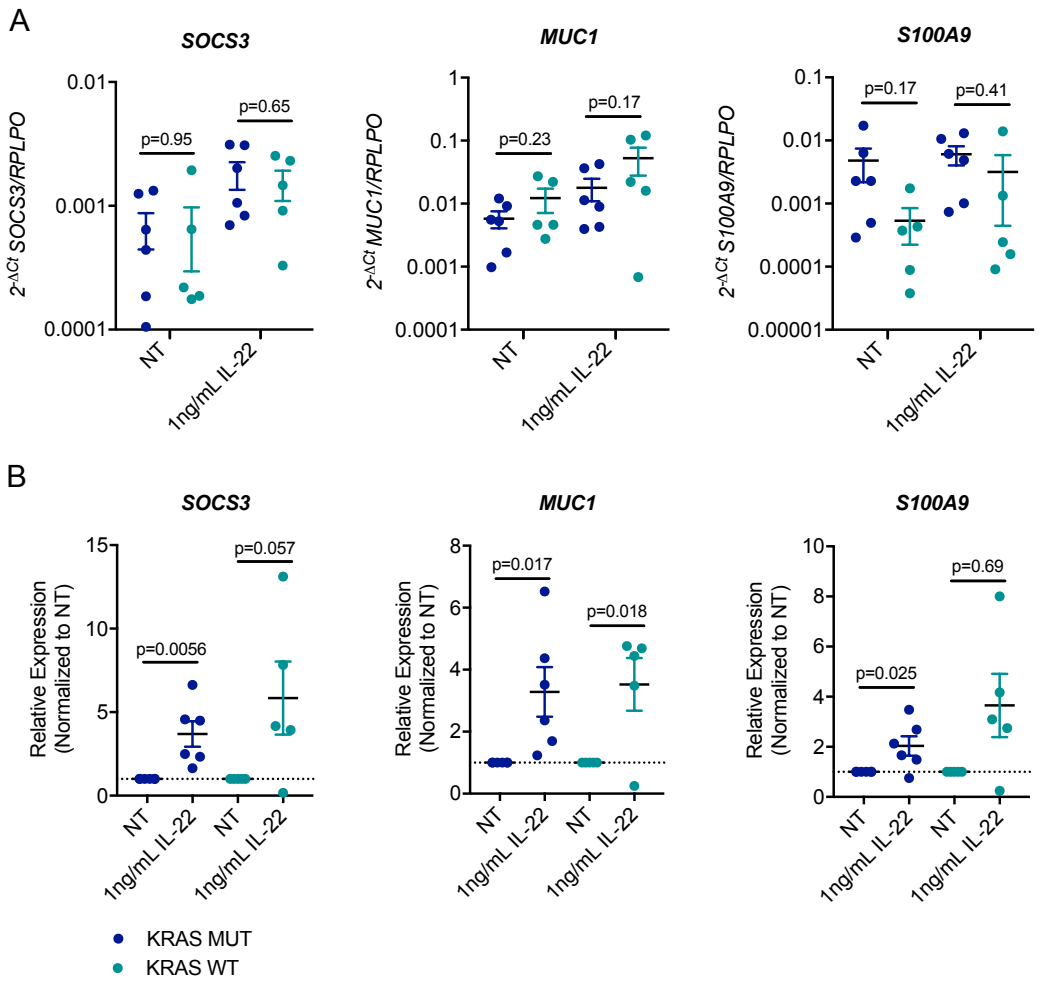


Figure 4.19 *S100A9* expression is elevated at baseline in *KRAS* mutant compared to *KRAS* wild type CRC derived organoids and is induced by IL-22.

CRC *KRAS* MUT and WT organoids generated from prospectively collected resection tissue were stimulated between passages 2-4 for 24h with 1ng/mL, 10ng/mL IL-22. qPCR analysis was performed for key IL-22 target genes:

(A) Relative *SOCS3, MUC1, S100A9* expression. Statistical significance was evaluated using unpaired T-tests comparing expression in *KRAS* MUT to *KRAS* WT CRC derived organoids in the NT and IL-22 stimulation conditions. P <0.05 is considered significant.

(B) Fold change in relative expression of *SOCS3, MUC1, S100A9*. Statistical significance was evaluated unpaired T-tests comparing IL-22 stimulation to the NT condition for *KRAS* MUT and *KRAS* WT CRC derived organoids independently. P <0.05 is considered significant.

Each dot represents the mean expression from technical duplicates of a *KRAS* MUT (N=6) or WT (N=5) organoid line derived from an independent patient.

Having observed a comparable pattern of IL-22 responses in *KRAS* mutant and wild type organoids that supported observations made in the CRC lines, we next sought to determine whether IL-22 preferentially promotes proliferation in *KRAS* mutant organoids. A panel of *KRAS* mutant and wild type organoids were trypsinised to single cells and seeded into organoid culture conditions in the presence or absence of 1ng/mL IL-22 for 96 hours. We focussed specifically on organoids harbouring clinically relevant mutations in codons 12 and 13 of the *KRAS* gene that are known to constitutively activate the Ras pathway. Proliferation was assessed by spectrophotometric detection of Alamar blue reduction. *IL22RA1* expression, as assessed by qPCR, was no different between the assessed *KRAS* mutant and wild type organoids. Interestingly, IL-22 reproducibly promoted proliferation in the *KRAS* mutant organoids (Figure 4.20 B). By contrast the proliferative response to IL-22 in the *KRAS* wild type organoids was highly variable (Figure 4.20 B).

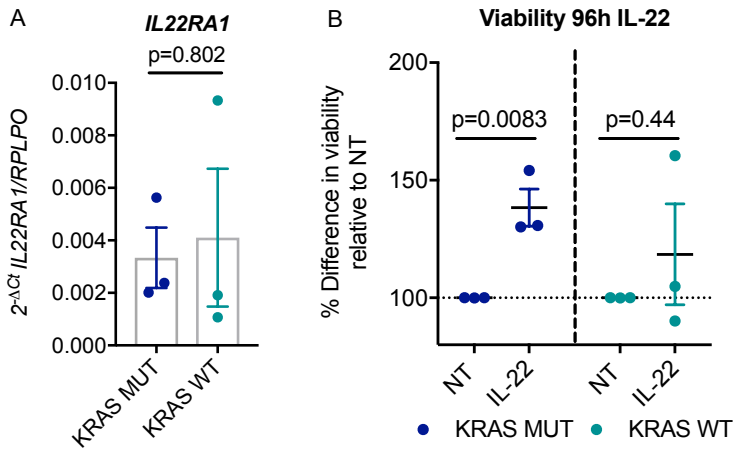


Figure 4.20 IL-22 consistently induces proliferation of *KRAS* mutant organoids.

KRAS G12D/G12V MUT or *KRAS* WT organoids were seeded in 96 well plates and treated with 1ng/mL IL-22 for 96h. 5h prior to the end of the IL-22 incubation, Alamar Blue was added to each well. Proliferation was measured by assessing the reduction of resazurin to resorufin by measuring absorbance at 570 and 600nm after 5 hours.

(A) *IL22RA1* expression in *KRAS* MUT and WT organoids used in proliferation assay.
(B) Proliferation of *KRAS* MUT and WT organoids with IL-22.

Each data point represents an independent CRC organoid derived line and is the average of n=3 technical replicates for that line. Data are normalised to the NT condition for each organoid line. Statistical significance was assessed using unpaired T-tests to compare the IL-22 stimulation to NT condition. P<0.05 is significant.

We next sought to determine whether IL-22 could support the proliferation of *KRAS* mutant organoids in the absence of the critical growth factor EGF. To address this, the same panel of organoids described above was cultured in organoid media lacking EGF in the presence or absence of 1ng/mL IL-22 for 96 hours. Proliferation was again assessed by spectrophotometric detection of Alamar blue reduction. Organoids were also macroscopically observed using brightfield microscopy. In two of the three *KRAS* G12D/G12V mutant organoids assessed, IL-22 supported proliferation in the absence of EGF (Figure 4.21 A). Interestingly, one *KRAS* wild type line also proliferated in response to IL-22 in the absence but not the presence of EGF (Figure 4.21 B). Based on clinical molecular diagnostic data, this line harboured an activating mutation in *BRAF*. Macroscopic observation of the organoids under the various stimulation conditions revealed a pronounced phenotype in the *BRAF* mutant line, whereby extensive organoid death was observed in the absence of EGF, while treatment with IL-22 restored organoid growth (Figure 4.21 C). Thus it seems that mutations in components of pathways downstream of Ras, such as *BRAF*, may promote IL-22 responses that that resemble those of *KRAS* mutants. Continued prospective accrual of CRC resections and establishment of organoids is required to validate these preliminary observations and to enable stratification not only based *KRAS* mutation, but also IL-22RA1 expression.

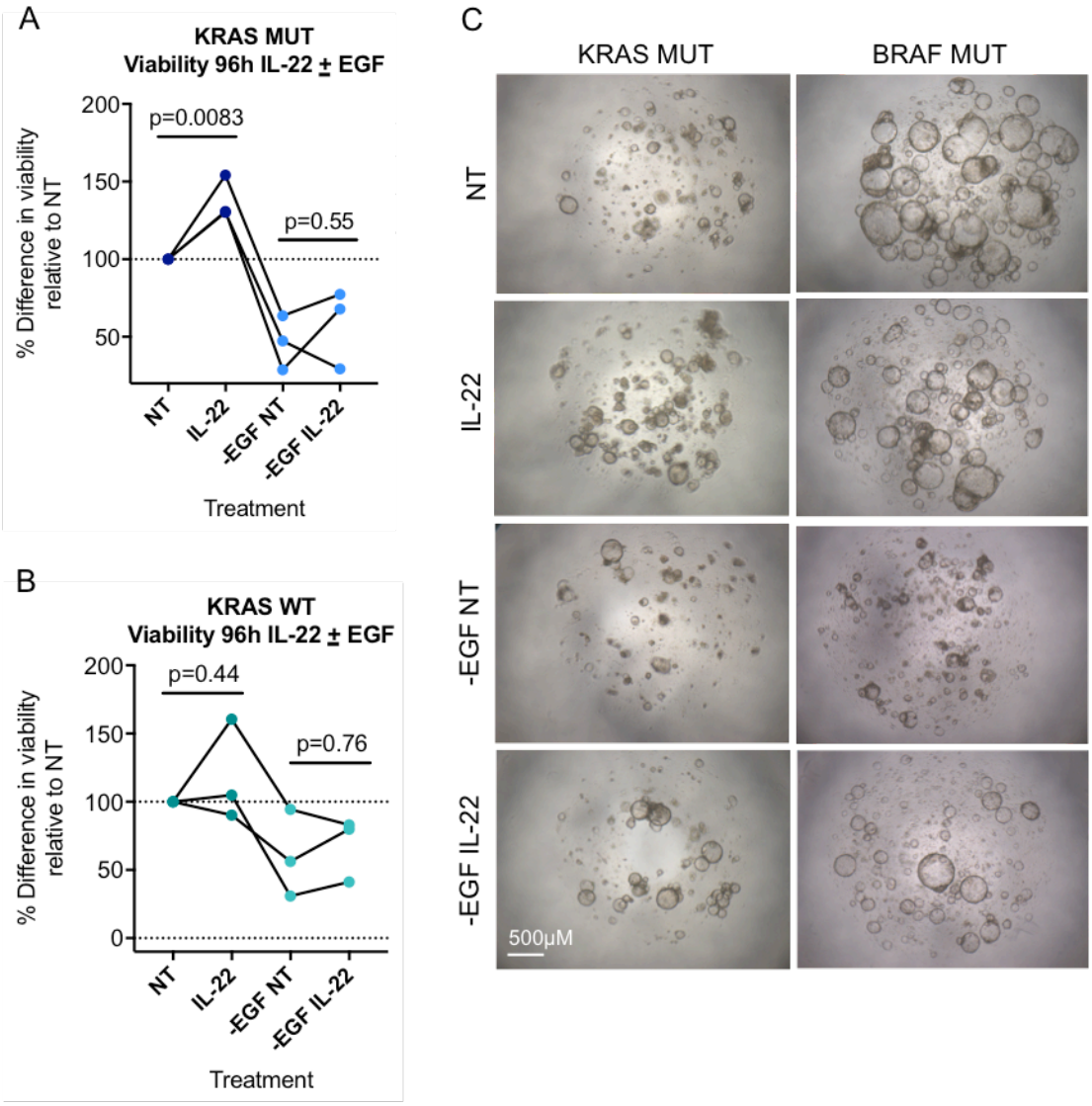


Figure 4.21 IL-22 consistently promotes proliferation of *KRAS* mutant orgnaoids in the presence of EGF, but variably promotes proliferation in absence of EGF.

KRAS G12D/G12V MUT or *KRAS* WT organoids were seeded in 96 well plates and treated with 1ng/mL IL-22 for 96h in the presence or absence of EGF. 5h prior to the end of the IL-22 incubation, Alamar Blue was added to each well. Proliferation was measured by assessing the reduction of resazurin to resorufin by measuring absorbance at 570 and 600nm after 5 hours.

(A) Proliferation of *KRAS* MUT organoids with IL-22.
(B) Proliferation of *KRAS* WT organoids with IL-22.
(C) Representative brightfield microscopy (4x magnification) of a *KRAS* MUT and *BRAF* MUT (grouped with *KRAS* WT organoids) line after 72h IL-22 stimulation in the presence or absence of EGF.

Each data point represents an independent CRC organoid derived line and is the average of n=3 technical replicates for that line. Data are normalised to the EGF containing NT condition for each organoid line. Statistical significance was assessed using unpaired T-tests to compare the IL-22 stimulation to NT condition for the EGF-containing and deficient conditions separately. $P<0.05$ is significant.

4.3 Discussion

4.3.1 Main conclusions

Here we have presented evidence of a direct biological link between IL-22 signalling and mutant *KRAS* which promotes malignant processes in three independent human colorectal cancer experimental systems. Using a panel of CRC cell lines that represent the clinical molecular subtypes of interest, we demonstrated that IL-22 enhances chemoresistance, clonogenic outgrowth, and proliferation specifically in cells bearing high levels of IL-22RA1 and mutated *KRAS*. These findings were validated in an isogenic cell line pair with identical IL-22RA1 expression, differing only in the presence or absence of mutant *KRAS*. Moreover, IL-22 reproducibly induced proliferation in *KRAS* mutant primary colorectal cancer-derived organoids. While activation of STAT3 (Y705) by IL-22 was not dependent on the CRC cell genotype, IL-22 uniquely induced AKT (S473) and ribosomal protein S6 (S235/236) phosphorylation in IL-22RA1-high, *KRAS* mutant and not wild type cells. Furthermore, transcriptional induction of the antimicrobial peptide, *S100A9* was most striking in *KRAS* mutant cell lines following IL-22 stimulation. To our knowledge this is the first evidence suggesting a functional synergy between IL-22 and mutant *KRAS*.

4.3.2 IL-22 promotes chemoresistance, clonogenic outgrowth, and proliferation in a *KRAS*-dependent manner

Cytokines do not induce neoplasia in the absence of oncogenic mutations. In the two murine models of IL-22-dependent CRC, the presence of an existing oncogenic mutation or treatment with a mutagenic agent was required for carcinogenesis (Huber *et al.*, 2012; Kirchberger *et al.*, 2013b). It seems logical that the presence of activating mutations in components of cytokine signalling pathways would change the way that a cytokine signal is interpreted by a cancer cell. However, this is one of the few

reports to specifically investigate the influence of underlying oncogenic mutations in cytokine signalling.

The reduced relapse-free survival observed in *IL22RA1*-high, *KRAS* mutant patients in the PETACC3 confirmation cohort—who uniformly received adjuvant 5-FU therapy—identified this molecular subgroup to be chemoresistant. In line with this, our functional studies in a panel of CRC lines revealed that IL-22 pretreatment had a direct chemoprotective effect specifically in IL-22RA1-high, *KRAS* mutant CRC cells. We confirmed that this effect was dependent on the presence of *KRAS* mutation in an isogenic cell line pair with matched IL-22RA1 expression. IL-22 promoted chemoresistance only in the *KRAS* mutant isogenic and not wild type cells. We are not the first to report that IL-22 can have chemoprotective effects. Pretreatment of SW620 and SW480 CRC cells (Wu *et al.*, 2013) and A549 lung adenocarcinoma cells (Zhang *et al.*, 2008) with IL-22 enhanced survival after 5-FU treatment. Notably, although not a focus of the aforementioned studies, each of the cell lines used is known to harbour an activating mutation in *KRAS*. Furthermore, Wu *et al.* began their study investigating IL-22-induced chemoresistance in Colo205, HCT116, SW620, and SW480 cells. However, after preliminary experiments, focussed only on the SW620 and SW480 lines in which IL-22 showed a pronounced chemoprotective effect (Wu *et al.*, 2013). Thus, like Wu *et al.,* we observed no significant chemo protective effect of IL-22 in IL-22RA1-high, *KRAS* WT Colo205 or IL-22RA1-low, *KRAS* MUT HCT116 cells. In contrast to Wu's findings however, IL-22 was not chemoprotective in the SW480 CRC line in our hands, likely due to its low expression of IL-22RA1.

There is reported evidence that *IL22RA1* expression is enhanced by radiation (Lindemans *et al.*, 2015) and some standard chemotherapies (Kobold *et al.*, 2013). This therapy-induced *IL22RA1* may be a physiologic response to cytotoxic stress, enhancing IL-22-mediated rescue of damaged cells. However, it has important implications for the effectiveness of therapy in patients with metastatic disease, since chemotherapy may augment *IL22RA1* expression in metastasising CRC cells. In future studies, it will be important to assess IL-22RA1 expression in biopsies of resected metastases from patients who receive adjuvant chemotherapy to determine whether IL-22RA1 expression is higher than that of the primary tumour. Given our observations of the direct chemoprotective effect of IL-22 and its dual dependency on *KRAS* mutation and IL-22RA1 expression, we would hypothesise that therapy-enhanced IL-22RA1 expression will only further promote IL-22-induced chemoresistance in *KRAS* mutant CRC.

In agreement with the findings of Kryczek *et al.*, we observed that IL-22 promotes the clonogenic outgrowth of DLD-1 cells in three-dimensional culture (Kryczek *et al.*, 2014). Although not specifically mentioned in their study, DLD-1 cells harbour an endogenous *KRAS* G13D mutation and express high levels of IL-22RA1. We similarly found that IL-22 promotes clonogenic outgrowth in IL-22RA1-high, *KRAS* mutant T84 cells but not other IL-22RA1-high, *KRAS* WT or IL-22RA1-low, *KRAS* MUT lines studied, implicating an IL-22-*KRAS* interaction. Kryczek *et al.* attributed the enhanced DLD-1 clonogenic outgrowth they observed to IL-22-induced stemness. They reported elevated *NANOG, SOX2,* and *POU5F1* expression after 24 hour IL-22 stimulation with 20ng/mL IL-22. Using half the concentration of IL-22 for the same period of time, we observed modest induction of *NANOG* in the T84 line, but did not

observe any significant induction of *NANOG, SOX2,* or *POU5F1* in the other cell lines studied. It is possible that the difference in cytokine concentrations used may account in part for this discrepancy. Interestingly, in our hands, IL-22, but not IL-6, profoundly upregulated *OLFM4* in an IL-22-specific, but *KRAS* independent manner. *OLFM4* has been coined a stem cell marker by the Clevers' group, who first developed an *OLFM4*-Cre mouse to label and track intestinal epithelial stem cells in 2014 (van der Flier *et al.*, 2009; Merlos-Suárez *et al.*, 2011; Schuijers *et al.*, 2014). While OLFM4 expression is indeed restricted to the base of the crypts at steady state, its expression extends the length of the crypt in active Crohn's and colitis (Gersemann *et al.*, 2012). Whether OLFM4 plays a beneficial or deleterious role in colorectal cancer may depend on the stage of tumourigenesis as it is typically more highly expressed in early disease and reduced or lost in advanced stages (Besson *et al.*, 2011). The dramatic and IL-22-specific induction of OLFM4 warrants further investigation, however it would be inappropriate to conclude that IL-22-induced *OLFM4* represents induction of cancer stemness. Therefore, unlike Kryczek *et al.*, we reason that the enhanced clonogenic outgrowth capacity of *IL22RA1*-high, *KRAS* mutant cells reflects the capacity of IL-22 to promote survival, inhibition of apoptosis, and anchorage independent growth, rather than stemness per se.

In line with the enhanced proliferation induced by IL-22 in *KRAS* mutant isogenic DLD-1 cells, when primary human CRC organoids were dissociated to single cells and then seeded into organoid culture conditions in the presence or absence of IL-22, IL-22 reproducibly enhanced proliferation of *KRAS* mutant CRC organoids. The proliferative response to IL-22 in *KRAS* wild type organoids was highly variable, however. One potential explanation for this variability is the presence of mutations in

the *KRAS* wild type organoids in cell signalling components downstream of Ras or in independent pathways that exert overlapping function (ie. PI3K/Akt). For instance, one of the *KRAS* WT organoid lines that we generated has an activating mutation in *BRAF*. *BRAF* mutations are mutually exclusive with *KRAS* mutations and this has long been assumed a consequence of functional redundancy (Roth *et al.*, 2010). As with mutations that abolish the GTPase activity of *KRAS,* activating mutations in the serine/threonine kinase *BRAF* can lead to constitutive activation of Raf-MEK-ERK signalling (Roth *et al.*, 2010). Although *KRAS* mutations are not prognostic in Stage II/III CRC, *BRAF* mutations predict poor overall survival in microsatellite stable tumours (Roth *et al.*, 2010). While our multivariate analysis of the prognostic *IL22RA1-KRAS* interaction revealed that it was independent of *BRAF* mutation, there were not enough *BRAF* mutant patients in the cohorts we have studied to test for a specific interaction between *IL22RA1* and *BRAF*. Interestingly, when CRC organoids were grown in the absence of EGF, which is typically present in organoid media and required for successful culture, organoid growth was diminished in both *KRAS* mutant and WT organoids. While IL-22 supported the growth and survival of some *KRAS* mutant organoids in the absence of EGF, the phenotype was most striking in the *BRAF* mutant organoid line. The *BRAF* mutant organoids failed to grow in absence of EGF, but growth was restored upon IL-22 treatment. This observation suggests that the IL-22-*KRAS* synergy may be dependent on ERK1/2 signalling rather than another Ras downstream effector pathway. Pharmacologic inhibition of ERK1/2 or MEK in IL-22 stimulated organoids will be used to specifically test this.

A major caveat to this study at present is that we do not have sufficient CRC organoid numbers to stratify based on both *KRAS* mutation status and *IL22RA1* expression

level. As we continue to generate CRC organoids from prospectively collected tissue, this dual stratification will be possible. Based on our evidence from clinical cohorts and CRC lines, we hypothesise that the relative strength of the IL-22-enhanced proliferation in *KRAS* mutant organoids will be more profound when the organoids are also stratified based on *IL22RA1* expression. Furthermore, inadequate numbers have made it impossible to stratify organoids derived from proximal versus distal tumours. At this point, it is not clear whether differences in IL-22 responses between proximal and distal tumours would be observable in an *ex vivo* organoid system, due to the loss of *in vivo* environmental cues that distinguish these anatomical regions. Despite the current numerical limitations, most importantly, this work has systematically validated the organoid system as an accurate *ex vivo* model in which to study the IL-22-*KRAS* synergy and has provided early evidence confirming observations derived from cell lines. Moving forward this organoid system will provide a unique functional model to use in early phase clinical trials, which test therapeutic intervention in the IL-22 pathway. In the interval between diagnosis and colectomy, patients will receive a single dose of an IL-22 pathway-modulating therapy and functional differences as a consequence of IL-22 pathway modulation will be explored in organoids derived from pre-treatment diagnostic biopsies and post-treatment colectomy resection tissue.

4.3.3 Convergence of IL-22 signalling and mutant *KRAS* on AKT, ribosomal protein S6, and *S100A9* activation and induction hint at possible mechanisms mediating malignant progression

Existing evidence from murine IL-22-driven CRC models—both colitis-associated and sporadic—attributed the pro-tumourigenic activity of IL-22 to its STAT3 activating capacity, though a direct mechanistic link was not proven (Huber *et al.*, 2012; Kirchberger *et al.*, 2013b). IL-22-induced colorectal cancer stemness was

driven by STAT3 mediated induction of the methyltransferase DOT1L, which promoted stem cell gene expression (Kryczek *et al.*, 2014). Interestingly, we observed no difference in the amount of STAT3 (Y705) phosphorylation over a range of doses of IL-22 between *KRAS* mutant and wild type DLD-1 isogenic cells. Based on our current experimental evidence, we cannot conclude that the interaction between IL-22 and *KRAS* is STAT3-independent, but simply that it is not strictly dependent on the amount of STAT3 activation. It is possible that STAT3 may drive specific pathways in conjunction with mutant *KRAS* that is does not in a *KRAS* wild type cell.

IL-22 has been shown to activate AKT in *KRAS* mutant A549 lung cancer cells (Bi *et al.*, 2016). Furthermore, IL-22-induced proliferation of keratinocytes was dependent on active PI3K/AKT/mTOR signalling (Mitra, Raychaudhuri and Raychaudhuri, 2012). We similarly observed IL-22-induced AKT phosphorylation and this induction occurred only in *KRAS* mutant cells. AKT activates mTORC1, which phosphorylates S6 kinases, resulting in ribosomal S6 protein phosphorylation (Hannan *et al.*, 2011). In our hands IL-22 induced pS6 (S235/236) specifically in *KRAS* mutant and not wild type isogenic cells. This induction was rapamycin sensitive in a preliminary experiment and may be mTORC1-dependent. Moreover, in line with evidence of Ras/ERK-dependent phosphorylation of ribosomal protein S6 on its serine 235/236 residues (Roux *et al.*, 2007), pS6 (S235/236) was modestly elevated in *KRAS* mutant versus wild type isogenic cells at baseline. Therefore, pS6 (235/236) may represent a convergent target of Ras/ERK and AKT signalling. Given the well studied role that ribosomal protein S6 plays in translation initiation and consequent cell growth (Roux *et al.*, 2007; LoRusso, 2016), it is plausible that the pro-proliferative effects of IL-22 in *KRAS* mutant cells may be dependent on convergent Ras/ERK and IL-22-induced

AKT signalling. IL-22 proliferation assays performed in the presence of specific S6 kinase inhibitors will be necessary to confirm that the pro-proliferative effect of IL-22 in *KRAS* mutant cells is dependent on this pathway.

IL-22 signalling in *KRAS* mutant cells markedly induces *S100A9*, a molecule with well-documented roles in primary tumourigenesis and malignant progression. S100A9 is a calcium binding protein that exists as a homodimer or heterodimer with S100A8 (Markowitz and Carson, 2013). S100A9 has known roles in seeding the pre-metastatic niche, directly promoting cancer cell migration and metastasis, and promoting drug resistance (Bresnick, Weber and Zimmer, 2015). Some reports have also suggested that S100A9 can have direct neutrophil chemotactic activity (Ryckman *et al.*, 2003). S100A9 is predominately expressed by cells of myeloid lineages and due to its inhibitory effect on macrophage and dendritic cell differentiation, has been found to promote myeloid-derived suppressor cell (MDSC) accumulation in syngeneic colorectal cancer models (Cheng *et al.*, 2008). In DSS/AOM colitis-associated cancer models, S100A9 can function in a paracrine fashion by binding RAGE and carboxylated glycans on tumour cells, which promotes activation of pro-tumourigenic MAPK and NF-κB signalling pathways (Turovskaya *et al.*, 2008; Ichikawa *et al.*, 2011). A role for tumour cell specific expression of *S100a9* was recently elucidated in a syngeneic MC38 CRC model. shRNA mediated knockdown of *S100a8* and *S100a9* in the cancer cells had no impact on subcutaneous tumour growth but dramatically reduced liver metastases after intrasplenic injection (Lim *et al.*, 2016). Furthermore, an elegant paracrine mechanism through which S100A9 and/or S100A8 promotes chemoresistance was demonstrated in a murine breast cancer model. Chemotherapy-induced TNFα release from cancer stroma induced CXCL1 expression by breast

tumour cells, leading to recruitment of $CD11b^{+}GR1^{+}$ myeloid cells and the consequent release of S100A9 and S100A8 in the tumour microenvironment. S100A9 signalling led to activation of ERK1/2 and ribosomal protein S6 kinase-β1 (P70S6K), which facilitated the expansion of chemoresistant breast cancer cells at the primary and distant metastatic sites (Acharyya *et al.*, 2012). The only direct link between S100A9 and *KRAS* that has been made to our knowledge comes from a murine $Kras^{G12D/+}$ inducible glioma model in which hyperactivation of Ras was found to induce overexpression of S100A8 and S100A9 in postmitotic neurons and astrocytes. S100A8-S100A9 heterodimers were found to directly promote astrocyte growth and their overexpression was deemed a critical early event in oncogenic KRAS induced gliosis (Ryu *et al.*, 2012). Therefore, tumour cell-specific induction of S100A9 may represent a plausible mechanism by which IL-22 synergises with mutant *KRAS* to promote primary tumourigenesis, chemoresistance, and metastatic progression.

4.3.4 Oncogenic *KRAS* does not directly modulate IL-22RA1 expression or dynamic regulation

Oncogenic *KRAS* was found to directly induce IL-17 receptor A expression in pancreatic epithelium in a mouse model (McAllister *et al.*, 2014). DLD-1 cells with or without mutant *KRAS* have nearly identical IL-22RA1 expression, suggesting that KRAS does not directly modulate IL-22RA1 basal expression. However, although IL22RA1 is more highly expressed by normal tissue than tumour tissue in patients with *KRAS* wild type CRC, tumour and matched normal *IL22RA1* expression is unchanged in *KRAS* mutant patients. A recent report in a *KRAS* mutant lung cancer model demonstrated that enhanced AKT and GSK3β activation can sustain IL-22RA1 through phosphorylation of its cytoplasmic tail, thus preventing proteasomal degradation (Metz *et al.*, 2016). Though the AKT-GSK3β-mediated sustainment of IL-22RA1 expression is active in murine epithelial cells (Weathington *et al.*, 2014),

the human protein is not likely regulated through this mechanism due to absence of the consensus GSK3β sequence (Franz *et al.*, 2015). This may explain why despite AKT activation downstream of IL-22 in *KRAS* mutant cells, we did not observe any differences in the dynamic regulation of IL-22RA1 protein with ligand stimulation between *KRAS* MUT and WT isogenic cells. Unexpectedly, however, *IL22RA1* mRNA expression was repressed in the wild type cells despite *IL22RA1* mRNA recovery in *KRAS* mutant cells upon removal of the stimulus. The only existing reported evidence of posttranscriptional control of *IL22RA1* demonstrated that *IL22RA1* is a direct target of IL-22-induced miR-197 in human keratinocytes (Lerman *et al.*, 2014). Downregulation of miR-197 in psoriasis led to deregulated IL-22 signalling (Lerman *et al.*, 2014). It will be necessary to conduct longer time course experiments in the DLD-1 isogenic pair to determine whether this transcriptional repression ultimately leads to lower surface IL-22RA1 expression in the presence of its ligand. Furthermore, studies which directly compare IL-22RA1 dynamic regulation in tumour and matched normal adjacent tissue-derived organoids from *KRAS* mutant and wild type patients may shed light on the reason for the observed differences between whole tissue *IL22RA1* expression in *KRAS* mutant versus wild type patients, when comparing tumour to matched normal tissue.

4.3.5 The study of primary normal adjacent and CRC organoids reveals unique differences between homeostasis and malignancy

Primary organoids from matched normal and CRC tissue present a unique experimental system in which to examine differences between homeostasis and malignancy. One of our initial findings when comparing tumour to matched normal adjacent-derived organoids was that *IL23A* expression is elevated in tumour-derived organoids compared to normal adjacent-derived organoids. Given that the organoid

cultures are exclusively epithelial, this provides definitive evidence that at least some portion of the transcriptional elevation of *IL23A* observed by ourselves and others (Langowski *et al.*, 2006; Grivennikov *et al.*, 2012) in CRC compared to matched normal tissue is derived from an mRNA signal in the epithelium. The key question that remains is whether the epithelium produces functional IL-23. Experiments to measure IL-23 protein in supernatant from tumour and normal adjacent derived organoids are currently underway.

Study of normal adjacent and CRC organoids has also highlighted the potential global de-regulation of cytokine signalling pathways in CRC. Specifically, in line with evidence that SOCS3 can be epigenetically suppressed in multiple cancer types (Ying *et al.*, 2010; Pierconti *et al.*, 2011; Yoshimura and Yasukawa, 2012; Yu *et al.*, 2015), we observed elevated *SOCS3* expression in normal adjacent compared to tumour organoids at baseline and with IL-22 stimulation. Though *SOCS3* cannot negatively regulate IL-22 signalling, it is an important negative regulator of signalling for cytokines that signal via gp130-containing receptors (e.g. IL-6, IL-11, oncostatin M) and its downregulation can enhance tumour aggressiveness and metastatic progression (Yoshimura and Yasukawa, 2012).

Somewhat paradoxically, we have also observed that mRNA expression of the well-described oncoprotein *MUC1* is basally elevated in normal compared to tumour-derived organoids. However, it is induced upon IL-22 signalling normal and CRC-derived organoids. MUC1 plays divergent roles in homeostasis and cancer that are largely dictated by differences in cellular localisation and post-translational glycosylation (Nath and Mukherjee, 2014). While MUC1 is a critical component of

the mucous barrier that protects epithelial cells from direct microbial contact in the gut under homeostatic settings, hypoglycosylated MUC1 in colorectal tumours can activate mitogenic pathways (Nath and Mukherjee, 2014). Our observations underscore that if used as a biomarker, specific detection of aberrantly glycosylated protein forms rather than *MUC1* transcript would be most appropriate. Much like *MUC1*, *OLFM4* was also elevated at baseline in normal compared to tumour-derived organoids. Though conflicting evidence exists in the literature at present, loss of *OLFM4* in colorectal tumours may in fact promote malignancy or be a marker of advanced disease (Liu *et al.*, 2016).

Finally, in line with its known pro-tumourigenic and pro-metastatic function (Markowitz and Carson, 2013), *S100A9* is broadly elevated in tumour compared to normal adjacent organoids at baseline and upon IL-22 stimulation, and trends toward being basally elevated in *KRAS* mutant versus wild type CRC organoids.

4.3.6 Concluding remarks

In summary, we have demonstrated that IL-22 promotes chemoresistance, clonogenic outgrowth, and proliferation specifically in *KRAS* mutant cells expressing high levels of the IL-22 receptor. The presence of a mechanistic link between IL-22 signalling and mutant *KRAS* has important implications for the poor prognosis subtype of colorectal cancers that that exhibit high IL-22 receptor expression and oncogenic *KRAS* mutations. Rather than stratifying patients based on IL-22 receptor expression and *KRAS* mutation for purely prognostic purposes, our data suggest that pharmacologically interfering with the IL-22 pathway may enhance responsiveness to standard of care chemotherapy and limit cancer cell proliferation. While the evidence presented here points to the unique activation of AKT and ribosomal protein S6, the

precise mechanism of synergy between IL-22 and *KRAS* remains to be determined. Here, we have observed how mutant *KRAS* can modulate the interpretation of an IL-22 signal to have consequences on cancer-cell intrinsic properties like growth and survival. It is also plausible, however, that IL-22 signalling in a *KRAS* mutant cell may have non-cell autonomous consequences on malignant progression that involve modulation of the inflammatory microenvironment. Elucidation of the precise mechanism of synergy between IL-22 and *KRAS* will be the focus of the next chapter of this thesis.

5 Elucidation of the mechanisms of IL-22-*KRAS* synergy

5.1 Introduction

Thus far, we have identified a subset of colorectal cancer patients with coincident high tumoural IL-22 receptor expression and *KRAS* mutation, whose prognosis is very poor compared to their *KRAS* wild type counterparts (Chapter 3). Patients with *KRAS* mutant tumours and high expression of both subunits of the heterodimeric IL-22 receptor had diminished 5-year survival compared to those with high expression of either subunit alone (Chapter 3). It seems that rather than a spurious association, there is a direct biological link between IL-22 signalling and mutant *KRAS* that enhances chemoresistance, clonogenic outgrowth, and proliferation in *IL22RA1*-high, *KRAS* mutant but not wild type cells (Chapter 4). However, the precise molecular mechanisms by which IL-22 interacts with mutant *KRAS* to promote malignancy remain unknown.

IL-22 is a pleiotropic cytokine capable of activating JAK/STAT (Dumoutier *et al.*, 2009; Lim and Savan, 2014), MAPK, PI3K (Mitra, Raychaudhuri and Raychaudhuri, 2012; Xu *et al.*, 2014), and NF-κB (Lim and Savan, 2014) signalling pathways in different contexts. Independently, gain of function mutations in *KRAS* which result in its constitutive activation, trigger stimulus-independent activation of the RAF/MEK/ERK, PI3K/AKT, and RAL-GTP pathways, promoting cellular proliferation and neoplastic transformation (Vojtek and Der, 1998).

However, the impact of mutant *KRAS* on malignant progression is not restricted to its cell-autonomous effects. In lung cancer models, mutant *KRAS* has been shown to directly induce chemokine expression, particularly those that attract neutrophils (Ji *et al.*, 2006). Similarly, Ras-dependent IL-8 (CXCL8) secretion was found to be

required for initiation of tumour associated inflammation and neovascularisation in subcutaneous tumour models (Sparmann and Bar-Sagi, 2004). Interestingly, IL-22 also induces expression of neutrophil chemokines as part of its physiologic function to recruit neutrophils to sites of infection (Andoh *et al.*, 2005). Mutant *KRAS* can also directly induce ICAM-1 expression in pancreatic acinar cells, resulting in macrophage recruitment and precancerous acinar-to-ductal metaplasia (Liou *et al.*, 2015). Moreover, oncogenic *KRAS,* in conjunction with persistent inflammation, is known to accelerate malignant progression in pancreatic cancer through various mechanisms. Previous studies have demonstrated that STAT3 is indispensible for *KRAS*-driven pancreatic ductal adenocarcinoma, though the precise mechanisms are poorly understood (Corcoran *et al.*, 2011). One proposed mechanism involves coordinated inflammation and Ras-induced NFATc1 complexing with STAT3 to enhance expression of cyclins, EGFR, and WNT family members that accelerate $Kras^{G12D}$-driven carcinogenesis (Baumgart *et al.*, 2014). In our experimental system, activation of STAT3 (Y705) by IL-22 was comparable in cells with matched IL-22 receptor expression, independent of *KRAS* mutation status (Chapter 4, Figure 4.10 B). However, IL-22 uniquely augmented AKT (S473) and ribosomal protein S6 (S235/236) phosphorylation in IL-22RA1-high, *KRAS* mutant cells (Chapter 4, Figure 4.6 D, 4.10 C). Both AKT-dependent mTORC1 activation (Hannan *et al.*, 2011) and Ras/ERK signalling (Roux *et al.*, 2007) are known to induce ribosomal S6 (S235/236) phosphorylation. Activated ribosomal protein S6 plays an important role in translation initiation and resultant cell growth (Roux *et al.*, 2007; LoRusso, 2016). Thus, convergence of IL-22 and mutant *KRAS* signalling on this pathway represents a plausible mechanism of synergistic promotion of malignant behaviour.

Clearly however, IL-22 activates multiple intracellular signalling pathways, each of which can be independently augmented by constitutively active Ras signalling. The primary aim of this chapter is to identify gene/protein modules that are uniquely regulated by IL-22 in *KRAS* mutant but not wild type cells that may promote malignant behaviour. Taking an unbiased approach, we hypothesised that coordinated IL-22 and Ras signalling activates both cell autonomous and non-cell autonomous pathways to drive carcinogenesis. Using target identification and validation methodology, we performed the following sequence of analyses:

1. RNA-sequencing and label-free proteomic analysis of IL-22 stimulated DLD-1 isogenic cells with matched IL-22 receptor expression, differing only in the presence or absence of mutant *KRAS*.
2. Differential expression analysis to identify single genes/proteins uniquely regulated by IL-22 in *KRAS* mutant cells. These targets were confirmed by direct IL-22 stimulation of primary human organoids.
3. Stimulation of isogenic cells and organoids with conditioned supernatants generated from polyclonally expanded $CD4^+$ T cells from primary human colorectal tumours in the presence or absence of IL-22 blockade. Using this *ex vivo* system, we determined whether differences in IL-22 signalling in *KRAS* mutant versus wild type cells persisted in a complex cytokine milieu.
4. We then performed pathway analysis on RNA-sequencing and proteomic samples to identify candidate pathways that were uniquely regulated by IL-22 in *KRAS* mutant cells. Using the DLD-1 isogenic system and siRNA knockdown approaches, we performed functional experiments to assess the possibility that malignant behaviour was dependent on IL-22-mediated activation of the candidate pathway in *KRAS* mutant but not wild type cells.

5.2 Results

5.2.1 Unbiased RNA-sequencing and proteomic approaches to identify potential mechanisms of IL-22-*KRAS* synergy.

In order to identify the precise mechanisms of synergy between IL-22 and *KRAS*, we sought to identify candidate gene and protein modules that are uniquely modulated by IL-22 signalling in *KRAS* mutant cells. Taking advantage of the DLD-1 isogenic pair with matched IL-22 receptor expression differing only in the presence or absence of mutant *KRAS*, global transcriptomic and proteomic changes were explored in an unbiased manner following IL-22 stimulation. Specifically, RNA-sequencing was performed on DLD-1 isogenic cells stimulated with 10ng/mL IL-22 in serum-free conditions for 2 hours, to identify early gene induction, and 24 hours to explore secondary transcriptomic changes (Figure 5.1 A, B). Due to the fact that IL-6 receptor expression does not interact with mutant *KRAS* in a prognostically meaningful manner (Chapter 3, Table 3.2), as is the case for the IL-22 receptor, cells were also stimulated with 10ng/mL IL-6 for 2 or 24 hours to identify pathways that are uniquely regulated by IL-22 and not IL-6 (Figure 5.1 A, B). Three independent experiments were performed with three successive passages (P6, 7, 8) of the DLD-1 isogenic cells. To determine whether transcriptional changes were reflected at the protein level, label free proteomic analysis (LC-MS/MS) was performed on DLD-1 isogenic cells stimulated with 10ng/mL IL-22 for 24 hours, using cells from the same cell passages as those used for RNA-sequencing (Figure 5.1 A, B). RNA-sequencing and proteomic data were analysed using two different approaches. First, we identified individual genes/proteins uniquely regulated by IL-22 in *KRAS* mutant but not wild type cells. Then, we performed pathway analysis (Gene set enrichment analysis (GSEA) and Protein set enrichment analysis (PSEA-Quant)) to identify pathways uniquely regulated by IL-22 in *KRAS* mutant cells. These IL-22-*KRAS* regulated modules were

validated by direct IL-22 stimulation of DLD-1 isogenic cells and primary organoids. Furthermore, to determine whether these modules were differentially regulated by IL-22 in a more complex immune milieu, supernatants from polyclonally expanded $CD4^+$ T cells isolated from tumour and matched normal tissue were used to treat DLD-1 isogenic cells and organoids in the presence or absence of IL-22 blockade (Figure 5.1 C).

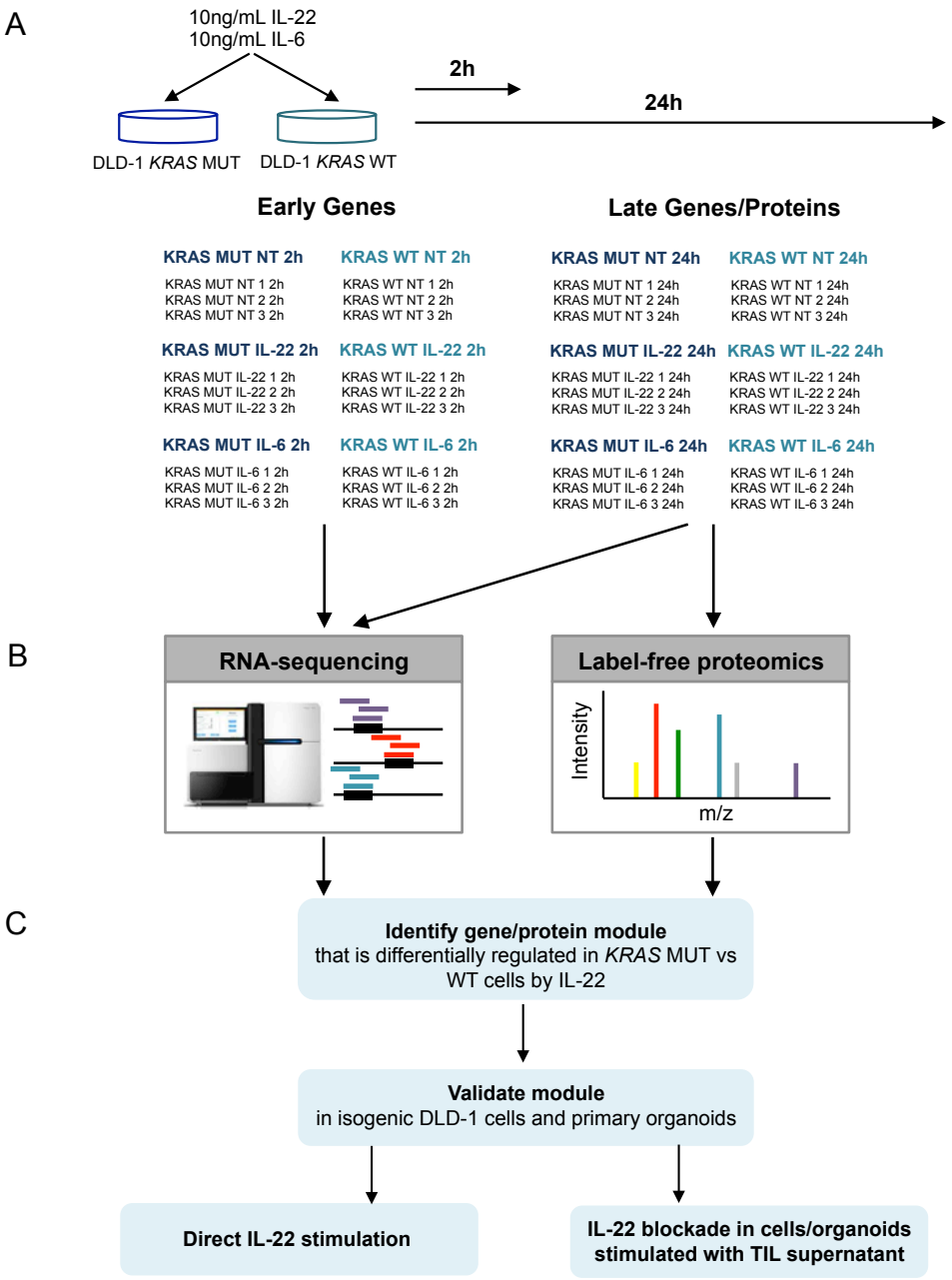


Figure 5.1 Experimental workflow for RNA-sequencing and proteomic analysis.

(A) DLD-1 *KRAS* mutant and wild type isogenic cells were stimulated for 2h or 24h with 10ng/mL IL-22 or 10ng/mL IL-6, a comparative STAT3, activator in serum free conditions. RNA was extracted from the 2h and 24h samples. Total protein was extracted from the 24h samples. 3 independent experiments were performed with cells from 3 successive passages (denoted by 1, 2, 3). (NT = no treatment) [n=36 samples]

(B) RNA-sequencing was performed on the 2h and 24h RNA samples. Label-free proteomic analysis (LC-MS/MS) was performed on the 24h protein samples.

(C) RNA-sequencing and proteomic data was analysed by examining specific genes/proteins and pathways differentially regulated by IL-22 in *KRAS* mutant versus wild type cells. These modules were validated by direct IL-22 stimulation experiments in DLD-1 isogenic cells and primary human organoids. Furthermore DLD-1 isogenic cells and organoids were treated with supernatant generated from primary $CD4^+$ tumour infiltrating leukocytes (TIL) with and without IL-22 blockade to determine whether these modules were similarly differentially regulated by IL-22 in a complex cytokine milieu.

5.2.2 ELR$^+$ CXC chemokines are potently induced by IL-22 in *KRAS* mutant compared to *KRAS* wild type cells

Initial unsupervised hierarchical clustering analysis of all RNA-sequenced samples revealed that *KRAS* mutation status drives the greatest gene expression differences in DLD-1 isogenic cells, regardless of the cytokine stimulation applied, as all *KRAS* mutant samples clustered together (Figure 5.2 A). This observation was confirmed by performing principal component analysis (PCA), in which genotype (*KRAS* MUT, WT), cytokine stimulation (no treatment (NT), IL-22, IL-6), and time (2h, 24h) were the principal modes of variation. PCA analysis demonstrated that genotype was the first principal component (1st PC); the component with the largest contribution to variance in the dataset (Figure 5.2 B). The cytokine stimulation condition was the second principal component (2nd PC) (Figure 5.2 B). Interestingly, all samples stimulated with IL-22 clustered further from the untreated samples than those stimulated with IL-6, suggesting that IL-22 drives greater gene expression changes in DLD-1 isogenic cells than IL-6, regardless of *KRAS* mutation status (Figure 5.2 B). Stimulation time formed the third principal component. While all 2h and 24h samples clustered separately, as the third principal component, stimulation time conferred the lowest amount of transcriptional variation of all variables in the dataset (Figure 5.2 B). This suggests that some of the transcriptional changes at 2 hours are sustained over 24 hours of cytokine stimulation.

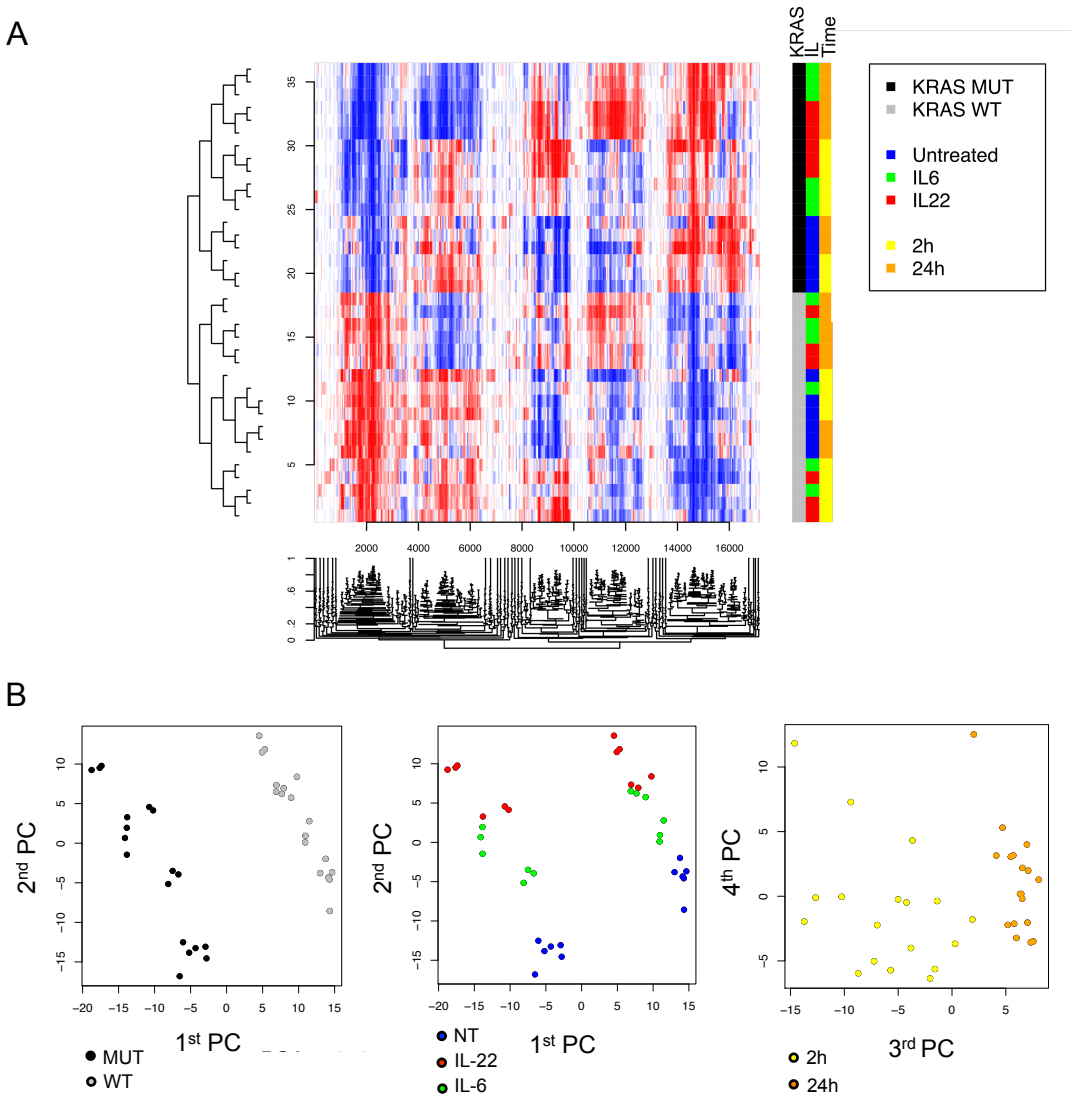


Figure 5.2 *KRAS* mutation confers the greatest gene expression differences in DLD-1 isogenic cells stimulated with IL-22 or IL-6.

(A) Unsupervised hierarchical clustering analysis using correlation distance metrics and the average linkage agglomeration algorithm of genes detected by RNA-sequencing of all samples (Chapter 2.5.3). Heatmap represents log2(RPKM+1) values. Numbers on y-axis indicate number of samples, numbers on x-axis indicate number of genes. This clustering was performed by D. Barras.

(B) Principal component analysis (PCA) on all samples (n=36) in dataset. 1st principal component separates *KRAS* mutant versus wild type cells. 2nd principal component separates the cytokine stimulation conditions. 3rd principal component separates the 2h versus 24h-stimulated samples. (PC = principal component, NT = no treatment)

To first identify transcriptional changes induced by IL-22 in *KRAS* mutant and wild type cells, simple differential expression analysis comparing IL-22 stimulated to untreated (NT) cells independently in *KRAS* mutant and wild type cells after 2 and 24 hours stimulation was performed. The top differentially expressed genes were determined by employing a stringent cut off of genes for which log 2 fold changes with IL-22 stimulation were greater than 2 with a false discovery rate (FDR) of less than $1x10^{-5}$. Upon initial observation, many of the top differentially expressed genes were similar in *KRAS* mutant and wild type cells (Figure 5.3 A). Notably however, while the myeloid chemoattractants *CXCL2* and *CXCL3* were induced in both *KRAS* mutant and wild type cells after 2 hour IL-22 stimulation, *CXCL5* was uniquely induced in *KRAS* mutant cells (Figure 5.3 A). Furthermore, *CXCL2* and *CXCL5* expression was sustained after 24 hour IL-22 stimulation in *KRAS* mutant cells, but no significant chemokine induction was observed in *KRAS* wild type cells (Figure 5.3 A). *CXCL1, CXCL2, CXCL3,* and *CXCL5* are all myeloid chemoattractants of the ELR^+ CXC chemokine family and ligands for the chemokine receptor CXCR2. CXCR2 is expressed predominately by neutrophils and is reportedly expressed by myeloid-derived suppressor cells (Eash *et al.*, 2010; Katoh *et al.*, 2013; Highfill *et al.*, 2014). To confirm the observations made in the RNA-sequencing analysis, DLD-1 isogenic cells were stimulated for 24 hours with 10ng/mL IL-22 and qPCR was performed to assess expression of *CXCL2, CXCL3,* and *CXCL5*. While these three chemokines were induced in both *KRAS* mutant and wild type cells upon IL-22 stimulation, the magnitude of the induction and the expression relative to the endogenous control (*RPLPO*) was higher in *KRAS* mutant cells (Figure 5.3 B). To independently validate this observation in primary human colorectal cancer, organoids derived from *KRAS* mutant and wild type colorectal tumours were stimulated for 24 hours with 1ng/mL

IL-22. The fold induction of *CXCL5* with IL-22 stimulation in *KRAS* mutant organoids was significantly higher than that in *KRAS* wild type organoids (Figure 5.3 C).

Therefore, direct IL-22 stimulation more strongly induces the expression of ELR^+ chemokines, particularly *CXCL5,* in *KRAS* mutant cells and primary organoids. It remains to be determined however, whether induction of these chemokines is IL-22-dependent in *KRAS* mutant cells in a more complex cytokine milieu.

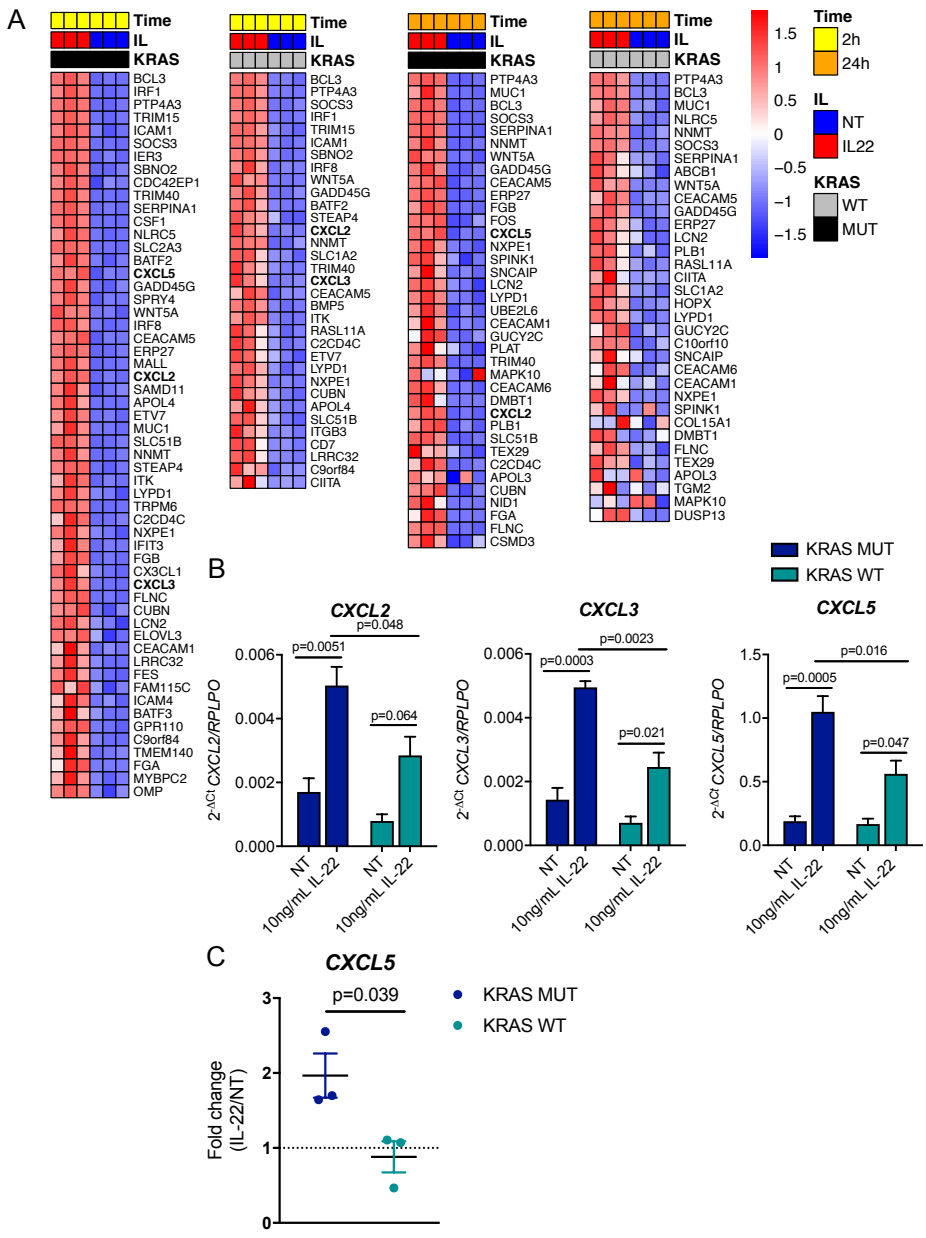


Figure 5.3 ELR$^+$ CXC chemokines are induced in *KRAS* mutant cells after 2h and 24h IL-22 stimulation.

(A) Differential expression analysis comparing IL-22 stimulated to untreated (NT) cells for both DLD-1 *KRAS* MUT and WT cells after 2h and 24h stimulation. Differential expression analysis was performed using the generalised linear model of the edgeR R package. Heatmaps represent the top differentially expressed genes (log2FC > 2, FDR < 1x10^{-5}) for each cell line at each time point. Colours are based on row normalised log2(RPKM+1) expression values for the 3 experimental replicates for each condition.

(B) qPCR confirmation of chemokine induction (*CXCL2, CXL3, CXCL5*) in DLD-1 *KRAS* MUT and WT cells after 24h 10ng/mL IL-22 stimulation. Data are means ± SEM (n=3 independent experiments). Statistical significance was determined using two-way ANOVA with Tukey's post-test for multiple comparisons. P<0.05 is considered significant.

(C) qPCR analysis of *CXCL5* expression in *KRAS* MUT and WT organoids (N=6) stimulated with 1ng/mL IL-22 for 24h. Each data point represents the average of technical duplicates normalised to the mean of the no treatment condition for each independent patient. Statistical significance was determined using an unpaired T-test comparing *KRAS* MUT to WT organoids. P<0.05 is considered significant.

5.2.3 IL-17A expression is elevated in CD4$^+$ T cells from tumour compared to matched normal adjacent tissue

Chemokines that signal through CXCR2 (*CXCL1, 2, 3, 5*) are known to be highly induced by TNFα and IL-17A (Liu *et al.*, 2011). Therefore, we sought to determine whether induction of these chemokines in *KRAS* mutant CRC cells is IL-22-dependent in a complex immune milieu containing high concentrations of the cytokines TNFα, IL-17A, and IFNγ. Supernatants were generated from CD4$^+$ T cells polyclonally expanded from tumours and matched normal adjacent tissue. These supernatants were used to stimulate DLD-1 isogenic cells and organoids in the presence or absence of blocking antibodies against cytokines of interest. Briefly, tumour biopsies and pieces of matched normal adjacent mucosa were digested in collagenase. Lamina propria leukocytes were isolated and cultured with anti-CD3/anti-CD28 coated beads and IL-2 for 11-20 days to promote T cell expansion (Figure 5.4 A). Non-T cells died out over the course of this culture period. A small fraction of the expanded T cells were re-stimulated with PMA/ionomycin and phenotypically assessed by flow cytometry (Figure 5.4 B, C). CD4$^+$ T cells were subsequently isolated by MACs separation from the remaining expanded T cells. The CD4$^+$ T cells were plated at a density of 1 million cells/mL and re-stimulated for 24 hours with PMA/ionomycin to generate T cell supernatants. These supernatants were then used to stimulate the DLD-1 isogenic cells and organoids (Figure 5.4 A).

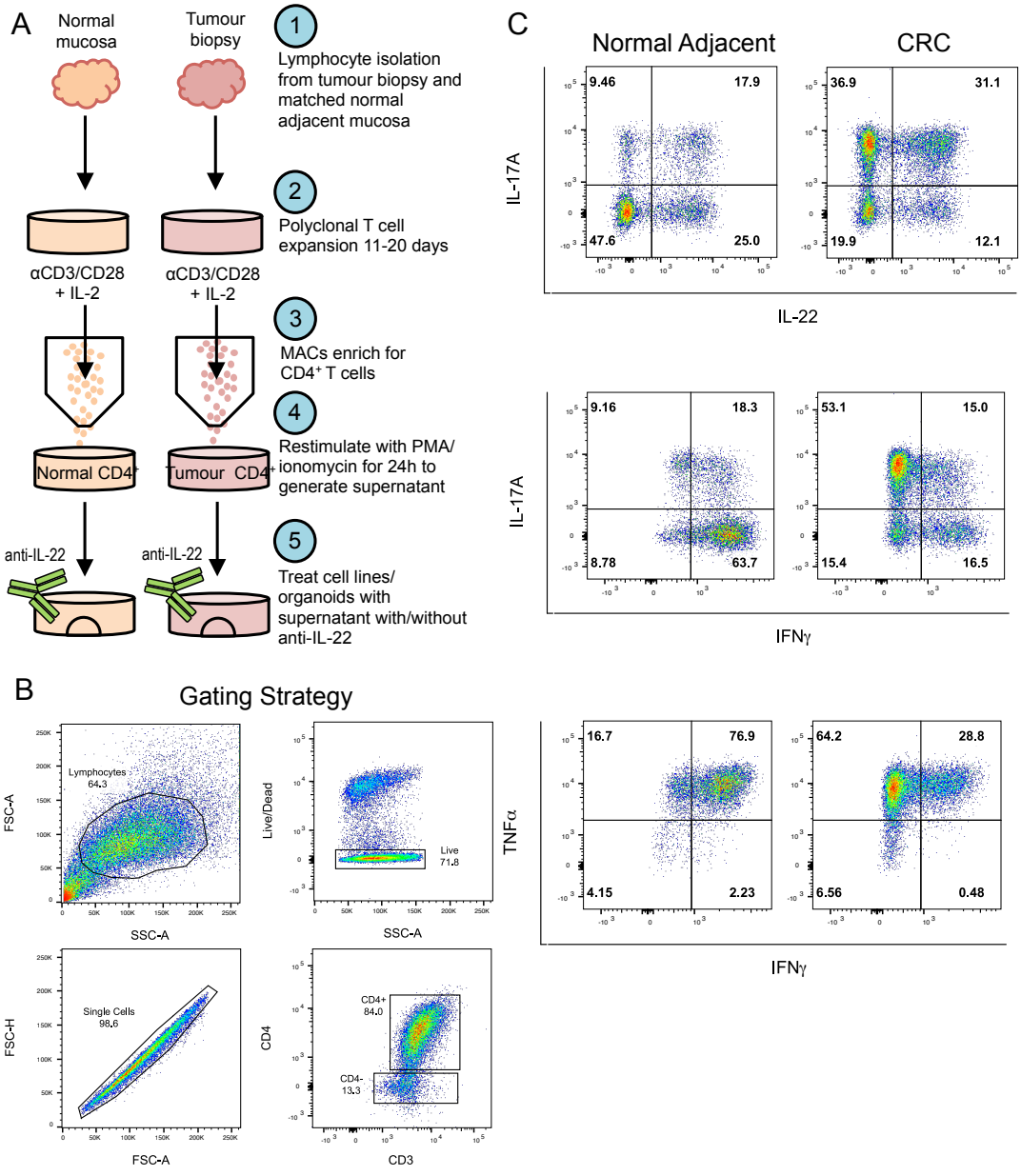


Figure 5.4 Polyclonal expansion of tumour infiltrating and matched normal adjacent leukocytes to generate supernatants for cell line and organoid stimulation.

(A) Workflow for the generation of CD4$^+$ T cell supernatants using biopsies from primary human CRC tumours and matched normal adjacent mucosa. Isolated leukocytes were polyclonally expanded for 11-20 days. MACS enrichment was performed to isolate the CD4$^+$ cells. Cells were re-stimulated with PMA/ionomycin for 24h to generate supernatants for use in CRC cell line and organoid stimulation experiments.

(B) Flow cytometric gating strategy used for cytokine profiling of polyclonally-expanded tumour infiltrating leukocytes (TIL) and matched normal adjacent leukocytes following 3h PMA/ionomycin re-stimulation.

(C) Cytokine expression in live, single, CD4$^+$ TIL and matched normal adjacent leukocytes from one representative patient. Expression of IL-22, IL-17A, IFNγ, and TNFα is displayed.

Though immunophenotyping of tumour and matched normal leukocytes from primary human tumours was not the primary focus of this study, some striking differences were notable despite the relatively small number of patients assessed (N=6). Following 3 hours of re-stimulation with PMA/ionomycin, the percentage of IFNγ$^+$ cells was markedly lower in tumour infiltrating compared to matched normal adjacent CD4$^+$ T cells (Figure 5.5 A). By contrast, IL-17A$^+$ cells were more frequent among T cells expanded from tumours compared to matched normal tissue (Figure 5.5 A). Similarly, IL-17F expressing CD4$^+$ cells were more abundant among tumour CD4$^+$ T cells, yet they represented a small percentage of the total CD4$^+$ cells (Figure 5.5 A). TNFα$^+$ cells were very abundant in both tumour and normal adjacent-derived CD4$^+$ cells. Interestingly, the percentage of CD4$^+$ cells expressing IL-22 was no different between tumour and normal adjacent-derived cells (Figure 5.5 A). However, in 4 of the 6 patients assessed, the percentage of IL-22$^+$IL-17A$^+$ cells was elevated in tumour compared to matched normal CD4$^+$ T cells (Figure 5.5 B). Most strikingly, IFNγ$^-$IL-17A$^+$ CD4$^+$ T cells from tumours were significantly elevated relative to normal tissue, while the percentage of IFNγ$^+$IL-17A$^+$ CD4$^+$ cells was unchanged (Figure 5.5 B). To confirm whether these observations of cytokine production at the protein level were reflected at the mRNA level, qPCR analysis was performed on unstimulated CD4$^+$ cells. Indeed, *IL17A* and *IL17F* expression was significantly higher in CD4$^+$ cells expanded from tumour compared to matched normal adjacent tissue. Expression of *IL26*, an IL-10 cytokine superfamily member that is often co-expressed with IL-22 and is produced predominately by Th17 cells (Rutz, Wang and Ouyang, 2014), was similarly elevated in CD4$^+$ TIL (Figure 5.5 C). However, expression of *IL22* itself was highly variable, with certain patients displaying dramatically elevated amounts of *IL22* in CD4$^+$ TIL and others showing no difference between CD4$^+$ TIL and matched

normal expanded $CD4^+$ cells (Figure 5.5 C). Several key proinflammatory mediators, *IFNG, IL11, TNF, IL6*, were unchanged or, in the case of *IL6*, significantly lower in $CD4^+$ TIL compared to matched normal $CD4^+$ cells (Figure 5.5 C). In line with the strong IL-17 dominated phenotype, transcription factor analysis revealed elevated expression of the master transcriptional regulator of the Th17 lineage, *RORC* (encoding RORγt), and diminished expression of *TBX21* (encoding T-bet), which controls Th1 cell differentiation (Figure 5.5 D).

Thus these preliminary data demonstrate a pattern of elevated Th17-related cytokine expression and diminished IFNγ expression in $CD4^+$ T cells expanded from tumours compared to matched normal adjacent leukocytes. Additional patients are required to confirm these results.

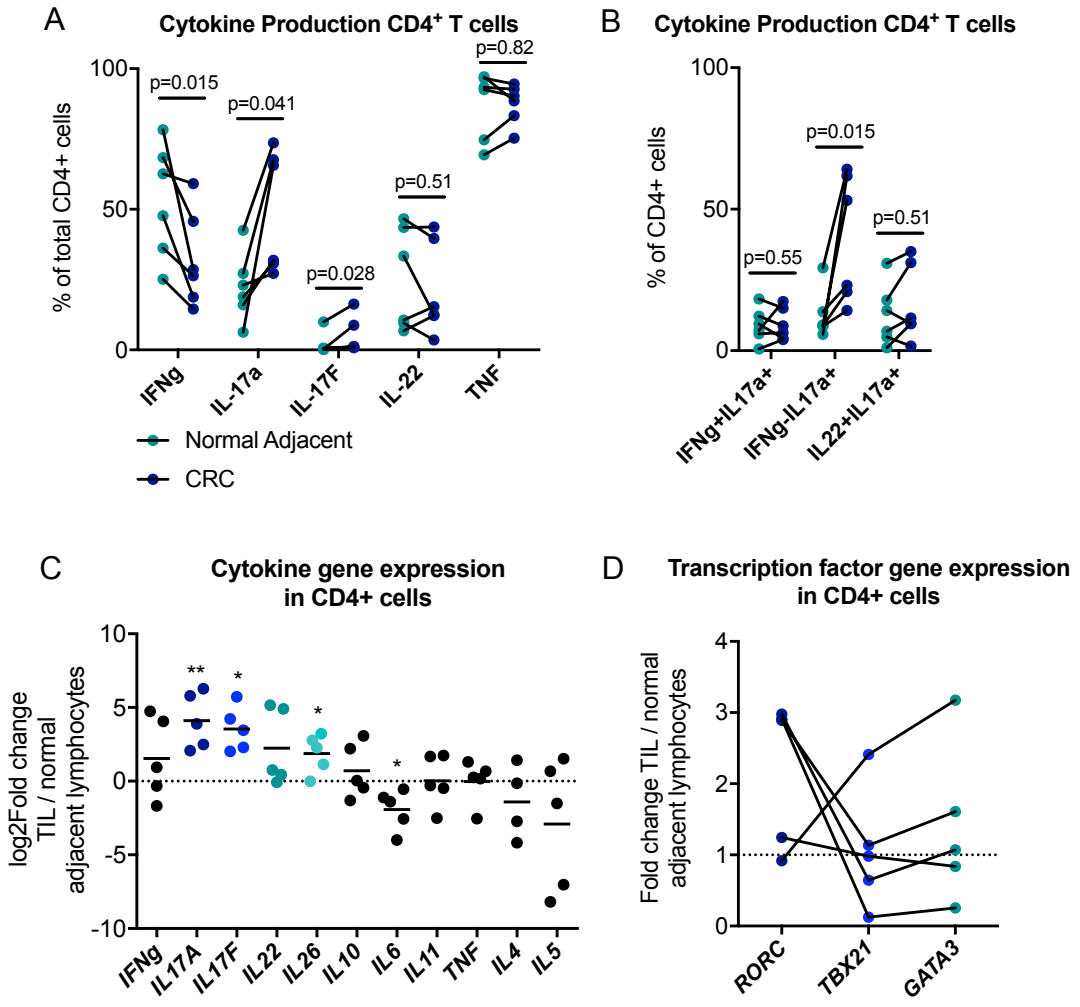


Figure 5.5 Expression of IL-17A is elevated in CD4$^+$ T cells expanded from tumour infiltrating leukocytes (TIL) compared to matched normal adjacent tissue leukocytes.

(A) (B) Percentage of total CD4$^+$ T cells expressing each of the indicated cytokines or combinations of cytokines following 3h PMA/ionomycin re-stimulation after 11-20 days of polyclonal expansion from CRC biopsies and matched normal adjacent mucosa. Dots adjoined by lines indicate matched normal adjacent and TIL expanded from a single patient (N=6 patients). Statistical significance was determined using ratio paired T-tests comparing cytokine expression in normal adjacent to matched TIL. P<0.05 is considered significant.

(C) qPCR analysis of cytokine gene expression in unstimulated CD4$^+$ T cells polyclonally expanded from normal adjacent mucosa and TIL. Each data point represents the log2 fold change in expression of a given cytokine gene comparing CD4$^+$ TIL to matched normal adjacent leukocytes for one patient (N=5 patients). Statistical significance was determined using one-sample T-tests to compare the fold change of cytokine gene expression to the reference value 0 (no difference between TIL and normal adjacent leukocytes). *p<0.05, **p<0.01.

(D) qPCR analysis of expression of key T-cell transcription factors *RORC* (RORγt), *TBX21* (T-bet), *GATA3* (Gata3) in matched normal leukocytes and TIL as described in (C). Each data point represents the log2 fold change in expression of a given transcription factor gene comparing TIL to matched normal adjacent leukocytes for one patient (N=5 patient). Connecting lines indicate expression of each transcription factor in the same patient.

5.2.4 ELR$^+$ CXC chemokines are induced in *KRAS* mutant cells and organoids by supernatant from tumour-infiltrating CD4$^+$ T cells in an IL-22-dependent manner

To begin to understand the role that IL-22 plays in the context of a complex cytokine environment, DLD-1 isogenic cells were stimulated with conditioned supernatant derived from expanded tumour-infiltrating CD4$^+$ T cells (Figure 5.4 C). Since numerous reports have pointed toward synergisms between STAT3 and NF-κB in CRC (Grivennikov and Karin, 2011; De Simone *et al.*, 2015), we explored the consequences of IL-22 blockade alone or in combination with TNFα and/or IFNγ blockade in DLD-1 cells stimulated for 24 hours with TIL supernatant. Specifically, expression of the key IL-22 target genes *SOCS3, S100A9, MMP1, CXCL1, MUC1* and the IL-22 receptor components (*IL22RA1, IL10RB*) were analysed. We were particularly interested in identifying genes for which the response to TIL supernatant stimulation was divergent between *KRAS* mutant and wild type isogenic cells. Most strikingly, TIL supernatant stimulation induced *CXCL1* in *KRAS* mutant but not wild type DLD-1 cells and this induction was partially IL-22-dependent (Figure 5.6 A, B). We next determined whether expression of other CXC chemokines which signal through CXCR2 was also enhanced in *KRAS* mutant versus wild type cells in an IL-22-dependent manner. Expression of *CXCL2, CXCL3,* and *CXCL5* was analysed, as RNA-sequencing analysis pointed towards their enhanced expression in *KRAS* mutant cells following direct IL-22 stimulation. Similar to *CXCL1,* the induction of *CXCL2, 3, 5* upon stimulation with TIL supernatant was greater in *KRAS* mutant versus wild type cells (Figure 5.6 B, C, D, E). However, only *CXCL1* and *CXCL5* induction was dependent on IL-22 (Figure 5.6 B, E).

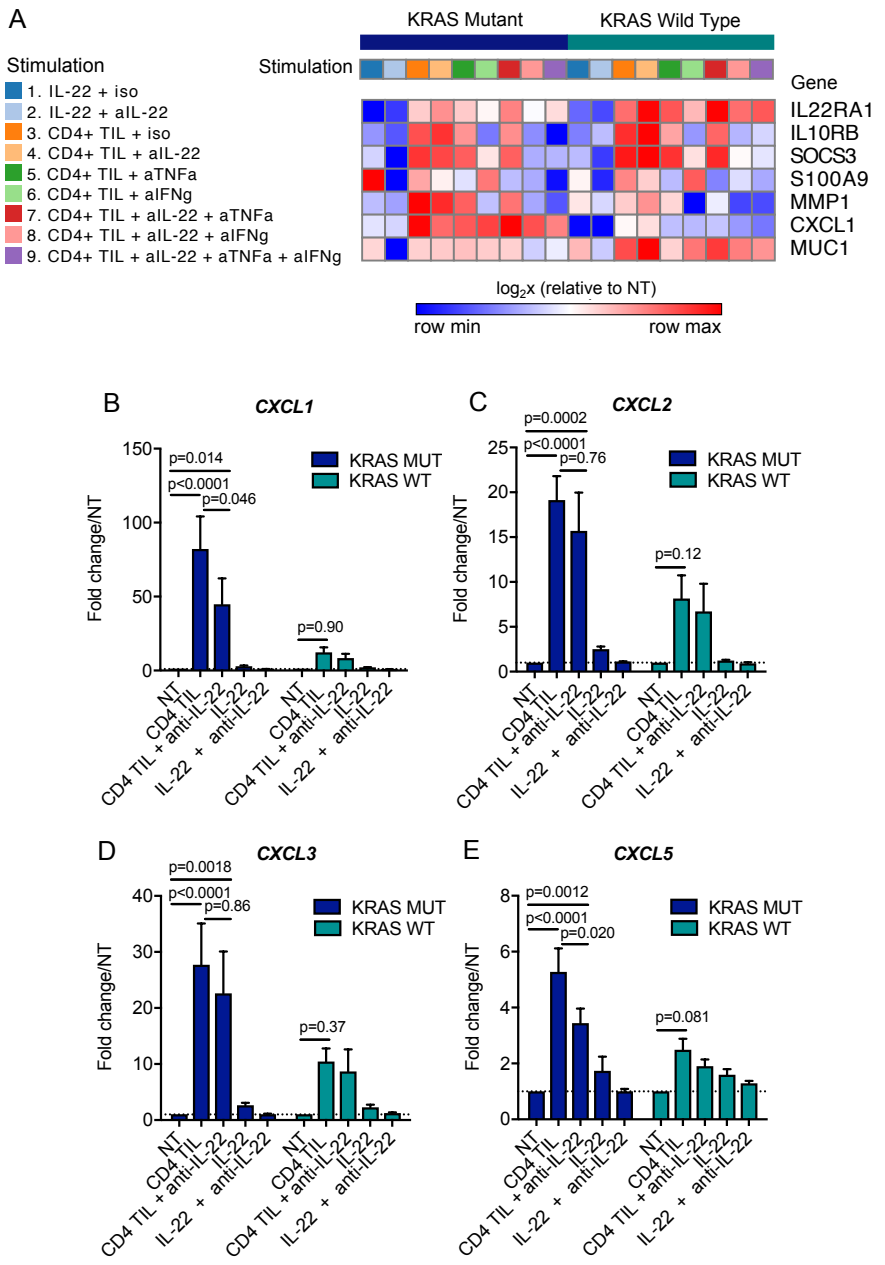


Figure 5.6 *CXCL1* and *CXCL5* are significantly induced by TIL supernatant in DLD-1 *KRAS* mutant isogenic cells in an IL-22-dependent manner.

DLD-1 *KRAS* MUT and WT cells were treated with supernatant generated from $CD4^+$ tumour infiltrating leukocytes (TIL) expanded from one candidate CRC patient (T cell cytokine expression profiles for this patient in **Figure 5.4 C**). Supernatants were used at 1:100 and cells were stimulated for 24 hours in the presence or absence of IL-22, TNFα, and/or IFNγ blocking antibodies.

(A) qPCR was performed to assess the expression of *IL22RA1, IL10RB,* and a panel of known IL-22 target genes (*SOCS3, S100A9, MMP1, CXCL1, MUC1*) following TIL supernatant stimulation. Heat map displays log_2 expression of each gene relative to the no treatment (vehicle control) condition for n=3 independent experiments.

(B) *CXCL1* (C) *CXCL2* (D) *CXCL3* (E) *CXLC5* expression assessed by qPCR. Data represent means ± SEM (n=4 independent experiments), of the fold change for each stimulation relative to the no treatment (vehicle control) condition. Statistical significance was assessed by one-way ANOVA with Tukey's post-test for multiple comparisons within each genotype. P<0.05 is considered significant.

Interestingly, ELR$^+$ chemokine expression, highlighted here using *CXCL1* as an example, was not as significantly induced by supernatant generated from matched normal CD4$^+$ T cells (Figure 5.7 A). Moreover, *CXCL1* induction by matched normal CD4$^+$ T cell supernatant was not IL-22-dependent (Figure 5.7 A). This could be a consequence of the lower proportion of IL-17A$^+$IL-22$^+$ CD4$^+$ T cells in the matched normal compared to tumour-derived supernatant (17.9% normal, 31.1% tumour) (Figure 5.5 C).

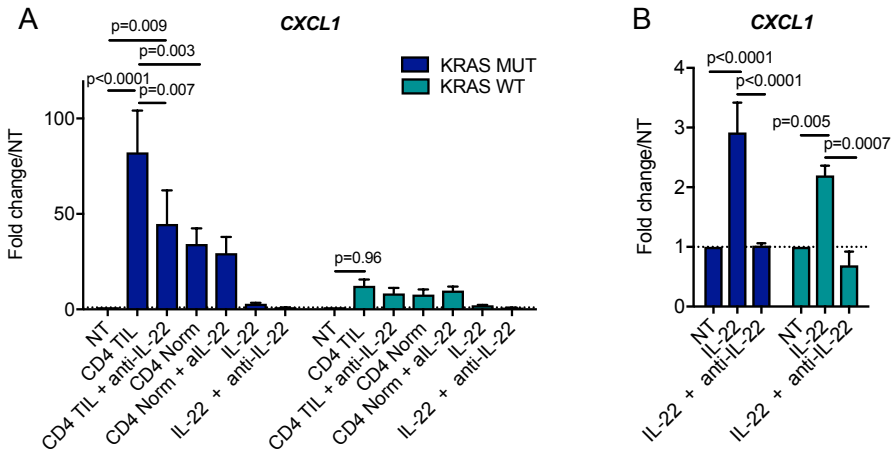


Figure 5.7 *CXCL1* is more significantly induced by supernatant generated from tumour infiltrating, compared to matched normal CD4$^+$ T cells.

DLD-1 *KRAS* MUT and WT cells were treated with supernatant generated from CD4$^+$ tumour infiltrating (TIL) and matched normal adjacent mucosal leukocytes expanded from one candidate CRC patient (T cell cytokine expression profiles for this patient in **Figure 5.4 C**). Supernatants were used at 1:100 and cells were stimulated for 24 hours in the presence or absence of IL-22 blocking antibodies.

(A) qPCR was performed to assess *CXCL1* expression following TIL and matched normal leukocyte supernatant stimulation in the presence or absence of IL-22 blockade. Data represent means ± SEM (n=4 independent experiments), of the fold change for each stimulation relative to the no treatment (vehicle control) condition. Statistical significance was assessed by one-way ANOVA with Tukey's post-test for multiple comparisons within each genotype. P<0.05 is considered significant.

(B) Expanded Y-axis displaying data from the control IL-22 stimulation and IL-22 + anti-IL-22 conditions from (A) to demonstrate efficacy of the anti-IL-22 blocking antibody.

To determine whether the observed IL-22-dependent *CXCL1* and *CXCL5* induction in *KRAS* mutant cells applied beyond the DLD-1 isogenic cells, primary CRC organoids were stimulated with TIL supernatant in the presence or absence of IL-22 blockade. Three *KRAS* G12D/G13D mutant and three *KRAS* wild type organoid lines derived from independent patients were utilised. Overall, *IL22RA1* expression did not differ between the *KRAS* mutant and wild type organoids, though there was variability between individual lines (Figure 5.8 A). Efficacy of IL-22 blockade in the organoid culture system was confirmed by observing abrogation of *SOCS3* expression following direct IL-22 stimulation in both *KRAS* mutant and wild type organoids (Figure 5.8 B). Following TIL supernatant stimulation, *CXCL1, CXCL2,* and *CXCL5* were significantly induced in *KRAS* mutant organoids (Figure 5.8 C, D, F). However, when combined with IL-22 blockade, TIL supernatant did not significantly augment expression of these chemokines (Figure 5.8 C, D, F). Though *CXCL1, CXCL2, CXCL3,* and *CXCL5* expression was elevated in *KRAS* wild type organoids following TIL supernatant stimulation, IL-22 blockade had no impact on the expression of each chemokine and in fact if anything, chemokine expression was elevated upon IL-22 blockade (Figure 5.8 C, D, E, F). Thus, in line with observations made in the DLD-1 isogenic pair, in the context of a complex cytokine milieu, expression of ELR^+ CXC chemokines that signal through CXCR2 is elevated in *KRAS* mutant organoids and there is a trend toward attenuation of *CXCL1, CXCL2,* and *CXCL5* expression with IL-22 blockade. Increased sample sizes of each molecular subtype are required to confirm these observations.

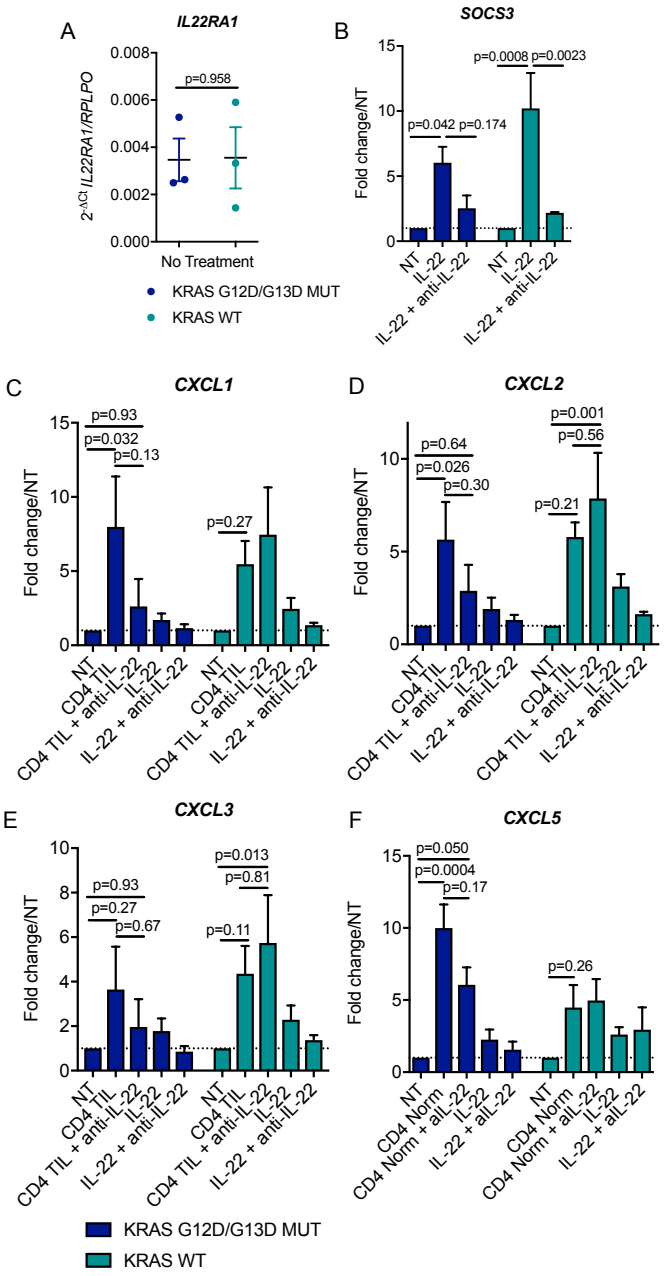


Figure 5.8 *CXCL1*, *CXCL2,* and *CXCL5* are induced in a partially IL-22-dependent manner in *KRAS* mutant but not wild type organoids treated with TIL supernatant.

KRAS G12D/G13D MUT and WT organoids were treated with supernatant generated from $CD4^+$ tumour infiltrating (TIL) leukocytes expanded from one candidate CRC patient (T cell cytokine expression profiles for this patient in **Figure 5.4 C**). Supernatants were used at 1:100 and cells were stimulated for 24 hours in the presence or absence of IL-22 blocking antibodies.

(A) Baseline *IL22RA1* expression in the *KRAS* MUT and WT organoids used in this experiment. Statistical significance was assessed using an unpaired T-test. $P<0.05$ is considered significant.

(B) *SOCS3* induction following control IL-22 stimulation and IL-22 blockade.

(C) *CXCL1* (D) *CXCL2* (E) *CXCL3* (F) *CXCL5* assessed by qPCR.

Data represent means ± SEM (n=3 organoid lines per genotype), of the fold change for each stimulation relative to the no treatment (vehicle control) condition. Statistical significance was assessed by one-way ANOVA with Tukey's post-test for multiple comparisons within each genotype. $P<0.05$ is considered significant.

5.2.5 *CD274* (PD-L1) is induced by IL-22 and not IL-6, specifically in *KRAS* mutant cells and organoids

The IL-22-*KRAS*-specific induction of ELR$^+$ CXC chemokines presents a potential cell extrinsic modality by which IL-22 signalling into a *KRAS* mutant cell may perpetuate tumour-promoting inflammation to promote malignancy. The initial identification of this chemokine signature came from basic analysis of the top differentially expressed genes upon IL-22 stimulation in *KRAS* mutant and wild type DLD-1 isogenic cells (Figure 5.3 A). However, since our analysis in tumour transcriptomic datasets from patient cohorts and clinical trials did not reveal a specific interaction between the IL-6 pathway and mutant *KRAS*, we were interested in identifying genes uniquely regulated by IL-22 and not IL-6, another STAT3 activator, in *KRAS* mutant cells. Thus differential expression analysis to test for genes specifically induced by IL-22 and not IL-6, in *KRAS* mutant but not wild type cells was performed (see Chapter 2.5.3.1 for methodology).

Among the top 15 differentially expressed genes following 2 hours of IL-22 stimulation, we identified *CD274*, which encodes programmed death-ligand 1 (PD-L1), to be uniquely induced by IL-22 and not IL-6 in *KRAS* mutant but not wild type cells (Figure 5.9 A). By conducting an IL-22 stimulation time course and measuring *CD274* induction by qPCR, we found that relative to *KRAS* wild type cells, *KRAS* mutant DLD-1 cells expressed high levels of *CD274* with peak expression at 2 hours, a trough at 8 hours, and a second peak of expression after 24 hours (Figure 5.9 B). Next, using a panel of *KRAS* G12D/G13D (N=3) and *KRAS* wild type (N=3) organoids, we similarly observed *CD274* induction in *KRAS* mutant but not wild type organoids following 24 hours of 1ng/mL IL-22 stimulation (Figure 5.9 D).

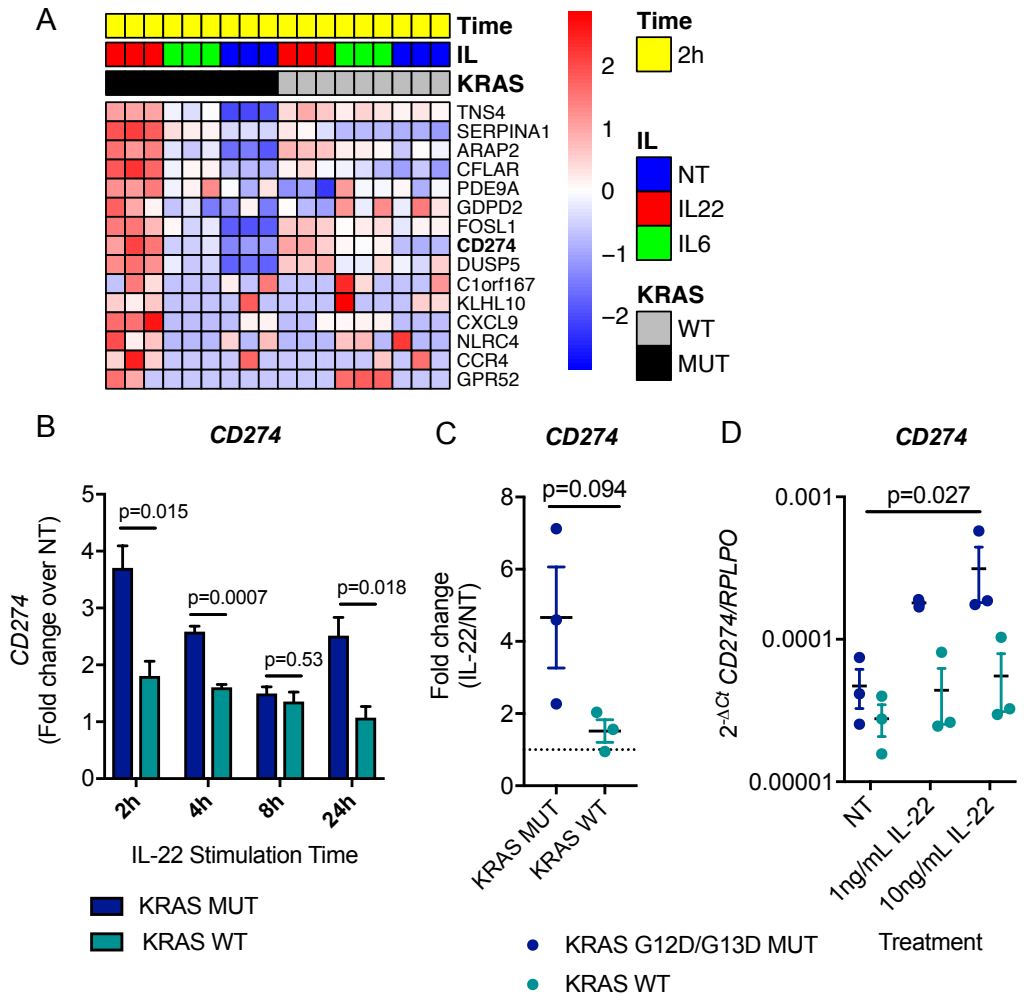


Figure 5.9 *CD274* (PD-L1) is induced by IL-22 and not IL-6, specifically in *KRAS* mutant cells and primary organoids.

(A) Differential expression interaction analysis was performed on RNA-sequencing data to assess genes induced by IL-22, and not IL-6, in specifically in *KRAS* MUT and not WT cells for 2h treated samples. Heatmap represents the top 15 differentially expressed genes (ordered by increasing FDR) for each cell line at each time point. Colours are based on row normalised log2(RPKM+1) expression values for each of the 3 experimental replicates for each condition.

(B) Confirmation of *CD274* induction upon 10ng/mL IL-22 stimulation in DLD-1 *KRAS* MUT and WT isogenic cells over a time course of 2-24h. Data are means ± SEM (n=3 independent experiments) of the fold change in *CD274* expression with IL-22 stimulation over NT (no treatment). Statistical significance was determined using unpaired T-tests comparing the *KRAS* MUT and WT *CD274* induction at each timepoint. P<0.05 is considered significant.

(C) Fold induction of *CD274* in *KRAS* G12D/G13D MUT and WT organoids stimulated for 24h with 1ng/mL IL-22. Each data point represents an organoid derived from an independent patient (n=3 orgaonids per genotype). Statistical significance was assessed using unpaired T-tests comparing the *KRAS* MUT and WT *CD274* induction. P<0.05 is considered significant.

(D) Expression of *CD274* relative to the endogenous control (*RPLPO*) following 24h stimulation with 1ng/mL or 10ng/mL IL-22. Each data point represents an organoid derived from an independent patient (n=3 orgaonids per genotype). Statistical significance was assessed using a two-way ANOVA with Dunnett's post-test for multiple comparisons. P<0.05 is considered significant.

5.2.6 The Myc pathway is uniquely induced by IL-22 and not IL-6 in *KRAS* mutant cells based on RNA-sequencing analysis

Next, we performed pathway analysis for a more comprehensive picture of core cellular pathways that are modulated uniquely by IL-22 in *KRAS* mutant cells. Single sample gene set enrichment analysis (ssGSEA) was performed on each sample in the RNA-sequencing dataset. The resultant enrichment score was used to perform differential analyses for the comparisons of interest. The Hallmark Collection pathways from the Molecular Signature Database (MSigDB, http://software.broadinstitute.org/gsea/msigdb), which are the most robustly annotated, were used for this analysis. Basic analysis of pathways upregulated with IL-22 stimulation in *KRAS* mutant and wild type cells revealed some similarities. For example, the "IL-6_JAK_STAT3" signalling and "Interferon_gamma_reponse" pathways were induced by IL-22 in *KRAS* mutant and wild type isogenic cells after 2 and 24 hours stimulation (Appendix 3, Figure 3.2). To focus on specific pathways regulated by IL-22 and not IL-6 in *KRAS* mutant and not wild type cells, differential analysis of ssGSEA enrichment scores was performed according to the following comparison:

[(*KRAS* MUT IL-22 – *KRAS* MUT NT) – (*KRAS* MUT IL-6 – *KRAS* MUT IL-6)] -

[(*KRAS* WT IL-22 – *KRAS* WT NT) – (*KRAS* WT IL-6 – *KRAS* WT IL-6)]

Following this stringent analysis, only the Myc pathway ("MYC_TARGETS_V2") was uniquely induced by IL-22 and not IL-6 in *KRAS* mutant but not wild type cells following 24-hour stimulation (Figure 5.10 A). *MYC*, which encodes c-Myc, is one of the earliest described proto-oncogenes and was first discovered over 35 years ago based on its homology to the avian retroviral oncogene *v-Myc* (Vennstrom *et al.*, 1982) in Burkitt lymphoma (Dalla-Favera *et al.*, 1982). The c-Myc protein is a basic helix-loop-helix, leucine zipper (bHLH-LZ) transcription factor and master regulator

of the transcription of genes involved in cellular growth, proliferation, metabolism, and numerous biosynthetic processes (Kress, Sabò and Amati, 2015). Assessment of the expression of all genes in the annotated "MYC_TARGETS_V2" pathway revealed that *MYC* itself is highly induced by IL-22 in *KRAS* mutant cells after 2 hours, along with the rate limiting glycolytic enzyme, hexokinase 2 (*HK2*) (Figure 5.10 B). Then, after 24 hour IL-22 stimulation, Myc target genes were potently upregulated in *KRAS* mutant but not wild type isogenic cells (Figure 5.10 B). This temporal *MYC* induction was confirmed by independent qPCR analysis of *MYC* in the DLD-1 isogenic cells following 2, 4, 8, and 24-hour IL-22 stimulation. Indeed, *MYC* transcriptional induction was significantly higher in *KRAS* mutant versus wild type cells after 2 and 4 hours IL-22 stimulation, but no difference was observed at later time points (8 and 24 hours) (Figure 5.10 C). Furthermore, induction of a selection of the Myc target genes contained in the "MYC_TARGETS_V2" signature (*HSPD1, GNL3, DCTPP1*) were confirmed by independent qPCR analysis to be significantly elevated in *KRAS* mutant versus wild type DLD-1 cells (Figure 5.10 D). In fact, no IL-22-dependent induction of *HSPD1, GNL3,* or *DCTPP1* was observed after 24-hour IL-22 stimulation in the *KRAS* wild type cells (Figure 5.10 D).

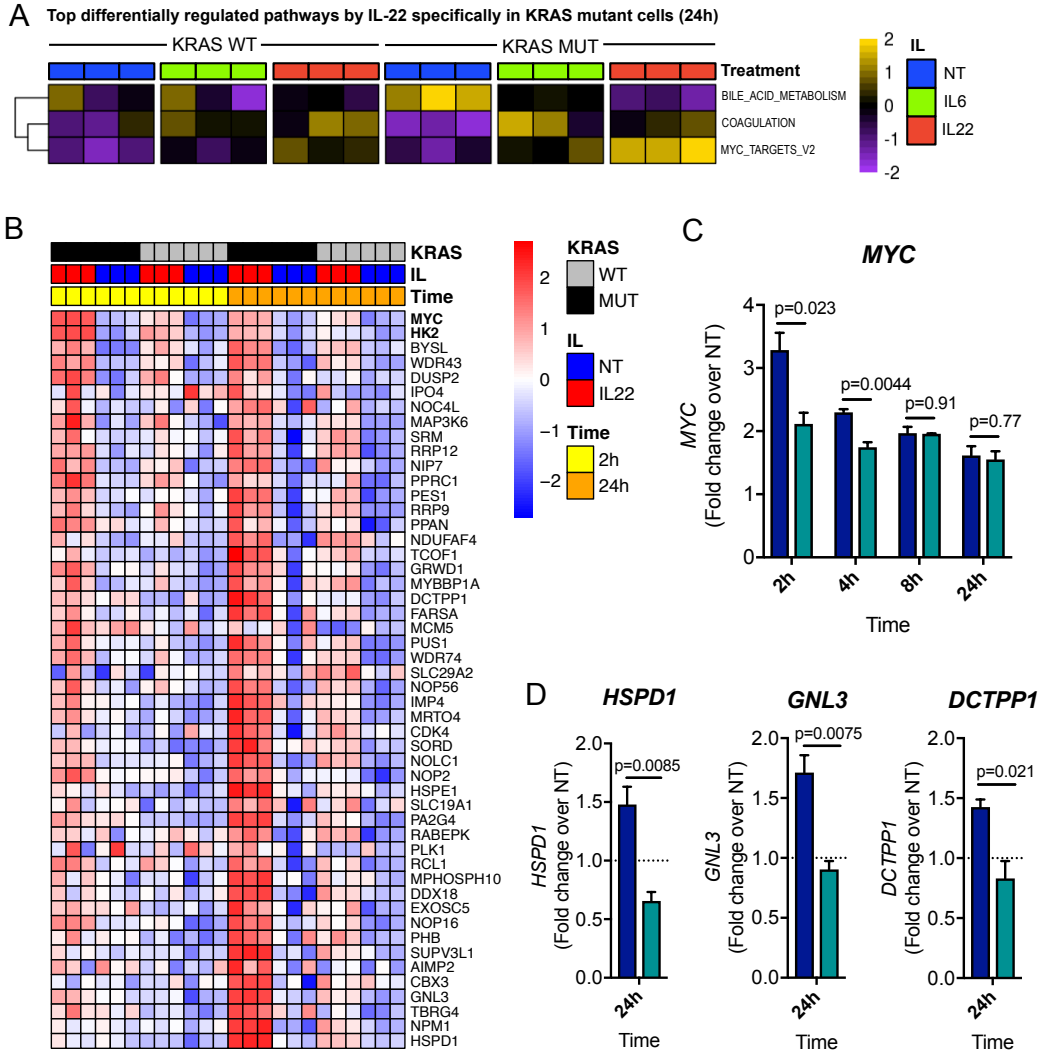


Figure 5.10 The Myc pathway is uniquely induced by IL-22 and not IL-6 in *KRAS* mutant but not wild type isogenic DLD-1 cells.

(A) Identification of pathways that are specifically induced by IL-22 and not IL-6 in *KRAS* MUT but not WT cells using an interaction analysis of single sample GSEA analysis (ssGSEA) scores computed for the DLD-1 isogenic cells stimulated with IL-22 or IL-6 for 24h. Heatmap is based on ssGSEA scores for each sample and displays the only significantly differentially regulated pathways for the described interaction analysis (p adjusted p<0.01). This analysis was performed by D. Barras.

(B) Heatmap based on row normalised log2(RPKM+1) values for genes in "MYC_TARGETS_V2" MSigDB Hallmark signature in DLD-1 isogenic cells stimulated with IL-22 for 2h or 24h.

(C) Confirmation of *MYC* induction following 10ng/mL IL-22 stimulation in DLD-1 *KRAS* MUT and WT isogenic cells over a time course of 2-24h. Data are means ± SEM (n=3 independent experiments) of the fold change in *MYC* expression with IL-22 stimulation over NT (no treatment). Statistical significance was determined using unpaired T-tests comparing the *KRAS* MUT and WT *MYC* induction at each timepoint. P<0.05 is considered significant.

(D) Confirmation of Myc target gene induction (*HSPD1, GNL3, DCTPP1*) after 24h 10ng/mL IL-22 stimulation in DLD-1 *KRAS* MUT and WT isogenic cells. Data are means ± SEM (n=3 independent experiments) of the fold change in Myc target gene expression with IL-22 stimulation over NT (no treatment). Statistical significance was

determined using unpaired T-tests comparing the *KRAS* MUT and WT gene induction at each timepoint. $P<0.05$ is considered significant.

In some cancers, the oncogenic activity of Myc is a direct consequence of gene amplification or translocation, which results in its overexpression (Beroukhim *et al.*, 2010). However, Myc overexpression is a hallmark of many human cancers since the pathways that regulate *MYC* transcription and c-Myc protein stability/activity are often mutated or de-regulated in cancer (Dang, 2012). For example, the Ras/Raf/ERK pathway has been shown to prolong the half-life of c-Myc protein by enhancing phosphorylation at an activating serine 62 residue and reducing phosphorylation at a threonine 58 residue that targets c-Myc for rapid proteasomal degradation (Sears, 2000). Given that we have observed enhanced IL-22-dependent *MYC* transcription in *KRAS* mutant cells and that the Ras/Raf/ERK pathway is known to stabilise active c-Myc protein, we hypothesised that c-Myc protein expression would be elevated in *KRAS* mutant versus wild type cells upon IL-22 stimulation. *KRAS* mutant and wild type isogenic cells were stimulated for 15 minutes to 24 hours with 10ng/mL IL-22 and total c-Myc protein was assayed in whole cell lysates by Western blot analysis. c-Myc protein was dramatically induced in *KRAS* mutant cells, reaching a maximum at 8 and 24 hours (Figure 5.11 A). Using fluorescently conjugated secondary antibodies and LI-COR-based detection, quantification of c-Myc protein revealed that c-Myc expression was elevated at baseline in *KRAS* mutant versus wild type cells and was significantly induced in *KRAS* mutant but not wild type cells upon IL-22 stimulation (Figure 5.11 B). The amount of c-Myc protein that had accumulated following 24 hours of IL-22 stimulation was nearly 3 times higher in *KRAS* mutant versus wild type cells (Figure 5.11 B). Using an antibody that specifically recognises the phosphorylated S62 residue (and may not recognise doubly S62 and T58 phosphorylated c-Myc), preliminary experiments revealed enhanced c-Myc S62

phosphorylation after 24 hour IL-22 stimulation in *KRAS* mutant versus wild type isogenic cells (Figure 5.11 C). Given our experimental approach, we cannot however determine whether given the same amount of c-Myc substrate, phosphorylation at S62 is enhanced in *KRAS* mutant versus wild type cells. The enhanced c-Myc S62 observed is likely is a consequence of elevated total c-Myc protein in *KRAS* mutant versus wild type cells following IL-22 stimulation. Previous reports have suggested that AKT-mediated phosphorylation of GSK-3β on its S9 residue prevents GSK-3β-mediated phosphorylation of c-Myc on the inactivating T58 residue (Sears, 2000). Since we have previously observed elevated pAKT (S473) following IL-22 stimulation in *KRAS* mutant versus wild type DLD-1 cells (Chapter 4, Figure 4.6 D), we hypothesised that T58 c-Myc phosphorylation may be reduced following IL-22 stimulation. Using a polyclonal antibody that specifically recognises the T58 residue on c-Myc, we performed western blot analysis to assess its expression following 24-hour IL-22 stimulation. Due to the presence of multiple bands with the antibody used, we could not definitively determine the impact of IL-22 on c-Myc T58 phosphorylation (Figure 5.11 D). Phosphorylation at this T58 inactivating residue requires further investigation with a monoclonal antibody.

In summary total c-Myc protein accumulates in *KRAS* mutant cells over 24 hours specifically in *KRAS* mutant and not wild type cells and preliminary observations have revealed enhanced phosphorylation at the activating S62 residue after 24 hour IL-22 stimulation in *KRAS* mutant cells.

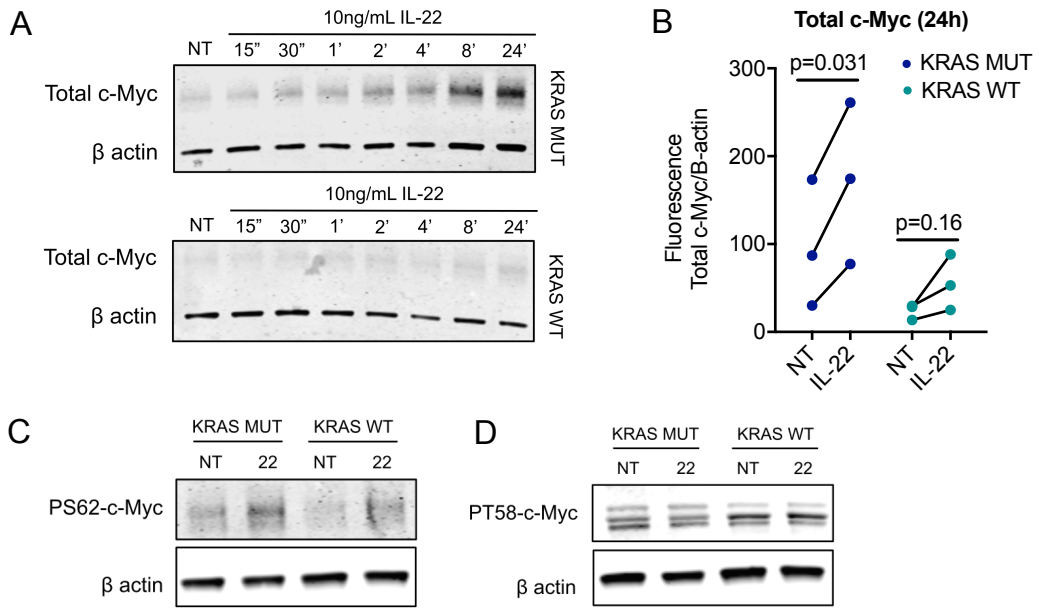


Figure 5.11 c-Myc protein is significantly induced in *KRAS* mutant cells after 24h IL-22 stimulation.

DLD-1 *KRAS* MUT and WT isogenic cells were stimulated with 10ng/mL IL-22 for 15 minutes (15") to 24 hours (24'). Total protein was extracted and assessed by Western blot.

(A) Representative western blot for total c-Myc in *KRAS* MUT and WT DLD-1 isogenic cells.

(B) Quantification of c-Myc protein relative to β-actin using LI-COR fluorescence detection of fluorophore-conjugated secondary antibodies. Data represent mean ± SEM for n=3 independent experiments after 24h IL-22 stimulation. Statistical significance was assessed using paired T-tests comparing IL-22 stimulation to NT (no treatment) for each cell line in each independent experiment. $P<0.05$ is considered significant.

(C) Representative western blot for PS62-c-Myc in *KRAS* MUT and WT DLD-1 isogenic cells (n=1 experiment representative of 2).

(D) Representative western blot for PT58-c-Myc in *KRAS* MUT and WT DLD-1 isogenic cells (n=1 experiment representative of 3).

To determine whether this IL-22-*KRAS* specific *MYC* induction was generalisable beyond the DLD-1 isogenic pair, we assessed *MYC* expression following 24-hour 1ng/mL IL-22 treatment in primary organoids (N=8). *MYC* has previously been reported to be overexpressed broadly in human colorectal cancer (Cancer Genome Atlas Network and Muzny, 2012). Therefore, we first compared induction of *MYC* following IL-22 stimulation in CRC-derived organoids and organoids derived from normal adjacent colonic mucosa. The induction of *MYC* following IL-22 stimulation was not significantly different between CRC and normal adjacent-derived organoids, however there was marked heterogeneity in *MYC* induction in the CRC organoids

(Figure 5.12 A). If the CRC organoids were stratified according to their *KRAS* mutation status, *MYC* induction following IL-22 stimulation was significantly greater in *KRAS* mutant compared to wild type organoids (Figure 5.11 B). *KRAS* mutant organoids assayed in these experiments included 3 lines with canonical *KRAS* G12D/G13D mutations that result in constitutive activation of the Ras pathway, as well as two lines with *KRAS* mutations for which there is no currently known clinical significance (Figure 5.11 B). We additionally confirmed this c-Myc induction at the protein level by confocal microscopic analysis of total c-Myc protein in *KRAS* mutant organoids (Figure 5.12 C).

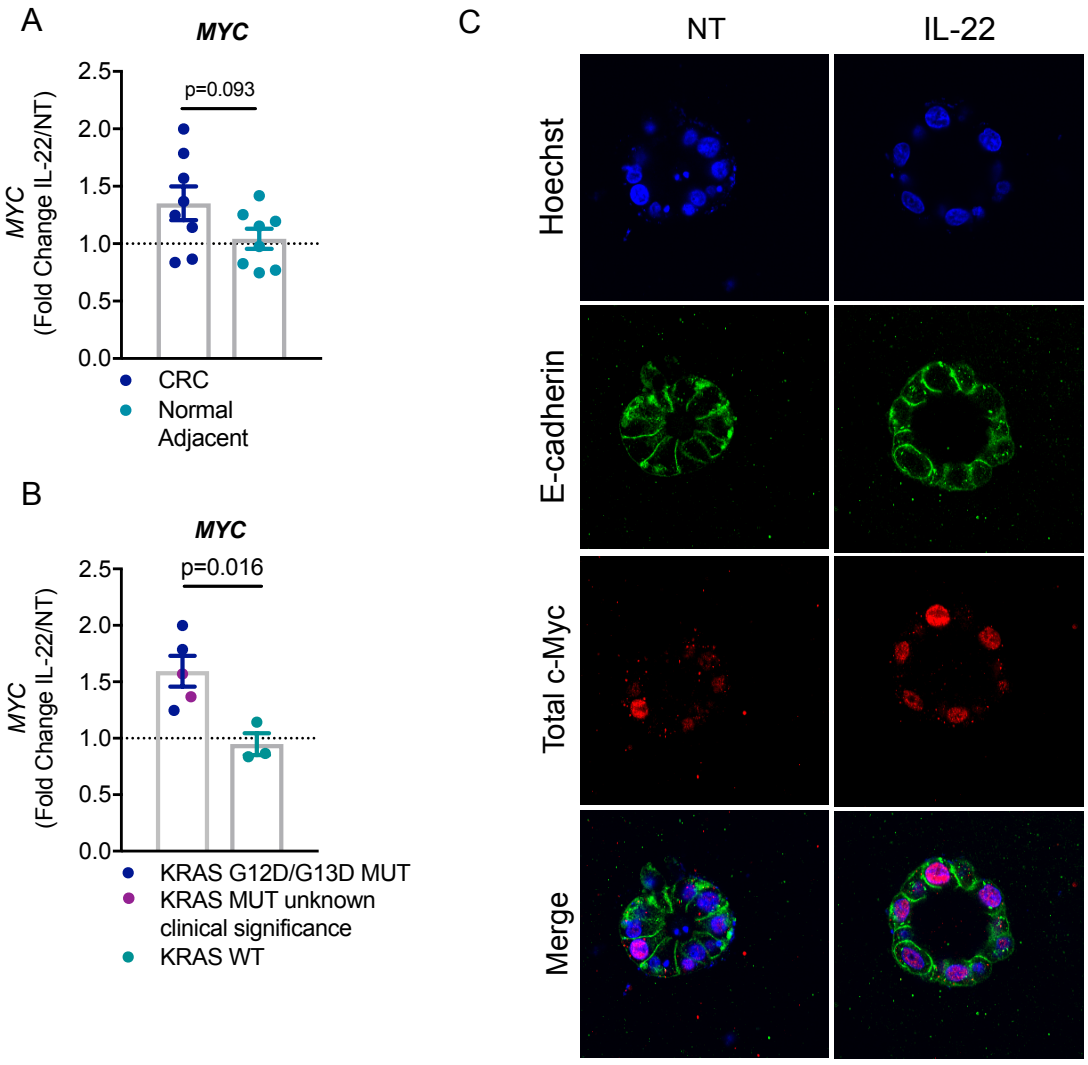


Figure 5.12 IL-22 induces c-Myc specifically in *KRAS* mutant but not wild type primary organoids.

(A) qPCR analysis of *MYC* induction in primary tumour-derived (N=8) or normal adjacent-derived (N=8) organoids after 24h 1ng/mL IL-22 stimulation. Each data point represents expression of technical duplicates normalised to the mean of the NT (no treatment) condition for each independent patient-derived organoid. Statistical significance was assessed by an unpaired T-test. P<0.05 is considered significant.

(B) qPCR analysis of *MYC* induction in *KRAS* MUT (N=5) versus WT (N=3) primary tumour-derived organoids after 24h 1ng/mL IL-22 stimulation. Each data point represents expression of technical duplicates normalised to the mean of the NT (no treatment) condition for each independent patient-derived organoid. Statistical significance was assessed by an unpaired T-test. P<0.05 is considered significant. Organoids derived from patients with mutations in *KRAS* with no known clinical significance (N=2) are indicated in pink.

(C) Representative confocal imaging for total c-Myc (red) in *KRAS* mutant organoids stimulated with 1ng/mL IL-22 for 24h. 60X magnification. Hoechst (blue) stains nuclei; E-cadherin (green) stains epithelial cells.

5.2.7 Myc knockdown attenuates *KRAS* mutant cell proliferation at baseline and following IL-22 stimulation

Having confirmed that c-Myc is induced by IL-22 specifically in *KRAS* mutant isogenic cells and primary organoids, we next sought to determine whether the IL-22-induced proliferation we have previously observed in *KRAS* mutant cells (Chapter 4, Figure 4.9) was c-Myc-dependent. Since basal c-Myc expression in the *KRAS* mutant isogenic line is higher than that in the matched wild type line, DLD-1 *KRAS* mutant isogenic cells were transfected with *MYC* targeting siRNA or control oligos with no known specificity for human genes (siscr) for 48 hours to reduce c-Myc expression in the *KRAS* mutant line to a level comparable to that of wild type cells. Optimal siRNA concentration and transfection time was determined using time course and dose response assays. An approximately 50% reduction in c-Myc protein was observed following 48 hour transfection of *KRAS* mutant isogenic cells with 40nM *MYC* siRNA (Figure 5.13 A, B) compared to mock transfected and no treatment controls. Importantly, the transfection itself did not alter basal c-Myc expression (Figure 5.13 A, B). Following *MYC* knockdown, c-Myc protein expression in the *KRAS* mutant line was more comparable to that in the *KRAS* wild type isogenic line, which was the desired outcome of the *MYC* knockdown (Figure 5.13 A, B).

Next, a series of experiments was performed in which *MYC* was knocked down for 48 hours in *KRAS* mutant cells that were subsequently stimulated with IL-22 for 24 hours, to assess protein and gene expression. Cell proliferation was then assessed after 48-hour IL-22 stimulation. As we previously observed, IL-22 significantly induced c-Myc protein after 24-hour stimulation in mock-transfected *KRAS* mutant cells (Figure 5.13 C). By contrast, *KRAS* mutant cells transfected with *MYC* siRNA showed no significant c-Myc induction following 24-hour IL-22 stimulation, similar to mock

transfected *KRAS* wild type cells (Figure 5.13 C). qPCR analysis of gene expression revealed that *MYC* knockdown had no impact on IL-22-induced *SOCS3* expression in the *KRAS* mutant line (Figure 5.13 D). However, while the Myc target gene *GNL3* was significantly induced following IL-22 stimulation in mock transfected *KRAS* mutant cells, its induction was partially attenuated in *MYC* siRNA transfected cells, similar to the mock-transfected *KRAS* wild type cells (Figure 5.13 E). Finally, on a functional level, *MYC* siRNA transfection reduced IL-22-induced *KRAS* mutant cell proliferation to the level of unstimulated mock-transfected *KRAS* mutant cells (Figure 5.13 F). It would be erroneous however, to conclude that this effect is strictly IL-22-dependent, as *MYC* knockdown also modestly reduced basal proliferation in the *KRAS* mutant cells compared to mock transfected controls, though this difference did not reach statistical significance (Figure 5.13 F). Furthermore, a modest increase in proliferation was observed following IL-22 stimulation in *MYC* knockdown *KRAS* mutant cells, though again this was not statistically significant (Figure 5.13 F). On global observation, the pattern of proliferation in the *KRAS* mutant *MYC* knockdown cells was more similar to the mock-transfected *KRAS* wild type cells than the mock-transfected *KRAS* mutant cells (Figure 5.13 F). Thus, *MYC* knockdown attenuates *KRAS* mutant cell proliferation at baseline and following IL-22 stimulation and may represent one potential cell intrinsic mechanism by which IL-22 and *KRAS* interact to promote malignancy.

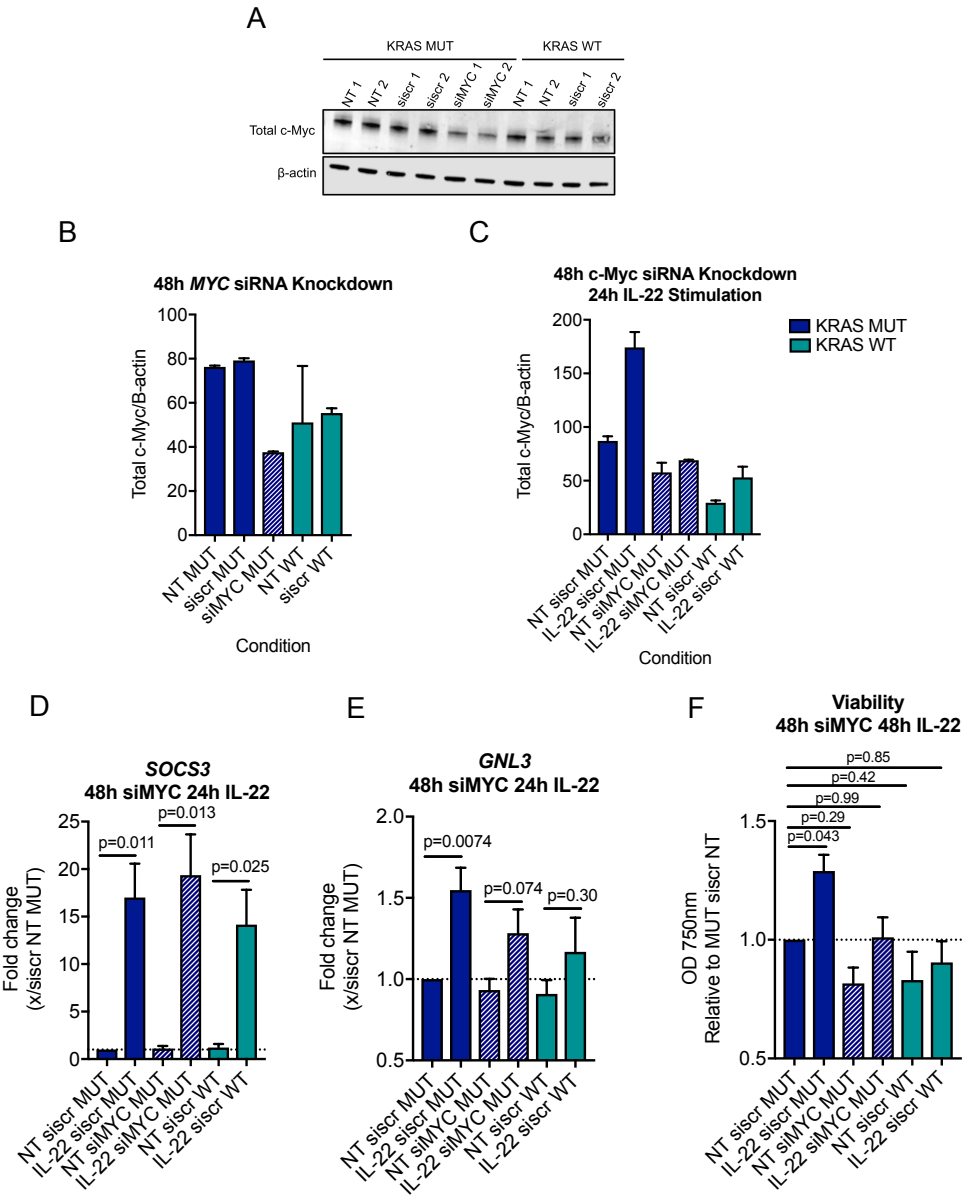


Figure 5.13 *MYC* knockdown attenuates *KRAS* mutant cell proliferation at baseline and following IL-22 stimulation.

c-Myc expression was knocked down in DLD-1 *KRAS* MUT cells by transfection with 40nM *MYC* siRNA (siMYC) for 48h. Cells were subsequently stimulated with 10ng/mL IL-22 for 24h and 48h. (NT = no treatment, siscr = transfected with non-targeting control siRNA)

(A) Representative western blot for total c-Myc following 48h *MYC* knockdown in *KRAS* MUT cells. Technical duplicates are displayed.

(B) Quantification of c-Myc protein relative to β-actin using LI-COR fluorescence detection of fluorophore-conjugated secondary antibodies. Data represent mean ± SEM for n=2 independent experiments after 48h si*MYC* transfection.

(C) Western blots were performed for total c-Myc following 48h *MYC* knockdown in *KRAS* MUT cells and 24h 10ng/mL IL-22 stimulation. Quantification of c-Myc protein relative to β-actin using LI-COR fluorescence detection of fluorophore-conjugated secondary antibodies. Data represent mean ± SEM for n=2 independent experiments after 48h si*MYC* transfection and 24h IL-22 stimulation.

(D) (E) qPCR analysis of *SOCS3* and *GNL3* expression following 48h *MYC* knockdown in *KRAS* MUT cells and 24h 10ng/mL IL-22 stimulation. Data represent mean ± SEM for

n=3 independent experiments. Statistical significance was assessed using unpaired T tests comparing the relevant pairs of samples. P<0.05 is considered significant.

(F) Viability of DLD-1 isogenic cells assessed by MTT assays after 48h *MYC* knockdown in *KRAS* MUT cells followed by 48h 10ng/mL IL-22 treatment. Data represent mean ± SEM of n=5 independent experiments (each experiment performed in technical triplicates) normalised to the MUT siscr NT condition. Statistical significance was assessed using a one-way ANOVA comparing each condition to the MUT siscr NT condition. P<0.05 is considered significant.

5.2.8 Preliminary evidence suggests that *MYC* transcriptional induction by IL-22 is not STAT3 dependent

The elevated c-Myc protein levels observed following IL-22 stimulation of *KRAS* mutant cells is likely a consequence of both transcriptional and post-translational mechanisms of IL-22-*KRAS* synergy to sustain elevated levels of active c-Myc in the cell. Historical studies from nearly two decades ago demonstrated that STAT3 can directly induce *MYC* transcription (Bromberg *et al.*, 1999; Kiuchi *et al.*, 1999; Bowman *et al.*, 2001). Since STAT3 is the major transcription factor activated downstream of IL-22 signalling, we sought to determine whether the transcriptional induction of *MYC* in *KRAS* mutant cells was STAT3-dependent. DLD-1 *KRAS* mutant cells were transfected with *STAT3* targeting siRNA for 48 hours and subsequently stimulated for 24 hours with 10ng/mL IL-22. *STAT3* knockdown was confirmed by qPCR (Figure 5.14 A) and western blot (Figure 5.14 B, C). 50% STAT3 knockdown was obtained at both the gene expression and protein level compared to mock transfected controls (Figure 5.14 A, B, C). IL-22 induced the expression of STAT3 itself in both control transfected and *STAT3* siRNA transfected cells; however, in *STAT3* knockdown cells, STAT3 mRNA and protein expression after IL-22 stimulation was comparable to the basal expression in mock transfected cells (Figure 5.14 A, B, C). To confirm that *STAT3* knockdown cells were impaired in their capacity to induce STAT3 target gene expression, induction of *SOCS3*, a known STAT3 target, was assessed by qPCR following 24-hour IL-22 stimulation. The fold induction of *SOCS3* with IL-22 stimulation relative to baseline was diminished by

more than 50% in *STAT3* knockdown cells (Figure 5.14 D). By contrast, *MYC* induction was unchanged between IL-22 stimulated mock transfected and *STAT3* siRNA transfected cells (Figure 5.14 E). Although we did not specifically explore the consequences of STAT3 knockdown on c-Myc protein expression, our preliminary evidence indicates that the IL-22-induced transcription of *MYC* in *KRAS* mutant cells is not STAT3-dependent.

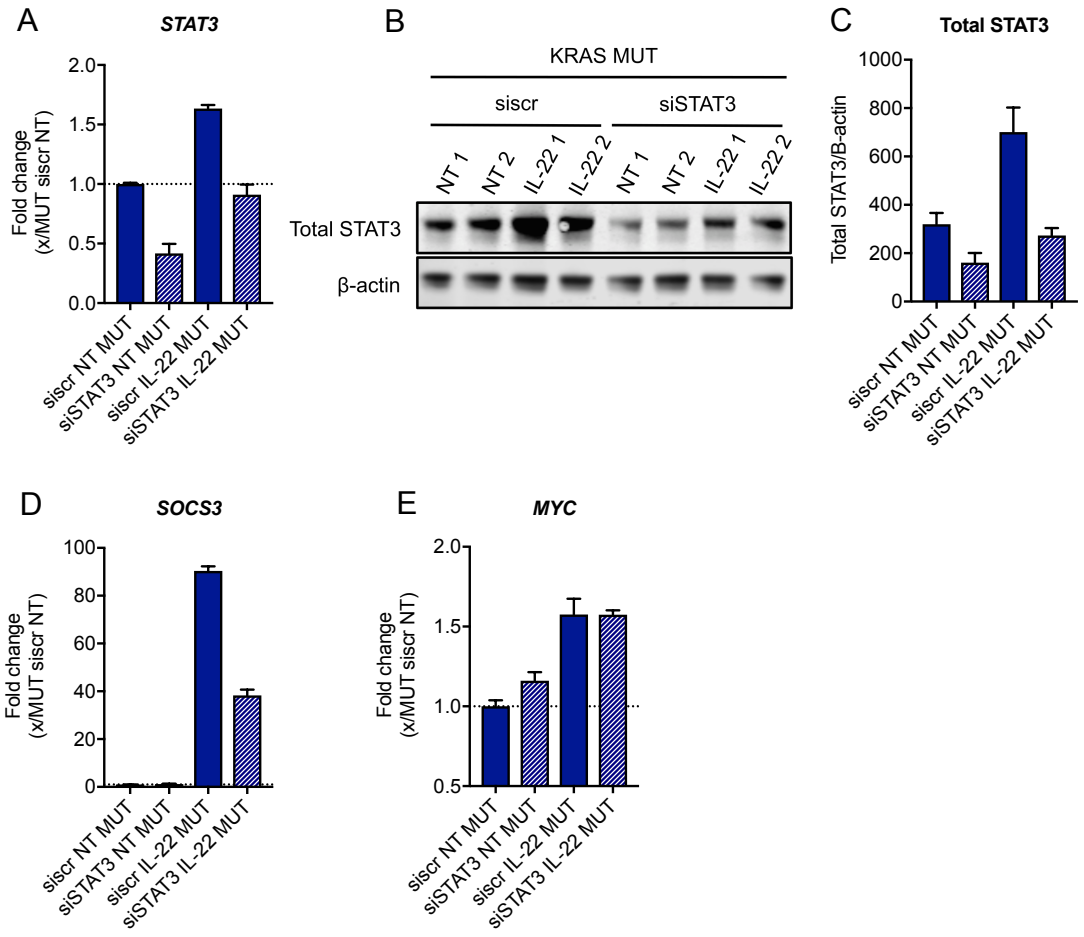


Figure 5.14 Preliminary evidence reveals that *MYC* transcriptional induction by IL-22 is not STAT3-dependent.

STAT3 expression was knocked down in DLD-1 *KRAS* MUT cells by transfection with 20nM *STAT3* siRNA (siSTAT3) for 48h. Cells were subsequently stimulated with IL-22 for 24h. (NT = no treatment, siscr = transfected with non-targeting control siRNA)

(A) qPCR analysis of *STAT3* expression. Data represent mean ± SEM for n=2 independent experiments performed with technical duplicates. *STAT3* expression was normalised to the mock transfected no treatment condition (siscr NT MUT).

(B) Representative western blot for total STAT3. Technical duplicates are displayed.

(C) Quantification of STAT3 protein relative to β-actin using LI-COR fluorescence detection of fluorophore-conjugated secondary antibodies. Data represent mean ± SEM for n=2 independent experiments performed with technical duplicates.

(D) (E) qPCR analysis of *SOCS3* and *MYC* expression. Data represent mean ± SEM for n=2 independent experiments performed with technical duplicates. Gene expression was normalised to the mock transfected no treatment condition (siscr NT MUT).

5.2.9 *MYC* expression is correlated with *IL22RA1* expression

In functional experiments, we have observed more significant induction of *MYC* mRNA and c-Myc protein in IL-22 stimulated *KRAS* mutant versus wild type cells and organoids. Therefore, we sought to determine whether in whole tissue transcriptomic analysis *MYC* expression is elevated in patients with *IL22RA1*-high, *KRAS* mutant versus wild type tumours. One key limitation in whole tissue analysis is that multiple cells types that are not responsive to IL-22 in the tumour express *MYC*. c-Myc for instance is a critical regulator of growth and proliferation in immune cells (Douglas *et al.*, 2001) and therefore the interpretation of whole tissue *MYC* expression is complicated by the representation of other cell types in the complex tumour microenvironment. Nonetheless, when we assessed *MYC* expression in the tumour transcriptomic training cohort (GSE39582), *MYC* expression was elevated in *IL22RA1*-high, *KRAS* mutant versus wild type tumours (Figure 5.15 A). This appeared by be driven by the significantly elevated *MYC* expression in *KRAS* mutant tumours generally (Figure 5.15 A). A key limitation in this analysis is that the dynamic range of the *MYC* probe on the HGU133 Affymetrix human array used for transcriptomics is very narrow and thus detecting reliable differences in expression may be problematic. Therefore, we turned to qPCR-based analysis of *MYC* expression in whole tumour tissue that we prospectively collected. To date, a cutpoint for high and low *IL22RA1* expression that stratifies patients in terms of prognosis has not been prospectively defined. This is, however, part of our ongoing study as we await survival data for the patients from whom we have collected tissue thus far. Therefore, for simplicity, in this analysis we defined the tumours above the 67th percentile of *IL22RA1* expression to be *IL22RA1*-high. We did not detect elevated *MYC* expression in *IL22RA1*-high, *KRAS* mutant tumours (Figure 5.15 B). At present, this may either be a consequence of an inappropriately defined cutpoint, or simply inadequate power

to detect differences due to low numbers. Moreover, we did not observe a difference in *MYC* expression between *KRAS* mutant and wild type tumours broadly (Figure 5.15 B). However, *MYC* expression was significantly higher in *IL22RA1*-high compared to *IL22RA1*-low tumours (Figure 5.15 B). Furthermore, when we performed Pearson correlation analysis comparing *MYC* to *IL22RA1* expression, the two were highly correlated regardless of *KRAS* mutation status (Figure 5.15 C). This elevated *MYC* in tumours with higher *IL22RA1* expression could be a functional consequence of more active IL-22 signalling, resulting in elevated *MYC* transcription. Alternatively, *IL22RA1* could be a transcriptional target of c-Myc. To determine whether *IL22RA1* transcription was directly regulated by c-Myc, *IL22RA1* expression was assessed in DLD-1 *KRAS* mutant cells following 48-hour transfection with *MYC* targeting siRNA or control siRNA. No significant difference in *IL22RA1* expression was observed between *MYC* knockdown and mock transfected cells (Figure 5.15 D). Therefore, it seems that the correlation between *MYC* and *IL22RA1* in whole tumour tissue is not due to c-Myc mediated transcriptional control of *IL22RA1*.

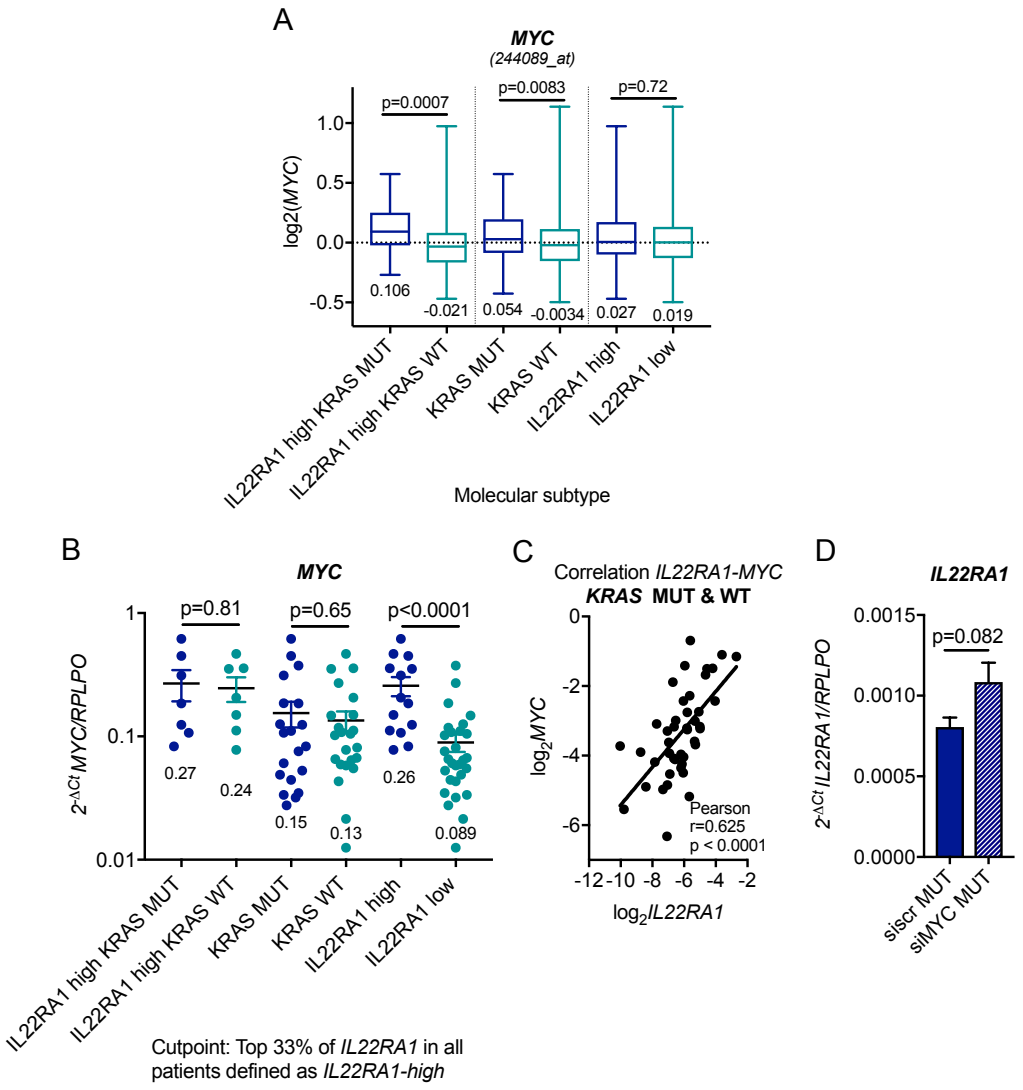


Figure 5.15 *MYC* expression is correlated with *IL22RA1* expression, but c-Myc does not directly control *IL22RA1* expression.

(A) Analysis of *MYC* expression in transcriptomic data from GSE39582 training cohort (Probe: 244089_at) in the molecular subtypes of interest: *IL22RA1*-high, KRAS MUT (N=49), *IL22RA1*-high, *KRAS* WT (N=104), *KRAS* MUT (N=169), *KRAS* WT (N=279), *IL22RA1*-high (N=158), *IL22RA1*-low (N=311). Box and whisker plots represent the mean ± min/max value in each subgroup. Statistical significance was assessed by unpaired T tests comparing the two subgroups of interest. P<0.05 is considered significant. Mean log2 *MYC* expression for each subgroup is indicated below the corresponding box and whisker.

(B) qPCR whole tissue RNA analysis of *MYC* expression in prospectively collected CRC biopsies in the molecular subtypes of interest: *IL22RA1*-high, KRAS MUT (N=7), *IL22RA1*-high, *KRAS* WT (N=7), *KRAS* MUT (N=20), *KRAS* WT (N=23), *IL22RA1*-high (N=14), *IL22RA1*-low (N=29). Each dot represents an individual patient. Statistical significance was assessed by unpaired T tests comparing the two subgroups of interest. P<0.05 is considered significant. Mean relative *MYC* expression for each subgroup is indicated below the data points.

(C) Pearson Correlation analysis of *IL22RA1* and *MYC* in prospectively collected CRC biopsies regardless of genotype (N=49).

(D) *IL22RA1* expression assessed by qPCR in DLD-1 *KRAS* MUT cells transfected with *MYC* siRNA (siMYC) or control siRNA (siscr) for 48h. Data represent the mean ± SEM

for n=4 independent experiments, *IL22RA1* expression relative to the endogenous control (*RPLPO*). Statistical significance was assessed using an unpaired T test. P<0.05 is considered significant.

5.2.10 IL-22 enhances lactate production in *KRAS* mutant cells that is diminished by *MYC* knockdown

Since ssGSEA analysis revealed that the Myc pathway ("MYC_TARGETS_V2") is upregulated in *KRAS* mutant but not wild type cells following IL-22 stimulation, we next sought to determine whether this signature was also enriched in *IL22RA1*-high, *KRAS* mutant versus wild type tumours. GSEA analysis was performed on samples from the combined CRC transcriptomic cohort comparing *IL22RA1*-high, *KRAS* MUT (N=178) to *IL22RA1*-high, *KRAS* WT (N=367) tumours. Enrichment of Myc target signatures from the Molecular Signatures Database (MSigDB) Hallmark collection was not observed in *IL22RA1*-high, *KRAS* mutant tumour (data not shown). However, we then went on to examine other pathways that were specifically enriched in *IL22RA1*-high, *KRAS* mutant tumours and enrichment of a glycolysis signature ("HALLMARK_GLYCOLYSIS") was observed (Figure 5.16 A). c-Myc is well known to enhance glycolytic flux and the Warburg effect by increasing glucose uptake and lactate production. Furthermore, c-Myc enhances the production of glycolytic intermediates used for the biosynthesis of nucleotides and amino acids (Dang, 2013). To determine whether IL-22-induced c-Myc modulates glycolytic pathways in our experimental system, we specifically explored lactate production in IL-22 stimulated cells in which *MYC* was knocked down by siRNA. In mock-transfected *KRAS* isogenic cells, IL-22 significantly induced lactate production following 48-hour stimulation (Figure 5.16 B). By contrast, lactate production was not enhanced by IL-22 in mock-transfected *KRAS* wild type cells (Figure 5.16 B). When *MYC* was knocked down in *KRAS* mutant cells, IL-22-induced lactate

production was significantly lower than that in mock transfected, IL-22 stimulated *KRAS* mutant cells (Figure 5.16 B). Lactate production at baseline in *MYC* knockdown cells was also modestly, though not significantly lower than that in mock transfected *KRAS* mutant cells (Figure 5.16 B).

Therefore, a glycolysis signature is enriched in *IL22RA1*-high, *KRAS* mutant compared to wild type patients in the combined CRC tumour transcriptomic cohort. IL-22 enhances lactate production in *KRAS* mutant but not wild type cells and knock down of *MYC* in *KRAS* mutant cells abrogates IL-22-enhanced lactate production.

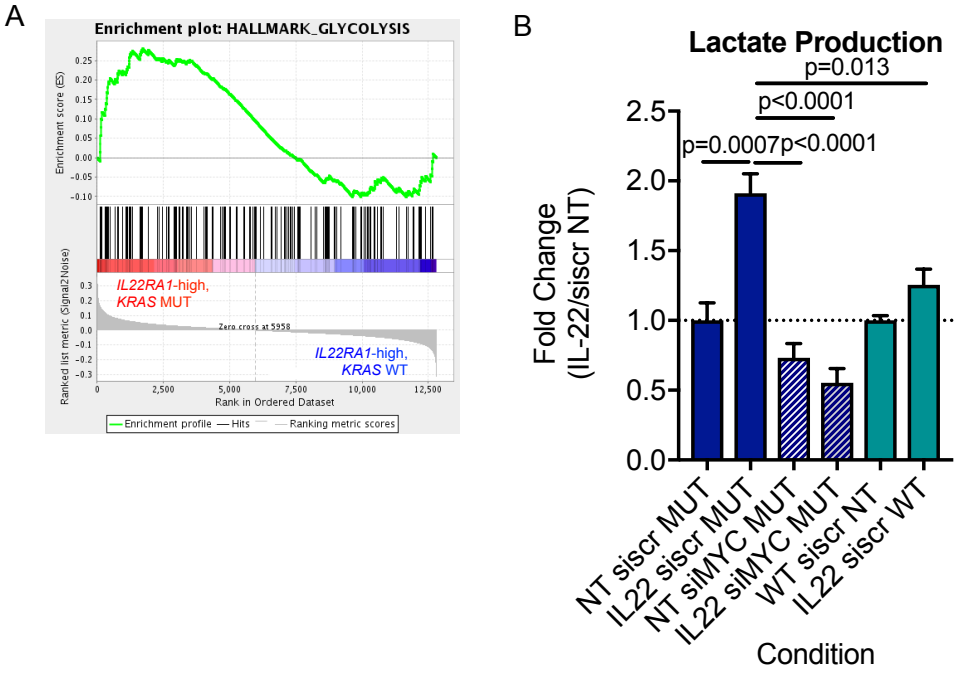


Figure 5.16 A glycolysis signature is enriched in *IL22RA1*-high, *KRAS* mutant compared to *IL22RA1*-high, *KRAS* WT tumours and lactate production is enhanced by IL-22 in *KRAS* mutant cells and this induction is diminished by *MYC* knockdown.

(A) GSEA analysis analysis was performed to compare enrichment of MSigDB Hallmark pathways in *IL22RA1*-high, *KRAS* MUT (N=178) versus *IL22RA1*-high, *KRAS* WT tumours (N=367) from the combined cohort. The Glycolysis pathway is enriched in *IL22RA1*-high, *KRAS* MUT versus WT tumours. Analysis performed by D. Barras.

(B) Analysis of lactate production in *KRAS* MUT and WT DLD-1 isogenic cells following 48h *MYC* siRNA transfection (or non-targeting control siRNA transfection) and 48h 10ng/mL IL-22 treatment. Data represent means ± SEM (one experiment representative of 4 independent experiments performed in technical triplicates) of the fold change in lactate production normalised to the mean of the no treatment condition (siscr NT) for each line. Statistical significance was assessed by a one-way ANOVA with Tukey's post-test for multiple comparisons. P<0.05 is considered significant.

5.2.11 The high capacity glucose transporter, GLUT3, is highly induced by IL-22 in *KRAS* mutant cells based on proteomic and RNA-sequencing analyses

c-Myc is known to induce the expression of cell surface glucose transporters as one mechanism of increasing cellular glycolytic rate (Miller *et al.*, 2012). Incidentally, when we explored the top differentially expressed proteins in *KRAS* mutant and wild type isogenic cells following 24 hour IL-22 stimulation, label free proteomic analysis revealed that SLC2A3 (also known as GLUT3), a high capacity glucose transporter, was significantly induced in *KRAS* mutant but not wild type cells (Figure 5.17 A, B). Interestingly, in parallel RNA sequencing interaction analysis, *SLC2A3* mRNA transcript was also significantly induced by IL-22 in *KRAS* mutant but not wild type cells following 2-hour IL-22 stimulation (Appendix 3, Figure 3.1). This elevated *SLC2A3* transcription was confirmed in *KRAS* mutant isogenic cells following IL-22 stimulation over a 2-24 hour period (Figure 5.17 C). Interestingly, the fold induction of *SLC2A3* mRNA diminished from 2-24 hours, though at 8 and 24 hours the fold induction in *KRAS* mutant cells was still elevated compared to wild type cells (Figure 5.17 C). Temporally, it is logical that following significant mRNA induction at early timepoints (2h), elevated SLC2A3 protein is observed at later timepoints (24h). It is also worth noting that on a whole, IL-22 significantly induced a greater number of proteins in *KRAS* mutant compared to wild type cells (Figure 5.17 A). Many of the proteins that were induced by IL-22 regardless of cell genotype (ie. BCL3, CEACAM1, CEACAM5, SERPINA1, ICAM1) were also induced in both genotypes at the transcript level based on RNA-sequencing analysis (Figure 5.3 A). Intriguingly, one of the proteins that was uniquely induced by IL-22 in *KRAS* wild type but not mutant cells was FOXO1 (Figure 5.17 A). FOXO1 is a transcription factor that has

previously been shown to negatively regulate MYC signalling and downstream target gene induction (Peck, Ferber and Schulze, 2013; Wilhelm *et al.*, 2016).

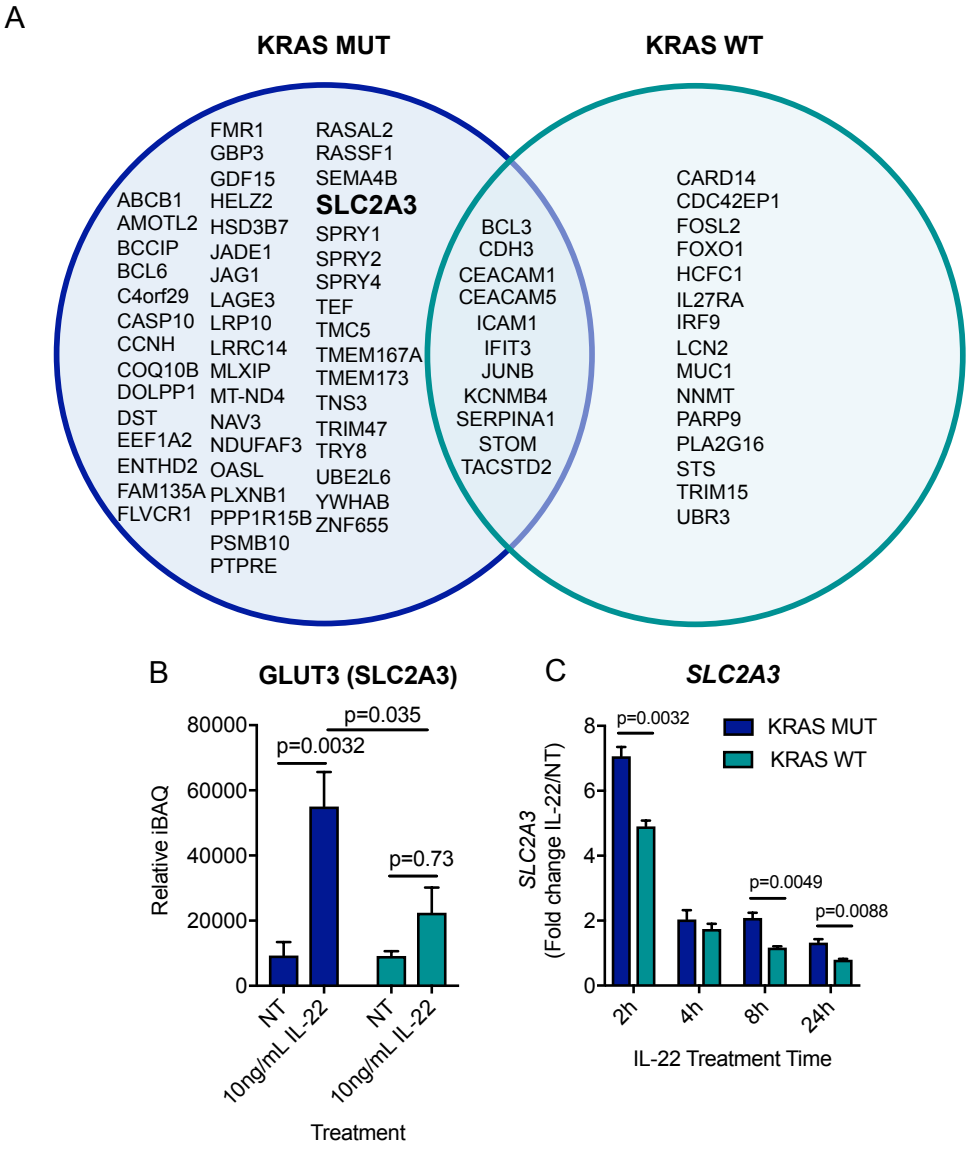


Figure 5.17 Proteomic and RNA-sequencing analyses reveal that the high capacity glucose transporter GLUT3 (*SLC2A3*) is highly induced by IL-22 in *KRAS* mutant compared to wild type cells.

(A) Venn diagram displaying the top (log2FC>1, P<0.05) IL-22-induced proteins detected by label free proteomic analysis (LC-MS/MS) in DLD-1 *KRAS* MUT and WT cells stimulated for 24h with 10ng/mL IL-22.

(B) Quantification of GLUT3 (*SLC2A3*) expression by LC-MS/MS using MaxQuant. Data are means ± SEM for n=4 independent experiments displaying relative iBAQ (a normalised measure of molar abundance) quantities. Statistical significance was assessed using a two-way ANOVA with Tukey's post-test for multiple comparisons. P<0.05 is considered significant.

(C) qPCR validation of observed IL-22-*KRAS* specific induction of *SLC2A3* by interaction analyses of RNA-sequencing data (refer to Appendix 3, Figure 3.1) in DLD-1 isogenic cells stimulated with 10ng/mL IL-22 over a time course of 2-24h. Data are means ± SEM (n=3 independent experiments) of the fold change in *SLC2A3* expression with IL-

22 stimulation over NT (no treatment). Statistical significance was determined using unpaired T-tests comparing the *KRAS* MUT and WT *SLC2A3* induction at each timepoint. P<0.05 is considered significant.

5.2.12 Myc target protein signatures are enriched in IL-22 stimulated *KRAS* mutant compared to wild type cells based on proteomic analysis

Given that ssGSEA analysis revealed an enriched Myc signature in *KRAS* mutant cells following IL-22 stimulation and the elevated FOXO1 protein expression in IL-22 stimulated *KRAS* wild type cells, we sought to determine whether at the protein level, Myc and its downstream targets were elevated in IL-22 stimulated *KRAS* mutant versus wild type cells. Unfortunately, Myc protein itself was not detected by LC-MS/MS in any of the samples assessed. This is likely a technical consequence of the c-Myc tryptic peptides not efficiently travelling to the mass spectrometer detector. Therefore, we utilised an algorithm analogous to GSEA developed by Lavallee-Adam *et al.* called Protein Set Enrichment Analysis (PSEA-Quant) (Lavallée-Adam *et al.*, 2014; Lavallée-Adam and Yates, 2016) to assess pathways differently induced in *KRAS* mutant versus wild type cells following IL-22 stimulation. Inherent in the PSEA-Quant algorithm is a permutation scheme that models protein abundance dependencies and annotation biases that has been validated for label-free proteomic analysis (Lavallée-Adam *et al.*, 2014). PSEA-Quant was used to compare the fold changes in iBAQ (intensity based absolute quantification) values with IL-22 stimulation (fold change IL-22/no treatment) for *KRAS* mutant versus *KRAS* wild type cells. The pathways for which P<0.001, with an FDR-q value of less than 0.05 were considered significant in this relative analysis. A full list of differentially induced pathways can be found in Appendix 3.2.2. Notably, five Myc target signature pathways annotated in the MSigDB were significantly induced by IL-22 in *KRAS* mutant compared to wild type cells (Figure 5.18 A).

Therefore, we have confirmed both at the mRNA and protein level that the Myc pathway is induced by IL-22 in *KRAS* mutant compared to wild type cells and that induction of c-Myc itself and its downstream targets is a plausible cell intrinsic mechanism by which IL-22 may synergise with mutant *KRAS* to promote malignancy.

A

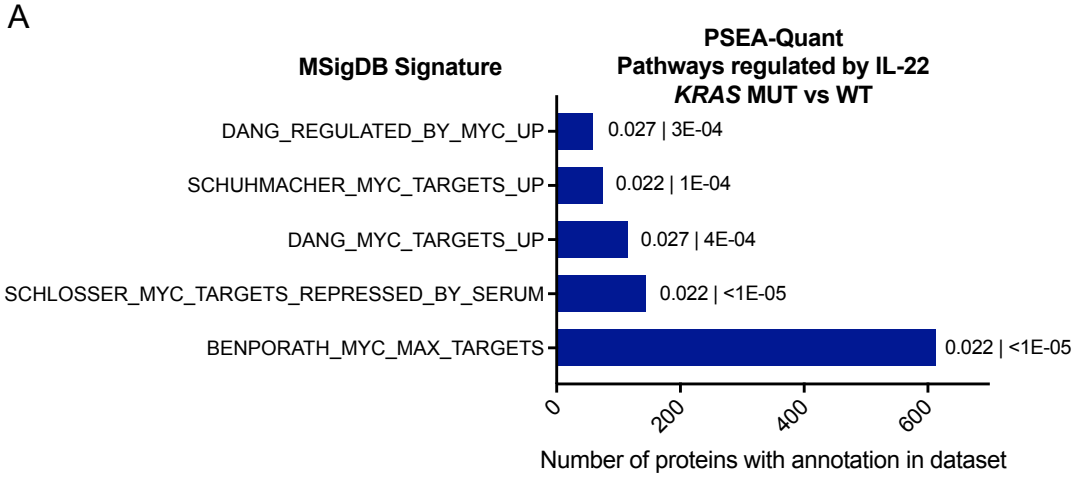


Figure 5.18 Myc targets are induced by IL-22 in *KRAS* mutant compared to wild type isogenic cells at the protein level.

(A) Protein set enrichment analysis (PSEA-Quant) [http://pseaquant.scripps.edu/] of abundance ratios comparing the proteome from *KRAS* MUT IL-22/NT to *KRAS* WT IL-22/NT to identify protein sets from the MSigDB that are enriched in *KRAS* MUT cells by IL-22. 5 MYC target signatures were among significantly enriched pathways in the *KRAS* MUT IL-22 stimulated cells. The numbers of proteins detected by LC-MS/MS with an annotation in each dataset are indicated by horizontal bars. FDR-q values and corresponding P-values are indicated beside each bar. FDR-q <0.05 is considered significant. P <0.001 is considered significant.

5.3 Discussion

5.3.1 Main conclusions

Here, we have outlined the unbiased transcriptomic and proteomic approaches taken to identify candidate modes of synergy between IL-22 signalling and mutant *KRAS*. Our evidence points towards both non-cell autonomous (cell extrinsic) and cell autonomous (cell intrinsic) consequences of IL-22 signalling into a *KRAS* mutant cell which may promote malignancy (Figure 5.19).

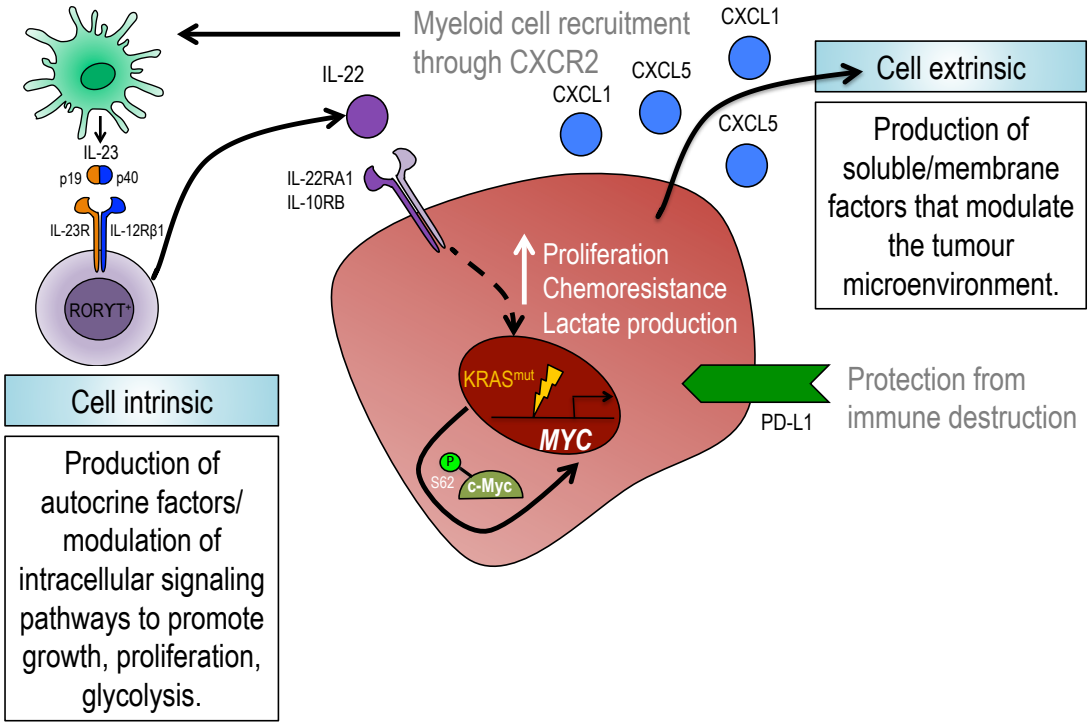


Figure 5.19 Proposed cell extrinsic and intrinsic mechanisms by which IL-22 interacts with *KRAS* to promote malignancy.

IL-22 signalling into a *KRAS* mutant cell results in CXCL1 and CXCL5 production and PD-L1 expression to, in a non-cell autonomous (cell extrinsic) manner, condition a pro-tumourigenic immune microenvironment. IL-22 induces *MYC* transcription and maintains elevated active c-Myc (c-Myc P-S62) levels in *KRAS* mutant cells. This results in enhanced Myc target gene expression, proliferation, and lactate production and represents a potential cell autonomous (cell intrinsic) mechanism by which IL-22 and *KRAS* may synergise to promote malignancy.

Analysis of the top differentially regulated genes in *KRAS* mutant and wild type isogenic cells following IL-22 stimulation, revealed that specific ELR^+ CXC chemokines (*CXCL1, CXCL5*) that signal through CXCR2 are potently induced in

KRAS mutant but not wild type cells (Figure 5.20). Moreover, when cells and organoids were stimulated with supernatants generated from $CD4^+$ T cells polyclonally expanded from human tumours, induction of *CXCL1* and *CXCL5* was partially IL-22-dependent. Given that neutrophils, myeloid-derived-suppressor cells, and some dendritic cell populations express CXCR2, we hypothesise that the elevated expression of ELR^+ CXC chemokines in *KRAS* mutant versus wild type cells upon IL-22 stimulation may result in recruitment of myeloid cells to the tumour microenvironment. Some of these myeloid populations may be capable of producing IL-23, which induces the production of IL-22 from $CD4^+$ T cells and innate lymphoid cells, and perpetuates the pro-tumourigenic inflammatory cycle. Furthermore, stringent differential expression interaction analysis revealed that IL-22 induces *CD274*, encoding PD-L1, specifically in *KRAS* mutant cells. Upregulation of PD-L1 on tumours subverts anti-tumour immune responses, tipping the balance towards pro-tumourigenic inflammation. Thus, IL-22 signalling into a *KRAS* mutant cell results in the production of myeloid chemoattractants and expression of immune suppressive receptors that in a non-cell autonomous fashion may sculpt the immune microenvironment to favour tumour survival and growth (Figure 5.20).

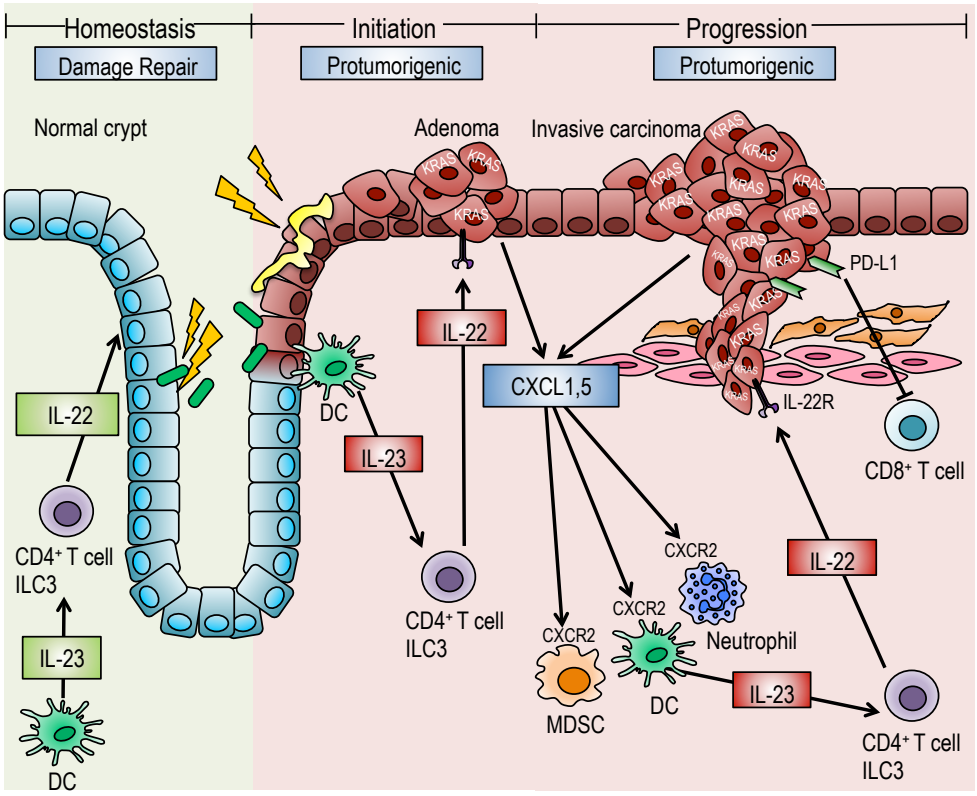


Figure 5.20 IL-22 and *KRAS* may interact to promote a self-sustaining pro-tumourigenic inflammatory loop.

Under homeostatic settings IL-22, produced by $CD4^+$ T cells and type 3 innate lymphoid cells (ILC3) in response to IL-23, protects the intestinal epithelium from microbial insult and repairs the epithelium after damage. When IL-22 signals into a *KRAS* mutant cell it induces production of the ELR^+ CXC chemokines CXCL1 and CXCL5. CXCL1/5 signal through CXCR2 expressed on neutrophils, dendritic cells (DC), and myeloid derived suppressor cells (MDSC) resulting in their recruitment to the tumour microenvironment. Some of these CXCR2-expressing populations, particularly DCs, produce IL-23, which induces IL-22 production from $CD4^+$ T cells and ILC3s. IL-22 signals into the *KRAS* mutant CRC cells to induce further production of CXCL1/5, resulting in a self-sustaining inflammatory loop. Concomitantly, IL-22 induces PD-L1 expression on *KRAS* mutant CRC cells, preventing immune recognition by cytotoxic $CD8^+$ T cells.

In addition to identification of IL-22-induced inflammatory mediators, pathway analysis of the RNA-sequencing data identified induction of the Myc pathway as a possible cell-intrinsic mechanism of tumour promotion. Notably, the Myc pathway was induced by IL-22 and not IL-6 in *KRAS* mutant but not wild type cells. Protein set enrichment analysis similarly identified multiple Myc target signatures with enhanced induction in *KRAS* mutant versus wild type IL-22 stimulated cells. *MYC* itself was induced at the mRNA and protein level in *KRAS* mutant cells and primary organoids

following IL-22 stimulation and its knockdown limited basal and IL-22-induced *KRAS* mutant cell proliferation. While a broad Myc signature was not significantly enriched in *IL22RA1*-high, *KRAS* mutant tumours, these tumours displayed an enhanced glycolysis signature, consistent with increased Myc activity. IL-22 stimulation drove lactate production in *KRAS* mutant cells in a Myc-dependent fashion. Furthermore, GLUT3, a high capacity glucose transporter, was uniquely induced by IL-22 in *KRAS* mutant cells at the transcript and protein level. Thus our evidence suggests that IL-22 signalling into a *KRAS* mutant cell leads to the induction of c-Myc and its downstream targets, with diverse potential consequences on cell growth, proliferation, apoptosis, glycolysis and energy metabolism. Thus the convergence of IL-22 signalling and mutant *KRAS* on c-Myc is a plausible cell intrinsic modality by which IL-22 and mutant *KRAS* synergise to promote malignancy.

5.3.2 Conditioning a pro-tumourigenic immune microenvironment: cell extrinsic mechanisms by which IL-22 interacts with mutant *KRAS* to promote malignancy

Initial simple differential expression analysis of RNA-sequencing data from IL-22-stimulated DLD-1 isogenic cells revealed a panel of CXC chemokines to be induced by IL-22; *CXCL2*, *3*, *5*. The expression of these chemokines was enhanced in *KRAS* mutant versus wild type cells in particular after 24-hour IL-22 stimulation. Under homeostatic settings, chemokines are known to play important roles in regulating inflammation and wound healing. In particular, the family of ELR^+ CXC chemokines comprised of CXCL1, 2, 3, 5, 6, 7, 8, which are characterised by a Glu-Leu-Arg (ELR) sequence followed by a canonical Cys-X-Cys motif, recruit myeloid cells via engagement with the G-protein coupled receptor CXCR2 to sites on infection or damage and elicit a localised immune response (Keeley, Mehrad and Strieter, 2010).

Thus, IL-22-induced ELR^+ CXC chemokine production likely contributes to its homeostatic damage repair function. For example, in acute epithelial damage models, such as bleomycin-induced lung injury, IL-22 has been shown to act synergistically with IL-17A to increase *Cxcl1* expression and neutrophil influx to the site of injury (Sonnenberg *et al.*, 2010).

However, inappropriately elevated or sustained ELR^+ CXC chemokine expression is known to promote malignancy. In fact, CXCL1, 2, and 3 were initially identified in culture supernatants from melanoma cell lines (Richmond *et al.*, 1988). Two important studies in murine CRC models revealed the functional contribution of chemokine signalling through CXCR2 to malignant progression. Elevated *Cxcl1,2,5,7* and modestly increased *Cxcr2* transcripts were detected in colonic polyps compared to matched normal tissue from mice with DSS/AOM-induced CAC (Jamieson *et al.*, 2012). Furthermore, DSS/AOM-treated $Cxcr2^{-/-}$ animals had reduced tumour burden as a consequence of diminished CXCR2-expressing granulocytic cell (defined as: $CD11b^+Ly6G^{high}CD11c^-F4/80^-$ cells) infiltration (Jamieson *et al.*, 2012; Katoh *et al.*, 2013). Adoptive transfer of wild type granulocytic cells (defined by the investigators as MDSCs) into $Cxcr2^{-/-}$ animals restored tumourigenesis in DSS/AOM-treated mice (Katoh *et al.*, 2013). CXC chemokines were not however strictly important in CRCs arising in an overtly inflammatory context. In more classical sporadic CRC models such as $Apc^{Min/+}$, supernatants from cultured intestinal crypts of $Apc^{Min/+}$ adenomas contained CXCL1, CXCL2, CXCL5, and CXCL7 and were among the top 6 most highly elevated proteins comparing adenoma and normal crypts (Jamieson *et al.*, 2012). Blockade of ELR^+ CXC chemokine signalling using a CXCR1/2 blocking pepducin decreased tumour burden in $Apc^{Min/+}$ mice (Jamieson *et*

al., 2012). Interestingly, in the *Helicobater hepaticus,* AOM-driven colitis-associated cancer model found to be dependent on IL-22, *Cxcl1* and *Cxcl2* were elevated in the colonic tissue of tumour bearing mice and expression was diminished following anti-IL-22 treatment (Kirchberger *et al.*, 2013a). It remains to be determined whether therapeutic CXCR2 blockade in this model could prevent tumourigenesis. Overall, there is abundant evidence from murine colitis-associated and sporadic CRC models implicating ELR^+ CXC chemokines in colorectal tumourigenesis.

In human colorectal cancer functional studies are limited, yet expression of CXCL1 and CXCR2 were found to be elevated in sporadic CRC (Wang *et al.*, 2006; Wen *et al.*, 2006; Rubie *et al.*, 2008; Oladipo *et al.*, 2011) and CXCL1 expression in the malignant epithelium was inversely associated with relapse free survival in stage III patients (N=91) (Oladipo *et al.*, 2011). Moreover, serum CXCL5 levels were found to be higher in preoperative CRC patients (N=250) compared to healthy controls (N=33) and high serum CXCL5 was highly predictive of the presence of liver metastases (Kawamura *et al.*, 2012). Despite the evidence demonstrating elevated ELR^+ CXC chemokine expression in human CRC, the upstream signals that induce this elevated expression have not been systematically explored. Furthermore, whether chemokine expression is enhanced in specific mutational subtypes of human CRC, remains to be determined.

Our functional studies in the DLD-1 isogenic cell line and primary human organoids point toward a unique synergy between IL-22 and mutant *KRAS* that enhances *CXCL1* and *CXCL5* expression in particular. Independent of IL-22 signalling, oncogenic *KRAS* has previously been found to directly induce CXCL1 and CXCL8 production

(O'Hayer, Brady and Counter, 2009). Furthermore, blockade of chemokine signalling through CXCR2 has functional consequences in Ras-driven tumourigenesis. For example, genetic ablation of CXCR2 reduced Ras-driven tumourigenesis in the DMBA/TPA skin papilloma model (O'Hayer, Brady and Counter, 2009). Neutralisation of CXCR2 similarly decreased the size of $KRAS^{G12D}$-driven murine lung tumours (Wislez *et al.*, 2006). Mechanistically, Ras-induced CXCL8 required the concurrent activation of MAPK and PI3K pathways (Sparmann and Bar-Sagi, 2004). Though no studies have specifically explored an IL-22-*KRAS* interaction as it relates to chemokine production, Metz *et al.* recently found that IL-22 accounts for most, but not all CXC chemokine production in *Kras/Irs-1-/-* lung tumours (Metz *et al.*, 2016). Moreover, in line with our data, they demonstrated that IL-22 induced CXC chemokine production in *KRAS* mutant lung cancer cell lines (A549, H460), but not *KRAS* WT cell lines (201T, H1650) (Metz *et al.*, 2016). Administration of either a JAK1 selective antagonist or a JAK1/2 antagonist, reduced CXC chemokine expression in *Kras/Irs-1-/-* lung tumours, suggesting that the JAK/STAT pathway downstream of IL-22 is involved in the elevated CXC chemokine expression (Metz *et al.*, 2016). To date, we have not explored the biochemical mechanisms mediating the enhanced ELR^+ CXC chemokine expression following IL-22 stimulation in *KRAS* mutant human CRC cells and organoids. Therefore, IL-22 stimulation experiments using a panel of inhibitors which block JAK/STAT, NF-κB, ERK1/2, and PI3K pathways in *KRAS* mutant compared to wild type cell lines and organoids are warranted to determine which pathways are responsible for the synergistic or additive effect of IL-22 and mutant *KRAS* with respect to CXC chemokine production.

Several reports from lung inflammation and pancreatic cancer models have demonstrated that CXC chemokine production is highly TNFα/NF-κB-dependent (Liu *et al.*, 2011; Chao, Furth and Vonderheide, 2016). Moreover, some studies have highlighted a synergistic link between TNFα and IL-17A signalling in CXCL5 production in particular (Liu *et al.*, 2011). Therefore, it was surprising that in *KRAS* mutant but not wild type cells and organoids stimulated with supernatant generated from $CD4^+$ tumour infiltrating leukocytes, IL-22 blockade still partially diminished *CXCL1* and *CXCL5* expression. In the candidate TIL from which the supernatant used in these experiments was generated, the percentage of $CD4^+TNF\alpha^+$ and $CD4^+$IL-$17A^+$ cells was far greater than those expressing IL-22. Blockade of TNFα, but not IL-22, almost completely abrogated TIL-mediated *CXCL1* induction in *KRAS* wild type isogenic cells. By contrast, TNFα blockade reduced TIL-mediated *CXCL1* induction in *KRAS* mutant cells to a similar extent as IL-22 blockade. Moreover, enhanced *CXCL1* downregulation following dual TNFα and IL-22 blockade was not observed in *KRAS* mutant TIL-stimulated cells, suggesting the involvement of another factor. Given the known NF-κB dependency for ELR^+ CXC chemokine production, blockade of an IL-17A-driven NF-κB signal in combination with IL-22 blockade may be necessary for complete abrogation of TIL-induced chemokine production in *KRAS* mutant cells. If indeed, dual IL-17A/IL-22 blockade can attenuate ELR^+ CXC chemokine production in *KRAS* mutant cells, this would provide rationale to block upstream IL-23, which induces both IL-22 and IL-17A, in *KRAS* mutant CRC patients.

A key limitation of our current study is that the functional consequences of elevated ELR^+ CXC chemokine production following IL-22 stimulation in *KRAS* mutant CRC

have not been explored. *Ex vivo* assays using supernatants generated from IL-22-stimulated *KRAS* mutant versus wild type cells or organoids could be used in migration assays with human blood, to determine whether the chemotactic activity is higher in *KRAS* mutant compared to wild type cell-derived supernatant. Moreover, detailed FACS analysis of myeloid populations from freshly isolated CRC biopsies, comparing patients with *IL22RA1*-high, *KRAS* mutant to *IL22RA1*-high, *KRAS* wild type tumours is warranted. Transcriptomic analysis in the training cohort (GSE39582) revealed only modestly elevated *CXCR2* expression in proximal, *IL22RA1*-high, *KRAS* mutant versus proximal, *IL22RA1*-high, *KRAS* wild type tumours and an enriched neutrophil metagene signature was not detected (data not shown). However, we hypothesise that CXCR2 expressing myeloid populations would be enriched in *IL22RA1*-high, *KRAS* mutant tumours. The further difficulty in studying heterocellular signalling in human CRC *ex vivo* is that linking IL-22-enhanced ELR^+ chemokine expression to increased CXCR2-expressing myeloid infiltrates and the consequent impact on patient prognosis can only be done in a correlative manner. In a meta-analysis of nearly 4000 human tumours, high levels of tumour infiltrating neutrophils (the dominant CXCR2-expressing myeloid population) were found to confer poor relapse-free and overall survival across many cancer types (Shen *et al.*, 2014). Therefore, one might predict that a signalling program that potentiates neutrophil recruitment to tumours may confer poor prognosis. Importantly, in future studies using flow cytometric analysis to characterise myeloid infiltrates in *IL22RA1*-high, *KRAS* mutant versus wild type tumours, concurrent analysis of T cell populations is critical. Recently, CXCR2 blockade in the KPC murine pancreatic cancer model was shown to promote T cell infiltration into tumours and increase sensitivity to anti-PD-1 treatment (Steele *et al.*, 2016). Similarly, in a syngeneic

pancreatic ductal adenocarcinoma model, anti-tumourigenic IFNγ$^+$ CD4$^+$ and CD8$^+$ T cells were elevated in *Cxcr2-/-* compared to *Cxcr2+/+* hosts (Chao, Furth and Vonderheide, 2016). Moreover, in a rhabdomyosarcoma model, CXCR2 blockade reduced trafficking of CD11b$^+$Ly6G^{hi} MDSCs to tumours and increased the efficacy of delayed anti-PD1 treatment (Highfill *et al.*, 2014). Clearly, CXCR2 blockade can tip the balance to favour anti-tumour immunity. One might thus predict that IFNγ$^+$ CD4$^+$ and CD8$^+$ T cells in *IL22RA1*-high, *KRAS* mutant tumours may be reduced compared to their *KRAS* wild type counter parts. In the small cohort of polyclonally expanded T cells assessed in this study, we did not stratify patients based on *IL22RA1* or *KRAS* mutation due to insufficient numbers. Nevertheless, we reproducibly detected elevated IL-17$^+$IFNγ$^-$ CD4$^+$ T cells when comparing T cells expanded from tumour to matched normal adjacent tissue. Though to date, FACS-based immunophenotyping studies in human colorectal cancer are relatively limited; our data is consistent with cellular and gene expression data demonstrating that IL-17$^+$ T cells and Th17 cytokines are enriched in human CRC while Th1 cytokines (ie. IFNγ) are comparatively low (Blatner *et al.*, 2012; De Simone *et al.*, 2013, 2015; Girardin *et al.*, 2013). This enhanced Th17 signature in CRC has been associated with poor prognosis (Tosolini *et al.*, 2011).

Another mechanism by which IL-22 may favour an immune suppressive microenvironment in *KRAS* mutant CRC is through induction of *CD274*, encoding PD-L1. Differential expression interaction analysis revealed that *CD274* was uniquely induced by IL-22 and not IL-6 in *KRAS* mutant but not wild type DLD-1 isogenic cells. We validated this IL-22-dependent *CD274* induction in *KRAS* mutant organoids. Though these differences need to be confirmed at the protein level, this is

to our knowledge, the first report that IL-22 can induce transcription of *CD274* in colorectal cancer. However, through STAT3 occupation of the PD-L1 promoter, IL-25 has previously been shown to induce *CD274* transcription (Wang *et al.*, 2015). Interestingly, reports have demonstrated in human hepatocellular carcinoma and murine intestinal injury models that myeloid PD-L1 expression can favour IL-17A$^+$ versus IFNγ^+ Th22 cells and promote IL-22 production (Kuang *et al.*, 2014; Scandiuzzi *et al.*, 2014). Therefore, it is possible that tumoural PD-L1 expression, may similarly favour skewing toward IL-17A$^+$IL-22$^+$ T cell populations in the tumour microenvironment and actively suppress anti-tumour immunity. It is also interesting that this IL-22-induced *CD274* expression is specific to *KRAS* mutant cells. Ongoing efforts to study the relationship between oncogenic driving mutations and the expression of PD-L1 have not revealed that canonical *KRAS* mutations are associated with enhanced PD-L1 expression nor that oncogenic *KRAS G12D* can directly induce PD-L1 (Akbay *et al.*, 2013; Rech and Vonderheide, 2013). However, a recent study demonstrated for the first time that c-Myc can directly bind the *CD274* promoter in leukemia and lymphoma lines and induce *CD274* expression in hepatocellular carcinoma cells (Casey *et al.*, 2016; Casey, Baylot and Felsher, 2017). This rasies the possibility that the convergence of IL-22 and *KRAS* signalling on c-Myc is causal in the enhanced *CD274* expression observed. qPCR and flow cytometric assessment of *CD274*/PD-L1 following *MYC* knockdown and IL-22 stimulation is ongoing to test this.

In summary, our evidence points toward a unique interaction between IL-22 signalling and mutant *KRAS* that induces ELR$^+$ CXC chemokine production and tumour cell *CD274* expression. In a non-cell autonomous manner, these induced

factors may condition the tumour immune microenvironment to favour self-perpetuating protumourigeneic inflammation and subvert anti-tumour immunity.

5.3.3 IL-22-*KRAS* dependent induction of the master transcriptional regulator and proto-oncogene c-Myc: cell intrinsic mechanisms by which IL-22 synergises with mutant *KRAS* to promote malignancy

In addition to the non-cell autonomous mechanisms by which IL-22 and mutant *KRAS* may interact to promote malignancy, RNA-sequencing and proteomic analysis of IL-22 stimulated DLD-1 isogenic cells revealed the Myc pathway to be uniquely induced by IL-22 in *KRAS* mutant cells. In fact, differential interaction analysis of ssGSEA enrichment scores from RNA-sequenced samples, demonstrated that the Myc pathway was the only pathway induced by IL-22 and not IL-6 in *KRAS* mutant but not wild type cells. We have previously described (Chapter 3, Figure 3.16) that *IL22RA1*-high, *KRAS* mutant tumours preferentially classify as CMS2. Interestingly, CMS2 tumours are characterised by high expression of WNT and MYC downstream targets (Guinney *et al.*, 2015). Expression of *MYC* itself was elevated in *IL22RA1*-high, *KRAS* mutant compared to wild type tumours in the training cohort (GSE39582), though due to the narrow dynamic range of expression from the *MYC* probe on the Affymetrix array platform used, this requires confirmation prospectively. Likely due to low patient numbers in the subgroups of interest, we did not detect differences in *MYC* expression between *IL22RA1*-high, *KRAS* mutant and wild type tumours in whole tumour tissue collected prospectively. Interestingly however, *MYC* expression was highly correlated with *IL22RA1* expression, regardless of *KRAS* mutation status. This falls in line with our previous observation that independent of *KRAS* mutation status, *IL22RA1*-high tumours were enriched in CMS2 compared to *IL22RA1*-low tumours (Chapter 3, Figure 3.16). This observation was puzzling however, given that induction of *MYC* mRNA and protein upon IL-22 stimulation was greater in *KRAS*

mutant versus wild type cells and primary organoids. Though little is known about regulation of *IL22RA1* expression, to our knowledge there are no reports that it is a direct transcriptional target of c-Myc. We indeed confirmed following siRNA-mediated *MYC* knockdown that basal *IL22RA1* expression was unchanged in *KRAS* mutant DLD-1 cells. Therefore, we hypothesise that the correlation between *MYC* and *IL22RA1* is a consequence of active IL-22 signalling inducing *MYC* transcription. As we prospectively collect primary tumour tissue, giving more power to subgroup analyses, differences in *MYC* expression between *IL22RA1*-high, *KRAS* mutant and wild type tumours may emerge. Moreover, in subgroup analysis of prospectively collected tumour tissue, *IL22RA1*-high tumours were arbitrarily classified as those with *IL22RA1* expression in the top 33% of all specimens analysed to date. Since the specimens used for the analysis presented here were all collected in the past two years, survival data is not yet available to determine a proper cut-point on that basis.

It is important to emphasise that IL-22 modestly induces *MYC* at the transcript and protein level in *KRAS* wild type cells, but the magnitude of the induction is consistently lower than that in *KRAS* mutant cells. Indeed, the capacity of IL-22 to induce c-Myc, which is a critical lynchpin in cell proliferation, growth, and energy metabolism (Kress, Sabò and Amati, 2015), is part of the homeostatic function of IL-22 to facilitate damage repair. For many oncogenes, mutations in their coding regions that alter protein structure and function dictate their oncogenic behaviour. By contrast, the oncogenic activity of c-Myc is largely dictated by its aberrant overexpression and, in colorectal cancer, mutations within its coding sequence are very rare (Lang *et al.*, 1988; Kress, Sabò and Amati, 2015). Therefore dosing is important. c-Myc expression and stability is regulated at both the transcriptional and post-translational

level. Our evidence points toward both direct transcriptional induction and post-translational stabilization of c-Myc by IL-22 in *KRAS* mutant cells that results in sustained higher levels of active c-Myc. Previous reports have highlighted that *Myc* is a direct and possibly indirect STAT3 transcriptional target in transformed cells (Bromberg *et al.*, 1999; Kiuchi *et al.*, 1999; Bowman *et al.*, 2001). Logically, given that IL-22 is a well-described STAT3 activator, we predicted that *MYC* induction by IL-22 is STAT3-dependent. However, our preliminary analysis of *MYC* transcriptional induction following *STAT3* siRNA-mediated knockdown did not reveal that *MYC* induction in *KRAS* mutant cells was STAT3-dependent. This perhaps is not unexpected given that in our system, the induction of *MYC* and its downstream targets was uniquely regulated by IL-22 and not IL-6, another key STAT3 inducer. Moreover, activation of STAT3, as assessed by Y705 phosphorylation, was comparable between *KRAS* mutant and wild type isogenic cells (Chapter 4, Figure 4.10 B) and thus could not explain the differences in transcriptional induction following only 2 hour IL-22 stimulation in *KRAS* mutant versus wild type cells. Transcriptional regulation of the human *MYC* gene is complex (Lang *et al.*, 1988) and to date, not clearly understood. In haematological malignancies, transcriptional control of *MYC* by Notch1 has been reported (Palomero *et al.*, 2006; Sharma *et al.*, 2006; Weng *et al.*, 2006), while in medulloblastoma Hedgehog-dependent *MYC* transcription has been observed (Berman *et al.*, 2002). However in colorectal cancer, both *in vitro* in human cells lines and *in vivo* in murine models, *MYC/Myc* was found to be a target of the Wnt pathway. Specifically, β-catenin-bound T cell factor-4 (Tcf-4) transcriptionally activated *MYC/Myc* (He, 1998; van de Wetering *et al.*, 2002). Moreover the adenomatous phenotype in murine small intestine following loss of *Apc* could be rescued if *Myc* was simultaneously deleted (Sansom *et al.*, 2007). Future

experiments will explore the direct impact of the Wnt pathway on IL-22-mediated *MYC* transcription, however this may not explain the enhanced induction in *KRAS* mutant versus wild type cells.

Activated Ras was shown to increase the accumulation of transcriptionally active Myc nearly two decades ago (Sears *et al.*, 1999). Mechanistically, mitogen stimulation results in rapid activation of Ras and induction of Raf/ERK and PI3K/AKT pathways. c-Myc was found to be stabilized by ERK-mediated phosphorylation on its S62 residue (Sears, 2000). Concomitantly, AKT phosphorylates GSK3β on its S9 residue, that prevents GSK3β-mediated c-Myc phosphorylation on its T58 residue, which targets it for rapid proteasomal degradation (Sears, 2000). In our system, experiments in the *KRAS* mutant and wild type isogenic pair were performed in serum free conditions. Thus IL-22 served as the mitogen in this setting. Accumulation of c-Myc protein was observed over a 24-hour timecourse of IL-22 stimulation, specifically in *KRAS* mutant cells, suggesting enhanced c-Myc protein stability. Though we did not systematically dissect the biochemical mechanisms mediating this c-Myc accumulation, preliminary observations showed enhanced phosphorylation of c-Myc on its stabilizing S62 residue in *KRAS* mutant compared to wild type cells following 24 hour IL-22 stimulation. However at this time point, this is likely a consequence of enhanced c-Myc substrate in *KRAS* mutant versus wild type cells. Moreover, we have previously observed enhanced AKT (S473) phosphorylation following IL-22 stimulation in *KRAS* mutant versus wild type cells (Chapter 4, Figure 4.6 D). Theoretically, this could result in enhanced GSK3β (S9) phosphorylation and reduced c-Myc phosphorylation on its destabilising T58 residue (Figure 5.21). Unfortunately, our evaluation of c-Myc T58 phosphorylation was inconclusive due to multiple bands

detected with the polyclonal antibody used and needs to be evaluated with a cleaner monoclonal antibody. Interestingly, we have observed enhanced IL-22-mediated ribosomal S6 protein phosphorylation specifically in *KRAS* mutant cells that is rapamycin sensitive and thus potentially mTORC1-dependent (Chapter 4, Figure 4.10 C, D). S6K1 activity, downstream of mTORC1, has been shown to enhance c-Myc translation efficiency (Csibi *et al.*, 2014), presenting another potential pathway by which IL-22 and *KRAS* may synergise to aberrantly express c-Myc. These signalling networks are complex and multiple feed-forward mechanisms are likely present. For instance Wnt-driven ribosomal S6 expression has been found to be Myc-dependent (Faller *et al.*, 2014). Systematic inhibition of each of the aforementioned pathways in IL-22-stimulated *KRAS* mutant and wild type isogenic cells and organoids is necessary to determine which pathway(s) are responsible for the elevated stable c-Myc expression in IL-22 stimulated *KRAS* mutant versus wild type cells.

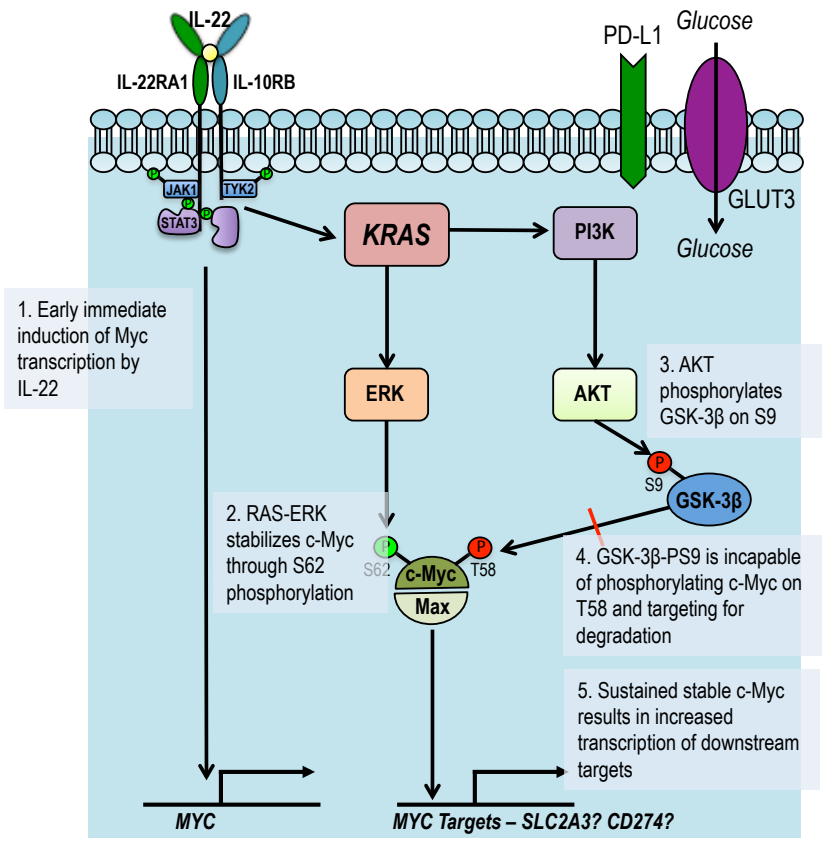


Figure 5.21 Theoretical mechanism by which IL-22 and *KRAS* signalling may sustain elevated levels of stable, active c-Myc.

1. *MYC* transcription is induced by IL-22 specifically in *KRAS* mutant cells after 2h IL-22 stimulation in an apparently non-STAT3-dependent manner. **2.** Elevated ERK1/2 signalling due to constitutively active *KRAS* phosphorylates c-Myc on an activating S62 residue. **3.** IL-22 induces AKT signalling resulting in phosphorylation of GSK-3β on an S9 residue. **4.** pGSK-3β cannot phosphorylate c-Myc on a T58 residue which targets it for proteasomal degredation. **5.** The result of these combined inputs is elevated levels of stable active c-Myc, resulting in enhanced transcription of Myc target genes. Recent reports have suggested that *CD274,* encoding PD-L1, is a direct Myc target (Casey *et al.*, 2016). *SLC2A3*, encoding GLUT3, may be a Myc target and its induction may enhance glycolytic rate upon IL-22 stimulation in *KRAS* mutant cells.

By solely focusing on positive regulation of c-Myc by IL-22 in *KRAS* mutant cells however, we may neglect the absence of induction of important Myc negative regulatory pathways. Intriguingly, FOXO1 was one of the mere 15 significantly differently regulated proteins in IL-22-stimulated *KRAS* wild type but not mutant cells. FOXO1 is a transcription factor and known negative regulator of c-MYC transcriptional activity (Peck, Ferber and Schulze, 2013; Wilhelm *et al.*, 2016). In *KRAS* wild type cells, it would be interesting to determine whether *FOXO1*

knockdown results in enhanced Myc target activation following IL-22 stimulation that is more comparable to *KRAS* mutant cells.

On a functional level, knockdown of *MYC* in *KRAS* mutant cells led to reduced basal and IL-22-induced cell proliferation. Following *MYC* knockdown, IL-22-induced *KRAS* mutant cell proliferation was more comparable to that in mock-transfected *KRAS* wild type isogenic cells. While c-Myc may be an important mediator of IL-22-induced cellular proliferation in *KRAS* mutant cells, this experiment does not provide definitive proof, as c-Myc is a critical regulator of basal cell growth. Following IL-22 stimulation in *MYC* knockdown *KRAS* mutant cells, c-Myc is still induced and there were modest, albeit insignificant, increases in cellular proliferation. Thus we can only infer, but not decisively conclude that Myc is a key driver of IL-22-induced cellular proliferation in *KRAS* mutant cells.

Myc target genes are diverse and abundant. Historically, there has been some controversy over whether c-Myc binds specific target genes or causes global transcriptional activation of genes with open loci (Lin *et al.*, 2012; Nie *et al.*, 2012; Kress, Sabò and Amati, 2015). Regardless, Myc is a well-established modulator of cellular metabolism and in malignant settings has been shown to enhance aerobic glycolysis (Dang, 2013). Mechanistically, Myc enhances expression of glucose transporters, promoting cellular glucose uptake. The glucose is then rapidly phosphorylated by the rate-limiting glycolytic enzyme, hexokinase 2, culminating in the production of pyruvate and release of ATP. Glycolytic intermediates are important substrates for amino acid, lipid, and nucleic acid biosynthesis and enhanced glycolytic flux increases their availability, providing the building blocks for cellular growth

(Dang, 2013). Given the rate of rapid glycolytic flux, pyruvate is converted to lactate in order to regenerate NAD^+ from NADH; a classical example of the Warburg effect (Dang, 2012, 2013; Carroll *et al.*, 2015). GSEA analysis of tumour transcriptomic data from the combined cohort revealed an enhanced glycolysis signature in *IL22RA1*-high, *KRAS* mutant versus wild type tumours. Functionally, RNA-sequencing analysis demonstrated that IL-22 rapidly induced transcription of *MYC, HK2* (encoding hexokinase 2), and *SLC2A3* (encoding the high capacity glucose transporter, GLUT3 (Simpson *et al.*, 2008)) specifically in *KRAS* mutant cells. Furthermore, proteomic analysis revealed enhanced GLUT3 protein expression following 24-hour IL-22 stimulation in *KRAS* mutant but not wild type cells. Lactate production was also enhanced with IL-22 stimulation in *KRAS* mutant cells and *MYC* knockdown attenuated this induced lactate production. Collectively, this evidence points toward enhanced glycolytic flux following IL-22-stimulation in *KRAS* mutant cells, possibly as a downstream consequence of IL-22-induced c-Myc. However, several questions still remain. First, it remains to be determined, using labelled glucose and GLUT3 knockdown, whether glucose uptake is enhanced in *KRAS* mutant cells upon IL-22 stimulation due to induced GLUT3 expression. If indeed this is the case, it would be very interesting to compare PET (positron emission tomography) scans of patients with *IL22RA1*-high, *KRAS* mutant versus wild type tumours to evaluate whether glucose consumption is elevated. Furthermore, in our experimental system, we have not definitively proven that GLUT3 protein induction is Myc-dependent (Figure 5.21). Simple western blot analysis of GLUT3 expression following *MYC* knockdown and IL-22 stimulation could provide the decisive evidence.

Thus here we have identified a plausible cell intrinsic mechanism by which IL-22 signalling into a *KRAS* mutant cell drives aberrant c-Myc expression, which may enhance cellular proliferation and glycolytic flux to drive malignant progression.

5.3.4 Concluding Remarks

In summary, taking unbiased approaches to identify candidate genes, proteins, and pathways that are uniquely regulated by IL-22 in *KRAS* mutant but not wild type cells, we have identified several plausible cell extrinsic and intrinsic modalities by which IL-22 drives malignancy in *KRAS* mutant CRC (Figure 5.19). The poor prognosis of *IL22RA1*-high, *KRAS* mutant patients is likely a consequence of the complex interplay between IL-22-induced secreted factors that sculpt a permissive inflammatory microenvironment, and direct modulation of intracellular signalling and metabolic pathways to promote tumour cell proliferation and survival.

The important question moving forward is whether any of the aforementioned pathways could be targeted in the clinic in combination with IL-22 or IL-23 blockade in *IL22RA1*-high, *KRAS* mutant tumours to enhance therapeutic efficacy. Certainly, a clinically relevant small molecule CXCR2 antagonist (AZ13381758) was recently shown to prolong survival and protect against metastasis in a murine pancreatic cancer model (Steele *et al.*, 2016) and CXCR2 antagonists are being investigated in early phase human trials. Careful dissection of the biochemical mechanisms mediating enhanced c-Myc protein stability in IL-22-stimulated *KRAS* mutant cells may lead to the identification of druggable intracellular targets in the upstream signalling pathways (ie. GSK3β or mTORC1). However, it was recently demonstrated that a small molecule inhibitor of the translation initiation factor eIF4A, which enhances Myc translation, was more efficacious than blockade of upstream signalling

pathways in reducing Myc expression in human CRC lines and suppressing tumour growth in murine models (Wiegering *et al.*, 2015). This small molecule inhibitor, silvestrol, may have clinical utility in *IL22RA1*-high, *KRAS* mutant CRC.

6 Final Discussion

6.1 Summary of findings

Despite evidence from murine models of both sporadic and colitis-associated colorectal cancer implicating IL-22 and upstream IL-23 in the initiation and progression of disease (Grivennikov *et al.*, 2012; Huber *et al.*, 2012; Kirchberger *et al.*, 2013a), an understanding of the consequences of IL-22 signalling in human CRC is limited. The work presented in this thesis was motivated by a primary aim to uncover the cellular and molecular mechanisms by which IL-22 contributes to the development and progression of human colorectal cancer.

Initially, we observed that mRNA expression of the upstream molecule responsible for IL-22 induction, *IL23A*, is almost universally elevated in human colorectal tumours compared to matched normal adjacent tissue. This finding is in accordance with previous observations made in smaller patient cohorts previously (Langowski *et al.*, 2006; Grivennikov *et al.*, 2012). It seems however, that the consequences of this elevated *IL23A* expression may be dependent on the mutational context of the tumour. By examining tumour transcriptomic data from training and validation cohorts totaling nearly 2000 CRC patients, we identified a novel and prognostically important interaction between the downstream IL-22 pathway and *KRAS* mutation. While neither IL-22 receptor expression nor *KRAS* mutation alone were strongly prognostic, the prognosis of patients with coincident high tumoural expression of *IL22RA1* and *KRAS* mutation was extremely poor. In an unbiased screen for other cytokines and cytokine receptors that interact with *KRAS* to influence prognosis, *IL10RB*, the second subunit of the heterodimeric IL-22R, was the highest hit next to *IL22RA1* itself. Patients with high expression of both IL-22R subunits in the context of mutant *KRAS* had reduced 5-year survival compared to those with high expression of either subunit

alone. Moreover, the detrimental effect of having a *KRAS* mutation in the context of high *IL22RA1* expression preferentially affected tumours in the proximal colon. Unlike in the distal colon, expression of *IL22* itself was significantly higher in proximal, *IL22RA1*-high, *KRAS* mutant tumours compared to proximal, *IL22RA1*-high, *KRAS* wild type tumours. While identification of this poor prognosis subtype of CRC may provide clinical utility in identifying patients who are predicted to be resistant to standard of care chemotherapy, this evidence also suggested a potential biological synergism between oncogenic *KRAS* and IL-22 signalling that promotes colorectal cancer progression.

Indeed, using a panel of CRC cell lines mirroring the clinical molecular subtypes of interest, we demonstrated that IL-22 enhances chemoresistance, clonogenic outgrowth and proliferation specifically in cells harbouring *KRAS* mutations with high IL-22RA1 expression. These findings were validated in an isogenic cell line pair with matched IL-22RA1 expression, differing only in the presence or absence of mutant *KRAS*. Moreover, IL-22 reproducibly induced proliferation in *KRAS* mutant primary colorectal cancer-derived organoids. This is, to our knowledge, the first evidence demonstrating a functional interaction between IL-22 and mutant *KRAS* in CRC. These findings underscore, perhaps unsurprisingly, that mutations in components of cytokine signalling pathways can alter the interpretation of a given cytokine signal to promote aberrant responses.

To identify the precise molecular mechanisms mediating this IL-22-*KRAS* interaction, we took unbiased transcriptomic and proteomic approaches to identify genes, proteins, and pathways uniquely regulated by IL-22 in *KRAS* mutant but not wild type

cells. ELR^+ CXC chemokines (*CXCL1*, *CXCL5*) were uniquely induced by IL-22 in *KRAS* mutant cells and primary organoids even in the context of a complex cytokine milieu derived from tumour-infiltrating leukocytes. These myeloid chemoattractants may recruit IL-23-expressing myeloid populations to the tumour microenvironment, resulting in increased IL-22 production and perpetuation of the protumourigenic inflammatory cycle. Additionally, the Myc pathway was the only pathway uniquely induced by IL-22 and not IL-6 in *KRAS* mutant but not wild type cells. c-Myc itself was induced in *KRAS* mutant IL-22-stimulated cells and primary organoids and its knockdown limited basal and IL-22-induced *KRAS* mutant cell proliferation and lactate production. Expression of the high capacity glucose transporter GLUT3, was augmented in *KRAS* mutant but not wild type cells and *IL22RA1*-high, *KRAS* mutant tumours displayed an enhanced glycolysis signature compared to their *KRAS* wild type counterparts. Thus, IL-22 may support malignancy in *KRAS* mutant cells through non-cell autonomous pathways that promote a permissive immune microenvironment, as well as through cell autonomous pathways that modulate master intracellular regulators of cell growth and metabolism.

Collectively, the evidence presented here points toward a method to both identify a subset of poor prognosis *KRAS* mutant CRC patients and to target these patients using immunomodulatory therapeutic blockade of the IL-22 pathway.

While the opportunities for clinical translation of this new knowledge are promising a number of unanswered scientific questions exist. The questions that directly follow on from the work presented in this thesis are summarized in Appendix 1 with descriptions of experimental methodology to approach each question.

6.2 Clinical translation

Ras mutations, were the first gain of function somatic mutations to be identified in human cancers (June, 2016). Activating mutations in *KRAS* occur in 40-45% of colorectal cancers (Sinicrope *et al.*, 2014). These patients are refractory to EGFR targeting therapies and variably resistant to some standard chemotherapies and therefore constitute a large population with unmet clinical need (Karapetis *et al.*, 2008; Bokemeyer and Bondarenko, 2011; Van Cutsem *et al.*, 2015). Despite decades of careful study, pharmacological targeting of mutant Ras with selective and safe inhibitors has hitherto been unsuccessful (McCormick, 2015). Thus Ras has been deemed an undruggable target. Attempts to block the downstream RAF-MAPK and PI3K pathways have had their own limitations due to redundancy and cross talk in these complex intracellular signalling networks. In the case of MEK inhibition for example, blockade of MEK in Ras mutant tumours results in loss of ERK1/2-dependent feedback inhibition and restores activation of the MEK-ERK pathway (Caunt *et al.*, 2015). Novel strategies to target mutant Ras have been tested in preclinical models and presented in clinical case reports in recent years. Nanoparticles carrying *KRAS*-targeting siRNA mediated regression of colorectal cancer in *KRAS*-driven xenograft models (Yuan *et al.*, 2014). Moreover, a patient with metastatic colorectal cancer was recently treated with *ex vivo* expanded autologous $CD8^+$ T cells with an HLA-C restricted T cell receptor that specifically recognized KRAS G12D and not wild type KRAS peptides. This adoptive transfer therapy initially mediated regression of seven lung metastases (Tran *et al.*, 2016), demonstrating the potential of immunotherapy for tumours with *KRAS* mutations. Despite the promise of immune checkpoint blockade in certain malignancies, until now only patients with microsatellite instable (MSI) colorectal cancer have shown objective responses (Le *et*

al., 2015; Llosa *et al.*, 2015). Emerging data from early stage clinical studies suggest that MEK-inhibition combined with anti-PD-L1 treatment in microsatellite stable, *KRAS* mutant colorectal tumours may augment MHCI expression on tumour cells, enhance T cell infiltration and improve responsiveness to anti-PD-L1. Though of 23 CRC patients enrolled in the study, responses were observed in only 3 patients after 4-7 months of treatment (Bendell, 2016). Perhaps in part because T cells infiltrating CRC tumours seem to be skewed toward a Th17 phenotype, despite potentiating T cell infiltration, the recruited T cells populations may not promote anti-tumour immunity. Strategies that block pro-tumourigenic immune responses, while augmenting anti-tumour immunity may be required for optimal therapeutic efficacy.

Abundant evidence from preclinical models of both colitis-associated and sporadic CRC point toward blockade of IL-22 or upstream IL-23 as a possible therapeutic strategy (Langowski *et al.*, 2006; S. Wu *et al.*, 2009; Grivennikov *et al.*, 2012; Huber *et al.*, 2012; Hyun *et al.*, 2012; Kirchberger *et al.*, 2013a; K. Wang *et al.*, 2014; Wang *et al.*, 2017). We have expanded on these studies by providing the first evidence (to our knowledge) in support of therapeutically targeting IL-23/IL-22 in a specific subset of human colorectal cancer patients, defined by tumours with high IL-22 receptor expression and oncogenic *KRAS* mutations. These patients are refractory to standard of care FOLFOX chemotherapy and have dramatically worsened relapse free and overall survival compared to their *KRAS* wild type counterparts. Our evidence predicts that roughly 19% of CRC patients fall into this poor prognosis subtype. *KRAS* mutation typing is already a component of routine clinical diagnostic assessment in colorectal cancer in the UK as *KRAS* mutations are contraindications to EGFR targeting therapies according to NICE guidelines (NICE, 2013). Current work

in our laboratory in collaboration with clinical pathologists is underway to prospectively determine a clinically relevant prognostic cutpoint of IL-22RA1 expression to use in a diagnostic immunohistochemical assay. Combining routine *KRAS* mutation typing with IL-22RA1 expression analysis would enable the identification of patients who might benefit from immunomodulatory IL-22/IL-23 blockade. Expedited clinical translational is in theory possible in this setting since monoclonal antibodies which target IL-22 and IL-23 have been developed for inflammatory indications and have proven safe in Phase I and II studies (NCT00563524, NCT00883896, NCT01866007, NCT02203032, NCT01225731). In particular, a new class of anti-IL-23p19 antibodies have shown remarkable success in psoriasis in the past two years (Gordon *et al.*, 2015; Kopp *et al.*, 2015). We have proposed and obtained funding for a novel Phase 0 window trial with biological endpoints utilising an existing IL-22/IL-23p19 targeting agent. Enrolled patients will receive a single infusion of anti-IL-22/anti-IL-23p19 in the window between diagnosis and colectomy. Pre-treatment endoscopic biopsies will be compared to post-treatment surgical resection tissue by performing whole tissue analysis and functional experiments in organoids to determine whether the therapeutic intervention modulated induction of genes/proteins (e.g. ELR^+ CXC chemokines) or pathways (e.g. Myc pathway) that are synergistically induced by IL-22 and mutant *KRAS*. Results from this study will guide the design of anti-IL-22/anti-23p19 trials with efficacy endpoints in CRC. The FOCUS4-C arm of the multi-site, molecularly stratified FOCUS-4 colorectal cancer trial lead by Professor Tim Maughan will recruit KRAS mutant patients and represents a clear pathway to efficacy testing of anti-IL-22/anti-IL23p19 therapy in stage IV patients. The results of these studies may define new guidelines for stratification of patients with *KRAS* mutant CRC and allow clinicians to stratify

patients to targeted therapy based not only upon a genetic signature, but the unique integration of a genetic and immune signature. Further pre-clinical work is required to determine whether blockade of CXCR2 (for which clinical grade agents are in early phase studies) or targeting c-Myc (with eIF4A targeting silvestrol, for example) may be used in combination with IL-22/IL-23p19 blockade to enhance therapeutic efficacy.

6.3 Limitations and new avenues

The promise of clinical translation also raises important questions about safety and efficacy across multiple cancer types. First, IL-22 has clear protective functions in models of acute intestinal epithelial damage (Zindl *et al.*, 2013) and in Th2-driven colitis (Sugimoto *et al.*, 2008). Moreover, two recent studies with combined evidence from pre-clinical models (DSS and T cell transfer colitis) and IBD patient samples have identified IL-22 binding protein (IL-22BP), which is overexpressed in IBD, to be a tractable therapeutic target (Martin *et al.*, 2016; Pelczar *et al.*, 2016). Overexpression of IL-22BP was found to limit the tissue protective function of IL-22 and exacerbate disease (Martin *et al.*, 2016; Pelczar *et al.*, 2016). Therefore, determining the appropriate timing to deploy IL-22 blockade in an overt cancer setting is critical. In an endpoints trial in stage IV patients, anti-IL-22 would be administered in the adjuvant setting (that is, following surgical resection). Given the importance of IL-22 for regeneration of intestinal tissue, it may be important to allow sufficient time for mucosal healing after colectomy before an IL-22 antagonist is administered.

It should be noted that all studies (including our own) linking IL-22 to CRC are based solely on analysis of primary tumours. Given that primary colorectal tumours are resectable in the majority of cases and do not often recur locally, distant metastases are ultimately the primary cause of CRC-related mortality (Read *et al.*, 2002). Therefore, it will be necessary to determine whether the IL-22-*KRAS* synergy observed in primary colorectal cancers is conserved in metastases. Interestingly, the two most common metastatic sites in colorectal cancer are the liver and lung (Riihimäki *et al.*, 2016). Some of the earliest descriptions of the physiologic function of IL-22 and its cognate receptor, IL-22RA1, came from the study of its capacity to induce acute-phase responses in the liver (Tachiiri *et al.*, 2003). Moreover, IL-22 has been shown to promote hepatocellular carcinoma (Jiang *et al.*, 2011). In the lung, IL-22 has important anti-microbial and tissue protective functions during acute infection (Aujla *et al.*, 2008), but many studies have implicated IL-22 in lung cancer development and progression, particularly in tumours driven by mutant *KRAS* (Kobold *et al.*, 2013; Khosravi *et al.*, 2016; Metz *et al.*, 2016). Thus the IL-22 pathway is active in the predominant metastatic sites of CRC. Lymphocyte-replete murine models of spontaneously metastasising CRC that harbour *KRAS* mutations will enable mechanistic dissection of the role of IL-22 in metastatic disease. This pre-clinical work must be coupled with the study, where possible, of paired biopsies from primary CRC and distant metastases to understand whether IL-22 receptor expression is stable or perhaps even elevated in metastases. Moreover, though difficult to obtain, organoids generated from fresh metastatic biopsy tissue would be valuable tools for exploring the IL-22-*KRAS* synergy.

Beyond metastatic CRC, expression of the IL-22 receptor is higher in the pancreas than in any other tissue (Gurney, 2004; Wolk *et al.*, 2004). Moreover, greater than 90% of pancreatic cancers harbour *KRAS* mutations and acquisition of *KRAS* mutations is thought to be an initiating event in the development of pancreatic ductal adenocarcinoma (McCormick, 2015). Though less frequent than CRC, pancreatic cancer is far more lethal and effective therapeutic strategies are limited (Ilic and Ilic, 2016). Furthermore, innate inflammation is a hallmark of pancreatic cancer and a driver of malignant progression (Elinav *et al.*, 2013). Thus investigation of the IL-22-*KRAS* interaction in pancreatic cancer is a logical next step and may lead to wider clinical utility of IL-22 pathway blockade in cancer.

Importantly, the data presented in this thesis have highlighted how cytokine responses can be quantitatively and qualitatively altered by specific oncogenic mutations. Synergies between cytokines and oncogenic driving mutations are not limited to IL-22 and *KRAS*. Exploration and exploitation of cytokine-oncogene interactions more broadly will be critical for precise patient stratification and the application of immunomodulatory therapies in cancer.

References

Acharyya, S., Oskarsson, T., Vanharanta, S., Malladi, S., Kim, J., Morris, P. G., Manova-Todorova, K., Leversha, M., Hogg, N., Seshan, V. E., Norton, L., Brogi, E. and Massagué, J. (2012) 'A CXCL1 paracrine network links cancer chemoresistance and metastasis', *Cell*, 150(1), pp. 165–178. doi: 10.1016/j.cell.2012.04.042.

Aden, K., Rehman, A., Falk-Paulsen, M., Secher, T., Kuiper, J., Tran, F., Pfeuffer, S., Sheibani-Tezerji, R., Breuer, A., Luzius, A., Jentzsch, M., H??sler, R., Billmann-Born, S., Will, O., Lipinski, S., Bharti, R., Adolph, T., Iovanna, J. L., Kempster, S. L., Blumberg, R. S., Schreiber, S., Becher, B., Chamaillard, M., Kaser, A. and Rosenstiel, P. (2016) 'Epithelial IL-23R Signaling Licenses Protective IL-22 Responses in Intestinal Inflammation', *Cell Reports*, 16(8), pp. 2208–2218. doi: 10.1016/j.celrep.2016.07.054.

Ahern, P. P., Schiering, C., Buonocore, S., McGeachy, M. J., Cua, D. J., Maloy, K. J. and Powrie, F. (2010) 'Interleukin-23 drives intestinal inflammation through direct activity on T cells.', *Immunity*, 33(2), pp. 279–288. doi: 10.1016/j.immuni.2010.08.010.

Akbay, E. A., Koyama, S., Carretero, J., Altabef, A., Tchaicha, J. H., Christensen, C. L., Mikse, O. R., Cherniack, A. D., Beauchamp, E. M., Pugh, T. J., Wilkerson, M. D., Fecci, P. E., Butaney, M., Reibel, J. B., Soucheray, M., Cohoon, T. J., Janne, P. A., Meyerson, M., Hayes, D. N., Shapiro, G. I., Shimamura, T., Sholl, L. M., Rodig, S. J., Freeman, G. J., Hammerman, P. S., Dranoff, G. and Wong, K.-K. (2013) 'Activation of the PD-1 Pathway Contributes to Immune Escape in EGFR-Driven Lung Tumors', *Cancer Discovery*, 3(12), pp. 1355–1363. doi: 10.1158/2159-8290.CD-13-0310.

Ancrile, B., Lim, K. K. and Counter, C. C. M. (2007) 'Oncogenic Ras-induced secretion of IL6 is required for tumorigenesis', *Genes & Development*, 21(919), pp. 1714–1719. doi: 10.1101/gad.1549407.1714.

Andoh, A., Zhang, Z., Inatomi, O., Fujino, S., Deguchi, Y., Araki, Y., Tsujikawa, T., Kitoh, K., Kim-Mitsuyama, S., Takayanagi, A., Shimizu, N. and Fujiyama, Y. (2005) 'Interleukin-22, a member of the IL-10 subfamily, induces inflammatory responses in colonic subepithelial myofibroblasts', *Gastroenterology*, 129(3), pp. 969–984. doi: 10.1053/j.gastro.2005.06.071.

Andtbacka, R. H. I., Kaufman, H. L., Collichio, F., Amatruda, T., Senzer, N., Chesney, J., Delman, K. A., Spitler, L. E., Puzanov, I., Agarwala, S. S., Milhem, M., Cranmer, L., Curti, B., Lewis, K., Ross, M., Guthrie, T., Linette, G. P., Daniels, G. A., Harrington, K., Middleton, M. R., Miller, W. H., Zager, J. S., Ye, Y., Yao, B., Li, A., Doleman, S., Van Der Walde, A., Gansert, J. and Coffin, R. S. (2015) 'Talimogene laherparepvec improves durable response rate in patients with advanced melanoma', *Journal of Clinical Oncology*, 33(25), pp. 2780–2788. doi: 10.1200/JCO.2014.58.3377.

Angevin, E., Tabernero, J., Elez, E., Cohen, S. J., Bahleda, R., van Laethem, J.-L., Ottensmeier, C., Lopez-Martin, J. a, Clive, S., Joly, F., Ray-Coquard, I., Dirix, L., Machiels, J.-P., Steven, N., Reddy, M., Hall, B., Puchalski, T. a, Bandekar, R., van de Velde, H., Tromp, B., Vermeulen, J. and Kurzrock, R. (2014) 'A Phase I/II, Multiple-Dose, Dose-Escalation Study of Siltuximab, an Anti-Interleukin-6 Monoclonal Antibody, in Patients with Advanced Solid Tumors', *Clinical Cancer Research*, 20(8), pp. 2192–2204. doi: 10.1158/1078-0432.CCR-13-2200.

Apte, R. N. and Voronov, E. (2002) 'Interleukin-1--a major pleiotropic cytokine in tumor-host interactions.', *Seminars in Cancer Biology*, 12(4), pp. 277–90.

Arnold, M., Sierra, M. S., Laversanne, M., Soerjomataram, I., Jemal, A. and Bray, F. (2017) 'Global patterns and trends in colorectal cancer incidence and mortality', *Gut*, 66(4), pp. 683–691. doi: 10.1136/gutjnl-2015-310912.

Artis, D. and Spits, H. (2015) 'The biology of innate lymphoid cells', *Nature*, 517(7534), pp. 293–301. doi: 10.1038/nature14189.

Asfaha, S., Dubeykovskiy, A. N., Tomita, H., Yang, X., Stokes, S., Shibata, W., Friedman, R. a., Ariyama, H., Dubeykovskaya, Z. a., Muthupalani, S., Ericksen, R., Frucht, H., Fox, J. G. and Wang, T. C. (2013) 'Mice that express human interleukin-8 have increased mobilization of immature myeloid cells, which exacerbates inflammation and accelerates colon carcinogenesis', *Gastroenterology*, 144(1), pp. 155–166. doi: 10.1053/j.gastro.2012.09.057.

Aujla, S. J., Chan, Y. R., Zheng, M., Fei, M., Askew, D. J., Pociask, D. A., Reinhart, T. A., McAllister, F., Edeal, J., Gaus, K., Husain, S., Kreindler, J. L., Dubin, P. J., Pilewski, J. M., Myerburg, M. M., Mason, C. A., Iwakura, Y. and Kolls, J. K. (2008) 'IL-22 mediates mucosal host defense against Gram-negative bacterial pneumonia', *Nature Medicine*, 14(3), pp. 275–81. doi: 10.1038/nm1710.

Balkwill, F. (2009) 'Tumour necrosis factor and cancer.', *Nature Reviews Cancer*, 9(5), pp. 361–71. doi: 10.1038/nrc2628.

Barker, N., Ridgway, R. a, van Es, J. H., van de Wetering, M., Begthel, H., van den Born, M., Danenberg, E., Clarke, A. R., Sansom, O. J. and Clevers, H. (2009) 'Crypt stem cells as the cells-of-origin of intestinal cancer', *Nature*, 457(7229), pp. 608–611. doi: 10.1038/nature07602.

Baumgart, S., Chen, N.-M., Siveke, J. T., König, A., Zhang, J.-S., Singh, S. K., Wolf, E., Bartkuhn, M., Esposito, I., Heßmann, E., Reinecke, J., Nikorowitsch, J., Brunner, M., Singh, G., Fernandez-Zapico, M. E., Smyrk, T., Bamlet, W. R., Eilers, M., Neesse, A., Gress, T. M., Billadeau, D. D., Tuveson, D., Urrutia, R. and Ellenrieder, V. (2014) 'Inflammation-Induced NFATc1-STAT3 Transcription Complex Promotes Pancreatic Cancer Initiation by KrasG12D.', *Cancer Discovery*, pp. 688–701. doi: 10.1158/2159-8290.CD-13-0593.

Becker, C., Fantini, M. C., Schramm, C., Lehr, H. A., Wirtz, S., Nikolaev, A., Burg, J., Strand, S., Kiesslich, R., Huber, S., Ito, H., Nishimoto, N., Yoshizaki, K., Kishimoto, T., Galle, P. R., Blessing, M., Rose-John, S. and Neurath, M. F. (2004) 'TGF-beta suppresses tumor progression in colon cancer by inhibition of IL-6 trans-signaling.', *Immunity*, 21(4), pp. 491–501. doi: 10.1016/j.immuni.2004.07.020.

Van Belle, A. B., de Heusch, M., Lemaire, M. M., Hendrickx, E., Warnier, G., Dunussi-Joannopoulos, K., Fouser, L. a, Renauld, J.-C. and Dumoutier, L. (2012) 'IL-22 Is Required for Imiquimod-Induced Psoriasiform Skin Inflammation in Mice', *The Journal of Immunology*, 188(1), pp. 462–469. doi: 10.4049/jimmunol.1102224.

Bendell, J. et al. (2016) 'Clinical activity and safety of cobimetinib (cobi) and atezolizumab in colorectal cancer (CRC)', *Journal of Clinical Oncology*, 34(suppl absr 3502).

Berman, D. M., Karhadkar, S. S., Hallahan, A. R., Pritchard, J. I., Eberhart, C. G., Watkins, D. N., Chen, J. K., Cooper, M. K., Taipale, J., Olson, J. M. and Beachy, P. A. (2002) 'Medulloblastoma Growth Inhibition by Hedgehog Pathway Blockade', *Science*, 297(5586), pp. 1559–1561. doi:

10.1126/science.1073733.

Beroukhim, R., Mermel, C. H., Porter, D., Wei, G., Raychaudhuri, S., Donovan, J., Barretina, J., Boehm, J. S., Dobson, J., Urashima, M., Mc Henry, K. T., Pinchback, R. M., Ligon, A. H., Cho, Y.-J., Haery, L., Greulich, H., Reich, M., Winckler, W., Lawrence, M. S., Weir, B. A., Tanaka, K. E., Chiang, D. Y., Bass, A. J., Loo, A., Hoffman, C., Prensner, J., Liefeld, T., Gao, Q., Yecies, D., Signoretti, S., Maher, E., Kaye, F. J., Sasaki, H., Tepper, J. E., Fletcher, J. A., Tabernero, J., Baselga, J., Tsao, M.-S., Demichelis, F., Rubin, M. A., Janne, P. A., Daly, M. J., Nucera, C., Levine, R. L., Ebert, B. L., Gabriel, S., Rustgi, A. K., Antonescu, C. R., Ladanyi, M., Letai, A., Garraway, L. A., Loda, M., Beer, D. G., True, L. D., Okamoto, A., Pomeroy, S. L., Singer, S., Golub, T. R., Lander, E. S., Getz, G., Sellers, W. R. and Meyerson, M. (2010) 'The landscape of somatic copy-number alteration across human cancers', *Nature*, 463(7283), pp. 899–905. doi: 10.1038/nature08822.

Besson, D., Pavageau, A.-H. A.-H., Valo, I., Bourreau, A., Belanger, A., Eymerit-Morin, C., Mouliere, A., Chassevent, A., Boisdron-Celle, M., Morel, A., Solassol, J., Campone, M., Gamelin, E., Barre, B., Coqueret, O., Guette, C., Bélanger, A., Eymerit-Morin, C., Moulière, A., Chassevent, A., Boisdron-Celle, M., Morel, A., Solassol, J., Campone, M., Gamelin, E., Barré, B., Coqueret, O. and Guette, C. (2011) 'A quantitative proteomic approach of the different stages of colorectal cancer establishes OLFM4 as a new nonmetastatic tumor marker.', *Molecular & cellular proteomics : MCP*, 10(12), p. M111.009712. doi: 10.1074/mcp.M111.009712.

Bi, Y., Cao, J., Jin, S., Lv, L., Qi, L., Liu, F., Geng, J. and Yu, Y. (2016) 'Interleukin-22 promotes lung cancer cell proliferation and migration via the IL-22R1/STAT3 and IL-22R1/AKT signaling pathways', *Molecular and Cellular Biochemistry*, 415(1–2). doi: 10.1007/s11010-016-2663-8.

Bindea, G., Mlecnik, B., Tosolini, M., Kirilovsky, A., Waldner, M., Obenauf, A. C., Angell, H., Fredriksen, T., Lafontaine, L., Berger, A., Bruneval, P., Speicher, M. R., Trajanoski, Z., Fridman, W. H., Becker, C., Page, F., Pagès, F., Speicher, M. R., Trajanoski, Z. and Galon, J. (2013) 'Spatiotemporal dynamics of intratumoral immune cells reveal the immune landscape in human cancer.', *Immunity*, 39(4), pp. 782–95. doi: 10.1016/j.immuni.2013.10.003.

Biswas, S., Chytil, A., Washington, K., Romero-Gallo, J., Gorska, A. E., Wirth, P. S., Gautam, S., Moses, H. L. and Grady, W. M. (2004) 'Transforming growth factor beta receptor type II inactivation promotes the establishment and progression of colon cancer.', *Cancer Research*, 64(14), pp. 4687–92. doi: 10.1158/0008-5472.CAN-03-3255.

Blatner, N. R., Bonertz, A., Beckhove, P., Cheon, E. C., Krantz, S. B., Strouch, M., Weitz, J., Koch, M., Halverson, A. L., Bentrem, D. J. and Khazaie, K. (2010) 'In colorectal cancer mast cells contribute to systemic regulatory T-cell dysfunction', *Proceedings of the National Academy of Sciences*, 107(14), pp. 6430–6435. doi: 10.1073/pnas.0913683107.

Blatner, N. R., Mulcahy, M. F., Dennis, K. L., Scholtens, D., Bentrem, D. J., Phillips, J. D., Ham, S., Sandall, B. P., Khan, M. W., Mahvi, D. M., Halverson, A. L., Stryker, S. J., Boller, A.-M., Singal, A., Sneed, R. K., Sarraj, B., Ansari, M. J., Oft, M., Iwakura, Y., Zhou, L., Bonertz, A., Beckhove, P., Gounari, F. and Khazaie, K. (2012) 'Expression of ROR t Marks a Pathogenic Regulatory T Cell Subset in Human Colon Cancer', *Science Translational Medicine*, 4(164). doi: 10.1126/scitranslmed.3004566.

Bogaert, J. and Prenen, H. (2014) 'Molecular genetics of colorectal cancer', *Annals of Gastroenterology*, 27, pp. 9–14. doi: 10.1146/annurev-pathol-011110-130235.

Bokemeyer, C. and Bondarenko, I. (2011) 'Efficacy according to biomarker status of cetuximab plus FOLFOX-4 as first-line treatment for metastatic colorectal cancer: the OPUS study', *Annals of Oncology*, 22(7), pp. 1535–46.

Bollrath, J., Phesse, T. J., von Burstin, V. a, Putoczki, T., Bennecke, M., Bateman, T., Nebelsiek, T., Lundgren-May, T., Canli, O., Schwitalla, S., Matthews, V., Schmid, R. M., Kirchner, T., Arkan, M. C., Ernst, M. and Greten, F. R. (2009) 'gp130-mediated Stat3 activation in enterocytes regulates cell survival and cell-cycle progression during colitis-associated tumorigenesis.', *Cancer Cell*, 15(2), pp. 91–102. doi: 10.1016/j.ccr.2009.01.002.

Bowman, T., Broome, M. A., Sinibaldi, D., Wharton, W., Pledger, W. J., Sedivy, J. M., Irby, R., Yeatman, T., Courtneidge, S. A. and Jove, R. (2001) 'Stat3-mediated Myc expression is required for Src transformation and PDGF-induced mitogenesis', *Proceedings of the National Academy of Sciences*, 98(13), pp. 7319–7324. doi: 10.1073/pnas.131568898.

Brahmer, J. R., Tykodi, S. S., Chow, L. Q. M., Hwu, W.-J., Topalian, S. L., Hwu, P., Drake, C. G., Camacho, L. H., Kauh, J., Odunsi, K., Pitot, H. C., Hamid, O., Bhatia, S., Martins, R., Eaton, K., Chen, S., Salay, T. M., Alaparthy, S., Grosso, J. F., Korman, A. J., Parker, S. M., Agrawal, S., Goldberg, S. M., Pardoll, D. M., Gupta, A. and Wigginton, J. M. (2012) 'Safety and Activity of Anti–PD-L1 Antibody in Patients with Advanced Cancer', *New England Journal of Medicine*, 366(26), pp. 2455–2465. doi: 10.1056/NEJMoa1200694.

Brand, S., Beigel, F., Olszak, T., Zitzmann, K., Eichhorst, S. T., Otte, J.-M., Diepolder, H., Marquardt, A., Jagla, W., Popp, A., Leclair, S., Herrmann, K., Seiderer, J., Ochsenkühn, T., Göke, B., Auernhammer, C. J. and Dambacher, J. (2006) 'IL-22 is increased in active Crohn's disease and promotes proinflammatory gene expression and intestinal epithelial cell migration.', *AJP: Gastrointestinal and Liver Physiology*, 290(4), pp. G827-38. doi: 10.1152/ajpgi.00513.2005.

Bresnick, Weber and Zimmer (2015) 'S100 proteins in cancer', *Nature Reviews Cancer*, 15(2), pp. 96–109. doi: 10.1038/nrc3893.

Bromberg, J. F., Wrzeszczynska, M. H., Devgan, G., Zhao, Y., Pestell, R. G., Albanese, C. and Darnell, J. E. (1999) 'Stat3 as an oncogene.', *Cell*, 98(3), pp. 295–303.

Brown, C. E., Alizadeh, D., Starr, R., Weng, L., Wagner, J. R., Naranjo, A., Ostberg, J. R., Blanchard, M. S., Kilpatrick, J., Simpson, J., Kurien, A., Priceman, S. J., Wang, X., Harshbarger, T. L., D'Apuzzo, M., Ressler, J. A., Jensen, M. C., Barish, M. E., Chen, M., Portnow, J., Forman, S. J. and Badie, B. (2016) 'Regression of Glioblastoma after Chimeric Antigen Receptor T-Cell Therapy', *New England Journal of Medicine*, 375(26), pp. 2561–2569. doi: 10.1056/NEJMoa1610497.

Buonocore, S., Ahern, P. P., Uhlig, H. H., Ivanov, I. I., Littman, D. R., Maloy, K. J. and Powrie, F. (2010) 'Innate lymphoid cells drive interleukin-23-dependent innate intestinal pathology.', *Nature*, 464(7293), pp. 1371–1375. doi: 10.1038/nature08949.

Burkett, P. R., Zu Horste, G. M. and Kuchroo, V. K. (2015) 'Pouring fuel on the fire: Th17 cells, the environment, and autoimmunity', *Journal of Clinical Investigation*, 125(6), pp. 2211–2219. doi: 10.1172/JCI78085.

Burnet, F. M. (1970) 'The concept of immunological surveillance.', *Progress in*

Experimental Tumor Research, 13, pp. 1–27.

Calon, A., Espinet, E., Palomo-Ponce, S., Tauriello, D. V. F., Iglesias, M., Céspedes, M. V., Sevillano, M., Nadal, C., Jung, P., Zhang, X. H.-F., Byrom, D., Riera, A., Rossell, D., Mangues, R., Massagué, J., Sancho, E. and Batlle, E. (2012) 'Dependency of colorectal cancer on a TGF-β-driven program in stromal cells for metastasis initiation.', *Cancer Cell*, 22(5), pp. 571–584. doi: 10.1016/j.ccr.2012.08.013.

Calon, A., Lonardo, E., Berenguer-Llergo, A., Espinet, E., Hernando-Momblona, X., Iglesias, M., Sevillano, M., Palomo-Ponce, S., Tauriello, D. V. F., Byrom, D., Cortina, C., Morral, C., Barceló, C., Tosi, S., Riera, A., Attolini, C. S.-O., Rossell, D., Sancho, E. and Batlle, E. (2015) 'Stromal gene expression defines poor-prognosis subtypes in colorectal cancer', *Nature Genetics*, 47(4), pp. 320–329. doi: 10.1038/ng.3225.

Cancer Genome Atlas Network and Muzny, D. M. (2012) 'Comprehensive molecular characterization of human colon and rectal cancer', *Nature*, 487(7407), pp. 330–337. doi: 10.1038/nature11252.

Carroll, P. A., Diolaiti, D., McFerrin, L., Gu, H., Djukovic, D., Du, J., Cheng, P. F., Anderson, S., Ulrich, M., Hurley, J. B., Raftery, D., Ayer, D. E. and Eisenman, R. N. (2015) 'Deregulated Myc Requires MondoA/Mlx for Metabolic Reprogramming and Tumorigenesis', *Cancer Cell*, 27(2), pp. 271–285. doi: 10.1016/j.ccell.2014.11.024.

Casey, S., Baylot, V. and Felsher, D. W. (2017) 'MYC: Master Regulator of Immune Privilege', *Trends in Immunology*, 38(4), pp. 298–305. doi: 10.1016/j.it.2017.01.002.

Casey, S., Tong, L., Li, Y., Do, R., Walz, S., Fitzgerald, K. N., Gouw, A. M., Baylot, V., Gutgemann, I., Eilers, M. and Felsher, D. W. (2016) 'MYC regulates the antitumor immune response through CD47 and PD-L1', *Science*, 352(6282), pp. 227–231. doi: 10.1126/science.aac9935.

Cassier, P. A., Italiano, A., Gomez-Roca, C. A., Le Tourneau, C., Toulmonde, M., Cannarile, M. A., Ries, C., Brillouet, A., Müller, C., Jegg, A.-M., Bröske, A.-M., Dembowski, M., Bray-French, K., Freilinger, C., Meneses-Lorente, G., Baehner, M., Harding, R., Ratnayake, J., Abiraj, K., Gass, N., Noh, K., Christen, R. D., Ukarma, L., Bompas, E., Delord, J.-P., Blay, J.-Y. and Rüttinger, D. (2015) 'CSF1R inhibition with emactuzumab in locally advanced diffuse-type tenosynovial giant cell tumours of the soft tissue: a dose-escalation and dose-expansion phase 1 study', *The Lancet Oncology*, 16(8), pp. 949–956. doi: 10.1016/S1470-2045(15)00132-1.

Caunt, C. J., Sale, M. J., Smith, P. D. and Cook, S. J. (2015) 'MEK1 and MEK2 inhibitors and cancer therapy: the long and winding road.', *Nature Reviews Cancer*, 15(10), pp. 577–92. doi: 10.1038/nrc4000.

Cendrowski, J., Mamińska, A. and Miaczynska, M. (2016) 'Endocytic regulation of cytokine receptor signaling', *Cytokine & Growth Factor Reviews*, 32, pp. 63–73. doi: 10.1016/j.cytogfr.2016.07.002.

Chae, W.-J., Gibson, T. F., Zelterman, D., Hao, L., Henegariu, O. and Bothwell, A. L. M. (2010) 'Ablation of IL-17A abrogates progression of spontaneous intestinal tumorigenesis', *Proceedings of the National Academy of Sciences*, 107(12), pp. 5540–5544. doi: 10.1073/pnas.0912675107.

Chao, T., Furth, E. E. and Vonderheide, R. H. (2016) 'CXCR2-Dependent Accumulation of Tumor-Associated Neutrophils Regulates T-cell Immunity in Pancreatic Ductal Adenocarcinoma', *Cancer Immunology Research*, 4(11), pp.

968–982. doi: 10.1158/2326-6066.CIR-16-0188.

Cheng, L., Eng, C., Nieman, L. Z., Kapadia, A. S. and Du, X. L. (2011) 'Trends in Colorectal Cancer Incidence by Anatomic Site and Disease Stage in the United States From 1976 to 2005', *American Journal of Clinical Oncology*, 34(6).

Cheng, P., Corzo, C. a, Luetteke, N., Yu, B., Nagaraj, S., Bui, M. M., Ortiz, M., Nacken, W., Sorg, C., Vogl, T., Roth, J. and Gabrilovich, D. I. (2008) 'Inhibition of dendritic cell differentiation and accumulation of myeloid-derived suppressor cells in cancer is regulated by S100A9 protein', *The Journal of Experimental Medicine*, 205(10), pp. 2235–2249. doi: 10.1084/jem.20080132.

Choi, S. Y. C., Gout, P. W., Collins, C. C. and Wang, Y. (2012) 'Epithelial immune cell-like transition (EIT): A proposed transdifferentiation process underlying immune-suppressive activity of epithelial cancers', *Differentiation*, 83(5), pp. 293–298. doi: 10.1016/j.diff.2012.02.005.

Chung, A. S., Wu, X., Zhuang, G., Ngu, H., Kasman, I., Zhang, J., Vernes, J., Jiang, Z., Meng, Y. G., Peale, F. V, Ouyang, W. and Ferrara, N. (2013) 'An interleukin-17–mediated paracrine network promotes tumor resistance to anti-angiogenic therapy', *Nature Medicine*, 19(9), pp. 1114–1123. doi: 10.1038/nm.3291.

Cooks, T., Harris, C. C. and Oren, M. (2014) 'Caught in the cross fire: p53 in inflammation.', *Carcinogenesis*, 35(8), pp. 1680–1690. doi: 10.1093/carcin/bgu134.

Cooks, T., Pateras, I. S., Tarcic, O., Solomon, H., Schetter, A. J., Wilder, S., Lozano, G., Pikarsky, E., Forshew, T., Rosenfeld, N., Rozenfeld, N., Harpaz, N., Itzkowitz, S., Harris, C. C., Rotter, V., Gorgoulis, V. G. and Oren, M. (2013) 'Mutant p53 prolongs NF-κB activation and promotes chronic inflammation and inflammation-associated colorectal cancer.', *Cancer Cell*, 23(5), pp. 634–46. doi: 10.1016/j.ccr.2013.03.022.

Corcoran, R. B., Contino, G., Deshpande, V., Tzatsos, A., Conrad, C., Benes, C. H., Levy, D. E., Settleman, J., Engelman, J. a and Bardeesy, N. (2011) 'STAT3 plays a critical role in KRAS-induced pancreatic tumorigenesis.', *Cancer Research*, 71(14), pp. 5020–9. doi: 10.1158/0008-5472.CAN-11-0908.

Couzin-Frankel, J. (2013) 'Cancer Immunotherapy', *Science*, 342(6165), pp. 1432–1433. doi: 10.1126/science.342.6165.1432.

Csibi, A., Lee, G., Yoon, S. O., Tong, H., Ilter, D., Elia, I., Fendt, S. M., Roberts, T. M. and Blenis, J. (2014) 'The mTORC1/S6K1 pathway regulates glutamine metabolism through the eif4b-dependent control of c-Myc translation', *Current Biology*, 24(19), pp. 2274–2280. doi: 10.1016/j.cub.2014.08.007.

Cua, D. J. and Tato, C. M. (2010) 'Innate IL-17-producing cells: the sentinels of the immune system', *Nature Reviews Immunology*, 10(7), pp. 479–489. doi: 10.1038/nri2800.

Cui, G., Yuan, A., Goll, R. and Florholmen, J. (2012) 'IL-17A in the tumor microenvironment of the human colorectal adenoma-carcinoma sequence.', *Scandinavian Journal of Gastroenterology*, 47(11), pp. 1304–1312. doi: 10.3109/00365521.2012.725089.

Van Cutsem, E., Lenz, H.-J., Kohne, C.-H., Heinemann, V., Tejpar, S., Melezinek, I., Beier, F., Stroh, C., Rougier, P., van Krieken, J. H. and Ciardiello, F. (2015) 'Fluorouracil, Leucovorin, and Irinotecan Plus Cetuximab Treatment and RAS Mutations in Colorectal Cancer', *Journal of Clinical Oncology*, 33(7), pp. 692–700. doi: 10.1200/JCO.2014.59.4812.

Dalla-Favera, R., Bregni, M., Eriksont, J. A. N., Pattersonf, D., Gallo, R. C. and

Crocet, C. M. (1982) 'Human c-myc onc gene is located on the region of chromosome 8 that is translocated in Burkitt lymphoma cells', *Proceedings of the National Academy of Sciences*, 79(24), pp. 7824–7827.

Damo, S. M., Kehl-Fie, T. E., Sugitani, N., Holt, M. E., Rathi, S., Murphy, W. J., Zhang, Y., Betz, C., Hench, L., Fritz, G., Skaar, E. P. and Chazin, W. J. (2013) 'Molecular basis for manganese sequestration by calprotectin and roles in the innate immune response to invading bacterial pathogens', *Proceedings of the National Academy of Sciences*, 110(10), pp. 3841–3846. doi: 10.1073/pnas.1220341110.

Dang, C. V. (2012) 'MYC on the Path to Cancer', *Cell*, 149(1), pp. 22–35. doi: 10.1016/j.cell.2012.03.003.

Dang, C. V. (2013) 'MYC, Metabolism, Cell Growth, and Tumorigenesis', *Cold Spring Harbor Perspectives in Medicine*, 3(8), pp. a014217–a014217. doi: 10.1101/cshperspect.a014217.

Dejea, C. M., Wick, E. C., Hechenbleikner, E. M., White, J. R., Mark Welch, J. L., Rossetti, B. J., Peterson, S. N., Snesrud, E. C., Borisy, G. G., Lazarev, M., Stein, E., Vadivelu, J., Roslani, A. C., Malik, A. a, Wanyiri, J. W., Goh, K. L., Thevambiga, I., Fu, K., Wan, F., Llosa, N., Housseau, F., Romans, K., Wu, X., McAllister, F. M., Wu, S., Vogelstein, B., Kinzler, K. W., Pardoll, D. M. and Sears, C. L. (2014) 'Microbiota organization is a distinct feature of proximal colorectal cancers', *Proceedings of the National Academy of Sciences*, 111(51), pp. 18321–18326. doi: 10.1073/pnas.1406199111.

Douglas, N. C., Jacobs, H., Bothwell, A. L. M. and Hayday, A. C. (2001) 'Defining the specific physiological requirements for c-Myc in T cell development', *Nature Immunology*, 2(4), pp. 307–315.

Drewes, J. L., Housseau, F. and Sears, C. L. (2016) 'Sporadic colorectal cancer: microbial contributors to disease prevention, development and therapy.', *British journal of cancer*, 115(3), pp. 273–80. doi: 10.1038/bjc.2016.189.

Duerr, R. H., Taylor, K. D., Brant, S. R., Rioux, J. D., Silverberg, M. S., Daly, M. J., Steinhart, A. H., Abraham, C., Regueiro, M., Griffiths, A., Dassopoulos, T., Bitton, A., Yang, H., Targan, S., Datta, L. W., Kistner, E. O., Schumm, L. P., Lee, A. T., Gregersen, P. K., Barmada, M. M., Rotter, J. I., Nicolae, D. L. and Cho, J. H. (2006) 'A Genome-Wide Association Study Identifies IL23R as an Inflammatory Bowel Disease Gene', *Science*, 314(5804), pp. 1461–1463. doi: 10.1126/science.1135245.

Dulai, P. S., Sandborn, W. J. and Gupta, S. (2016) 'Colorectal Cancer and Dysplasia in Inflammatory Bowel Disease: A Review of Disease Epidemiology, Pathophysiology, and Management', *Cancer Prevention Research*, 9(12), pp. 887–894. doi: 10.1158/1940-6207.CAPR-16-0124.

Dumoutier, L., de Meester, C., Tavernier, J. and Renauld, J.-C. (2009) 'New Activation Modus of STAT3: A Tyrosine-less region of the interleukin-22 receptor recruits STAT3 by interacting with its coiled-coil domain', *Journal of Biological Chemistry*, 284(39), pp. 26377–26384. doi: 10.1074/jbc.M109.007955.

DuPage, M. and Bluestone, J. A. (2016) 'Harnessing the plasticity of CD4+ T cells to treat immune-mediated disease', *Nature Reviews Immunology*, 16(3), pp. 149–163. doi: 10.1038/nri.2015.18.

Dvorak, H. F. (1986) 'Tumors: Wounds that do not heal. Similarities between tumor stroma generation and wound healing', *New England Journal of Medicine*, 315(26), pp. 1650–1659.

Eash, K. J., Greenbaum, A. M., Gopalan, P. K. and Link, D. C. (2010) 'CXCR2 and CXCR4 antagonistically regulate neutrophil trafficking from murine bone marrow', *Journal of Clinical Investigation*, 120(7), pp. 2423–2431. doi: 10.1172/JCI41649.

Ehrlich, P. (1909) 'The current state of cancer research (Über den jetzigen Stand der Karzinomforschung)', *Ned Tijdschr Geneeskd*, 5, pp. 273–90.

Elinav, E., Nowarski, R., Thaiss, C. a, Hu, B., Jin, C. and Flavell, R. a (2013) 'Inflammation-induced cancer: crosstalk between tumours, immune cells and microorganisms.', *Nature Reviews Cancer*, 13(11), pp. 759–71. doi: 10.1038/nrc3611.

Endam, L. M., Bossé, Y., Filali-Mouhim, A., Cormier, C., Boisvert, P., Boulet, L.-P., Hudson, T. J. and Desrosiers, M. (2009) 'Polymorphisms in the interleukin-22 receptor alpha-1 gene are associated with severe chronic rhinosinusitis.', *Otolaryngology--head and neck surgery*, 140(5), pp. 741–7. doi: 10.1016/j.otohns.2008.12.058.

Erdman, S. E., Rao, V. P., Poutahidis, T., Rogers, a B., Taylor, C. L., Jackson, E. a, Ge, Z., Lee, C. W., Schauer, D. B., Wogan, G. N., Tannenbaum, S. R. and Fox, J. G. (2009) 'Nitric oxide and TNF- trigger colonic inflammation and carcinogenesis in Helicobacter hepaticus-infected, Rag2-deficient mice', *Proceedings of the National Academy of Sciences*, 106(4), pp. 1027–1032. doi: 10.1073/pnas.0812347106.

Faller, W. J., Jackson, T. J., Knight, J. R. P., Ridgway, R. A., Jamieson, T., Karim, S. A., Jones, C., Radulescu, S., Huels, D. J., Myant, K. B., Dudek, K. M., Casey, H. A., Scopelliti, A., Cordero, J. B., Vidal, M., Pende, M., Ryazanov, A. G., Sonenberg, N., Meyuhas, O., Hall, M. N., Bushell, M., Willis, A. E. and Sansom, O. J. (2014) 'mTORC1-mediated translational elongation limits intestinal tumour initiation and growth', *Nature*, 517(7535), pp. 497–500. doi: 10.1038/nature13896.

Fearon, E. R. (2011) 'Molecular Genetics of Colorectal Cancer', *Annual Review of Pathology: Mechanisms of Disease*, 6(1), pp. 479–507. doi: 10.1146/annurev-pathol-011110-130235.

Fearon, E. R. and Vogelstein, B. (1990) 'A genetic model for colorectal tumorigenesis.', *Cell*, 61(5), pp. 759–67.

Finkelman, F. D., Pearce, E. J., Urban, J. F. and Sher, A. (1991) 'Regulation and biological function of helminth-induced cytokine responses', *Immunology Today*, 12(3), pp. A62–A66. doi: 10.1016/S0167-5699(05)80018-0.

Fleming, N. I., Jorissen, R. N., Mouradov, D., Christie, M., Sakthianandeswaren, A., Palmieri, M., Day, F., Li, S., Tsui, C., Lipton, L., Desai, J., Jones, I. T., McLaughlin, S., Ward, R. L., Hawkins, N. J., Ruszkiewicz, A. R., Moore, J., Zhu, H.-J., Mariadason, J. M., Burgess, A. W., Busam, D., Zhao, Q., Strausberg, R. L., Gibbs, P. and Sieber, O. M. (2013) 'SMAD2, SMAD3 and SMAD4 mutations in colorectal cancer.', *Cancer Research*, 73(2), pp. 725–35. doi: 10.1158/0008-5472.CAN-12-2706.

van der Flier, L. G., Haegebarth, A., Stange, D. E., van de Wetering, M. and Clevers, H. (2009) 'OLFM4 Is a Robust Marker for Stem Cells in Human Intestine and Marks a Subset of Colorectal Cancer Cells', *Gastroenterology*, 137(1), pp. 15–17. doi: 10.1053/j.gastro.2009.05.035.

Flores, M. B. S., Rocha, G. Z., Damas-Souza, D. M., Osório-Costa, F., Dias, M. M., Ropelle, E. R., Camargo, J. A., de Carvalho, R. B., Carvalho, H. F., Saad, M. J. A. and Carvalheira, J. B. C. (2012) 'Obesity-induced increase in tumor necrosis

factor-α leads to development of colon cancer in mice.', *Gastroenterology*, 143(3), pp. 741-53–4. doi: 10.1053/j.gastro.2012.05.045.

Foran, E., Garrity-Park, M. M., Mureau, C., Newell, J., Smyrk, T. C., Limburg, P. J. and Egan, L. J. (2010) 'Upregulation of DNA Methyltransferase-Mediated Gene Silencing, Anchorage-Independent Growth, and Migration of Colon Cancer Cells by Interleukin-6', *Molecular Cancer Research*, 8(4), pp. 471–481. doi: 10.1158/1541-7786.MCR-09-0496.

Franz, J., Jerome, J., Lear, T., Gong, Q. and Weathington, N. M. (2015) 'The Human IL-22 Receptor Is Regulated through the Action of the Novel E3 Ligase Subunit FBXW12, Which Functions as an Epithelial Growth Suppressor', *Journal of Immunology Research*, 2015, pp. 1–9. doi: 10.1155/2015/912713.

Gaffen, S. L., Jain, R., Garg, A. V and Cua, D. J. (2014) 'The IL-23–IL-17 immune axis: from mechanisms to therapeutic testing', *Nature Reviews Immunology*, 14(9), pp. 585–600. doi: 10.1038/nri3707.

Galandiuk, S., Rodriguezjusto, M., Jeffery, R., Nicholson, A. M., Cheng, Y., Oukrif, D., Elia, G., Leedham, S. J., McDonald, S. A. C., Wright, N. A. and Graham, T. A. (2012) 'Field cancerization in the intestinal epithelium of patients with Crohn's ileocolitis', *Gastroenterology*, 142(4), p. 855–864.e8. doi: 10.1053/j.gastro.2011.12.004.

Gao, C., Kozlowska, A., Nechaev, S., Li, H., Zhang, Q., Hossain, D. M. S., Kowolik, C. M., Chu, P., Swiderski, P., Diamond, D. J., Pal, S. K., Raubitschek, A. and Kortylewski, M. (2013) 'TLR9 signaling in the tumor microenvironment initiates cancer recurrence after radiotherapy.', *Cancer Research*, 73(24), pp. 7211–21. doi: 10.1158/0008-5472.CAN-13-1314.

Garfall, A. L., Maus, M. V., Hwang, W.-T., Lacey, S. F., Mahnke, Y. D., Melenhorst, J. J., Zheng, Z., Vogl, D. T., Cohen, A. D., Weiss, B. M., Dengel, K., Kerr, N. D. S., Bagg, A., Levine, B. L., June, C. H. and Stadtmauer, E. A. (2015) 'Chimeric Antigen Receptor T Cells against CD19 for Multiple Myeloma', *New England Journal of Medicine*, 373(11), pp. 1040–1047. doi: 10.1056/NEJMoa1504542.

Gazzinelli, R. T., Hakim, F. T., Hieny, S., Shearer, G. M. and Sher, A. (1991) 'Synergistic role of CD4+ and CD8+ T lymphocytes in IFN-gamma production and protective immunity induced by an attenuated Toxoplasma gondii vaccine', *J Immunol*, 146(1), pp. 286–292.

Gelebart, P., Zak, Z., Dien-Bard, J., Anand, M. and Lai, R. (2011) 'Interleukin 22 signaling promotes cell growth in mantle cell lymphoma.', *Translational oncology*, 4(1), pp. 9–19. doi: http://dx.doi.org/10.1593/tlo.10172.

Geremia, A., Arancibia-Cárcamo, C. V, Fleming, M. P. P., Rust, N., Singh, B., Mortensen, N. J., Travis, S. P. L. and Powrie, F. (2011) 'IL-23-responsive innate lymphoid cells are increased in inflammatory bowel disease.', *The Journal of Experimental Medicine*, 208(6), pp. 1127–1133. doi: 10.1084/jem.20101712.

Germain, R. N. (1994) 'MHC-dependent antigen processing and peptide presentation: Providing ligans for T lymphocyte activation', *Cell*, 76, pp. 287–299. doi: 10.1016/0092-8674(94)90336-0.

Germain, R. N. (2002) 'T-cell development and the CD4–CD8 lineage decision', *Nature Reviews Immunology*, 2(5), pp. 309–322. doi: 10.1038/nri798.

Gersemann, M., Becker, S., Nuding, S., Antoni, L., Ott, G., Fritz, P., Oue, N., Yasui, W., Wehkamp, J. and Stange, E. F. (2012) 'Olfactomedin-4 is a glycoprotein secreted into mucus in active IBD', *Journal of Crohn's and Colitis*, 6(4), pp.

425–434. doi: 10.1016/j.crohns.2011.09.013.

Ghoreschi, K., Laurence, A., Yang, X.-P., Tato, C. M., McGeachy, M. J., Konkel, J. E., Ramos, H. L., Wei, L., Davidson, T. S., Bouladoux, N., Grainger, J. R., Chen, Q., Kanno, Y., Watford, W. T., Sun, H.-W., Eberl, G., Shevach, E. M., Belkaid, Y., Cua, D. J., Chen, W. and O'Shea, J. J. (2010) 'Generation of pathogenic TH17 cells in the absence of TGF-β signalling', *Nature*, 467(7318), pp. 967–971. doi: 10.1038/nature09447.

Girardin, A., McCall, J., Black, M. A., Edwards, F., Phillips, V., Taylor, E. S., Reeve, A. E. and Kemp, R. a (2013) 'Inflammatory and regulatory T cells contribute to a unique immune microenvironment in tumor tissue of colorectal cancer patients', *International Journal of Cancer*, 132(8), pp. 1842–1850. doi: 10.1002/ijc.27855.

González-Aguilera, J. J., Oliart, S., Azcoita, M. M. and Fernández-Peralta, A. M. (2004) 'Simultaneous Mutations in K-ras and TP53 Are Indicative of Poor Prognosis in Sporadic Colorectal Cancer.', *American Journal of Clinical Oncology*, 27(1), pp. 39–45.

Gordon, K. B., Duffin, K. C., Bissonnette, R., Prinz, J. C., Wasfi, Y., Li, S., Shen, Y.-K., Szapary, P., Randazzo, B. and Reich, K. (2015) 'A Phase 2 Trial of Guselkumab versus Adalimumab for Plaque Psoriasis', *New England Journal of Medicine*, 373(2), pp. 136–144. doi: 10.1056/NEJMoa1501646.

Gordon, M. A., Gil, J., Lu, B., Zhang, W., Yang, D., Yun, J., Schneider, S., Groshen, S., Iqbal, S., Press, O. A., Rhodes, K. and Lenz, H.-J. (2005) 'Genomic profiling associated with recurrence in patients with rectal cancer treated with chemoradiation', *Pharmacogenomics*, 7(1), pp. 67–88. doi: 10.2217/14622416.7.1.67.

Grady, W. M. and Carethers, J. M. (2008) 'Genomic and Epigenetic Instability in Colorectal Cancer Pathogenesis', *Gastroenterology*, 135(4), pp. 1079–1099. doi: 10.1053/j.gastro.2008.07.076.

Gravina, G. L., Festuccia, C., Marampon, F., Popov, V. M., Pestell, R. G., Zani, B. M. and Tombolini, V. (2010) 'Biological rationale for the use of DNA methyltransferase inhibitors as new strategy for modulation of tumor response to chemotherapy and radiation.', *Molecular Cancer*, 9(1), p. 305. doi: 10.1186/1476-4598-9-305.

Grivennikov, S., Greten, F. R. and Karin, M. (2010) 'Immunity, Inflammation, and Cancer', *Cell*. doi: 10.1016/j.cell.2010.01.025.

Grivennikov, S., Karin, E., Terzic, J., Mucida, D., Yu, G.-Y., Vallabhapurapu, S., Scheller, J., Rose-John, S., Cheroutre, H., Eckmann, L. and Karin, M. (2009) 'IL-6 and Stat3 Are Required for Survival of Intestinal Epithelial Cells and Development of Colitis-Associated Cancer', *Cancer Cell*, 15(2), pp. 103–113. doi: 10.1016/j.ccr.2009.01.001.

Grivennikov, S. and Karin, M. (2010) 'Dangerous liaisons: STAT3 and NF-kappaB collaboration and crosstalk in cancer.', *Cytokine & Growth Factor Reviews*, 21(1), pp. 11–9. doi: 10.1016/j.cytogfr.2009.11.005.

Grivennikov, S. and Karin, M. (2011) 'Inflammatory cytokines in cancer: tumour necrosis factor and interleukin 6 take the stage', *Annals of the Rheumatic Diseases*, 70(Suppl 1), pp. i104–i108. doi: 10.1136/ard.2010.140145.

Grivennikov, S., Wang, K., Mucida, D., Stewart, C. A., Schnabl, B., Jauch, D., Taniguchi, K., Yu, G.-Y., Osterreicher, C. H., Hung, K. E., Datz, C., Feng, Y., Fearon, E. R., Oukka, M., Tessarollo, L., Coppola, V., Yarovinsky, F., Cheroutre, H., Eckmann, L., Trinchieri, G. and Karin, M. (2012) 'Adenoma-

linked barrier defects and microbial products drive IL-23/IL-17-mediated tumour growth.', *Nature*, 491(7423), pp. 254–8. doi: 10.1038/nature11465.

Gu, L., Talati, P., Vogiatzi, P., Romero-Weaver, A. L., Abdulghani, J., Liao, Z., Leiby, B., Hoang, D. T., Mirtti, T., Alanen, K., Zinda, M., Huszar, D. and Nevalainen, M. T. (2014) 'Pharmacologic suppression of JAK1/2 by JAK1/2 inhibitor AZD1480 potently inhibits IL-6-induced experimental prostate cancer metastases formation.', *Molecular Cancer Therapeutics*, 13(5), pp. 1246–1258. doi: 10.1158/1535-7163.MCT-13-0605.

Guidoboni, M., Gafà, R., Viel, a, Doglioni, C., Russo, a, Santini, a, Del Tin, L., Macrì, E., Lanza, G., Boiocchi, M. and Dolcetti, R. (2001) 'Microsatellite instability and high content of activated cytotoxic lymphocytes identify colon cancer patients with a favorable prognosis.', *The American journal of pathology*, 159(1), pp. 297–304. doi: 10.1016/S0002-9440(10)61695-1.

Guinney, J., Dienstmann, R., Wang, X., de Reyniès, A., Schlicker, A., Soneson, C., Marisa, L., Roepman, P., Nyamundanda, G., Angelino, P., Bot, B. M., Morris, J. S., Simon, I. M., Gerster, S., Fessler, E., De Sousa E Melo, F., Missiaglia, E., Ramay, H., Barras, D., Homicsko, K., Maru, D., Manyam, G. C., Broom, B., Boige, V., Perez-Villamil, B., Laderas, T., Salazar, R., Gray, J. W., Hanahan, D., Tabernero, J., Bernards, R., Friend, S. H., Laurent-Puig, P., Medema, J. P., Sadanandam, A., Wessels, L., Delorenzi, M., Kopetz, S., Vermeulen, L. and Tejpar, S. (2015) 'The consensus molecular subtypes of colorectal cancer', *Nature Medicine*, 21(11), pp. 1350–1356. doi: 10.1038/nm.3967.

Gurney, A. L. (2004) 'IL-22, a Th1 cytokine that targets the pancreas and select other peripheral tissues.', *International Immunopharmacology*, 4(5), pp. 669–77. doi: 10.1016/j.intimp.2004.01.016.

Hale, L. P. and Greer, P. K. (2012) 'A novel murine model of inflammatory bowel disease and inflammation-associated colon cancer with ulcerative colitis-like features.', *PloS one*, 7(7), p. e41797. doi: 10.1371/journal.pone.0041797.

Halvorsen, T. B. and Seim, E. (1988) 'Degree of differentiation in colorectal adenocarcinomas: a multivariate analysis of the influence on survival.', *Journal of Clinical Pathology*, 41(5), pp. 532–537. doi: 10.1136/jcp.41.5.532.

Hanahan, D. and Weinberg, R. a (2011) 'Hallmarks of cancer: the next generation.', *Cell*, 144(5), pp. 646–74. doi: 10.1016/j.cell.2011.02.013.

Hanash, A. M., Dudakov, J. a, Hua, G., O'Connor, M. H., Young, L. F., Singer, N. V, West, M. L., Jenq, R. R., Holland, A. M., Kappel, L. W., Ghosh, A., Tsai, J. J., Rao, U. K., Yim, N. L., Smith, O. M., Velardi, E., Hawryluk, E. B., Murphy, G. F., Liu, C., Fouser, L. A., Kolesnick, R., Blazar, B. R. and van den Brink, M. R. M. (2012) 'Interleukin-22 protects intestinal stem cells from immune-mediated tissue damage and regulates sensitivity to graft versus host disease.', *Immunity*, 37(2), pp. 339–50. doi: 10.1016/j.immuni.2012.05.028.

Hannan, K. M., Sanij, E., Hein, N., Hannan, R. D. and Pearson, R. B. (2011) 'Signaling to the ribosome in cancer-It is more than just mTORC1', *IUBMB Life*, 63(2), pp. 79–85. doi: 10.1002/iub.428.

Harrington, L. E., Hatton, R. D., Mangan, P. R., Turner, H., Murphy, T. L., Murphy, K. M. and Weaver, C. T. (2005) 'Interleukin 17-producing CD4+ effector T cells develop via a lineage distinct from the T helper type 1 and 2 lineages.', *Nature Immunology*, 6(11), pp. 1123–32. doi: 10.1038/ni1254.

Harrison, O. J., Srinivasan, N., Pott, J., Schiering, C., Krausgruber, T., Ilott, N. E. and Maloy, K. J. (2015) 'Epithelial-derived IL-18 regulates Th17 cell differentiation and Foxp3^{+} Treg cell function in the intestine.', *Mucosal Immunology*, 8(6), pp.

1226–36. doi: 10.1038/mi.2015.13.

Hawinkels, L. J. A. C., Paauwe, M., Verspaget, H. W., Wiercinska, E., van der Zon, J. M., van der Ploeg, K., Koelink, P. J., Lindeman, J. H. N., Mesker, W., ten Dijke, P. and Sier, C. F. M. (2014) 'Interaction with colon cancer cells hyperactivates TGF-β signaling in cancer-associated fibroblasts.', *Oncogene*, 33(1), pp. 97–107. doi: 10.1038/onc.2012.536.

He, D., Li, H., Yusuf, N., Elmets, C. a, Li, J., Mountz, J. D. and Xu, H. (2010) 'IL-17 Promotes Tumor Development through the Induction of Tumor Promoting Microenvironments at Tumor Sites and Myeloid-Derived Suppressor Cells', *The Journal of Immunology*, 184(5), pp. 2281–2288. doi: 10.4049/jimmunol.0902574.

He, T.-C. (1998) 'Identification of c-MYC as a Target of the APC Pathway', *Science*, 281(5382), pp. 1509–1512. doi: 10.1126/science.281.5382.1509.

Hickish, T., Andre, T., Wyrwicz, L., Saunders, M., Sarosiek, T., Kocsis, J., Nemecek, R., Rogowski, W., Lesniewski-Kmak, K., Petruzelka, L., Apte, R. N., Mohanty, P., Stecher, M., Simard, J. and de Gramont, A. (2017) 'MABp1 as a novel antibody treatment for advanced colorectal cancer: a randomised, double-blind, placebo-controlled, phase 3 study', *The Lancet Oncology*, 18(2), pp. 192–201. doi: 10.1016/S1470-2045(17)30006-2.

Highfill, S. L., Cui, Y., Giles, A. J., Smith, J. P., Zhang, H., Morse, E., Kaplan, R. N. and Mackall, C. L. (2014) 'Disruption of CXCR2-Mediated MDSC Tumor Trafficking Enhances Anti-PD1 Efficacy', *Science Translational Medicine*, 6(237), p. 237ra67-237ra67. doi: 10.1126/scitranslmed.3007974.

Hoogwater, F. J. H., Nijkamp, M. W., Smakman, N., Steller, E. J. a, Emmink, B. L., Westendorp, B. F., Raats, D. a E., Sprick, M. R., Schaefer, U., Van Houdt, W. J., De Bruijn, M. T., Schackmann, R. C. J., Derksen, P. W. B., Medema, J.-P., Walczak, H., Borel Rinkes, I. H. M. and Kranenburg, O. (2010) 'Oncogenic K-Ras turns death receptors into metastasis-promoting receptors in human and mouse colorectal cancer cells.', *Gastroenterology*, 138(7), pp. 2357–2367. doi: 10.1053/j.gastro.2010.02.046.

Hu, W.-H., Chen, H.-H., Yen, S.-L., Huang, H.-Y., Hsiao, C.-C. and Chuang, J.-H. (2017) 'Increased expression of interleukin-23 associated with progression of colorectal cancer', *Journal of Surgical Oncology*, 115(2), pp. 208–212. doi: 10.1002/jso.24505.

Huang, L., Hu, B., Ni, J., Wu, J., Jiang, W., Chen, C., Yang, L., Zeng, Y., Wan, R., Hu, G. and Wang, X. (2016) 'Transcriptional repression of SOCS3 mediated by IL-6/STAT3 signaling via DNMT1 promotes pancreatic cancer growth and metastasis', *Journal of Experimental & Clinical Cancer Research*, 35(1), p. 27. doi: 10.1186/s13046-016-0301-7.

Hubbard, J., O'Neil, B., Jonker, D., Halfdanarson, T., Starodub, A., Grothey, A., Borodyansky, L. and Li, C. (2016) 'Phase Ib study of cancer stem cell (CSC) pathway inhibitor BBI-608 administered in combination with FOLFIRI with and without bevacizumab (Bev) in patients (pts) with advanced colorectal cancer (CRC)', *Journal of Clinical Oncology*, 34(suppl 4S), p. abstr 569.

Huber, S., Gagliani, N., Zenewicz, L. a, Huber, F. J., Bosurgi, L., Hu, B., Hedl, M., Zhang, W., O'Connor, W., Murphy, A. J., Valenzuela, D. M., Yancopoulos, G. D., Booth, C. J., Cho, J. H., Ouyang, W., Abraham, C. and Flavell, R. A. (2012) 'IL-22BP is regulated by the inflammasome and modulates tumorigenesis in the intestine.', *Nature*, 491(7423), pp. 259–63. doi: 10.1038/nature11535.

Hussain, S. P., Amstad, P., Raja, K., Ambs, S., Nagashima, M., Bennett, W. P.,

Shields, P. G., Ham, A. J., Swenberg, J. A., Marrogi, A. J. and Harris, C. C. (2000) 'Increased p53 mutation load in noncancerous colon tissue from ulcerative colitis: a cancer-prone chronic inflammatory disease.', *Cancer Research*, 60(13), pp. 3333–7.

Hwang, W., Yang, M., Tsai, M., Lan, H., Su, S., Chang, S., Teng, H., Yang, S., Lan, Y., Chiou, S. and Wang, H. (2011) 'SNAIL regulates interleukin-8 expression, stem celllike activity, and tumorigenicity of human colorectal carcinoma cells', *Gastroenterology*, 141, pp. 279–291. doi: 10.1053/j.gastro.2011.04.008.

Hyun, Y. S., Han, D. S., Lee, A. R., Eun, C. S., Youn, J. and Kim, H.-Y. (2012) 'Role of IL-17A in the development of colitis-associated cancer', *Carcinogenesis*, 33(4), pp. 931–936. doi: 10.1093/carcin/bgs106.

Ichikawa, M., Williams, R., Wang, L., Vogl, T. and Srikrishna, G. (2011) 'S100A8/A9 Activate Key Genes and Pathways in Colon Tumor Progression', *Molecular Cancer Research*, 9(2), pp. 133–148. doi: 10.1158/1541-7786.MCR-10-0394.

Ilic, M. and Ilic, I. (2016) 'Epidemiology of pancreatic cancer', *World Journal of Gastroenterology*, 22(44), pp. 9694–9705. doi: 10.3748/wjg.v22.i44.9694.

Ivanov, I. I., McKenzie, B. S., Zhou, L., Tadokoro, C. E., Lepelley, A., Lafaille, J. J., Cua, D. J. and Littman, D. R. (2006) 'The Orphan Nuclear Receptor ROR-gamma t Directs the Differentiation Program of Proinflammatory IL-17+ T Helper Cells', *Cell*, 126(6), pp. 1121–1133. doi: 10.1016/j.cell.2006.07.035.

Iwasaki, A. and Medzhitov, R. (2015) 'Control of adaptive immunity by the innate immune system', *Nature Immunology*, 16(4), pp. 343–353. doi: 10.1038/ni.3123.

Jamieson, T., Clarke, M., Steele, C. W., Samuel, M. S., Neumann, J., Jung, A., Huels, D., Olson, M. F., Das, S., Nibbs, R. J. B. and Sansom, O. J. (2012) 'Inhibition of CXCR2 profoundly suppresses inflammation-driven and spontaneous tumorigenesis', *Journal of Clinical Investigation*, 122(9), pp. 3127–3144. doi: 10.1172/JCI61067.

Janeway, C. a (1989) 'Approaching the asymptote? Evolution and revolution in immunology.', *Cold Spring Harbour Symposium Quantitative Biology*, 54, pp. 1–13.

Janeway, C. a (1992) 'The T Cell Receptor as a Multicomponent Signalling Machine: CD4/CD8 Coreceptors and CD45 in T Cell Activation', *Annual Review of Immunology*, 10(1), pp. 645–674. doi: 10.1146/annurev.iy.10.040192.003241.

Jatoi, A., Dakhil, S. R., Nguyen, P. L., Sloan, J. a, Kugler, J. W., Rowland, K. M., Soori, G. S., Wender, D. B., Fitch, T. R., Novotny, P. J. and Loprinzi, C. L. (2007) 'A placebo-controlled double blind trial of etanercept for the cancer anorexia/weight loss syndrome: results from N00C1 from the North Central Cancer Treatment Group.', *Cancer*, 110(6), pp. 1396–1403. doi: 10.1002/cncr.22944.

Jess, T., Rungoe, C. and Peyrin–Biroulet, L. (2012) 'Risk of Colorectal Cancer in Patients With Ulcerative Colitis: A Meta-analysis of Population-Based Cohort Studies', *Clinical Gastroenterology and Hepatology*, 10(6), pp. 639–645. doi: 10.1016/j.cgh.2012.01.010.

Ji, H., Houghton, a M., Mariani, T. J., Perera, S., Kim, C. B., Padera, R., Tonon, G., McNamara, K., Marconcini, L. a, Hezel, a, El-Bardeesy, N., Bronson, R. T., Sugarbaker, D., Maser, R. S., Shapiro, S. D. and Wong, K.-K. (2006) 'K-ras activation generates an inflammatory response in lung tumors.', *Oncogene*, 25(14), pp. 2105–12. doi: 10.1038/sj.onc.1209237.

Jiang, R., Tan, Z., Deng, L., Chen, Y., Xia, Y., Gao, Y., Wang, X. and Sun, B. (2011) 'Interleukin-22 promotes human hepatocellular carcinoma by activation of STAT3', *Hepatology*, 54(3), pp. 900–909. doi: 10.1002/hep.24486.

Johnson, C. H., Dejea, C. M., Edler, D., Hoang, L. T., Santidrian, A. F., Felding, B. H., Ivanisevic, J., Cho, K., Wick, E. C., Hechenbleikner, E. M., Uritboonthai, W., Goetz, L., Casero, R. A., Pardoll, D. M., White, J. R., Patti, G. J., Sears, C. L. and Siuzdak, G. (2015) 'Metabolism links bacterial biofilms and colon carcinogenesis', *Cell Metabolism*. Elsevier Inc., 21(6), pp. 891–897. doi: 10.1016/j.cmet.2015.04.011.

Johnson, W. E., Li, C. and Rabinovic, A. (2007) 'Adjusting batch effects in microarray expression data using empirical Bayes methods', *Biostatistics*, 8, pp. 118–127. doi: 10.1093/biostatistics/kxj037.

June, C. H. (2016) 'Drugging the Undruggable Ras — Immunotherapy to the Rescue?', *New England Journal of Medicine*, 375(23), pp. 2286–2289. doi: 10.1056/NEJMe1612215.

Kaler, P., Augenlicht, L. and Klampfer, L. (2009) 'Macrophage-derived IL-1beta stimulates Wnt signaling and growth of colon cancer cells: a crosstalk interrupted by vitamin D3.', *Oncogene*, 28(44), pp. 3892–902. doi: 10.1038/onc.2009.247.

Kamanaka, M., Huber, S., Zenewicz, L. A., Gagliani, N., Rathinam, C., O'Connor, W., Wan, Y. Y., Nakae, S., Iwakura, Y., Hao, L. and Flavell, R. A. (2011) 'Memory/effector (CD45RB(lo)) CD4 T cells are controlled directly by IL-10 and cause IL-22-dependent intestinal pathology.', *The Journal of Experimental Medicine*, 208(5), pp. 1027–40. doi: 10.1084/jem.20102149.

Karapetis, C., Khambata-Ford, S., Jonker, D., O'Callaghan, C., Tu, D. and Tebbutt, N. (2008) 'K-ras Mutations and Benefit from Cetuximab in Advanced Colorectal Cancer', *New England Journal of Medicine*, 359(17), pp. 1757–1765.

Katoh, H., Wang, D., Daikoku, T., Sun, H., Dey, S. K. and DuBois, R. N. (2013) 'CXCR2-Expressing Myeloid-Derived Suppressor Cells Are Essential to Promote Colitis-Associated Tumorigenesis', *Cancer Cell*, 24(5), pp. 631–644. doi: 10.1016/j.ccr.2013.10.009.

Kawamura, M., Toiyama, Y., Tanaka, K., Saigusa, S., Okugawa, Y., Hiro, J., Uchida, K., Mohri, Y., Inoue, Y. and Kusunoki, M. (2012) 'CXCL5, a promoter of cell proliferation, migration and invasion, is a novel serum prognostic marker in patients with colorectal cancer', *European Journal of Cancer*, 48(14), pp. 2244–2251. doi: 10.1016/j.ejca.2011.11.032.

Keeley, E. C., Mehrad, B. and Strieter, R. M. (2010) 'CXC Chemokines in Cancer Angiogenesis and Metastases', in *Advances in Cancer Research*. 1st edn, pp. 91–111. doi: 10.1016/S0065-230X(10)06003-3.

Kennedy, R. D., Bylesjo, M., Kerr, P., Davison, T., Black, J. M., Kay, E. W., Holt, R. J., Proutski, V., Ahdesmaki, M., Farztdinov, V., Goffard, N., Hey, P., McDyer, F., Mulligan, K., Mussen, J., O'Brien, E., Oliver, G., Walker, S. M., Mulligan, J. M., Wilson, C., Winter, A., O'Donoghue, D., Mulcahy, H., O'Sullivan, J., Sheahan, K., Hyland, J., Dhir, R., Bathe, O. F., Winqvist, O., Manne, U., Shanmugam, C., Ramaswamy, S., Leon, E. J., Smith, W. I., McDermott, U., Wilson, R. H., Longley, D., Marshall, J., Cummins, R., Sargent, D. J., Johnston, P. G. and Harkin, D. P. (2011) 'Development and independent validation of a prognostic assay for stage ii colon cancer using formalin-fixed paraffin-embedded tissue', *Journal of Clinical Oncology*, 29(35), pp. 4620–4626. doi:

10.1200/JCO.2011.35.4498.

Khare, V., Paul, G., Movadat, O., Frick, A., Jambrich, M., Krnjic, A., Marian, B., Wrba, F. and Gasche, C. (2015) 'IL10R2 Overexpression Promotes IL22/STAT3 Signaling in Colorectal Carcinogenesis.', *Cancer immunology research*, 3(11), pp. 1227–35. doi: 10.1158/2326-6066.CIR-15-0031.

Khosravi, N., Cumpian, A. M., Daliri, S., Caetano, M. S. and Moghaddam, S. J. (2016) 'Impact of interleukin-22 on K-ras mutant lung cancer promotion and stemness properties', *Journal of Thoracic Oncology*, 11(2), pp. S26–S27. doi: 10.1016/j.jtho.2015.12.044.

Kim, H.-J. and Cantor, H. (2014) 'CD4 T-cell Subsets and Tumor Immunity: The Helpful and the Not-so-Helpful', *Cancer Immunology Research*, 2(2), pp. 91–98. doi: 10.1158/2326-6066.CIR-13-0216.

Kim, S. J., Im, Y. H., Markowitz, S. D. and Bang, Y. J. (2000) 'Molecular mechanisms of inactivation of TGF-beta receptors during carcinogenesis.', *Cytokine & Growth Factor Reviews*, 11(1–2), pp. 159–68.

Kinugasa, T., Sakaguchi, T., Gu, X. and Reinecker, H. C. (2000) 'Claudins regulate the intestinal barrier in response to immune mediators', *Gastroenterology*, 118(6), pp. 1001–1011. doi: 10.1053/gast.2000.8314.

Kirchberger, S., Royston, D. J., Boulard, O., Thornton, E., Franchini, F., Szabady, R. L., Harrison, O. and Powrie, F. (2013a) 'Innate lymphoid cells sustain colon cancer through production of interleukin-22 in a mouse model', *Journal of Experimental Medicine*, 210(5), pp. 917–931. doi: 10.1084/jem.20122308.

Kirchberger, S., Royston, D. J., Boulard, O., Thornton, E., Franchini, F., Szabady, R. L., Harrison, O. and Powrie, F. (2013b) 'Innate lymphoid cells sustain colon cancer through production of interleukin-22 in a mouse model', *The Journal of Experimental Medicine*, 210(5), pp. 917–931. doi: 10.1084/jem.20122308.

Kiuchi, N., Nakajima, K., Ichiba, M., Fukada, T., Narimatsu, M., Mizuno, K., Hibi, M. and Hirano, T. (1999) 'STAT3 Is Required for the gp130-mediated Full Activation of the c- myc Gene', *The Journal of Experimental Medicine*, 189(1), pp. 63–73. doi: 10.1084/jem.189.1.63.

Kobold, S., Völk, S., Clauditz, T., Küpper, N. J., Minner, S., Tufman, A., Düwell, P., Lindner, M., Koch, I., Heidegger, S., Rothenfußer, S., Schnurr, M., Huber, R. M., Wilczak, W. and Endres, S. (2013) 'Interleukin-22 Is Frequently Expressed in Small- and Large-Cell Lung Cancer and Promotes Growth in Chemotherapy-Resistant Cancer Cells', *Journal of Thoracic Oncology*, 8(8), pp. 1032–1042. doi: 10.1097/JTO.0b013e31829923c8.

Kopp, T., Riedl, E., Bangert, C., Bowman, E. P., Greisenegger, E., Horowitz, A., Kittler, H., Blumenschein, W. M., McClanahan, T. K., Marbury, T., Zachariae, C., Xu, D., Hou, X. S., Mehta, A., Zandvliet, A. S., Montgomery, D., van Aarle, F. and Khalilieh, S. (2015) 'Clinical improvement in psoriasis with specific targeting of interleukin-23', *Nature*, 521(7551), pp. 222–226. doi: 10.1038/nature14175.

Kress, T. R., Sabò, A. and Amati, B. (2015) 'MYC: connecting selective transcriptional control to global RNA production.', *Nature Reviews Cancer*, 15(10), pp. 593–607. doi: 10.1038/nrc3984.

Kryczek, I., Lin, Y., Nagarsheth, N., Peng, D., Zhao, L., Zhao, E., Vatan, L., Szeliga, W., Dou, Y., Owens, S., Zgodzinski, W., Majewski, M., Wallner, G., Fang, J., Huang, E. and Zou, W. (2014) 'IL-22(+)CD4(+) T cells promote colorectal cancer stemness via STAT3 transcription factor activation and induction of the methyltransferase DOT1L.', *Immunity*, 40(5), pp. 772–784. doi:

10.1016/j.immuni.2014.03.010.

Kuang, D.-M., Xiao, X., Zhao, Q., Chen, M.-M., Li, X.-F., Liu, R.-X., Wei, Y., Ouyang, F.-Z., Chen, D.-P., Wu, Y., Lao, X.-M., Deng, H. and Zheng, L. (2014) 'B7-H1–expressing antigen-presenting cells mediate polarization of protumorigenic Th22 subsets', *Journal of Clinical Investigation*, 124(10), pp. 4657–4667. doi: 10.1172/JCI74381.

Lal, N., Beggs, A. D., Willcox, B. E. and Middleton, G. W. (2015) 'An immunogenomic stratification of colorectal cancer: Implications for development of targeted immunotherapy', *OncoImmunology*, 4(3), p. e976052. doi: 10.4161/2162402X.2014.976052.

Lang, J. C., Whitelaw, B., Talbot, S. and Wilkie, N. M. (1988) 'Transcriptional regulation of the human c-myc gene', *British Journal of Cancer*, 58(IX), pp. 62–66.

Langowski, J. L., Zhang, X., Wu, L., Mattson, J. D., Chen, T., Smith, K., Basham, B., McClanahan, T., Kastelein, R. a and Oft, M. (2006) 'IL-23 promotes tumour incidence and growth.', *Nature*, 442(7101), pp. 461–5. doi: 10.1038/nature04808.

Langrish, C. L., Chen, Y., Blumenschein, W. M., Mattson, J., Basham, B., Sedgwick, J. D., McClanahan, T., Kastelein, R. a and Cua, D. J. (2005) 'IL-23 drives a pathogenic T cell population that induces autoimmune inflammation', *The Journal of Experimental Medicine*, 201(2), pp. 233–240. doi: 10.1084/jem.20041257.

Lavallée-Adam, M., Rauniyar, N., McClatchy, D. B. and Yates, J. R. (2014) 'PSEA-Quant: A Protein Set Enrichment Analysis on Label-Free and Label-Based Protein Quantification Data', *Journal of Proteome Research*, 13(12), pp. 5496–5509. doi: 10.1021/pr500473n.

Lavallée-Adam, M. and Yates, J. R. (2016) 'Using PSEA-Quant for Protein Set Enrichment Analysis of Quantitative Mass Spectrometry-Based Proteomics', in *Current Protocols in Bioinformatics*, p. 13.28.1-13.28.16. doi: 10.1002/0471250953.bi1328s53.

Le, D. T., Uram, J. N., Wang, H., Bartlett, B. R., Kemberling, H., Eyring, A. D., Skora, A. D., Luber, B. S., Azad, N. S., Laheru, D., Biedrzycki, B., Donehower, R. C., Zaheer, A., Fisher, G. A., Crocenzi, T. S., Lee, J. J., Duffy, S. M., Goldberg, R. M., de la Chapelle, A., Koshiji, M., Bhaijee, F., Huebner, T., Hruban, R. H., Wood, L. D., Cuka, N., Pardoll, D. M., Papadopoulos, N., Kinzler, K. W., Zhou, S., Cornish, T. C., Taube, J. M., Anders, R. A., Eshleman, J. R., Vogelstein, B. and Diaz, L. A. (2015) 'PD-1 Blockade in Tumors with Mismatch-Repair Deficiency', *New England Journal of Medicine*, 372(26), pp. 2509–2520. doi: 10.1056/NEJMoa1500596.

Lee, J.-H., Kang, M.-J., Han, H.-Y., Lee, M.-G., Jeong, S.-I., Ryu, B.-K., Ha, T.-K., Her, N.-G., Han, J., Park, S. J., Lee, K. Y., Kim, H.-J. and Chi, S.-G. (2011) 'Epigenetic Alteration of PRKCDBP in Colorectal Cancers and Its Implication in Tumor Cell Resistance to TNF -Induced Apoptosis', *Clinical Cancer Research*, 17(24), pp. 7551–7562. doi: 10.1158/1078-0432.CCR-11-1026.

Lee, J.-H., Park, K.-S., Alberobello, A. T., Kallakury, B., Weng, M.-T., Wang, Y. and Giaccone, G. (2013) 'The Janus Kinases Inhibitor AZD1480 Attenuates Growth of Small Cell Lung Cancers In Vitro and In Vivo', *Clinical Cancer Research*, 19(24), pp. 6777–6786. doi: 10.1158/1078-0432.CCR-13-1110.

Lejeune, D., Dumoutier, L., Constantinescu, S., Kruijer, W., Schuringa, J. J. and Renauld, J. C. (2002) 'Interleukin-22 (IL-22) activates the JAK/STAT, ERK,

JNK, and p38 MAP kinase pathways in a rat hepatoma cell line: Pathways that are shared with and distinct from IL-10', *Journal of Biological Chemistry*, 277(37), pp. 33676–33682. doi: 10.1074/jbc.M204204200.

Lerman, G., Sharon, M., Leibowitz-Amit, R., Sidi, Y. and Avni, D. (2014) 'The crosstalk between IL-22 signaling and miR-197 in human keratinocytes', *PLoS ONE*, 9(9). doi: 10.1371/journal.pone.0107467.

Li, H., Rodriguez-Canales, J., Liu, W., Zhu, J., Hanson, J. C., Pack, S., Zhuang, Z., Emmert-Buck, M. R. and Rodgers, G. P. (2013) 'Deletion of the Olfactomedin 4 Gene Is Associated with Progression of Human Prostate Cancer', *The American Journal of Pathology*, 183(4), pp. 1329–1338. doi: 10.1016/j.ajpath.2013.06.028.

Li, Y., Deuring, J., Peppelenbosch, M. P., Kuipers, E. J., de Haar, C. and van der Woude, C. J. (2012) 'IL-6-induced DNMT1 activity mediates SOCS3 promoter hypermethylation in ulcerative colitis-related colorectal cancer', *Carcinogenesis*, 33(10), pp. 1889–1896. doi: 10.1093/carcin/bgs214.

Li, Y., Wang, L., Pappan, L., Galliher-Beckley, A. and Shi, J. (2012) 'IL-1β promotes stemness and invasiveness of colon cancer cells through Zeb1 activation.', *Molecular cancer*, 11(1), p. 87. doi: 10.1186/1476-4598-11-87.

Liang, S. C., Tan, X.-Y., Luxenberg, D. P., Karim, R., Dunussi-Joannopoulos, K., Collins, M. and Fouser, L. a (2006) 'Interleukin (IL)-22 and IL-17 are coexpressed by Th17 cells and cooperatively enhance expression of antimicrobial peptides', *The Journal of Experimental Medicine*, 203(10), pp. 2271–2279. doi: 10.1084/jem.20061308.

Lim, C. and Savan, R. (2014) 'The role of the IL-22/IL-22R1 axis in cancer.', *Cytokine & Growth Factor Reviews*, 25(3), pp. 257–71. doi: 10.1016/j.cytogfr.2014.04.005.

Lim, S. Y., Yuzhalin, A. E., Gordon-Weeks, A. N. and Muschel, R. J. (2016) 'Tumor-infiltrating monocytes/macrophages promote tumor invasion and migration by upregulating S100A8 and S100A9 expression in cancer cells', *Oncogene*, 35(44), pp. 5735–5745. doi: 10.1038/onc.2016.107.

Lin, C. Y., Lovén, J., Rahl, P. B., Paranal, R. M., Burge, C. B., Bradner, J. E., Lee, T. I. and Young, R. A. (2012) 'Transcriptional amplification in tumor cells with elevated c-Myc', *Cell*, 151(1), pp. 56–67. doi: 10.1016/j.cell.2012.08.026.

Lin, J.-T., Wang, J.-Y., Chen, M.-K., Chen, H.-C., Chang, T.-H., Su, B.-W. and Chang, P.-J. (2013) 'Colon cancer mesenchymal stem cells modulate the tumorigenicity of colon cancer through interleukin 6.', *Experimental Cell Research*, 319(14), pp. 2216–29. doi: 10.1016/j.yexcr.2013.06.003.

Lindemans, C. A., Calafiore, M., Mertelsmann, A. M., O'Connor, M. H., Dudakov, J. A., Jenq, R. R., Velardi, E., Young, L. F., Smith, O. M., Lawrence, G., Ivanov, J. A., Fu, Y.-Y., Takashima, S., Hua, G., Martin, M. L., O'Rourke, K. P., Lo, Y.-H., Mokry, M., Romera-Hernandez, M., Cupedo, T., Dow, L. E., Nieuwenhuis, E. E., Shroyer, N. F., Liu, C., Kolesnick, R., van den Brink, M. R. M. and Hanash, A. M. (2015) 'Interleukin-22 promotes intestinal-stem-cell-mediated epithelial regeneration', *Nature*, 528(7583), pp. 560–564. doi: 10.1038/nature16460.

Ling, J., Kang, Y., Zhao, R., Xia, Q., Lee, D. F., Chang, Z., Li, J., Peng, B., Fleming, J. B., Wang, H., Liu, J., Lemischka, I. R., Hung, M. C. and Chiao, P. (2012) 'Kras G12D-Induced IKK2/β/NF-κB Activation by IL-1α and p62 Feedforward Loops Is Required for Development of Pancreatic Ductal Adenocarcinoma', *Cancer Cell*, 21, pp. 105–120. doi: 10.1016/j.ccr.2011.12.006.

Liou, G.-Y., Doppler, H., Necela, B., Edenfield, B., Zhang, L., Dawson, D. W. and Storz, P. (2015) 'Mutant KRAS-Induced Expression of ICAM-1 in Pancreatic Acinar Cells Causes Attraction of Macrophages to Expedite the Formation of Precancerous Lesions', *Cancer Discovery*, 5(1), pp. 52–63. doi: 10.1158/2159-8290.CD-14-0474.

Liu, W., Li, H., Hong, S.-H., Piszczek, G. P., Chen, W. and Rodgers, G. P. (2016) 'Olfactomedin 4 deletion induces colon adenocarcinoma in ApcMin/+ mice', *Oncogene*, 35(40), pp. 5237–5247. doi: 10.1038/onc.2016.58.

Liu, W., Liu, Y., Zhu, J., Wright, E., Ding, I. and Rodgers, G. P. (2008) 'Reduced hGC-1 Protein Expression Is Associated with Malignant Progression of Colon Carcinoma', *Clinical Cancer Research*, 14(4), pp. 1041–1049. doi: 10.1158/1078-0432.CCR-07-4125.

Liu, Y., Mei, J., Gonzales, L., Yang, G., Dai, N., Wang, P., Zhang, P., Favara, M., Malcolm, K. C., Guttentag, S. and Worthen, G. S. (2011) 'IL-17A and TNF-Exert Synergistic Effects on Expression of CXCL5 by Alveolar Type II Cells In Vivo and In Vitro', *The Journal of Immunology*, 186(5), pp. 3197–3205. doi: 10.4049/jimmunol.1002016.

Llosa, N. J., Cruise, M., Tam, A., Wicks, E. C., Hechenbleikner, E. M., Taube, J. M., Blosser, R. L., Fan, H., Wang, H., Luber, B. S., Zhang, M., Papadopoulos, N., Kinzler, K. W., Vogelstein, B., Sears, C. L., Anders, R. a, Pardoll, D. M. and Housseau, F. (2015) 'The Vigorous Immune Microenvironment of Microsatellite Instable Colon Cancer Is Balanced by Multiple Counter-Inhibitory Checkpoints', *Cancer Discovery*, 5(1), pp. 43–51. doi: 10.1158/2159-8290.CD-14-0863.

Longo, D. L., Beaugerie, L. and Itzkowitz, S. H. (2015) 'Cancers Complicating Inflammatory Bowel Disease', *New England Journal of Medicine*, 372(15), pp. 1441–1452. doi: 10.1056/NEJMra1403718.

Longo, D. L. and Strum, W. B. (2016) 'Colorectal Adenomas', *New England Journal of Medicine*, 374(11), pp. 1065–1075. doi: 10.1056/NEJMra1513581.

LoRusso, P. M. (2016) 'Inhibition of the PI3K/AKT/mTOR pathway in solid tumors', *Journal of Clinical Oncology*, 34(31), pp. 3803–3815. doi: 10.1200/JCO.2014.59.0018.

Lotti, F., Jarrar, A. M., Pai, R. K., Hitomi, M., Lathia, J., Mace, A., Gantt, G. a., Sukhdeo, K., DeVecchio, J., Vasanji, A., Leahy, P., Hjelmeland, A. B., Kalady, M. F. and Rich, J. N. (2013) 'Chemotherapy activates cancer-associated fibroblasts to maintain colorectal cancer-initiating cells by IL-17A', *Journal of Experimental Medicine*, 210(13), pp. 2851–72. doi: 10.1084/jem.20131195.

Lurje, G., Zhang, W., Schultheis, A. M., Yang, D., Groshen, S., Hendifar, A. E., Husain, H., Gordon, M. A., Nagashima, F., Chang, H. M. and Lenz, H.-J. (2008) 'Polymorphisms in VEGF and IL-8 predict tumor recurrence in stage III colon cancer', *Annals of Oncology* , 19(10), pp. 1734–1741. doi: 10.1093/annonc/mdn368.

Ma, H., Liang, S., Li, J., Napierata, L., Brown, T., Benoit, S., Senices, M., Gill, D., Dunussi-Joannopoulos, K., Collins, M., Nickerson-Nutter, C., Fouser, L. a and Young, D. a (2008) 'IL-22 is required for Th17 cell–mediated pathology in a mouse model of psoriasis-like skin inflammation', *Journal of Clinical Investigation*, 118(2), pp. 597–607. doi: 10.1172/JCI33263.

Maloy, K. J. and Kullberg, M. C. (2008) 'IL-23 and Th17 cytokines in intestinal homeostasis', *Mucosal Immunology*, 1(5), pp. 339–349. doi: 10.1038/mi.2008.28.

Mangan, P. R., Harrington, L. E., O'Quinn, D. B., Helms, W. S., Bullard, D. C., Elson, C. O., Hatton, R. D., Wahl, S. M., Schoeb, T. R. and Weaver, C. T. (2006) 'Transforming growth factor-β induces development of the TH17 lineage', *Nature*, 441(7090), pp. 231–234. doi: 10.1038/nature04754.

Margalef, P., Colomer, C., Villanueva, A., Montagut, C., Iglesias, M., Bellosillo, B., Salazar, R., Martinez-Iniesta, M., Bigas, A. and Espinosa, L. (2015) 'BRAF-induced tumorigenesis is IKK -dependent but NF-kB-independent', *Science Signaling*, 8(373). doi: 10.1126/scisignal.2005886.

Marisa, L., de Reyniès, A., Duval, A., Selves, J., Gaub, M. P., Vescovo, L., Etienne-Grimaldi, M.-C., Schiappa, R., Guenot, D., Ayadi, M., Kirzin, S., Chazal, M., Fléjou, J.-F., Benchimol, D., Berger, A., Lagarde, A., Pencreach, E., Piard, F., Elias, D., Parc, Y., Olschwang, S., Milano, G., Laurent-Puig, P. and Boige, V. (2013) 'Gene expression classification of colon cancer into molecular subtypes: characterization, validation, and prognostic value.', *PLoS medicine*, 10(5), p. e1001453. doi: 10.1371/journal.pmed.1001453.

Markowitz, J. and Carson, W. E. (2013) 'Review of S100A9 biology and its role in cancer', *Biochimica et Biophysica Acta (BBA) - Reviews on Cancer*, 1835(1), pp. 100–109. doi: 10.1016/j.bbcan.2012.10.003.

Martin, J. C., Bériou, G., Heslan, M., Bossard, C., Jarry, A., Abidi, A., Hulin, P., Ménoret, S., Thinard, R., Anegon, I., Jacqueline, C., Lardeux, B., Halary, F., Renauld, J.-C., Bourreille, A. and Josien, R. (2016) 'IL-22BP is produced by eosinophils in human gut and blocks IL-22 protective actions during colitis', *Mucosal Immunology*, 9(2), pp. 539–549. doi: 10.1038/mi.2015.83.

Maus, M. K. H., Hanna, D. L., Stephens, C. L., Astrow, S. H., Yang, D., Grimminger, P. P., Loupakis, F., Hsiang, J. H., Zeger, G., Wakatsuki, T., Barzi, A. and Lenz, H.-J. (2015) 'Distinct gene expression profiles of proximal and distal colorectal cancer: implications for cytotoxic and targeted therapy', *The Pharmacogenomics Journal*, 15(4), pp. 354–362. doi: 10.1038/tpj.2014.73.

McAllister, F., Bailey, J., Alsina, J., Nirschl, C., Sharma, R., Fan, H., Rattigan, Y., Roeser, J. C. C., Lankapalli, R. H. H., Zhang, H., Jaffee, E. M. M., Drake, C. G. G., Housseau, F., Maitra, A., Kolls, J. K. K., Sears, C. L. L., Pardoll, D. M. M. and Leach, S. D. D. (2014) 'Oncogenic Kras Activates a Hematopoietic-to-Epithelial IL-17 Signaling Axis in Preinvasive Pancreatic Neoplasia', *Cancer Cell*, 25(5), pp. 621–637. doi: 10.1016/j.ccr.2014.03.014.

McCormick, F. (2015) 'KRAS as a Therapeutic Target', *Clinical Cancer Research*, 21(8), pp. 1797–1801. doi: 10.1158/1078-0432.CCR-14-2662.

McGeachy, M. J., Chen, Y., Tato, C. M., Laurence, A., Joyce-Shaikh, B., Blumenschein, W. M., McClanahan, T. K., O'Shea, J. J. and Cua, D. J. (2009) 'The interleukin 23 receptor is essential for the terminal differentiation of interleukin 17–producing effector T helper cells in vivo', *Nature Immunology*, 10(3), pp. 314–324. doi: 10.1038/ni.1698.

Medler, T. R., Cotechini, T. and Coussens, L. M. (2015) 'Immune Response to Cancer Therapy: Mounting an Effective Antitumor Response and Mechanisms of Resistance', *Trends in Cancer*, 1(1), pp. 66–75. doi: 10.1016/j.trecan.2015.07.008.

Merlos-Suárez, A., Barriga, F. M., Jung, P., Iglesias, M., Céspedes, M. V., Rossell, D., Sevillano, M., Hernando-Momblona, X., da Silva-Diz, V., Muñoz, P., Clevers, H., Sancho, E., Mangues, R. and Batlle, E. (2011) 'The intestinal stem cell signature identifies colorectal cancer stem cells and predicts disease relapse.', *Cell stem cell*, 8(5), pp. 511–24. doi: 10.1016/j.stem.2011.02.020.

Metz, H. E., Kargl, J., Busch, S. E., Kim, K.-H., Kurland, B. F., Abberbock, S. R., Randolph-Habecker, J., Knoblaugh, S. E., Kolls, J. K., White, M. F. and Houghton, A. M. (2016) 'Insulin receptor substrate-1 deficiency drives a proinflammatory phenotype in KRAS mutant lung adenocarcinoma', *Proceedings of the National Academy of Sciences*, 113(31), pp. 8795–8800. doi: 10.1073/pnas.1601989113.

Miller, D. M., Thomas, S. D., Islam, A., Muench, D. and Sedoris, K. (2012) 'c-Myc and Cancer Metabolism', *Clinical Cancer Research*, 18(20), pp. 5546–5553. doi: 10.1158/1078-0432.CCR-12-0977.

Missiaglia, E., Jacobs, B., D'Ario, G., Di Narzo, a F., Soneson, C., Budinska, E., Popovici, V., Vecchione, L., Gerster, S., Yan, P., Roth, a D., Klingbiel, D., Bosman, F. T., Delorenzi, M. and Tejpar, S. (2014) 'Distal and proximal colon cancers differ in terms of molecular, pathological, and clinical features', *Annals of Oncology*, 25(10), pp. 1995–2001. doi: 10.1093/annonc/mdu275.

Mitra, A., Raychaudhuri, S. K. and Raychaudhuri, S. P. (2012) 'IL-22 induced cell proliferation is regulated by PI3K/Akt/mTOR signaling cascade.', *Cytokine*, 60(1), pp. 38–42. doi: 10.1016/j.cyto.2012.06.316.

Mlecnik, B., Bindea, G., Angell, H. K., Sasso, M. S., Obenauf, A. C., Fredriksen, T., Lafontaine, L., Bilocq, A. M., Kirilovsky, A., Tosolini, M., Waldner, M., Berger, A., Fridman, W. H., Rafii, A., Valge-Archer, V., Pagès, F., Speicher, M. R. and Galon, J. (2014) 'Functional network pipeline reveals genetic determinants associated with in situ lymphocyte proliferation and survival of cancer patients.', *Science Translational Medicine*, 6(228), p. 228ra37. doi: 10.1126/scitranslmed.3007240.

Mosmann, T. R., Cherwinski, H., Bond, M. W., Giedlin, M. A. and Coffman, R. L. (1986) 'Two types of murine helper T cell clone. I. Definition according to profiles of lymphokine activities and secreted proteins.', *The Journal of Immunology*, 136(7), pp. 2348–57. doi: 10.1111/j.1442-9071.2011.02672.x.

Muñoz, M., Heimesaat, M. M., Danker, K., Struck, D., Lohmann, U., Plickert, R., Bereswill, S., Fischer, A., Dunay, I. R., Wolk, K., Loddenkemper, C., Krell, H.-W., Libert, C., Lund, L. R., Frey, O., Hölscher, C., Iwakura, Y., Ghilardi, N., Ouyang, W., Kamradt, T., Sabat, R. and Liesenfeld, O. (2009) 'Interleukin (IL)-23 mediates Toxoplasma gondii –induced immunopathology in the gut via matrixmetalloproteinase-2 and IL-22 but independent of IL-17', *The Journal of Experimental Medicine*, 206(13), pp. 3047–3059. doi: 10.1084/jem.20090900.

Murphy, C. A., Langrish, C. L., Chen, Y., Blumenschein, W., McClanahan, T., Kastelein, R. A., Sedgwick, J. D. and Cua, D. J. (2003) 'Divergent Pro- and Antiinflammatory Roles for IL-23 and IL-12 in Joint Autoimmune Inflammation', *The Journal of Experimental Medicine*, 198(12), pp. 1951–1957. doi: 10.1084/jem.20030896.

Nagalakshmi, M. L., Rascle, A., Zurawski, S., Menon, S. and de Waal Malefyt, R. (2004) 'Interleukin-22 activates STAT3 and induces IL-10 by colon epithelial cells.', *International immunopharmacology*, 4(5), pp. 679–91. doi: 10.1016/j.intimp.2004.01.008.

Nagasaki, T., Hara, M., Nakanishi, H., Takahashi, H., Sato, M. and Takeyama, H. (2014) 'Interleukin-6 released by colon cancer-associated fibroblasts is critical for tumour angiogenesis: anti-interleukin-6 receptor antibody suppressed angiogenesis and inhibited tumour-stroma interaction.', *British Journal of Cancer*, 110(2), pp. 469–78. doi: 10.1038/bjc.2013.748.

Nath, S. and Mukherjee, P. (2014) 'MUC1: a multifaceted oncoprotein with a key role

in cancer progression', *Trends in Molecular Medicine*, 20(6), pp. 332–342. doi: 10.1016/j.molmed.2014.02.007.

Nebiker, C., Han, J., Eppenberger-Castori, S., Iezzi, G., Hirt, C., Amicarella, F., Cremonesi, E., Huber, X., Padovan, E., Angrisani, B., Droeser, R. a, Rosso, R., Bolli, M., Oertli, D., von Holzen, U., Adamina, M., Muraro, M. G., Mengus, C., Zajac, P., Sconocchia, G., Zuber, M., Tornillo, L., Terracciano, L. and Spagnoli, G. C. (2014) 'GM-CSF Production by Tumor Cells Is Associated with Improved Survival in Colorectal Cancer', *Clinical Cancer Research*, 20(12), pp. 3094–3106. doi: 10.1158/1078-0432.CCR-13-2774.

Ngiow, S. F., Teng, M. W. L. and Smyth, M. J. (2013) 'A balance of interleukin-12 and -23 in cancer', *Trends in Immunology*, 34(11), pp. 548–555. doi: 10.1016/j.it.2013.07.004.

Nguyen, L. T. and Ohashi, P. S. (2014) 'Clinical blockade of PD1 and LAG3 — potential mechanisms of action', *Nature Reviews Immunology*, 15(1), pp. 45–56. doi: 10.1038/nri3790.

NICE (2013) 'Diagnostics Assessment Programme KRAS mutation testing of tumours in adults with metastatic colorectal cancer Final scope', *National Insitute for Health and Clinical Excellence*, (January), pp. 1–29.

NICE (2014) 'Colorectal cancer : diagnosis and management', *National Insitute for Health and Clinical Excellence*, (December), pp. 1–48.

Nie, Z., Hu, G., Wei, G., Cui, K., Yamane, A., Resch, W., Wang, R., Green, D. R., Tessarollo, L., Casellas, R., Zhao, K. and Levens, D. (2012) 'c-Myc Is a Universal Amplifier of Expressed Genes in Lymphocytes and Embryonic Stem Cells', *Cell*, 151(1), pp. 68–79. doi: 10.1016/j.cell.2012.08.033.

Ning, Y., Labonte, M. J., Zhang, W., Bohanes, P. O., Gerger, a., Yang, D., Benhaim, L., Paez, D., Rosenberg, D. O., Nagulapalli Venkata, K. C., Louie, S. G., Petasis, N. a., Ladner, R. D. and Lenz, H.-J. (2012) 'The CXCR2 Antagonist, SCH-527123, Shows Antitumor Activity and Sensitizes Cells to Oxaliplatin in Preclinical Colon Cancer Models', *Molecular Cancer Therapeutics*, 11, pp. 1353–1364. doi: 10.1158/1535-7163.MCT-11-0915.

Ning, Y., Manegold, P. C., Hong, Y. K., Zhang, W., Pohl, A., Lurje, G., Winder, T., Yang, D., LaBonte, M. J., Wilson, P. M., Ladner, R. D. and Lenz, H. J. (2011) 'Interleukin-8 is associated with proliferation, migration, angiogenesis and chemosensitivity in vitro and in vivo in colon cancer cell line models', *International Journal of Cancer*, 128, pp. 2038–2049. doi: 10.1002/ijc.25562.

Nosho, K., Baba, Y., Tanaka, N., Shima, K., Hayashi, M., Meyerhardt, J. a, Giovannucci, E., Dranoff, G., Fuchs, C. S. and Ogino, S. (2010) 'Tumour-infiltrating T-cell subsets, molecular changes in colorectal cancer, and prognosis: cohort study and literature review.', *The Journal of Pathology*, 222(4), pp. 350–366. doi: 10.1002/path.2774.

O'Hayer, K. M., Brady, D. C. and Counter, C. M. (2009) 'ELR+ CXC chemokines and oncogenic Ras-mediated tumorigenesis', *Carcinogenesis*, 30(11), pp. 1841–1847. doi: 10.1093/carcin/bgp198.

Ogawa, A., Andoh, A., Araki, Y., Bamba, T. and Fujiyama, Y. (2004) 'Neutralization of interleukin-17 aggravates dextran sulfate sodium-induced colitis in mice.', *Clinical Immunology*, 110(1), pp. 55–62. doi: 10.1016/j.clim.2003.09.013.

Oladipo, O., Conlon, S., O'Grady, A., Purcell, C., Wilson, C., Maxwell, P. J., Johnston, P. G., Stevenson, M., Kay, E. W., Wilson, R. H. and Waugh, D. J. J. (2011) 'The expression and prognostic impact of CXC-chemokines in stage II and III colorectal cancer epithelial and stromal tissue', *British Journal of*

Cancer, 104(3), pp. 480–487. doi: 10.1038/sj.bjc.6606055.

Oppmann, B., Lesley, R., Blom, B., Timans, J. C., Xu, Y., Hunte, B., Vega, F., Yu, N., Wang, J., Singh, K., Zonin, F., Vaisberg, E., Churakova, T., Liu, M., Gorman, D., Wagner, J., Zurawski, S., Liu, Y.-J., Abrams, J. S., Moore, K. W., Rennick, D., de Waal-Malefyt, R., Hannum, C., Bazan, J. F. and Kastelein, R. A. (2000) 'Novel p19 Protein Engages IL-12p40 to Form a Cytokine, IL-23, with Biological Activities Similar as Well as Distinct from IL-12', *Immunity*, 13(5), pp. 715–725. doi: 10.1016/S1074-7613(00)00070-4.

Palomero, T., Lim, W. K., Odom, D. T., Sulis, M. L., Real, P. J., Margolin, A., Barnes, K. C., O'Neil, J., Neuberg, D., Weng, A. P., Aster, J. C., Sigaux, F., Soulier, J., Look, a T., Young, R. a, Califano, A. and Ferrando, A. a (2006) 'NOTCH1 directly regulates c-MYC and activates a feed-forward-loop transcriptional network promoting leukemic cell growth', *Proceedings of the National Academy of Sciences*, 103(48), pp. 18261–18266. doi: 10.1073/pnas.0606108103.

Parham, C., Chirica, M., Timans, J., Vaisberg, E., Travis, M., Cheung, J., Pflanz, S., Zhang, R., Singh, K. P., Vega, F., To, W., Wagner, J., O'Farrell, A.-M., McClanahan, T., Zurawski, S., Hannum, C., Gorman, D., Rennick, D. M., Kastelein, R. a, de Waal Malefyt, R. and Moore, K. W. (2002) 'A receptor for the heterodimeric cytokine IL-23 is composed of IL-12Rbeta1 and a novel cytokine receptor subunit, IL-23R', *The Journal of Immunology*, 168(11), pp. 5699–5708.

Park, H., Li, Z., Yang, X. O., Chang, S. H., Nurieva, R., Wang, Y.-H., Wang, Y., Hood, L., Zhu, Z., Tian, Q. and Dong, C. (2005) 'A distinct lineage of CD4 T cells regulates tissue inflammation by producing interleukin 17', *Nature Immunology*, 6(11), pp. 1133–1141. doi: 10.1038/ni1261.

Pastrana, E., Silva-Vargas, V. and Doetsch, F. (2011) 'Eyes wide open: A critical review of sphere-formation as an assay for stem cells', *Cell Stem Cell*, 8(5), pp. 486–498. doi: 10.1016/j.stem.2011.04.007.

Peck, B., Ferber, E. C. and Schulze, A. (2013) 'Antagonism between FOXO and MYC Regulates Cellular Powerhouse', *Frontiers in Oncology*, 3(April), p. 96. doi: 10.3389/fonc.2013.00096.

Pelczar, P., Witkowski, M., Perez, L. G., Kempski, J., Hammel, A. G., Brockmann, L., Kleinschmidt, D., Wende, S., Haueis, C., Bedke, T., Witkowski, M., Krasemann, S., Steurer, S., Booth, C. J., Busch, P., König, A., Rauch, U., Benten, D., Izbicki, J. R., Rösch, T., Lohse, A. W., Strowig, T., Gagliani, N., Flavell, R. A. and Huber, S. (2016) 'A pathogenic role for T cell-derived IL-22BP in inflammatory bowel disease.', *Science*, 354(6310), pp. 358–362. doi: 10.1126/science.aah5903.

Pickert, G., Neufert, C., Leppkes, M., Zheng, Y., Wittkopf, N., Warntjen, M., Lehr, H.-A., Hirth, S., Weigmann, B., Wirtz, S., Ouyang, W., Neurath, M. F. and Becker, C. (2009) 'STAT3 links IL-22 signaling in intestinal epithelial cells to mucosal wound healing', *The Journal of Experimental Medicine*, 206(7), pp. 1465–1472. doi: 10.1084/jem.20082683.

Pierconti, F., Martini, M., Pinto, F., Cenci, T., Capodimonti, S., Calarco, A., Bassi, P. F. and Larocca, L. M. (2011) 'Epigenetic silencing of SOCS3 identifies a subset of prostate cancer with an aggressive behavior', *Prostate*, 71(3), pp. 318–325. doi: 10.1002/pros.21245.

Popivanova, B. K., Kitamura, K., Wu, Y., Kondo, T., Kagaya, T., Kaneko, S., Oshima, M., Fujii, C. and Mukaida, N. (2008) 'Blocking TNF-alpha in mice

reduces colorectal carcinogenesis associated with chronic colitis.', *The Journal of Clinical Investigation*, 118(2), pp. 560–70. doi: 10.1172/JCI32453.

Popovici, V., Budinska, E., Tejpar, S., Weinrich, S., Estrella, H., Hodgson, G., Van Cutsem, E., Xie, T., Bosman, F. T., Roth, A. D. and Delorenzi, M. (2012) 'Identification of a poor-prognosis BRAF-mutant - Like population of patients with colon cancer', *Journal of Clinical Oncology*, 30(12), pp. 1288–1295. doi: 10.1200/JCO.2011.39.5814.

Porter, D., Levine, B., Kalos, M., Bagg, A. and June, C. H. (2011) 'Chimeric Antigen Receptor–Modified T Cells in Chronic Lymphoid Leukemia', *New England Journal of Medicine*, 365(8), pp. 725–733. doi: 10.1056/NEJMoa1103849.

Powrie, F., Leach, M. W., Mauze, S., Caddle, L. B. and Coffman, R. L. (1993) 'Phenotypically distinct subsets of CD4+ T cells induce or protect from chronic intestinal inflammation in C.B-17 scid mice', *International Immunology*, 11(11), pp. 1461–1471.

Preston, S. L., Wong, W., Chan, A. O., Poulsom, R., Jeffery, R., Goodlad, R. A., Mandir, N., Elia, G., Novelli, M., Bodmer, W. F., Tomlinson, I. P. and Wright, N. A. (2003) 'Bottom-up histogenesis of colorectal adenomas: origin in the monocryptal adenoma and initial expansion by crypt fission.', *Cancer Research*, 63(13), pp. 3819–25.

Punt, C. J. A., Koopman, M. and Vermeulen, L. (2016) 'From tumour heterogeneity to advances in precision treatment of colorectal cancer', *Nature Reviews Clinical Oncology*, 14(4), pp. 235–246. doi: 10.1038/nrclinonc.2016.171.

Putoczki, T., Thiem, S., Loving, A., Busuttil, R., Wilson, N., Ziegler, P. K., Nguyen, P. M., Preaudet, A., Farid, R., Edwards, K. M., Boglev, Y., Luwor, R. B., Jarnicki, A., Horst, D., Boussioutas, A., Heath, J. K., Sieber, O. M., Pleines, I., Kile, B. T., Nash, A., Greten, F. R., McKenzie, B. S. and Ernst, M. (2013) 'Interleukin-11 is the dominant IL-6 family cytokine during gastrointestinal tumorigenesis and can be targeted therapeutically.', *Cancer Cell*, 24(2), pp. 257–71. doi: 10.1016/j.ccr.2013.06.017.

Pylayeva-Gupta, Y., Lee, K. E., Hajdu, C. H., Miller, G. and Bar-Sagi, D. (2012) 'Oncogenic Kras-induced GM-CSF production promotes the development of pancreatic neoplasia.', *Cancer Cell*, 21(6), pp. 836–847. doi: 10.1016/j.ccr.2012.04.024.

Radaeva, S., Sun, R., Pan, H. N., Hong, F. and Gao, B. (2004) 'Interleukin 22 (IL-22) Plays a Protective Role in T Cell-mediated Murine Hepatitis: IL-22 Is a Survival Factor for Hepatocytes via STAT3 Activation', *Hepatology*, 39(5), pp. 1332–1342. doi: 10.1002/hep.20184.

Read, T. E., Mutch, M. G., Chang, B. W., McNevin, M. S., Fleshman, J. W., Birnbaum, E. H., Fry, R. D., Caushaj, P. F. and Kodner, I. J. (2002) 'Locoregional recurrence and survival after curative resection of adenocarcinoma of the colon.', *Journal of the American College of Surgeons*, 195(1), pp. 33–40.

Rech, A. J. and Vonderheide, R. H. (2013) 'Dynamic Interplay of Oncogenes and T Cells Induces PD-L1 in the Tumor Microenvironment', *Cancer Discovery*, 3(12), pp. 1330–1332. doi: 10.1158/2159-8290.CD-13-0775.

Richmond, A., Balentien, E., Thomas, H. G., Flaggs, G., Barton, D. E., Spiess, J., Bordoni, R., Francke, U. and Derynck, R. (1988) 'Molecular characterization and chromosomal mapping of melanoma growth stimulatory activity, a growth factor structurally related to beta-thromboglobulin', *Embo J*, 7(7), pp. 2025–2033.

Ries, C. H., Cannarile, M. A., Hoves, S., Benz, J., Wartha, K., Runza, V., Rey-Giraud, F., Pradel, L. P., Feuerhake, F., Klaman, I., Jones, T., Jucknischke, U., Scheiblich, S., Kaluza, K., Gorr, I. H., Walz, A., Abiraj, K., Cassier, P. A., Sica, A., Gomez-Roca, C., de Visser, K. E., Italiano, A., Le Tourneau, C., Delord, J.-P., Levitsky, H., Blay, J.-Y. and Rüttinger, D. (2014) 'Targeting Tumor-Associated Macrophages with Anti-CSF-1R Antibody Reveals a Strategy for Cancer Therapy', *Cancer Cell*, 25(6), pp. 846–859. doi: 10.1016/j.ccr.2014.05.016.

Riihimäki, M., Hemminki, A., Sundquist, J. and Hemminki, K. (2016) 'Patterns of metastasis in colon and rectal cancer', *Scientific Reports*, 6(1), p. 29765. doi: 10.1038/srep29765.

Rochman, Y., Spolski, R. and Leonard, W. J. (2009) 'New insights into the regulation of T cells by gamma(c) family cytokines.', *Nature Reviews Immunology*, 9(7), pp. 480–490. doi: 10.1038/nri2580.

Rokavec, M., Öner, M. G., Li, H., Jackstadt, R., Jiang, L., Lodygin, D., Kaller, M., Horst, D., Ziegler, P. K., Schwitalla, S., Slotta-huspenina, J., Bader, F. G., Greten, F. R. and Hermeking, H. (2014) 'IL-6R/STAT3/miR-34a feedback loop promotes EMT-mediated colorectal cancer invasion and metastasis', *The Journal of Clinical Investigation*, 124(4), pp. 1853–1867. doi: 10.1172/JCI73531DS1.

Roth, A. D., Delorenzi, M., Tejpar, S., Yan, P., Klingbiel, D., Fiocca, R., D'Ario, G., Cisar, L., Labianca, R., Cunningham, D., Nordlinger, B., Bosman, F. and Van Cutsem, E. (2012) 'Integrated analysis of molecular and clinical prognostic factors in stage II/III colon cancer', *Journal of the National Cancer Institute*, 104, pp. 1635–1646. doi: 10.1093/jnci/djs427.

Roth, A. D., Tejpar, S., Delorenzi, M., Yan, P., Fiocca, R., Klingbiel, D., Dietrich, D., Biesmans, B., Bodoky, G., Barone, C., Aranda, E., Nordlinger, B., Cisar, L., Labianca, R., Cunningham, D., Van Cutsem, E. and Bosman, F. (2010) 'Prognostic Role of KRAS and BRAF in Stage II and III Resected Colon Cancer: Results of the Translational Study on the PETACC-3, EORTC 40993, SAKK 60-00 Trial', *Journal of Clinical Oncology*, 28(3), pp. 466–474. doi: 10.1200/JCO.2009.23.3452.

Roux, P. P., Shahbazian, D., Vu, H., Holz, M. K., Cohen, M. S., Taunton, J., Sonenberg, N. and Blenis, J. (2007) 'RAS/ERK signaling promotes site-specific ribosomal protein S6 phosphorylation via RSK and stimulates cap-dependent translation', *Journal of Biological Chemistry*, 282(19), pp. 14056–14064. doi: 10.1074/jbc.M700906200.

Rubie, C., Frick, V. O., Wagner, M., Schuld, J., Gräber, S., Brittner, B., Bohle, R. M. and Schilling, M. K. (2008) 'ELR+ CXC chemokine expression in benign and malignant colorectal conditions', *BMC Cancer*, 8(1), p. 178. doi: 10.1186/1471-2407-8-178.

Rutz, S., Wang, X. and Ouyang, W. (2014) 'The IL-20 subfamily of cytokines — from host defence to tissue homeostasis', *Nature Reviews Immunology*, 14(12), pp. 783–795. doi: 10.1038/nri3766.

Ruvinsky, I. and Meyuhas, O. (2006) 'Ribosomal protein S6 phosphorylation: from protein synthesis to cell size', *Trends in Biochemical Sciences*, 31(6), pp. 342–348. doi: 10.1016/j.tibs.2006.04.003.

Ryan, D. P., Hong, T. S. and Bardeesy, N. (2014) 'Pancreatic Adenocarcinoma', *New England Journal of Medicine*, 371(11), pp. 1039–1049. doi: 10.1056/NEJMra1404198.

Ryckman, C., Vandal, K., Rouleau, P., Talbot, M. and Tessier, P. a (2003) 'Proinflammatory Activities of S100: Proteins S100A8, S100A9, and S100A8/A9 Induce Neutrophil Chemotaxis and Adhesion', *The Journal of Immunology*, 170(6), pp. 3233–3242. doi: 10.4049/jimmunol.170.6.3233.

Ryu, M. J., Liu, Y., Zhong, X., Du, J., Peterson, N., Kong, G., Li, H., Wang, J., Salamat, S., Chang, Q. and Zhang, J. (2012) 'Oncogenic Kras expression in postmitotic neurons leads to S100A8-S100A9 protein overexpression and gliosis', *Journal of Biological Chemistry*, 287(27), pp. 22948–22958. doi: 10.1074/jbc.M112.357772.

Sabat, R., Ouyang, W. and Wolk, K. (2014) 'Therapeutic opportunities of the IL-22-IL-22R1 system.', *Nature Reviews Drug Discovery*, 13(1), pp. 21–38. doi: 10.1038/nrd4176.

Sakaguchi, S., Takahashi, T. and Nishizuka, Y. (1982) 'Study on cellular events in postthymectomy autoimmune oophoritis in mice. I. Requirement of Lyt-1 effector cells for oocytes damage after adoptive transfer.', *The Journal of Experimental Medicine*, 156(6), pp. 1565–76.

Salcedo, R., Worschech, A., Cardone, M., Jones, Y., Gyulai, Z., Dai, R., Wang, E., Ma, W., Haines, D., O'hUigin, C., Marincola, F. M. and Trinchieri, G. (2010) 'MyD88-mediated signaling prevents development of adenocarcinomas of the colon: role of interleukin 18.', *The Journal of Experimental Medicine*, 207(8), pp. 1625–1636. doi: 10.1084/jem.20100199.

Sangiorgi, E. and Capecchi, M. R. (2008) 'Bmi1 is expressed in vivo in intestinal stem cells', *Nature Genetics*, 40(7), pp. 915–920. doi: 10.1038/ng.165.

Sano, T., Huang, W., Hall, J. A., Yang, Y., Chen, A., Gavzy, S. J., Lee, J. Y., Ziel, J. W., Miraldi, E. R., Domingos, A. I., Bonneau, R. and Littman, D. R. (2015) 'An IL-23R/IL-22 Circuit Regulates Epithelial Serum Amyloid A to Promote Local Effector Th17 Responses', *Cell*, 163(2), pp. 381–393. doi: 10.1016/j.cell.2015.08.061.

Sansom, O. J., Meniel, V. S., Muncan, V., Phesse, T. J., Wilkins, J. a, Reed, K. R., Vass, J. K., Athineos, D., Clevers, H. and Clarke, A. R. (2007) 'Myc deletion rescues Apc deficiency in the small intestine', *Nature*, 446(7136), pp. 676–679. doi: 10.1038/nature05674.

Sato, T., Stange, D. E., Ferrante, M., Vries, R. G. J., Van Es, J. H., Van den Brink, S., Van Houdt, W. J., Pronk, A., Van Gorp, J., Siersema, P. D. and Clevers, H. (2011) 'Long-term expansion of epithelial organoids from human colon, adenoma, adenocarcinoma, and Barrett's epithelium.', *Gastroenterology*, 141(5), pp. 1762–72. doi: 10.1053/j.gastro.2011.07.050.

Scandiuzzi, L., Ghosh, K., Hofmeyer, K. A., Abadi, Y. M., Lázár-Molnár, E., Lin, E. Y., Liu, Q., Jeon, H., Almo, S. C., Chen, L., Nathenson, S. G. and Zang, X. (2014) 'Tissue-Expressed B7-H1 Critically Controls Intestinal Inflammation', *Cell Reports*, 6(4), pp. 625–632. doi: 10.1016/j.celrep.2014.01.020.

Schiechl, G., Bauer, B., Fuss, I., Lang, S. a, Moser, C., Ruemmele, P., Rose-John, S., Neurath, M. F., Geissler, E. K., Schlitt, H., Strober, W. and Fichtner-Feigl, S. (2011) 'Tumor development in murine ulcerative colitis depends on MyD88 signaling of colonic F4/80+CD11bhighGr1low macrophages', *Journal of Clinical Investigation*, 121(5), pp. 1692–1708. doi: 10.1172/JCI42540.

Schuijers, J., van der Flier, L. G., van Es, J., Clevers, H., van der Flier, L. G., van Es, J. and Clevers, H. (2014) 'Robust Cre-Mediated Recombination in Small Intestinal Stem Cells Utilizing the Olfm4 Locus.', *Stem Cell Reports*, 3(2), pp. 234–241. doi: 10.1016/j.stemcr.2014.05.018.

Schumacher, T. N., Kesmir, C. and van Buuren, M. M. (2015) 'Biomarkers in Cancer Immunotherapy', *Cancer Cell*, 27(1), pp. 12–14. doi: 10.1016/j.ccell.2014.12.004.

Schwitalla, S., Fingerle, A. a, Cammareri, P., Nebelsiek, T., Göktuna, S. I., Ziegler, P. K., Canli, O., Heijmans, J., Huels, D. J., Moreaux, G., Rupec, R. a, Gerhard, M., Schmid, R., Barker, N., Clevers, H., Lang, R., Neumann, J., Kirchner, T., Taketo, M. M., van den Brink, G. R., Sansom, O. J., Arkan, M. C. and Greten, F. R. (2013) 'Intestinal tumorigenesis initiated by dedifferentiation and acquisition of stem-cell-like properties.', *Cell*, 152(1–2), pp. 25–38. doi: 10.1016/j.cell.2012.12.012.

Schwitalla, S., Ziegler, P. K., Horst, D., Becker, V., Kerle, I., Begus-Nahrmann, Y., Lechel, A., Rudolph, K. L., Langer, R., Slotta-Huspenina, J., Bader, F. G., Prazeres da Costa, O., Neurath, M. F., Meining, A., Kirchner, T. and Greten, F. R. (2013) 'Loss of p53 in Enterocytes Generates an Inflammatory Microenvironment Enabling Invasion and Lymph Node Metastasis of Carcinogen-Induced Colorectal Tumors', *Cancer Cell*, 23(1), pp. 93–106. doi: 10.1016/j.ccr.2012.11.014.

Sears, R. (2000) 'Multiple Ras-dependent phosphorylation pathways regulate Myc protein stability', *Genes & Development*, 14(19), pp. 2501–2514. doi: 10.1101/gad.836800.

Sears, R., Leone, G., DeGregori, J. and Nevins, J. R. (1999) 'Ras enhances Myc protein stability', *Molecular Cell*, 3(2), pp. 169–179. doi: 10.1016/S1097-2765(00)80308-1.

Shaked, H., Hofseth, L. J., Chumanevich, A., Chumanevich, A. A., Wang, J., Wang, Y., Taniguchi, K., Guma, M., Shenouda, S., Clevers, H., Harris, C. C. and Karin, M. (2012) 'Chronic epithelial NF-kB activation accelerates APC loss and intestinal tumor initiation through iNOS up-regulation', *Proceedings of the National Academy of Sciences*, 109(35), pp. 14007–14012. doi: 10.1073/pnas.1211509109.

Shalapour, S. and Karin, M. (2015) 'Immunity, inflammation, and cancer: An eternal fight between good and evil', *Journal of Clinical Investigation*, 125(9), pp. 3347–3355. doi: 10.1172/JCI80007.

Sharma, V. M., Calvo, J. a, Draheim, K. M., Cunningham, L. a, Hermance, N., Beverly, L., Krishnamoorthy, V., Bhasin, M., Capobianco, A. J. and Kelliher, M. a (2006) 'Notch1 contributes to mouse T-cell leukemia by directly inducing the expression of c-myc.', *Molecular and Cellular Biology*, 26(21), pp. 8022–8031. doi: 10.1128/MCB.01091-06.

Shen, M., Hu, P., Donskov, F., Wang, G., Liu, Q. and Du, J. (2014) 'Tumor-Associated Neutrophils as a New Prognostic Factor in Cancer: A Systematic Review and Meta-Analysis', *PLoS ONE*, 9(6). doi: 10.1371/journal.pone.0098259.

Sher, A. and Coffman, R. L. (1992) 'Regulation of immunity to parasites by T cells and T cell-derived cytokines.', *Annual Review of Immunology*, 10(6), pp. 385–409. doi: 10.1146/annurev.iy.10.040192.002125.

Shih, I.-M., Wang, T.-L., Traverso, G., Romans, K., Hamilton, S. R., Ben-Sasson, S., Kinzler, K. W. and Vogelstein, B. (2001) 'Top-down morphogenesis of colorectal tumors', *Proceedings of the National Academy of Sciences*, 98(5), pp. 2640–2645. doi: 10.1073/pnas.051629398.

Shin, S. Y., Choi, C., Lee, H. G., Lim, Y. and Lee, Y. H. (2012) 'Transcriptional regulation of the interleukin-11 gene by oncogenic Ras.', *Carcinogenesis*,

33(12), pp. 2467–2476. doi: 10.1093/carcin/bgs297.

Siegel, R. L., Fedewa, S. A., Anderson, W. F., Miller, K. D., Ma, J., Rosenberg, P. S. and Jemal, A. (2017) 'Colorectal Cancer Incidence Patterns in the United States, 1974–2013', *JNCI: Journal of the National Cancer Institute*, 109(8), pp. 27–32. doi: 10.1093/jnci/djw322.

De Simone, V., Franzè, E., Ronchetti, G., Colantoni, A., Fantini, M. C., Di Fusco, D., Sica, G. S., Sileri, P., MacDonald, T. T., Pallone, F., Monteleone, G. and Stolfi, C. (2015) 'Th17-type cytokines, IL-6 and TNF-α synergistically activate STAT3 and NF-kB to promote colorectal cancer cell growth', *Oncogene*, 34(27), pp. 3493–3503. doi: 10.1038/onc.2014.286.

De Simone, V., Pallone, F., Monteleone, G. and Stolfi, C. (2013) 'Role of T H 17 cytokines in the control of colorectal cancer', *OncoImmunology*, 2(12), p. e26617. doi: 10.4161/onci.26617.

Simpson, I. A., Dwyer, D., Malide, D., Moley, K. H., Travis, A. and Vannucci, S. J. (2008) 'The facilitative glucose transporter GLUT3: 20 years of distinction', *AJP: Endocrinology and Metabolism*, 295(2), pp. E242–E253. doi: 10.1152/ajpendo.90388.2008.

Sinicrope, F., Shi, Q., Smyrk, T. C., Thibodeau, S. N., Dienstmann, R., Guinney, J., Bot, B. M., Tejpar, S., Delorenzi, M., Goldberg, R. M., Mahoney, M., Sargent, D. J. and Alberts, S. R. (2014) 'Molecular Markers Identify Subtypes of Stage III Colon Cancer Associated With Patient Outcomes.', *Gastroenterology*, 148(1), pp. 88–99. doi: 10.1053/j.gastro.2014.09.041.

Smyth, G. K. (2004) 'Linear models and empirical bayes methods for assessing differential expression in microarray experiments.', *Statistical applications in genetics and molecular biology*, 3(1), pp. 1–25. doi: 10.2202/1544-6115.1027.

Song, X., Gao, H., Lin, Y., Yao, Y., Zhu, S., Wang, J., Liu, Y., Yao, X., Meng, G., Shen, N., Shi, Y., Iwakura, Y. and Qian, Y. (2014) 'Alterations in the microbiota drive interleukin-17c production from intestinal epithelial cells to promote tumorigenesis', *Immunity*, 40(1), pp. 140–152. doi: 10.1016/j.immuni.2013.11.018.

Sonnenberg, G. F., Nair, M. G., Kirn, T. J., Zaph, C., Fouser, L. A. and Artis, D. (2010) 'Pathological versus protective functions of IL-22 in airway inflammation are regulated by IL-17A', *The Journal of Experimental Medicine*, 207(6), pp. 1293–1305. doi: 10.1084/jem.20092054.

Sparmann, A. and Bar-Sagi, D. (2004) 'Ras-induced interleukin-8 expression plays a critical role in tumor growth and angiogenesis.', *Cancer Cell*, 6(5), pp. 447–58. doi: 10.1016/j.ccr.2004.09.028.

Spits, H., Artis, D., Colonna, M., Diefenbach, A., Di Santo, J. P., Eberl, G., Koyasu, S., Locksley, R. M., McKenzie, A. N. J., Mebius, R. E., Powrie, F. and Vivier, E. (2013) 'Innate lymphoid cells — a proposal for uniform nomenclature', *Nature Reviews Immunology*, 13(2), pp. 145–149. doi: 10.1038/nri3365.

Starczynowski, D. T., Lockwood, W. W., Deléhouzée, S., Chari, R., Wegrzyn, J., Fuller, M., Tsao, M., Lam, S., Gazdar, A. F., Lam, W. L. and Karsan, A. (2011) 'TRAF6 is an amplified oncogene bridging the RAS and NF- κ B pathways in human lung cancer', *Journal of Clinical Investigation*, 121(10), pp. 4095–4105. doi: 10.1172/JCI58818.cations.

Steele, C. W., Karim, S. A., Leach, J. D. G., Bailey, P., Upstill-Goddard, R., Rishi, L., Foth, M., Bryson, S., McDaid, K., Wilson, Z., Eberlein, C., Candido, J. B., Clarke, M., Nixon, C., Connelly, J., Jamieson, N., Carter, C. R., Balkwill, F., Chang, D. K., Evans, T. R. J., Strathdee, D., Biankin, A. V., Nibbs, R. J. B.,

Barry, S. T., Sansom, O. J. and Morton, J. P. (2016) 'CXCR2 Inhibition Profoundly Suppresses Metastases and Augments Immunotherapy in Pancreatic Ductal Adenocarcinoma', *Cancer Cell*, 29(6), pp. 832–845. doi: 10.1016/j.ccell.2016.04.014.

Steele, N., Anthony, A., Saunders, M., Esmarck, B., Ehrnrooth, E., Kristjansen, P. E. G., Nihlén, A., Hansen, L. T. and Cassidy, J. (2012) 'A phase 1 trial of recombinant human IL-21 in combination with cetuximab in patients with metastatic colorectal cancer.', *British Journal of Cancer*, 106(5), pp. 793–798. doi: 10.1038/bjc.2011.599.

Stingl, J. (2009) 'Detection and analysis of mammary gland stem cells', *The Journal of Pathology*, 217(2), pp. 229–241. doi: 10.1002/path.2457.

Stockinger, B. and Veldhoen, M. (2007) 'Differentiation and function of Th17 T cells', *Current Opinion in Immunology*, 19(3), pp. 281–286. doi: 10.1016/j.coi.2007.04.005.

Sugimoto, K., Ogawa, A., Mizoguchi, E., Shimomura, Y., Andoh, A., Bhan, A. K., Blumberg, R. S., Xavier, R. J. and Mizoguchi, A. (2008) 'IL-22 ameliorates intestinal inflammation in a mouse model of ulcerative colitis', *Journal of Clinical Investigation*, 118(2), pp. 534–44. doi: 10.1172/JCI33194.

Swain, S. L. (1983) 'T cell subsets and the recognition of MHC class', *Immunological Reviews*, Vol. 74.

Tachiiri, a, Imamura, R., Wang, Y., Fukui, M., Umemura, M. and Suda, T. (2003) 'Genomic structure and inducible expression of the IL-22 receptor α chain in mice', *Genes and Immunity*, 4(2), pp. 153–159. doi: 10.1038/sj.gene.6363934.

Taniguchi, K. and Karin, M. (2014) 'IL-6 and related cytokines as the critical lynchpins between inflammation and cancer.', *Seminars in Immunology*, 26(1), pp. 54–74. doi: 10.1016/j.smim.2014.01.001.

Tanoue, T., Atarashi, K. and Honda, K. (2016) 'Development and maintenance of intestinal regulatory T cells', *Nature Reviews Immunology*, 16(5), pp. 295–309. doi: 10.1038/nri.2016.36.

Teng, M. W. L., Bowman, E. P., McElwee, J. J., Smyth, M. J., Casanova, J.-L., Cooper, A. M. and Cua, D. J. (2015) 'IL-12 and IL-23 cytokines: from discovery to targeted therapies for immune-mediated inflammatory diseases.', *Nature Medicine*, 21(7), pp. 719–729. doi: 10.1038/nm.3895.

Terzić, J., Grivennikov, S., Karin, E. and Karin, M. (2010) 'Inflammation and colon cancer.', *Gastroenterology*, 138(6), p. 2101–2114.e5. doi: 10.1053/j.gastro.2010.01.058.

Thompson, C. L., Plummer, S. J., Tucker, T. C., Casey, G. and Li, L. (2010) 'Interleukin-22 genetic polymorphisms and risk of colon cancer.', *Cancer causes & control : CCC*, 21(8), pp. 1165–70. doi: 10.1007/s10552-010-9542-5.

Tong, Z., Yang, X. O. X., Yan, H., Liu, W., Niu, X., Shi, Y., Fang, W., Xiong, B., Wan, Y. and Dong, C. (2012) 'A Protective Role by Interleukin-17F in Colon Tumorigenesis', *PLoS One*, 7(4), pp. 1–8. doi: 10.1371/journal.pone.0034959.

Topalian, S. L., Hodi, F. S., Brahmer, J. R., Gettinger, S. N., Smith, D. C., McDermott, D. F., Powderly, J. D., Carvajal, R. D., Sosman, J. A., Atkins, M. B., Leming, P. D., Spigel, D. R., Antonia, S. J., Horn, L., Drake, C. G., Pardoll, D. M., Chen, L., Sharfman, W. H., Anders, R. A., Taube, J. M., McMiller, T. L., Xu, H., Korman, A. J., Jure-Kunkel, M., Agrawal, S., McDonald, D., Kollia, G. D., Gupta, A., Wigginton, J. M. and Sznol, M. (2012) 'Safety, Activity, and Immune Correlates of Anti–PD-1 Antibody in Cancer', *New England Journal of Medicine*, 366(26), pp. 2443–2454. doi: 10.1056/NEJMoa1200690.

Tosolini, M., Kirilovsky, A., Mlecnik, B., Fredriksen, T., Mauger, S., Bindea, G., Berger, A., Bruneval, P., Fridman, W.-H., Pagès, F. and Galon, J. (2011) 'Clinical impact of different classes of infiltrating T cytotoxic and helper cells (Th1, Th2, Treg, Th17) in patients with colorectal cancer.', *Cancer Research*, 71(4), pp. 1263–71. doi: 10.1158/0008-5472.CAN-10-2907.

Tran, E., Robbins, P. F., Lu, Y.-C., Prickett, T. D., Gartner, J. J., Jia, L., Pasetto, A., Zheng, Z., Ray, S., Groh, E. M., Kriley, I. R. and Rosenberg, S. A. (2016) 'T-Cell Transfer Therapy Targeting Mutant KRAS in Cancer', *New England Journal of Medicine*, 375(23), pp. 2255–2262. doi: 10.1056/NEJMoa1609279.

Trinchieri, G. (2003) 'Interleukin-12 and the regulation of innate resistance and adaptive immunity.', *Nature Reviews Immunology*, 3(2), pp. 133–46. doi: 10.1038/nri1001.

Tseng-Rogenski, S. S., Hamaya, Y., Choi, D. Y. and Carethers, J. M. (2014) 'Interleukin 6 Alters Localization of hMSH3, Leading to DNA Mismatch Repair Defects in Colorectal Cancer Cells.', *Gastroenterology*, 148(3), pp. 579–589. doi: 10.1053/j.gastro.2014.11.027.

Turovskaya, O., Foell, D., Sinha, P., Vogl, T., Newlin, R., Nayak, J., Nguyen, M., Olsson, A., Nawroth, P. P., Bierhaus, A., Varki, N., Kronenberg, M., Freeze, H. H. and Srikrishna, G. (2008) 'RAGE, carboxylated glycans and S100A8/A9 play essential roles in colitis-associated carcinogenesis', *Carcinogenesis*, 29(10), pp. 2035–2043. doi: 10.1093/carcin/bgn188.

Tyanova, S., Temu, T. and Cox, J. (2016) 'The MaxQuant computational platform for mass spectrometry-based shotgun proteomics.', *Nature protocols*, 11(12), pp. 2301–2319. doi: 10.1038/nprot.2016.136.

Uhlig, H. H., McKenzie, B. S., Hue, S., Thompson, C., Joyce-Shaikh, B., Stepankova, R., Robinson, N., Buonocore, S., Tlaskalova-Hogenova, H., Cua, D. J. and Powrie, F. (2006) 'Differential activity of IL-12 and IL-23 in mucosal and systemic innate immune pathology.', *Immunity*, 25(2), pp. 309–318. doi: 10.1016/j.immuni.2006.05.017.

Urdinguio, R. G., Fernandez, A. F., Moncada-Pazos, A., Huidobro, C., Rodriguez, R. M., Ferrero, C., Martinez-Camblor, P., Obaya, A. J., Bernal, T., Parra-Blanco, A., Rodrigo, L., Santacana, M., Matias-Guiu, X., Soldevilla, B., Dominguez, G., Bonilla, F., Cal, S., Lopez-Otin, C. and Fraga, M. F. (2013) 'Immune-dependent and independent antitumor activity of GM-CSF aberrantly expressed by mouse and human colorectal tumors', *Cancer Research*, 73, pp. 395–405. doi: 10.1158/0008-5472.CAN-12-0806.

Vennstrom, B., Sheiness, D., Zabielski, J. and Bishop, J. M. (1982) 'Isolation and characterization of c-myc, a cellular homolog of the oncogene (v-myc) of avian myelocytomatosis virus strain 29.', *Journal of Virology*, 42(3), pp. 773–9.

Vogelstein, B. and Kinzler, K. W. (2004) 'Cancer genes and the pathways they control', *Nature Medicine*, 10(8), pp. 789–799. doi: 10.1038/nm1087.

Vojtek, A. B. and Der, C. J. (1998) 'Increasing Complexity of the Ras Signaling Pathway', *Journal of Biological Chemistry*, 273(32), pp. 19925–19928. doi: 10.1074/jbc.273.32.19925.

Volpe, E., Servant, N., Zollinger, R., Bogiatzi, S. I., Hupé, P., Barillot, E. and Soumelis, V. (2008) 'A critical function for transforming growth factor-β, interleukin 23 and proinflammatory cytokines in driving and modulating human TH-17 responses', *Nature Immunology*, 9(6), pp. 650–657. doi: 10.1038/ni.1613.

Wan, Y. Y. and Flavell, R. A. (2007) '"Yin–Yang" functions of transforming growth

factor-β and T regulatory cells in immune regulation', *Immunological Reviews*, 220(1), pp. 199–213. doi: 10.1111/j.1600-065X.2007.00565.x.

Wang, C., Gong, G., Sheh, A., Muthupalani, S., Bryant, E. M., Puglisi, D. A., Holcombe, H., Conaway, E. A., Parry, N. A. P., Bakthavatchalu, V., Short, S. P., Williams, C. S., Wogan, G. N., Tannenbaum, S. R., Fox, J. G. and Horwitz, B. H. (2017) 'Interleukin-22 drives nitric oxide-dependent DNA damage and dysplasia in a murine model of colitis-associated cancer', *Mucosal Immunology*, (February), pp. 1–14. doi: 10.1038/mi.2017.9.

Wang, D., Wang, H., Brown, J., Daikoku, T., Ning, W., Shi, Q., Richmond, A., Strieter, R., Dey, S. K. and DuBois, R. N. (2006) 'CXCL1 induced by prostaglandin E 2 promotes angiogenesis in colorectal cancer', *The Journal of Experimental Medicine*, 203(4), pp. 941–951. doi: 10.1084/jem.20052124.

Wang, H., Wang, H.-S., Zhou, B.-H., Li, C.-L., Zhang, F., Wang, X.-F., Zhang, G., Bu, X.-Z., Cai, S.-H. and Du, J. (2013) 'Epithelial-mesenchymal transition (EMT) induced by TNF-α requires AKT/GSK-3β-mediated stabilization of snail in colorectal cancer.', *PloS One*, 8(2), p. e56664. doi: 10.1371/journal.pone.0056664.

Wang, K., Kim, M. K., Di Caro, G., Wong, J., Shalapour, S., Wan, J., Zhang, W., Zhong, Z., Sanchez-Lopez, E., Wu, L.-W., Taniguchi, K., Feng, Y., Fearon, E., Grivennikov, S. and Karin, M. (2014) 'Interleukin-17 receptor A signaling in transformed enterocytes promotes early colorectal tumorigenesis', *Immunity*, 41(6), pp. 1052–1063. doi: 10.1016/j.immuni.2014.11.009.

Wang, W.-B., Yen, M.-L., Liu, K.-J., Hsu, P.-J., Lin, M.-H., Chen, P.-M., Sudhir, P.-R., Chen, C.-H., Chen, C.-H., Sytwu, H.-K. and Yen, B. L. (2015) 'Interleukin-25 Mediates Transcriptional Control of PD-L1 via STAT3 in Multipotent Human Mesenchymal Stromal Cells (hMSCs) to Suppress Th17 Responses', *Stem Cell Reports*, 5(3), pp. 392–404. doi: 10.1016/j.stemcr.2015.07.013.

Wang, Y., Han, G., Wang, K., Liu, G., Wang, R., Xiao, H., Li, X., Hou, C., Shen, B., Guo, R., Li, Y. and Chen, G. (2014) 'Tumor-derived GM-CSF promotes inflammatory colon carcinogenesis via stimulating epithelial release of VEGF', *Cancer Research*, 74, pp. 716–726. doi: 10.1158/0008-5472.CAN-13-1459.

Wang, Y., Wang, K., Han, G.-C., Wang, R.-X., Xiao, H., Hou, C.-M., Guo, R.-F., Dou, Y., Shen, B.-F., Li, Y. and Chen, G.-J. (2014) 'Neutrophil infiltration favors colitis-associated tumorigenesis by activating the interleukin-1 (IL-1)/IL-6 axis', *Mucosal Immunology*, 7(5), pp. 1106–1115. doi: 10.1038/mi.2013.126.

Waugh, D. J. J. and Wilson, C. (2008) 'The Interleukin-8 Pathway in Cancer', *Clinical Cancer Research*, 14(21), pp. 6735–6741. doi: 10.1158/1078-0432.CCR-07-4843.

Weathington, N. M., Snavely, C. a, Chen, B. B., Zhao, J., Zhao, Y. and Mallampalli, R. K. (2014) 'Glycogen Synthase Kinase-3β Stabilizes the Interleukin (IL)-22 Receptor from Proteasomal Degradation in Murine Lung Epithelia', *Journal of Biological Chemistry*, 289(25), pp. 17610–17619. doi: 10.1074/jbc.M114.551747.

de Weerd, N. A. and Nguyen, T. (2012) 'The interferons and their receptors—distribution and regulation', *Immunology and Cell Biology*, 90(5), pp. 483–491. doi: 10.1038/icb.2012.9.

Weiss, A. and Attisano, L. (2013) 'The TGFbeta Superfamily Signaling Pathway', *Wiley Interdisciplinary Reviews: Developmental Biology*, 2(1), pp. 47–63. doi: 10.1002/wdev.86.

Wen, W., Liang, W., Wu, J., Kowolik, C. M., Buettner, R., Scuto, A., Hsieh, M.-Y.,

Hong, H., Brown, C. E., Forman, S. J., Horne, D., Morgan, R., Wakabayashi, M., Dellinger, T. H., Han, E. S., Yim, J. H. and Jove, R. (2014) 'Targeting JAK1/STAT3 signaling suppresses tumor progression and metastasis in a peritoneal model of human ovarian cancer.', *Molecular Cancer Therapeutics*, 13(12), pp. 3037–3048. doi: 10.1158/1535-7163.MCT-14-0077.

Wen, Y., Giardina, S. F., Hamming, D., Greenman, J., Zachariah, E., Bacolod, M. D., Liu, H., Shia, J., Amenta, P. S., Barany, F., Paty, P., Gerald, W. and Notterman, D. (2006) 'GRO Is Highly Expressed in Adenocarcinoma of the Colon and Down-Regulates Fibulin-1', *Clinical Cancer Research*, 12(20), pp. 5951–5959. doi: 10.1158/1078-0432.CCR-06-0736.

Weng, A. P., Millholland, J. M., Yashiro-Ohtani, Y., Arcangeli, M. L., Lau, A., Wai, C., Del Bianco, C., Rodriguez, C. G., Sai, H., Tobias, J., Li, Y., Wolfe, M. S., Shachaf, C., Felsher, D., Blacklow, S. C., Pear, W. S. and Aster, J. C. (2006) 'c-Myc is an important direct target of Notch1 in T-cell acute lymphoblastic leukemia/lymphoma', *Genes and Development*, 20(15), pp. 2096–2109. doi: 10.1101/gad.1450406.

West, N. R., McCuaig, S., Franchini, F. and Powrie, F. (2015) 'Emerging cytokine networks in colorectal cancer', *Nature Reviews Immunology*, 15(10), pp. 615–629. doi: 10.1038/nri3896.

Westra, J. L., Schaapveld, M., Hollema, H., De Boer, J. P., Kraak, M. M. J., De Jong, D., Ter Elst, A., Mulder, N. H., Buys, C. H. C. M., Hofstra, R. M. W. and Plukker, J. T. M. (2005) 'Determination of TP53 mutation is more relevant than microsatellite instability status for the prediction of disease-free survival in adjuvant-treated stage III colon cancer patients', *Journal of Clinical Oncology*, 23(24), pp. 5635–5643. doi: 10.1200/JCO.2005.04.096.

van de Wetering, M., Francies, H. E., Francis, J. M., Bounova, G., Iorio, F., Pronk, A., van Houdt, W., van Gorp, J., Taylor-Weiner, A., Kester, L., McLaren-Douglas, A., Blokker, J., Jaksani, S., Bartfeld, S., Volckman, R., van Sluis, P., Li, V. S. W., Seepo, S., Sekhar Pedamallu, C., Cibulskis, K., Carter, S. L., McKenna, A., Lawrence, M. S., Lichtenstein, L., Stewart, C., Koster, J., Versteeg, R., van Oudenaarden, A., Saez-Rodriguez, J., Vries, R. G. J., Getz, G., Wessels, L., Stratton, M. R., McDermott, U., Meyerson, M., Garnett, M. J. and Clevers, H. (2015) 'Prospective Derivation of a Living Organoid Biobank of Colorectal Cancer Patients', *Cell*, 161(4), pp. 933–945. doi: 10.1016/j.cell.2015.03.053.

van de Wetering, M., Sancho, E., Verweij, C., de Lau, W., Oving, I., Hurlstone, A., van der Horn, K., Batlle, E., Coudreuse, D., Haramis, A. P., Tjon-Pon-Fong, M., Moerer, P., van den Born, M., Soete, G., Pals, S., Eilers, M., Medema, R. and Clevers, H. (2002) 'The beta-catenin/TCF-4 complex imposes a crypt progenitor phenotype on colorectal cancer cells.', *Cell*, 111(2), pp. 241–50.

Wiegering, A., Uthe, F. W., Jamieson, T., Ruoss, Y., Huttenrauch, M., Kuspert, M., Pfann, C., Nixon, C., Herold, S., Walz, S., Taranets, L., Germer, C.-T., Rosenwald, A., Sansom, O. J. and Eilers, M. (2015) 'Targeting Translation Initiation Bypasses Signaling Crosstalk Mechanisms That Maintain High MYC Levels in Colorectal Cancer', *Cancer Discovery*, 5(7), pp. 768–781. doi: 10.1158/2159-8290.CD-14-1040.

Wiener, Z., Band, A. M., Kallio, P., Hogstrom, J., Hyvonen, V., Kaijalainen, S., Ritvos, O., Haglund, C., Kruuna, O., Robine, S., Louvard, D., Ben-Neriah, Y. and Alitalo, K. (2014) 'Oncogenic mutations in intestinal adenomas regulate Bim-mediated apoptosis induced by TGF-', *Proceedings of the National*

Academy of Sciences, 111(21), pp. E2229–E2236. doi: 10.1073/pnas.1406444111.

Wilhelm, K., Happel, K., Eelen, G., Schoors, S., Oellerich, M. F., Lim, R., Zimmermann, B., Aspalter, I. M., Franco, C. A., Boettger, T., Braun, T., Fruttiger, M., Rajewsky, K., Keller, C., Brüning, J. C., Gerhardt, H., Carmeliet, P. and Potente, M. (2016) 'FOXO1 couples metabolic activity and growth state in the vascular endothelium', *Nature*, 529(7585), pp. 216–220. doi: 10.1038/nature16498.

Wilson, N. J., Boniface, K., Chan, J. R., McKenzie, B. S., Blumenschein, W. M., Mattson, J. D., Basham, B., Smith, K., Chen, T., Morel, F., Lecron, J.-C., Kastelein, R. A., Cua, D. J., McClanahan, T. K., Bowman, E. P. and de Waal Malefyt, R. (2007) 'Development, cytokine profile and function of human interleukin 17–producing helper T cells', *Nature Immunology*, 8(9), pp. 950–957. doi: 10.1038/ni1497.

Wing, J. B. and Sakaguchi, S. (2012) 'Multiple Treg suppressive modules and their adaptability', *Frontiers in Immunology*, 3. doi: 10.3389/fimmu.2012.00178.

Wislez, M., Fujimoto, N., Izzo, J. G., Hanna, A. E., Cody, D. D., Langley, R. R., Tang, H., Burdick, M. D., Sato, M., Minna, J. D., Mao, L., Wistuba, I., Strieter, R. M. and Kurie, J. M. (2006) 'High expression of ligands for chemokine receptor CXCR2 in alveolar epithelial neoplasia induced by oncogenic Kras', *Cancer Research*, 66(8), pp. 4198–4207. doi: 10.1158/0008-5472.CAN-05-3842.

Wolk, K., Kunz, S., Witte, E., Friedrich, M., Asadullah, K. and Sabat, R. (2004) 'IL-22 increases the innate immunity of tissues', *Immunity*, 21(2), pp. 241–254. doi: 10.1016/j.immuni.2004.07.007.

Wolk, K., Witte, E., Hoffmann, U., Doecke, W.-D., Endesfelder, S., Asadullah, K., Sterry, W., Volk, H.-D., Wittig, B. M. and Sabat, R. (2007) 'IL-22 Induces Lipopolysaccharide-Binding Protein in Hepatocytes: A Potential Systemic Role of IL-22 in Crohn's Disease', *The Journal of Immunology*, 178(9), pp. 5973–5981. doi: 10.4049/jimmunol.178.9.5973.

Wolk, K., Witte, E., Wallace, E., Döcke, W.-D., Kunz, S., Asadullah, K., Volk, H.-D., Sterry, W. and Sabat, R. (2006) 'IL-22 regulates the expression of genes responsible for antimicrobial defense, cellular differentiation, and mobility in keratinocytes: a potential role in psoriasis', *European Journal of Immunology*, 36(5), pp. 1309–1323. doi: 10.1002/eji.200535503.

Wood, L. D., Parsons, D. W., Jones, S., Lin, J., Sjoblom, T., Leary, R. J., Shen, D., Boca, S. M., Barber, T., Ptak, J., Silliman, N., Szabo, S., Dezso, Z., Ustyanksky, V., Nikolskaya, T., Nikolsky, Y., Karchin, R., Wilson, P. A., Kaminker, J. S., Zhang, Z., Croshaw, R., Willis, J., Dawson, D., Shipitsin, M., Willson, J. K. V., Sukumar, S., Polyak, K., Park, B. H., Pethiyagoda, C. L., Pant, P. V. K., Ballinger, D. G., Sparks, A. B., Hartigan, J., Smith, D. R., Suh, E., Papadopoulos, N., Buckhaults, P., Markowitz, S. D., Parmigiani, G., Kinzler, K. W., Velculescu, V. E. and Vogelstein, B. (2007) 'The Genomic Landscapes of Human Breast and Colorectal Cancers', *Science*, 318(5853), pp. 1108–1113. doi: 10.1126/science.1145720.

Wu, P., Wu, D., Ni, C., Ye, J., Chen, W., Hu, G., Wang, Z., Wang, C., Zhang, Z., Xia, W., Chen, Z., Wang, K., Zhang, T., Xu, J., Han, Y., Zhang, T., Wu, X., Wang, J., Gong, W., Zheng, S., Qiu, F., Yan, J. and Huang, J. (2014) 'γδT17 cells promote the accumulation and expansion of myeloid-derived suppressor cells in human colorectal cancer', *Immunity*, 40(5), pp. 785–800. doi:

10.1016/j.immuni.2014.03.013.

Wu, S., Rhee, K.-J., Albesiano, E., Rabizadeh, S., Wu, X., Yen, H., Huso, D. L., Brancati, F. L., Wick, E., McAllister, F., Housseau, F., Pardoll, D. M. and Sears, C. L. (2009) 'A human colonic commensal promotes colon tumorigenesis via activation of T helper type 17 T cell responses', *Nature Medicine*, 15(9), pp. 1016–1022. doi: 10.1038/nm.2015.

Wu, T., Cui, L., Liang, Z., Liu, C., Liu, Y. and Li, J. (2013) 'Elevated serum IL-22 levels correlate with chemoresistant condition of colorectal cancer.', *Clinical Immunology*, 147(1), pp. 38–9. doi: 10.1016/j.clim.2013.02.007.

Wu, T., Wang, Z., Liu, Y., Mei, Z., Wang, G., Liang, Z., Cui, A., Hu, X., Cui, L., Yang, Y. and Liu, C.-Y. (2014) 'Interleukin 22 protects colorectal cancer cells from chemotherapy by activating the STAT3 pathway and inducing autocrine expression of interleukin 8', *Clinical Immunology*, 154(2), pp. 116–126. doi: 10.1016/j.clim.2014.07.005.

Wu, Y., Deng, J., Rychahou, P. G., Qiu, S., Evers, B. M. and Zhou, B. P. (2009) 'Stabilization of Snail by NF-κB Is Required for Inflammation-Induced Cell Migration and Invasion', *Cancer Cell*, 15(5), pp. 416–428. doi: 10.1016/j.ccr.2009.03.016.

Xie, M. H., Aggarwal, S., Ho, W. H., Foster, J., Zhang, Z., Stinson, J., Wood, W. I., Goddard, a D. and Gurney, a L. (2000) 'Interleukin (IL)-22, a novel human cytokine that signals through the interferon receptor-related proteins CRF2-4 and IL-22R.', *The Journal of Biological Chemistry*, 275(40), pp. 31335–9. doi: 10.1074/jbc.M005304200.

Xu, M.-J., Feng, D., Wang, H., Guan, Y., Yan, X. and Gao, B. (2014) 'IL-22 ameliorates renal ischemia-reperfusion injury by targeting proximal tubule epithelium.', *Journal of the American Society of Nephrology : JASN*, 25(5), pp. 967–77. doi: 10.1681/ASN.2013060611.

Xu, W., Presnell, S. R., Parrish-Novak, J., Kindsvogel, W., Jaspers, S., Chen, Z., Dillon, S. R., Gao, Z., Gilbert, T., Madden, K., Schlutsmeyer, S., Yao, L., Whitmore, T. E., Chandrasekher, Y., Grant, F. J., Maurer, M., Jelinek, L., Storey, H., Brender, T., Hammond, A., Topouzis, S., Clegg, C. H. and Foster, D. C. (2001) 'A soluble class II cytokine receptor, IL-22RA2, is a naturally occurring IL-22 antagonist', *Proceedings of the National Academy of Sciences*, 98(17), pp. 9511–9516. doi: 10.1073/pnas.171303198.

Yao, Z., Fanslow, W. C., Seldin, M. F., Rousseau, A. M., Painter, S. L., Comeau, M. R., Cohen, J. I. and Spriggs, M. K. (1995) 'Herpesvirus Saimiri encodes a new cytokine, IL-17, which binds to a novel cytokine receptor', *Immunity*, 3(6), pp. 811–821. doi: 10.1016/1074-7613(95)90070-5.

Yen, D., Cheung, J., Scheerens, H., Poulet, F., Mcclanahan, T., Mckenzie, B., Kleinschek, M. A., Owyang, A., Mattson, J., Blumenschein, W., Murphy, E., Sathe, M., Cua, D. J., Kastelein, R. A. and Rennick, D. (2006) 'IL-23 is essential for T cell – mediated colitis and promotes inflammation via IL-17 and IL-6', 116(5). doi: 10.1172/JCI21404.1310.

Ying, M., Li, D., Yang, L., Wang, M., Wang, N., Chen, Y., He, M. and Wang, Y. (2010) 'Loss of SOCS3 expression is associated with an increased risk of recurrent disease in breast carcinoma', *Journal of Cancer Research and Clinical Oncology*, 136(10), pp. 1617–1626. doi: 10.1007/s00432-010-0819-6.

Yoshimura, A., Naka, T. and Kubo, M. (2007) 'SOCS proteins, cytokine signalling and immune regulation', *Nature Reviews Immunology*, 7(6), pp. 454–465. doi: 10.1038/nri2093.

Yoshimura, A. and Yasukawa, H. (2012) 'JAK's SOCS: a mechanism of inhibition.', *Immunity*, 36(2), pp. 157–9. doi: 10.1016/j.immuni.2012.01.010.

Yu, H., Liu, Y., McFarland, B. C., Deshane, J. S., Hurst, D. R., Ponnazhagan, S., Benveniste, E. N. and Qin, H. (2015) 'SOCS3 Deficiency in Myeloid Cells Promotes Tumor Development: Involvement of STAT3 Activation and Myeloid-Derived Suppressor Cells', *Cancer Immunology Research*, 3(7), pp. 727–740. doi: 10.1158/2326-6066.CIR-15-0004.

Yu, H., Pardoll, D. and Jove, R. (2009) 'STATs in cancer inflammation and immunity: a leading role for STAT3', *Nature Reviews Cancer*, 9(11), pp. 798–809. doi: 10.1038/nrc2734.

Yuan, T. L., Fellmann, C., Lee, C.-S., Ritchie, C. D., Thapar, V., Lee, L. C., Hsu, D. J., Grace, D., Carver, J. O., Zuber, J., Luo, J., McCormick, F. and Lowe, S. W. (2014) 'Development of siRNA Payloads to Target KRAS-Mutant Cancer', *Cancer Discovery*, 4(10), pp. 1182–1197. doi: 10.1158/2159-8290.CD-13-0900.

Zaki, M. H., Vogel, P., Body-Malapel, M., Lamkanfi, M. and Kanneganti, T.-D. (2010) 'IL-18 Production Downstream of the Nlrp3 Inflammasome Confers Protection against Colorectal Tumor Formation', *The Journal of Immunology*, 185(8), pp. 4912–4920. doi: 10.4049/jimmunol.1002046.

Zenewicz, L. a, Yancopoulos, G. D., Valenzuela, D. M., Murphy, A. J., Karow, M. and Flavell, R. a (2007) 'Interleukin-22 but not interleukin-17 provides protection to hepatocytes during acute liver inflammation.', *Immunity*, 27(4), pp. 647–659. doi: 10.1016/j.immuni.2007.07.023.

Zenewicz, L. a, Yancopoulos, G. D., Valenzuela, D. M., Murphy, A. J., Stevens, S. and Flavell, R. a (2008) 'Innate and Adaptive Interleukin-22 Protects Mice from Inflammatory Bowel Disease', *Immunity*, 29(6), pp. 947–957. doi: 10.1016/j.immuni.2008.11.003.

Zhang, M., Yao, Z., Dubois, S., Ju, W., Muller, J. R. and Waldmann, T. a (2009) 'Interleukin-15 combined with an anti-CD40 antibody provides enhanced therapeutic efficacy for murine models of colon cancer', *Proceedings of the National Academy of Sciences*, 106(18), pp. 7513–7518. doi: 10.1073/pnas.0902637106.

Zhang, W., Chen, Y., Wei, H., Zheng, C., Sun, R., Zhang, J. and Tian, Z. (2008) 'Antiapoptotic activity of autocrine interleukin-22 and therapeutic effects of interleukin-22-small interfering RNA on human lung cancer xenografts', *Clinical Cancer Research*, 14(20), pp. 6432–6439. doi: 10.1158/1078-0432.CCR-07-4401.

Zhang, X., Yue, P., Page, B. D. G., Li, T., Zhao, W., Namanja, A. T., Paladino, D., Zhao, J., Chen, Y., Gunning, P. T. and Turkson, J. (2012) 'Orally bioavailable small-molecule inhibitor of transcription factor Stat3 regresses human breast and lung cancer xenografts', *Proceedings of the National Academy of Sciences*, 109(24), pp. 9623–9628. doi: 10.1073/pnas.1121606109.

Zheng, Y., Danilenko, D. M., Valdez, P., Kasman, I., Eastham-Anderson, J., Wu, J. and Ouyang, W. (2007) 'Interleukin-22, a TH17 cytokine, mediates IL-23-induced dermal inflammation and acanthosis', *Nature*, 445(7128), pp. 648–651. doi: 10.1038/nature05505.

Zheng, Y., Valdez, P. a, Danilenko, D. M., Hu, Y., Sa, S. M., Gong, Q., Abbas, A. R., Modrusan, Z., Ghilardi, N., de Sauvage, F. J. and Ouyang, W. (2008) 'Interleukin-22 mediates early host defense against attaching and effacing bacterial pathogens', *Nature Medicine*, 14(3), pp. 282–289. doi: 10.1038/nm1720.

Zhuang, Y., Peng, L.-S., Zhao, Y.-L., Shi, Y., Mao, X.-H., Guo, G., Chen, W., Liu, X.-F., Zhang, J.-Y., Liu, T., Luo, P., Yu, P.-W. and Zou, Q.-M. (2012) 'Increased intratumoral IL-22-producing CD4(+) T cells and Th22 cells correlate with gastric cancer progression and predict poor patient survival.', *Cancer Immunology, Immunotherapy : CII*, 61(11), pp. 1965–75. doi: 10.1007/s00262-012-1241-5.

Zindl, C. L., Lai, J.-F., Lee, Y. K., Maynard, C. L., Harbour, S. N., Ouyang, W., Chaplin, D. D. and Weaver, C. T. (2013) 'IL-22-producing neutrophils contribute to antimicrobial defense and restitution of colonic epithelial integrity during colitis', *Proceedings of the National Academy of Sciences*, 110(31), pp. 12768–12773. doi: 10.1073/pnas.1300318110.

1 Appendix: Future Experiments

1.1 Unanswered scientific questions

While the opportunities for clinical translation of the new knowledge presented in this thesis were discussed in Chapter 6.3 and 6.4, it is important to highlight a number of unanswered scientific questions that if answered, will enhance our understanding of the IL-23/IL-22 pathways in human CRC and may inform combinatorial therapeutic strategies in this poor prognosis molecular subtype of CRC.

1.2 IL-22RA1 expression and regulation

1.2.1 Why do some patients have elevated tumoural and matched normal adjacent IL-22RA1 expression compared to others? Is this microbiota dependent?

IL22RA1 expression between tumour and matched normal tissue was highly correlated, but there was vast heterogeneity between patients (Chapter 3). It remains unclear whether this heterogeneity is dictated by underlying genetic or epigenetic factors or is a consequence of signals from the microenvironment. *IL22RA1* expression was induced with TIL supernatant stimulation and was not dependent on TNFα, IFNγ, or IL-22 (Chapter 5, Figure 5.6 A), suggesting the involvement of another factor in the milieu (ie. IL-1β, IL-17A). One possibility is that the microbiota, which is very heterogeneous between individuals, conditions the immune microenvironment to influence *IL22RA1* expression or that it directly interacts with epithelial cells and modulates basal *IL22RA1* expression. A recent study identified that proximal colorectal tumours are almost universally associated with biofilms (Dejea *et al.*, 2014). Moreover, regardless of location, mucosa adjacent to biofilm-associated tumours was also biofilm-associated (Dejea *et al.*, 2014). Since previous reports have suggested that LPS stimulation can induce IL-22RA1 expression (Tachiiri *et al.*, 2003), we wonder whether the presence or absence of biofilms on tumour and adjacent mucosa influences IL-22RA1 expression. By collaborating with

Dr. Cynthia Sears *et al.* we plan to stain for IL-22RA1 expression by IHC on banked samples from two independent cohorts of tumours and matched normal tissue with known biofilm +/- status.

1.2.2 Why is *IL22* expression elevated in proximal, *IL22RA1*-high, *KRAS* mutant versus wild type tumours? Is this microbiota dependent?

We observed elevated *IL22* transcript (and a trend toward elevated *IL23A*) in *KRAS* mutant versus wild type, *IL22RA1*-high proximal tumours, but this difference between genotypes in *IL22RA1*-high distal tumours was not present. We question whether this difference in *IL22* expression may be microbe-dependent and again possibly a consequence of the biofilm status of the tumour. Therefore in the cohorts described in the previous section, with known biolfilm status, we will assess *IL22* and *IL23A* expression likely using RNA-scope versus IHC, as IHC-based detection of cytokines is historically difficult and inconsistent and relate this to the *KRAS* mutation status of the tumours.

1.2.3 Are the cell types, which express IL-22RA1 in the tumour the same as those in the normal adjacent tissue?

Universally we observed that *IL22RA1* expression is lower in tumours compared to matched normal tissue (this was also the case for IL-10RB) (Chapter 3). Some studies have suggested that IL-22RA1 is predominately expressed on differentiated epithelial cell subtypes such goblet cells and enteroendocrine cells, but expression has also been observed on intestinal epithelial stem cells (Hanash *et al.*, 2012; Lindemans *et al.*, 2015). Tumours that are well-differentiated tend to be associated with better prognosis, which presents a paradox if indeed *IL22RA1* is predominately expressed on more differentiated cell types in the tumour. Thus, single cell sequencing analysis of the epithelial compartment from paired tumour and matched normal adjacent tissue

should be conducted to determine the transcriptional signature associated with *IL22RA1*-high cells in the tumour versus matched normal adjacent tissue. Are these signatures similar or different and what are the implications?

1.2.4 How does regulation of IL-22RA1 differ in *KRAS* mutant versus wild type tumours?

Preliminary functional studies of IL-22RA1 dynamics were presented in this thesis (Chapter 4, Figure 4.12). Preliminary observations of IL-22 stimulation and subsequent withdrawl in the DLD-1 isogenic pair revealed that *IL22RA1* mRNA recovery is slower in *KRAS* wild type versus mutant cells (Chapter 4, Figure 4.12 F). These experiments need to be repeated to confirm this observation. Moreover, we observed that while *IL22RA1* expression was diminished in *KRAS* wild type tumours compared to matched normal adjacent tissue, no differences were observed in *KRAS* mutant tumours and matched normal tissue (Chapter 4, Figure 4.11). These observations need to be confirmed in larger patient cohorts. The single cell sequencing analysis described in the previous section should be conducted with both *KRAS* mutant and wild type tumours to again identify whether there is a difference in the transcriptional profiles of the cell types expressing *IL22RA1* in *KRAS* mutant versus wild type tumours and if there is more or less divergence from the normal adjacent tissue in one genotype versus the other.

1.2.5 What is the prognostically important cutpoint that defines high and low IL-22RA1 expression?

We continue to accrue patient tumour and matched normal adjacent tissue prospectively and are working with Clare Verrill and Dr. Robert Pell in molecular pathology to develop a diagnostic IHC assay to be scored using digital pathology methods. This would be used in combination with *KRAS* mutation typing to identify patients in the poor prognosis subgroup. Once survival data becomes available for the

patients we have collected prospectively, a cutpoint that stratifies patients based on prognosis will be determined.

1.3 Elevated IL-23 in CRC

1.3.1 Is IL-23 protein elevated in human CRC tumours compared to matched normal tissue and what is the dominant cellular source?

While we and others have observed elevated *IL23A* mRNA in CRC tumours compared to matched normal tissue in whole tissue RNA analysis (Chapter 3, Figure 3.1), it remains unknown whether these differences are reflected at the protein level and what the dominant cellular source of IL-23 in the tumour microenviorment is. IL-23 analysis by flow cytometry is difficult, but Dominik Aschenbrenner, a post doc in Holm Uhlig's lab, has a working IL-23p19 staining protocol for human PBMCs. We propose combining IL-23p19 staining of fresh resected CRC and matched normal tissue with broad cell lineage markers (EpCAM, CD45, CD31, gp38) and a detailed myeloid staining panel to both determine whether IL-23 protein expression in higher in tumours versus matched normal tissue and what dominant cellular source is.

1.3.2 Is functional IL-23 produced by malignant CRC cells?

If IL-23p19 is indeed produced at the protein level, the key question is whether it is functional and can modulate the tumour immune milieu. Supernatant from CRC cell lines or organoids should first be assayed by ELISA to determine whether IL-23 is secreted. Then these supernatants can be used to treat naïve $CD4^+$ T cells from human PBMCs in the presence and absence of a preclinical IL-23p19 antibody (MTA for use of antibody from Janssen currently being finalized) and determine whether there is Th17 skewing and consequent elevated IL-22 and IL-17A production. If this is the case, then IL-23 production by malignant epithelial cells represents a novel strategy acquired by cancer cells to condition an immune suppressive microenvironment.

1.4 IL-22-*KRAS*-enhanced ELR$^+$ CXC chemokines

1.4.1 What are the functional consequences of enhanced ELR$^+$ CXC chemokine expression in *KRAS* mutant versus wild type cells following IL-22 stimulation?

While we have observed enhanced induction of *CXCL1* and *CXCL5* in KRAS mutant cells and organoids following IL-22 stimulation, the functional consequences have not been elucidated (Chapter 5). *Ex vivo* assays using supernatants generated from IL-22 stimulated *KRAS* mutant versus wild type cells or organoids could be used in migration assays with human blood, to determine whether the chemotactic activity is higher in *KRAS* mutant compared to wild type cell-derived supernatant in the presence and absence of a CXCR2 blocking agent. Moreover, detailed FACS analysis of myeloid populations from freshly isolated CRC biopsies, comparing patients with *IL22RA1*-high, *KRAS* mutant to *IL22RA1*-high, *KRAS* wild type tumours is warranted to determine whether there is enhanced infiltration of CXCR2 expressing myeloid populations in *IL22RA1*-high, *KRAS* mutant tumours. In the *Hh*, AOM CAC model found by previous lab members to be IL-22 dependent (Kirchberger *et al.*, 2013b), CXCR2 blockade could be deployed to determine whether like IL-22 blockade, it can rescue mice with established disease.

1.5 IL-22-*KRAS*-enhanced Myc pathway

1.5.1 Is *MYC* expression elevated in IL-22RA1-high, *KRAS* mutant compared to wild type tumours?

Our subgroup analysis of *MYC* expression was limited by low patient numbers (Chapter 5, Figure 5.15 B), therefore as we continue to prospectively collect tumour resection tissue, qPCR analysis of *MYC* expression should be included in the panel of other markers to determine whether indeed its expression is elevated in *KRAS* mutant versus wild type, *IL22RA1*-high tumours.

1.5.2 What mediates the elevated IL-22-induced transcription of *MYC* in *KRAS* mutant versus wild type cells?

Based on our functional studies of in *KRAS* mutant cells, *MYC* mRNA induction following IL-22 stimulation was not affected by *STAT3* knockdown, suggesting that transcriptional induction by IL-22 is not *STAT3*-dependent (Chapter 5, Figure 5.14). Another plausible pathway that may regulate *MYC* transcription in CRC is the Wnt pathway. We propose use of inhibitors of Wnt pathway components to determine if following IL-22 stimulation, *MYC* induction is reduced. Furthermore, chromatin immunoprecipitation analysis using antibodies against the β-catenin/Tcf-4 complex followed by qPCR for *MYC* could be used to determine if the *MYC* promoter is directly bound by β-catenin/Tcf-4 following IL-22 stimulation.

1.5.3 Is T58 c-Myc phosphorylation diminished by IL-22 in *KRAS* mutant cells? Is this GSK-3β-dependent?

Our analysis of T58 c-Myc phosphorylation following IL-22 stimulation was inconclusive due to multiple bands detected with the polyclonal antibody used (Chapter 5, Figure 5.11 D). Therefore, we propose using a cleaner, monoclonal antibody that specifically detects PT58 be used in conjunction with a GSK-3β-PS9 antibody. We hypothesise that GSK-3β-PS9 will be enhanced with IL-22 stimulation and that c-Myc-PT58 will consequently be reduced, however the kinetics of this regulation requires careful dissection. Moreover, we propose treating *KRAS* mutant and wild type cells with IL-22 in conjunction with a GSK-3β inhibitor to determine whether c-Myc PT58 is enhanced and total c-Myc levels are reduced due to more rapid degradation. If this is the case, then GSK-3β inhibitors could also be used in functional assays to determine whether proliferation and lactate production following IL-22 stimulation are reduced in *KRAS* mutant cells.

1.5.4 Is the enhanced IL-22-induced *CD274* expression in *KRAS* mutant cells versus wild type cells mediated by c-Myc?

A recent study demonstrated that c-Myc can directly bind the *CD274* promoter and induce its transcription (Casey *et al.*, 2016). In our system, we propose analysis of *CD274* expression following *MYC* knockdown and IL-22 stimulation to determine whether the enhanced *CD274* expression in *KRAS* mutant cells following IL-22 stimulation is due to enhanced active c-Myc. This analysis should couple investigation of *CD274* expression at the mRNA level and PD-L1 expression at the cell surface level by flow cytometry.

1.5.5 Is glucose uptake by *KRAS* mutant cells enhanced by IL-22 in a GLUT3-dependent manner? Is GLUT3 induction Myc-dependent?

RNA-sequencing and proteomic analysis revealed elevated GLUT3 expression in *KRAS* mutant cells following IL-22 stimulation (Chapter 5, Figure 5.17). We also observed enhanced lactate production in *KRAS* mutant cells following IL-22 stimulation pointing toward enhanced glycolytic flux (Chapter 5, Figure 5.16 B). It remains to be determined whether enhanced GLUT3 expression augments glucose uptake following IL-22 stimulation. We propose investigating differences in glucose uptake between *KRAS* mutant and wild type cells using a fluorometric glucose uptake assay. If enhanced glucose uptake is indeed observed in *KRAS* mutant cells following IL-22 stimulation, we propose knocking down GLUT3 to determine if this enhanced uptake can be abrogated. Furthermore, it remains to be determined whether induction of GLUT3 by IL-22 in *KRAS* mutant cells is Myc-dependent. Thus, we will explore GLUT3 protein and mRNA expression following *MYC* knockdown and IL-22 stimulation to determine if a mechanistic link exists.

1.6 IL-22-*KRAS* synergy in metastatic disease

1.6.1 Is this IL-22-*KRAS* synergy active at metastatic sites?

In colorectal cancer, the primary tumour is seldom the cause of mortality, thus it is absolutely critical to study this IL-22-*KRAS* synergy in metastatic disease. Functionally, we propose use of new spontaneously metastasizing CRC murine models (e.g. The KPN (*Kras, tp53, Notch* mutant) model developed by Owen Sansom's group) to investigate whether IL-22/IL-23 blockade can limit metastasis. In human disease, it is critical to determine using paired primary tumour biopsies and those from metastatic sites whether IL-22RA1 expression in the primary tumour reflects that in the metastasis. Furthermore, when it is possible to obtain fresh metastatic tissue, growing organoids and performing functional experiments comparing *KRAS* mutant to wild type metastases and examining *MYC, CXCL1, CXCL5, SLC2A3, CD275* induction following IL-22 stimulation will be necessary to determine whether the IL-22-*KRAS* synergy is active at metastatic sites.

2 Appendix: Extended Materials and Methods

2.1 Confirmation of specificity of IL-22RA1 antibodies used in this study

2.1.1 *IL22RA1* siRNA knockdown to confirm specificity

In order to confirm the specificity of the antibodies used for both IHC and FACS based analysis of the human IL-22RA1, *IL22RA1* siRNA (ON-TARGETplus Human IL22RA1 (58985) SMARTpool, Dharmacon) was used to knockdown *IL22RA1* in the T84 colon adenocarcinoma cell line. T84 cells were plated at a density of 30,000 cells per well in 48 well plates and allowed to adhere overnight. Cells were transfected with 20nM *IL22RA1* siRNA or 20nM control siRNA (ON TARGET plus control pool b-001810-10-05, Dharmacon) prepared in Opti-MEM (Thermo Fisher) with 0.8uL Dharmafect 2 (Dharmacon) per well. Prior to transfection, siRNAs were incubated at room temperature for 20 minutes with Dharmafect transfection reagent to allow complexes to form. siRNA complexes were incubated with cells for 48h. Following transfection, cells were trypsinised and:

A) RNA was extracted from triplicate wells of *IL22RA1* siRNA transfected and control siRNA transfected cells. qPCR analysis was performed to assess the efficiency of the *IL22RA1* knockdown. 50% *IL22RA1* mRNA knockdown was observed (Figure 2.1 A).

B) Cells were stained with PE conjugated IL-22RA1 antibody (1:10, R&D; 305405) or matched isotype control (1:10, R&D, 11711) (Chapter 2, Table 2.1) for 30 minutes at room temperature in FACS buffer. Cells were washed in FACS buffer and DAPI was added (1:100 for live/dead analysis). Flow cytometric analysis was performed on a BD LSR Fortessa X-20. IL-22RA1 protein was 50% lower in the *IL22RA1* siRNA transfected compared to control siRNA transfected cells (Figure 2.1 B, C).

C) Cells were seeded on 12 well microscope slides (CA Hendley Essex) in 50uL media per well. Cells were incubated at 37°C for 3h to allow cells to adhere. Slides

were washed in 1x PBS and submerged in 1:1 Methanol: Acetone for 30 seconds to fix. Slides were blocked with 10% goat serum in 1x TBS (50uL/well) for 1 hour at room temperature to prevent non-specific binding. Slides were stained with anti-human IL-22RA1 (1:750, Atlas Antibodies; HPA042399 lot: R38731) or no primary antibody (secondary only control) and incubated at 4°C overnight. Following incubation, slides were washed 3 times for 5 minutes in 1x TBS and then stained with goat anti-rabbit IgG Alexa Fluor 555 conjugated secondary antibody (1:400, Life Technologies; A32732) for 1 hour at room temperature. Slides were washed and stained with Hoechst (1:20,000, Life Technologies) for 10 minutes at room temperature. Finally slides were washed and coverslips were mounted and sealed. Images were acquired at 20x magnification on an Olympus BX51 Osteometric microscope. IL-22RA1 staining was significantly reduced in the *IL22RA1* siRNA transfected as compared to the control siRNA transfected cells (Figure 2.1 D).

Given the reduction in IL-22RA1 staining using both the flow cytometry and IHC anti-human IL-22RA1 in the *IL22RA1* siRNA transfected versus control transfected cells, we concluded that the antibodies were IL-22RA1 specific. Due to the absence of IL-22RA1 knockout human cells, this *IL22RA1* siRNA knockdown approach was deemed the best method for assessing antibody specificity.

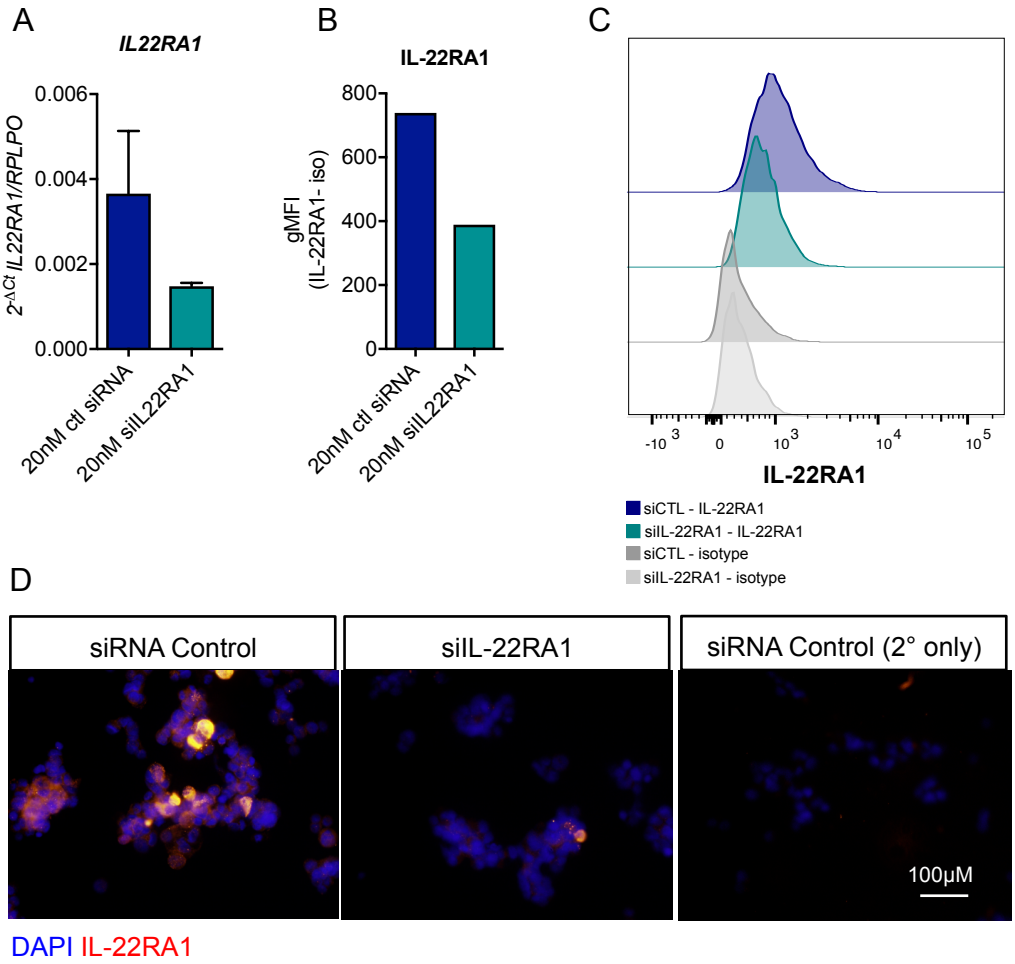


Figure 2.1 *IL22RA1* siRNA knockdown to confirm the specificity of the IL-22RA1 FACS and IHC antibodies

T84 colon adenocarcinoma cells were transfected with 20nM *IL22RA1* siRNA or control siRNA for 48h.

(A) qPCR analysis of *IL22RA1* expression in *IL22RA1* siRNA or control siRNA transfected cells. Data represent one experiment performed in technical triplicates.

(B) Quantification of IL-22RA1 protein expression in *IL22RA1* siRNA or control siRNA transfected cells based on flow cytometric analysis. Data represent the geometric mean fluorescence intensity (gMFI) of the isotype subtracted IL-22RA1 staining for one experiment performed in technical duplicates.

(C) Representative histograms displaying IL-22RA1 and matched isotype flow cytometric control staining of *IL22RA1* siRNA or control siRNA transfected cells.

(D) Representative images of immune fluorescent staining of IL-22RA1 in *IL22RA1* siRNA or control siRNA transfected cells and control siRNA transfected cells stained with secondary antibody only. 20x magnification.

2.1.2 IL-22RA1 immunohistochemistry staining controls

To further confirm antibody specificity when used for immunohistochemical anaylsis on FFPE sections, negative control staining was performed by omitting the primary antibody from the staining procedure described in Chapter 2.1.3 (Figure 2.2 A). However, secondary antibody staining and HRP-based detection was performed as in the full staining protocol (Figure 2.2 A). Compared to fully stained sections from the same patient (Figure 2.2 B), no positive staining was observed in the secondary only control (Figure 2.2 A). Since the IL-22RA1 antibody used is a polyclonal antibody, a specific isotype control does not exist. To confirm that the IL-22RA1 was specific, fully stained sections from the same patient featuring areas of lymphocytic infiltrate were examined as lymphocytes are not reported to express IL-22RA1 (Figure 2.2 C). Modest background staining was observed in the lymphocytic infiltrate (Figure 2.2 C), though no specific staining was observed, as was the case in the same section in an area featuring epithelium (Figure 2.2 B). Therefore, we concluded that the IL-22RA1 staining was specific.

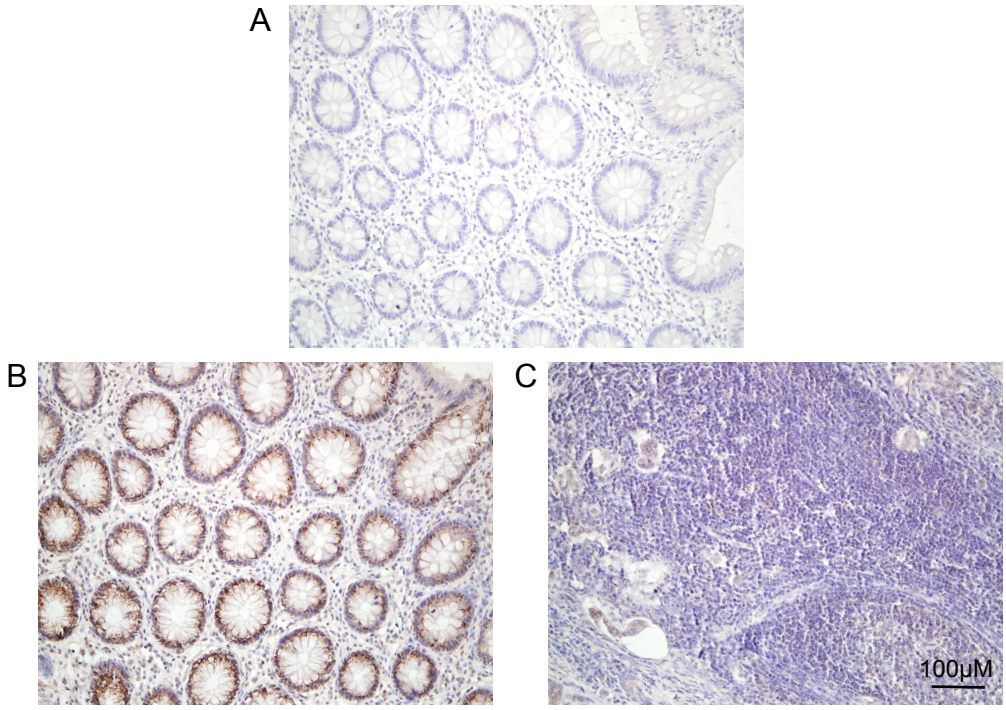


Figure 2.2 IL-22RA1 immunohistochemical staining controls.

Immunohistochemical analysis was performed on FFPE colon matched normal tissue sections as described in Chapter 2.1.3. Sections from one individual patient are displayed showing:

(A) Negative control staining performed by omitting the primary antibody with nuceli stained by haematoxylin counterstain.
(B) Fully stained section using primary IL-22RA1 antibody at 0.27ug/mL.
(C) Fully stained section displaying lymphocytic infiltrate using primary IL-22RA1 antibody at 0.27ug/mL.

Images were acquired on an Olympus BX51 Osteometric microscope at 20X magnification.

2.2 T cell supernatant titration experiments

Initial T cell supernatant dose response stimulations were performed to determine the concentration of supernatant generated from restimulation of polycloncally expanded $CD4^+$ tumour infiltrating and matched normal adjacent lymphocytes that elicited maximal functional responses but minimal cytotoxicity. DLD-1 isogenic cells were stimulated for 24 hours with T cell supernatants at 1:20, 1:100, and 1:200. MTT assays were used to assess viability following stimulation and qPCR analysis was performed to assess induction of the control gene *SOCS3*. Vehicle control media containing PMA/ionomycin at the concentrations used in the T cell restimulations was

also used at 1:20, 1:100, 1:200 as appropriate. Supernatants used at 1:20 were cytotoxic, but cytotoxicity decreased with lower supernatant concentrations Figure 2.3 A, B). While supernatants used at 1:200 had the least impact on cell viability, induction of *SOCS3* was significantly lower as compared to supernatants used at 1:100 or 1:20 (Figure 2.3 C). In fact, the induction of *SOCS3* increased in a dose-dependent manner with increasing concentrations of T cell supernatant used 20 (Figure 2.3 C). Supernatants used at 1:100 both elicited gene expression changes and did not significantly alter cell viability and therefore downstream experiments were conducted with T cell supernatants used at 1:100.

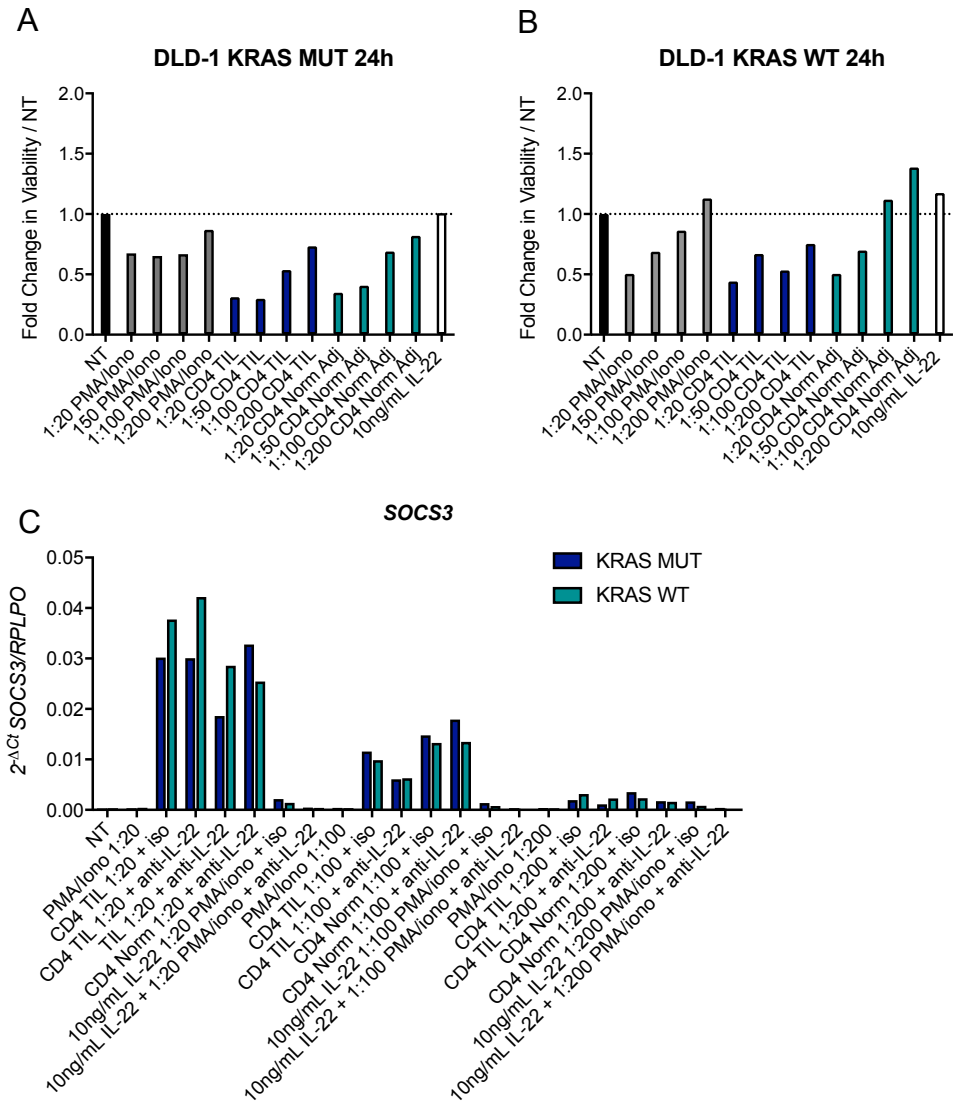


Figure 2.3 Titration of TIL and matched normal adjacent CD4$^+$ supernatant on DLD-1 isogenic pair

(A) (B) DLD-1 isogenic cells were stimulated with tumour infiltrating lymphocyte (TIL) and matched normal adjacent CD4$^+$ T cell supernatant for 24 hours. Supernatants and vehicle control (PMA/ionomycin) were used at 1:20, 1:100, and 1:200. Viability following 24h stimulation was assessed by MTT assay. Data represent n=1 experiment.

(C) qPCR analysis of *SOCS3* induction following 24h stimulation of DLD-1 isogenic cells with TIL and matched normal adjacent CD4$^+$ T cell supernatant. Supernatants and vehicle control (PMA/ionomycin) were used at 1:20, 1:100, and 1:200. Data represent n=1 independent experiment.

TNFα and IFNγ are known to be cytotoxic at high concentrations. To determine whether these factors in the cytokine supernatant were responsible for the observed cytotoxicity, DLD-1 isogenic cells were stimulated with T cell supernatants at 1:100 in the presence or absence of TNFα and/or IFNγ blocking antibodies. Combined

blockade of TNFα and IFNγ restored cell viability to that in the vehicle control condition (Figure 2.4 A, B). Thus TNFα and IFNγ are the dominant cytotoxic factors in the T cell supernatant.

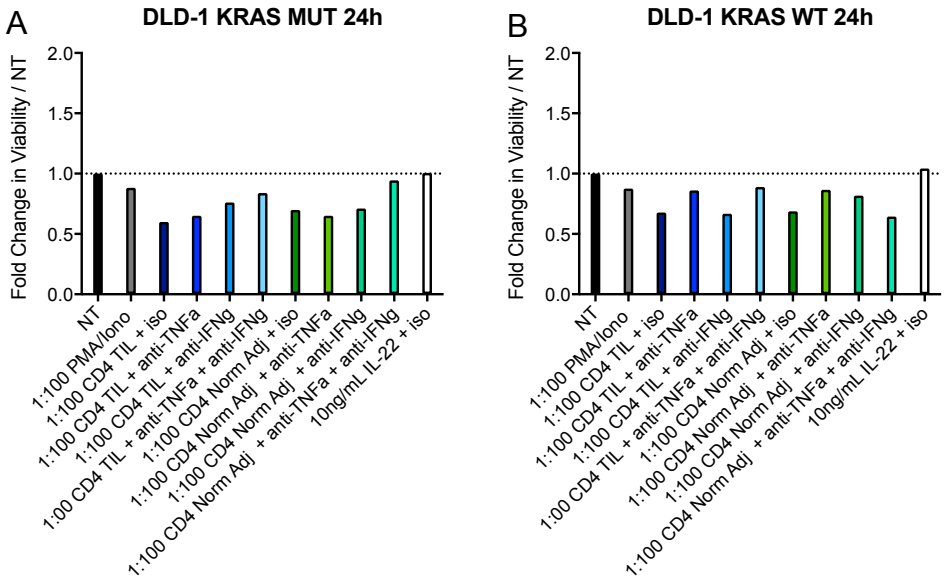


Figure 2.4 Cytotoxicity induced by CD4$^+$ T supernatant is TNFα and IFNγ dependent.

(A) (B) DLD-1 isogenic cells were stimulated for 24 hours with TIL and matched normal adjacent CD4$^+$ T cell supernatant in the presence or absence of TNFα and/or IFNγ blockade. Viability following 24h stimulation was assessed by MTT assay. Data represent n=1 experiment.

2.3 Production of Noggin, R-spondin, Wnt3A conditioned media

2.3.1 Rspondin and Noggin conditioned media production

HEK293T cells stably transfected with Rspo1-FC were obtained from Dr. Kalvin Kuo (Stanford, USA) under MTA. HEK293T cells stably transfected with Noggin-FC were obtained from Gijs Van den Brink (Academisch Medisch Centrum, Netherlands). Cell lines were cultured in DMEM (Life Technologies), 10% FBS, 1% Pen/Strep (Sigma), 2mM Glutamine (Life Technologies), 10mM HEPES (Sigma) [herein termed DMEM^{full}] in 25cm^2 flasks with 0.3µg/mL Zeocin (Invitrogen) for Rspo1-FC cells and 10 µg/mL Puromycin (Sigma) for Noggin-FC cells. Once cells reached confluency in 25cm^2 flasks, cells were trypsinised and split 1:5 into 1x75cm^2

flask with Zeocin or Puromycin for the Rspo1-FC or Noggin-FC cells respectively and 4x75cm^2 flasks without antibiotics in DMEM^{full}. When cells reached confluence in the larger flasks, the cells cultured in four 75cm^2 without Zeocin/Puromycin were trypsinised and 2x75cm^2 flasks were combined into 1x175cm^2 flask and cultured in 55mL of Advanced DMEM/F-12 (Life Technologies) with 1x Glutamax (Invitrogen), 10mM HEPES (Sigma), 1% Pen/Strep (Sigma) [herein referred to as ADF^{+++}] and cultured for 7 days. 5% FBS was added to Noggin-FC cultures. The remaining 1x75cm^2 flask was split 1:5 as described above, to repeat another cycle of conditioned media production. After 7 days, supernatants from the two 175 cm^2 flasks were harvested, combined and spun at 3000 RPM for 5 minutes. Supernatant was collected and filtered through a 0.22µM filter. Conditioned media was aliquoted into 10mL aliquots and frozen at -20°C for subsequent organoid media preparation.

2.3.2 Wnt-3A conditioned media preparation

L cells stably transfected with Wnt-3A were obtained from ATCC (CRL-2647). Cells were grown in DMEM^{full} with 0.4mg/mL G418/Geniticin (Invitrogen) in 75cm^2 flasks. Once cells reached confluence, cells were trypsinised, split 1:10 into 75cm^2 flasks, and cultured in DMEM^{full} without G418 for 4 days. After 4 days, the culture medium was collected, pooled and sterile filtered through a 0.22µM filter. An additional 10mL of fresh DMEM^{full} without G418 was added to each flask. Culture medium was collected after an additional 3 days and sterile filtered through a 0.22µM filter. The first and second batches of Wnt-3A medium were combined in a 1:1 ratio. Conditioned media was aliquoted into 10mL aliquots and frozen at -20°C for subsequent organoid media preparation.

2.4 Taqman probes used in this study

Gene Name	Gene Symbol	ABI Assay ID
CD274 molecule;PD-L1;B7-H1	*CD274*	Hs01125301_m1
chemokine (C-X-C Motif) ligand 1	*CXCL1*	Hs00605382_gH
chemokine (C-X-C Motif) ligand 2	*CXCL2*	Hs00601975_m1
chemokine (C-X-C Motif) ligand 3	*CXCL3*	Hs00171061_m1
chemokine (C-X-C Motif) ligand 5	*CXCL5*	Hs01099660_g1
dCTP pyrophosphatase 1	*DCTPP1*	Hs00225433_m1
GATA binding protein 3	*GATA3*	Hs00231122_m1
G protein nucleolar 3	*GNL3*	Hs00205071_m1
heat shock protein family D (Hsp60) member 1	*HSPD1*	Hs01036753_g1
interferon gamma	*IFNG*	Hs00989291_m1
interleukin 10	*IL10*	Hs00961622_m1
interleukin 10 receptor beta	*IL10RB*	Hs00175123_m1
interleukin 11	*IL11*	Hs01055413_g1
interleukin 12 alpha subunit (p35)	*IL12A*	Hs01073447_m1
interleukin 12 beta subunit (p40)	*IL12B*	Hs01011518_m1
interleukin 17A	*IL17A*	Hs00174383_m1
interleukin 17F	*IL17F*	Hs00369400_m1
interleukin 1 beta	*IL1B*	Hs01555413_m1
interleukin 22	*IL22*	Hs01574154_m1
interleukin 22 receptor alpha	*IL22RA1*	Hs00222035_m1
interleukin 23 alpha subunit (p19)	*IL23A*	Hs00900828_g1
interleukin 26	*IL26*	Hs00218189_m1
interleukin 4	*IL4*	Hs00174122_m1
interleukin 5	*IL5*	Hs00174200_m1
interleukin 6	*IL6*	Hs00985639_m1
leucine-rich repeat containing GPCR 5	*LGR5*	Hs00969422_m1
mucin 1 cell surface associated	*MUC1*	Hs00159357_m1
v-myc avian myelocytomatosis viral oncogene homolog	*MYC*	Hs00153408_m1
nanog homeobox	*NANOG*	Hs04260366_g1
olfactomedin 4	*OLFM4*	Hs00197437_m1
POU class 5 homeobox 1 (OCT4)	*POU5F1*	Hs04260367_gH
RAR related orphan receptor C	*RORC*	Hs01076112_m1
large ribosomal protein	*RPLPO*	Hs04189669_g1
S100 calcium-binding protein A9	*S100A9*	Hs00610058_m1
solute carrier family 2 member 3 (GLUT3)	*SLC2A3*	Hs00359840_m1
suppressor of cytokine signaling 3	*SOCS3*	Hs02330328_s1
SRY (sex determining region Y)-box 2	*SOX2*	Hs01053049_s1
signal transducer and activator of transcription 3	*STAT3*	Hs00374280_m1
T-Box 21	*TBX21*	Hs00203436_m1
tumour necrosis factor	*TNF*	Hs01113624_g1

2.5 DLD-1 isogenic cell line generation

The DLD-1 isogenic pair was purchased from the Horizon Discovery Group (Cambridge, UK). The parental line carries an endogenous heterozygous *KRAS* G13D mutation (Parental Line (KRAS G13D): HD PAR-111 Passage 4). An adeno-associated virus was used to knockout the mutant *KRAS* allele by homologous recombination to revert the *KRAS* mutant parental line to "wild type" (wild type reverted line (KRAS+/-): HD 105-040 Passage 4). The isogenic pair purchased is the parental and matched reverted line generated from DLD-1 cells at the same passage. The recombinant adeno-associated virus (rAAV) uses an exchange of nucleotides to enable deletion of DNA sequences without causing a double-strand break, but instead stimulates endogenous homologous recombination for precise DNA repair. Professor David Russell developed this technology and it is a proprietary technology used by Horizon Discovery (https://www.horizondiscovery.com/gene-editing/raav).

3 Appendix: RNA-sequencing and proteomics extended data

3.1 RNA-Sequencing

3.1.1 Differential expression analysis

KRAS WT IL-22-NT 2h		
Gene Symbol	log2FC	p-value
BCL3	3.547840497	1.79E-155
PTP4A3	4.933928058	6.12E-117
SOCS3	5.744853663	2.74E-97
IRF1	2.3864175	3.20E-95
TRIM15	2.314636545	1.58E-81
ICAM1	2.045680676	1.01E-72
SBNO2	2.010776292	2.72E-70
IRF8	2.981899428	3.31E-42
WNT5A	3.499499015	2.11E-38
GADD45G	2.362874121	5.64E-31
BATF2	2.684787275	2.41E-30
STEAP4	2.38744012	7.57E-27
CXCL2	2.70356434	7.75E-26
NNMT	3.079024468	4.29E-24
SLC1A2	2.334104501	3.25E-23
TRIM40	5.408833927	2.87E-22
CXCL3	2.814979331	2.66E-21
CEACAM5	3.022268654	1.17E-20
BMP5	3.18373444	4.58E-17
ITK	2.677502994	4.83E-17
RASL11A	2.232859256	1.97E-16
C2CD4C	3.34408203	3.44E-15
ETV7	2.331107021	6.43E-15
LYPD1	2.219831115	1.51E-14
NXPE1	3.456613948	1.57E-14
CUBN	2.152820524	2.09E-14
APOL4	2.925523428	3.48E-14
SLC51B	3.247703811	5.85E-13
ITGB3	3.63171889	2.05E-12
LRRC32	4.436950714	1.16E-11
CD7	3.152371069	1.17E-11
C9orf84	2.768301358	5.93E-11
CIITA	5.234678704	2.03E-09
MYO1H	2.544557391	3.22E-08
TMEM140	2.065689233	3.56E-08
NFE2	2.81856843	1.11E-07
CXCL1	2.75401326	6.05E-07
CEACAM6	2.061535001	8.31E-07
PAPPA	2.051827288	1.66E-06
LBP	5.946920961	1.95E-06
NID1	4.079721196	2.24E-06
CHST15	2.767395275	5.59E-06
SPP1	5.204316506	4.47E-05
SH2D3C	2.319840677	0.000148544
FGB	3.416054274	0.000250228
GBP1	2.326664531	0.000567217
KRT6A	4.593158593	0.000727625
BATF3	2.282290943	0.00111998
HSF5	2.205954238	0.001990391
C2CD4A	3.096615918	0.002080122
ADAMTS9	2.275494136	0.002218509
WFDC3	2.075717028	0.002287486
CASP1	3.196950115	0.002412883
PARP15	4.247693028	0.002659495
NCF4	2.525859774	0.002931496
RNF183	2.296695284	0.003202536
PAX5	2.205498946	0.003355803
FAM101B	4.260509432	0.003872975
KRT36	2.424288456	0.004189633
CTD-2583A14.1	4.038239183	0.005204211
GRK1	4.03745889	0.005275511
ZNF705A	4.036140217	0.005563033
CALB1	4.04323262	0.005709068
C20orf202	4.043962377	0.006301146
TOMM20L	2.848671789	0.007512163
LRRC73	2.057967779	0.008790663
RP11-181C3.1	2.439444638	0.009488354
BIRC7	2.701484467	0.009968828

KRAS MUT IL-22-NT 2h		
Gene Symbol	log2FC	p-value
BCL3	3.964672728	1.68E-192
IRF1	2.958970526	2.97E-140
PTP4A3	5.459798103	6.81E-138
TRIM15	2.995783515	3.00E-134
ICAM1	2.759400885	2.06E-124
SOCS3	7.279363242	1.21E-123
IER3	2.413054361	1.08E-121
SBNO2	2.4943682	6.21E-104
CDC42EP1	2.070180715	1.68E-82
TRIM40	8.145868939	6.95E-80
SERPINA1	3.441759891	9.85E-78
CSF1	2.133320182	1.35E-71
NLRC5	2.237122665	5.48E-68
SLC2A3	2.521047326	1.19E-54
CXCL5	2.14549958	2.64E-54
BATF2	3.734673852	4.42E-54
SPRY4	2.142365401	2.51E-52
GADD45G	3.23236725	2.86E-52
WNT5A	3.78566495	5.96E-49
IRF8	2.510492992	5.50E-41
CEACAM5	2.988319681	2.08E-40
ERP27	2.982867332	2.19E-40
MALL	2.154436588	4.66E-35
CXCL2	2.77153651	7.36E-32
SAMD11	2.825187454	8.46E-31
APOL4	8.481605592	6.66E-30
MUC1	2.112197955	1.66E-29
ETV7	3.477163339	1.75E-29
SLC51B	3.612179634	3.22E-29
NNMT	3.921756326	1.47E-28
STEAP4	2.431941473	2.18E-27
ITK	4.776659696	4.21E-26
LYPD1	3.699088289	1.31E-25
TRPM6	2.47085496	4.11E-24
C2CD4C	4.46027747	5.69E-24
NXPE1	2.572682192	1.82E-23
IFIT3	2.230825321	5.85E-23
FGB	4.614753171	1.57E-22
CX3CL1	2.481661913	6.15E-19
CXCL3	2.35496909	8.93E-19
FLNC	4.811984268	2.37E-18
CUBN	2.392066742	1.93E-16
LCN2	2.153025892	2.84E-16
ELOVL3	2.731227517	8.67E-16
CEACAM1	3.296202064	1.79E-15
LRRC32	4.496903612	3.16E-12
FES	2.82952789	8.04E-12
FAM115C	2.107385306	3.89E-11
ICAM4	3.759804454	4.95E-10
BATF3	4.24909576	9.51E-10
GPR110	2.185003124	1.12E-09
C9orf84	2.70736584	1.22E-09
TMEM140	2.640299299	1.65E-09
FGA	7.233907755	6.21E-09
MYBPC2	3.805720512	6.74E-09
OMP	2.195829489	1.13E-08
NID1	5.973773232	5.88E-08
BMP5	2.802028028	1.74E-07
PAPPA	2.428040795	1.96E-07
CHRD	3.335218793	3.83E-07
CD7	2.285892936	5.01E-07
KRT36	3.175057379	5.88E-07
ADAMTS9	5.593225796	5.25E-06
FEZF1	5.5490144	6.45E-06
MUC4	3.166740766	7.36E-06
SLC47A2	3.791843902	1.12E-05
TEK	3.790103584	1.21E-05
PELI2	2.414659018	1.24E-05

KRAS MUT IL-22-NT 2h continued		
Gene Symbol	log2FC	p-value
ADRA1D	2.090615247	3.96E-05
CXCL1	2.077164262	6.70E-05
IL37	2.306929574	7.54E-05
HTR3A	3.558736631	0.000111329
DSCAM	4.905783245	0.000130485
SPINK1	2.738626326	0.000283373
LRRC73	2.452698082	0.000522921
SOX14	4.61311265	0.000761895
CIITA	2.899518371	0.001140164
ROPN1L	4.472918485	0.001186819
DMBT1	4.487488747	0.001204348
TGM2	2.090528307	0.001660244
GBP1	4.590529916	0.001682272
DRD1	4.309290666	0.002288049
CRIP2	2.17559066	0.003151826
TF	4.164844018	0.003516255
MMP13	2.88141205	0.003957434
CCR2	2.887110369	0.004070948
SAMD7	2.887436278	0.004580883
ZBP1	2.164909347	0.006213646
SPATA18	3.952983209	0.006549136
WFDC10B	3.946212805	0.006551694
PAPLN	3.963446095	0.006648294
SCIMP	3.945502037	0.006763768
RP11-542C16.2	2.887933568	0.006814073
SH2D1B	3.935446919	0.006993064
SPN	3.917623698	0.007942919
TTBK1	2.323641317	0.008718489
KLRK1	2.784112569	0.009009155
GRIN3A	2.116927611	0.009580605

Table 3.1 Significantly up-regulated genes following 2h IL-22 stimulation

KRAS WT IL-6-NT 2h		
Gene Symbol	log2FC	p-value
BCL3	2.241596505	5.14E-65
PTP4A3	3.781388829	1.41E-61
SOCS3	3.847272973	1.35E-32
WNT5A	2.619455773	4.78E-20
IRF8	2.024972962	9.68E-18
C2CD4C	2.418327715	7.38E-08
TRIM40	3.675509413	3.56E-07
CIITA	4.356124968	4.12E-06
SLC51B	2.288000874	9.38E-06
MYO1H	2.094315783	1.84E-05
LRRC32	3.263982921	2.86E-05
NXPE1	2.185026904	6.03E-05
WFDC3	2.316912422	0.000538381
MSLNL	4.596495695	0.000760911
AP000275.65	3.269895128	0.000787255
VHLL	4.199956828	0.003549721
RP5-1021I20.4	2.478956952	0.004511312
HSF5	2.085957648	0.004682124
LBP	4.20011079	0.005116258
IYD	4.189666224	0.005162582
FUT6	2.870635447	0.006448128
AC093157.1	3.953554242	0.007307949
ANKRD20A1	2.286128003	0.007382058
SATL1	3.953848319	0.00755066
DCDC1	3.952399	0.007809372
EPGN	2.083232737	0.007937742
AC114546.1	2.35407513	0.008230842
SPP1	3.956065911	0.008291558
HOXD1	3.950293006	0.008301476
MROH7	3.947791634	0.008594286

KRAS MUT IL-6-NT 2h		
Gene Symbol	log2FC	p-value
PTP4A3	4.1934813	5.63E-73
BCL3	2.32246678	1.85E-71
SOCS3	4.97566374	5.84E-39
TRIM40	5.42453864	2.96E-22
WNT5A	2.61249019	7.07E-22
ERP27	2.13469192	4.89E-19
APOL4	6.92573639	3.32E-13
ITK	3.4124566	9.43E-10
C2CD4C	2.76362587	1.11E-08
LYPD1	2.30076215	3.28E-08
NNMT	2.03616767	4.06E-07
C9orf84	2.18350257	4.64E-06
BMP5	2.45848062	2.14E-05
LRRC32	3.24938705	2.81E-05
ROPN1L	4.96084249	0.00017221
SLC47A2	3.39936678	0.00028554
KRT36	2.52837362	0.00042002
ICAM4	2.52980873	0.00054817
SBSN	2.60094911	0.00077433
FLNC	2.70465013	0.00082051
NTN3	2.60550316	0.00207059
MYBPC2	2.37568135	0.00243461
RSPH6A	4.33503323	0.00267675
SERPINI2	4.33332119	0.00280261
BPIFC	4.12414814	0.00428008
KCNN1	4.1245562	0.00435538
FGA	4.33552321	0.00441815
AKT3	4.12448376	0.00457692
KIAA1210	2.09895464	0.00580028
AC093157.1	3.87774239	0.00873239
KIF5A	4.12717127	0.00890525
DSCAM	3.8781005	0.00893076
GOLGA8I	3.87738739	0.00910943
KCNIP4	3.87777023	0.00920211
IL2RB	3.87761657	0.00933381
C6orf100	2.26982854	0.00991659

Table 3.2 Significantly up-regulated genes following 2h IL-6 stimulation

	KRAS WT IL-22-NT 2h		KRAS MUT IL-22-NT 2h		KRAS WT IL-6-NT 2h		KRAS MUT IL-6-NT 2h	
Gene Symbol	log2FC	p-value	log2FC	p-value	log2FC	p-value	log2FC	p-value
MYC	0.81528227	3.60E-25	1.25126965	8.16E-57	0.34629822	1.09E-05	0.59791946	2.22E-14
CD274	0.93694251	1.92E-11	1.58210939	1.30E-29	0.51174732	0.00046813	0.48656444	0.00159016
SLC2A3	1.31664852	9.12E-15	2.52104733	1.19E-54	0.33966494	0.06642347	1.11687563	1.09E-10

Table 3.3 Differential expression of key genes of interest following 2h IL-22 stimulation

KRAS WT IL-22-NT 2h		
Gene Symbol	log2FC	p-value
PDE4B	-3.1383632	4.20E-06
SIX1	-2.0226482	7.01E-05
DDC	-4.9497678	0.00013582
ALPL	-2.0307879	0.00048653
SPATA4	-4.5039277	0.00077773
C6orf58	-4.6581793	0.0008239
SLC22A14	-3.2324191	0.00083462
KMO	-3.1087243	0.00149913
RP11-279O9.4	-4.3188847	0.00165913
INHBC	-3.1042913	0.00186467
MYPN	-4.314772	0.00200494
GALNT5	-4.1109824	0.00346291
AC124890.1	-4.1080509	0.00362582
RPL3L	-2.9767797	0.00399925
WFDC9	-2.8283433	0.00592774
MYBPC3	-4.1511795	0.00606506
ITGAL	-4.0732155	0.00768332
RP11-195B21.3	-3.8608071	0.00786077
PODN	-3.8639615	0.00788461
UBE2F-SCLY	-3.8630347	0.0079538
CPXM1	-3.8688428	0.00823956
GAPDHS	-3.8647813	0.00825167
TAS2R46	-3.8576154	0.00829055
PTPN20A	-3.8518576	0.00879259
EXOC3L4	-2.3252738	0.00948418

KRAS MUT IL-22-NT 2h		
Gene Symbol	log2FC	p-value
CYP1A1	-2.6293341	1.39E-17
TET1	-2.4116626	1.42E-06
RASL11B	-4.2809023	1.43E-06
AUTS2	-2.3366933	5.48E-05
RP11-455G16.1	-2.9515614	0.00031927
S1PR4	-2.0436506	0.00063747
AC110615.1	-4.3287309	0.00124668
TMEM176A	-4.3353054	0.00128374
CHRNB2	-4.3242378	0.00145492
SLITRK6	-2.2008263	0.00181748
C14orf166B	-4.1205981	0.00271492
C1orf177	-4.1193043	0.00287153
PLA2G3	-4.1237091	0.00310611
CYP3A5	-2.9067747	0.00441452
C9orf139	-2.9077259	0.00533034
IL27	-3.8797425	0.00662068
AMZ1	-3.8678745	0.00685488
NXF3	-3.8770369	0.00729781
HIST1H2AM	-2.7432825	0.00830781
PCDHB16	-3.8352443	0.00983721
TEX101	-2.2940703	0.00997127

KRAS WT IL-6-NT 2h		
Gene Symbol	log2FC	p-value
EXOC3L4	-4.9429748	0.00021283
RPL3L	-4.8135423	0.00043069
SYNGR3	-3.3173738	0.00050358
SIGLEC6	-4.5026565	0.00134255
AQP1	-4.5153944	0.00171444
RNASE6	-4.3170646	0.00275439
COL8A2	-4.3259547	0.00313487
BRSK2	-2.696621	0.00314319
ASB3	-2.1157657	0.00432158
TMEM176B	-2.4143565	0.00499583
C1orf222	-2.4136516	0.0051755
HOXB1	-4.1013234	0.00593473
UGT1A8	-2.8535797	0.00606375
SMPX	-4.1058195	0.0060814
OR2AE1	-2.846049	0.00618921
TAS2R3	-4.1006162	0.0062091
ZSCAN5B	-4.0901702	0.00748322
HOXC9	-2.3036462	0.00927435
ZDHHC19	-2.8350941	0.00965492

KRAS MUT IL-6-NT 2h		
Gene Symbol	log2FC	p-value
RASL11B	-3.357438	3.37E-05
AC093677.1	-3.3907799	0.00045244
RETNLB	-2.4474209	0.00089538
CD226	-3.1758576	0.00105463
CCR7	-4.6542036	0.00107039
OPRL1	-2.3640016	0.00124984
HOGA1	-4.3339573	0.00217695
C12orf42	-2.3531838	0.00236869
SPEG	-2.1861882	0.00401233
DPCR1	-3.0528112	0.00417409
GRID1	-4.1170184	0.00443433
FAM19A3	-4.1196459	0.00453422
OLFM2	-4.1134813	0.00456738
PLA2G3	-4.1237091	0.00470255
FRY	-4.1125438	0.00471301
SP140	-2.7734898	0.00784455
CCM2L	-2.0859506	0.00807194
SLC5A5	-3.8742454	0.00903679
C9orf139	-2.778011	0.00905082
SLA2	-2.7820552	0.00916
SAMD14	-3.8718066	0.00942628
LGI3	-3.8685165	0.00951483
C6orf164	-2.2585948	0.00954276
CCL17	-3.8808338	0.00960682
AMZ1	-3.8678745	0.00976561

Table 3.4 Significantly down-regulated genes following 2h IL-22 or IL-6 stimulation

KRAS WT IL-22-NT 24h		
Gene Symbol	log2FC	p-value
PTP4A3	6.26855474	3.03E-284
BCL3	2.50001319	4.19E-211
MUC1	2.73692133	2.01E-162
NLRC5	2.02521454	1.58E-112
NNMT	3.99726436	9.66E-84
SOCS3	4.22867942	2.79E-81
SERPINA1	2.31130076	1.14E-61
ABCB1	2.10420579	1.52E-57
WNT5A	3.00045028	4.33E-43
CEACAM5	5.31133599	3.65E-41
GADD45G	2.06402712	2.82E-40
ERP27	2.7398792	6.30E-39
LCN2	3.82239649	5.02E-32
PLB1	2.09610437	4.29E-29
RASL11A	2.09751887	4.97E-21
CIITA	6.02333847	1.38E-20
SLC1A2	2.00630627	5.28E-20
HOPX	2.89771446	5.75E-20
LYPD1	2.29314962	8.55E-20
GUCY2C	3.79074742	2.07E-19
C10orf10	2.10796135	8.10E-18
SNCAIP	2.22158097	6.11E-17
CEACAM6	3.88864439	2.24E-16
CEACAM1	2.54406298	1.64E-15
NXPE1	4.06242221	3.91E-13
SPINK1	3.68881669	5.02E-13
COL15A1	3.53471843	1.18E-12
DMBT1	4.37291415	2.21E-11
FLNC	3.99351723	4.14E-11
TEX29	2.04975231	8.05E-11
APOL3	2.11813415	3.22E-10
TGM2	2.21908917	8.67E-10
MAPK10	2.16007014	3.21E-09
DUSP13	3.06728605	8.38E-09
FGB	3.83335323	2.66E-07
RARRES3	2.12814515	9.03E-07
MYO1H	2.15980714	3.10E-06
BMP5	2.23595701	1.08E-05
SLC51B	2.20567459	2.10E-05
GBP1	2.1336959	2.15E-05
AL590708.2	2.27383448	4.58E-05
CHST15	2.62204566	5.47E-05
BEND7	5.05207179	0.00011072
LRRC32	4.93264337	0.00012862
MUC4	4.93256491	0.00013078
EPYC	5.05216461	0.00025828
IL13	4.79890091	0.00029087
SLC17A8	4.65279659	0.00055927
SLCO2A1	2.76187215	0.00074354
A2M	4.65263618	0.00080428
ABCB11	4.49090902	0.00121573
LBP	3.15398958	0.00150326
AC120194.1	3.15598108	0.00201893
BIRC7	4.30687172	0.00230112
SORCS3	4.30813485	0.00238837
MYO3B	2.25160606	0.00263992
CCL22	2.57497982	0.00265236
ADAMTS9	4.09668646	0.00450444
SLC34A1	4.09664601	0.00453859
RP11-321F6.1	4.09666165	0.00459512
KMO	4.09600415	0.00462621
C10orf82	4.09774058	0.00469555
CLCA2	4.09776438	0.00470974
CPED1	4.0979099	0.00479808
IL17REL	3.03133265	0.00505967
LPAR6	2.47484227	0.00534404
AC012313.1	2.35975645	0.0056452
PCYT1B	4.09447974	0.0058748
TRIM40	2.06549244	0.00714267
SORCS2	2.89912185	0.00721567
OR2B6	2.75181745	0.0078851
RP11-426L16.1	2.75209683	0.00860972
SUN3	2.75253346	0.00874042
KRT36	3.850527	0.00903729
CXCL17	3.85046128	0.00924015
UGT2B7	3.85038182	0.00926351
GNAT1	3.85044098	0.00936399
DNALI1	3.85070718	0.00949602
PAPPA-AS1	3.85024468	0.00963277
GBP2	2.89679348	0.00965192

KRAS MUT IL-22-NT 24h		
Gene Symbol	log2FC	p-value
PTP4A3	7.39700238	0
MUC1	2.88988877	2.85E-201
BCL3	2.23239379	6.09E-192
SOCS3	5.56018876	1.81E-135
SERPINA1	3.20469219	2.91E-124
NNMT	5.2675223	5.29E-93
WNT5A	3.41145299	8.75E-90
GADD45G	2.87453256	1.07E-73
CEACAM5	4.67080223	4.98E-67
ERP27	2.9721313	4.46E-52
FGB	10.6372241	6.31E-52
FOS	2.17331677	6.69E-45
CXCL5	2.80207682	3.37E-41
NXPE1	3.32791812	1.79E-35
SPINK1	3.83758216	4.82E-35
SNCAIP	2.46307175	8.27E-32
LCN2	3.89138577	1.12E-31
LYPD1	4.21670126	2.60E-28
UBE2L6	2.01750304	3.82E-28
CEACAM1	3.10293817	6.31E-28
GUCY2C	2.53424443	1.61E-25
PLAT	3.21945999	6.12E-25
TRIM40	4.02805366	7.00E-23
MAPK10	2.55616994	8.09E-23
CEACAM6	2.94084767	4.08E-22
DMBT1	8.34491706	7.79E-22
CXCL2	2.51705366	1.27E-21
PLB1	2.1603666	2.89E-20
SLC51B	3.27846532	2.35E-16
TEX29	2.30076806	9.84E-16
C2CD4C	2.39346294	2.38E-14
APOL3	2.43026087	9.67E-13
CUBN	2.23684695	1.57E-12
FGA	3.39102069	1.43E-08
NID1	4.47669744	1.46E-08
FLNC	3.3608842	2.64E-08
CSMD3	2.79172377	6.37E-08
HTR3A	3.79892006	8.58E-08
CFI	5.58187009	4.98E-07
A2M	5.79400618	5.91E-07
COL15A1	2.79183979	5.69E-06
BMP5	2.56735504	3.74E-05
GIF	5.00877353	4.06E-05
KIAA1210	4.75739044	0.00016848
TCN1	4.76497015	0.000366
MCC	4.60950508	0.00037089
FGG	2.27607791	0.00039794
MPZ	3.35036045	0.00054772
WFDC3	2.07843495	0.00057405
C9orf84	2.57918264	0.00068098
ZFP91-CNTF	4.44747414	0.00069955
CCDC103	4.44739421	0.00071099
BATF3	4.44703637	0.00072221
S100A9	4.44910959	0.00076989
CYP3A7	2.45309568	0.00078041
LPHN3	2.42397787	0.00122986
REG1A	4.45947492	0.00138992
ASIC2	4.26503224	0.00152671
SULT4A1	4.26477578	0.00154137
CFB	4.26552493	0.0016738
FAP	2.00505971	0.00177387
CTSE	4.05352132	0.0034046
ZNF439	4.05485271	0.0035745
LUM	4.05298973	0.00384894
RP11-87C12.2	4.04852564	0.00447731
ADAM20	2.45257817	0.00468853
AL591479.1	4.05648272	0.00698175
C1orf189	2.34104548	0.00713621
SLC25A52	3.80871178	0.0072919
WFDC10B	3.80907198	0.00729666
DDX4	3.80867086	0.00734637
RP4-734P14.4	3.80865495	0.00736775
UGT2B11	4.07497875	0.00742136
CD86	3.8094262	0.0074562
KL	3.81014254	0.0078806
CYP2C18	2.33812345	0.00788457
SYNPO2	2.47369511	0.00939387

Table 3.5 Significantly up-regulated genes following 24h IL-22 stimulation

KRAS WT IL-6-NT 24h		
Gene Symbol	log2FC	p-value
PTP4A3	5.3446083	2.24E-179
SOCS3	3.46969901	4.55E-46
NNMT	2.9585064	1.15E-41
WNT5A	2.52406643	8.97E-28
CEACAM5	4.31965239	8.96E-24
ERP27	2.05309928	3.04E-20
LCN2	2.68562764	6.07E-18
GUCY2C	3.05667501	1.74E-11
HOPX	2.02146332	6.67E-10
CIITA	4.78835411	6.95E-10
TGM2	2.09054856	1.72E-08
SPINK1	3.1497242	2.49E-08
MAPK10	2.06894208	2.82E-08
FGB	3.88317947	1.91E-07
FLNC	3.05124605	2.40E-06
COL15A1	2.64355673	4.06E-06
DMBT1	3.28158212	6.01E-06
CEACAM6	2.39081944	1.71E-05
NXPE1	2.9032343	1.85E-05
LRRC32	4.57008311	0.00082447
LPAR6	2.85240902	0.00082499
CDX1	4.57405497	0.00084379
GBP4	4.57259204	0.00089902
BIRC7	4.56935294	0.00090438
CD36	3.23122636	0.00101288
SLC35G5	4.58574685	0.00117136
CHST15	2.16367229	0.00160131
PPP1R1B	2.01899519	0.00172826
CTC-786C10.1	4.38590736	0.00174778
ZNF345	4.38623468	0.00174833
C11orf72	4.39021453	0.00196888
SUN3	3.1102495	0.00197673
ANGPT1	2.12165653	0.00200194
COLEC11	2.04606136	0.00308861
GPR128	4.17349809	0.00370741
IL13	4.1760246	0.00387145
CLCA2	4.1753445	0.00392614
AC012313.1	2.43789795	0.00415389
IL17REL	3.08770818	0.00424224
TEK	2.835234	0.00681497
KRT36	3.92563443	0.0077315
CXCL17	3.92602229	0.007908
WFDC10B	3.9242139	0.00802172
RP11-248J23.6	3.92771781	0.00807109
SLC17A8	3.92607144	0.00821265
KMO	3.92030778	0.00831215
ABCB11	3.93104059	0.00845339
BEND7	3.92020618	0.00905434
SPP1	3.9291668	0.00913008

KRAS MUT IL-6-NT 24h		
Gene Symbol	log2FC	p-value
PTP4A3	6.54334053	1.84E-285
MUC1	2.3025887	1.06E-120
SERPINA1	2.71866378	1.90E-92
SOCS3	4.55165204	1.13E-72
WNT5A	2.60399062	1.98E-47
FGB	10.1310946	4.68E-45
NNMT	4.00905567	3.38E-44
CEACAM5	3.52319977	1.32E-38
GADD45G	2.08871221	2.75E-37
NXPE1	3.33323742	2.63E-35
CXCL5	2.16860422	1.58E-26
TRIM40	4.17955579	3.57E-25
ERP27	2.10593256	3.65E-24
CEACAM1	2.73467469	4.53E-22
LCN2	2.95947718	4.74E-20
GUCY2C	2.04498433	3.93E-17
SPINK1	2.97766649	1.42E-16
LYPD1	3.44564527	1.94E-15
MAPK10	2.15439868	2.58E-15
CXCL2	2.03858127	3.15E-14
DMBT1	7.16955717	1.95E-13
SLC51B	2.85828974	9.75E-12
FGA	3.64380689	6.78E-10
CUBN	2.00491329	1.29E-09
PLAT	2.11280731	2.46E-09
TGM2	2.36408356	3.37E-09
COL15A1	2.96411778	9.25E-07
CFI	5.3031839	5.74E-06
CSMD3	2.4703118	6.53E-06
CYP3A7	3.01640462	7.73E-06
NID1	3.61863985	7.35E-05
KRT36	2.21859895	7.57E-05
A2M	4.96563574	0.00011734
MYO3B	2.01376533	0.00031325
BMP5	2.31229287	0.00042946
GIF	4.52314319	0.0005871
FLNC	2.23444242	0.00078354
C9orf84	2.5194452	0.00101626
FGF12	3.19135425	0.00117396
BATF3	4.33867542	0.00124815
HTR3A	2.64142672	0.0018417
TCN1	4.33307217	0.00202717
RP11-1084J3.4	3.05206212	0.00214197
AP002884.2	3.05201143	0.00218998
FGG	2.0129298	0.00269003
LRRC32	4.12789217	0.0027794
RYR3	4.12791126	0.00285669
CD86	4.12696923	0.00287531
TRPM8	2.16327451	0.00383833
ZFP91-CNTF	3.88096198	0.00617349
C8orf44-SGK3	3.88240114	0.00630916
C1QTNF8	3.88049588	0.00640615
TVP23C-CDRT	3.88195973	0.00643033
FOXJ1	3.87958947	0.00678109
TAS2R30	3.87780843	0.0069898
GPRC6A	3.89211694	0.00791671
PPP1R3C	3.87767544	0.00797916
CYP3A5	2.74013588	0.00945396

Table 3.6 Significantly up-regulated genes following 24h IL-6 stimulation

KRAS WT IL-22-NT 24h		
Gene Symbol	log2FC	p-value
KRTAP3-1	-6.6078571	1.54E-06
UPK3A	-3.6902078	3.49E-05
GPR68	-2.2575229	8.90E-05
ENPP2	-3.8651178	9.25E-05
LOXL4	-4.9692425	0.00011832
MMP28	-4.9624619	0.00012733
KRT83	-4.6791469	0.00042162
ALPL	-2.1766743	0.00042502
PCDHGA6	-4.6806186	0.00043835
CITED4	-2.1517129	0.00048125
C17orf82	-3.5128093	0.00079367
SLC5A12	-3.195057	0.0012576
AC110771.1	-4.3333816	0.0018221
FBN3	-4.3309922	0.00187006
FLT4	-4.32656	0.00202622
THSD7A	-4.3310841	0.00214868
PHOSPHO1	-2.0131911	0.00235303
SLC45A1	-3.0628365	0.00265487
WIF1	-2.5215966	0.00277936
KRT4	-3.0770815	0.00389515
DMP1	-4.1218535	0.00416718
EYA4	-4.1174148	0.00417025
CDCP2	-4.116117	0.00422043
CORO6	-2.7986309	0.00678425
USH1G	-3.8754091	0.00838399
XCR1	-3.8771019	0.00848074
CACNA1S	-3.8777437	0.00848219
CPSF4L	-3.8734004	0.00851112
KAAG1	-3.8789085	0.00858842
RP11-195B21.3	-3.8742154	0.00863712
TMEM92	-3.8730584	0.00871302
GPC5	-3.8794881	0.00871531
P2RY4	-3.8721652	0.00899005
PTGDS	-3.8689545	0.00900064
NHLRC4	-3.8716513	0.0091293
COX6B2	-3.8907092	0.00913304

KRAS MUT IL-22-NT 24h		
Gene Symbol	log2FC	p-value
HMGCS2	-2.8059703	1.38E-35
FMO5	-2.0714021	9.90E-23
NTF4	-2.4794604	9.05E-20
REG4	-2.5565196	4.65E-14
CYP1A1	-2.1689894	8.21E-14
OR51E1	-3.8157333	5.41E-12
BCAS1	-2.2777499	1.72E-11
TP53INP1	-2.5124964	5.11E-11
ZNF185	-2.0572541	1.22E-10
C9orf117	-3.0586285	3.13E-10
CDH2	-2.5522304	1.84E-09
GLI2	-2.1745319	6.70E-09
MAFB	-2.7051698	7.19E-09
CST1	-2.0705484	8.74E-09
CAMK2B	-2.3687252	1.08E-08
GPR133	-2.0534198	1.38E-08
COL27A1	-2.2861423	1.40E-08
GNG13	-2.2118512	1.97E-08
AOC1	-3.0914276	2.09E-08
CCR1	-2.879573	5.91E-08
COLCA1	-2.3855695	1.26E-07
PDE9A	-2.1109415	1.54E-07
C1orf127	-2.0896844	2.44E-07
FRMD1	-4.310931	2.59E-07
CDH7	-2.0757154	3.43E-07
FSCN2	-2.0482297	3.45E-07
COL10A1	-2.1681433	4.73E-07
NPFFR1	-2.4545779	5.25E-07
ALOX15	-3.4390556	1.07E-06
GNAZ	-2.1558211	1.11E-06
RINL	-2.2447213	1.36E-06
ASIC5	-4.7325234	1.59E-06
KCND3	-5.6487676	1.80E-06
SMPD3	-2.052532	4.70E-06
RAMP1	-3.015463	4.81E-06
GPR68	-2.7192386	5.20E-06
IL36RN	-2.0719198	6.64E-06
AQP5	-2.1187869	1.68E-05
MRC2	-2.5968273	1.91E-05
SMTNL2	-2.8591051	1.98E-05
SIX1	-2.0637056	2.14E-05
SLITRK6	-2.7603775	2.18E-05
SHANK1	-2.12759	3.17E-05
ATP2A3	-2.7478387	3.49E-05
PTPRO	-2.6079217	4.74E-05
UGT2B10	-3.680109	4.91E-05
EMID1	-3.0708919	5.57E-05
HOGA1	-3.6126427	6.16E-05
PHOSPHO1	-2.2017341	6.52E-05
TMPRSS11E	-2.0239812	7.29E-05
TRIM74	-2.0820811	7.33E-05
KLK11	-2.6889482	7.67E-05
KLK12	-2.124646	8.23E-05
ALPL	-2.0754174	8.41E-05
UGT2B4	-2.0337842	0.00010048
CPAMD8	-2.3465791	0.00010699
LHB	-2.0650366	0.0001299
NFATC1	-2.200352	0.00013901
CHRNB4	-2.9300865	0.00017662
BPIFB1	-4.7858117	0.00018277
LOXL4	-4.798839	0.00019515

KRAS MUT IL-22-NT 24h continued		
Gene Symbol	log2FC	p-value
OPRL1	-4.7844422	0.00019716
C17orf72	-2.1093723	0.0002191
SRRM3	-2.1441521	0.00026605
RPS4Y1	-2.0370732	0.00027806
CSTL1	-4.6602627	0.00029623
DACT3	-4.657215	0.0003321
STAP1	-2.1623367	0.00044304
RBMS3	-2.8537825	0.00044554
ZNF385C	-2.8114952	0.00050967
PRTN3	-2.1516826	0.00062478
TMEM92	-4.5138269	0.00071256
ATP12A	-2.3481279	0.00071662
RAB44	-4.5551805	0.00079275
CELF2	-3.1793597	0.00095134
CIB2	-2.1848562	0.00097352
MYO7B	-2.8623145	0.00098823
MYBPC3	-4.4697577	0.00106492
RCAN2	-2.2050001	0.0012133
DNASE1L3	-4.3542666	0.00128433
AK7	-2.4411991	0.00129095
PIPOX	-2.2312675	0.00140724
MYCBPAP	-2.3794481	0.0014298
GJB1	-4.3682625	0.00145907
ART1	-4.3245843	0.00166712
SLC14A1	-2.4747572	0.00170055
LRIG1	-3.051179	0.00183196
DGKI	-2.2600252	0.00194193
C1orf222	-3.0631678	0.00201726
WNT2B	-2.0930088	0.00213125
IL36G	-2.3011306	0.00250532
CTB-50L17.14	-2.5161864	0.00300801
MME	-2.1508716	0.00365133
TRIM39-RPP21	-2.9942842	0.00376444
MEGF11	-2.5677413	0.003966
CSF2RA	-2.9193178	0.00441435
C6orf165	-2.1941195	0.00454183
SLC24A2	-3.9586976	0.00527711
WIF1	-2.8116657	0.00531794
TTLL6	-2.2137005	0.0053284
PCDHGB3	-3.965309	0.00536515
AKT3	-3.9649283	0.00537264
CYP4B1	-3.172038	0.00541051
C12orf74	-2.8116461	0.00541939
ARHGDIG	-3.9958633	0.00552181
AC016559.1	-3.9568291	0.0055855
FAM221B	-2.8121746	0.00576719
SNTN	-3.9556606	0.00582767
PARVG	-2.8840344	0.00585685
ALOX5AP	-2.0825568	0.00586408
FBXO43	-2.8275967	0.00588165
RBP5	-2.1971635	0.00598861
CBS	-3.9445836	0.00604917
AVPR1B	-2.8000228	0.00619396
SLC6A2	-4.0255272	0.00620017
GLYATL3	-2.8395937	0.00663373
TEX101	-2.7857129	0.00731427
LY6G6E	-2.2806802	0.00815349
SLC34A2	-2.2726322	0.00852676
C5orf60	-2.2656985	0.00910602
PROKR1	-2.6651528	0.00989703
TRPM3	-2.6648107	0.00998278

Table 3.7 Significantly down-regulated genes following 24h IL-22 stimulation

KRAS WT IL-6-NT 24h		
Gene Symbol	log2FC	p-value
KRTAP3-1	-3.8433077	0.00022711
NODAL	-3.4427103	0.00040163
KRT83	-4.6791469	0.00054875
PCDHGA6	-4.6806186	0.00056936
PALM2	-2.2351569	0.00086927
TAS2R10	-3.1402644	0.00121065
SLITRK6	-2.7851171	0.00131725
GOLGA8K	-4.5196326	0.00135873
PCDHGA12	-3.1377275	0.00139665
SLC5A12	-3.135315	0.00171247
SLC5A1	-4.331873	0.00222574
HTRA4	-4.3335006	0.00234737
THSD7A	-4.3310841	0.00262905
WIF1	-2.4520326	0.00386554
NCAN	-2.4499182	0.00415034
CCDC147	-2.4513673	0.00449323
COL25A1	-2.8863452	0.00464505
DKFZP434H05	-4.1208361	0.00479558
IPCEF1	-2.8873456	0.00482324
GSTM1	-2.4609055	0.00485501
FNDC5	-4.1177252	0.00495159
RP11-613M10.(	-4.1301706	0.0049607
EYA4	-4.1174148	0.00498693
TTC36	-2.8806147	0.00502904
CNTN2	-4.1170605	0.00536244
LCN15	-4.1032403	0.00773424
FOXF1	-2.0479275	0.00780679
CORO6	-2.7390687	0.00864701
DRC1	-2.7348186	0.00909901
SLC34A2	-3.8773755	0.00976973
EDARADD	-3.8777345	0.00988631
THEG	-3.8777661	0.00989671
C11orf91	-3.8772439	0.0099654

KRAS MUT IL-6-NT 24h		
Gene Symbol	log2FC	p-value
GNG13	-2.1326563	6.82E-08
CACNA1I	-3.7690557	2.63E-05
IL12B	-2.676478	8.39E-05
AK7	-2.8818175	0.00046643
CPAMD8	-2.063681	0.00046857
ALOX15	-2.0571602	0.00050883
TRPM3	-4.5137508	0.00082674
KLK11	-2.0729317	0.00103499
KRTAP1-1	-4.3393841	0.00183408
CHRM4	-4.3269529	0.0020117
GAS2	-3.0085952	0.00212685
TMEM176A	-2.0422706	0.00223966
HOGA1	-2.252461	0.00245432
HIST1H4D	-2.2881748	0.00246268
KLK4	-2.5243558	0.0026242
NEUROG2	-2.517488	0.0028203
RPEL1	-4.1908697	0.00335142
MYBPHL	-4.183511	0.00360342
POU2AF1	-4.1471379	0.00379456
BPIFB1	-2.8795361	0.00423899
GPNMB	-3.9624253	0.00604677
CLCN1	-3.9635746	0.00617735
SLC24A2	-3.9586976	0.00623433
CTC-786C10.1	-3.9586748	0.00623972
NUTM2E	-3.9588894	0.00635108
AL359091.2	-3.9767879	0.00650732
SLC5A12	-3.9486737	0.0067036
CBS	-3.9445836	0.00710212
FAM221B	-2.7564915	0.00732429
C17orf98	-3.9293876	0.00751168

Table 3.8 Significantly down-regulated genes following 24h IL-6 stimulation

The tables in this section are the result of differential expression analysis using the generalised linear model implemented in the *edgeR* package (version 3.16.0). Significantly differentially expressed genes for the comparisons of interest were those genes with log2 fold change >2 (up-regulation) or <-2 (down-regulation) with an adjusted p value of less than 0.01.

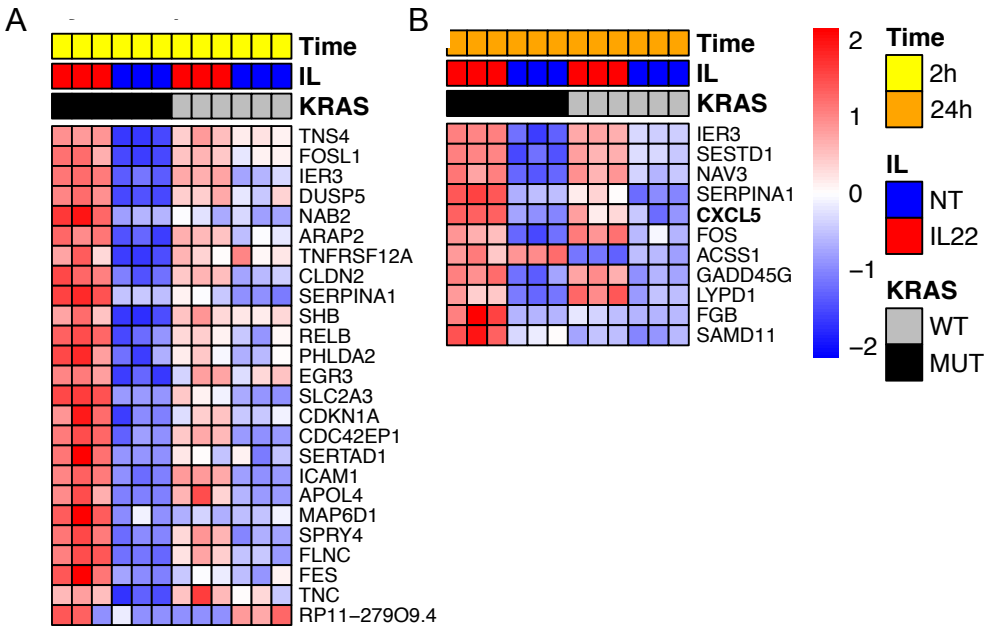


Figure 3.1 Interaction analysis genes significantly induced by IL-22 in *KRAS* mutant but not wild type cells.

Differential expression analysis was performed to assess genes induced by IL-22 in specifically in *KRAS* MUT and not WT cells [(KRAS MUT IL-22 – KRAS MUT NT) – (KRAS WT IL-22 – KRAS WT NT)] for 2h and 24h treated samples. Heatmaps represent the top differentially expressed genes (log2FC > 0.7, FDR < 0.05) for each cell line at each time point. Colours are based on log2(RPKM)+1 expression values for each of the 3 experimental replicates for each condition.

(A) Differentially regulated genes at 2h.
(B) Differentially regulated genes at 24h.

3.1.2 Pathway analysis

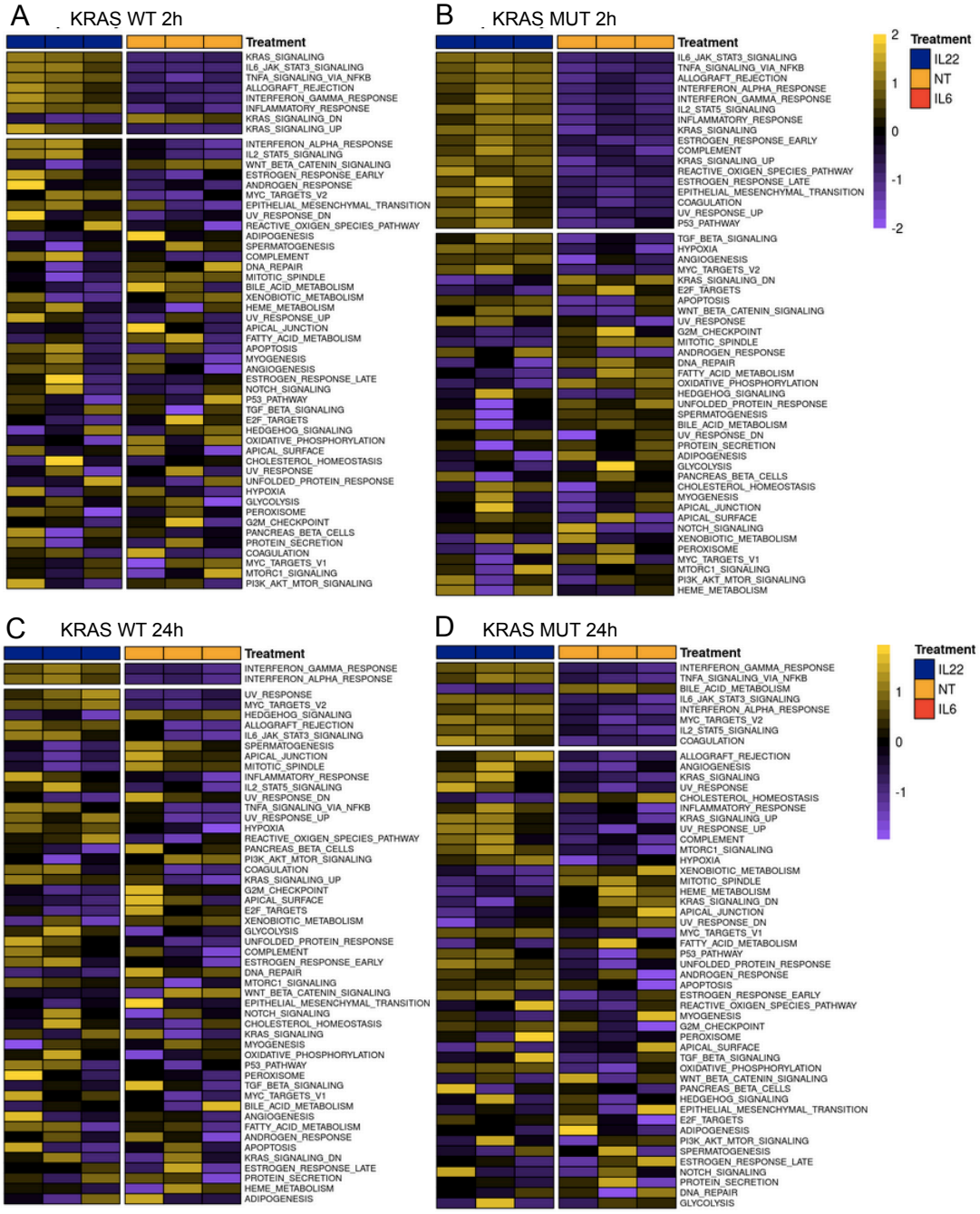


Figure 3.2 Differential analysis of single sample GSEA enrichment scores for comparisons of IL-22 to NT for each cell genotype at 2h and 24h.

Single sample GSEA (ssGSEA) was performed using the MSigDB "Hallmark Pathways" on each sample and enrichment scores were used to perform differential analysis of these scores for the comparisons of interest. The vertical gap in the heatmap indicates the significance threshold. Pathways for which the adjusted p value was less than 0.01 were considered significant.

(A) Enriched pathways KRAS WT DLD-1 isogenic cells 2h.
(B) Enriched pathways KRAS MUT DLD-1 isogenic cells 2h.
(C) Enriched pathways KRAS WT DLD-1 isogenic cells 24h.
(D) Enriched pathways KRAS MUT DLD-1 isogenic cells 24h.

This analysis was performed by D. Barras.

3.2 Proteomics

3.2.1 Differential expression analysis

KRAS WT IL-22-NT 24h			
Protein Name	Gene Symbol	log2FC	p-value
B-cell lymphoma 3 protein	BCL3	3.69507563	0.00012752
Cadherin-3	CDH3	1.06966739	0.00045415
Signal transducer and activator of transcription 3	STAT3	1.29275357	0.00053931
Transcription factor jun-B	JUNB	1.63292643	0.00120206
Tumor-associated calcium signal transducer 2	TACSTD2	1.24691297	0.00197425
Poly [ADP-ribose] polymerase 9	PARP9	1.03532463	0.00476539
Carcinoembryonic antigen-related cell adhesion molecule 1	CEACAM1	3.13902607	0.00605613
Tripartite motif-containing protein 15	TRIM15	2.6652586	0.00672117
Intercellular adhesion molecule 1	ICAM1	1.04389692	0.00768587
Fos-related antigen 2	FOSL2	1.05409582	0.00856549
Nicotinamide N-methyltransferase	NNMT	5.68761551	0.00919639
Interferon regulatory factor 9	IRF9	2.51117092	0.01249135
Carcinoembryonic antigen-related cell adhesion molecule 5	CEACAM5	5.57606995	0.01481846
Calcium-activated potassium channel subunit beta-4	KCNMB4	1.59931411	0.01618465
Caspase recruitment domain-containing protein 14	CARD14	1.12988013	0.01842515
HRAS-like suppressor 3	PLA2G16	1.48173784	0.01976971
Cdc42 effector protein 1	CDC42EP1	1.34066965	0.02341551
Neutrophil gelatinase-associated lipocalin	LCN2	4.51806001	0.02734811
Mucin-1;Mucin-1 subunit alpha;Mucin-1 subunit beta	MUC1	3.11256339	0.02799161
Interferon-induced protein with tetratricopeptide repeats 1	IFIT1	1.01606236	0.02844994
Steryl-sulfatase	STS	2.04775732	0.03233889
Host cell factor 1;HCF N-terminal chain 1	HCFC1	1.20787137	0.03247324
Erythrocyte band 7 integral membrane protein	STOM	1.79239368	0.03494951
Forkhead box protein O1	FOXO1	1.27895035	0.03822694
Alpha-1-antitrypsin;Short peptide from AAT	SERPINA1	2.27640277	0.04124411
Interleukin-27 receptor subunit alpha	IL27RA	2.3854417	0.04868942
Ubiquitin *Protein* Ligase E3 Component N-Recognin 3	UBR3	1.35801709	0.04892549

Table 3.9 Significantly up-regulated proteins following 24h IL-22 stimulation

KRAS MUT IL-22-NT 24h			
Protein Name	Gene Symbol	log2FC	p-value
Intercellular adhesion molecule 1	ICAM1	1.50206021	0.0007922
Trypsin-2	TRY8;PRSS2	1.56580023	0.0008661
B-cell lymphoma 6 protein	BCL6	1.1812498	0.0010889
Tumor-associated calcium signal transducer 2	TACSTD2	1.00143471	0.00148218
Guanylate-binding protein 3	GBP3	1.08101978	0.00160945
Caspase-10;Caspase-10 subunit p23/17;Caspase-10 subunit p12	CASP10	1.25670308	0.00177723
Carcinoembryonic antigen-related cell adhesion molecule 5	CEACAM5	5.32585696	0.00248446
Cadherin-3	CDH3	1.69606377	0.00346719
Coenzyme Q-binding protein COQ10 homolog B, mitochondrial	COQ10B	1.2234691	0.00592974
Fragile X mental retardation protein 1	FMR1	1.17026841	0.00649433
Alpha-1-antitrypsin;Short peptide from AAT	SERPINA1	3.77711644	0.00684113
Transcription factor jun-B	JUNB	1.67708754	0.00865561
Protein sprouty homolog 2	SPRY2	1.09506534	0.00892785
Proteasome subunit beta type-10	PSMB10	1.13866499	0.01112671
BRCA2 and CDKN1A-interacting protein	BCCIP	1.47799533	0.01205909
Protein sprouty homolog 1	SPRY1	1.7928524	0.01304637
Zinc finger protein 655	ZNF655	1.7393339	0.01327048
Erythrocyte band 7 integral membrane protein	STOM	1.81022287	0.01336139
Interferon-induced protein with tetratricopeptide repeats 3	IFIT3	1.17151951	0.01472064
Plexin-B1	PLXNB1	1.78260169	0.01639273
Carcinoembryonic antigen-related cell adhesion molecule 1	CEACAM1	4.7452558	0.01669716
Solute carrier family 2, facilitated glucose transporter member 3	SLC2A3	2.56098816	0.01697817
Receptor-type tyrosine-protein phosphatase epsilon;Protein-tyrosine-p	PTPRE	1.48360065	0.01714085
Tripartite motif-containing protein 47	TRIM47	1.02891054	0.01717034
Sp110 nuclear body protein	SP110	1.08014648	0.01733643
Dystonin	DST	1.95965275	0.01862271
3 beta-hydroxysteroid dehydrogenase type 7	HSD3B7	1.65672518	0.01884714
NADH dehydrogenase [ubiquinone] 1 alpha subcomplex assembly fact	NDUFAF3	1.44697833	0.01970671
EKC/KEOPS complex subunit LAGE3	LAGE3	1.03439575	0.02186615
Neuron navigator 3	NAV3	2.4522099	0.02195488
Ras GTPase-activating protein nGAP	RASAL2	1.18104599	0.02454173
Transmembrane channel-like protein 5	TMC5	1.04373953	0.02509365
Helicase with zinc finger domain 2	HELZ2	1.20705596	0.02557727
Angiomotin-like protein 2	AMOTL2	1.82625119	0.02653253
Low-density lipoprotein receptor-related protein 10	LRP10	1.05556832	0.02675428
Semaphorin-4B	SEMA4B	1.08041663	0.02693136
Protein Jade-1	JADE1	1.47006611	0.03097116
NADH-ubiquinone oxidoreductase chain 4	MT-ND4	1.1200816	0.03100516
AP-4 complex accessory subunit tepsin	ENTHD2	1.97618468	0.03111376
Ubiquitin/ISG15-conjugating enzyme E2 L6	UBE2L6	1.55872532	0.03300701
Feline leukemia virus subgroup C receptor-related protein 1	FLVCR1	1.20212149	0.03314358
Thyrotroph embryonic factor	TEF	2.16775979	0.03377069
Multidrug resistance protein 1	ABCB1	2.05267882	0.03409997
Dolichyldiphosphatase 1	DOLPP1	1.67951966	0.0342578
B-cell lymphoma 3 protein	BCL3	3.73187645	0.03674575
Protein jagged-1	JAG1	1.07309022	0.0367795
14-3-3 protein beta/alpha;14-3-3 protein beta/alpha	YWHAB	1.29925937	0.03767699
Cyclin-H	CCNH	1.292832	0.03833028
MLX-interacting protein	MLXIP	1.107273	0.03923509
2-5-oligoadenylate synthase-like protein	OASL	2.05482869	0.03969211
Protein kish-A	TMEM167A	2.2116782	0.04046947
Leucine-rich repeat-containing protein 14	LRRC14	1.35172548	0.04064778
Protein FAM135A	FAM135A	1.45808436	0.0423098
Calcium-activated potassium channel subunit beta-4	KCNMB4	2.50589433	0.0434806
Uncharacterized protein C4orf29	C4orf29	1.1559155	0.0456079
Protein sprouty homolog 4	SPRY4	1.62226178	0.04589882
Ras association domain-containing protein 1	RASSF1	1.93465866	0.0463317
Elongation factor 1-alpha 2	EEF1A2	1.6780244	0.04799145
Tensin 3	TNS3	2.99110743	0.0482279
Growth/differentiation factor 15	GDF15	1.29568151	0.04832125
Protein phosphatase 1 regulatory subunit 15B	PPP1R15B	1.17787217	0.049224
Stimulator of interferon genes protein	TMEM173	1.16373722	0.04947026

Table 3.10 Significantly up-regulated proteins following 24h IL-22 stimulation

KRAS WT IL-22-NT 24h			
Protein Name	Gene Symbol	log2FC	p-value
Unconventional myosin-X	MYO10	-1.6002608	0.00058706
Myotonin-protein kinase	DMPK	-1.3372425	0.00505833
Type I inositol 1,4,5-trisphosphate 5-phosphatase	INPP5A	-1.246568	0.00983342
Zinc finger and BTB domain-containing protein 4	ZBTB4	-1.0016196	0.01063938
Hydroxymethylglutaryl-CoA synthase, mitochondrial	HMGCS2	-1.1611682	0.0121995
Inositol 1,4,5-trisphosphate receptor type 1	ITPR1	-1.9658193	0.01224742
Glutaminyl-peptide cyclotransferase	QPCT	-1.0969215	0.01907758
DNA (cytosine-5)-methyltransferase 1	DNMT1	-2.8984673	0.02218707
Spindlin-3	SPIN3	-1.4491554	0.02439966
Uncharacterized protein KIAA1328	KIAA1328	-1.0844826	0.02502118
ADP-ribosylation factor-like protein 4C	ARL4C	-1.7267024	0.02774807
Polyamine-modulated factor 1	PMF1-BGLAP;I	-1.4175064	0.0352486
Histone-lysine N-methyltransferase SUV420H2	SUV420H2	-1.2136855	0.03542521
Zinc finger protein 561	ZNF561	-1.2961501	0.04151352
Acetyl-CoA carboxylase 2;Biotin carboxylase	ACACB	-1.7698513	0.04514836
Transmembrane protein 69	TMEM69	-1.7828427	0.04689809

KRAS MUT IL-22-NT 24h			
Protein Name	Gene Symbol	log2FC	p-value
Actinin Alpha 4	ACTN4	-1.06884	0.00264491
B-raf	BRAF	-1.7302589	0.00461628
Signal-induced proliferation-associated protein 1	SIPA1	-1.8868629	0.01876189
5-azacytidine-induced protein 2	AZI2	-1.1281955	0.02418866
Protein GPR107	GPR107	-1.577693	0.02757379
SRR1-like protein	SRRD	-1.3274277	0.0312764
Breast carcinoma-amplified sequence 1	BCAS1	-1.7308211	0.03224022
Centrosomal protein of 68 kDa	CEP68	-1.0307886	0.03568207
Nephronectin	NPNT	-1.0471107	0.0375264
Mast/stem cell growth factor receptor Kit	KIT	-1.5619459	0.04542298
CXXC-type zinc finger protein 5	CXXC5	-2.920876	0.04564729
Aprataxin and PNK-like factor	APLF	-1.0203593	0.04760591
Battenin	CLN3	-1.0676006	0.04824446
Kelch-like protein 12	KLHL12	-1.5007879	0.04910745

Table 3.11 Significantly down-regulated proteins following 24h IL-22 stimulation

The tables in this section represent the results from two-tailed, paired T-tests used to compare relative iBAQ intensities for the IL-22 stimulated versus no treatment condition for the *KRAS* mutant and wild type DLD-1 isogenic line. Proteins for which log2 fold change > 1 and P<0.05 were considered significantly differentially regulated.

3.2.2 Pathway analysis

Annotation Description	PES	p-value	FDR	Number of proteins with annotation in dataset	Total number of proteins with annotation
PILON_KLF1_TARGETS_DN	650.257	0	0.02	1482	1972
PUJANA_BRCA1_PCC_NETWORK	548.3245	0	0.02	1214	1652
DIAZ_CHRONIC_MEYLOGENOUS_LEUKEMIA_UP	513.6105	0	0.02	1144	1382
DODD_NASOPHARYNGEAL_CARCINOMA_DN	423.8485	0	0.02	948	1375
PUJANA_ATM_PCC_NETWORK	405.4865	0	0.02	912	1442
KINSEY_TARGETS_OF_EWSR1_FLII_FUSION_UP	402.258	0	0.02	906	1278
BLALOCK_ALZHEIMERS_DISEASE_DN	359.6895	0	0.02	806	1237
LEE_BMP2_TARGETS_DN	309.0365	0	0.02	689	882
KRIGE_RESPONSE_TO_TOSEDOSTAT_24HR_DN	302.961	3.00E-04	0.03	685	1011
DACOSTA_UV_RESPONSE_VIA_ERCC3_DN	300.9405	0	0.02	676	855
ACEVEDO_LIVER_CANCER_UP	289.36	4.00E-04	0.03	655	973
PUJANA_CHEK2_PCC_NETWORK	295.831	0	0.02	649	779
GRADE_COLON_CANCER_UP	274.9605	0	0.02	618	871
BENPORATH_MYC_MAX_TARGETS	272.693	0	0.02	613	775
WEI_MYCN_TARGETS_WITH_E_BOX	266.0565	0	0.02	593	795
RODRIGUES_THYROID_CARCINOMA_ANAPLASTIC_UP	246.742	0	0.02	555	722
CAIRO_HEPATOBLASTOMA_CLASSES_UP	239.7925	0	0.02	525	605
CASORELLI_ACUTE_PROMYELOCYTIC_LEUKEMIA_DN	227.6985	0	0.02	502	663
KIM_ALL_DISORDERS_OLIGODENDROCYTE_NUMBER_CORR_UP	224.5355	0	0.02	501	756
REACTOME_IMMUNE_SYSTEM	219.6035	2.00E-04	0.03	492	933
SCHLOSSER_SERUM_RESPONSE_DN	218.7715	2.00E-04	0.03	490	712
KIM_BIPOLAR_DISORDER_OLIGODENDROCYTE_DENSITY_CORR_UP	213.5895	0	0.02	475	682
TIEN_INTESTINE_PROBIOTICS_24HR_UP	207.7855	1.00E-04	0.02	466	557
SPIELMAN_LYMPHOBLAST_EUROPEAN_VS_ASIAN_DN	204.136	1.00E-04	0.02	457	584
HAMAI_APOPTOSIS_VIA_TRAIL_UP	193.154	0	0.02	424	584
FEVR_CTNNB1_TARGETS_DN	191.0325	0	0.02	422	553
MILI_PSEUDOPODIA_HAPTOTAXIS_UP	189.276	0	0.02	422	518
BERENJENO_TRANSFORMED_BY_RHOA_UP	184.5865	1.00E-04	0.02	413	536
FLECHNER_BIOPSY_KIDNEY_TRANSPLANT_OK_VS_DONOR_UP	184.254	0	0.02	408	555
ENK_UV_RESPONSE_KERATINOCYTE_DN	174.9875	0	0.02	390	485
FLECHNER_BIOPSY_KIDNEY_TRANSPLANT_REJECTED_VS_OK_DN	165.238	0	0.02	366	546
SHEN_SMARCA2_TARGETS_UP	162.8515	0	0.02	359	424
GARY_CD5_TARGETS_DN	160.683	0	0.02	352	431
KIM_ALL_DISORDERS_CALB1_CORR_UP	156.7115	2.00E-04	0.03	349	548
HSIAO_HOUSEKEEPING_GENES	141.7525	0	0.02	311	389
ROME_INSULIN_TARGETS_IN_MUSCLE_UP	137.954	2.00E-04	0.03	306	442
PENG_GLUTAMINE_DEPRIVATION_DN	135.6075	0	0.02	291	337
WONG_EMBRYONIC_STEM_CELL_CORE	131.3255	3.00E-04	0.03	291	335
RHEIN_ALL_GLUCOCORTICOID_THERAPY_DN	130.607	0	0.02	287	362
WANG_TUMOR_INVASIVENESS_UP	129.4475	0	0.02	284	374
TARTE_PLASMA_CELL_VS_PLASMABLAST_DN	118.624	1.00E-04	0.02	261	309
BORCZUK_MALIGNANT_MESOTHELIOMA_UP	115.2985	0	0.02	249	305
MANALO_HYPOXIA_DN	109.24	3.00E-04	0.03	242	289
REACTOME_METABOLISM_OF_RNA	108.1385	0	0.02	232	330
GRADE_COLON_AND_RECTAL_CANCER_UP	105.3405	0	0.02	232	285
FOURNIER_ACINAR_DEVELOPMENT_LATE_2	104.006	0	0.02	230	277
ZHANG_TLX_TARGETS_60HR_DN	103.1425	0	0.02	227	277
PENG_RAPAMYCIN_RESPONSE_DN	94.3729997	0	0.02	206	245
ENK_UV_RESPONSE_EPIDERMIS_UP	90.7879998	0	0.02	199	293
REACTOME_METABOLISM_OF_MRNA	89.2830002	0	0.02	191	284
GSE15930_NAIVE_VS_48H_IN_VITRO_STIM_CD8_TCELL_DN	81.6569999	1.00E-04	0.02	177	200
BOYAULT_LIVER_CANCER_SUBCLASS_G3_UP	80.1975002	0	0.02	173	188
GSE14000_TRANSLATED_RNA_VS_MRNA_DC_UP	79.0975	0	0.02	171	200
GSE22886_UNSTIM_VS_STIM_MEMORY_TCELL_DN	77.4710001	2.00E-04	0.03	170	200
GSE22886_NEUTROPHIL_VS_MONOCYTE_DN	77.2840001	0	0.02	168	200
GSE22886_NAIVE_CD4_TCELL_VS_48H_ACT_TH1_DN	77.3590003	1.00E-04	0.02	168	200
GSE22886_UNSTIM_VS_IL2_STIM_NKCELL_DN	76.4785002	4.00E-04	0.03	168	200
REACTOME_DNA_REPLICATION	76.301	1.00E-04	0.02	167	192
GSE24634_TEFF_VS_TCONV_DAY5_IN_CULTURE_UP	75.9844999	3.00E-04	0.03	167	200
GSE22886_NAIVE_TCELL_VS_NEUTROPHIL_UP	76.3709999	0	0.02	165	200
GSE3982_MEMORY_CD4_TCELL_VS_TH2_DN	75.274	0	0.02	165	200
GSE14000_TRANSLATED_RNA_VS_MRNA_4H_LPS_DC_UP	74.9915001	2.00E-04	0.03	165	200
PENG_LEUCINE_DEPRIVATION_DN	76.771	0	0.02	163	187
REACTOME_HIV_INFECTION	74.8620002	1.00E-04	0.02	163	207
GSE10239_MEMORY_VS_DAY4.5_EFF_CD8_TCELL_DN	74.3879998	3.00E-04	0.03	163	199
GSE12845_NAIVE_VS_PRE_GC_TONSIL_BCELL_DN	73.6439998	0	0.02	159	200
CHIANG_LIVER_CANCER_SUBCLASS_UNANNOTATED_DN	71.5210003	1.00E-04	0.02	156	193
WELCSH_BRCA1_TARGETS_UP	70.5355	0	0.02	153	198

continued on next page

Annotation Description	PES	p-value	FDR	Number of proteins with annotation in dataset	Total number of proteins with annotation
GSE12845_NAIVE_VS_DARKZONE_GC_TONSIL_BCELL_DN	69.5275001	2.00E-04	0.03	152	200
GSE12845_IGD_NEG_BLOOD_VS_DARKZONE_GC_TONSIL_BCELL_DN	69.0225001	3.00E-04	0.03	151	200
GSE27786_NKTCELL_VS_MONO_MAC_UP	67.3369998	0	0.02	146	200
GSE12845_IGD_NEG_BLOOD_VS_NAIVE_TONSIL_BCELL_UP	66.9229998	3.00E-04	0.03	146	200
SCHLOSSER_MYC_TARGETS_REPRESSED_BY_SERUM	68.1405	0	0.02	145	159
GSE22886_NAIVE_BCELL_VS_BLOOD_PLASMA_CELL_DN	66.3004998	2.00E-04	0.03	145	200
GSE3982_NKCELL_VS_TH2_DN	65.7175001	1.00E-04	0.02	143	200
REACTOME_MRNA_PROCESSING	66.3320001	0	0.02	142	161
GSE24634_TREG_VS_TCONV_POST_DAY10_IL4_CONVERSION_UP	63.1335	4.00E-04	0.03	138	200
GSE17721_POLYIC_VS_GARDIQUIMOD_12H_BMDM_DN	62.5050001	1.00E-04	0.02	136	200
GNF2_FBL	64.2265001	0	0.02	134	147
GSE13411_NAIVE_VS_MEMORY_BCELL_DN	61.8384998	0	0.02	132	200
REACTOME_PROCESSING_OF_CAPPED_INTRON_CONTAINING_PRE_MRNA	60.1570001	0	0.02	127	140
REACTOME_TRANSLATION	60.0355	0	0.02	126	222
GSE12845_IGD_NEG_BLOOD_VS_PRE_GC_TONSIL_BCELL_DN	57.9550003	4.00E-04	0.03	126	200
LI_WILMS_TUMOR_VS_FETAL_KIDNEY_1_DN	56.517	0	0.02	122	163
REACTOME_INFLUENZA_LIFE_CYCLE	56.3595001	0	0.02	121	203
KEGG_SPLICEOSOME	53.6535	2.00E-04	0.03	116	128
DANG_MYC_TARGETS_UP	52.804	4.00E-04	0.03	115	143
GSE16522_ANTI_CD3CD28_STIM_VS_UNSTIM_NAIVE_CD8_TCELL_UP	49.6589998	2.00E-04	0.03	107	200
GCM_NPM1	49.4065	0	0.02	105	116
REACTOME_HOST_INTERACTIONS_OF_HIV_FACTORS	49.1905	0	0.02	105	132
TOOKER_GEMCITABINE_RESISTANCE_DN	47.2205002	1.00E-04	0.02	102	122
REACTOME_MRNA_SPLICING	46.3080001	0	0.02	98	111
REACTOME_SRP_DEPENDENT_COTRANSLATIONAL_PROTEIN_TARGETING_T	44.216	0	0.02	94	179
HOSHIDA_LIVER_CANCER_SUBCLASS_S2	43.9425001	1.00E-04	0.02	94	115
RB_P130_DN.V1_DN	43.5274999	0	0.02	93	139
REACTOME_NONSENSE_MEDIATED_DECAY_ENHANCED_BY_THE_EXON_JU	43.4805001	1.00E-04	0.02	93	176
KARLSSON_TGFB1_TARGETS_UP	43.0164999	1.00E-04	0.02	92	127
REACTOME_3_UTR_MEDIATED_TRANSLATIONAL_REGULATION	42.9114999	0	0.02	91	176
REACTOME_SYNTHESIS_OF_DNA	38.493	2.00E-04	0.03	83	92
SEIDEN_ONCOGENESIS_BY_MET	35.4955001	3.00E-04	0.03	76	88
SCHUHMACHER_MYC_TARGETS_UP	34.813	1.00E-04	0.02	74	80
BHATTACHARYA_EMBRYONIC_STEM_CELL	28.967	0	0.02	61	89
BILANGES_SERUM_AND_RAPAMYCIN_SENSITIVE_GENES	28.6805001	1.00E-04	0.02	60	68
ZHANG_RESPONSE_TO_CANTHARIDIN_DN	27.4540001	2.00E-04	0.03	58	69
DANG_REGULATED_BY_MYC_UP	27.2774999	3.00E-04	0.03	58	72
RHODES_CANCER_META_SIGNATURE	26.3750001	0	0.02	55	64
REACTOME_METABOLISM_OF_NUCLEOTIDES	25.5245	2.00E-04	0.03	54	72
REACTOME_TRANSPORT_OF_MATURE_TRANSCRIPT_TO_CYTOPLASM	24.3555	3.00E-04	0.03	51	54
TARTE_PLASMA_CELL_VS_B_LYMPHOCYTE_UP	24.1290001	4.00E-04	0.03	51	78
REACTOME_ACTIVATION_OF_THE_MRNA_UPON_BINDING_OF_THE_CAP_BIN	23.0319998	1.00E-04	0.02	48	84
MULLIGHAN_NPM1_MUTATED_SIGNATURE_2_DN	21.376	3.00E-04	0.03	45	77
REACTOME_FORMATION_OF_THE_TERNARY_COMPLEX_AND_SUBSEQUENT	20.0704998	4.00E-04	0.03	42	74
RIZKI_TUMOR_INVASIVENESS_2D_DN	19.6799998	2.00E-04	0.03	41	64
KEGG_VALINE_LEUCINE_AND_ISOLEUCINE_DEGRADATION	19.1064999	3.00E-04	0.03	40	44
ABRAMSON_INTERACT_WITH_AIRE	19.387	0	0.02	39	45
GRADE_METASTASIS_DN	16.4434999	2.00E-04	0.03	34	45
WIERENGA_PML_INTERACTOME	15.842	3.00E-04	0.03	33	42
MODY_HIPPOCAMPUS_PRENATAL	15.016	1.00E-04	0.02	31	42
GREENBAUM_E2A_TARGETS_UP	12.2665	2.00E-04	0.03	25	33
MELLMAN_TUT1_TARGETS_UP	6.65099993	2.00E-04	0.03	13	19
REACTOME_PURINE_RIBONUCLEOSIDE_MONOPHOSPHATE_BIOSYNTHESIS	5.5845001	1.00E-04	0.02	11	11

Table 3.12 Significantly upregulated pathways in KRAS mutant IL-22 stimulated versus KRAS wild type IL-22 stimulated cells PSEA-Quant analysis

Protein set enrichment analysis (PSEA-Quant) (http://pseaquant.scripps.edu/) (Lavallée-Adam et al. 2014; Lavallée-Adam and Yates 2016) was used to perform pathway analysis. Analysis of the ratio of the fold changes in iBAQ values for *KRAS* mutant IL-22 stimulated over unstimulated cells compared to *KRAS* wild type IL-22 stimulated over unstimulated cells was performed.

The positional, curated, motif, computational, oncogenic, immunologic pathways from the MSigDB (totaling 11,812) were used in this analysis. The pathways from the MSigDB for which P<0.001, with an FDR-q value of less than 0.05 were considered significant.

PES – Protein enrichment score of the protein set: an internal score used by PSEA-Quant to compute the *p*-value of the protein set.

p-value – Statistical significance enrichment *p*-value of protein set. *p*-value generally overestimates significance therefore FDR-q value computed.

FDR-*q*-value – False discovery rate associated with protein set.

Number of proteins with annotation in dataset: number of proteins in the annotated signature that are contained in the input data.

Total number of proteins with annotation – number of proteins in the annotated signature

.

4 Appendix: Clinical Data

Sample #	ORB #	Tumour vs matched normal	Clinical Diagnosis/location	Tumour Stage (TNM Classification)	Age	Sex	Neoadjuvent Therapy	Oxford Molecular Diagnostics Mutational Analysis
Prospectively collected fresh resections								
1	0108563/4	CRC	moderately differentiated mucinous adenocarcinoma/ascending colon	pT3 N0(0/32) M0	57	F	None	KRAS (c.34G>T, p.(G12C), COSM516).
1	0108565	Adjacent Normal			57	F	None	
2	0108571/2	CRC	moderately differentiated mucinous adenocarcinoma/caecum	pT4a N0(0/46) Mx	46	F	None	PIK3CA (c.1633G>A, p.(E545K), COSM763). Mutation of uncertain clinical significance detected in PTEN (c.963delA, p.(N323fs)).
2	0108573	Adjacent Normal			46	F	None	
3	0108576/7	CRC	moderately differentiated adenocarcinoma/rectosigmoid	pT3 N0(0/35) M0	52	M	None	Mutation not detected in the KRAS, NRAS and BRAF genes.
3	0108578	Adjacent Normal			52	M	None	
4	0108595/6	CRC	moderately differentiated adenocarcinoma/ascending colon	pT3 N0(0/21) M0	79	F	None	BRAF (c.1799T>A, p.(V600E), COSM476).
4	0108597	Adjacent Normal			79	F	None	
5	0108598/9	CRC	poorly differentiated adenocarcinoma/anorectal junction	ypT3 N1(1/10) M0	77	M	Yes	FAILED TEST
5	0108600	Adjacent Normal			77	M	Yes	
6	0108610	CRC	moderately differentiated adenocarcinoma/ascending colon	pT3 N2(4/28) M0	77	M	None	NOT TESTED
6	0108611	Adjacent Normal			77	M	None	
7	0108614/5	CRC	moderately differentiated adenocarcinoma/caecum	pT3 N0(0/11) M0	55	M	None	NOT TESTED
7	0108616	Adjacent Normal			55	M	None	
8	0108650	CRC	moderately differentiated adenocarcinoma/transverse colon	pT4b N2(33/48) M1	69	M	None	TP53 (c.404G>T, p.(Cys135Phe), COSM10647).
8	0108651	Adjacent Normal			69	M	None	
9	0108654	CRC	moderately differentiated adenocarcinoma/sigmoid colon	pT3 N2(5/54) M0	78	M	None	TP53 (c.659A>G, p.(Tyr220Cys), COSM10758).
9	0108655	Adjacent Normal			78	M	None	
10	0108659	CRC	moderately differentiated mucinous adenocarcinoma/proximal ascending colon	pT3 N2(4/18) Mx	79	F	None	BRAF (c.1799T>A, p.(Val600Glu), COSM476).
10	0108660	Adjacent Normal			79	F	None	
11	0108666	CRC	moderately differentiated adenocarcinoma/rectum	pT2 N1(2/15) M0	71	M	None	KRAS (c.38G>A, p.(Gly13Asp), COSM532). TP53 (c.1050_1051insT, p.(Lys351*)).
11	0108667	Adjacent Normal			71	M	None	
12	0108668	CRC	moderately differentiated adenocarcinoma/caecum	pT3 N1(2/11) M0	68	F	None	KRAS (c.38G>A, p.(Gly13Asp), COSM532).
12	0108669	Adjacent Normal			68	F	None	
13	0108674	CRC	moderately differentiated adenocarcinoma/sigmoid colon	pT3 N0(0/24) Mx	72	F	None	TP53 (c.818G>T, p.(Arg273Leu), COSM10779).
13	0108675	Adjacent Normal			72	F	None	
14	0108679	CRC	moderately differentiated adenocarcinoma/sigmoid colon	pT2 N0(0/34) M0	34	M	None	Mutation detected in the KRAS gene (c.35G>A, p.(Gly12Asp), COSM521). Mutation detected in the PIK3CA gene (c.1637A>T, p.(Gln546Leu), COSM25041). Mutation of uncertain clinical significance detected in the PTEN gene (c.800_800delA, p.(Lys267fs), COSM5809, NM_000314.4). Mutation of uncertain clinical significance detected in the KIT gene (c.1702T>A, p.(Tyr568Asn), NM_000222.2).
14	0108680	Adjacent Normal			34	M	None	
15	0108689	CRC	moderately differentiated adenocarcinoma/rectosigmoid colon	pT3 N0(0/20) Mx	1963	M	None	Mutation of uncertain clinical significance detected in the KRAS gene (c.35_36insAGCTGG, p.(Ala11_Gly12dup), COSM1562186). Mutation detected in the TP53 gene (c.524G>A, p.(Arg175His), COSM10648).
15	0108690	Adjacent Normal			1963	M	None	
16	0108691	CRC	moderately differentiated adenocarcinoma/rectosigmoid colon	pT3 N0(0/20) Mx	1963	M	None	Mutation of uncertain clinical significance detected in the KRAS gene (c.35_36insAGCTGG, p.(Ala11_Gly12dup), COSM1562186). Mutation detected in the TP53 gene (c.524G>A, p.(Arg175His), COSM10648).
16	0108692	Adjacent Normal			1963	M	None	
17	0108693	CRC	moderately differentiated adenocarcinoma/distal sigmoid colon	pT3 N0(0/18) M0	1935	M	None	Mutation detected in the KRAS gene (c.35G>T, p.(Gly12Val), COSM520). Mutation detected in the TP53 gene (c.659A>G, p.(Tyr220Cys), COSM10758).
17	0108694	Adjacent Normal			1935	M	None	
18	0108698	CRC	moderately differentiated adenocarcinoma/distal sigmoid colon	pT3 N0(0/15) M0	1964	F	None	Mutation not detected in the KRAS, NRAS and BRAF genes.
18	0108699	Adjacent Normal			1964	F	None	
19	0108704	CRC	moderately differentiated adenocarcinoma/distal sigmoid colon	pT2 N1(1/26) M0	1947	M	None	NOT TESTED
19	0108705	Adjacent Normal			1947	M	None	
20	0108707	CRC	moderately differentiated adenocarcinoma/distal sigmoid colon	pT4b N1(1/13) M0	1931	M	None	Mutation of uncertain clinical significance detected in the BRAF gene (c.1781A>G, p.(Asp594Gly), COSM467). Mutation detected in the TP53 gene (c.488A>G, p.(Tyr163Cys), COSM10808).
20	0108708	Adjacent Normal			1931	M	None	
21	0108709	CRC	moderately differentiated adenocarcinoma/transverse colon	pT3 N0(0/36) M0	1978	M	None	Mutation detected in the KRAS gene (c.35G>A p.(Gly12Asp), COSM521). Mutation of uncertain clinical significance detected in the PIK3CA gene (c.1258T>C, p.(Cys420Arg), COSM757).
21	0108710	Adjacent Normal	caecum		1978	M	None	
21	0108711	Min UC sigmoid	inflammed UC sigmoid colon		1978	M	None	
22	0108712	CRC	moderately differentiated adenocarcinoma/sigmoid colon	pT3 N0(0/26) M0	1939	M	None	Mutation detected in the PIK3CA gene (c.1633G>A, p.(Glu545Lys), COSM763). Mutation detected in the TP53 gene (c.524G>A, p.(Arg175His), COSM10648).
22	0108713	Adjacent Normal	sigmoidal		1939	M	None	

Sample #	ORB #	Tumour vs matched normal	Clinical Diagnosis/location	Tumour Stage (TNM Classification)	Age	Sex	Neoadjuvent Therapy	Oxford Molecular Diagnostics Mutational Analysis
Prospectively collected fresh resections								
23	0108719	CRC	moderately differentiated adenocarcinoma/mid sigmoid colon	(pT3). N0(0/26) M0	1943	M	None	NOT TESTED
23	0108720	Adjacent Normal	sigmoidal		1943	M	None	
24	0108723	CRC	moderately differentiated adenocarcinoma/sigmoid colon	(pT2). N0(0/19) M0	1950	M	None	Mutation detected in the TP53 gene (c.743G>A, p.(Arg248Gln), COSM10662).
24	0108724	Adjacent Normal	sigmoidal		1950	M	None	
25	0108728	CRC	moderately differentiated adenocarcinoma/ascending colon	(pT3). N1(1/18) M0	1942	F	None	Mutation not detected in the KRAS, NRAS and BRAF genes.
25	0108729	Adjacent Normal	caecum		1942	F	None	
26	0108733	CRC	moderately differentiated adenocarcinoma/descending colon	(pT4b). N1(2/38)	1971	F	None	Mutation detected in the TP53 gene (c.586C>T, p.(Arg196Ter), COSM10705).
26	0108734	Adjacent Normal	descending colon		1971	F	None	
27	0108737	CRC	poorly differentiated adenocarcinoma/ascending colon	(pT4a). N1(1/21) M0	1947	F	None	Mutation detected in the BRAF gene (c.1799T>A, p.(Val600Glu), COSM476). Mutation of uncertain clinical significance detected in the PIK3CA gene (c.323G>A, p.(Arg108His), COSM27497). Mutation detected in the TP53 gene (c.817C>T, p.(Arg273Cys), COSM10659).
27	0108736	Adjacent Normal			1947	F	None	
28	0108740	CRC	moderately differentiated adenocarcinoma/transverse colon	(pT3). N1(3/33) M0	1957	F	None	Mutation detected in the KRAS gene (c.35G>A, p.(Gly12Asp), COSM521). Mutation detected in the PIK3CA gene (c.1624G>A, p.(Glu542Lys), COSM760).
28	0108741	Adjacent Normal	Ascending/transverse colon		1957	F	None	
29	0108742	CRC	moderately differentiated adenocarcinoma/splenic flexure	(pT3). N0(0/15) Mx	1940	M	None	Mutation detected in the NRAS gene (c.176C>A, p.(Ala59Asp), COSM253327). Mutation detected in the TP53 gene (c.395A>G, p.(Lys132Arg), COSM11582).
29	0108743	Adjacent Normal	splenic flexure		1940	M	None	
30	0108748	CRC	moderately differentiated adenocarcinoma/ascending colon	(pT3). N0(0/31) M0	1951	F	None	Mutation detected in the KRAS gene (c.35G>C, p.(Gly12Ala), COSM522). Mutation detected in the TP53 gene (c.824G>T, p.(Cys275Phe), COSM10701).
30	0108749	Adjacent Normal			1951	F	None	
31	0108753	CRC	moderately differentiated adenocarcinoma/transverse colon	(pT3). N0 (0/26) M0	1936	M	None	Mutation detected in the KRAS gene (c.35G>A, p.(Gly12Asp), COSM521). Mutation detected in the PIK3CA gene (c.1633G>A, p.(Glu545Lys), COSM763).
31	0108754	Adjacent Normal			1936	M	None	
32	0108756	CRC	moderately differentiated adenocarcinoma/caecum	(pT3). N1 (1/28) M0	1940	M	None	Mutation detected in the KRAS gene (c.32_34delinsCTG>TTT, p.(Ala11_Gly12delinsValCys), COSM5369708). Mutation detected in the TP53 gene (c.916C>T, p.(Arg306*), COSM10663).
32	0108755	Associated Normal			1940	M	None	
33	0108757	CRC	poorly differentiated mucinous adenocarcinoma/ascending colon	(pT3). N0 (0/23) M0	1960	M	None	Mutations of uncertain clinical significance detected in the PTEN gene (c.70G>T, p.(Asp24Tyr), COSM5237; c.389G>A, p.(Arg130Gln), COSM5033). Mutation of uncertain clinical significance detected in the PDGFRA gene (c.2041G>T, p.(Asp681Tyr).
33	0108758	Adjacent Normal			1960	M	None	
34	0108767	CRC	moderately differentiated adenocarcinoma/ascending colon	(pT3). N0 (0/25) M0	1935	F	None	Mutation detected in the PIK3CA gene (c.1637A>G, p.(Gln546Arg), COSM12459).
34	0108768	Adjacent Normal			1935	F	None	
35	0108769	CRC	moderately differentiated adenocarcinoma/sigmoid colon	(pT3). N2 (9/21) M0	1951	M	None	Mutation detected in the NRAS gene (c.37G>C, p.(Gly13Arg), COSM569). Mutation detected in the TP53 gene (c.818G>A, p.(Arg273His), COSM10660).
35	0108770	Adjacent Normal	rectosigmoidal		1951	M	None	
36	0108772	CRC	moderately differentiated adenocarcinoma	pT3 N2 (4/59) M0	1978	F	Unknown	Mutation detected in the KRAS gene (c.183A>C, p.(Gln61His), COSM554). Mutation detected in the TP53 gene (c.701A>G, p.(Tyr234Cys), COSM10725).
36	0108773	Adjacent Normal	sigmoidal		1978	F		
37	0108774	CRC	moderately differentiated adenocarcinoma	pT2 N0 (0/23) M0	1944	F	Unknown	Mutation detected in the BRAF gene (c.1799T>A, p.(Val600Glu), COSM476).
37	0108775	Adjacent Normal	ascending colon		1944	F		
38	0108780	CRC	No residual tumour: RG-2	ypT0 N1 (1/27) M0	1949	M	Yes	NOT TESTED
38	0108781	Adjacent Normal	Recto-sigmoidal		1949	M		
39	0108790	CRC	moderately differentiated adenocarcinoma	pT4b N1 (1/25) M0	1949	M	Unknown	Mutation detected in the KRAS gene (c.35G>A, p.(Gly12Asp), COSM521). Mutation detected in the PIK3CA gene (c.1624G>A, p.(Glu542Lys), COSM760).
39	0108791	Adjacent Normal	sigmoidal		1949	M		
40	0108800	CRC	moderately differentiated adenocarcinoma	pT2 N0 (0/14) M0	1950	F	Unknown	Mutation not detected in the KRAS, NRAS and BRAF genes.
40	0108801	Adjacent Normal	sigmoidal		1950	F		
41	0108802	CRC	moderately differentiated adenocarcinoma	pT2 N1 (2/33) M0	1928	M	Unknown	Mutation not detected in the KRAS, NRAS and BRAF genes.
41	0108802	Adjacent Normal	sigmoidal		1928	M		
42	0108806	CRC	moderately differentiated adenocarcinoma	pT3 N0 (0/21) M0	1955	F	Unknown	Mutation detected in the BRAF gene (c.1799T>A, p.(Val600Glu), COSM476).
42	0108807	Adjacent Normal			1955	F		
43	0108813	CRC	moderately differentiated adenocarcinoma	pT1 N0 (0/12) M0	1968	F	Unknown	Mutation not detected in the KRAS, NRAS and BRAF genes.
43	0108815	Adjacent Normal			1968	F		
44	0108819	CRC	moderately differentiated adenocarcinoma	pT4b N1 (2/42) M0	1957	F	Unknown	NOT TESTED
44	0108820	Adjacent Normal	right colon		1957	F		
45	0108822	CRC	poorly differentiated adenocarcinoma	pT3 N0 (0/40) M0	1946	F	Unknown	Mutation detected in the BRAF gene (c.1799T>A, p.(Val600Glu), COSM476).
45	0108823	Adjacent Normal			1946	F		
46	0108825	CRC	moderately differentiated adenocarcinoma	pT3 N0 (0/12) M0	1930	M	Unknown	NOT TESTED
46	0108826	Adjacent Normal	ascending colon		1930	M		
47	0108833	CRC	moderately differentiated adenocarcinoma	pT3 N2 (8/27) M0	1954	M	Unknown	Mutation not detected in the KRAS, NRAS and BRAF genes.
47	0108834	Adjacent Normal			1954	M		
48	0108837	CRC	well differentiated adenocarcinoma	pT3 N0 (0/27) Mx	1948	M	Unknown	Mutation detected in the KRAS gene (c.35G>C, p.(Gly12Ala), COSM522).
48	0108838	Adjacent Normal	rectal		1948	M		
49	0108841	CRC	moderately differentiated adenocarcinoma	pT2 N0 (0/20) M0	1941	F	Unknown	Mutation detected in the KRAS gene (c.38G>A, p.(Gly13Asp), COSM532).
49	0108842	Adjacent Normal	ceacum		1941	F		

Sample #	ORB #	Tumour vs matched normal	Clinical Diagnosis/location	Tumour Stage (TNM Classification)	Age	Sex	Neoadjuvent Therapy	Oxford Molecular Diagnostics Mutational Analysis
Prospectively collected fresh resections								
50	0108846	CRC	moderately differentiated adenocarcinoma	pT4a N0 (0/22) M0	1944	M	Unknown	Mutation detected in the KRAS gene (c.436G>A, p.(Ala146Thr), COSM19404). Mutation detected in the PIK3CA gene (c.1624G>A, p.(Glu542Lys), COSM760). Mutation of uncertain clinical significance detected in the PTEN gene (c.388C>T, p.(Arg130Ter), COSM5152).
50	0108847	Adjacent Normal			1944	M		
51	0108850	CRC	moderately differentiated adenocarcinoma	pT2 N1 (1/12) Mx	1980	M	Unknown	Mutation detected in the KRAS gene (c.179G>A, p.(Gly60Asp), COSM87290). Mutation detected in BRAF gene (c.1781A>G, p.(Asp594Gly), COSM467). Mutation detected in the TP53 gene (c.844C>T, p.(Arg282Trp), COSM10704).
51	0108851	Adjacent Normal	sigmoid		1980	M		
52	0108858	CRC	moderately differentiated adenocarcinoma	pT4a N1 (2/58) Mx	1931	M	Unknown	Mutation detected in the KRAS gene (c.38G>A, p.(Gly13Asp), COSM532).
52	0108859	Adjacent Normal			1931	M		
53	0108862	CRC	poorly differentiated adenocarcinoma	pT4b N0 (0/35) M0	1935	F	Unknown	Mutation not detected in the KRAS and NRAS genes. Mutation detected in the BRAF gene (c.1799T>A, p.(Val600Glu), COSM476). Mutation of uncertain clinical significance detected in the PIK3CA gene (c.1030G>A, p.(Val344Met),COSM253279).
53	0108863	Normal Adjacent			1935	F		
54	0108870	CRC	poorly differentiated adenocarcinoma	pT4a L0 V0 N0 (0/27) Mx	1957	M	Unknown	Mutation detected in the KRAS gene (c.35G>T, p.(Gly12Val), COSM520). Mutation detected in the TP53 gene (c.742C>T, p.(Arg248Trp), COSM10656).
54	0108871	Normal Adjacent			1957	M		
55	0108898	CRC	moderately differentiated mucinous adenocarcinoma	pT3 N0 (0/30)	1947	M	Unknown	Mutation detected in the BRAF gene (c.1799T>A, p.(Val600Glu), COSM476). Mutation not detected in the KRAS and NRAS genes.
55	0108899	Normal Adjacent			1947	M		
56	0108901	CRC	moderately differentiated adenocarcinoma	pT4b N0 (0/21) Mx	1944	F	Unknown	Mutation not detected in the KRAS, NRAS and BRAF genes. Mutation detected in the TP53 gene (c.826_827delGCinsTT, p.(Ala276Phe).
56	0108902	Normal Adjacent			1944	F		
57	0108904	CRC	mucinous adenocarcinoma	pT2 N1 (3/25) Mx	1944	F	Unknown	Mutation not detected in the KRAS, NRAS and BRAF genes. Mutation detected in the TP53 gene (c.818G>A, p.(Arg273His), COSM10660)
57	0108905	Normal Adjacent			1944	F		
58	0108908	CRC	No evidence of primary tumour: RG-1	ypT0 N0 (0/16) M0	1959	M	Yes	NOT TESTED
58	0108909	Normal Adjacent			1959	M		
Fresh-frozen samples obtained from OCHRe								
59	0104758	CRC	moderately differentiated adenomcarcinoma	pT3 N1(2/23) M0	1934	F	None	--
59	0104757	Normal Adjacent			1934	F		--
60	0104528	CRC	moderately differentiated adenomcarcinoma	pT3 N0 MX	1930	M	None	--
60	0104532	Normal Adjacent			1930	M		--
61	0104518	CRC	moderately differentiated adenomcarcinoma	pT2 N0(0/32) MX	1926	M	Unknown	--
61	0104507	Normal Adjacent			1926	M		--
62	0104456	CRC	ulcerated signet ring cell adenocarcinoma	pT4b N2(5/13) MX	1966	F	None	--
62	0104453	Normal Adjacent			1966	F		--
63	0104423	CRC	moderately differentiated adenomcarcinoma	PT3 N0(0/16) M0	1927	F	None	--
63	0104421	Normal Adjacent			1927	F		--
64	0105836	CRC	moderately differentiated adenomcarcinoma	pT2 N0(0/24) M0	1969	M	None	--
64	0105832	Normal Adjacent			1969	M		--
65	0105726	CRC	moderately differentiated adenomcarcinoma	pT3 NT(15/26) M0	1960	M	None	--
65	0105721	Normal Adjacent			1960	M		--
66	0105473	CRC	moderately differentiated adenomcarcinoma	pT4 N0(0/28) Mx	1930	F	None	--
66	0105470	Normal Adjacent			1930	F		--
67	0105349	CRC	tubulovillous adenoma high grade dysplasia	N/A	1939	M	None	--
67	0105358	Normal Adjacent			1939	M		--

**Missing clinical data from N=2 patients
-- Denotes data not available